

Delineation of channel networks from Digital Elevation Models

ASHRAF AFANA
Ph.D. Dissertation



Departamento de
Biología Vegetal y Ecología
UNIVERSIDAD DE ALMERIA



CSIC

Estación
Experimental
de Zonas Áridas

Departamento de
Desertificación y
Geocología



University of Almeria
Experimental Station of Arid Zones (EEZA)

Delineation of channel networks from Digital Elevation Models (DEMs)

By:
ASHRAF AFANA

Submitted for the degree of Ph.D. in Landscape Ecology of
the University of Almeria

SUPERVISED BY: DR. GABRIEL DEL BARRIO

“Although the river and hillslope waste do not resemble each other at first sight, they are only the extreme members of a continuous series and when this generalization is appreciated one may fairly extend the ‘river’ all over its basin and up to its very divide. Ordinarily treated the river is like the veins of a leaf; broadly viewed it is the entire leaf”.

William M. Davis, 1899

إهداء:

إلى والدي العزيز.....

إلى والدي الحبيب.....

إلى إخوتي و أخواتي الأحباء.....

إلى رفيقة الدرب و العمر, زوجتي الغالية.....

Para mis queridos padres

Omar & Faiqa

Para mis hermanos

Ishraf, Mohamad & Olfat

Pero sobre todo para Maite con el mismo amor y la misma ilusión desde hace 11 años

Acknowledgements

While a completed Ph.D. thesis bears the single name of the student, it is always accomplished with the help of other people. I wish to express my acknowledgment to certain people who help to reach this stage.

First and for most I want to thank Dr. Gabriel del Barrio supervisor of this thesis. I appreciate all of his contributions in ideas and suggestions, which made my Ph.D. experience productive and meaningful. He has been very helpful to me during the entire period of my studies. The enthusiasm he has for his research was a continuous motivation for me, even when the pursuit of my Ph.D. became daunting. I believe that without his help this dissertation would have been a wish.

I am grateful to Dr. Albert Solé-Benet (neighbour in the old *Chumbo* and boss in the new centre) for his time and support, helping and providing insights on the working of academic research.

Many thanks go to the member of the Geo-Ecology and Desertification Research Group at the Experimental Station of Arid Zones (EEZA-CSIC), mainly Dr. Roberto Lázaro and Dr. Paco Domingo. The group has been a good source for advice and collaboration. Special thanks to Dr. Yolanda Cantón who provided excellent timely advice. My sincere thanks and gratitude goes to Marieta Sanjuan, my old office mate and my first GIS teacher, for her incessant help and courage, affection and sympathy, worry and concern, and for her countless advices not only at work but also in my daily life. I would also like to acknowledge Sebastian Marquez and Alberto Ruiz for their advice and willingness to share in GIS. Special thanks go to Isabel our librarian for her contiguous help and efforts in preparing the large list of references in this work. Also, I would like to thank Dr. Monica García for all the support and help during her stay in the centre.

I would also like to thank Dr. Matthias Boer and Dr. Juan Puigdefábregas for the first advices in my initial studies. It was a great honour for me to share with them ideas, work and company.

Special thanks to Alfredo Duran for the help and advices in the field and for the continuous encouragements and willingness that makes every moment I spend in and out of the work glad and joyful. More thanks to Teresa Abaigar for all the sweet moments that I spend with her, with special and intense discussions on the dilemma of the life.

In addition to the CANOA project, the present PhD thesis was partially supported by other projects and programs we would like to acknowledge: *i)* A scholarship from the Spanish Agency of

International Cooperation (AECD); *ii*) Global Coherence Analysis of the Red Natura 2000 in Spain (Ref. CSIC: 2006X0365) and financed by the Ministry of Environment and TRAGSA enterprise; *iii*) Habitat Conservation and Land Degradation in Andalusia (MesoTopos) and financed by the Andalusia Autonomous Region (Excellency Project P08-RNM-04023); *iv*) Experimental soil restoration in limestone quarries under arid climates, financed by the Andalusia Autonomous Region (Excellency Project RNM-5887); *v*) Plan of Ecologic Restoration and Landscape Integration of Quarry Limestone in the Sierra of Gador, contract with HOLCIM-Spain; and, *vi*) project DESIRE (Desertification Mitigation and Remediation of Land– a global approach for local Solutions), financed by the EC-DG RTD (Ref. 037046).

I gratefully acknowledge all the Grand family of the Chumbo for the sweet, warm environment and the unforgotten moments in every corner of the centre. I would like to show my gratitude to all my friends, with them my stay in Almeria was made enjoyable.

Of course, I can't forget my best friends and housemates, Luis and Carlos, for their warm kindness and the endless hospitality that they showed and continue so far during my presence in Almeria, they are more than friends they are my brothers.

Last but not least, my family deserves special mention in this work. My father is the person who taught me the meaning of the life, who showed me the way to follow, who awarded me the spirit of being honest, patient, glad and grateful in this life, and who raised me with a love of learning and working hard. My mother, with her continued love, affection, warmth and care I keep on hope day and night. To both of you thank you very much for grooming me to be what I am now. Also, I would like to show my great love, gratitude and thanks to my family, both in Salfit and in Zamora. Lastly, my wife Maite, with her every moment is a new inspiration of love and happiness. Thanks a lot for your spirit, support and cheering up which made this work a real enjoyable journey.

Ashraf,

Agradecimientos

Cualquier trabajo en el mundo no solamente lleva la huella de su autor, sino también de otras personas que han sido autores indirectos y que forman parte de su contenido. Me gustaría expresar toda mi gratitud y consideración a ciertas personas que me han ayudado a lo largo de este trabajo.

En primer lugar, mi reconocimiento al Dr. Gabriel del Barrio, el Director de esta tesis. Todo mi agradecimiento por su contribución en ideas y sugerencias, que han hecho de mi tesis doctoral una experiencia muy productiva y significativa. Durante todo el tiempo de mi tesis doctoral, su ayuda ha sido para mí de gran utilidad y provecho. El entusiasmo que tiene hacia su trabajo ha sido una de las motivaciones que me han guiado y empujado, incluso en los momentos de más desasosiego y cuando más difícil era proseguir con mi trabajo de tesis. Creo que sin su ayuda este trabajo hubiera sido solo un anhelo.

Mi enorme gratitud al Dr. Albert Solé-Benet (vecino en el antiguo *Chumbo*, jefe y compañero en el nuevo centro) por su tiempo y el apoyo constante, ayudando y proporcionando ideas e informaciones sobre este trabajo en particular y sobre los trabajos académicos en general.

Después, mi gran agradecimiento a todos los miembros del equipo de investigación del departamento de Geo-Ecología y Desertificación en la Estación Experimental de Zonas Áridas (EEZA), especialmente al Dr. Roberto Lázaro y al Dr. Paco Domingo. Para mí, el grupo ha sido un apoyo constante y una fuente de consejos y de colaboración. Mi especial gratitud a la Dra. Yolanda Cantón quien me ha proporcionado excelentes y oportunos consejos desde el primer día de conocerla. Mi más sincero agradecimiento para Marieta Sanjuan, mi antigua compañera de despacho y mi primera profesora de GIS, por su incesante ánimo y apoyo, por su afecto y simpatía, y por sus consejos y ayuda en todo momento, no solo en el trabajo sino también en la vida cotidiana. Sinceramente, es una fantástica amiga y compañera. Igualmente, me gustaría agradecer a Sebastián Márquez y Alberto Ruiz por los consejos y la información compartida en los SIG. Especial gratitud a Isabel (nuestra indispensable bibliotecaria) por la continua ayuda y esfuerzo en la preparación de la enorme lista de referencias de este trabajo. También, mi gratitud a la Dra. Mónica García por todo el apoyo y la ayuda durante su estancia en el Chumbo.

Asimismo me gustaría agradecer al Dr. Juan Puigdefábregas y al Dr. Matthias Boer por los primeros consejos al inicio de este trabajo; ha sido para mí un gran honor compartir con ellos ideas, trabajo y compañía.

Me gustaría también dar las gracias a dos grandes amigos: el primero, Alfredo Durán, por la ayuda y los consejos en el campo y por el continuo ánimo, apoyo y fino sentido del humor que hacía de cualquier momento, dentro y fuera del trabajo, algo alegre y gustoso; y la segunda, Teresa Abaigar, por todos los momentos dulces que he pasado con ella, llevando a cabo las más intensas discusiones sobre el dilema de la vida.

Del mismo modo, me gustaría agradecer a toda la gran familia del Chumbo por la gran amabilidad, su hospitalidad y los momentos inolvidables en cada esquina de este centro. Me gustaría dar y mostrar mi gratitud a todos mis amigos (fuera y dentro del trabajo, compañeros o colegas, almerienses o forasteros, negros o moros, autóctonos o guiris), con ellos mi estancia en Almería ha sido la experiencia más dulce, divertida y agradable.

Además del proyecto CANOA, la actual tesis doctoral ha sido apoyada por otros proyectos y programas que nos gustaría agradecer: *i*) una beca de la Agencia Española de Cooperación Internacional (AECI); *ii*) Análisis de Coherencia Global de la Red Natura 2000 en España (Ref. CSIC: 2006X0365), financiado por el ministerio de Medio Ambiente y TRAGSA; *iii*) Conservación de Hábitats y Degradación de Tierras en Andalucía (MesoTopos), financiado por la Junta de Andalucía (Proyecto de Excelencia P08-RNM-04023); *iv*) Restauración experimental de suelos en Canteras de roca calcárea en ambientes áridos (Proyecto de Excelencia de la Junta de Andalucía, RNM-5887); *d*) Plan de restauración ecológica e integración paisajística de las canteras de caliza de la Sierra de Gádor (contrato con HOLCIM-España); y, *e*) Proyecto DESIRE (Desertification Mitigation and Remediation of land – a global approach for local Solutions) financiado por EC-DG RTD (Ref. 037046).

Pero sobre todo, no puedo olvidar mis amigos y compañeros de piso, Carlos y Luis, por su cálida amabilidad y la interminable hospitalidad que me han mostrado y siguen mostrando durante todo este tiempo. La verdad más que amigos, son mis hermanos.

Por último, pero no por ello menos importante, mi familia merece una especial mención en este trabajo. Mi padre, la persona que me ha enseñado el significado de la vida, el camino a seguir, quién me ha infundido el espíritu de ser honesto, paciente, alegre y agradecido, y me ha criado con el amor de aprender y trabajar duro en la vida. Mi Madre, cuyo continuo amor, afición y fervor me mantiene con esperanza día y noche. Para ambos muchas gracias por haberme educado y por enseñarme los valores de la vida que me han permitido llegar a lo que ahora soy. También, quisiera mostrar todo mi gratitud y cariño para mi familia, ambas en Salfit y en Zamora. Por último, mi querida Maite, con ella cada momento es una nueva inspiración de amor y felicidad. Gracias, cariño, por tu espíritu de apoyo y alegría que hace de este trabajo y de todos los momentos un verdadero viaje de felicidad.

Ashraf.

Contents

1. INTRODUCTION TO THE GENERAL CONTEXT OF THE WORK	9
1.1. General approach: motivation	9
1.2. Problem definition: needs for new approaches	11
1.3. Aims and objectives	15
1.4. Thesis outline	16
2. ASSESSMENT OF DIGITAL ELEVATION MODELS (DEMS) FOR STREAM NETWORK EXTRACTION	19
2.1. Introduction	19
2.2. Background	20
2.2.1. Origin, Sources and Structure	20
2.2.2. Errors, uncertainties and accuracy	22
2.2.3. Importance and utilities	25
2.2.4. Scale and resolution	27
2.2.4.1. Concepts	27
2.2.4.2. Importance and consequence	29
2.2.4.3. Multi-scale approach	36
2.2.4.4. Integration of scale and resolution in the approach model	38
2.2.4.5. Resolution and accuracy in DEMs	39
2.2.5. River basins from DEMs	46
2.3. Location and general characteristics of the study area	48
2.3.1. Tabernas Basin site location and general characteristics	48
2.3.2. La Rambla Honda site location and general characteristics	55
2.3.3. El Cautivo site location and general characteristics	57

2.4. DEMs of the study area.....	60
2.4.1. Introduction	60
2.4.2. Methodology	62
2.4.3. Low resolution DEM (complex & heterogeneous landscape)	62
2.4.4. High resolution DEMs (homogeneous landscape).....	71
2.4.5. Conclusions	74
3. GEOMORPHOMETRIC QUANTIFICATION OF CHANNEL NETWORK STRUCTURE..	77
3.1. Introduction.....	77
3.2. Background	77
3.2.1. Features, relations and processes in landscape.....	77
3.2.2. Hydrology	78
3.2.3. Geomorphology.....	79
3.2.3.1. Introduction.....	79
3.2.3.2. Fluvial geomorphology.....	80
3.2.3.3. Geomorphometry	81
3.3. Characteristics of catchment and channel network.....	85
3.3.1. Definition of hydrological basins and drainage networks.....	85
3.3.2. Drainage basins and channel networks classification	87
3.3.2.1. Ordering system.....	92
3.3.3. Geometry of stream networks	94
3.3.4. Relief characteristics	107
3.3.5. Fractal and scaling laws in channel networks	110
3.3.6. Multifractal approach	113
3.3.7. Channel network evolution	114
3.3.8. Geomorphic concept of landscape change	116
3.4. A reduced quantitative approach for channel network properties.....	120
3.4.1. Introduction	120
3.4.2. Treatment for methodological comparison	123

3.4.3. Selection parameters	124
3.4.4. Conclusions	129
4. AUTOMATIC STREAM NETWORK DELINEATION FROM DEMS	131
4.1. General revision	131
4.2. Manual derivation of channel networks	132
4.3. Automatic derivation of channel networks	133
4.3.1. O’Callaghan and Mark’s method	137
4.3.2. Band’s method	139
4.4. Threshold definition mode (Channel initiation)	140
4.4.1. Automatic thresholds with local factors (indirect models)	142
4.4.2. Automatic thresholds without local factors (direct models)	145
4.5. Multifractal approach in stream network delineation	153
4.6. Validation procedures in channel networks	155
4.7. Conclusions	157
5. INTRINSIC HIERARCHICAL STRATIFICATION OF LANDSCAPE AND THE ADAPTIVE MODEL	159
5.1. Introduction	159
5.1.1. General revision	159
5.1.2. Importance of selecting the optimum threshold	160
5.2. Aims and objectives	163
5.3. Methodology	164
5.3.1. Introduction	164
5.3.2. Origin of the model approach	166
5.3.3. A conceptual framework	166
5.3.4. Model derivation	170
5.3.5. The concept of stability zones and the hierarchical stratification approach	172
5.3.6. Quantitative characterization of channel networks	176

5.3.7. Model validation and auxiliary interpretations	178
5.4. Analysis and Results	180
5.4.1. Introduction	180
5.4.2. The analysis of Tabernas Basin at 30m.....	181
5.4.2.1. Drainage network delineation.....	181
5.4.2.2. The comparison mode between techniques	186
5.4.3. The analysis of El Cautivo and La Rambla Honda Basins.....	195
5.4.3.1. Introduction.....	195
5.4.3.2. Drainage network delineation.....	196
5.4.3.3. Geomorphometrical indices analysis	199
5.4.4. Physical validation process	200
5.4.4.1. Experimental comparison	202
5.4.4.2. Visual interpretation	208
5.5. Discussion and Analysis	211
5.5.1. Introduction	211
5.5.2. The adaptive model and the <i>HSP</i>	211
5.5.3. Comparison between techniques.....	230
5.5.4. Physical validation process	235
5.6. Conclusions.....	239
6. SPATIAL ANALYSIS AND LANDFORM DEPICTION IN SIMULATED AND REAL LANDSCAPES.....	247
6.1. Introduction.....	247
6.2. Background.....	252
6.2.1. Introduction	252
6.2.2. The spatial analysis and semivariogram approach.....	253
6.2.3. Laser scanning techniques.....	259
6.2.4. Workflow for <i>TLS</i> data.....	263
6.2.4.1. Field data collection.....	264

6.2.4.2. Data processing.....	265
6.2.4.3. Model creation.....	267
6.3. Aims and objectives.....	269
6.4. Data acquisition and site location.....	269
6.4.1. Introduction to site location.....	269
6.4.2. Data acquisition and preparation.....	270
6.5. Methodology.....	273
6.6. Analysis and results.....	276
6.6.1. Introduction.....	276
6.6.2. Spatial analysis in ridge formations.....	277
6.6.2.1. Ridge analysis with trend.....	277
6.6.2.2. Ridge analysis without trend.....	280
6.6.3. Spatial analysis in hillslope formations.....	281
6.6.3.1. Hillslope formations with trend.....	282
6.6.3.2. Hillslope formations without trend.....	283
6.6.4. Spatial analysis in channels and valley formations.....	287
6.6.4.1. Channel formations with trend.....	288
6.6.4.2. Channel formations without trend.....	290
6.6.5. Spatial analysis at channel heads (channel initiation).....	291
6.6.5.1. Channel head formations with trend.....	292
6.6.5.2. Channel head formations without trend.....	294
6.6.6. Interpretation of the directional analysis for the examined formations.....	295
6.6.7. Spatial analysis in a stream-hillslope transect (toposequence profile).....	299
6.6.7.1. Toposequence profile with clear limits (case A).....	300
6.6.7.2. Toposequence profile with smooth limits (case B).....	307
6.6.8. Spatial analysis in simulated landscape (DLSTM).....	310
6.6.9. Delineation and validation of stream network limits.....	314
6.7. Discussion.....	319

6.7.1. Introduction	319
6.7.2. Landform analysis in real data structures.....	319
6.7.3. Toposequence profile analysis in real landscapes	324
6.7.4. Toposequence profile analysis in simulated landscapes	325
6.7.5. Validation of stream limits based on directional analysis.....	327
6.8. Conclusions and recommendations.....	328
7. GENERAL CONCLUSIONS AND RECOMMENDATIONS	333
7.1. Introduction	333
7.2. Evaluation of the data and the proposed approach.....	333
7.3. Synthesis conclusion	335
7.4. Partial Conclusions.....	337
7.5. Suggestions for further research.....	338
BIBLIOGRAPHY	341
Appendix 1	377

List of Figures

1.1	Schematic flowchart representation of the thesis structure	18
2.1	The main tasks associated with DEMs.....	26
2.2	Scales in hydrology and geomorphology	34
2.3	DEMs of different origins and resolution and varied landform complexities	49
2.4	Geomorphologic scheme of the Tabernas Basin.....	51
2.5	The digitized channel network or Blue Lines (<i>BLs</i>) for the Tabernas Basin.....	53
2.6	Values of normalized difference vegetation index (NDVI) in Tabernas Basin.....	55
2.7	Catena scheme in the Rambla Honda catchment	57
2.8	Digitized- <i>BLs</i> in La Rambla Honda catchment obtained by a topographic map at 1:500	58
2.9	Digitized- <i>BLs</i> in El Cautivo Catchment obtained by a topographic map at 1:500	61
2.10	Aerial photograph of El Cautivo badland system.....	61
2.11	Generalized DEMs with systematically declining horizontal resolution.....	66
2.12	Probability depressions from the application of Stochastic Shape Analysis	67
2.13	DEM of Tabernas at 30 m grid spacing corrected by the SSA analysis.....	68
2.14	Scatterplot of RMSE in DEM-data matrix against resolution and catchment areas.....	69
2.15	Resolution effect on changes in catchment size. The curve shows tow different scales	69
2.16	Stochastic Shape analysis in El Cautivo catchment	72
2.17	Drainage networks in El Cautivo catchment, extracted by a threshold value of 20 cells.....	72
2.18	Stochastic shape analysis in La Rambla Honda catchment.....	73
2.19	Drainage networks in La Rambla Honda catchment, extracted by a threshold value of 50 cells.....	74
3.1	The idealized fluvial system.....	85
3.2	Watershed areas of different outlets and hence different sizes.....	86
3.3	Watershed classification based on dominates channel patterns	88
3.4	Illustration of sinuosity concept.....	89
3.5	A schematic illustration of a longitudinal stream profile	90
3.6	Two ordering systems of stream channel networks	93

3.7	The <i>HI</i> curves of different sub-catchments of Tabernas Basin	109
3.8	Projection of factor coordinates (1 & 2) in relation variables and cases	125
3.9	Projection of factor coordinates (1 & 2) in relation to cases below and above 1 km ²	126
4.1	A Schematic representation of landscape dominant channel initiation processes.....	143
4.2	Slope-area relationship approach for stream network delineation with two phase regression	147
4.3	Channel networks delineated by the Constant Drop Analysis (CDA)	148
4.4	Slope-area relationship approach for stream network delineation with reversal and inflection.....	152
5.1	A conceptual framework for R'_A behaviour.....	172
5.2	A schematic flowchart representing the $R'_A t$ approach and related processes.	177
5.3	Channel networks delineated by <i>CDA</i> procedure with $A_S = 500$ cells.	181
5.4	The curve relationship between R'_A and A_S for Tabernas Basin	182
5.5	Hypsometric integral (<i>HI</i>) curve for Tabernas Basin DEM at 30 m resolution.	183
5.6	Order and classification of Tabernas Basin defined by the <i>MRC</i>	184
5.7	Channel networks for Tabernas Basin after reconnecting the reconstructed parts.....	185
5.8	Tabernas sub-basins mentioned earlier in table 4.10 classified according to Pennock	185
5.9	Curves relationship between catchment area and drainage density without the <i>HSP</i>	189
5.10	Fractal dimensions of Hack's and Melton's laws for the <i>BLs</i> in Tabernas Basin	189
5.11	Curve relationship between catchment area and drainage area density with the <i>HSP</i>	191
5.12	Comparison between channel networks in Tabernas Basin	193
5.13	Observed sub-catchment within Tabernas Basin and its corresponding drainage networks	193
5.14	Estimation of Melton's value of ϕ for <i>BLs</i> in the sub-catchments of Tabernas Basin	195
5.15	The Cautivo Basin field site with different channel networks	197
5.16	The Rambla Honda Basin field site with different channel networks	198
5.17	Quantification of first order streams of the digitized <i>BLs</i> in the Cautivo and Rambla Honda.....	202
5.18	Two possible sketches for a modified channel network according to different A_S in the Cautivo	205
5.19	Two possible sketches for a modified channel network according to different A_S in Rambla Honda	205
5.20a	Channel networks of the Cautivo basin constructed by mean A_S values	206
5.20b	Channel networks of the Cautivo basin constructed by median A_S values.....	206
5.21a	Channel networks of the Rambla Honda basin constructed by mean A_S values.....	207

5.21b	Channel networks in the Rambla Honda basin constructed by median A_S values.....	207
5.22	A direct comparison between the BLs and the automated channel networks.....	209
5.23	Visualized channel networks using orthophotographs for the El Cautivo catchment	210
5.24	Visualized channel networks using orthophotographs for the Rambla Honda catchment	210
5.25	DEMs capacity in relation to its resolution in detection the range of the critical threshold.....	213
5.26	Curve relationship for the adaptive model in the Cautivo Catchment.....	214
5.27	Channel networks delineated by different A_S values localized in the order level 4.....	215
5.28	Channel networks delineated with different A_S values localized in the third order level	216
5.29	Channel stream network in the Cautivo catchment with $A_S = 21$	216
5.30	Generated sub-catchments in the Cautivo basin using the HSP procedure	217
5.31	A schematic of the transition between channelled and unchanneled areas.	221
5.32	Curve relationships between A_S and R'_A in the Rambla Honda Basin	225
5.33	The digitized BLs and the channel network in the Cautivo delineated by different A_S values	225
5.34	Main sub-catchments of the Rambla Honda basin resulted from the $R'_A t$ procedure.....	226
5.35	Direct comparison between channel network limits delineated by the CDA and R'_A procedure	227
5.36	Form and type of the curve tendency relationship between A_S and R'_A in the sub-basin B.....	229
5.37	3D structure visualization of the drainage networks in Tabernas Basin.....	230
6.1	Experimental variogram with basic characteristics.....	255
6.2	A representation of a geometric anisotropy	256
6.3	The three most commonly used transition models (spherical, exponential, and Gaussian)	257
6.4	A “point cloud” representing a hydrographic unit basin	263
6.5	Location of the study area and its position within El Cautivo field site.....	270
6.6	Data registration for the 3 point clouds of the studied area.....	272
6.7	Dissimilarity in point cloud density in relation to the direction and orientation of the landform	273
6.8	A pure ridge formation structure or a divide line from the mini-catchment in the study area	277
6.9	Direct comparison between different sub-hierarchical scales for ridge formations with trend.....	279
6.10	Direct comparison between different sub-hierarchical scales for ridge formations without trend.....	281
6.11	Hillslope sample data set location in the studied mini catchment.....	281
6.12	Direct comparison between different sub-hierarchical scales for hillslope with trend.....	282

6.13	Directional autocorrelation in hillslope formation without trend.....	284
6.14	Semivariograms of the hillslope feature of the 1 m unit	286
6.15	3D representations of hillslope formations without trend for the four sub-units.....	287
6.16	Location, form and limits of the channel sample dataset within the studied catchment	288
6.17	Comparisons between semivariogram parameters for channel formations with trend.....	289
6.18	Comparisons between semivariogram parameters for stream formations without trend.....	291
6.19	A Sample data set of channel initiation form structure	292
6.20	Comparison between semivariogram parameters for channel initiation with trend	293
6.21	Comparison between semivariogram parameters for channel initiation without trend	295
6.22	3D representations of the analyzed sample datasets of channel initiation without trend	295
6.23	Location of the profile transects in the studied mini-catchment.....	300
6.24	Schematic representations for the semivariogram parameters in toposequence profile A.....	301
6.25	Nested curve structure formed in the second transition zone	304
6.26	Kriging interpolation for the second transition zone.....	304
6.27	Zonal anisotropy observed in the second transition zone.....	305
6.28	Channel-hillslope toposequence for a smooth transition zone in toposequence B.....	308
6.29	Schematic representations for the semivariogram parameters in toposequence B	309
6.30	Interpolation of the sample datasets of the toposequence profile B	310
6.31	Schematic representations for the semivariogram parameters using DEM data in the profile A	311
6.32	Semivariogram parameters for hillslope formation 2 using DEM data in the profile A.....	312
6.33	Degree of inclination in the two sample datasets that represents hillslope 1 & 2	313
6.34	3D reconstructions of stream formations representing stream bank and bed effects	314
6.35	3D representation of the channel network delineated by the (CDA) approach	315
6.36	3D representation of the channel network delineated by the $R'_A t$ approach.....	316
6.37	Stream networks delineated by (a) CDP and (b) the $R'_A t$ approach in the Cautivo basin	318

List of Tables

2.1	Spatial scales of applications of DEMs and common sources	40
2.2	Main characteristics of four main monitored soil surfaces.....	60
2.3	RMSE for the different resolution with different degradation DEM procedures	63
2.4	Change Catchment size values and the differences in relation to the average	65
2.5	Change Catchment size values at different resolutions	70
3.1	Channel network properties adapted from Strahler.....	97
3.2	Geomorphometrical indices proposed for the comparison and validation procedure	121
3.3	Main factor coordinates of the 27 geomorphometrical indices used in the <i>PCA</i> analysis.....	125
3.4	Main factor coordinates of the 27 geomorphometrical indices with basin size > 1km ²	127
3.5	Correlation matrix for the topologic properties in the first factor.	128
3.6	Correlation matrix between attributed of the third factor.....	128
3.7	Indices used in the comparison test between <i>BLs</i> and channel networks defined from DEMs.....	129
4.1	Main GIS systems that treat directly or incorporated basic models	154
5.1	Rank order correlation index of Spearman (<i>R</i>) between Relief indices and catchment area.....	175
5.2	Tabernas Basin and the main sub-catchments presented in figure 5.6.....	183
5.3	Degrees of result enhancement (%) in comparison between geomorphometrical parameters	188
5.4	Direct comparison values for Tabernas Basin without using the <i>HCP</i>	188
5.5	Values of partial comparison between α and ϕ for the studied catchments in Tabernas Basin	190
5.6	Degrees of result enhancement in partial comparison between geomorphometrical parameters	191
5.7	Direct comparison values for Tabernas Basin using <i>HCP</i>	192
5.8	Comparison values of α and ϕ and their <i>GM</i> test of association for the total comparison	194
5.9	Dimensions of Melton's value (ϕ) for channel networks delineated by <i>CDA</i> and R'_{At}	195
5.10	Direct comparison values for the Cautivo Basin.....	199
5.11	Direct comparison values for La Rambla Honda Basin	200

5.12	Direct comparison between first order streams of the <i>BLs</i> in El Cautivo Basin	203
5.13	Direct comparison between first order streams of the <i>BLs</i> in La Rambla Honda	203
5.14	Description of the general statistics of length (<i>L</i>) and threshold value (<i>A_S</i>) of first order streams	203
5.15	The optimum <i>A_S</i> value defined according to the <i>R'_At</i> approach in the Cautivo Basin	217
5.16	Changes in geomorphometric indices before and after applying the new <i>A_S</i> value.....	223
5.17	Number and percentage of catchments in which used techniques failed to detach a valid <i>A_S</i>	232
5.18	Fluctuations of Hack's value extracted from the <i>BLs</i> in relation to the basin area.....	235
5.19	Descriptive statistics of contributing source area for first order streams of the <i>BLs</i>	236
6.1	Specifications and system performance characteristics of Leica ScanStation 2 Laser System	265
6.2	Parameters of the anisotropic models fitted to variograms for ridge formations with trend	278
6.3	Parameters of the anisotropic models fitted to variograms for hillslope with trend.....	283
6.4	Parameters of the anisotropic models fitted to variograms for hillslopes without trend	285
6.5	Values of fractal dimension and the Brownian motion for the analysed sub-scales	287
6.6	Parameters of the anisotropic models fitted to variograms for all formations at 1 m.....	297
6.7	Summary of semivariogram parameters and their interpretation from the analysed formations.....	298
6.8	Parameters of the anisotropic models fitted to experimental variograms in four directions	302
6.9	Slope and sill variance for profile sample set data in the studied area	307
6.10	Parameters of the anisotropic models fitted to variograms channel heads in figure 6.35	317
6.11	Parameters of the anisotropic models fitted to variograms channel heads in figure 6.36	317

ABSTRACT

Since the early work of W.W. Davis in 1899, channel networks and their drainage basins have formed one of the main scientific endeavours to understand landscape evolution, mainly the geomorphological and hydrological functions and processes that control the actual earth shape and aspect. Stream network extraction and delineation is one of the main tasks to understand the above roles and processes. Based on manual methods and eye observations, earlier scientists delineated channel networks from either topographic maps or aerial photographs. In this case, manual delineation depends on relief contrasts and is highly subjective leading to considerable errors at high resolutions. An alternative approach is the automated extraction of drainage networks from Digital Elevation Models (DEMs), based on the wide notion of the hydrological properties of topographic surfaces. Whilst extraction of channel networks is broadly simple and direct, delineation of stream limits is still a matter of debate because of the inherent challenge of formalising overland flow with respect to surface features. In general, methods of stream limits definition propose the use of a constant threshold drainage area to define where channels begin in the landscape. However, such a threshold depends on the topographic complexity, and consequently the majority of these methods fail to perform consistently wherever the basin is made up of heterogeneous sub-zones, as they only work lumped. In this study, the critical threshold value has been defined by the analysis of dominant geometric and topologic properties of stream network formations. In addition, a recursive stratification process has been integrated in the model to detect homogeneous hierarchical sub-basins in relation to dominant intrinsic properties. Such approach (i.e. adaptive model) provides with the necessary critical thresholds in relation to DEM-data resolution and to diversity of dominant landforms. All these assumptions are based on a basic notion that “DEMs are self-contained structures which reflect the geomorphic and hydrologic processes that form them, and therefore encompass the necessary information to extract and delineate the channel networks by using algorithms and models capable of processing such information.

While delineation of stream limits has received a considerable attention from scientists, validation of the achieved results is still in lagging behind. How and what to validate were between the several questions that opened debates between researchers. The complex structure of natural stream systems makes it somewhat complicated to adapt a particular approach over the others. In general, two main approaches for stream network validation are widespread between geomorphologists: quantitative and qualitative methods. The former uses geomorphometrical indices that describe stream network structure properties, extracted from different sources (e.g. topographic maps, DEMs, etc.)

which are statistically compared. The latter involve field visits and visual interpretation of the resulting data, and its post comparison with information from other sources (e.g. orthophotographs, 3D structures, etc.). In the present work, emphasis has been placed on the quantitative approach, because of the direct effect of geomorphometrical parameters on hydrological and geomorphological models.

The work has been carried out in various catchments with different lithology and geomorphic processes. The studied area comprises the Tabernas basin (SE Spain) representing a heterogeneous complex landscape, and the El Cautivo and Rambla Honda sub-basins representing respective homogeneous relief formations of different types and origins. High-resolution DEMs of 6 cm and 1 m were used to obtain the best detailed drainage network that the algorithm can generate at these homogeneous landscapes, whereas a medium-resolution DEM (30 m) was applied to the general heterogeneous landscape. The used DEMs are of diverse origins. The 6 cm DEM was obtained by laser scanning technique (*LST*), the 1 m DEMs were interpolated from isohyets and contour maps, whereas the 30-m DEM was obtained by photogrammetric restitution and interpolation. The wide range and origin of those analysed DEMs should provide deeper insights on errors and uncertainties effect on stream network delineation. In addition, detailed DEMs may allow for a direct quantitative comparison as well indirect qualitative ones.

Uncertainty in the analysed dataset was treated in relation to the original data resolution and construction procedure (i.e. vertical and horizontal accuracies). In addition, suitability of the DEMs to channel network extraction was tested by the average-drop-cell ratio. Since DEMs are of varying origin and resolutions, uncertainty was assessed with a comprehensive procedure for error quantification. In general, a combination between global (root square mean error-RMSE) and local (stochastic shape analysis-SSA) error measurements was applied to the data matrix. First, results of resolution effect over stream network extraction, in relation to the current RMSE value, showed that above 240 m the extracted drainage network losses reliability, and below the 120 m the resolution is widely optimal. Second, the SSA reduces local uncertainties in the analysed matrix leading to moderate modifications in the defined channel networks, mainly in areas that may be altered by local factors (e.g. vegetation cover, flat areas, valley formations, etc.).

The geomorphometric attributes are simple or compound parameters that describe drainage network structure properties, either partially or completely leading to redundancy and autocorrelation between these descriptors. Scientists used multivariate statistical techniques (e.g. factor or principle component analysis) to screen and reduce the amount of analysed inter-related attributes by using the highest loading parameter as representative index of each component of variation. Results of the current work demonstrated that such approach is somewhat erratic and unreliable, because parameters weight and presence in each factor is highly related to scale. In order to avoid these drawbacks, this study proposes the use of a combination of multivariate technique and a complementary correlation test. Herein, the selection of the indices is determined by the amount of correlation in each factor

rather than the highest weight one. In this case, similar geomorphometric properties are grouped and tested. By doing so, the selected indices summarises the geomorphometric components of the original matrix and explains the underlying relations and influences among the parameters.

Application of the adaptive model to the study area revealed a clear improvement in channel network depiction translated in great similarity to natural ones. In general, the adaptive model defines as many as necessary threshold values based on the intrinsic properties of the analysed drainage networks and the resolution of the original data structure. The former is underlined by the topological and geometrical properties of the stream network, whereas the latter is related to the DEM resolution. The provided thresholds depict landscape to different hydrological units in relation to relief complexity leading to multifractal and simple values in heterogeneous and homogeneous landscapes, respectively. The later comparison between the adaptive model and the constant drop analysis (*CDA*), an accepted and benchmark technique for delineating channel networks, revealed a better approximation to natural stream by the former, in approximately all the analysed catchments. The validation of the above results was carried out by the geomorphometrical indices, which should form part of any quantitative description and analysis of the channel network morphology. The geomorphometric descriptors were compared directly by the Gower Metric (*GM*) test, which enables pairwise comparisons of the selected indices. Validation results revealed that the above approach is adequate for describing terrain dissection, since its function depends on intrinsic properties of the drainage network, being at the same time objective and easy to implement. Likewise, it provides an enhanced approximation to empirical geomorphometric parameters used to describe stream network dimensions.

A second phase of this study was conducted in a mini-catchment of 956 m² in the Cautivo basin and is intended for a more precise validation of stream borders and limits. In this case, the topography was captured by a Terrestrial Laser Scanner (*TLS*) at 5 mm to generate a digital surface model (*DLSM*) and a DEM with an average of 6 cm gridded-data resolution. In order to achieve this aim, a geostatistical analysis of semivariograms was performed to define the exact spatial patterns that control landform types and to verify scale effect (i.e. scaling-up and -down) over the topographic features and limits between them. Thus, a comprehensive set of *TLS* sample data was processed to verify the spatial-domain effect in landform structures. First, within the domain structure itself, several samples of varying dimensions were selected to check for directional effects, i.e. anisotropy. In each sample data, several semivariogram parameters were defined and compared. In addition, another group of sample datasets containing more than one structural formation were analysed. Such sample data allows for a comprehensive understanding of semivariogram behaviour under multiple landform conditions. Finally, a sample dataset of stream-hillslope transect was used to identify convergent and divergent topography (i.e. channels and hillslopes), as well as the transition zone between both (i.e. channel initiation area). The results of the semivariogram analysis highlighted two important points.

The first one is the presence of a clear domain pattern in each landform component that could be used to identify similar landform structures and limits between adjacent ones. Secondly, such prevailing patterns are highly sensitive to the scale of the sample dataset. Direct applications of these results include a reliable validation approach for channel network extent in the landscape.

Finally, this work answers some questions on DEMs suitability and capacity for channel networks delineation. It is highly accepted that such datasets convey sufficient information to depict and describe the geomorphometry of a landscape. Beyond question, stream sources and limits exhibit an extreme complexity, where convergent and divergent flows become combined to produce a sensitive-feature element. Hence, errors and uncertainties should be handled throughout the study stages, as they are crucial for a reliable and efficient approach in stream network delineation.

Key words: Digital Elevation Models (DEMs), Drainage networks, Stream Channel Initiation, Specific Catchment Area, Intrinsic Properties, Adaptive Model, Geomorphometrical Indices, Terrestrial Laser Scanner (TLS), Digital Land Surface Model (DLSM), Geostatistical Analysis of Semivariograms.

RESUMEN

Desde los primeros trabajos de W.M. Davis en 1899, las redes de drenajes y sus cuencas hidrográficas han sido objeto de importantes esfuerzos científicos para comprender la evolución del paisaje, sobre todo los procesos geomorfológicos e hidrológicos que controlan el actual relieve de la Tierra. La extracción y la delineación automática de redes de drenajes es una de las tareas principales para comprender tales procesos. Basándose en métodos manuales y observaciones directas, los primeros trabajos emplearon mapas topográficos o fotografías aéreas. En estos casos, la delineación manual depende en gran medida del contraste topográfico y la subjetividad del cartógrafo, lo que conducía en muchos casos a considerables errores a altas resoluciones. Un enfoque alternativo es la extracción automática de redes de drenaje a partir de Modelos Digitales de Elevaciones (MDEs), basándose en el conocimiento previo de las propiedades hidrológicas de las superficies topográficas. Mientras que la extracción automática de redes de cauces y canales es relativamente sencilla, la delineación de sus límites es un tema de debate, por el desafío inherente en comprender y determinar el flujo superficial respecto a las características del relieve. En general, los métodos de delineación proponen el uso de un umbral constante de área de drenaje (umbral crítico) para definir donde empiezan los cauces en el paisaje. Sin embargo, dicho umbral depende de la complejidad topográfica, y por lo tanto, la mayoría de estos métodos son inconsistentes en cuencas compuestas por zonas heterogéneas. Este estudio usa también la noción de umbral crítico, que es definido por las propiedades geométricas y topológicas dominantes de la red de drenaje. Pero además, un proceso de estratificación recursiva se ha integrado en el modelo para detectar sub-cuencas homogéneas en relación con dichas propiedades. Este enfoque (“modelo adaptativo”) proporciona tantos umbrales críticos como sea necesario en relación con la resolución del MDE y la diversidad de las geoformas dominantes. Todas estas hipótesis se basan en la tesis básica de que los MDEs son estructuras autónomas que reflejan los procesos geomorfológicos e hidrológicos que han modelado el relieve que representan, y por lo tanto contienen la información necesaria para definir y delinear sus redes de drenaje mediante el uso de algoritmos y modelos capaces de procesar tal información.

Mientras que la delineación de los cauces ha recibido una considerable atención de los científicos, la validación de los resultados se encuentra todavía a la zaga. Con qué y cómo validar son algunas preguntas que han abierto el debate entre los científicos. La compleja estructura de las redes de drenajes naturales hace que sea complicado adaptar un enfoque

particular sobre los demás. En general, existen dos aproximaciones principales para la validación de cauces, según sus métodos sean cuantitativos o cualitativos. Los primeros utilizan índices geomorfométricos que describen las propiedades de las redes de drenajes extraídas de diferentes fuentes (ej. mapas topográficos, MDEs, etc.), y que son estadísticamente comparables. Los segundos consisten en visitas de campo e interpretaciones visuales de los datos, y su posterior comparación con información extraída de otras fuentes (ej. ortofotografías, estructuras 3D, etc.). En este estudio se ha puesto especial énfasis en el enfoque cuantitativo, debido al efecto directo de los parámetros geomorfométricos en la construcción de modelos geomorfológicos e hidrológicos.

El trabajo fue realizado en varias cuencas hidrográficas de diferentes litologías y dinámica geomórfica dominante. El área de estudio comprende la cuenca de Tabernas en el sudeste de España, que representa una cuenca heterogénea, y sus sub-cuencas de El Cautivo y Rambla Honda, que representan geoformas homogéneas pero de orígenes y tipos diferentes. Se usaron MDEs de 0.06 y 1 m de resolución para obtener la mejor red de drenaje que el algoritmo puede generar en relieves homogéneos, mientras que un MDE de media resolución (30 m) se aplicó para representar el paisaje heterogéneo. Los MDEs utilizados son de diversos orígenes. El de 6 cm fue obtenido mediante un láser escáner (*LST*), los de 1 m fueron interpolados a partir de curvas de nivel y puntos de apoyo, y el de 30 m fue construido a partir de un proceso de restitución fotogramétrica e interpolación. El amplio rango y origen de estos MDEs debería proporcionar una visión más profunda sobre el efecto de las incertidumbres en la delineación de redes de drenajes. Además, los MDEs de alta resolución pueden permitir una comparación directa tanto cuantitativa como cualitativa.

La incertidumbre de los datos fue tratada en relación a su resolución original y los procesos de construcción (precisión vertical y horizontal). Además, la idoneidad de los MDEs para la extracción de redes de drenajes fue comprobada por la razón de celdas de eliminación media (*average-drop-cell ratio*). En general, se aplicó una combinación entre medidas de errores globales (la raíz del error cuadrático medio o RECM) y locales (análisis estocástico). Los resultados del efecto de la resolución en relación con el RECM mostraron que la red de drenaje extraída pierde fiabilidad a resoluciones más gruesas que 240 m, mientras que tienden a ser óptimas a resoluciones más finas que 120 m. Por otra parte, el análisis estocástico redujo los errores locales mediante modificaciones moderadas en la red de drenaje definida, especialmente en las áreas alteradas por los factores locales (ej. cubierta vegetal, áreas planas, valles, etc.).

Los índices geomorfométricos son parámetros simples o compuestos que describen las propiedades, tanto parciales como totales, de la estructura de la red de drenaje, lo que lleva a redundancia y auto-correlación entre ellos. Antecedentes a este estudio han empleado técnicas de estadística multivariante (ej. análisis factorial o de componentes principales) para detectar y

reducir la cantidad de atributos interrelacionados mediante el uso del parámetro de más carga como índice representativo de cada componente de variación. Los resultados del presente trabajo demostraron que este enfoque es errático y poco fiable, ya que la presencia y peso de cada parámetro en cada factor está altamente relacionado con la escala. Con el fin de evitar estos inconvenientes, este estudio propone el uso de una combinación entre dichas técnicas multivariantes y un análisis de correlación complementario. Aquí, la selección de índices se determina por el grado de auto-correlación en cada factor, en vez del parámetro de mayor peso. Así, las mismas propiedades geomorfométricas son agrupadas y examinadas. De este modo, los índices seleccionados pueden resumir y representar los componentes geomorfométricos del MDE original, y al tiempo explicar las relaciones e influencias subyacentes entre parámetros.

La aplicación del modelo adaptativo a la zona de estudio reveló una mejora sustancial en la delineación de los cauces y canales, resultando en una gran similitud con las redes naturales. Los umbrales proporcionados dividen efectivamente el paisaje en diferentes unidades hidrográficas en relación a la complejidad del relieve, proporcionando valores fractales simples o múltiples en paisajes homogéneos y heterogéneos, respectivamente. La posterior comparación entre las técnicas del modelo adaptativo y el análisis por la razón de las propiedades de desnivel constante (*constant drop analysis*, un método de referencia para delinear redes de drenajes que ha sido aplicado sobre los mismos datos) reveló una mayor aproximación a las redes naturales por el primero de ellos en casi todas las cuencas analizadas. La validación de los resultados anteriores se realizó comparando las redes de drenaje extraídas en ambos casos con las existentes como líneas azules en el mapa topográfico. Se usaron índices geomorfométricos, que deberían formar parte de cualquier análisis y descripción cuantitativa de redes de drenajes. Los conjuntos de valores resultantes se compararon directamente mediante el índice Gower Metric (*GM*), el cual valora la disimilitud entre pares de parámetros. Los resultados de la validación mostraron que el modelo adaptativo es adecuado para describir la disección del paisaje (es decir, la densidad de la red de drenaje), ya que su función depende de las propiedades intrínsecas de la red de drenaje, siendo a su vez, objetivo y fácil de implementar. Asimismo, proporciona una mayor aproximación a los parámetros geomorfométricos empíricos utilizados en la descripción de las dimensiones de la estructura de la red de drenaje.

Una segunda fase de este estudio, destinada a una validación más precisa de los límites de los cauces, se llevó a cabo en una mini-cuenca de 956 m² en el área del Cautivo. En este caso, la topografía fue capturada mediante un laser escáner terrestre (*LST*) a 5 mm de resolución original para después generar un modelo digital de superficie (*MDS*) y un MDE con 6 cm de resolución. Sobre esos datos se realizó un análisis geoestadístico de semivariogramas para definir los patrones espaciales que controlan las geoformas dominantes, y verificar el efecto de la escala y los límites entre ellas. De esta manera, un conjunto de datos adquirido por el *LST* fue

procesado para verificar la estructura especial en las geoformas. Primero, dentro del dominio de la estructura en sí, varias muestras de diversos tamaños fueron seleccionadas para comprobar los efectos direccionales, es decir la anisotropía. En cada muestra, varios parámetros del semivariograma fueron definidos y comparados. Además, fue analizado otro conjunto de datos que contenía más de un tipo de relieve. Esto último, permitió adquirir una percepción global del comportamiento del semivariograma al ser aplicado a geoformas múltiples. Finalmente, un conjunto de datos que describe un transecto de cauce-ladera fue utilizado para identificar las geoformas convergentes y divergentes (cauces y laderas), así como la transición entre ambas (la zona de iniciación del cauce). Los resultados del análisis geoestadístico destacaron dos puntos importantes. En primer lugar, la presencia de un patrón claro en cada tipo de geoforma que puede ser utilizado para identificar otros elementos y estructuras similares y los límites entre ellos. En segundo lugar, estos patrones dominantes son altamente sensibles al cambio de la escala en cada conjunto de datos. Las aplicaciones directas de estos resultados constituyen un enfoque de validación fiable para los límites de las redes de drenajes en el paisaje.

Finalmente, este trabajo responde a algunas preguntas sobre la idoneidad y la capacidad de los MDEs como base para delinear redes de drenaje. En general, es aceptado que los datos matriciales de los MDEs conllevan suficiente información para definir y describir la morfometría de los componentes del paisaje. Indudablemente, las zonas de iniciación de los cauces muestran y exhiben una complejidad extrema, donde los flujos convergentes y divergentes se combinan para producir un elemento de relieve sensible. Por lo tanto, los errores e incertidumbres deberían ser tratados durante las fases iniciales del trabajo, ya que son cruciales para un enfoque de delineación de cauces eficiente y fiable.

Palabras claves: Modelos digitales de Elevaciones (MDEs), Redes de Drenaje, Zona de Iniciación del Cauce, Propiedades Intrínsecas, Modelo Adaptativo, Índices Geomorfométricos, Láser Escáner Terrestre (LST), Modelo Digital de Superficie (MDS), Análisis Geoestadístico de semivariogramas.

Chapter 1

INTRODUCTION TO THE GENERAL CONTEXT OF THE WORK

1.1. General approach: motivation

One of the long standing aims of science has been to impose a rational, internally consistent, framework upon 'nature'. The construction and implementation of such a framework is intended to help us to understand and predict the nature it describes (Wood, 1996a). It is evident that the study of any landscape discipline should include and resolve as much as possible intrinsic (actions between elements and processes within the studied object) and extrinsic (relation with the surrounding environment) factors that integrate and act in that discipline. The fluvial system, which forms part of nature, is at the head of these disciplines that generates unlimited feedback processes between input and output elements of the landscape.

In the last decades the progress of landscape disciplines, especially geomorphological and hydrological ones have generated revolutionary advances in landscape studies. Evans et al., (2003) have described this revolution as follows: *"in the last decades, the prospects for geomorphological modelling have been drastically improved by advances in information technology, especially by greatly increased processing speed and storage capacity. The development of new processing tools in Geomorphic Information Systems (GIS), the production and availability of comprehensive spatial data from remote sensing and of high resolution digital landform data such as Digital Elevation Models (DEMs), in addition to ongoing progress in statistical and mathematical methods have resolved many difficulties and permit new problems to be tackled. In various branches of geomorphology, analysis and models based on these new opportunities have tested many of the existing concepts and generated new ones. Both landforms and processes have been quantified, but they have also been interrelated and models have been developed to cover feedbacks, time lags and connections between different scales, so that we come closer to modelling systems and prediction of landform development."* Examples between various tools tackled are finite elements, scales and fractals, threshold definition, distributed modelling, entropy and energy expenditure, exploratory and inferential statistics, partial differential equations, and response time-analysis.

Depiction and definition of earth surface features is the first step to quantify feedback mechanisms in landscape disciplines. Water flows from hillslope to valleys, carrying out part of these features, moving it to lower parts, and generating new elements in the landscape; that is simply landscape evolution. These actions forms part of the natural balance or equilibrium, which give raise to basic relationships between features through the processes that act on them. In the current work, and in a general context, landscape features will be limited to hillslopes and valleys, together will forms

the basic unit of the landscape; that is drainage catchment or river basin. Movement of materials between these two parts are controlled by mechanisms and processes, that is in pertaining to the feature type relationships are denominated hillslope processes (processes that act on hillslopes) or fluvial processes (processes act on valleys and channels). So, the best the features are described the best the processes are modelled. That is the goal of any scientists; model efficiency is related to the parameters used in order to describe the exact relationships between variables.

Landscape depiction is usually described in relation to its dissection, interpreted in terms of the channel network extension. Channel and stream networks are defined, measured and classified in relation to distinct factors (e.g. geologic, hydrologic, geomorphologic, etc.). In the early nineteenth century, Playfair (1802) provided a comprehensive-didactical description to branching river systems, in which he stated that *“the most striking morphologic feature of fluvial eroded landscapes is the land surface tiling by valleys nested within large valleys, their bottoms forming a connected network with the appearance of a bifurcating arborization. Through the valley network extend the stream channels that carry flow and sediment from the landscape. The valley connectivity and continuity of slope show such -nice adjustment- that they appear designed to accommodate the network of channels testifying that the valley is the work of the stream which flows in it.”*

There is no doubt that channel network delineation is a crucial process in environmental studies, mainly hydrological response and modelling, erosion processes, impact assessment, restoration processes, landscape depiction and other related studies. Even desertification and land degradation processes are strongly related to such studies, since both concepts need a strictly direct definition of land surface features that acts as a theatre scene for such processes. For so, and under the framework of development of desertification monitoring systems, early intents to study relationships between topographic landforms and vegetation cover density highlighted the need to establish a clear parameters (i.e. topographic parameterization) for landscape elements. In which, the principle aim was to establish a clear limits between processes that act on landscape features (i.e. hillslopes and channels) and verify the effect of both on vegetation cover distribution. In our first attempts to establish a strictly defined limit between features, we found a group of models highly criticized as being too subjective, mainly when dealing with data obtained from a sole source. Moreover, the problem is exaggerated when handling digital-gridded data (e.g. Satellite imagery or Digital Terrain Models), which describes landform features in relation to mathematical models based on fixed parameters and variables. Reasons for such critics may be attributed to a clear rationality in the form in which such models define stream extent in the landscape.

On the same direction and under the need to develop a clear strategy in treating data uncertainty, spatial heterogeneity and temporal variability of processes in relation to process verification and catchment-models development, the CANOA (*Characterisation and modelling of hydrological processes and regimes in gauged catchments for the prediction in ungauged catchments*)

project have been launched to address such problems. The project was financed by the Ministry of Science and Education, with the following reference (CGL2004-04919-C02-01). The final objective of the project was the contributions to the International Decade (2003-2012) for “*Prediction in Ungauged Basins*” (PUB), launched by the International Association of Hydrological Sciences. One of the principle aims of the project was to enhance description capacity of theoretical models in hydrological catchments through landscape parameterization. This is compound of a series of analysis at distinct levels, mainly the morphometric analysis of hydrologic catchments (fluvial system) adjusted for the identification of streams and channels in relation to available scale and resolution. The current work forms part of this singular project, where, in general, emphasis on data uncertainty in river basin models forms the basis of a common strategy for a real process approximation at hillslope and catchment scale.

All above motivations highlighted a crucial and urgent need for an objective definition of limits between landscape elements (hillslope and channels), mainly in digital-gridded data. The importance of the boundary inflection limits between features is not only related to a problem of depiction or visualization, rather it integrates multi-functional dimension problems, that includes scale, resolution, optimality and complexity, as well patterns and dominate processes between landscape features. It is, hence the heterogeneity and homogeneity of elements to be identified and measured for optimum delineation of features. It's obvious that, models and algorithms for channel network delineation are widely treated by the scientific community; nonetheless we believe that, till writing the present lines, several gaps are presented in these models. Moreover, we are not trying to invalidate other algorithms rather it is an endeavour to enhance landscape depiction in order to achieve the optimum description of its features under the current roles of advances in computer devices, software packages, gridded datasets, processing models, and data-captures devices.

1.2. Problem definition: needs for a new approach

In landscape studies, delineation of channel networks is a major problem. Its effect goes farther than the boarder of one discipline and restrict, not only the results expected but also the methodologies used in the desired studies. Identification of channel networks, both permanents and ephemerals, are important from both a theoretical and practical perspective in geomorphologic and hydrologic disciplines, since it defines the relative extent of hillslope and channel processes in a catchment which, in turn, have important influences on watershed hydrological responses (Bischetti et al., 1998). Moreover, it can be used in various applications, such as studies of stream flow hydraulics (Monlar & Ramirez, 2002), prediction of flooding and modelling of chemical transportation and deposition of pollutants in surface waterways (e.g. Breilinger et al., 1993; Pitlick, 1994). Furthermore, characteristics of stream network can provide insight into surface and subsurface dominant processes (e.g. Horton, 1945; Leopold & Miller, 1956; Strahler, 1957, 1958; Kirkby, 1976; Beven, 1989) in the

landscape. Lately, incorporating the effects of three-dimensional terrain has become essential in surface hydrological modelling processes (Moore et al., 1991, 1993).

Early geomorphologists and hydrologists focused their efforts on understanding and interpreting landform structure, formation and related processes, and hence evolution and controlling factors. In this direction the first step was realized by Davis (1899) in studying landscape evolution based on the cycle erosion, where he put the core explanation in channel network de-formation. Since then, unlimited amount of works and studies have been realized to study channel network formation (e.g. Strahler, 1950; Howard, 1976), geometrical properties (e.g. Horton, 1945; Strahler, 1956; Shreve, 1966), geometric and hydraulic relationships (e.g. Hack, 1957; Melton, 1958a; Leopold & Maddock, 1953; Leopold et al., 1964), scaling properties (e.g. Mandelbrot, 1982; Goodchild & Mark, 1987; Tarboton et al., 1989), and their complex response to landscape evolution, e.g. optimality and energy expenditure and self-organized criticality (e.g. Bak et al., 1987, 1988; Rodriguez-Iturbe et al., 1992).

Since the early work of Horton (1945) and in order to analyze the development of landforms in relation to geologic history, the field site procedure was the basic method in determining the measurable elements of river basin. Horton realized 100 visits to achieve an eligible statistical test, in each site location 10 elements were verified, which mean 1000 measures for the related study. This procedure highlights the vast amount of efforts and times needed to realize such experiments. Moreover, because of the scale of most drainage basin studies, it is impossible to examine all channels in the field. Horton and earlier researchers in their depiction of drainage network characteristics (mainly planimetric) they made use of available topographic maps as data sources, with only occasional recourses to aerial photographs or to field studies (Mark, 1983). This reliance on topographic maps led to an intense debate over the differences between channels found in the field and those interpreted from maps. Several authors (e.g. Abrahams, 1984a) discussed the problems that arise frequently in relation to the accuracy of the required data which are obtained from maps, aerial photographs and measurements in the field. Such problems are mainly related to inefficiency of field measures with large scale studies (i.e. basin to continental scale), as well the subjectivity and the experience of the topographer. The drainage network that is shown by blue lines (*BLs*) on topographic maps is not a total representation of that network. Moreover, in many cases the *BLs* on topographic maps designate streams that contain water at the time that when the aerial photographs were taken (Chorley et al., 1984). It is logical, then, that depending on the time of the year, the total length of the *BLs* on topographic maps varies greatly. Nonetheless, and for geomorphic purposes, all drainage channels, whatever were the controlling conditions, must be measured or counted.

The advents in the last decades, mainly digital interpretation of cartographic data, have provided new tools and devices that opened the gates for a more efficient research and results with new dimensions and concepts. The widespread of digital representation of surface relief have made it possible to construct and simulate any part of the earth surface. Main rivers and basins, extreme

summits and valleys, and major plains and deserts all are available in a gridded digital format. In particular, traditional manual tasks in landscape studies, e.g. watershed delineation, are being replaced by methods that utilize spatial structure data (Saura et al., 2000). For channel networks, deeper insight into the structure, both two- and three-dimensional, have been gained after the introduction of Digital Elevation Models (DEMs). DEM, which is an ordered array of numbers that represents the spatial distribution of elevation above some arbitrary datum, in addition to digitized contour data and Triangular Irregular Networks (TINs) are principle type of data used for terrain and relief form description (Quinn et al., 1991). In particular, the analysis of large river networks obtained from DEMs has made it possible to acquire a completely new set of statistical analysis aimed at the determination of scaling properties of the observed field (e.g. Grayson & Blöschl, 2000).

The early procedures for describing channel network from DEMs were based on the early work of Peucker and Douglas (1975), revised later by Band (1986), and O'Callaghan and Mark (1984). The first is related to the basic notion that convex pixels in the terrain are related to divergent processes and hence hillslope formation, whereas concave ones are related to convergent processes and hence valleys and channel network formations. The second is related to the threshold concept of Schumm (1973, 1977), that is, quantifying the drainage accumulation (i.e. the approximate surface and subsurface water flow) at each cell in the DEM. Consequently, and for both cases, cells which had a specific-user threshold were considered to be on a drainage channel. The above two procedures are in highly concurrence in defining the main channels and valleys in the drainage network, but with well inconsistency on lateral streams that connect hillslopes to major streams. So, answering where channels begin in the landscape opened the debate between researchers on aptness of algorithms and procedures that best describe lateral or secondary streams (e.g. rills and gullies). In consequence, two major schemes in streams and channel networks limits delineation had emerged: the first incorporates local factors to DEM data, whereas the second uses DEMs exclusively to delineate stream networks.

It is evident that the first approach is more effective since it correlates stream channel initiation to related processes and corresponding factors that leads to channelization in the landscape, e.g. surface-runoff type, dominant lithology, vegetation cover, climate regime, land use (e.g. Kirkby 1976; Schumm, 1973, 1977; Schumm et al., 1984). In this direction several algorithms and models have been proposed, such as relating channel initiation to dominant sediment transport process or dominant erosion process (e.g. Dietrich et al., 1992, 1993; Tarboton et al., 1991; Montgomery & Dietrich, 1994). However, the problem is raised when there are no previous data on the terrain or when definition is realized over large scale terrain, or even at extremely limited terrain of high details when available topographic maps of highest available scale does not cover such limits. In this case, DEMs will be the unique available information to define channel networks, and other landform features.

The choice of the appropriate threshold used to define the optimum channel network is highly related to the scale and resolution of the original data (e.g. Walker & Willgoose, 1999; Thompson et

al., 2001; Hancock, 2005). Although it is true that DEMs may cloud the correct scale of channel initiation (Montgomery & Dietrich, 1988), at large enough sizes of the basin such features may lose relevance (Rodríguez-Iturbe & Rinaldo, 1997). This implies that natural channel networks are scale invariants, whereas streams derived from DEMs are scale dependent (e.g. Tarboton et al., 1989, 1991). Such problems should be treated and the dimension of scale dependency is to be defined in order to determine the appropriate resolution for the corresponding scale. Moreover, in the last three decades researchers (e.g. Ijjász-Vasquez et al., 1992; Rinaldo et al., 1992, 1993) appointed out to the appropriateness of the multiple approach over the simple one in depicting landscape dissection. In which, they asserted that complex heterogeneous landscapes are best described under the multiple approach, that is, different threshold values.

Channel heads represent a transitional stage between convergent (dominated-hillslope processes) and divergent processes (dominated-channel processes) giving rise to the quantitative theories of channel and hillslope evolution. Physically based theories for predicting source areas contributing to channel heads will consequently contribute to network models and provide a linkage between hillslope processes and network properties (Montgomery & Dietrich, 1989); for so, channel head or stream source is a key feature in quantifying drainage density (Moglen et al., 1998). Debates over the precise location of channel heads have occupied a considerable attention, both from field-survey data (e.g. Leopold & Miller, 1956) or DEMs data (e.g. Montgomery & Dietrich, 1988, 1994; Tarboton et al., 1991, 1992; Montgomery & Foulfoula-Georgiuo, 1993). Several questions have occupied the core discussion between scientists, such as; does one consider intermittent or ephemeral streams? Or if DEMs are appropriate tools for drainage network delineation, and if so what is the appropriate scale and resolution? Does valleys constitute stream network, or vice versa?

In relation to DEMs use in fluvial geomorphology, the great challenged to face was the ability of the scientific community in deriving models capable to describe the optimum stream channel networks under diverse conditions of local-data availability, scale dependency, and landscape heterogeneity (i.e. limited conditions). In this direction, several algorithms have been proposed, such as threshold connection value (e.g. Band, 1986; Tarboton & Ames, 2001), or the constant threshold area (e.g. Tarboton et al., 1991, 1992; Tribe, 1992; Montgomery & Dietrich, 1989). The majority of these models failed to depict landscape dissection under varied-diverse conditions and succeeded under particular conditions of diversity (e.g. homogeneous landscape of prevailing runoff and erosion process, heterogeneous landscape of different runoff processes).

In the same direction, delineation of stream limits has received a considerable attention from scientists, whilst validation of the achieved results is still in logging behind. How and what to validate were between the several questions that opened the debates between researchers (e.g. Mark, 1984; Chorley et al., 1984). The complex structure of natural stream system (i.e. geometric, topologic, fractality, self organization and optimality) makes it somewhat complicated to adapt a particular

approach over the others. In general, two main approaches for stream network validation are the widespread between geomorphologists: quantitative and qualitative methods. The former includes a group of geomorphometrical indices (i.e. parameters) that describe stream network structure properties, extracted from different sources (e.g. *BLs*, automated drainage networks defined from DEMs, etc.) and statistically compared. The latter include field visit and visual interpretation of the resulted data and the post comparison with other sources of data (e.g. orthophotographs, *3D* structures, etc.). Herein, it worth's to underline that validation procedures of stream limits and location is a complementary and important process in drainage network analysis; basically, because the optimum delineation of any part of the channel network is related directly to such process.

Hence, under these conditions, we believe that defining the optimum channel network using DEM-data under limited conditions of data availability and scale variability is still a basic requirement for hydrologic and geomorphologic studies. Herein, we propose a new compound model that delineates channel networks in relations to the intrinsic-landscape information. Such approach attains to depict landscape dissection in relation data availability (DEM resolution), presented heterogeneity (scale extension) and intrinsic information of landscape structure (landscape classification), which allows for terrain simplification (a simple model approach), in order *i*) to achieve the best approximation to natural streams and *ii*) to advance in channel networks validation procedures.

1.3. Aims and objectives

The current work tries to highlight the problems of usefulness of DEMs for describing landscape dissection, through the definition of the optimal automated channel network that best describe natural ones. The above optimality and usefulness are highly related to the scale and resolution of both area extension and the dataset dimensions, respectively. Heterogeneity of the surface landforms and dominant relationships between features and patterns of relief formations are the main aspects to concern in studying dynamic landscapes. The border limits between patterns in nature is not a strict line rather is diffuse interchange of multiple and complex dimensions. From micro-topographic surface boundaries to continental ones, scale is the key issue in defining these patterns and threshold is the measure dimension limits between such elements. Herein, and throughout the present work, we will seek for the appropriate threshold that best describe such limits, either between dominant processes (fluvial versus hillslope) or directly between the features itself (channel geometry versus hillslope geometry).

In general, two broad approaches are usually used to derive geomorphometrical characterization tool, theoretical and empirical (Wood, 1996a). The former is related to the construction of the tools themselves, whereas the latter is oriented toward the evaluation of the tools. The approach adopted here is the former, inspired basically on the construction of a new approach that fulfils the weakness of available methods for landscape dissection. The selection of the appropriate

threshold that allows for the definition of the optimum channel network that best represent natural ones is the core of the current work. For so, a new procedure have been proposed, approved (validated) and applied to a natural landscape. Throughout the present work, gridded digital elevation models (DEMs) will be used as a surrogate for landscape representation. Accordingly, the above approach has been formalized in the following goals and aims:

1. Understanding landscape function through the development of new tools that help to describe and study it.
2. Defining the limits between landscape features and hence dominant processes on these structures.
3. Enhancing predictive capacities against challenges in the semi-natural hydrological systems by the advances in the knowledge of hydrological processes.
4. Knowledge enhancement of hydrological models through data-uncertainty understanding and the comparison of hydrological system functions (water redistribution models).
5. Knowledge of implementing objective methods for channel network delineation, taking into account the spatial variation of scale associated with relief forms.
6. Highlighting the importance of local factors (tectonics, landforms, vegetation, etc.) and landscape heterogeneity as limiting agents for channel network delineation, mainly in models that uses DEMs as a unique source of information.

The above goals have been formulated and summarized in the following concrete (testable) objectives:

1. Defining a new technique for channel network delineation, as a starting point in landscape studies, using DEMs solely. Three sub-objectives will be treated to achieve this goal:
 - Exploring whether DEMs own sufficient information to define and describe the geomorphometry of the landscape (e.g. catchments and drainage networks)
 - Determining landform reclassification effect according to internal factors concerning the DEM capacity for terrain recognition.
 - Defining scale variation effect over channel network extraction.
2. Developing and implementing procedures based on the direct observation of the relief structure, which serve to validate stream networks regardless of their origin.
3. Understanding scale- and resolution-effect over different descriptors of catchment behaviour.

1.4. Thesis overview

The structure of the thesis reflects the steps that have been taken in this research to develop a valid procedure to define landscape dissection. This work consists of seven chapters reorganized in

three main sections (figure 1.1) that highlight the methodology used, the methods and the importance of channel network delineation.

Chapter one presents a general focus that comprises the motivations of the current work, the problem related to be resolved, general aims and goals that lead to particular objectives (testable ones), which allow for the reconstruction of the proposed procedure, and finally the present outlines.

Chapter two is dedicated to consider DEM definition and construction in great depth. The first part provides a brief entrance to DEMs, which include concepts, origin and structures, as well as uncertainties and accuracy. A crucial distinction between scale and resolution, the integration of both concepts in relation to DEMs use in landscape disciplines. The second part is the application of the anterior knowledge over the dataset of the study area; that is, the DEMs of different resolution over different heterogeneous areas.

Chapter three covers in some details the process of landscape parameterization. The first part provides a general introduction to landscape features, dominant processes, and available relationships between elements. The second part provides emphasis on drainage basins and channel network as the basic unit for landscape definition. Pattern types and classification methods for channel networks are highlighted, as well as geometrical properties and possible dimension measures used to define such characteristics. The third part describes theories of landscape and channel network evolution, which may provide a possible insight in understanding channel network behaviour in nature and the way in which threshold may be selected or defined. Finally, more emphasis has been added to the mode in which the geomorphometric indices should be selected, which allows for a quantitative and conventional comparison between several channel networks of different origins.

Chapter four provides a literature review that explains the major methods and lines used in channel network delineation. First, general approaches in channel network definition in relation to other landscape features are highlighted, from which the most used methods to define automated channel network skeleton from DEMs are considered. Then, the selection of the appropriate threshold value/s is conceptualized and attention is directed to separate between methods that use local factors and that does not. The emphasis in this direction is placed on methods and procedures that utilize DEMs solely. In each approximation, a group of arguments and justifications of the performance, drawbacks, and corresponding results of applying each method in the study area has been presented.

Chapter five is the core part of the current thesis that includes the formulation of a comprehensive approach to define landscape dissection. Basically, the procedure is based on an integrated model, which comprises two essential parts. The first consists of an algorithm that uses the geometric and topologic properties of the channel network provided by the studied landscape structure in order to derive an optimum threshold (i.e. adaptive model). The second part involves a hierarchical classification of the landscape based on the intrinsic information provided by the prevailing structure

characteristics. This step seeks to simplify the landscape to homogeneous units (i.e. sub-basins) so that the algorithm reaches the best efficiency and least possible errors. Finally, a statistical treatment in both directions descriptive and qualitative is realized, which can promise acceptable and satisfactory conclusions. The validation of results is based on the comparison between the Blue Lines (*BLs*) that represents natural streams and the automated channel networks delineated by different models and algorithms.

Chapter six goes farther in the validation of the model through the use of natural data obtained by laser scanning techniques. The capacity of the new technology and the geospatial analysis are the basic core of this chapter. Interpolated DEMs have been constructed from the provided digital data. Both, DEM and real data were used in the directional analysis of the semivariograms to define channel network isotropic/anisotropic properties through longitudinal and cross-section profiles. The final results of this chapter highlighted the importance of rationality between goals and data used to achieve such aims.

Chapter seven presents the final conclusions of the work that have been constructed from the previous chapters. In addition the final lines provides general recommendations that may help in future works and studies.

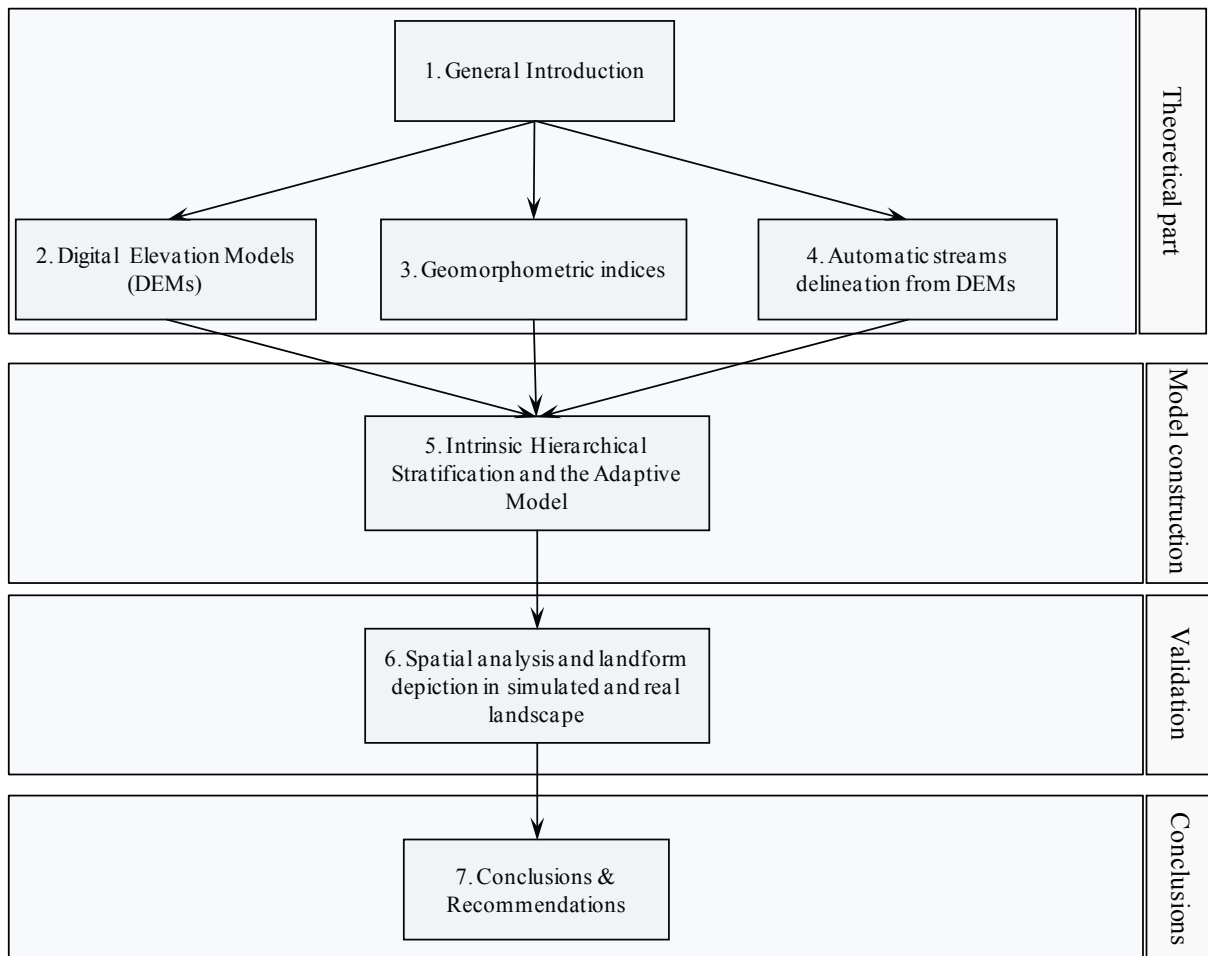


Figure 1.1 Schematic flowchart representation of the thesis structure.

Chapter 2

ASSESSMENT OF DIGITAL ELEVATION MODELS (DEMS) FOR STREAM NETWORK EXTRACTION

2.1. Introduction:

Since the early work of Miller and Laflamme (1958), Digital Terrain Models (DTMs) have obtained universal importance in managing technological, scientific and military problems. In their early work, they defined DTMs as “*a statistical representation for a continuous terrain surface, through an elevated number of selected points with a known coordinates (x,y,z), using an arbitrary coordinate system*”. Since then, scientists tried to use DTMs as a new tool for science research, and a large number of applications have emerged. Although the term DTM is used inconsistently in the literature (e.g. Burrough & McDonell, 1998), herein two definitions are detached; the first one is generic, and describes DTM as “ordered arrays of numbers that represent the spatial distribution of terrain attributes” (Moore et al., 1991); and the second is a formal definition, and depicts DTM as “a numeric structure of data that represents the spatial distribution of a quantitative and continuous variable” (Felicísimo, 1994). This formal definition implies that the quantitative and continuous variable could represent any relief property (i.e. elevation, slope, curvature, etc.), from which the elevation variable is detached as the main and habitual subset variable, known universally as Digital Elevation Model (DEM). Although, it is possible to observe in the bibliography the use of the term DTM as a synonym of DEM, they are exactly different. Accordingly, and throughout the present work, we will adapt Moore et al (1991) definition of DEMs, as “*an ordered array of numbers that represent the spatial distribution of elevations above some arbitrary datum in a landscape*”. This definition implies that these matrices may consist of elevations sampled at discrete points or the average elevation over a specified segment of the landscape, although in most cases it is the former.

For this entire study, Digital Elevation Models (DEMs) will be the base data unit for surface modelling, mainly channel network delineation. For which, deeper insights on DEMs characteristics and properties are highlighted and validated, mainly in relation to DEMs of the study area. The main aim of the present chapter is to consider anterior knowledge in DEMs in order to validate its capacity in hydrological applications. The certainty, with which we can assume a DEM represents the true surface from, is a function partly of the conceptual limitations of the model and partly the quality of the data provided. This chapter provides a description and some evaluation of uncertainty quantification methods commonly available. It is worthy to highlight that both source data and construction models used in DEM generations are continuously renovated, for which we tried to

achieve a compromise between conveniently measured quantification and simplicity in DEM-quality validation.

2.2. Background

2.2.1. Origin, Sources and Structure

The capture of the hypsometric information constitutes the first step in the construction process of DEMs (Felicísimo, 1994), that include the transformation phase from geographic reality to digital dataset structure. Most of the currently available digital elevation datasets are the products of photogrammetric data captures (Moore et al., 1991). These resources rely on the stereoscopic interpretation of aerial photographs or Satellite imagery (Carter, 1988; Weibel & Heller, 1991). Another important source of digital data set can be acquired by digitizing the contour lines on topographic maps (Wilson & Gallant, 2000), in some cases accompanied with conducting ground surveys. Global Positioning Systems (GPSs) can provide a collection of large number of special-purpose, a kind of elevation data sets (Fix & Burt, 1995; Twigg, 1998). Recently, the advanced in technology have permitted the use of other techniques for DEMs construction, such as Radar and Laser Altimeters technology (Rabus et al., 2003), or the Laser Scanners (both aerial and terrestrial versions) (Kilian et al., 1996; Lohr, 2003, etc.).

In general, the basic information unit in DEMs is a referenced point, defined as a ternate point compound of the altitude value, z , which goes with the correspondent values of x and y (Felicísimo, 1994). Variations appear when these data elements are organized in distinctive structures representing different spatial and topological relations. En function of the basic conception of data representation, DEMs are usually organized into one of two major structures: Vector and Raster

1. Vector structures: based on objects/entities, the most representative are two main structures:
 - a) Contour lines or isohypses (i.e. polylines of constant altitudes); and
 - b) Triangulated Irregular Networks (*TIN*) (Peucker et al., 1978).
2. Raster structures: based on localizations, also formed by two principle structures:
 - a) Uniform regular grids (i.e. regular matrices); and
 - b) Quadtrees or hierarchical matrices (Burrough & McDonnell, 1998).

Square-grid digital elevation models (DEMs) have emerged as the most widely used data structure during the past decades because of their simplicity (Wilson & Gallant, 2000) and ease of computer implementation (Moore et al., 1991). These advantages offset at least two disadvantages: First, square grids cannot handle abrupt changes in elevation easily and they will often skip important details of the land surface, mainly in flat areas (Carter, 1988). Second, the computed upslope flow paths will tend to zigzag across the landscape and increase the difficulty of calculating specific

catchment area accurately (Zevenbergen & Thornes, 1987). Several of these obstacles have been overcome in recent years. Several algorithms for treating flat areas and flow path direction have been proposed (Mark, 1984; O'Callaghan & Mark, 1984; Jenson & Domingue, 1988; Band, 1989; Freeman, 1991; Quinn et al., 1991, 1995; Tribe, 1991, 1992; Martz & Garbrecht, 1992, 1998; Lea, 1992; Costa-Cabral & Burges, 1994; Tarboton, 1997). Similarly, the advent of new compression techniques have reduced the storage capacity, improved computational efficiency and makes it possible to utilize all-type structures in reproducing real landscapes (i.e. 3D landscape structures).

Triangulated irregular Networks (*TINs*) have also found a widespread use (e.g. Yu et al., 1997; Tucker et al., 2001b) in landscape modelling, and lately in surface reconstruction. *TIN* is a digital data structure used for the representation of a surface, and are based on triangular elements (facets) with vertices at the sample point (Moore et al., 1991). The facets are made up of irregularly distributed nodes and lines with three dimensional coordinates (x, y, and z) that are arranged in a network of nonoverlapping triangles. A *TIN* is typically based on a Delaunay Triangulation but its utility will be limited by the selection of input data points; well-chosen points will be located so as to capture significant changes in surface form, such as topographical summits, breaks of slope, ridges, valley floors, pits and cols. So, the best *TIN* samples surface specific point, forming an irregular network of points store as a set of x, y and z values together with pointers to their neighbours in the net (Ware & Jones, 1997). An advantage of using a *TIN* over a DEM in mapping and analysis is that the points of a *TIN* are distributed variably based on an algorithm that determines which points are most necessary to an accurate representation of the terrain. Data input is therefore flexible and fewer points are needed to be stored than in a DEM with regularly distributed points. While a *TIN* may be less suited than a DEM raster for certain kinds of GIS applications (Wilson & Gallant, 2000), such as analysis of a surface's slope and aspect, *TINs* have the advantage of being able to portray terrain in three dimensions. In addition, *TINs* can easily incorporate discontinuities and may constitute efficient data structures because densities can be varied to match the roughness of the terrain (Moore et al., 1991). Other form structures, mentioned in literature, used in DEM generation, but to less extend, could be highlighted, such as Quadtrees or hierarchical matrix (Samet et al., 1984; Burrough & McDonnell, 1998), contour based networks (Moore et al., 1988; Moore & Grayson, 1991), profile representation (Yoeli, 1983), and polynomial equations (Roessel, 1988).

The construction of the DEMs, recognized as regular matrix, from vector datasets is basically a process of interpolation (Felicísimo, 1994). The widely-used interpolation processes for continuous surfaces is called “*kriging*” (i.e. interpolation with geostatistics, after *D.G. Krige*) (Burrough & McDonnell, 1998). Moore et al., (1991) mentioned that when discussing the use of DEM it is important to consider the way in which the surface representation is to be used. They mentioned that the ideal structure for a DEM may be different if it is used as a structure for dynamic hydrologic model than if it is used to determine the topographic attributes of the landscape. In this direction,

Hutchinson (1988, 1989) proposed a new approach to generate hydrologically corrected DEMs. His approach is basically to retain the underlying finite difference computational structure, while the minimum curvature interpolation criterion is replaced by a locally adaptive criterion which directly minimizes profile curvature, which is curvature of the modelled land surface in the down slope direction. The main advantage of this method is in its capacity to produce automatically match landforming processes and hence reserve drainage structure (i.e. hydrologically corrected DEMs).

However, the proliferation of digital elevation sources and pre-processing tools means that the initial choice of data structure is not as critical as was. Numerous methods have been proposed to convert digital elevation data from one structure to another (Wilson & Gallant, 2000). In addition, larger quantities of data do not necessarily produce better results (Wilson & Gallant, 1998). Attempts to make generalization about best model is tremendously difficult (Burrough & McDonnell, 1998) for the highly range of terrain types, sample structures and modelling routines. For which, scientists recommend that, mainly for less experienced users, it is more necessary to focus on the quality of the input data instead of learning sophisticated interpolation methods (Eklundh & Martensson, 1995). Thus, simpler interpolation methods will give satisfactory results as long as the input data are well sampled and sophisticated algorithms are likely to produce unsatisfactory results if applied to a poor data (Wilson et al., 1998).

2.2.2. Errors, uncertainties and accuracy

Since relatively little is known about handling the effect of changing spatial and temporal resolutions in landscape models, uncertainty in many modelling approaches remains a dominant factor. Moreover, digital data always appear to be of high accuracy, but in most cases information on data quality and error sources is neglected or is lacking (Milne et al., 2002). Considering DEMs as the basic source of information for developing other related models (e.g. hydrological or geomorphological models), usefulness and validity of the results obtained are intimately associated with the quality of the original model, as quality is measured in terms of kind and magnitude of its error (Felicísimo, 1994). The quality of a derived DEM (i.e. accuracy) can greatly depends upon the source of data, the spatial resolution that is grid spacing, and the technique used for its construction (Wood, 1996a; Hutchinson & Gallant, 2000). Many studies have examined the cause, detection, visualization, and correction of DEM errors (Wilson & Gallant, 2000). Therefore, depending on the desired quality and application, DEM should be created with care using the best available data sources and processing techniques. Yet, the presence of errors in DEMs is an assumed fact, mainly in the modelling process, which always implies a kind of reality simplification (Felicísimo et al., 1995). Thus, DEMs information usually contains a kind of inherent imprecise nature. So, in order to solve the problem, erroneous-aspects definition in the DEM is of vital importance, hence reliability of the results depends on. DEMs error could be divided in two main categories: a) Positional errors: affected mainly vector models, and implies a deficient problem in the geographic localization, and hence plane

situation (i.e. x and y position); and b) Attributive errors: affected both vector and raster models, and implies incorrect assignment of the altitude, and hence modify the value of the z-axis. These errors commonly appear in the creation process of DEMs, both by automatic and manual procedures. It is therefore necessary to apply systematically methods for their detection, measurement and correction (Felicísimo, 1994).

Depending on data type structure or/and purpose of use, error-detection methods have been evolved from visual inspection of perspective displays or shaded relief displays (e.g. Weibel & Heller, 1991), the integration between quantification and comprehensive description (e.g. Wood, 1993, 1996a), to systematic and exhaustive calculation analysis methods (e.g. Wechsler, 2003, 2007; Wechsler & Kroll, 2006; Lindsay & Evans, 2008). Visualization of data and data errors can provide a powerful mechanism for identifying the spatial distribution and possible causes in DEM uncertainty (Wood, 1995). Thus, visualizing spatial arrangement of DEM errors Wood (1996a) developed a deterministic error model based on local surface slope. Fisher (1998) argued that the best method for error modelling is based on conditional stochastic simulation. Darnell et al., (2008) claimed for more simple computation procedures to enable the ‘average’ DEM user to perform his/her assessment on the implications of choosing a particular dataset for their work. Their proposal was to design methodologies that adhere to the essential user-requirements, whilst maintaining the option of modifying defaults. Gousie (2005) in order to enhance error detection from DEMs have described a visualization system that computes two quantitative error measurements, that gives the user a three-dimensional representation of the DEM in conjunction with the computed errors. Estimation of the magnitude and/or the spatial distribution of errors are widely spread in text literatures (e.g. Felicísimo, 1994; Garbrecht & Starks, 1995; Fisher, 1998; Holmes et al., 2000; Gousie, 2005; Darnell et al., 2008) and the selection of the appropriate procedure for error detection is a matter of researchers’ inference. Desmet (1997) evaluated the suite of interpolation methods used to construct a DEM from irregularly spaced sample points, in terms of both ‘precision’ and ‘shape reliability’. For which, arguably, he suggested that positional operations seems to give reliable results, since errors and uncertainties in terrain analysis and modelling tools are important and sometimes distressingly high. Depending on the resolution of the input data, strategies have been implemented. In this direction, Van Rompaey et al., (1999) introduced the aggregation strategy in order to reduce the error on the output of spatial distributed models.

In catchment basins and channel network analysis, quality of DEMs must includes additional procedures for error detection and treatments, rather than a simply root mean square error (RMSE) measurement (i.e. moment description). While RMSE is a generally good error estimate (i.e. vertical accuracy), it is problematic in that it only gives a *global* measure of the validity of a DEM (Gousie, 2005). RMSE compares a DEM height point with a corresponding elevation from an accurate source (USGS, 1987; Rinehart & Coleman, 1988):

$$RMSE = \sqrt{\frac{1}{N} \sum_{i=1}^N (v_i - w_i)^2} \quad 2.1$$

where v_i is the interpolated DEM elevation of referenced point I and w_i is the true elevation of reference point i

However, researchers have reported on the limitations of a single value of accuracy, stressing that DEM error is spatially autocorrelated (Carter, 1989; Wood, 1993; Kyriakidis et al., 1999; Wechsler, 2007). Moreover, the RMSE has a dimension of $[L]$, and is, in consequently, usually measured in the same units as the original elevation data. This makes comparisons of RMSE values for areas with different relative relief values hazardous (Wood, 1995). The magnitude of the RMSE depends not only on our intuitive idea of error but also on the variance of the true elevation distribution. So, this “natural” variance will depend on relative relief as well as on the spatial scale of measurements. Wood (1995) described several methods for quantifying DEMs uncertainty, from which it is worthy to mention the spatial measures (e.g. spatial autocorrelation, variograms and correlograms, and accuracy surfaces), and Hypsometric analysis (i.e. based on the hypsometric curve of Strahler, 1952). Brown and Bara, (1994) used fractals and semivariograms to detect the presence of errors in 7.5' USGS 30 m DEMs, in which they applied several types of filters (i.e. interpolations) for reducing the magnitude of these errors. Florinsky (1998) derived formulas to calculate RMSEs based on the partial derivatives of elevation surface, where he argued that mapping is the most convenient and practical way to implement the derived algorithms. Fisher (1998) argued that, perhaps, the best method for error modelling is based on conditional stochastic simulation. Holmes et al., (2000) used stochastic conditional simulation (SCS) to generate multiple realizations of the DEM error surface that reproduce the error measurements at their original locations and sample statistics such as the histogram and semivariogram model. Hutchinson and Gallant (2000) argued that absolute measure of elevation error do not provide a complete assessment of DEM quality. Accordingly, they proposed to use graphical techniques (i.e. non-classical measures of data quality that offers means of confirmatory data analysis without the use of accurate reference data) for assessing data quality in addition to classical ones. For example, frequency histograms of elevation and aspect are used to detect deficiencies in the quality of DEMs. In the same direction, Wechsler and Kroll (2006) proposed a Monte Carlo methodology for evaluation of the effects of uncertainty on elevation and derived topographic parameters.

Stochastic simulation, or the Monte Carlo method, has been widely used to assess uncertainty in data derived from DEMs (Lindsay & Evans, 2008) because many terrain analysis functions are too complex for analytical approaches (Fisher, 1998). The technique has been used to study uncertainty in DEM-extracted stream networks (Lee et al., 1992; Gatzliolis & Fried, 2004; Lindsay, 2006) and to examine uncertainty in network geometric properties (Lindsay & Evans, 2008). The technique assumptions, as applied to error propagation study in the field of terrain analysis, are based on

(Wechsler, 2000): *i*) DEM error exist and constitutes uncertainty that is propagated with the manipulation of terrain data; *ii*) the exact nature of these errors is unknown; *iii*) DEM error can be represented by a distribution of topographic realizations; and *iv*) the true surface lies somewhere within this distribution of surfaces. In general, a stochastic simulation operates as follows. First, error distribution is assigned to each grid cell of the DEM. An error field is then generated by drawing a random sample from the individual grid cell error distributions. This error field can then be added to the DEM to create a new terrain realization. Data are extracted from the new DEM and the above procedure is repeated iteratively until a stopping condition (e.g. RMSE value) is met.

Hydrological connectivity is another important aspect for DEMs used in landscape disciplines, mainly hydrogeomorphic analysis. Regardless of their resolution and accuracy, however, grid-based DEMs will always contain numerous artefacts that should be removed from the data. Pits and depressions in key parts of the landscape are usually unnatural features and correspond to human artefacts. So, removal of such artefacts could be carried out as a priori step using particular interpolation procedures (e.g. using the ANUDEM approach), or posterior by pit removal models. Herein, several algorithms have been proposed to remove these artefacts (e.g. Jenson & Domingue, 1988). Lindsay and Creed (2006) appointed on the importance to distinguish between actual (i.e. natural) and artefact depressions in DEM data, since causation must be attained to these features for their potential effect on natural phenomena.

2.2.3. Importance and utilities

During the last decade, DEMs have emerged as the most widely used data structure in landscape construction (i.e. visualization) and modelling (i.e. interpretation), because of their simplicity (i.e. simple elevation matrices that record topological relationship between data points implicitly) and ease of computer implementation (Moore et al., 1991, 1993; Wise, 1998). The vast Importance of DEMs is attributed mainly to the unlimited utilities that offer these data matrices and the multiple uses of DEM data (Thompson et al., 2001), mainly for predictive models. Applications in merely all landscape disciplines mainly in hydrological, geomorphological, and biological studies (Moore et al., 1991), in addition to other climatic applications (Felicísimo, 1996), give DEMs a privileged position between different structure datasets. Their utilities are not limited to the explicit information that they contain (i.e. the elevation), but it extends to the spatial relations between their datasets (i.e. implicit information), giving rise to unlimited use in almost all landscape disciplines. Another point of major interest in DEMs and its derivative attributes utilities are the capacity to realize experimental simulation processes (Felicísimo, 1996), independently from the real system.

Terrain plays a fundamental role in modelling earth surface and atmospheric processes. Hutchinson and Gallant (2000) refers to this link as the core point for terrain visualization and structure interpretation; that is, this linkage is so strong that an understanding of the nature of terrain

can directly confer understanding of the nature of these processes, in both subjective and analytical one. For so, they placed DEMs in the centre of the flow chart diagram (figure 2.1) in order to represent the relationships between source data capture and applications.

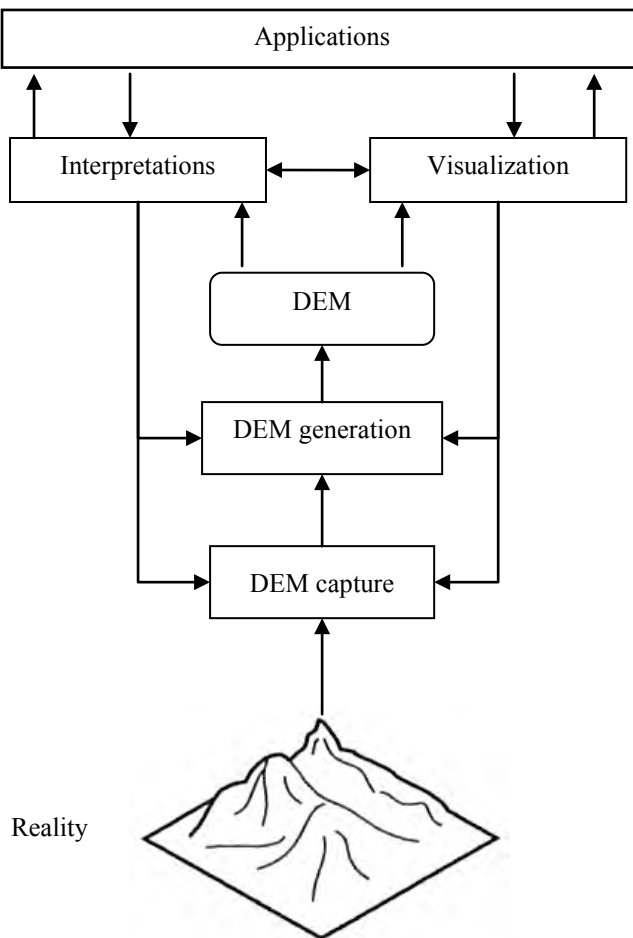


Figure 2.1 The main tasks associated with DEMs (after Hutchinson & Gallant, 2000).

The utility of the DEM is evidenced by the widespread availability of digital topographic data and by the ever-increasing list of uses for and products from DEM. A digital elevation model (DEM) is convenient for representing the continuously varying topographic surface of the earth, and it is a common data source for terrain analysis and other spatial applications. Common terrain attributes that are readily computed from a DEM include slope gradient, slope aspect, slope curvature, upslope length, specific catchment area (upslope contributing area divided by the grid cell size), and the compound topographic index $\ln(a/\tan \beta)$ (where a is drainage area per unit contour length and β is slope) a hydrologically based index that is related to zones of surface saturation (Moore et al., 1993). Terrain analysis also has applications in land use/land cover/vegetation mapping (e.g. Alexander & Millington, 2000; Cantón et al., 2004), precision agriculture (e.g. Bishop & McBratney, 2002), soil-landscape models (e.g. Thompson et al., 2001) and surrogate parameters for soil erosion equations (e.g. Moore et al., 1991), relief visualization (Wood, 1996a; Felicísimo, 1996); radiometric correction of satellite images (e.g. Sandmeier & Itten, 1997), orthophotos corrections (e.g. Jensen, 1995), etc.

Herein, as our main utility of DEMs will be the construction and definition of stream channel networks, we shall focus all the attention in hydrological applications. In hydrological studies, DEMs applications extends from the purely stream channel network and drainage basin delineation, routing analysis, and distributed hydrologic modelling (Beven & Morre, 1993), to results that can be linked to ecological models or global climate models (Beven, 1995). Within small watersheds and across individual catena, terrain analysis has also been used to predict surface saturation zones (e.g. O’Loughlin, 1986), zones of erosion and deposition (Moore et al., 1988), ground-water contribution (Gerla, 1999), and soil water content (Moore et al., 1993).

2.2.4. Scale and resolution

2.2.4.1. concepts

Curran et al., (1997) simplified the notion and the understanding of the concept of scaling in the following example: *“Places that are near to each other are more alike than that are further away and the degree of dissimilarity depends on both the environment and the nature of the observations. This view is one that we need to adopt if we wish to move measurements and understanding from the local to the regional scale. True, there are some phenomenon that can sometimes be studied in isolation because they show self-similarity with scale (e.g. drainage patterns) or can be considered spatially homogeneous (e.g. fresh snow), but in this diverse world of ours these are the exception rather than the true”*. In non-linear dynamics, microscopic events do not directly transform into macroscopic events, that is, in a non-linear world adequate scaling is necessary because phenomena not only may turn different when boundaries of a particular domain are crossed, by contrast, they do inevitably turn different (Haila, 2002).

The term scale can mean many things depending on what is described (Woodcock & Strahler, 1987; Lam & Quattrochi, 1992). Strictly, scale refers to the ratio of the size of a representation of an object to its actual size (Atkinson, 1997). Foody and Curran (1994) have distinguished between two equal valid definitions: the first is cartographic and the second is colloquial. In cartography, scale relates the distance on a map to the actual distance on the real world via the equation:

$$\text{scale} = \text{distance on map} / \text{actual distance on ground} \quad 2.2$$

Consequently, the convention is that a small-scale map has a relatively small size ratio (e.g. 1:100,000) and a large scale map has a relatively large size ratio (e.g. 1:10,000). The colloquial definition of scale is that it is a synonym of words such as size or area (e.g. landscape scale, hillslope scale, regional scale, etc.). Thereby, scale by this definition has no commonly accepted bounds (Curran et al., 1997) and so is relative to the observer (e.g. scale of analysis, scale of operation, etc.).

In addition to the above definitions, the term scale may refer to any one or combinations of several concepts, including grain (i.e. resolution or support), extent, and lag (i.e. spacing), mainly

related to digital terrain datasets and remotely-sensed data (Wiens, 1989; Lam & Quatrochi, 1992; Schneider, 2001; Dungan et al., 2002). Moreover, it is possible to distinguish scale in terms of the forms of underlying phenomena and the processes that create them, or the sampling framework that is used to measure them (Atkinson, 1997). Accordingly, the interaction between the underlying forms and processes, and the sampling frame determines the nature and scale of the observed phenomena. Herein, it is important to underline the above mentioned concepts of “*scale of measurement and scale of variation*”, since part of the study is reliant on.

From one hand, the scale of measurement depends on the sampling frame, which can be divided into the spatial or geometrical characteristics of each individual observation and the spatial coverage and spatial extent of the sample. In this context, several support-measurements could be stated such as size, geometry and the space on which an observation is defined, and the spatial coverage of the spatial extent of measurement. On the other hand, the scale of variation, which is related directly to spatial dependence, is simply its size. Mandelbrot (1982) mentioned that for most natural phenomena spatial variation exists, however, at a range of scales. Importance of spatial dependence in understanding scale is related to several factors: a) it simplifies our view of spatial variation; b) it identifies the scale of the underlying variation, forms and processes; and c) it provides a link between spatial variation and the sampling frame (i.e. sampling scheme, sampling intensity and sample size). In this context, it is also important to have in mind that scaling as a term, if used in directional form, could have two connotations; 1) the first one is scale invariance defined as processes behaving similarly at small and large scales; and 2) the second is upscaling / downscaling and related to the process of data handling, that is, upscaling refers to data aggregation and downscaling refers to data disaggregation. This problem arises mainly with remote sensing, where measurements or sampling frame coverage are to be synchronized between sampling ground coverage and remotely sensed images.

While resolution utility has extended to different disciplines, the antecedents of applying this notion to landscape studies get back to early 1952, where Chapman proposed the use of a regular matrix in the topographic analysis. Since then, application and use of resolution are restricted to more specialized usage techniques and measures in digital datasets. In general, resolution is a term that naturally applies to observations and analysis rather than to phenomena. Given that, our application of resolution will be limited to DEMs and remote sensing; spatial resolution concept will be the core concept in referring to such disciplines. In the world of remote sensing and DEMs spatial resolution boils down to cell size, and usually is the size of a raster pixel (*i.e. a raster file is a coding process for the units that are forming the studied object; in geography a raster is a digital representation of real geographical variation into discrete elements*) with respect to the actual ground distance represented by the pixel.

The dimension of the raster pixel is variable and can be changed according to several factors, such as detail of study, final goals, etc. In a real world, the higher the spatial resolution is the better the approximation of reality; that is, the minimum difference or distance between two independently measured or computed values or objects that can be distinguished by the measurement or analytical method, or sensor being considered or used. Such definition provides a limit to precision and accuracy in digital dataset structures. In general, resolution can be defined as the minimum linear dimension of the smallest unit of a geographic space for which data are recorded. Accordingly, high resolution refers to raster with small cell dimensions (i.e. a lot of details), whereas low resolution means large pixel dimensions. Herein, in the raster model, the smallest units are generally rectangular (occasionally systems have used hexagons or triangles), known as cells or pixels. In hydrological applications, O'Callaghan and Mark (1985) restricted the analysis of channel network to the most commonly used data structure for DEMs, that of the regular square grid. In such a grid, elevations are available as a matrix of points equally spaces in the two orthogonal directions. Spacing in each direction is not necessarily the same, that is, rectangular grids are commonplace (Rodríguez-Iturbe & Rinaldo, 1997). In contrast, map resolution is defined as the accuracy at which a given map-scale can depict the location and shape of map features; the larger the map scale is, the higher the possible resolution. As map scale decreases, resolution diminishes and feature boundaries must be smoothed, simplified, or even not shown at all (Brassel & Weibel, 1988). It is the size of the smallest feature that can be represented in a surface. On a larger scale map feature resolution more closely resembles real-world features.

Although, in literature, it is a common practice to use the two notions of scale and resolution as synonymous (e.g. Luoto & Hjort, 2006), however, separation of both is preferable. Nevertheless, it is important to be aware that no new artificial scale effects are introduced by modelling landscape processes at different scales (Schoorl, et al., 2000) and related spatial and temporal resolutions. For so, and to avoid confusion on the meaning of scale and resolution, we shall restrict, throughout this work, the use of scale to spatial extent of an area (e.g. total area) and resolution to spatial resolution of the grid pixel/cell size of the digital data set (e.g. DEM, satellite imagery, etc.).

2.2.4.2. Importance and consequence

In landscape disciplines the concept of scale is also of a changeable importance and depends heavily on objects, goals and measurement-tools of the study. Landscape ecology, as a conceptual approach, deals, in essence, with two important perspectives, single landscape components and the spatial relationships between them (Turner, 1989); the former is related to the structure (i.e. patterns), whereas the latter is related to the processes between patterns in the landscape.

In dealing with structures, two important attributes are to be identified: the unit of sampling and the cover of geographical space (Luoto & Hijort, 2006). The first attribute is defined by “grain”

and “focus”; grain being the size of the common analytical unit, and focus being the area represented by each data point (Turner, 1989; Scheiner, 2001). The first attribute is also often called “scale of analysis”. It refers to the size of the individual sampling units defined by the inference space to which each datum applies. The second attribute is “extent”, and refers to the inference space to which the entire set of sample units are applied, so as to describe the geographical space over which comparisons are made (Rahbek, 2005). Processes involved in landscape development are typically linked to certain spatial and temporal scales (Schoorl et al., 2000), which is caused by the non-linearity of landscape processes and the heterogeneity of the system (Beven, 1995; Wu, 2004). In addition, and due to the large number of processes operating over the wide range of spatial and temporal scales, modelling landscape disciplines are especially tedious and complex. This imposes important restrictions, mainly in the methodologies used and applied (e.g. physical, empirical), in such studies (e.g. hydrologic and geomorphologic modelling), that is referred as scale effects. Such restrictions have focus the attention of scientists and led to increasing discussions mainly in landscape processes and features (e.g. Beven, 1989; Bloeschl & Sivapalan, 1995; Thieken et al., 1999; Bloeschl & Grayson, 2002; Hancock, 2005).

On the other hand, spatial variability in earth surface processes and landforms is a crucial phenomenon and has formed the basis for numerous geomorphological studies. Wu (2004) mentioned that spatial heterogeneity is ever-present across all scales and forms the fundamental basis of the structure and function of landscapes, be they natural or cultural (Wu, 2004). In order to understand relations and processes between different landscape features, it is important to quantify the spatial heterogeneity and its scale dependence (i.e., how patterns change with scale). Two different but related connotations of scale dependence of spatial heterogeneity may be distinguished. The first implies that spatial heterogeneity exhibits various patterns at different scales, or patterns have distinctive “operational” scales (Lam & Quattrochi, 1992) at which they can be best characterized. The second connotation refers to the dependence of observed spatial heterogeneity on the scale of observation and analysis – often discussed in terms of scale effects on image classification and spatial pattern analysis. Scientists argued that representation of land surface features is linked inherently to the scale of analysis, and a variety of questions in physical geography now require the understanding of spatial scales of landscape patterns (Turner, 1989). Usually, spatial analysis problem is related to aggregation/disaggregation on area-based data, which includes two distinct but related aspects: the result of the statistical analysis is affected by both the level of data aggregation/disaggregation or grain size (so-called “scale problem”) mentioned earlier and by alternative ways of aggregating/disaggregating cells at a given grain size (often called the “zoning problem” or “aggregation problem”).

So, the importance of scale could be attributed to complex problems, which are associated mainly to methods and parameters used in defining operating processes and features of the landscape. Such problems may occur in each of the following situations: The first one of these problems is

associated with scale variation; that is, quantification, or the ability to analyze landscapes (Willgoose et al., 2003), is especially necessary in the evolving disciplines of hydrological and landscape evolution modelling (Hancock, 2005), where it is essential to be able to compare real and computer simulated landscapes using statistically defensible methodologies at appropriate scale (e.g. schoorl et al., 2000). The second problem is associated to models building at catchments scale (i.e. unverifiability of physical models). Physically based, distributed parameter models, have shown to be useful for the synthesis and interpretation of detailed data and for hypothesis testing (Beven, 2002) but for the purpose of prediction, many authors have argued that they must be used with a great deal of caution (e.g. Grayson et al., 1992a, b). This is because the difficulties in scaling occur not only between the research catchment and management area scales but also between the laboratory and research catchment scale (Grayson et al., 1993). Several researchers (e.g. Beven, 1989) have indicated that even at the research catchment scale, the algorithm used to represent hydrologic processes may not be valid and even when they are, their parameterization is uncertain (e.g. surface runoff models and uniform sheet flow). The third problem is associated to the distributed nature of scaling models (Beven, 1989). The distributed nature of the models complicates proper testing and validation procedures because the detail of information provided by the model is much greater than that measured in the catchment (Beven & Wood, 1983). So, not only are there problems associated with the large scale of management areas compared to research catchments but also of the fundamental premises of the original models (Thieken et al., 1999). Moreover, in watershed definition, the amount of data, parameterization effort and computation time increase enormously with the basin scale. As a result, physically based models are hardly to be applied to large catchments (Milne et al., 2002). Possible solutions could be found in reducing required-data volume, with the aim of saving computation time, which may be achieved by regionalization schemes that often include data aggregation. In order to minimize the parameterization effort, hydrological models are commonly coupled with a geographical information system (GIS).

Problems associated with selecting an appropriate scale for research and analysis emerged during the several stages of the work. Scale is not only a critical issue in designing a study and data-collection methods, but also in less recognized issues such as model development, data selection and data availability (Parsons & Thoms, 2007). Herein, its worth to mention that, changing scale, in landscape studies, implies not only shifting in dominant structural forms but also broken up in dominant processes. Parameters and processes important at one scale are frequently not important or predictive at another scale, and information is often lost as spatial data are considered at coarser scales (Turner, 1989). Furthermore, every geomorphological process may have its own optimal spatial and temporal scale of analysis (Luoto & Hjort, 2006). This has fundamental significance for the study of geomorphological systems, especially because increasing emphasis is placed on investigating regional to global scale land surface processes using remote sensing (Walsh et al., 1998).

Another problem related to scale variation is scale measurements and accuracy measurements. Observed patterns, in landscape, are usually obtained by multiple measurements at discrete locations, and discrete points in time (Blöschl & Grayson, 2000). This implies that their spatial dimensions can be characterized by three scales: the spacing, the extent, and the support and have been termed the “scale triplet” by Blöschl and Sivapalan (1995). Their importance is related to specify the space and time dimensions of the measurement of a pattern. The accuracy of measurements is related to the measurement error, both systematic random. In this case, averaging (or aggregation) could be a proper solution for the problem, such as in remote sensing.

Several authors have emphasized in the importance of scaling (i.e. scaling variance and up-down-scaling) in handling processes and structures in landscape disciplines (e.g. Ijjász-Vásquez & Bras, 1995; Haila, 2002; Montgomery, 2003; Schmidt & Andrew, 2005; Hancock, 2005;). The idea that different processes dominate hydrologic and geomorphic response at different scales is implicit in the literature describing the modelling of these systems (Moore et al., 1993). Several models have been proposed to model landscape structure from grid-based DEMs (e.g. first and second topographic attributes, Geomorphic Instantaneous Unit Hydrograph, etc.). For instance, grid approaches to subdivide the landscape provide the most common structure for dynamic, process-based hydrological modelling (Moore et al., 1991). For particular processes occurring in the landscape, indices values for topographic attributes need to be computed at the appropriate scale. If these scale effects are not considered, then the computed attributes may be meaningless or the process of interest may be masked so that the intended use of these attributes may not be realized (Moore et al., 1991). Scale effects on spatial pattern analysis in the grid approach may arise in each of the following three situations: 1) changing grain size (or resolution) only; 2) changing extent only; and 3) changing both grain and extent (Wu, 2004). Several studies have been proposed to handle the effect of altered grain size and the way of this alteration, as well as changing extent, a subject that will be treated lately in “DEM resolution and accuracy.

Although, DEMs are considered as one of the forcing engines in geomorphological and hydrological researches, several problems could emerged when using DEMs in defining dominant landscape features and processes (Hutchinson & Gallant, 2000). The first observation is that grid resolution is not, in particular, the appropriate representation of scale. This is related mainly to the process of scaling-up (i.e. aggregation) in the grid model. When we sub sample an elevation grid to obtain another grid at coarser resolution, we are not only removing fine scale features of the surface (the intended change) but also changing the number of square cells into which the surface is divided. The second is related to the number of grid cells used in defining topographic attributes and threshold points used for geomorphometrical applications. If grid resolution is used to study scale dependence of topographic attributes, the analysis is complicated by the different number of samples obtained from each resolution. Furthermore, specific catchment area is generally computed by accumulating cell

areas from adjacent cells, and this network of connections is changed when the grid resolution is changed, mainly with changing flow direction model. The minimum catchment area resolvable using the usual flow accumulation algorithms (i.e. single or multiple flow direction) is also dependent on grid size. So, grid resolution introduces a number of complicating artefacts to the analysis of scale dependence, which propagates throughout the calculation process. In order to avoid the effect of grid resolution in studying the scale properties of a topographic surface, it would be best to use a method that dealt with scale directly (Hutchinson & Gallant, 2000). One technique for studying scale effects is spectral analysis, which provides information on relative amounts of variation at different wavelengths or spatial frequencies (Gallant et al., 1994): wavelength is approximately equivalent to spatial scale. The positive wavelet decomposition presented here is a useful tool for analysis of scale dependence in topography. It explicitly identifies features at a range of scales, allowing generalization of a topographic surface to allow detailed study of the effect of scale on topographic attributes without introducing artefacts due to changes in grid resolution. The shapes and orientations of features identified in the landscape may also be useful for characterizing landforms and delineating regions of contrasting surface structure.

In hydrology, scaling problems have become more relevant through the need of valid hydrological models simulating the water balance of large areas. However, large scale models cannot incorporate detailed and physically based description of processes, because of unknown boundary conditions and limited computing capacities (Schmidt et al., 2000). Parameterization of boundary conditions and simplifications of models are therefore two necessary steps toward the development of hydrologic models for larger scales. In general, local scale, hillslope scale and catchment scale are often used to distinguish different spatial scales in hydrology (figure 2.2). Herein, parameters that describe effects of landform structure and topology on hydrologic processes are defined as geomorphometric parameters (Evans, 1972), a core base in understanding landscape structure, mainly watersheds of drainage basins and channel networks. Scaling effects have to be considered in quantifying and understanding the significance of geomorphometric properties in hydrology, meaning that (1) runoff-morphometry relations, which tends to be invariant over certain spatial ranges and (2) spatial thresholds affecting changes in these relations have to be determined (Schmidt et al., 2000).

Herein, figure (2.2) reveals different types of effects between dominant geomorphic features and dominant hydrologic processes in relation to scale effects (i.e. spatial and temporal). In the spatial scale, hydrological-processes effect is initiated at the fine toposcale (i.e. local slope) through infiltration processes and concluded at the macro-scales of large catchments or even landscapes as e.g. flood hydrographs or discharge regimes. In parallel, both (processes and features) act in arising temporal scale that ascend from few minutes to several decades or even ages. In hydrological modelling and at catchment scale, for instance, it is possible to distinguish several types of variables that operate and dominate within a hierarchical organization (i.e. different scales). For instance,

geology, discharge and land use operate at the catchment scale because these factors operate at large spatial scales and long-temporal scales to constrain the formation of lower level factors (Schumm & Lichty, 1965). Substrate and hydrologic processes operate at the hillslope scale because these factors operate at small spatial and temporal scales (Schumm & Lichty, 1965). Channel head formations operate at a finetopo scale because their formation depend on the turbulent energy generated from surface flow in rills and gullies, which operates at a limited part of the hillslope, mainly near divides. Finally, variables that indicate ground cover patterns are difficult to assign to scale since they are controlled directly by topographic attributes (Cantón et al., 2004). Each variable is assigned to a different level scale that operates independently but, in effect, is interchangeable within the catchment scale.

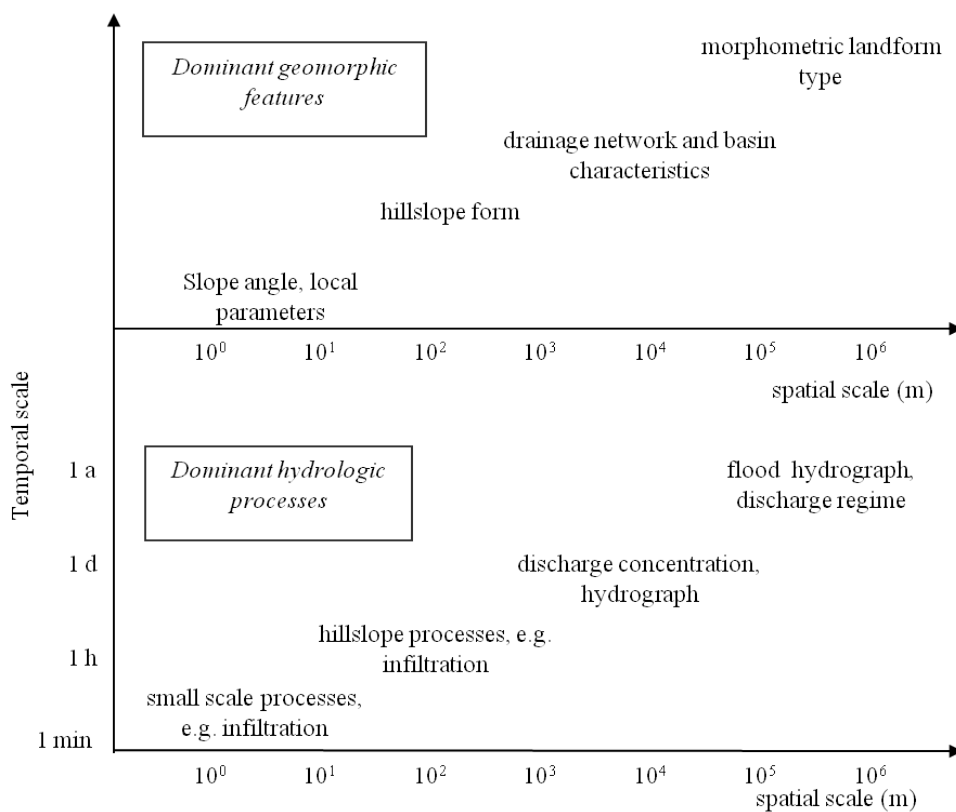


Figure 2.2 Scales in hydrology and geomorphology. The figure shows in a crude way some dominant features of each discipline in a spatial and spatio-temporal context (after, Schmidt et al., 2000).

Two general types of methods have been used in landscape pattern analysis – spatial statistics (including geostatistics) and pattern metrics. The former is the wide spread in hydrological and geomorphological disciplines, which includes the spatial interaction models. Herein, the scaling relationship between processes and features reveal a fractal dimension that describes the scale effect. While, the latter is a relatively new discipline (Turner & Gardner, 1991), which is founded on the idea that the spatial arrangement of phenomena in the landscape is a principal determinant of ecological process and landscape health (Turner, 1989). Scale effects have been increasingly studied using landscape metrics (or indices) in ecology, remote sensing, and geography in the past two decades (e.g.

Wu et al., 2000). These studies have shed new light on the problems of scale effects in pattern analysis as well as the multi-scaled nature of spatial heterogeneity. However, authors (e.g. Fisher et al., 2004) highlighted the incapacity of these patterns in special cases, mainly where the analysis of metrics provides limited degree of reassurance between boundaries (i.e. where the boundaries may have spatial extent). Other methods for studying scale effects include fractal geometry (treated in the next chapter), strange attractors, percolation theory, and chaos have focused the attention of researchers (e.g. Vicsek, 1992) as a primary target of their investigations.

Scaling relationships are widespread and frequently observed in hydrologic and geomorphic processes, such as area-channel frequency (Melton, 1958a), width function (Shreve, 1969), slope-area relationship (Flint, 1974), peak flow frequency in rivers (Leopold et al., 1964), etc. Power-law relationships have been widely used in the hydrologic and geomorphologic literature (e.g. Leopold & Miller, 1956; Gupta & Waymire, 1989) to describe the scaling of hydraulic-geometric variables (Tarboton et al., 1989). Such relationships may be derived from, e.g. fractal structures, or dimensional analysis (Rodríguez-Iturbe & Rinaldo, 1997). Wu (2004) analyzed effects of changing scale on landscape patterns analysis and found that, in general sense, scaling relations were more variable at the class level than at the landscape level, and more consistent and predictable with changing grain size than with changing extent at both levels. His conclusions highlight the need for multi-scale analysis in order to adequately characterize and monitor landscape heterogeneity, and provide insights into the scaling of landscape patterns.

In the sight of these notions, several questions have emerged, mainly related to scale problems, solutions, measures or even combinations of all. We can say that each question could represent a research line. Since scale problem is related to several disciplines (i.e. hydrology, geomorphology, ecology, etc.), questions are also variant (i.e. definitions, relations, measurements, etc.). For instance, here we highlight questions related to landscape ecology, such as, at what scales should landscape be examined, and what are the essential components of a landscape that allow us to re-engineer a stable, self-sustaining, landform that blends in with the surrounding distributed landscape (Hancock & Willgoose, 2002)? What is the appropriate scale for defining dominant hydrological processes? In the prediction of landscape erosion rates, what is the effect of scale and generalization processes, what problems are involved in the integration of different processes over long time-scale (e.g. Montgomery, 2003)? In extremely small scales (sub-meter) and extremely high scales (continental), how geomorphic and ecosystem processes are linked at these scales (Renschler et al., 2007). How do changing grain size and changing extent affect different landscape metrics for a given landscape (Wu, 2004)? What is the appropriate fractal dimension that describes best landscape dissection? Can scale invariance or “scaling” be viewed as a fundamental symmetry in nature that manifests under a scale change? In this study, we’ll try to answer some of these questions either

directly by the obtained results and their justifications or indirectly by the emphasis of the conclusions that could be highlighted.

2.2.4.3. Multi-scale approach

It has long been recognized that different landscape environments, different geologic and tectonic settings, and climate characteristics are related to different geomorphologic processes regimes and landform features (Schmidt & Andrew, 2005). From a philosophical point of view, features, boundary conditions and the class to which a location is allocated in one landscape are vague (e.g. Varzi, 2001; Fisher et al., 2004). Scientists argued that no meaningful answer can be clear-cut, and in the philosophy literature the argument persists as to whether this is due to human perception dividing a landscape into features, let's say, called mountains, or whether the mountains actually exist as vague objects (Sainsbury, 1995; Burgess, 1999). Similar arguments are appropriate to other landform features, such as ridges and valleys. It is easy to specify where these features are in a trivial sense, but to describe or understand the spatial extent of (or region associated with) the feature which people agree to give a particular label is much harder, but most have a spatial extent to some degree. At the location of the core concept they are definite, but that core concept fails to capture their full identity, and they have a spatial extent beyond that core area, where most people would to some extent say they exist (Fisher, et al., 2004). For instance, a core scale issue is related to the definition of land elements (i.e. the parameterization has to incorporate a specific spatial extent: a ridge is generally a larger land element than a hollow). Quantification of appropriate scales for local element is a crucial problem, which often is related to the context. Accordingly, and in order to obtain the best approximation for elements, features or even patterns quantification, multi-scale approach seems to have the answer. Wood (1996b) for instance proposed to use a variety of window sizes (i.e. surrogate for spatial scales) and derived the dominant element over all scales as a classifier, whereas Gallant and Dowling (2003) used a multi-scale index for modelling valley bottoms. Whereas Fisher et al., (2004) have used a novel method of multi-scale analysis to define landscape phenomena (i.e. modelling objects which are vague for scale reasons).

Important characteristics for land elements are, usually derived from the spatial context (i.e. neighbourhood relationships and landscape position in a higher scale context). For example, a ridge can be defined as a facet on a hill that is surrounded in two opposite directions by shoulders or backslopes. One should keep in mind that a unique, non-ambiguous classification into land elements will not be possible, as there is a high degree of uncertainty inherent in the semantic descriptions of land elements and the descriptor variables used: it is, for example, unclear what a hillslope is in semantic terms (Dehn et al., 2001). If a hillslope is simply defined as a high gradient area, it is still uncertain what 'high gradient' means in quantitative terms. Therefore, there are no clearly defined spatial boundaries, i.e. land elements are 'fuzzy objects' (MacMillan et al., 2000). Fisher et al., (2004) defined landscape features from a multi-scale analysis approach (i.e. toponym and synonym

interpretation) and concluded that knowledge of the spatial extent of named, but distinct, geographical locations is a scale-problem definition. Ting et al., (2007) argued that it is difficult to interpret structural characteristic under multiple scale for the behaviours of drainage proprieties. Motivated by solving the problems mentioned above, he proposed a methodology based on the use of two “lacunarity algorithms”. The first is used for interpreting spatial pattern at each examined scale and the second is used for acquiring accurate critical points of distinct scales. In which, he concluded that the method can effectively interpret multi-scale characteristic of channel network and helps to get better understanding of multi-scale structural characteristic, which is the essential to scaling.

In general, the impact of geomorphic processes with size and lifetime of landforms has been heavily investigated. Furthermore, identifying landform features at different spatial scales, related to their different forming processes is also a research point (Schmidt & Hewitt, 2004). Landscape features are characterized by a multitude of processes produced on different spatial scales (Schmidt & Andrew, 2005). This means that one feature in a landscape can potentially carry more than one type of information, that is landforms in general have multi-scale characteristics (Fisher et al., 2004;). Moreover, in the last decades, several papers have examined the effect of spatial variability of parameters on hillslope and catchment processes (e.g. Quinn et al., 1991; Yang, et al., 2000). Many of these studies have concluded that it is not possible to define a consistent effective parameter value to reproduce the response of a spatially variable pattern of parameters values (Beven, 1995). The primary reason is that a single parameter value cannot reproduce the heterogeneity of responses engendered by the variable catchment characteristics. This suggests therefore that it is not possible to use the small scale physics equations at the grid scale (Beven, 1989). Therefore, complex equations should be developed to take into account the effects of landscape heterogeneity (but in consequence have more parameter values to describe that heterogeneity). The effect of scale of the variability to be expected in parameter values at the model grid scale can be obtained by a process of “*block Kriging*” (journal & Huijbregts, 1978).

Scale effects do not necessarily have to be considered as problems because they can be used for understanding the multi-scale characteristics of landscapes (Wu et al., 2000). In principle, the relevant pattern is revealed only when the scale of analysis approaches the operational scale of the phenomenon under study (Wu, 1999). In order to achieve some enhancement in modelling topographic features, Kidner et al., (2000) proposed multi-scale implicit *TIN* construction-procedure that provides a flexible framework for digital surface modelling that allows multi-scale terrain models to be integrated with 3D topographic features. Deng et al., (2007) discussed the importance of multi-scale approaches for quantitative modelling between topographic attribute and vegetation cover, and concluded that, between topographic attributes and vegetation cover, relationships are more improved under the multi-scale approach for spatial scale dependence. A basis function which better represents the fundamental shapes in the landscape would provide more meaningful representation of scale. The

introduced multi-scale feature based representation of topography consists of a superposition of features at various scales (Hutchinson, 1996). A surface can be constructed by introducing broad-scale features first and refining the surface by adding finer features onto the broader features.

2.2.4.4. Integration of scale and resolution in the approach model

Hutchinson and Gallant (2000) appointed that the scale of source data should guide the choice of resolution of generated DEM, and the scales of DEM interpretation should match the natural scales of terrain-dependent applications. A simple criterion for matching the spatial resolution of the DEM to the information content of the data has led to a practical advance toward addressing scale issues in hydrological and environmental modelling (Hutchinson, 1996).

Integration of scale and resolution in landscape approach models is a basic task and active research issue (Hutchinson & Gallant, 2000). The rapid development of analytical cartography, GIS, and remote sensing (the mapping sciences) in the last decade has forced the issues of scale and resolution to be treated formally and better defined (Lam & Quattrochi, 2005), e.g. determine the appropriate scale for hydrological modelling (e.g. Zhang & Montgomery, 1994). Several models have been developed in order to combine resolution information with spatial scale data for more adequate hydrological models (e.g. Daniel et al., 1995). Incorporation of terrain structure into considerations of spatial scale is also an emerging issue in terrain analysis (Hutchinson, 1996). Both small- and large-scale features have been incorporated in terrain analysis (e.g. Zhou, et al., 2007) to achieve more enhance techniques that supports user-controlled terrain synthesis in a wide variety of styles, based upon the visual richness of real-world terrain data.

In nature, our ability to detect patterns is a function of both the extent and the grain of an investigation (O'Neil et al., 1986). In a global context, Wiens 1989 defined extent as the scale and grain as the size of the individual units of observation. In this definition Wiens explains that extent and grain define the upper and lower limits of resolution of the study; they are analogous to the overall size of a sieve and its mesh size, respectively. So, any inferences about scale-dependency in a system are constrained by the extent and grain of investigation, i.e. resolution.

In landscape disciplines, the relation between scale and resolution is somewhat ambiguous, since limits between landscape units are subjective. Hutchinson and Gallant (2000) tried to align spatial scale, DEM resolution, common topographic data, and possible corresponding eco-hydrological applications in order to understand the connections and limits between them (table 2.1). Herein, they tried to establish a connection between limits of landscape units in a feedback approach. Where studying a dynamic process on a concrete scale has its particular resolution, pass over data source information, finally in order to study a specific hydro-ecological application, and vice versa. There is naturally some overlap between the divisions mentioned in table 2.1, but a genuine distinction between fine and coarse toposcale is available, in terms of common topographic data sources and in

terms of modelling applications (Hutchinson & Gallant, 2000). Nowadays, and with vast advances in measurement technologies new dimensions may be obtained and hence new scales and resolutions are widely available. Laser scanning technology has allowed for millimetric or even sub-millimetre measurements, which may add new dimension scale to Hutchinson and Gallant scheme, for instance “microtoposcale”. Hence, new insights and perspectives on feedback processes at plot scale (i.e. 0.5-5m) are studied highlighting new hydrological applications (e.g. soil roughness and water infiltration).

Though actual terrain can vary across a wide range of spatial scales, source topographic data, terrain landforms and related hydrological processes are commonly acquired at a particular scale, and changed heavily if we move from one scale to another. Actually, this framework places certain limits on the range of DEM resolution, and hence corresponding spatial scale, and what researchers attain to achieve. The choice of the appropriate DEM resolution is shown to be important in minimizing errors in representation of terrain shape, as measured by various primary terrain attributes, as well as matching the true information connect to the source data.

2.2.4.5. Resolution and accuracy in DEMs

Different conceptual problems should be addressed when considering DEMs as models of surface form, mainly fidelity representation of the modelled surface and the final use of the DEM (Moore et al., 1991). First, the reliability with which the DEM conveys the true surface will depend on surface roughness and DEM resolution (Wood, 1996b). Fractal characteristics of surface derived from DEMs suggest that there will always be detail at a finer scale than that measured at the DEM resolution. This implies that all DEMs implicitly model at a certain scale involved by the grid cell resolution. Second, it is important to consider the way in which the surface representation will be used in the DEM (i.e. what each elevation value within and between gridded matrix represents?). Different interpolation procedures give rise to different elevation estimates, and hence different structure of DEMs (e.g. Fisher, 1993; Kumler, 1994; Wood, 1996a).

Inevitable question arise when using DEMs as a source data in landscape studies; that is "what grid resolution should I use for a particular modelling exercise?" Determination of the appropriate resolution of an interpolated or filtered DEM is usually a compromise between achieving fidelity to the true surface and respecting practical limits related to the density and accuracy of the source data (Hutchinson & Gallant, 2000). Since the ability to understand catchment processes is reliant on DEM scale and reliability of landscape data input (e.g. Kenward et al., 2000; Thompson et al., 2001; McMaster, 2002), modelling grid size used in landscape quantification is of considerable importance. In this direction, determination of the DEM resolution that matches the information content of the source data is desirable for several reasons; it facilitates efficient data inventory, permits interpretation of the horizontal resolution of the DEM as an index of information content, and it can facilitate the assessment of the scale dependence of terrain-dependent applications (Gessler et al., 1996).

Scale	DEM Resolution	Common topographic data sources	Hydrological and Ecological Applications
<i>Fine toposcale</i>	5-50 m	Contour and stream-line data from aerial photography and existing topographic maps at scales from 1:5,000 to 1:50,000	Spatially distributed hydrological modelling Spatial analysis of soil properties
		Surface-specific point and stream-line data obtained by ground survey using GPS	Topographic aspect corrections to remotely sensed data
		Remotely sensed elevation data using airborne and spaceborne radar and laser	Topographic aspect effects on solar radiation, evaporation and vegetation patterns
<i>Coarse toposcale</i>	50-200 m	Contour and stream-line data from aerial photography and existing topographic maps at scales from 1:50,000 to 1:200,000	Broader scale distributed parameter hydrological modelling
		Surface-specific point and stream-line data digitized from existing topographic maps at 1:100,000	Subcatchment analysis of lumped parameter hydrological modeling and assessment of biodiversity
<i>Mesoscale</i>	200 m-5 km	Surface-specific point and stream-line data digitized from existing topographic maps at scales from 1:100,000 to 1:250,000	Elevation-dependent representations of surface temperature and precipitation Topographic aspect effects on precipitation Surface roughness effects on wind
			Determination of continental drainage divisions
Macroscale	5-500 km	Surface-specific point data digitized from existing topographic maps at scale from 1:250,000 to 1:1,000,000 National archives of ground surveyed topographic data including trigonometric points and benchmarks	Major orographic barriers for general circulation models

Table 2.1 Spatial scales of applications of DEMs and common sources of topographic data for generation of DEMs (after Hutchinson & Gallant, 2000)

The scale of terrain features is highly sensitive to DEM data source and grid resolution (Wilson et al., 2000). Numerous studies have explored what resolution is needed to accurately represent the key hydrologic and geomorphologic processes operating in selected landscape (Quinn et al., 1991; Wolock & Price, 1994; Walker & Willgoose, 1999; Wolock & McCabe, 2000; Kienzle, 2004; Chaubey et al., 2005; etc.). For instance, Wilson et al., 2000 highlighted the sensitivity of selected primary and secondary topographic attributes to the choice of elevation data source, grid resolution and flow-routing method. Whereas, Thompson et al., (2001) studied DEM resolution effect on terrain attributes, in which they demonstrated that, at the field scale, the horizontal resolution, vertical precision of the DEM, and the source of the DEM data influence topographic-attribute values. Moreover, these effects are seen in both the overall distribution of terrain attributes and in the values of terrain attributes at specific points. In the same direction, scientists examined terrain attributes derived from multiple DEMs from identical sources, but of different horizontal resolutions, and their results always led to the same conclusions. As resolution decreased, slope gradients decreased, with differences prominent in areas of steeper slopes (e.g. Thielen et al., 1999). Whereas, other topographic attributes (e.g. specific catchment area) were found to increase as resolution decreased with errors concentrated in small catchment area, such as hillslope summits or headwaters (Wolock & Price, 1994). Zhang and Montgomery (1994) found that with increasing grid size, areas of predicted zones of surface saturation also increase. In addition, there was a tendency for hydrologic models to compute increase peak discharge with increasing grid size (Zhang & Montgomery, 1994), as well as increasing runoff volume and decreased time to peak flow (Thielen et al., 1999). Wang and Yin (1998) found that as DEM resolution decreased, there was a trend for decreasing total flow lengths and hence decreasing drainage density, similar conclusions have been confirmed later by researchers (e.g. Yin & Wang, 1999). Wolock and Price (1994) using a topographically based hydrologic model, found that changing grid size may affect water table configuration.

The accuracy of a DEM depends on several factors, including the horizontal resolution (i.e. the spatial resolution that is grid spacing) and vertical precision at which the elevation data are represented, and the source of the elevation data (Thompson et al., 2001). A dependency exists between the scale of the source materials and the level of grid-possible refinement. The source resolution is also a factor in determining the level of content that may be extracted during construction process (i.e. digitization). Another important factor influencing DEM accuracy is the horizontal and vertical dimension of the DEM (Felicísimo, 1996). Horizontal accuracy of DEM data is dependent upon the horizontal spacing of the elevation matrix. Within a standard DEM, most terrain features are generalized by being reduced to grid nodes spaced at regular intersections in the horizontal plane (Wood, 1996b). This generalization reduces the ability to recover positions of specific features less than the internal spacing throughout testing process, and results in a defect-surface filtering or smoothing during grid construction. Vertical accuracy of DEM data is dependent upon the spatial

resolution (horizontal grid spacing), quality of the source data, collection and processing procedures, digitizing systems, and interpolation procedures. For instance, Kenward et al., (2000) evaluated the effect of vertical accuracy of DEMs on hydrologic prediction accuracy by comparing three DEMs of different resolutions and their associated stream flow simulations. Their results revealed that the vertical accuracy of DEMs does affect the accuracy of hydrologic-prediction models, manifested in progressively reduced spatial coherence (more “scattering”) that is related directly to runoff peaks, timing, and volume as well as saturation and runoff production zones.

As with horizontal accuracy, the entire process, beginning with project authorization, compilation of the source data sets, and the final gridding process, must satisfy accuracy criteria usually applied to each system. Thompson et al., (2001) found a direct relationship effect between horizontal resolution and vertical precision. Their studies reveal that a DEM of 10 m horizontal resolution represent better topographic features than 30 m DEMs, whereas vertical precision affect more 10 m DEMs than 30 m ones, e.g. producing a less continuous landscape effect. So, they suggest that to properly characterize local topography the vertical precision must increase as the horizontal resolution increase, so that the vertical precision remains greater than the average difference in elevation between grid points in the DEM. Each source data set must qualify to be used in the next step of the process (Hutchinson & Gallant, 2000). Improving data structure seems to be one of the key challenges when dealing with accuracy and precision in DEMs (Felicísimo et al., 1995). Several methods have been proposed for matching DEM resolution and source data information content (e.g. Hutchinson, 1996; Kienzle, 2004), such methods provides more enhanced description of topographic features, highly reliable and free gross-errors gridded elevation data. Herein, it is worth to concrete some terminologies used throughout the work. ‘Precision’ may be defined as the accuracy with which the heights for unsampled points are predicted, and ‘reliability’ as the degree of fidelity with which the shape or the spatial pattern of the topography is maintained in the interpolated surface. Walker and Willsgoose (1999) tried to verify the reliability of DEMs for channel networks definition, and concluded that the maximum horizontal resolution for which the details of the drainage network are reliable is related to both vertical accuracy of the DEM and the slope. In addition, del Barrio et al (1993) concluded that the optimal resolution for a DEM is approximately between 1 and 2 times the equidistance of the source input contours, depending on surface complexity.

Herein, horizontal accuracy of the DEM could be expressed as an estimation of the (RMSE). Estimation of the RMSE is based upon horizontal accuracy tests of the DEM source materials which are selected as equal to or less than intended horizontal RMSE error of the DEM (Moore et al., 1991). The testing of horizontal accuracy of the source materials is accomplished by comparing the planimetric (x and y) coordinates of well-defined ground points with the coordinates of the same points as determined from a source of higher accuracy. The vertical RMSE statistic is used to describe the vertical accuracy of a DEM, encompassing both random and systematic errors introduced during

production of the data. Accuracy is computed by a comparison of linear interpolated elevations in the DEM with corresponding known elevations. In view of that, three types of DEM-vertical errors have been distinguished blunder, systematic and random (Wood, 1996a). These errors are reduced in magnitude by editing but cannot be completely eliminated. Blunder errors are those errors of major proportions and are easily identified and removed during interactive editing. Systematic errors are those errors that follow some fixed pattern and are introduced by data collection systems and procedures. These errors artefacts include: vertical elevation shifts, misinterpretation of terrain surface due to trees, buildings and shadows, and fictitious ridges, tops, benches or striations. Random errors result from unknown or accidental causes.

In general, the appropriate grid resolution used to derive geomorphological input parameters for hydrological modelling depends on the objective of the study and the type of indices and variables used (Thieken et al., 1999; Schoorl et al., 2000; Hancock, 2005). From one hand, the accuracy of the DEM and DEM-derived products may be critical when the DEM data are used for environmental modelling and prediction of the spatial distribution of hydrological, geomorphological and biological properties (Thompson et al., 2001). These scale issues are particularly important in hydrology and hydrologic modelling (Zhang & Montgomery, 1994; Bruneau et al., 1995). On the other hand, advances in numerical models to monitor and predict hydrology and geomorphology rely heavily on DEMs and their integrity (Hancock, 2005). Luoto and Hjort (2006) appointed to the importance of resolution in the design of the geomorphological studies, in which they concluded that if the details with which sample attributes are discriminated can affect the inferences of geomorphological studies, determination of the proper resolution of any analysis should be incorporated carefully into the study design.

The advent of new technologies has made it possible to construct high resolution DEMs for any part of the world (Rabus et al., 2003). In the last decades, the debate over the appropriate scale and resolution in landscape studies took a favourable tendency for high resolution grid data, i.e. >30 m, over coarse one, i.e. <30 m. In this direction, several authors studied landscape response to different grid size resolution and tried to provide generalized results for all landscape environments. For instance, Quinn et al., (1991) showed that the spatial patterns of the topographical index (i.e. wetness index) distribution computed from 12.5- and 50-m resolution DEMs for a watershed were different from each other. Zhang and Montgomery (1994) studied the effect of 2-, 4-, 10-, 30-, and 90-m resolution DEMs on the portrayal of the land surface and hydrologic simulation and conclude that for many landscapes, a 10m grid size presents a rational compromise between increasing resolution and data volume. They recommended using 10-m DEM for geomorphological and hydrological applications because the 10-m DEM performed much better than the 30- and 90-m data and only slightly worse than the 2- and 4-m DEMs. Most significant, the grid size of 50 m or more tend to ignore the existence of lower order streams and they artificially smooth landforms in complex

landscapes (Wilson et al., 2000) so that the terrain features that modulate key hydrologic processes are lost (Quinn et al., 1991). However, Bruneau et al., (1995) consider 50 m to be sufficient because model calibration is able to compensate aggregation effects to some degree. Wolock and Price (1994) showed that DEM map scale and data resolution affect prediction capacity of hydrological models, in which 30-m DEMs are a more detailed representation of the real land-surface topography than 60- and 90-m DEMs. It was concluded that changing the DEM grid size on average tended to affect the mean depth to the water table, the ratio of overland flow to total flow, peak flow, the variance of daily flow, the skew of daily flow and the maximum daily flow calculated from the TOPMODEL (Wolock & Price, 1994). Walker & Willgoose (1999) compared ground truth data set, obtained by ground surveys, to various grid resolution (6.25 m, 12.5 m, and 25 m) datasets of catchment sizes and stream networks statistics and found that, almost 60-90% of hydrological response fall consistently outside confidence limits, suggesting that several hydrological properties are poorly estimated of published DEMs. Nevertheless, their study indicates that published cartometric and photogrammetric DEMs may be used for determination of catchments and stream networks with caution by comparing the catchment and major stream network defined from the DEMs with that observed from a site inspection. They also suggest a method for predicting the maximum horizontal resolution, for which the details of the drainage network are reliable, is related to both the vertical accuracy of the DEM and the slope. In order to predict this maximum horizontal resolution for a DEM, it is necessary to estimate the vertical accuracy. If the vertical accuracy is consistent throughout the DEM, independent of elevation and slope, then the horizontal resolution will be governed by the topography in the flattest regions of the catchments. More concretely, Gyasi-Agyei et al., (1995) investigated the effects of vertical resolutions of DEMs on morphological parameters. Their results reveals that for most hydrological applications, the vertical resolution of a DEM is considered satisfactory if the ratio of the average drop per cell and vertical resolution is greater than unity. The average drop per cell was defined as the elevation between a pixel and the next in steepest descent. Accordingly, they proposed that this ratio criterion could be used to define the optimum horizontal resolution for geomorphometrical relationships.

In the same direction, Wang and Yin (1998) compared drainage networks derived from 30- and 130-m DEM resolution using various drainage network parameters. Their results revealed that goodness-of-fit between parameters estimates based on the DEMs varies. Where, for a group of parameters (i.e. mainly related to first order streams) 30 m grid resolution fits better than 130 m resolution, whereas 130 m grid resolution provides good estimates to some geometric and topologic parameters (i.e. mainly for higher order streams), such as stream length and frequency, as well as bifurcation ratio. Artan et al., (2000) propose that a modelling grid size of about 10 m deemed to be the best compromise between aimed objectives and reduction of computation time and the size of the support data, in spatially distributed hydrologic models. Thompson et al., (2001) revealed that decreasing the horizontal resolution of a DEM from 10 to 30 m tended to create a smoother, less

defined landscape, with more moderate slope gradient, reduced curvatures, and higher values in the specific catchment area. Guth (2003) went farther and concluded that Terrain variables computed from 10 m and 30 m USGS Level 2 DEMs are essentially identical. His conclusions attributed differences in DEMs values to physiographic and relief effects. In order to identify the grid resolution that matches the information content of the source data, Kienzle (2004) concluded that, depending on terrain complexity and terrain derivative, the optimum grid cell size is between 5 and 20 m. While, Hancock (2005) demonstrated that catchment DEM of 10 m grid size is the most appropriate for the reliable capture of hillslope properties. Nevertheless, he affirmed that considerable catchment information can be obtained from DEMs at larger grid scales. Consequently, he concluded that current available DEMs at grid scales greater than an appropriate grid scale for the catchment property of interest may have a considerable loss of catchment detail.

Studies over scale and resolution effect on channel network definition have received little attention from researchers, since definition where channels begin is vague. Moreover, channels and valleys are distinct geomorphological features but occupy approximately the same location. The majority of the available works study resolution effect in relation to model requirements, such as models that need an identification of channel network segments and their contributing sub-areas and hillslopes (Thiekin et al., 1999). Scale and resolution effect have been studied from two perspectives: the first study the effect of resolution and scale on the definition of the threshold used to define channel extension (e.g. Ijjász-Vasquez & Bras, 1995; Hancock, 2005). The second deals with the direct effect of scale and resolution over the definition of channel network as a geomorphological feature (e.g. Wood, 1996b; Desmet, 1997).

Two major factors can affect the accuracy of the stream network derived from DEMs: DEM resolution and drainage density, which is related to channel head definitions (Wang & Yin, 1998). Garbrecht and Martz (1994) found that the sensitivity to grid size of a DEM varied among the extracted drainage parameters after examining the impact of DEM resolution on extracted drainage properties using hypothetical configurations of drainage network. Geomorphologic properties (i.e. geometry and topology) of channel networks are highly sensitive to both DEM grid resolution and threshold area (A_s) used to defined channel heads. A_s is the minimum drainage area required to initiate the stream in the channel network, whereas DEM resolution depends on the available elevation data. As upstream area or drainage area (i.e. defined as a terrain feature) is highly sensitive to spatial grid spacing that is grid resolution, and hence A_s is directly related to DEM grid spacing (i.e. resolution). Walker and Willgoose (1999) tried to identify the maximum horizontal resolution for which the details of the channel network are reliable, in which they found that it is related to both the vertical accuracy of the DEM and slope. If the vertical accuracy is consistent throughout the DEM, independent of elevation and slope, then the horizontal resolution will be governed by topography in the flattest regions of the catchment. Yang et al., (2001) revealed that the channel networks generated with larger

threshold areas tend to lose detailed scaling information. Their results reveal that while increasing the DEM mesh sizes, the river networks extracted with the same threshold area become sparser and the topography tends to be smoother. So, they concluded that the appropriate threshold area for river generation is decided to be the largest threshold value that keeps the catchment scaling structure. Fractal dimension describes scale characteristics of landscape features, and channel networks are not an exception. As mentioned earlier, for surface features, there will always be detail at a finer scale than that measured at the DEM resolution. For so, the first question arises, when using DEMs to define channel networks; what is the appropriate resolution for channel network extraction? Or what resolution should I use to define the best drainage network that best describes landscape dissection? Answering this question will not be easy, mainly under the large amount of publications and opinions that provide more confusion than certainty. Moreover, the problem is exaggerated with drainage networks since channel networks are space-filling (Tarboton et al., 1988). For so, even the highest possible grid size (e.g. <5 m) will be insufficient for natural channel network simulation. For instance, Dietrich et al. (1993) detected that DEMs, even at very high resolution (e.g. 1 m) are so sparse to capture the local topography around typical small channel heads, which often are only decimeters in size at their tips. So, scale invariance in nature for drainage networks will be converted to scale dependence in channels networks defined by DEMs. Herein, in order to select the appropriate resolution for the proposed model approval, a logical approach will be established. The majority of published works agree in that above 30 m grid size is insufficient resolution for landscape modelling (i.e. topographic attributes and landscape features), whereas higher resolution (i.e. <30 m) are more appropriate for particular definition aspects (e.g. rill and gullies). For so, the 30 m grid size DEM resolution will be used throughout the work as the principle source data, in order to enhance and validate the model in heterogeneous landscapes. Whereas, the 1 m grid size DEM will be used to validate the model under homogeneous environmental conditions.

2.2.5. River basins from DEMs

The fluvial activities, on terrestrial landscapes include a group of important processes for land surface-modelling, in which the hydrographic catchments is the basic geomorphological unit (Felicísimo, 1996). The infinite application of channel network and corresponding basin catchments make it one of the basic tasks in landscape analysis (i.e. hydrology, geomorphology, topography, etc.). Additionally, characteristics of stream network can provide insight into various surface and subsurface processes (Horton, 1945; Strahler, 1957, 1958; Shreve, 1966, 1967; Smart, 1972a; Abrahams, 1972, 1977; etc.). More recently, incorporating the effects of three-dimensional terrain on hydrological processes (Wang & Yin, 1998) has become an important part in modelling surface processes (Moore et al., 1991, 1993).

Herein, and as mentioned earlier, the basic structure for DEMs used in delineating Channel networks, is the regular square grid. In this context, two basic treatments should be realized for the

posterior usage of data matrix: the first is to determine routing, i.e. assign drainage direction, and the second is related to DEM quality enhancement, that is, pit removal. In determine routing, the flow of material over a gridded surface is assigned by considering the direction of steepest downhill slope. There are several algorithms to calculate this, the simplest is called simple flow direction known as ($D8$) and the more sophisticated is called multiple flow direction designated as ($D\infty$). The first, assign the flow to one of eight directions and assumes that subsurface flow occurs only in the steepest downslope direction from any given point; whereas the second divide flow between directions and assumes that subsurface flow occurs in all downslope directions from any given point. Depending on the algorithm ($D8$ or $D\infty$) used flow direction will represent part or the total of adjacent neighbour cells. Pits (i.e. sinks or local depressions in DEMs) are anomalies manifested as sites lower than all surrounding neighbours. Pits are uncommon features of natural terrains, except in karst landscapes and some types of desert, so in many instances observed pits arise from errors in data capture and subsequent modelling of the surface. For hydrological analysis pits can be assumed to fill with water during flow and it is often convenient to remove them prior to analysis. This is an application-specific form of smoothing, but may be applied to any grid file, assuming that the result is meaningful for the problem at hand. Nowadays, several GIS programs (e.g. ANUDEM, IDRISI, SAGA, PCRaster, GRASS, ArcGIS, TAS, etc.) handle this problem in different ways; some of these implementations involve simple pit removal working on the assumption that such pits are likely to be minor errors in modelling the landscape, whilst many adopted a broader view of the hydrology, and try to distinguish between errors or artefacts, and true hydrological depressions (Lindsay & Creed, 2006).

Irrespective of the algorithm used to compute the flow directions, the result is to create a gridded overlay in which the surface topology has been made explicit (Burrough & McDonnell, 1998). The resulted dataset is extremely useful for computing other properties of a DEM because it explicitly contains information about the connectivity of different cells. The following steps of the pre-treatment process are simply mathematical operation and include: a) catchment area or accumulation area: calculated as the number of upstream cells draining to a target cell, that is to count the number of cells that drain through each cell.; b) Stream channels: defining channel networks from DEMs imply a kind of simplification to real-stream networks. Accordingly, cells which had total drainage area above a user-specific threshold area (A_S) were considered to be drainage channels. The identification of drainage basins and corresponding stream branching limits are both determined by the A_S value.

Ridges identification from the treated matrix will be a mere formality procedure. By definition, ridges have no upstream elements, so selecting all cells with an upstream accumulation value of 1 provides a first estimate of ridges. Although, new methods and GIS packages incorporate sophisticated algorithm (i.e. quadratic approximations or/and fractal dimensions) for ridges' definition, the base initial procedures still alike. Isolation of the drainage basin consists of identifying those cells that eventually drain through outlet cell, usually the lowest cell in the catchment. Because all cells that

drain through a given cell are part of the catchment of that cell, counting upstream area above the cell computes and defines automatically the catchment above that cell. Thus, channel network basin should include the outlet cell and all upstream area that drain into that cell. Once the drainage network is identified, computing channel network prosperities and watershed statistics (e.g. Magnitude, Order, lengths, perimeter, etc.) is straightforward.

2.3. Location and general characteristics of the study area

2.3.1. Tabernas Basin site Location and general characteristics

The study was conducted at the Tabernas Basin, located in the south eastern part of the Iberian Peninsula (figure 2.3a), which is widely known as “*The Desert of Tabernas*” attributed to the presence of badlands sector in the centre of the study area. However, it is not a real desert, but an arid zone with regular albeit low rainfall (Lázaro et al., 2004). The Tabernas basin occupies an area of about 572 km², with varying landform structure. This area extends from Filabres Mountains in the north with a 2168 m a. s. l. (the highest point in the study area) to Alhamilla in the south and between Sierra Nevada and Sierra de Gador in the west to Almanzora basin in the east. The lowest point reaches 111 m a.s.l. and is located near the Andarax River in the southern part of the study area.

- *Geology and tectonics*

The Tabernas basin is one of the intermountain basins of the Betic Cordillera, which is formed by mountains aligned in the W-E direction and which can be followed in the southern part of Spain for almost 600 km (Gutiérrez, 1994). The Tabernas Basin is bounded by the Sierra Filabres to the north, the Sierra Alhamilla to the south and the Sorbas Basin to the east. The mountain ranges to the north and south are dominated by Precambrian to Triassic micaschists and other high-grade metamorphic rocks of the Nevado–Filabrides complex (Nash & Smith, 2003). In the northern Sierra Alhamilla, those rocks are partly overlain by nappes of Palaeozoic to Triassic low-grade metamorphic and Triassic sedimentary rocks of the Alpujarride complex (Sanz de Galdeano et al., 2006). The tectonics of the area is essentially produced compression and release tensions of the African plate against the Iberian plate instilled during the Miocene which produced the rising of the Nevado-Filabride complex and the movement over it of the Alpujarride, creating topography of emerging mountains, separated by sedimentary basins, where very thick sequences of Neogene sediments accumulated. The Tabernas sedimentary basin is essentially formed by marine sediments, since the Tortonian, with predominance of marls deposited in deep water conditions, along with alternates of fine and coarse sediments (flysch facies) in shallow waters.

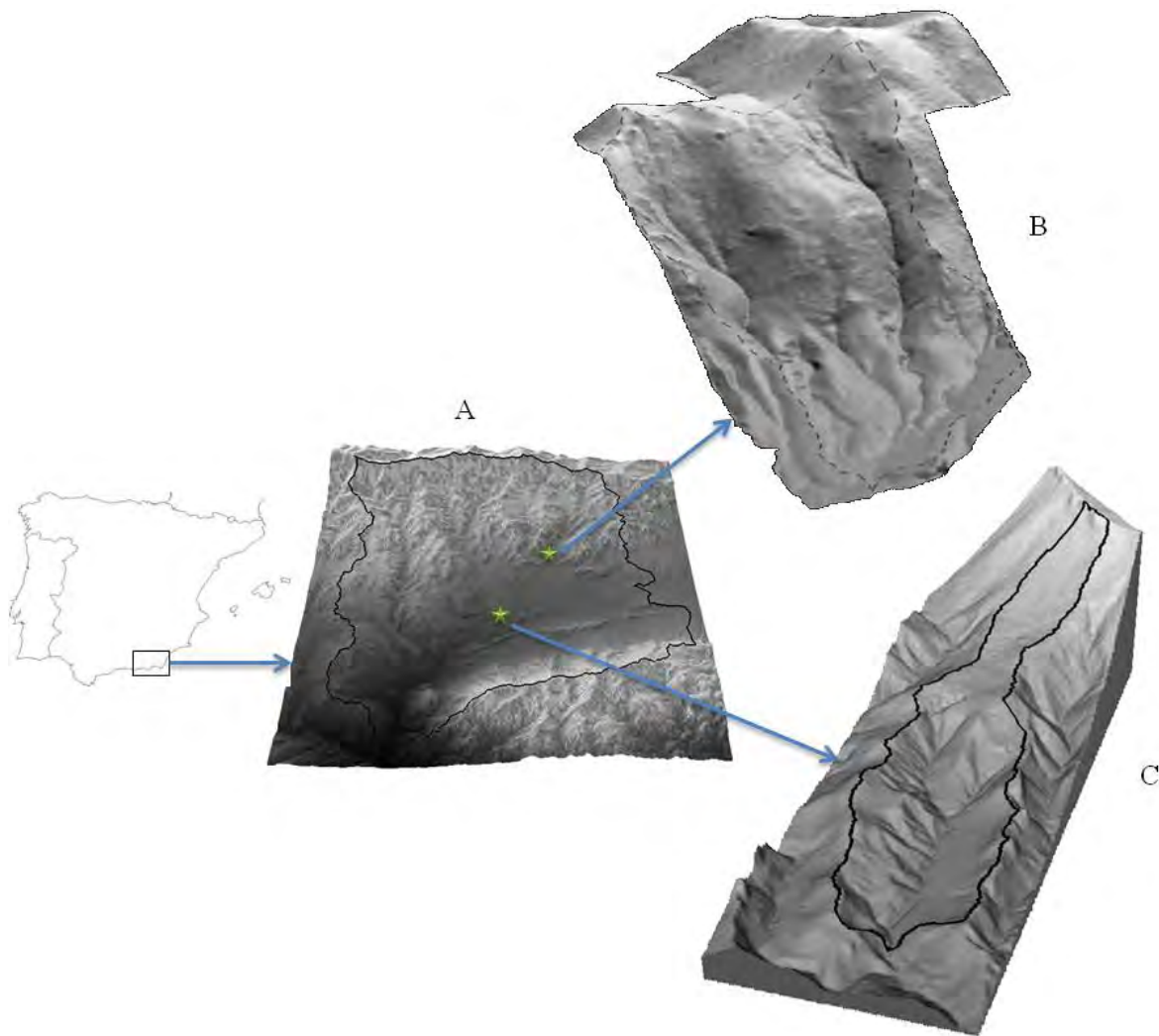


Figure 2.3 DEMs of different origins and resolution and varied landform complexities used to generate the channel networks. A) Tabernas Basin at 30m grid resolution with high heterogeneity. B) La Rambla Honda Basin (highly homogeneous landscape). C) El Cautivo Basin at 1m grid resolution (highly homogeneous landscape).

The Tabernas Basin has been formed by the repeated folding and faulting of the metamorphic basement of Serravallian age, which was filled from then until the Pleistocene by marine sediments first and continental ones at the end (Weijermars, 1991). Starting with the Pliocene, a tectonic compression and epirogenesis lift are initiated which provoked the emergence of the entire region. The marine deposits are limited to the present coast, with coastlines retreating toward the south, from the Sorbas basin. The sedimentary basins are fractured and suffer relative lifting (the maximum relative lifting may be seen in the Sorbas basin) and sinking, where strong differences in level are created between Vera to the east and Tabernas to the west to form the second morphostructural unit of the Betic Cordilleras (i.e. Neogene Sedimentary Basin and Quaternary Deposits).

- *Geomorphology, hydrology and erosion*

In general, the geomorphology of the region is influenced by two factors: active tectonics and Quaternary climatic change (Weijermars, 1991; Harvey, 2002), which characterizes the current form

context of Tabernas Basin in particular and the southeast of Spain in general. The quaternary landforms of the Tabernas Basin are characterized by a spectacular contrast between an almost wholly depositional landscape in the upper part of the basin and an almost wholly erosional one in the Tabernas badlands of the lower part of the basin (Harvey, 1987) linked by deeply entrenched canyons (Harvey et al., 2003). The most extensive forms of aggradation in the region are the glacis or pediments and the alluvial fans. Various surfaces from the lower Quaternary end in marine deposits also belong to the Quaternary. The Tabernas basin has been affected by a series of tectonic movements since the Miocene to the present, giving rise to a stepped landscape of Cuestas, which have been dissected by gullies starting at the footslopes of the Sierra Alhamilla. These gullies are found within the pediments and have formed younger alluvial fans in their interior. The largest alluvial fans are found at the contacts between Los Filabres and Alhamilla Mountains at the extreme east of the Tabernas basin on one side and, between the Alhamilla and Cabrera Mountains, with the central part of the Almería-Carboneras basin, on the other side (Harvey, 1996).

The development of the tectonic activity has conditioned the development of the drainage network in the landscape throughout the Quaternary period (Harvey, 2002). While the lifted mountain systems show a predominance of dissection along the main valleys (Solé-Benet & Cantón, 2004). The Neogenic basins present outstanding differences between the forms of dissection and aggradation. The forms of dissection are related to the incision of the drainage network and are especially significant on steep gradients that originate to the east and the west of the Sorbas basin, which experience a relative lift compared to its surroundings. The dissection has cut through the lower lake sediments, and through Tabernas canyon into the upper part of the basin. As a result, the fans in the upper part of the basin show differential coupling relationships (Harvey, 2002). Only in the south of the basin has the modern wave of dissection reached the mountain front. The southern group of fans are dissected throughout and coupled with the downstream channel network (figure. 2.4), while the Filabres fans remain decoupled (Harvey, 2002). Thus, the Aguas River on the east falls 160 m in 11 km and carves 160 m into the Messinian marls and captures the ancient Aguas-Feos system which originally drained the Sorbas basin to the south, by the Carboneras basin. In the west, the Tabernas Rambla falls 260m in 16 km and produces dissectional reliefs of 200 m into Tortonian marl sediments, giving rise to one of the largest areas of “*badlands*” in Spain (Solé-Benet et al., 2009).

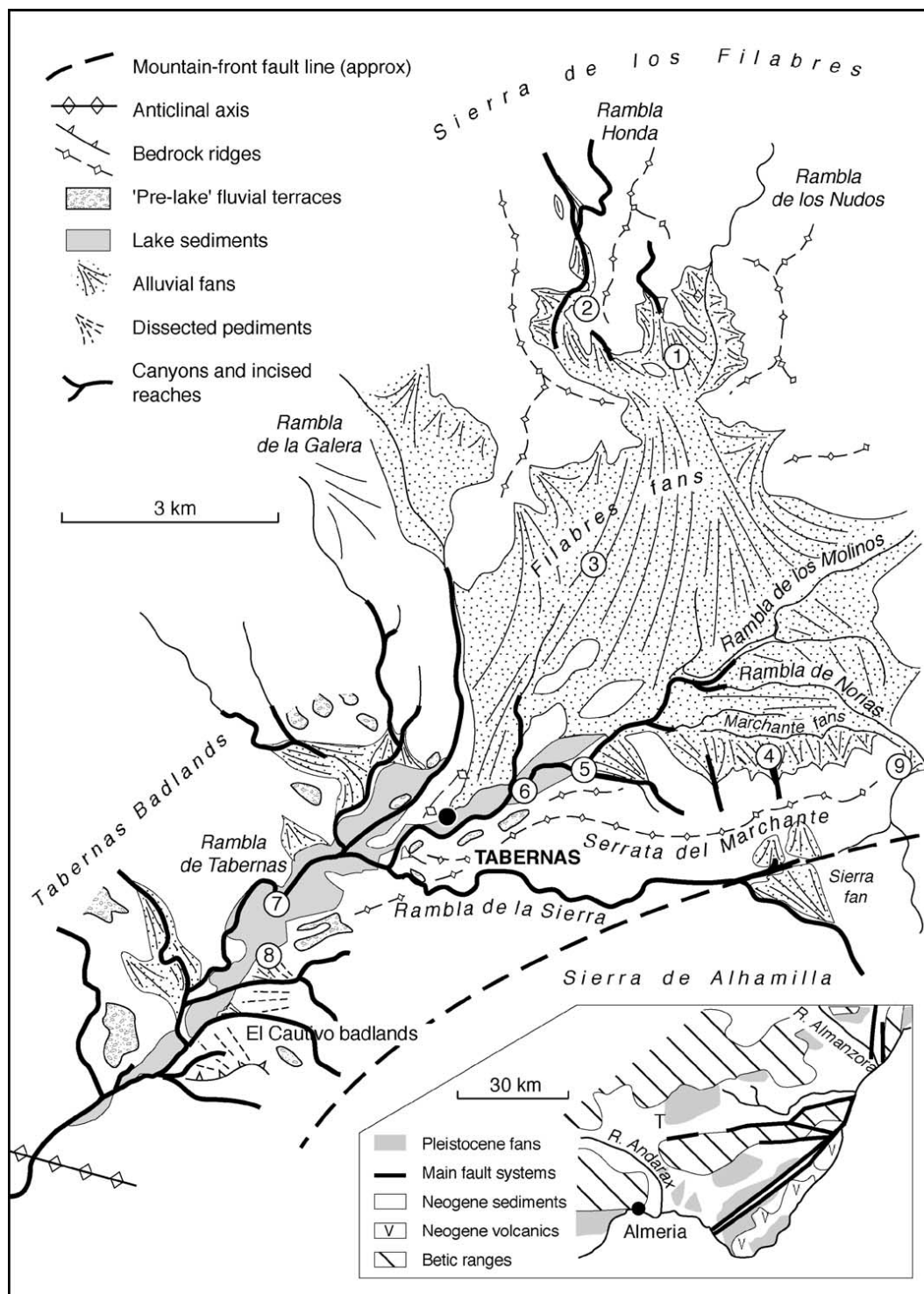


Figure 2.4 Geomorphologic scheme of the Tabernas Basin (after Harvey et al., 2003). Both site locations of Rambla Honda and Cautivo basins are located in number 2 and 8, respectively.

The main channels of the area are of the dry type (ephemeral streams) almost during all the year round, although some might flow during some months (Lázaro, 1995). In rainy years narrow streams (usually do not go over 1m wide and 20 cm deep) become braided streams and could flow during 10 months. On the other hand, in dry years, it is possible to remain more than ten months without water. Thornes (1976, 1996) provided some data about the nature of the ephemeral streams (channels) focusing on channel-bed sediments as they changed downstream. Drainage networks and

streams, catchments (or watersheds), drainage divides or ridges are important properties of real landscapes that contribute to the understanding of material flows (Burrough & McDonnell, 1998). The fluvial system of the area (figure 2.5) reveals a varying inconsistent dissected landscape. In general, the central part of the basin is highly dissected whereas the higher parts show elongated smooth hillslopes. This fits the theoretical interpretation of the hydrological network formation of the Tabernas Basin mentioned above and the construction for the so-called the great lake of Tabernas.

Five types of soil erosion were identified in the Tabernas badlands (Gallart et al., 2002), which could be representative for the whole study area: 1) Rainsplash,: the impacts of raindrops during rainstorms contribute to the destruction of the regolith layers and to the sealing of cracks, through the clogging role of detached regolith particles; 2) Piping: flow through a network of macropores detaches and erodes particles, enlarging the initial conduits towards a well developed network of pipes; 3) Rills, common micro-forms in badlands surface, usually reappear during rainfall events and are significant in sediment production and water and sediment conveyance; 4) Shallow mass movements, during rainfall events the regolith mass may flow towards the valley bottom in the form of small mud or debris flow; and, 5) Deeper mass movements, related to badlands initiation and evolution and their activity disorganizes the fluvial landscape characteristics.

The landscape of the study area suggests high rates of erosion (Lázaro, 1995) attributed to lithological and relief characteristics of the site. Wise et al., (1982), in a study of the southeast Iberian badlands, stated that there is a clear inconsistency between the high erosion rates, which one would expect from the visual appearance of the landscape and the persistent of appreciable inter-fluvial areas untouched by erosion during 4000 years. Because of precipitation scarcity, Tabernas watershed shows low active erosion rates (Solé-Benet et al., 2009). In the other hand, the rate of erosion, obtained by Solé-Benet et al., (1997) in the Cautivo site (southern part of the basin) oscillates between 10 g m^{-2} in areas of high vegetation cover and low inclination, and 567 g m^{-2} in the most eroded sites, lacking of vegetation and with exposed horizon C. In total, a twenty year period of erosion measurements has shown, in one hand, that the overall erosion in a small badlands catchment is quite reduced to $< 4 \text{ t ha}^{-1} \text{ yr}^{-1}$. On the other hand, and in quiet seldom years, the steep and bare south-southwest oriented slopes can produce over $100 \text{ t ha}^{-1} \text{ yr}^{-1}$, while plant covered north-northeast oriented slopes gives very low sediments $< 0.6 \text{ t h}^{-1} \text{ yr}^{-1}$. Nevertheless, south to north slopes are periodically eroded when enough regolith has been prepared by wetting- drying cycles prior to an intense rainfall event able to detach and remove it (Solé-Benet et al., 1997).

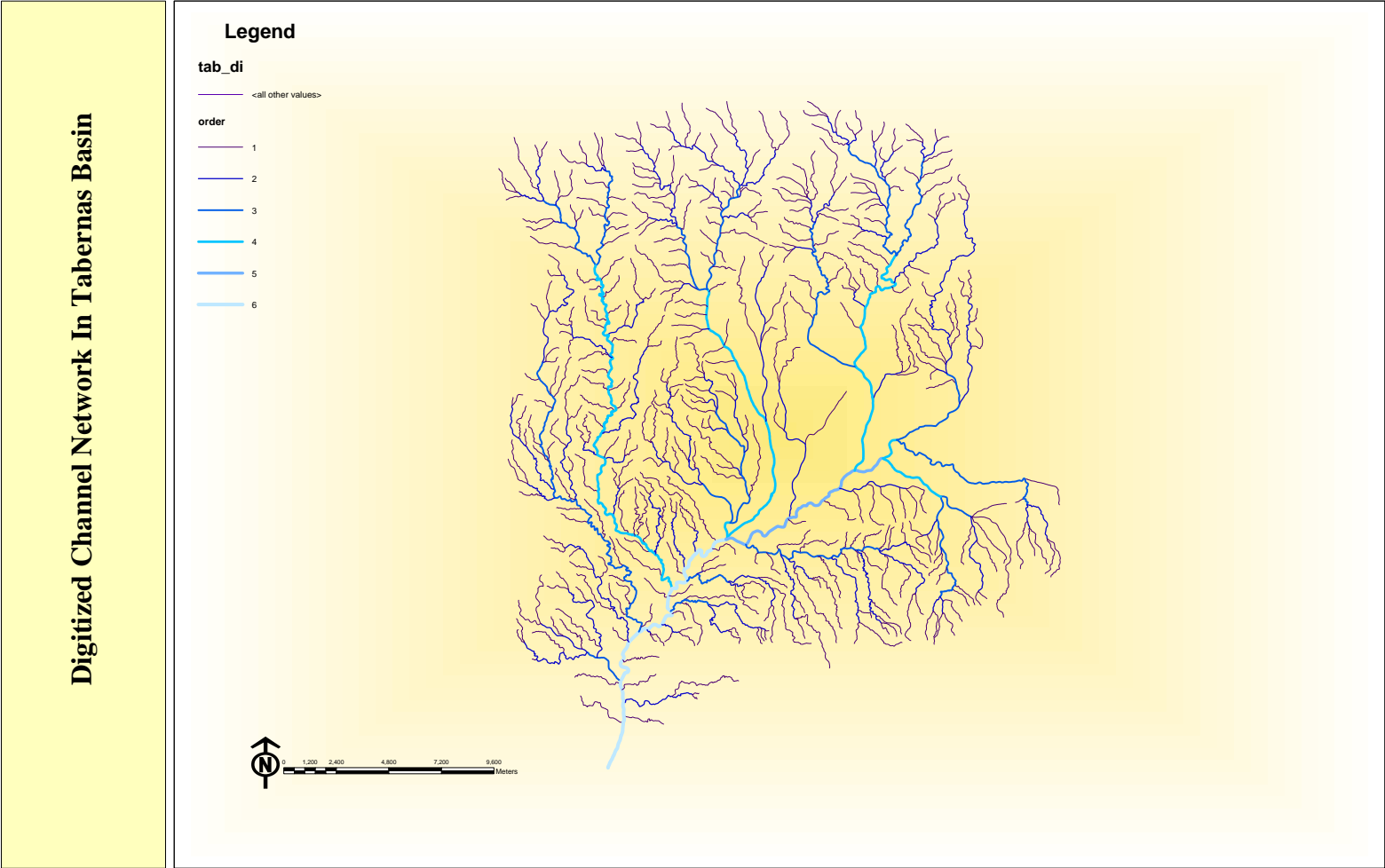


Figure 2.5 The digitized channel network or Blue Lines (BLs) for the Tabernas Basin.

- *Climate, soil and vegetation cover*

The climate of the region is thermo-Mediterranean semiarid. It has a mean annual precipitation of 239 mm (as recorded over a period of 30 years in Tabernas station, 1967-1997) (Solé-Benet et al., 2009). Regionally, average rainfall events vary from 331 mm year⁻¹ in Sierra Filabres in the north, 266.2 mm year⁻¹ in the Rambla Honda station in the center of the area, to 236 mm year⁻¹ in the Cautivo station in the south. The precipitation presents a high peak in winter, between 31-55% of the total annual precipitations, the rest is distributed between autumn and spring, and the summer is usually dry with occasional rain events between 1-10 mm yr⁻¹ (Cantón, 1999). Some of the rainfall events are of stormy type, where maximum intensities registered in the Cautivo station for distinct time intervals were 66.6 mm in 24 h, 108 mm in 5 minutes, and 83.8 mm in 10 minutes (Solé-Benet et al., 2009).

The soils formation in the Tabernas basin is controlled by a variety of factors, where the composition of the geologic formations that act as parent materials is one of the most relevant. Climatic condition, of high aridity, morphologic features and hillslope-dominant processes are also factors that influence the soil development (Palacio, 2002; Oyonarte, 2004). Shallow development of soil horizons is also attributed to high rates of soil erosion mentioned earlier (Solé-Benet et al., 2009). Five major taxonomic units (FAO, 1977) with their corresponding soil associations have been described in Tabernas area (LUCDEME, 1987). The taxonomic units include the followings: 1) Lithosols: They are well distributed in the study area but best located in the high and steep lands forming part of different associations; 2) Regosols: They are developed from either siliceous or calcareous rocks forming Calcaric Regosols and Eutric Calcaric Regosols, respectively; and with the Lithosolic Regosols are the most common associations in the area; 3) Lithosolic Regosols: They are developed from siliceous materials, micaschists and quartzites from the Nevada-Filabride Complex; 4) Calcaric Regosols: Are one of the most abundant type of soils. The parent materials are generally calcareous rocks, conglomerates and rocks from the Nevada Filabride Complex, such as micaschists and quartzites. They have abundant stones and the slope ranges from moderately titled to steep terrain; and, 5) Eutric Regols: they are developed from schists and quartzites with moderate to highly steep slopes.

The region's serial vegetation is floristically rich and with abundant endemism, since they are located in a broad ecotone between the European Mediterranean and arid African eco-regions and because of the great number of microhabitats that produce an intersection of climates together with the rough topography and lithological variety. The special distribution of the vegetation cover in Tabernas Basin is widely affected by main landform and prevailing relief structures of the area. Afana (2003) showed that the spatial distribution of vegetation cover (figure 2.6) is widely controlled by topographic formations that act as a major limiting factor. In general, the dispersed distribution of the species in patches that settle the zone followed certain patterns, which respond at

the special variation of the own heterogeneity of the zone (Gutiérrez, 2000). This heterogeneity acts as a damper for the human pressure and probably adapts the appearance and the actual permanent vegetation communities with different strategies to survive with the scarcity of water. This heterogeneity is the result of the geomorphic processes which operate at different rates over a single landform (Puigdefábregas et al., 1999).

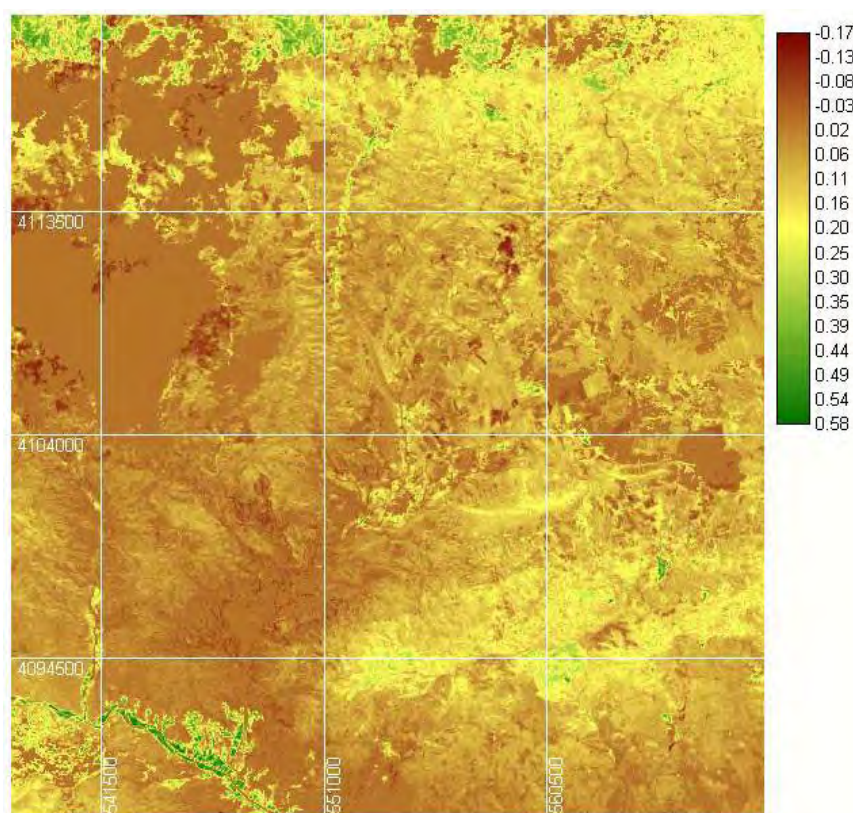


Figure 2.6 Values of normalized difference vegetation index (NDVI) in Tabernas Basin at 30 m grid resolution. Negative values indicate shade effect of clouds.

2.3.2. Rambla Honda site location and general characteristics

The Rambla Honda field site was selected as an ideal location for answering questions arising from the earlier MEDALUS project, which tries to identify regional key indicators and environmentally sensitive area of desertification (Brandt & Thornes, 1996). Moreover, the Rambla Honda is extremely well placed, both because of its semi-arid Mediterranean climate and because the essential basin information (e.g. climate, vegetation, soils, main topographic and geomorphic structures and processes, etc.) has already been acquired and available (e.g. Boer & Puigdefábregas, 2004).

The Rambla Honda basin is located in the contact zone between the Filabres range and the Neogene depression of Sorbas-Tabernas (figure 2.3b). In the lower sector of the Rambla Honda, an ephemeral river draining a basin of 154733m² (Puigdefábregas et al., 1996) will be used as an experimental catchment in order to prove the proposed model. It is important to underline that the Rambla Honda field site forms part of a large fan system prevailing in the lower parts of the

southern versant of the Filabres range. The experimental basin is formed by asymmetric valley formation, with a left gradient of a very steep and rocky hillslope and a smoother right one with alluvial fans system in its base, developed from the Pleistocene (Harvey, 1984a), and is destroyed slowly by the continuous incision of the present fluvial network.

- **Geology and Hydrology**

The Rambla Honda is an ephemeral river situated on the southern slopes of the “Sierra de los Filabres”, a core of Pre-Cambrian to Triassic metamorphic rocks (from Nevado-Filabride complex) in the eastern part of the Betic Cordillera. The river ends at the Honda fan, which is the backfilled portion of a coalescent mountain front fan complex (Puigdefábregas et al., 1999), which has developed since the Late Pliocene. The bed rock of the area is slaty micaschists, highly convoluted and fractured, dark grey, fine-grained, with graphite and garnets, crossed by abundant veins alternating with thin phyllite layers, all of Devonian-Carboniferous age (Puigdefábregas et al., 1996). When garnets and quartz proportions are high, spurs or shoulders are formed by differential erosion and colluvial debris is accumulated behind them. In the middle to low part of the catena, the slope colluvia gradate to an alluvial fan formation which connects with the large Rambla Honda fan system (Puigdefábregas et al., 1999). Altitudinal-transect holes in the rambla floor reveal the existence of a rather pronounced palaeo-relief, antecedent to the deposition of sediment (Harvey, 1984b). The sedimentary columns contain alternating beds of coarse and fine materials. Gravels and sands prevail in the upper section, whereas red loams with small sandy intercalations predominate in the lower section (Puigdefábregas et al., 1996).

- **Soils – Structural properties**

The soils are essentially alluvial and colluvial in origin. Those on the higher hillslopes have developed directly from micaschists and over inclined deposits (Puigdefábregas et al., 1998a). Steepness of slope and variability in hardness of bedrock influence soil thickness; for instance, soils are usually shallow (up to 15 cm) where slates with abundant quartz veins dominate (Eutric Leptosols according to the FAO-ISRIC-ISSS, 1998); however, soils are thicker (up to 60 cm) where phyllite strata are dominant (Eutric Regosols according to the FAO-ISRIC-ISSS, 1998). Those on alluvial fans have developed from bedded colluvia which have originated from the erosion and sedimentation of material from the slopes above them (Puigdefábregas et al., 1996).

In the Rambla Honda site, soil structural properties are well described by the catena hillslope concept or sequence (Puigdefábregas et al., 1998a, 1999). Soils from the scarce vegetated upper slopes, the alluvial fans at midslope position and the valley floor, are graded into each other to form a catena of increasing depth and coarseness of texture downslope (figure 2.7). Because of irregularities in rainfall, infiltration and runoff, soil moisture doesn't increase uniformly

downslope. However, the presence of deep-seated, relatively moist layers of soil in the valley bottom means that soil moisture is higher than upslope.

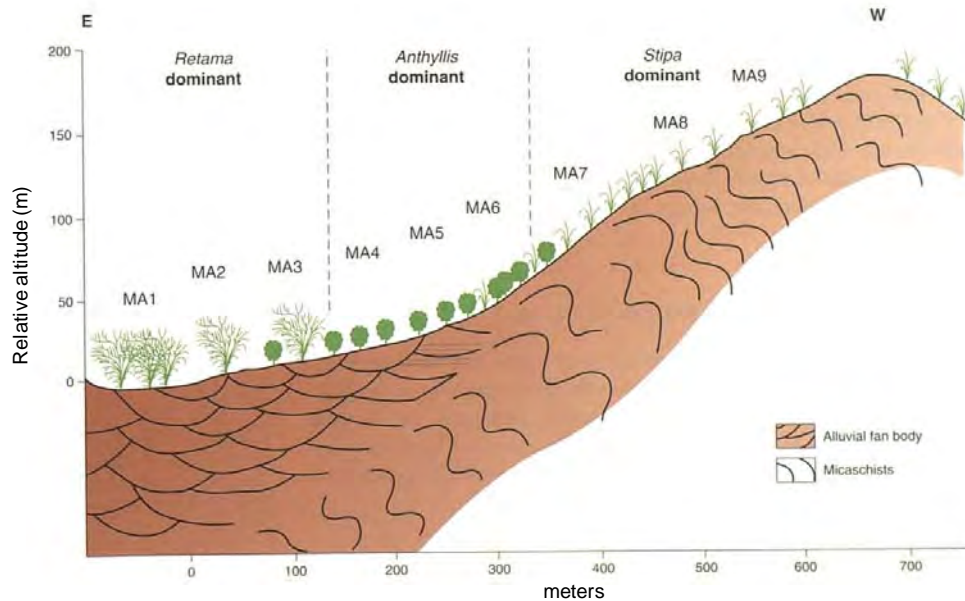


Figure 2.7 Catena scheme in the Rambla Honda catchment (after Puigdefábregas et al., 1998a).

- **Current drainage network**

Because of the scarcity and nature of precipitation, runoff along the hillslope is discontinuous, being at the same time ephemeral even in the main channel. The drainage network of the area is of dendritic type (figure 2.8). The landscape is smoothly dissected and stream branching is strongly conditioned by the local structure of both the prevailing schistosity and the folding axis of the faults (Puigdefábregas et al., 1998a). Such structures follow the lineal zones of high weakness, with the presence of good examples of differential erosion types giving rise to morphometric ridges and spurs near to thalweg of reduced dimensions, i.e. first-order links.

2.3.3. El Cautivo site location and general characteristics

El Cautivo field site is located in the southern part of Tabernas Basin (figure 2.3c), forming part of the “badlands” core of Tabernas Desert, with 19040 m² drainage area. Similar to the Rambla Honda, El Cautivo field site were selected for its own geo-ecological characteristics (e.g. active geomorphological processes within the Badlands of Tabernas, perfect examples for erosive forms and processes within a fluvial landscapes, arid to semiarid climate, etc.).

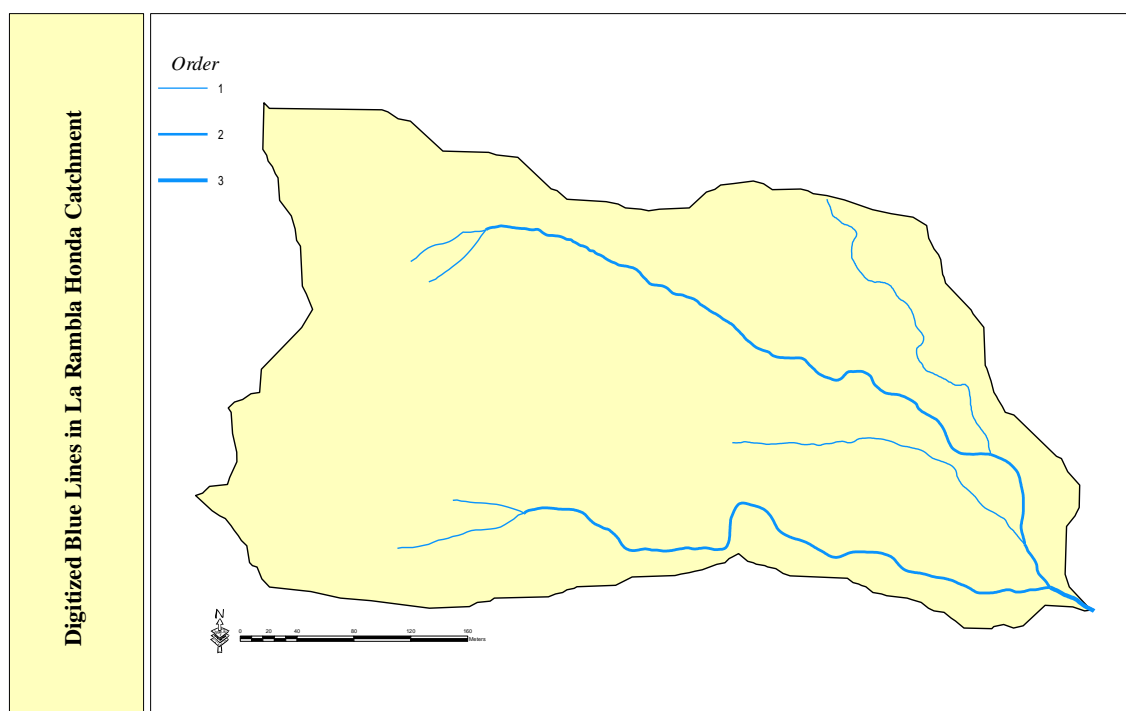


Figure 2.8 Digitized-BLs in La Rambla Honda catchment obtained by a topographic map at 1:500.

- **Geology**

Badlands of El Cautivo site are cut in an uplifted sequence of Tortonian (Upper Miocene) gypsiferous mudstone (Cantón et al., 2004). A multiple-age of stepped *badland* has resulted from episodic uplifting and dissection during the Quaternary (Harvey, 1987, Alexander et al., 1994). The basin is partially surrounded by the Betic Cordillera System and is located at the south of the Filabres mountain range, and at the leeward of the Nevada and Gádor ranges (Cantón et al., 2001, 2004). The stratigraphic series (i.e. the Totorrian-age Chozas formation) is about 150 m thick and include mudstone and some calcareous sandstone (Kleverlaan, 1989). As mentioned earlier, episodic tectonic uplift and alterations between dry and humid climate sequences (Harvey et al., 2003) during the quaternary led to the development of a multi-age badlands landscape (Alexander et al., 1994).

The parent material is a hard and compacted mudrock, petrographically identified as calcareous and gypsiferous, predominantly composed by silt-size (>60%) of siliceous minerals (mica, paragonite, chlorite, quartz and feldspar, in decreasing order of abundance) and the rest are calcite, gypsum and dolomite particles (Solé-Benet et al., 1997; Cantón et al., 2001). According to these authors, weathering of mudstone is caused by the combined effect of wetting–drying and gypsum solubilization–crystallization, once the unloading of the consolidated sediment has initiated the development of an extensive network of cracks which widen upwards, until the rock shatters into irregular pieces of a few centimeters. After extended wetting under saturation or after several wetting-drying cycles, these pieces further disintegrate into smaller grains, finally producing fine silt structures (Cantón et al., 2001).

- **Soils**

The soils of the area, formed under high aridity conditions over soft bedrock and predominated erosional processes, are little profound (Solé-Benet et al., 2009). Generally, in badlands, it is highly important to distinguish soil units in relation to different stages of evolution (i.e. developed soils and regolith stage). Highly-gradient slopes with S, SW and W orientations don't allow for a real soil structures (regolith) since soil erosion is frequent and/or intense. Whereas, soils with good differentiated horizons are located in the more stable surfaces, which could be attributed to the in-situ material evolution (Solé-Benet, et al., 2009), or because of sediment accumulation in gentle gradient formations (pediments or alluvial terraces) that favor its evolution (Gallart et al., 2002). En general, dominated soil types are of Leptosols, Ortic Solonchaks and Calcic Regosols, according to the existing cartography 1:100,000 (Perez Pujalte, 1987), whereas a further detailed field survey revealed soils of Epileptic Regosols, Endoleptic Regosol, Eutric Regosol, Eutric Gypsisols, Haplic Gypsisols, Haplic Calcisols and Gypsisols types (Cantón et al., 2003).

- **Topography and vegetation cover**

The topography varies sharply along and across relief landforms with altitudes that extend between 260 and 367 m a.s.l. In general, the landscape is made up of asymmetric NW-SE valleys (Cantón et al., 2004). Northeast-facing slopes are moderately steep with gradients averaging $28^\circ \pm 8^\circ$. Rills are rare on these hillslopes. Mass movements are not frequent but when they occur, large soil volumes can be affected (Solé-Benet et al., 1997). Southwest-facing hillslopes are much steeper (averaging $47^\circ \pm 9^\circ$), straighter in profile, and in general are bare (Cantón et al., 2001, 2003). Rills are quite frequent and develop almost from the top to the bottom of hillslopes. Very shallow mass movements have been frequently observed on such hillslope following rainfall events larger than 50 mm (Solé-Benet et al., 1997; 2009). At the foot of any hillslope, a pediment can form, more frequently and larger on north- and east-facing slopes; their gradient average 10° . Rills and mass movements are absent from these morphological units. Some pipes developing at the contact between the hard mudrock and the upper-layered sediment or soil can be observed (Solé-Benet et al., 1997).

The lithology and climate of the zone have confirmed a landscape of “*badlands*”, in which vast and matched valleys with marked (large and thin) ridges and divides are well observed (Solé-Benet et al., 2009). Observed patterns of the spatial distribution of soil cover are repeated all over the dissected landscape. Cantón et al., (2003) have distinguished four main soil surface types according to *i*) the type of the plant cover (or base ground); *ii*) differential hydrological behavior; *iii*) topographic characteristics; and *iv*) soil beneath them. These types are arranged topographically in table 2.2.

	Surface cover type	Topographic characteristics	Soil type
1	Disperse dwarf shrubs and annual plants	Pediments at the foot of NE facing slopes. Moderate curvature (concave) SLO = 21	<i>Haplic Calcisol</i> ; >1 m depth
2	Scattered cover of high perennial herbs (<i>Stipa tenacissima</i>) and other perennial plants and lichens in open areas	Steep slopes at the area's headwaters. Moderate curvature (concave). SLO=34	<i>Eutric Gypsisol</i> (at the higher part) and <i>Calcaric Regosol</i> ; >0.5 m; sandy
3	Almost continuous lichen crust along with a sparse cover of annual and perennial plants	Highest part of NE facing slopes, moderate to high curvature (convex) SLO = 29	<i>Endoleptic Regosol</i> ; <0.3 m
4	Bare marl regolith, sometimes covered by a crusted silty layer or with a degraded lichen crust	SW facing slopes with strong curvature. SLO = 40	<i>Epileptic Regosol</i> ; <0.3 m; apedal

Table 2.2 Main characteristics of four main monitored soil surfaces. SLO: slope angle in degrees (after Yolanda et al., 2003).

- **Current drainage network**

The drainage network of the studied zone proceeds from the Cautivo hills; that is, a faulting fold lifted up at the end of the Pliocene (Harvey, 1987). In fact, the entire drainage network in the Cautivo area forms part of the tributary branching system of the Tabernas rambla that fills into the Río Andarax. This rambla reaches the zone coming from northwestern part, after forming a meander of approximately 90°, then takes the southwestern direction; with an altitude of a bout 240 m, which constitutes the base level. The hydrologic network of El Cautivo area is of dendritic type (figure 2.9) formed by ramblas, rills and gullies of a reduced and stationary pattern, of torrential type, coming from Sierra Alhamilla in the south and the Filabres in the north (Solé-Benet et al., 2009). The landscape is strongly dissected (figure 2.10) leading to highly drainage density values (i.e. 0.281 m/m², in the study area).

2.4. DEMs of the study area

2.4.1. Introduction:

The methodological aim of the current work is to delineate optimal channel networks at the available resolution and scale from DEMs, solely. In order to accomplish this goal, several experimental DEMs of different origins and terrain-relief complexity conditions, i.e. homogeneity and heterogeneity, were employed. These DEMs are hierarchically organized representing different level of complexities and organized as follows. The first DEM covers the Tabernas Basin area, at 30 m grid resolution representing a complex heterogeneous landscape (figure 2.3a). The second resolution consists of two DEMs of 1 m grid size for El Cautivo and the Rambla Honda catchments, which represents homogeneous relief formations of different origins (figure 2.3b & c).

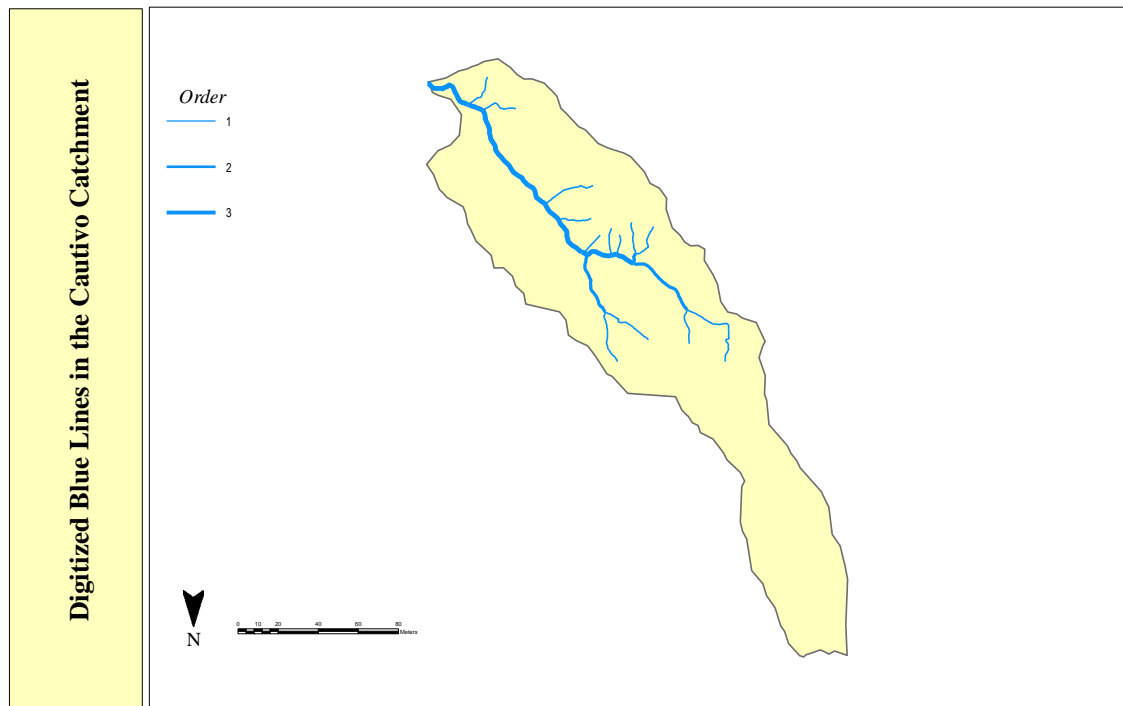


Figure 2.9 Digitized-BLs in El Cautivo Catchment obtained by a topographic map at 1:500.



Figure 2.10 Aerial photograph of El Cautivo badland system (source Chadwick).

The origin of the 30 m DEM resolution is a 10 m grid resolution, constructed by aerial photographs of colour high resolution fly (Junta de Andalucía, 2002). The flight was realized at a scale 1:60,000, with a focal distance of 150 mm, and elevation height of approximately 9,000 m. Consequently, a digitalization process for the photogramms was realized with a photogrammetric

scanner at a resolution of 21 micrometer (i.e. equivalent to 1.25 m in the terrain). The acquisition of the DEM has been realized through an automatic spatial correlation for the referenced photogramms to produce a network of points with 10 m equidistance over the terrain.

The second DEM is a high detailed one that describes the Badlands of the El Cautivo study site. Herein, the DEM was constructed using the ANUDEM program (Hutchinson, 1988). The original dataset was computed from 0.5 m contour lines derived from a topographic map at 1:500, based on aerial photographs at 1:3,500. In order to get the highly resolution DEM at 1 m grid size, ANUDEM interpolation technique was applied, which incorporates a drainage enforcement algorithm (i.e. imposing channel network to the original data). ANUDEM uses an iterative finite differences interpolation technique, which has the benefits of removing spurious pits and imposing a drainage network consistent with the original data (Hutchinson, 1989). The final RSME for the vertical resolution of El Cautivo DEM was 17.2 cm (Cantón et al., 2004). Tools and procedures used for the construction and treatment of the Rambla Honda DEM are alike to the Cautivo DEM. The horizontal resolution is 1 m, and the RMS vertical error is about 0.353 m (Cantón, 1999).

2.4.2. Methodology

The methodology presented here is intended for use in applications where data availability is limited to DEMs and its RMSE. In addition to certainty and errors in DEMs, items such as resolution and scale are also treated. Other previous knowledge, such as suitability of the DEMs to channel network extraction, was also commented and handled. The error in automated channel mapping is associated to several factors between which are the errors in the DEMs (Lindsay & Evans, 2006). In order to assess the amount of uncertainty in data matrix, a stochastic approach has been applied to the different DEMs that used in channel network delineation. Moreover, because the used DEMs have different origin and construction procedures, we will adapt a comprehensive procedure for error quantification. Accordingly, and throughout our work, we will adapt the spirit methodology of Darnell et al., (2008), that is “simplifying existing procedures to enable the ‘average’ DEM user to perform his/ her assessment on the implications of choosing a particular dataset for their work”. Hence, the stochastic method will be combined to other approaches in order to achieve a hydrologically connected DEM.

2.4.3. Low resolution DEM (complex & heterogeneous landscape)

In order to study resolution and scale effect, the original DEM was used to generate new models with systematically declining horizontal resolution. Hence, DEMs with various resolutions were created; these are 30 m, 60 m, 120 m, 240 m, 480 m, and 960 m grid size DEMs (Figure 2.11). The spatial resolution was reduced by averaging, i.e. aggregation or generalization or degradation, a reasonable operation under the assumption that digital elevation data at a given resolution, i.e. grid size, can be interpreted as averages over an area surrounding the point at which

elevation is reported (Helmlinger et al., 1993). The aggregation, that means a change of cell size, was performed by two algorithms: the resample and Contract functions within the reformat model of the IDRISI package. In the resample function option, two important operations have to be determined: the first is related to the method to be used in the interpolation process, nearest neighbour and bilinear. Bilinear produces a smoother result, but outputs values that are modified from the original. Nearest neighbour, on the other hand, only outputs values that were contained in the original. The second is related to the mapping function, i.e. the order of polynomial fit desired, which may be represented by linear (first order), quadratic (second order), or cubic (third order) functions. In general, one should use the lowest order of polynomial that provides a reasonable solution since the effect of poor control point specification gets dramatically worse as the order of equation used increases. Accordingly, the original DEM was resampled by the linear mapping function with the two interpolation methods producing two DEMs with the same resolution but from different interpolation methods. The RMSE was calculated for the original DEM and generalized ones (table 2.3). Alternatively, the contract function is a direct aggregation procedure, where the DEM (or any raster dataset) is generalized by reducing the number of rows and columns while simultaneously decreasing the cell resolution. Contraction may take place by pixel thinning or pixel aggregation, with the contraction factors in X and Y being independently defined. With pixel thinning, every nth pixel is kept. While with pixel aggregation, the new pixels represent averages of the n pixels specified by the reducing factor. Again, the original DEM of 10m were generalized by thinning and aggregation, and RMSE is calculated for both procedures (table 2.3).

Resolution	RMSE			
	Resample		Contract	
	Bilinear	Nearest neighbour	Thinning	Aggregation
10	3.506			
30	3.548	3.548	5.708	3.613
60	6.187	5.526	8.192	4.5316
120	7.564	7.159	12.323	6.145
240	12.308	12.208	24.579	11.794
480	19.353	19.551	43.799	20.534
960	42.377	42.003	96.585	43.124

Table 2.3 RMSE for the different resolution with different degradation DEM procedures.

Herein, the RMSE is related to the absolute vertical accuracy (i.e. feature to mean sea level), whereas the horizontal accuracy is related to the interpolation procedure used to obtain the desired resolution (i.e. feature to datum). It is obvious that, the resample function interpolation models (bilinear and nearest neighbour) provide similar results in almost all resolutions (table 2.3) with slightly advantage to the nearest neighbour algorithm. Whereas in the contract function the aggregation procedure produce a highly considerable improvements in RMSE compared to

thinning model (table 2.3), for which thinning procedures seems to be more appropriate for qualitative data. Such results confirm the ability of interpolation models, both bilinear and nearest neighbour, with other aggregation functions, e.g. aggregation (the output cell is the medium for the aggregated cells) to be used in DEM degradation, where similar results confirmed by Thielen (1999).

In general, the visualization process, which forms part of catchment-shape assessment, mainly catchment morphology, is another complementary process in quality evaluation. Visual examination of the Tabernas basin with different grid spacing reveals a loss of surface morphological details as grid resolution decrease (figure 2.11). At grid spacing over 240 m the catchment appears a set of linked linear facets with hillslope curvature being poorly represented. At 480 m resolution (and over), practically, much of the hillslope and channel networks detail has been lost. Not only stream networks are vanished, but also possible catchment limits are deformed totally, mainly in the 960 m grid dimensions, highlighting the presence of a non-complete hydrological unit. Such conclusions underline the need for a new scale dimensions that extended farther than the Tabernas-catchment limits in order to study stream network properties.

The global estimation of the RMSE of the studied DEMs allows for a new estimation of local uncertainty within spatial structures, that is, the stochastic simulation or the Monte Carlo approach (Wechsler & Kroll, 2006; Lindsay & Evans, 2008). Between the several stochastic approaches, Lindsay (2004) proposed a comprehensive one designated as stochastic shape analysis (SSA) based on Monte Carlo test. The selection of Lindsay approach is due to its efficiency in hydrologically corrected DEMs free of artefact depressions. The SSA conduct Monte Carlo tests to identify the most likely shape of depressions in a DEM based on a known error variance. Moreover, SSA can be used to identify which parts of a landscape are most likely to be affected by drainage topology interruptions caused by artefact depressions, mainly for hydrological applications. Another important aspect in the SSA analysis is the incorporation of spatial autocorrelation corrector which allows for a more rational error because elevation errors are widely known to be spatially autocorrelated. A direct disadvantage of the model, depending on the size of the DEM and the number of realizations used, the model needs to realize a huge amount of iterations, the needs to highly advanced facilities.

The final result of applying the SSA analysis in Tabernas basin is a spatial data matrix that describes the probability of a cell to have an artificial depression (figure 2.12a). From the SSA resulted grid, DEM error appeared to exert greater influence on planer and flat areas, where slope is reduced to minimum (i.e. less than 6 degrees), than upslope areas. Valley floor is another source of uncertainty where both natural and artificial depressions are localized within the same formation giving rise to the high probability values in figure 2.12a. Another important aspect is the approximately absence of depressions on upper hillslopes and mountain summits (upper and lower

parts of figure 2.12a). Such probability values can be expressed in depth measurements (2.12b), which may be added to the original DEM in order to remove such uncertainty. The impact of change in drainage network properties can be discerned through visual inspection of the result grids (figure 2.13). Herein, the change (or enhancement) in the modified DEM is widely appreciated by the change of the stream network position, direction or even structure form.

In relation to catchment scale variation, primary observations have revealed that basin size is changed irregularly with DEM resolution (table 2.4). This fact could be attributed to both, grid size and flow direction algorithm. The former is directly related to the form structure of the relief form and the capacity of grid size to define or represent a landform structure. The effect of grid dimension is observed in the whole catchment. The latter is related to lateral or border limits in the catchment and determine if a limiting cell is located within the catchment or corresponding to neighbour basins.

Resolution	Catchment size (km ²)	Differences in area size to the average (km ²)	Differences in area size to the average in cells
10	567.534	2.548	25480
30	567.265	2.817	3130
60	567.389	2.693	748.1
120	568.853	1.229	85.4
240	576.518	6.436	111.7
480	572.544	2.462	10.7
960	570.470	0.388	0.42
Average: 571.368			

Table 2.4 Changes in catchment size-values and the difference in relation to the average at different resolutions.

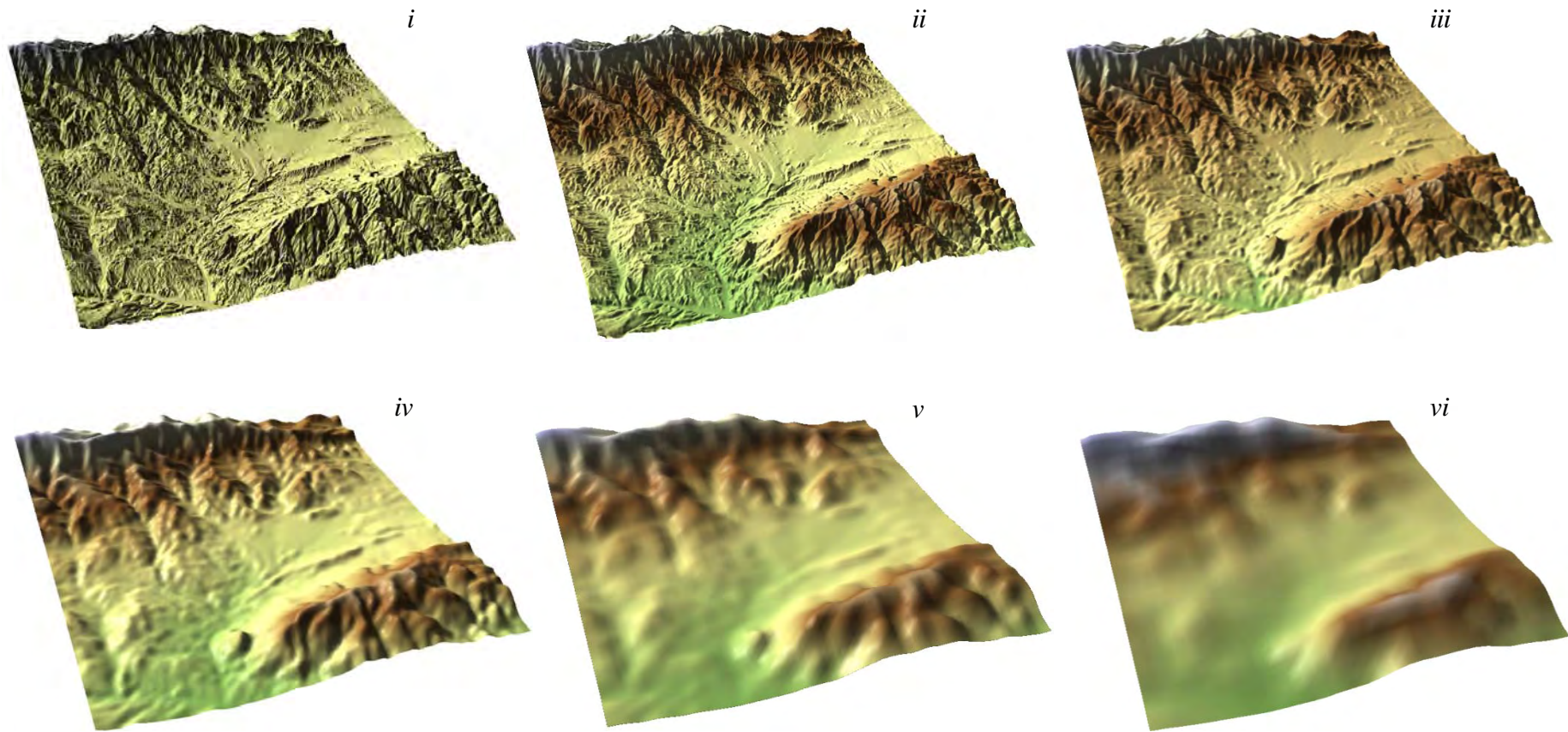


Figure 2.11 Generalized DEMs with systematically declining horizontal resolution. i) 30 m grid resolution, ii) 60 m grid resolution, iii) 120 m grid resolution, iv) 240 m grid resolution, v) 480 m grid resolution, vi) 960 m grid resolution.

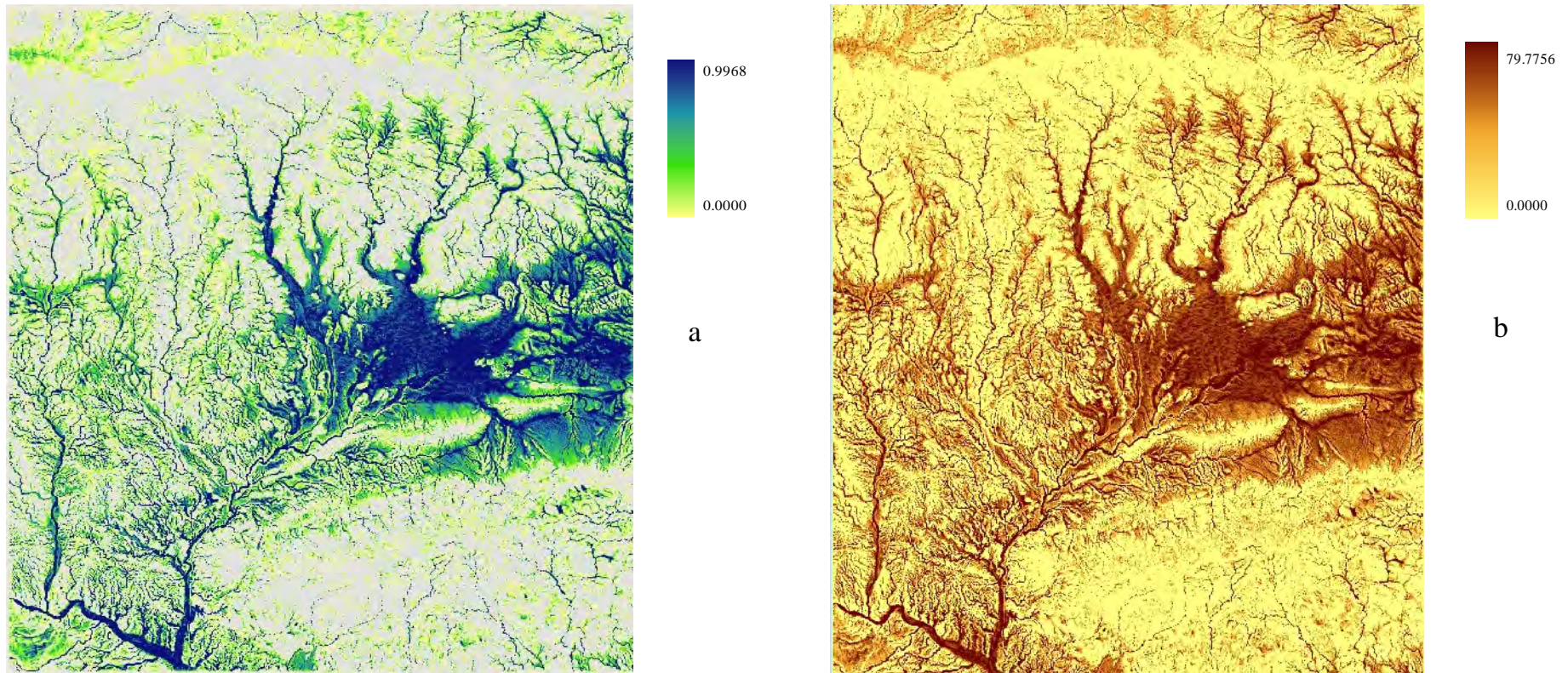


Figure 2.12 Probability depressions from the application of Stochastic Shape Analysis (SSA) in Tabernas Basin; a) pure probability values, and b) probability values expressed in depth values.

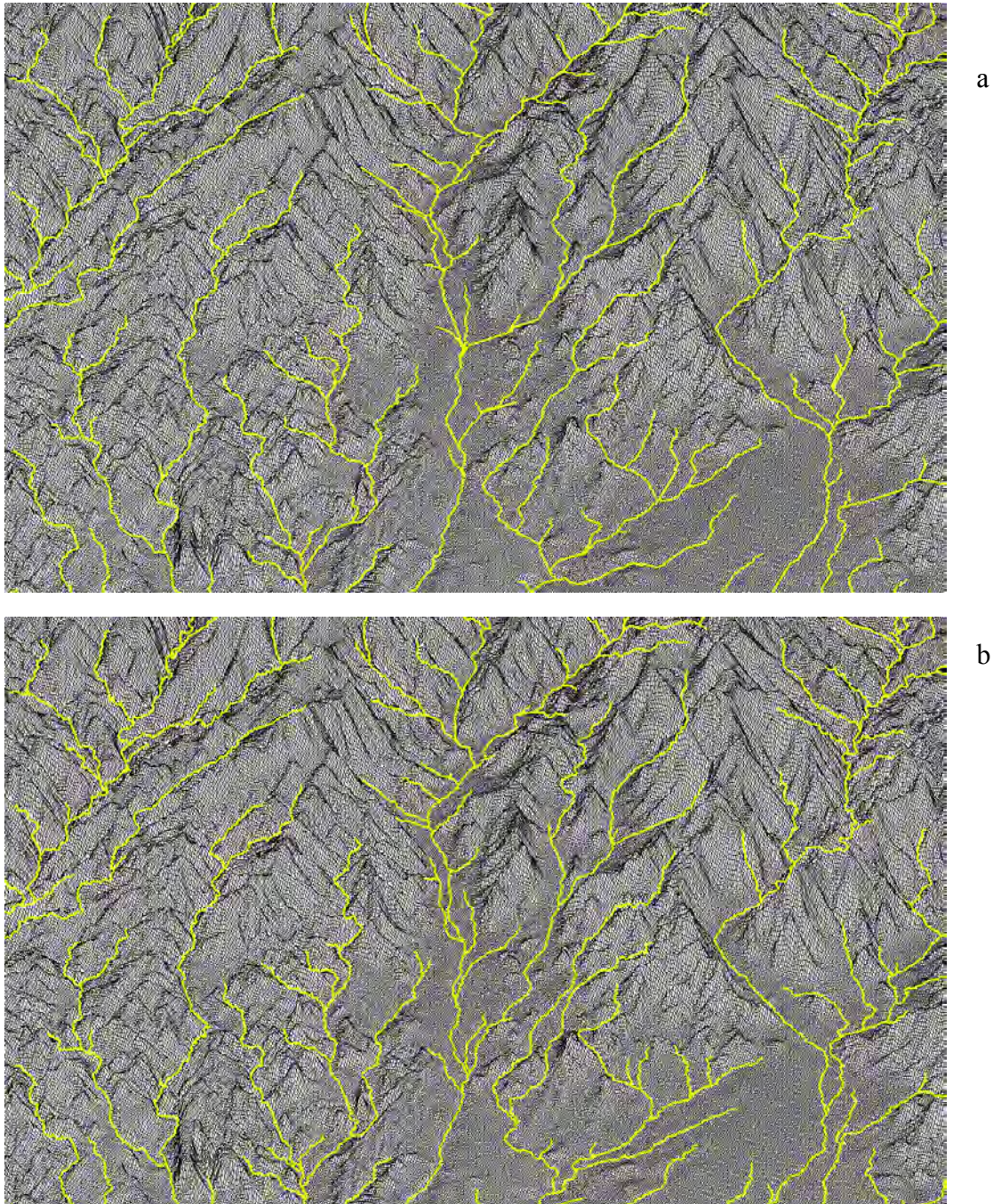


Figure 2.13 DEM of Tabernas at 30 m grid spacing corrected by the SSA analysis; a) 3D relief form before correction; and, b) 3D relief form after correction.

Lately, Oksanen and Sarjakoski (2005) underlined that drainage basin delineation is very sensitive to DEM uncertainty. They revealed two important aspects: the first one indicates that diffuseness (i.e. uncertainty) of the delineation was often a result of the flatness of the terrain, which is directly related to flow-direction algorithms; and, the second conclude that such sensitivity is not limited to specific dimension area. In our work, when plotting RMSE against resolution a strong relationship was detached (figure 2.14a), whereas such relationship was vanished when RMSE vales were plotted against catchment sizes (figure 2.14b) calculated by the different DEM-resolutions. The

results revealed that although RMSE is increased in relation to resolution, catchment area (defined by these resolutions) maintained unbiased in relation to resolution change. Conversely, catchment sizes of the different resolutions when plotted against RMSE revealed a clear enhancement in the degree of significance as it is limited to certain resolutions (figure 2.15). Such findings highlighted the importance of resolution in scale studies, mainly when DEMs are the unique source of information for catchment limitation.

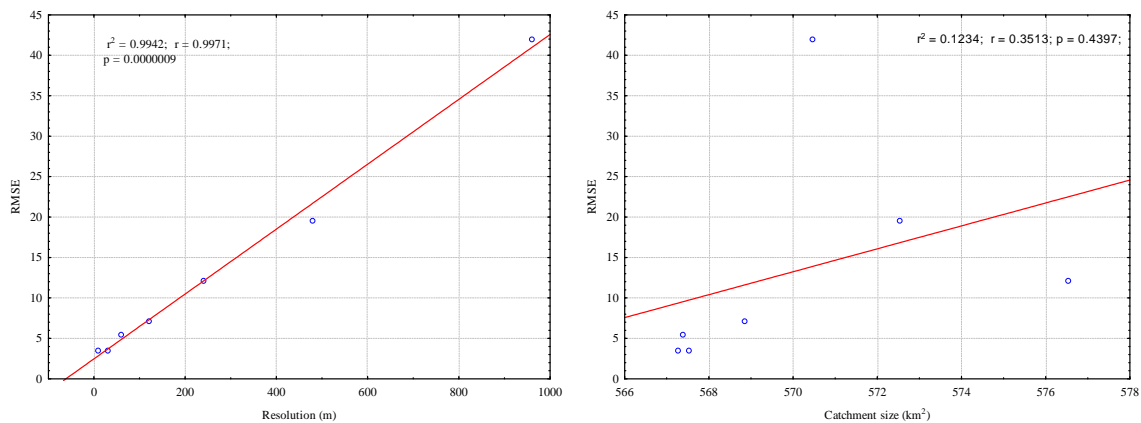


Figure 2.14 Scatterplot of RMSE in DEM-data matrix against resolution and catchment areas of the studied sites; a) linear significant relationship between resolution and RMSE, and b) relationship aspect and significance between catchment area and RMSE.

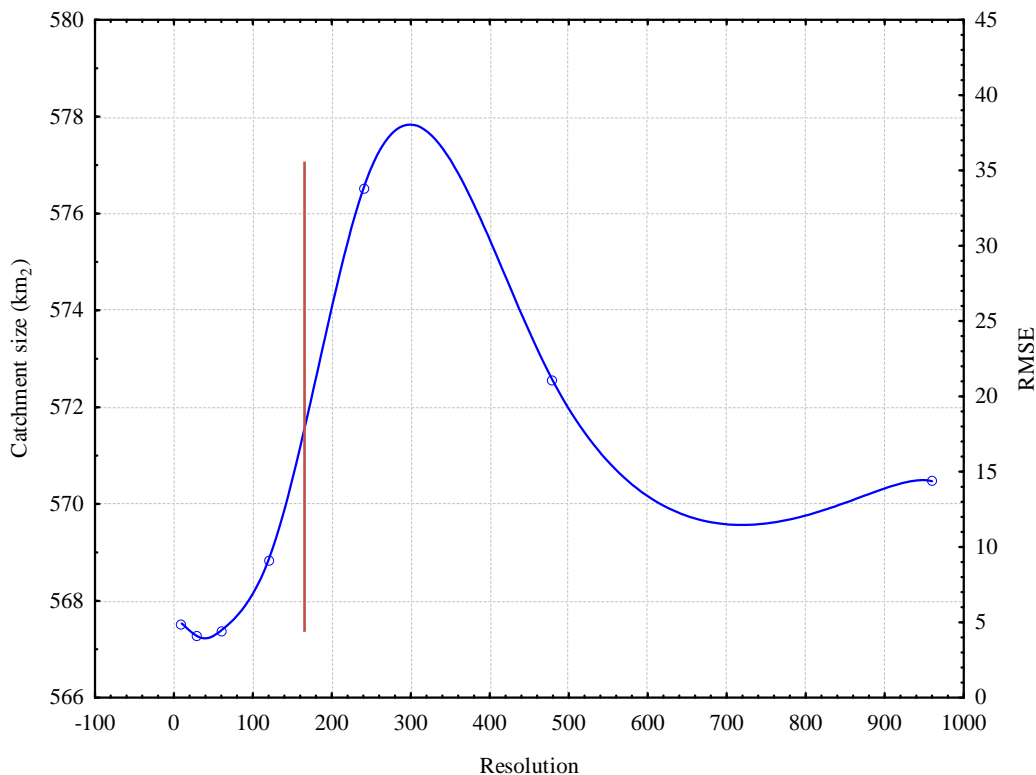


Figure 2.15 Resolution effect on changes in catchment size. The curve shows two different behaviours above and below the 240 m gridded-data dimension (underlined by the red line).

Another important aspect in DEMs characteristics is its suitability for stream network extraction. As mentioned previously, Gyasi-Agyei et al., (1995) suggested that a DEM is adequate for

extracting the channel network, if the ratio of average cell drop and vertical resolution is greater than unity. The average pixel drop can be determined from the average slope and grid spacing, whereas the vertical resolution can be considered as being approximately equal to the standard deviation of relative errors between points (Walker & Willgoose, 1999), and can be expressed by the following:

$$\frac{\text{average pixel drop}}{\text{vertical resolution}} \approx \frac{\alpha D_x}{\sigma_{\Delta Z}} > 1 \tag{2.3}$$

where α is the mean slope (m/m), D_x is the grid point spacing (m), and $\sigma_{\Delta Z}$ is the standard deviation of relative error in elevation (m).

In this way, the empirical relationship of Gyasi-Agyei et al., (1995) were tested (table 2.4) to check DEMs-adequacy used in the present study. It's evident that ratio of average drop pixel in relation to vertical resolution reveals a clearly two sets of resolutions, the first extends from 10 to less than 240 m grid size, and the second is at 240 m and all grid-dimensions above that resolution. These results highlighted the existence of two phase scale resolution related either to feature type (i.e. relief structure formation) or prevailing processes dominant at these scales and resolutions. These findings resemble that observed in grid size-effect over basin size (table 2.5).

Resolution	Ratio of average drop pixel to vertical resolution			
	Resample		Contract	
	Bilinear	Nearest neighbor	Thinning	Aggregation
10	2.433			
30	2.1644	2.1644	0.9121	2.1438
60	1.4619	1.1747	0.6998	2.2021
120	1.3359	1.2038	0.5227	1.5928
240	0.7251	0.6626	0.1938	0.7069
480	0.6239	0.6936	0.1552	0.7208
960	0.3736	0.3603	0.0559	0.3285

Table 2.5 Change in catchment size values at the different resolutions.

It seems that the resolution effect between 120- to 240-m grid-size is of considerable importance, mainly for comparison effects, in relation to landscape-features identification. If this is the case, then certainly dominant hillslope processes that act in these features are affected. Although the ratio average of drop pixel to vertical resolution is just an indicator of slight importance, since the final results depends on the errors of its components (vertical resolution and average drop pixel), it is still possible to be used as auxiliary data improvements. For resolutions higher than 240 m, DEMs seems to contain sufficient and adequate information to represent channel network related scale, exception just only founded in thinning procedures. Whereas, coarse DEMs resolutions (i.e. >240 m) may be considered as poor representatives for channel network extraction. This change of efficiency is attributed to the scale representation of the study area. Tabernas Basin is a highly complex landscape

that contain vast amount of information, i.e. features and processes. At high resolution, features are well represented and ratio-average components (vertical resolution and average drop pixel) are highly representative to the real catchment. While, features are badly represent by coarse resolution at the present scale, where the standard deviations of relative errors in elevation are merely high to represent catchment Tabernas features at that scale. Figure (2.11) reveals that coarse-resolution DEMs, mainly 450 m and 960 m, are inadequate to describe feature units of Tabernas Basin, since landscape patterns are indistinguishable at that scale. It is therefore, the effect of resolution aggregation process or the scale of the study area that may have a direct or indirect effect over resolution efficiency for channel network extraction. For instance, Zhang and Montgomery (1994) found that horizontal aggregation of elevation data leads to significant simplification and smoothing of the terrain.

Results of table 2.5 did not confirm a strict usefulness of some resolutions and the inefficiency of others, rather than adequacy for channel network extraction. Gyasi-Agyei et al., (1995) founded a negligible effect of vertical resolution in relatively high relief areas, but significant one in low relief zones and concluded that vertical precision of a DEM could be an issue in areas of flatter slopes. So, interpretation of results should be carried with caution, since one indicator is not sufficient to deduce adequacy of particular resolution to channel network extraction. Mutliframe approaches should lead these indicators, such as multifractal dimensions that relate scale and resolution to more than one landscape feature and process. Herein, it is not the scope of this work to prove scale and resolution effect, rather is a slightly description of these effects.

2.4.4. High resolution DEMs (homogeneous landscape)

Again, the same methodology and analysis have been carried out in the assessment of DEMs quality. In the Cautivo catchment, the data matrix of probability depressions confirms again the high concentration of probable artificial depressions mainly in channel and valley formations (figures 2.16a). Such uncertainty could be explained by the complexity of the stream network structure, the initial resolution (i.e. 0.5 m equidistance contour map) and the interpolation algorithm used to define such formations. Of course, the last two properties are directly related, the higher the initial resolution is the better the interpolation algorithm works. Another important aspect in the probability-data matrix is the considerable degree of uncertainty in the northern-direction hillslopes. This concentration of moderate errors in these directions may be attributed to the high vegetation cover in comparison to southern directions that are characterized by a scares vegetation or even naked soil cover. Again, the probability of depth values (figures 2.16b) was added to the original DEM, and the channel network was extracted by a constant threshold value from the two matrices (i.e. modified and original DEMs) (figure 2.17). The stream network of the modified structure reveals considerable restrained modifications in comparison to the original one. These changes are not restricted to one property rather they are diverse, e.g. some streams are disappeared and others are emerged, others are enlarged or decreased, and in some cases streams are displaced some meters to the right or to the left. For

example, the highlighted stream by an arrow in the northern hillslopes (figure 2.17) was completely removed, where later field visit confirms the presence of no channels in this location. Whereas, the upper part of the catchment reveal a confuse aspect of drainage network structure in both cases, where, in this case, DEM uncertainty is of trivial effect and the model used to define threshold area for stream delineation is the key domain.

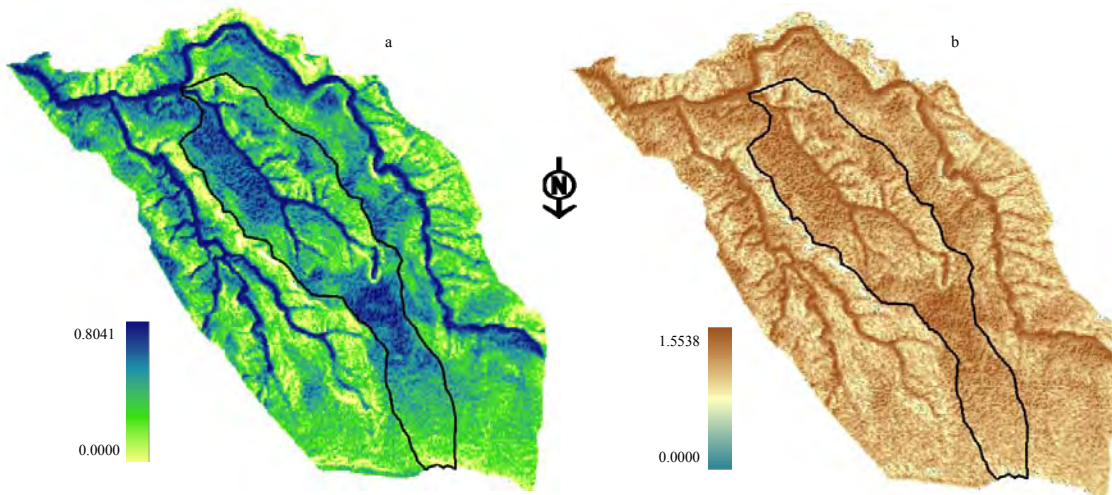


Figure 2.16 Stochastic Shape analysis in El Cautivo catchment; a) pure probability values, and b) probability values expressed in depth.

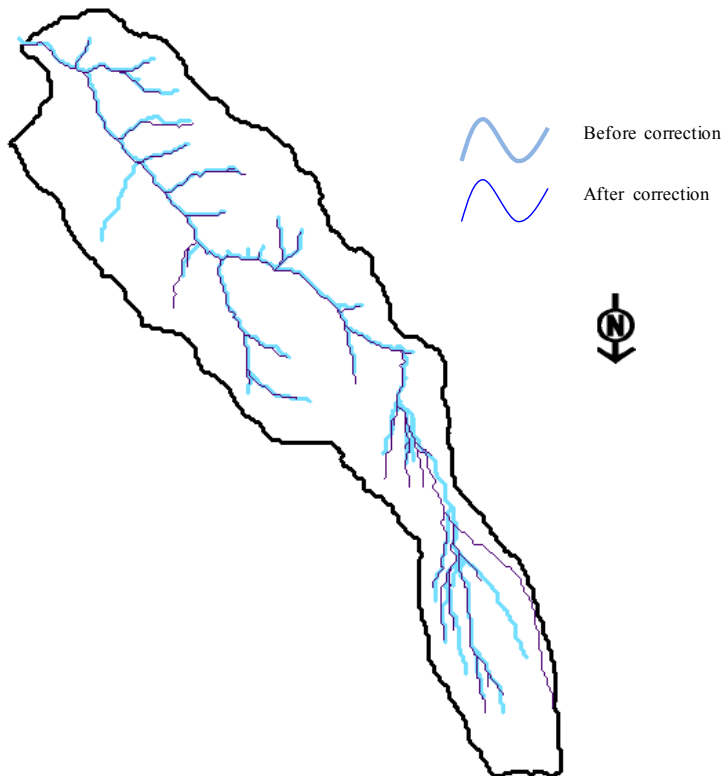


Figure 2.17 Drainage networks in El Cautivo catchment, extracted by a threshold value (A_s) of 20 cells, before and after applying the stochastic shape analysis (SSA) correction.

On the other hand, the Rambla Honda catchment reveals a more homogeneous aspect of the probability distribution of artificial depressions (figure 2.18a), but more slightly than the Cautivo basin

(i.e. 0.62 for the former and 0.80 for the latter). Again, the higher concentration are localized in the lower part of the catchment, but, in any cases, are not concentrated in the drainage network rather are extended to surrounding hillslopes. The upper part of the catchment maintains low values of uncertainties, but with no clear domain of complete uncertainty, such as the case of the Cautivo. This is widely clear for the general RMSE of the two areas (0.17 m for the Cautivo and 0.33 m for the Rambla Honda), highlighting the importance of the local factors, such as vegetation cover and relief contrast, in the final DEM quality and not only the initial data and the interpolation model effects. Again, the correction of the original DEM and the extraction of the channel network with a constant threshold (figure 2.19) highlighted smooth modifications between structures and less effect in comparison to Cautivo catchment. The slight modifications in the Rambla Honda DEM may be attributed to the smooth relief structure, where such slight modifications in the DEM matrix are little appreciated in the final drainage network.

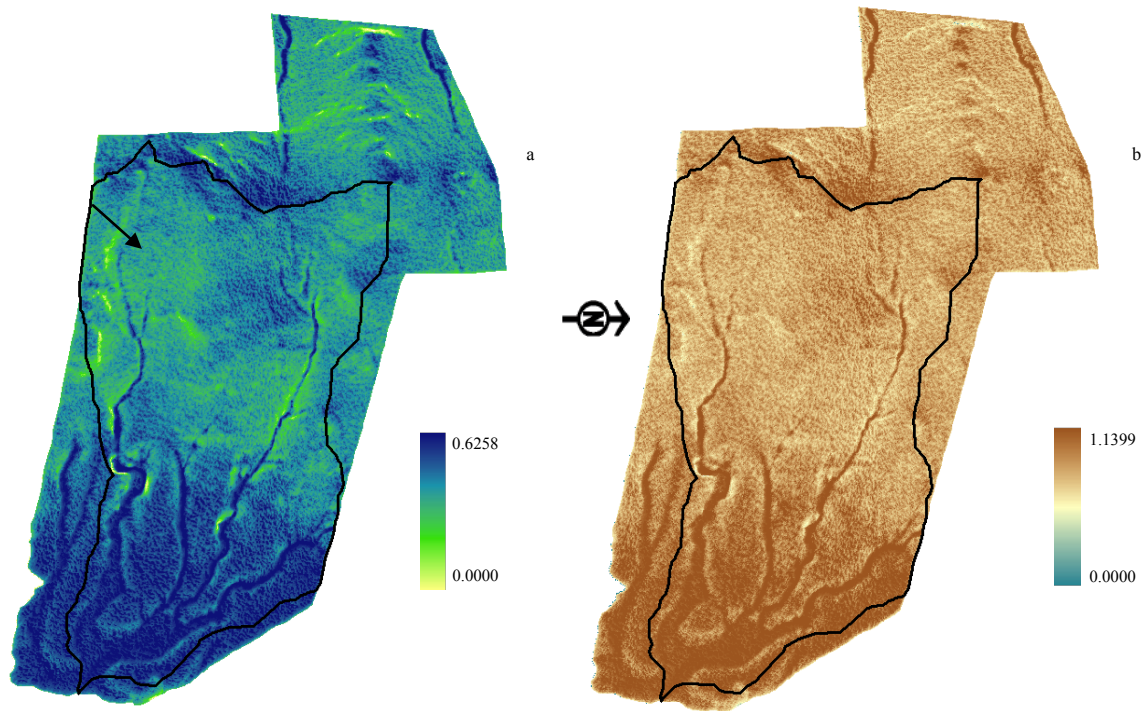


Figure 2.18 Stochastic shape analysis in La Rambla Honda catchment; a) pure probability values, and b) probability values expressed in depth.

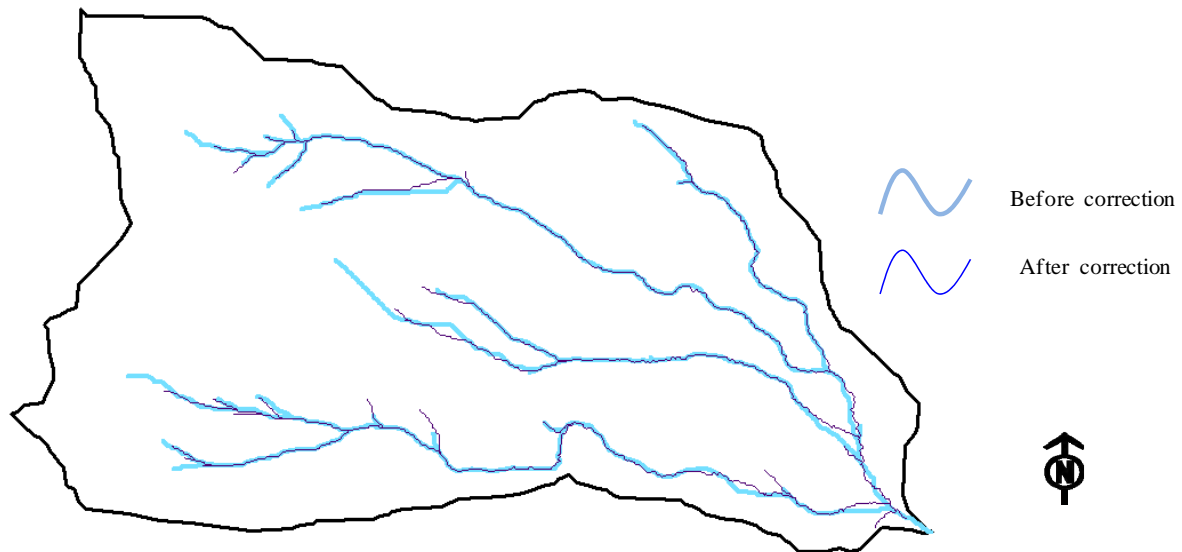


Figure 2.19 Drainage networks in La Rambla Honda catchment, extracted by a threshold value (A_s) of 50 cells, before and after applying the stochastic shape analysis (SSA) correction.

2.4.5. Conclusions:

DEMs serve as the base for several hydrologic and geomorphic studies and application. With fine enough resolutions, main landscape features, such as lateral streams and channels, are widely appreciated, either qualitatively (e.g. by scene) or quantitatively (e.g. models and algorithms). Obtaining an accurate spatial characterization of such features is relatively complicated and is widely related to accuracy and uncertainty of the DEM matrix. Error and uncertainty in DEMs structure is of considerable importance, since its effect modifies certain and considerable properties of the drainage networks extracted from these datasets. Both approaches of uncertainties (global and local) used in this study showed a considerable importance in DEM assessment and treatments as a priori step for hydrologic and topographic variables extraction.

In general, DEMs generalization or degradation is a common procedure between scientists to acquire lower resolutions. In relation to the mode of aggregation and the final resolution, such process may involve various degrees of uncertainties. The results showed that the interpolation procedures (i.e. Bilinear or Nearest Neighbour) provide a more constant and similar results with approximately the same RMSE values than direct generalization processes (i.e. thinning or aggregation). Moreover, the Thinning function confirmed a RMSE twice than the rest of the models highlighting higher uncertainties for the DEMs generalized by such approach.

The present study showed that resolutions above 240 m grid dimensions are useless for stream network representation. First, the ratio of average drop cell was too small indicating a clear inadequacy of the present grid dimension in relation to studied scale, which may be reflected in a lot of information lost, mainly that are related to stream properties. The 120-240 grid dimensions revealed a doubtful effect on landform extraction, because this range contains the border limits between

acceptable and improper average-drop-cell ratio. Higher resolutions (e.g. ≤ 120 m) revealed acceptable average-drop-cell ratios to be used as appropriate structures for stream channel extraction. These results were confirmed on catchment size extracted by different resolutions, where a considerable change has been detected on 240 m gridded-data. However, above that resolution catchment area is unpredictable confirming the sensitivity of the drainage basin delineation to DEMs uncertainty. Such findings highlighted the importance of resolution in scale studies, mainly when DEMs are the unique source of information for catchment limitation.

Finally, the SSA has introduced a good approximation to local uncertainty in the studied DEMs. The drainage network extracted from original and treated matrices underlines changeable modifications in relation to the structure homogeneity and the initial data used on the construction of these DEMs. While these modifications could be trivial or critical, final judgment to determine whether certainty in a DEM will affect results from specific analysis should be the responsibility of the DEM user.

Chapter 3

GEOMORPHOMETRIC QUANTIFICATION OF CHANNEL NETWORK STRUCTURE

3.1. Introduction

This chapter reviews and discusses some of the related topics that provide a basic context for terrain modelling (geomorphometry). A core subject in defining the locations of drainage basin and stream channel networks between earth-science disciplines. Moreover, we will define channel networks and drainage basins, explain their formations and evolution, and highlight the processes and relationships that act and control these features. In addition, measurement dimensions are explained and focused in relation to the feature type, dominant landscape processes, and available scale. Finally, scaling relationships and related power laws were approximated to be used as geomorphometric descriptors between different geomorphic properties.

The main objective of the current chapter is to review recent developments in geomorphometrical characteristics of drainage networks. More concretely, global and deeper insights on stream network properties that may provide concrete identification to each stream segment, in particular, and to the total river basin system, in general. In addition, this work provides a creative methodology on the pre-definition of a reduced and representative collection of the basic geomorphometric indices that may be used directly to identify and compare streams of different properties (e.g. dimension, structure, shape, etc.). The importance of such approach resides on the increasing need for a new methodology in defining stream heads or sources from DEMs, which are directly related to these attributes.

3.2. Back ground

3.2.1. Features, relations and processes in landscape

Landscape comprises the visible features of an area of land, which include a group of complex elements (such as physical elements or landforms, living elements, etc.) that inter- and intra-act to form the present natural world. Because of the various aspects in the landscape (components, processes, relations), landscape should be regarded as a multidisciplinary, better a transdisciplinary, science where different views and approaches are involved in a holistic manner (complex-system perspective). Herein, the physical elements of the landscape, widely known as landforms, comprise the basic structure on which relations and processes act in multi directional approach. Landform understanding, and hence verification, requires the definition of all disciplines that comprise the

landscape; this include geomorphology, hydrology or fluvial geomorphology and geometry or geomorphometry (i.e. tools of measurements between features and processes).

It is obvious that the final landscape structure is a matter of various (multi-) disciplines and not a particular approach. For instance, Richards (1982) referred to fluvial geomorphology as “*Fluvial geomorphology is fundamentally concerned with river channel form: documentation of channel change, construction of morphology-based sediment budgets and numerical modelling of flow and sediment transport all rely upon spatially distributed topographic information*”. Herein, nor we will go through all these disciplines neither we will define processes and models; instead the effect of the above disciplines on landscape dissection (stream and channel network) will be highlighted. Hence, the above disciplines we be treated in relation to drainage catchment formation. More concretely, Haschenburger and Souch (2004), based on historical literature, suggested six geomorphic landscape principles that describe key aspects of landscape structure and function, defined as follows: (1) The basic building block of a landscape is a landform; (2) Landscapes are organized assemblages of interconnected landforms; (3) Landscapes reflect interactions between driving forces and surface resistance; (4) Landscapes evolve under particular histories; (5) Landscapes respond to exogenic and endogenic perturbations and adjust to internal functioning; and, (6) Landscapes exhibit aspects of equilibrium, disequilibrium, and nonequilibrium behaviours. All these principles, on one way or another, have been mentioned and treated in the coming sections in relation to the importance of each discipline to the general objectives of the work.

3.2.2. Hydrology

Hydrology is the study of the movement of water throughout the physical environment. It embraces the occurrence, distribution, movement, and properties of the waters of the earth. In a mathematical sense an accounting may be made of the inputs, outputs and water storages of a region so that a history of water movement for the region can be estimated (Viessmann & Lewis, 1996). From the above definition, we will handle the output section, more concretely surface water hydrology. Herein, a group of concepts will be detached, mainly those considered to have a considerable utility for the present work. In the hydrologic cycle, runoff is the rainfall water transported from the land surface to water bodies, through channels and rivers. Runoff occur when rainfall and snowmelt moves across the land surface, some of which eventually reaches natural channel networks, the rest is lost by evaporation and infiltration processes. Runoff type is related to climatic factors (e.g. precipitation form and type) and physiographic factors (e.g. geometric properties of drainage basin). Surface runoff could be of “*Hortonian overland flow*” (i.e. occurred when rainfall intensity exceeds the infiltration capacity of the soil) or “*Saturated overland flow*” (describes the process of stream flow generation where rainfall over saturated areas near stream channels forms direct runoff). Surface runoff can be further subdivided into two distinct types: i) Overland flow (or sheet flow), which moves down slopes and is not confined to channels. Overland flow erodes

sediments from slopes and delivers them to stream valleys. ii) Stream flow, which is normally channelized (except during floods). One of the main consequences of runoff generation is sediment transportation (i.e. soil erosion). In general, streams erode their channel (and sometimes the surrounding floodplain), eventually carrying sediments downstream and out to the ocean by the force of gravity.

In general, since the core dataset that have been used throughout the work are DEMs, runoff type, amount, and routing flow (flow direction) will be defined directly of these datasets based on different methods and algorithms. Stream systems and channels are linear features and have a hierarchical organization based on gravity flow of water. Based on this concept, several algorithms and models have been proposed to define surface flow water, mainly amount and routine flow direction. The former is easy to calculate and depends on the resolution of the gridded-data used, since in digital data treatment there is no water loss (infiltration and evaporation = 0) and water flow freely between adjacent parts of the digital landscape. Whereas the latter is more complicated, this needs complex algorithms to define the surface topography on which water will flow. The routing of water over a surface of a landscape represents a fundamental geomorphological process that is intimately tied to its form. The subdivision of the continuous surface into discrete hydrological units provides an important step in the geomorphological treatment of gridded data (Wood, 1996a). Since the early introduction of digital data in hydrological modelling, several algorithms have been proposed to determine flow direction and related runoff (i.e. drainage accumulation). These models have enabled the construction of newly relationships between landscape disciplines, and the definition of vast number of geometrical indices. The literature on the derivation of hydrological variables is large (e.g. Moore et al., 1991; Tarboton1997), and will be treated with more details after DEMs definition and treatments in dataset description chapter.

3.2.3. Geomorphology

3.2.3.1. Introduction

In spite of the entire received appraisal, the work of William Morris Davis is still considered the father of the modern geomorphology. At the end of the last century Davis invented and designed the first method in geomorphological analysis, strictly speaking: his formulation don't leave doubts: *"All the varied forms of the lands are dependent on –or, as the mathematician says, are function of three variable quantities, which may be called structure, process and time"* (Davis, 1899). Moreover, Davis developed the evolution theory of landforms (i.e. the cycle of erosion), the parallel to Charles Darwin's *"Origin of Species"* (1859); a paradigm of the systems approach of geomorphology. Since then, geomorphology, as a science, has passed several evolutionary steps, two of which are of considerable importance: 1) the classic geomorphology, supported by the European school that tries to integrated all relieve associated aspects; and 2) the non-classic geomorphology, supported by the

American school that tries to analyze the geomorphological processes in a grouping form, proceeding its quantification, and defining geometrical parameters related to relief forms or dynamic relation of the process. The first consequence of non-classic line was the creation of the “quantitative geomorphology” or denominated as “geomorphometry”. The second consequence reached in form of high-evolutionary science related to vertices and fluvial geometry (Chang, 1988). The experience in the field of the geomorphological analysis has originated contrasting effects, till the moment; the catastrophe theory of dynamical systems and the fractal geometry (Mandelbrot, 1982).

Geomorphology as a science discipline could be defined as the study of the formation and structure of the earth’s surface features or the study of landforms and the nature of the materials underlying them (DeParry, 2004). Although the term is commonly restricted to those landforms that have developed at or above the sea level, geomorphology includes all aspects of the interface between the solid earth, the hydrosphere and the atmosphere (Chorley et al., 1984). In addition, geomorphology not only includes the Earth but also extend to other planets (e.g. Moon, Mars, etc.) giving geomorphology extraterrestrial aspect. Within these concepts, geomorphologic studies comprise two interrelated approaches: historical and functional. The former explains the existing landform assemblage as a mixture of effects resulting from the vicissitudes through which it has passed. The latter explains the existence of a landform in terms of the circumstances which surround it and allow it to be produced, sustained, or transformed such that the landform functions in a manner which reflects these circumstances (Chorley et al., 1984). It’s clear that most objects of geomorphic interest show evidence of both functional and historical influences, for so, usually, many geomorphic problems are open to widely differing approaches. Moreover, most functional explanation is directed towards prediction; whereas, historical explanation lies on retrodiction. However, both approaches require a description of the landform or landscape, either quantitatively or qualitatively. Two sub-disciplines of geomorphology are of capital and direct relation to the present work, fluvial geomorphology and geomorphometry, which will be detailed in the coming lines.

3.2.3.2. fluvial geomorphology

A landform can be considered as a part of a large system. This system is compound of both the landforms (morphologic systems) and the mass (sediments) and the energy flow through the landscape (cascading systems). A complete explanation of a landform must involve a description of the feature and an understanding of the processes involved in its formation, as well as its development through time (Chorley et al., 1984). A geomorphic system is a structure of interacting processes and landforms that function individually and jointly to form a landscape complex. The easiest landscape complex to visualize is that of a drainage basin with its interrelated summits (divides), hillslopes, drainage network and major alluvial channels. All mentioned aspects of landscape form part of the fluvial system, and the geomorphologic study related to the fluvial system are called “*fluvial*

geomorphology". Herein, stream channel networks definition (i.e. drainage network morphology) will form the core issue of our research and study (Schumm, 1977).

A fluvial system consists of the physical/abiotic (e.g. river networks, hillslopes, etc.) and biological/biotic (e.g. terrestrial vegetation, riparian habitats) elements, which interact across a range of nested scales in space and time (Molnar, 2006). From a geomorphological point of view, the physical template of the fluvial system is its main building block. It is a landscape unit consists of different morphological elements (e.g. hillslopes and channels), which are connected by fluvial processes driven by water and sediment transport through the system. DeParry (2004) defined fluvial geomorphology as the study of landforms (i.e. characteristics) and processes associated with rivers and streams, or a stream's definition based upon the climate, geology, soils (stream bank materials), vegetation, and topography of its watershed. These processes include rainfall/infiltration/runoff as they related to the formation, functioning and characteristics of the streams, and are crucial in properly managing a watershed's water resources. In the fluvial system, forms and processes are not only important to understand the relationships that control these aspects, but also are interrelated since both are action and reaction in the complex dynamic landscape. While Davis is considered as the father of modern geomorphology, Luna Leopold is, without doubt, the father of fluvial geomorphology. His early works in the mid of the past century (1950-1960) in the field of ephemeral streams geomorphology and hydraulic geometry forms the basic framework for understanding watershed/stream relationships. Yet, Rosgen and Silvey in (1996) culminate the advances in the fluvial geomorphology by publishing the groundbreaking book, "*Applied River Morphology*". In this line, it is important to highlight the essential information provided by Leopold, Rosgen and others in order to have a better conceptualization for fluvial geomorphology concepts and processes.

Understanding the dynamics of a fluvial system is only achieved when it is looked at in its entirety (Molnar, 2006). Any part of the system is influenced by upstream control (geology, hydrology, sediment source, etc.) and downstream control (e.g. base level change). From one hand, upstream controls are more apparent and easily understood. For instance, the channel shape and form at a given location are largely determined by the water and sediment load (and their variability) from upstream (Bull & Kirkby, 2002). However, also downstream controls may play an important role on longer time scales (Rosgen, 2001). For instance, in some rivers upstream knickpoint migration and adjustment of channel slope is a major concern for channel stability (Simon & Thomas, 2002).

3.2.3.3. Geomorphometry

One of the main consequences of the non-classic geomorphology, was the quantitative geomorphology or what called "geomorphometry". Chorley et al., (1957) defined geomorphometry as the science which treats the geometry of the landscape. In general, it is the science of quantitative land-surface analysis, which attempts to describe quantitatively the form of the land surface (Mark,

1975). It draws upon mathematical, statistical, and more recently computer science and image-processing techniques to quantify the shape of earth's topography at various spatial scales. The focus of geomorphometry is calculation of surface-form measures (land-surface parameters) and features (objects), which may be used to improve the mapping and modelling of landforms, soils, vegetation, land use, natural hazards, and other environmental information. The first attempts of the systematic measurement of topography from cartographic sources can be traced back to the mid-nineteenth century (Cayley, 1859). Significantly, the development of a science of surface measurement techniques has been accompanied and attains benefit from the development of surface storage and representation methods (Felicísimo, 1995). Although a substantial part of twentieth century geomorphology has been devoted to the measurement and quantification of topographic form, this has proved less successful than the characterization of geomorphological process (Pike, 2002).

Pike (2000) stated that macro-scale practice of surface-form quantification, which has been evolved independently from metrologic disciplines, is the equivalent designation to the geo-(morphometry), quantitative geomorphology, and terrain analysis. Lately, he annotated that “*terrain modelling*” is more appropriate (i.e. general and comprehensive) nomination (i.e. descriptor) for land surface quantification than geomorphometry, in which he defined terrain modelling as the practice of ground-surface quantification (Pike, 2002). According to internet-search results, the title of series incorporate terrain modelling is 15 times more frequent than geomorphometry. Other descriptors (such as surface modelling, surface topography, digital terrain modelling, morphometry, topographical analysis, etc.) are inapt, since it includes or excludes parts of the related essential characteristics. For example, digital terrain modelling would exclude pre- or non-computer work; terrain analysis has military and non quantitative connotations; surface modelling have specialized meaning in computer vision and image analysis; morphometry is a common practice in biology and palaeontology; and surface topography implies industrial micro- and nano-morphometry.

Evans (1972) made the distinction between two major types of geomorphometry: the first is “*general geomorphometry*”, the measurement and analysis of those characteristics of landforms which are applicable to any continuous rough surface; and, the second is “*specific geomorphometry*”, the measurements and analysis of specific types of landforms, e.g. stream channels or landform equations, which can be separated from adjacent parts of the land surface according to clear criteria of delimitation.

Mark (1975) established a general approach for land surface representation, in which he considered that all measures of land surface form can be considered in some way representative of the “roughness” of the surface. Accordingly, and in order to establish a rational classification of geomorphometric parameters, he focused upon two points: the amenability of the parameters to measurements based upon computer terrain storage systems, and the probable geomorphic significance of the measures. Thus, Mark considered that the most fundamental concepts of geomorphometry are

the basic horizontal and vertical scales of the topography. The horizontal variations are encompassed by the concepts of grain (i.e. the largest significant wavelength of a topographic surface) and texture (i.e. the shortest significant wavelength of a topographic surface). The vertical scale has been characterized by various measures of relief, mainly local relief, available relief, and drainage relief. Wood (1996a) criticized deeply this approach for the possible significant problems that could arise, mainly ambiguity in definitions and significant dimensional overlap between measurements. In order to avoid such problems, Evans (1980, 1984) introduced a more systematic parameterization procedure for vertical and horizontal variation based on the first and second derivatives of altitude (slope, aspect, profile convexity and plan convexity). The above approach is related to general geomorphometry, which is of trivial importance for the present work. Since the essential aim of this work is to delineate channel networks, specific geomorphology will be more detached and underlined in the coming paragraphs.

Terrain modelling (i.e. geomorphometry) and topographic surface description have been revolutionized by the advent of computer devices and related geographic-system packages (i.e. GIS), mainly by the adoption of DEMs (Pike, 1988; Moore et al., 1991). Terrain relief and pattern are measured to depict Earth's surface and to decipher structural processes. In addition, terrain data are gathered by geographers, geologists, and geomorphologists (landform specialists) to assess landscape features and processes. Thus, Pike (2002) affirmed that quantitative characterization of surface form, mainly from DEM data, is cross-disciplinary and can be applied at any scale. In which, he concluded that a unified approach to surface representation is necessary, and separation of industrial-surface metrology from its Earth-science counterpart, (digital) terrain modelling, is artificial. The computer implementation of geomorphometry provides geomorphologists with a digital representation of landforms that is now essential to process modelling (Dehn et al., 2001) at all levels of organization. Adediran et al., (2004) stated that computer morphometry contributes to various synoptic attempts at integrating land-surface form with remotely sensed spectral and other environmental data to facilitate broad-scale explanation physical processes. Reddy et al., (2004) demonstrated that remotely sensed data and GIS based approach is found to be more appropriate than conventional methods in evaluation and analysis of drainage morphometry and landforms and to understand their inter-relationships for planning and management at river basin level. Jordan et al., (2005) used digital terrain analysis based on structural geology and geomorphology to extract morphotectonic features from DEMs along known faults, in order to achieve an appropriate tectonic interpretation of his study area.

Several voices have claimed that drainage basin should represent the fundamental geomorphic unit (e.g. Horton, 1945; Strahler, 1956; Leopold et al., 1964), since it is related to the spatial basis for landform analysis (Chorley et al., 1984). Horton (1945) has described the morphometry of drainage basin based on physiographic approach, in which he explained how morphometric features are interrelated, for which he tried to rationalize these features (i.e. basically drainage density) on the basis

of hydrological processes. It is evident that, acceptance of the drainage basin as the basic geomorphic unit in many terrains is attributed to the following (Strahler, 1964): i) a limited, convenient, and usually clearly defined and unambiguous topographic unit, available in a nested hierarchy of scales on the basis of stream ordering; and, ii) a physical process-response system opened to cascade of inputs and outputs. If drainage basin and channel morphology are related to the geology, climate and hydrologic character of the basin, then it is necessary to describe these features quantitatively in order to investigate these relationships (Chorley et al., 1984). For these reasons, among others, numerous descriptors of basin morphology have been developed. In relation to specific geomorphometry, drainage basins and channel networks characteristics could be divided into two major lines: i) Geometrical (length properties): which involve the relationships among dimensional properties such as elevation, lengths, areas, and volumes; and, ii) Topological (Random properties): which relate numbers of objects in the drainage network.

Strahler (1964) appointed that all geometrical properties which describe form, or morphology, can be reduced to length dimensions (L), and hence dimensional analysis forms an operational basis for quantitative empirical science. Herein, Abrahams (1984a) appointed out that “*the actual progress of channel network development mainly the quantitative approach is the result of the concerned effort of A.N. Strahler and his Columbia University Association*”. He affirmed that their work was essentially empirical or inductive in character and led to the creation of an impressive battery of morphometric indices, to the recognition of numerous regularities and relationships among these indices, and to the beginning of a formal theory based on the concept of the drainage basin as an open system (Strahler, 1950), the application of dimensional analysis (Strahler, 1958), and the investigation of the process-form relationship (Melton, 1958a & b). On the other direction, Shreve (1966, 1967) introduced the concept of randomness in channel network (topological approach) definition, in which he tried to explain channel network properties based on its magnitude. This approach has an obvious advantage in overcoming the problem of distributive law (i.e. that is, there is no increase in order where confluence involve tributaries of unlike order). Paradoxically, this achievement of greater precision of topologic description has caused considerable problems in testing large networks for interregional and intraregional comparisons (Jarvis, 1972). Smart (1969a) cited that the definitions of network topology in relation to both Strahler and Shreve systems are often too extreme for practical purposes, the first method being too broad and the second too detailed. Whereas Strahler (1964) reviewed the advanced in geomorphometric quantification of channel networks, Abrahams (1984a) revised advances in both topological and geometrical approaches of channel network, and concluded that “both approaches are necessary to explain channel network forms and processes.

Herein, and in order to define the geometrical and topological properties of channel networks, it is important to define what a hydrological basin means, its components, ordering systems, and their general characteristics and classification types.

3.3. Characteristics of catchment and channel network

3.3.1. Definition of hydrological basins and drainage networks

In order to perceive the concept of a hydrological basin, it is important to clarify its concept and understand its forms and processes. What is a river basin? The whole picture of a river system may be divided in three loosely separated, but distinct regions (figure, 3.1). According to their main working purpose they are called the production zone, the transportation or transfer zone, and the delivery or deposition zone (Schumm, 1977). The production zone is what called the river basin or watershed. It originates most of the water and sediments that are then transported through the plains for their delivery to oceans and seas. Although each of these sections has its own peculiar properties, it is in the river basin where the greatest challenges and crucial phenomena are perceived, from the hydrological point of view (Rodríguez-Iturbe & Rinaldo, 1997).

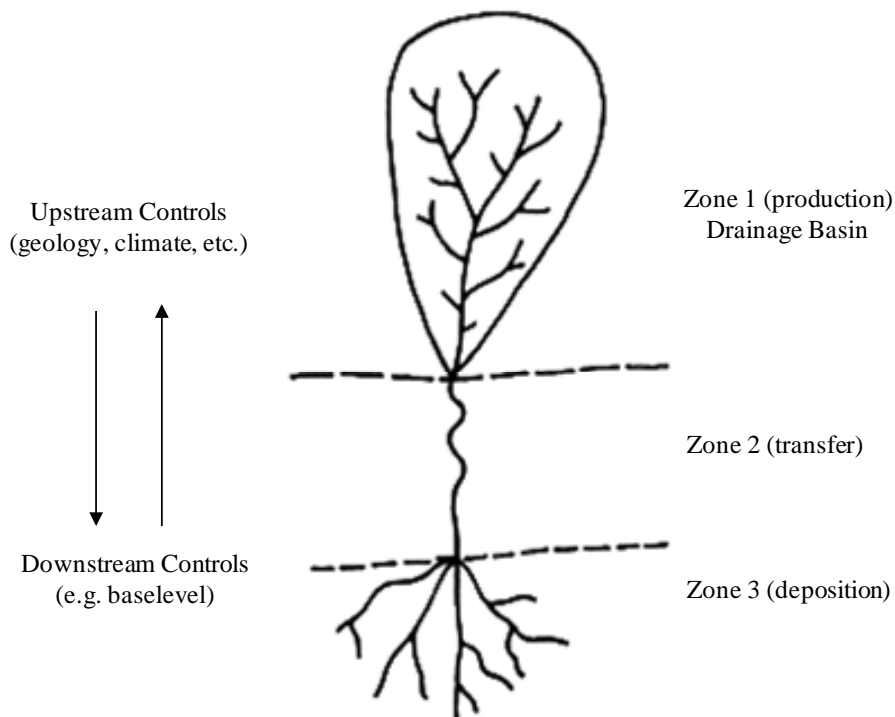


Figure 3.1 The idealized fluvial system (Schumm, 1977).

Accordingly, watershed can be defined and specified in several forms, general and particular (i.e. related to worker in the field of hydrology): the general form defined a watershed as an “*area of land that captures water in any form, such as rain, snow, or dew, and drains it to a common water body, i.e. stream, river, or lake*” (DeBarry, 2004). Whereas, the particular form defined a watershed as “*the area of land that drains water, sediment, and dissolved materials to a common outlet at some point along a stream channel*” (Dunne & Leopold, 1978). For this reason, watersheds are classified by size and complexity into other generalized terms such as drainage basins or sub-watersheds (DeBarry, 2004). Watersheds, catchments, and drainage basins are synonyms, which will be used

alternatively throughout the work. Natural drainage patterns vary significantly depending on topography, underlying geology, morphology, vegetation, soils, and climatic regime (e.g. Chorley et al., 1984; Tucker et al., 2001a). The ridges that separate the watersheds are referred to as divides or watershed boundaries. Limiting watershed boundaries (i.e. watershed assessment) is often defined to a particular point, often referred to as outlet. Watershed size or catchment drainage areas are determined to one or several outlets (figure 3.2). DeBarry (2004) affirmed that the general characteristics of watersheds are derived directly from the prevailing geology, soil, and landforms from which they originate. Thus, having a thorough understanding of these three major physical factors will enable a better understanding and analysis of dominant-features formation and evolution. Moreover, watershed analysis is important, not only for surface flow and runoff water, but also for subsurface and groundwater quantification (e.g. Beven, 1989). Infiltration type, definition of recharge areas, and accumulation flow area, in addition to dominant geology are in the middle of aquifer and groundwater management.

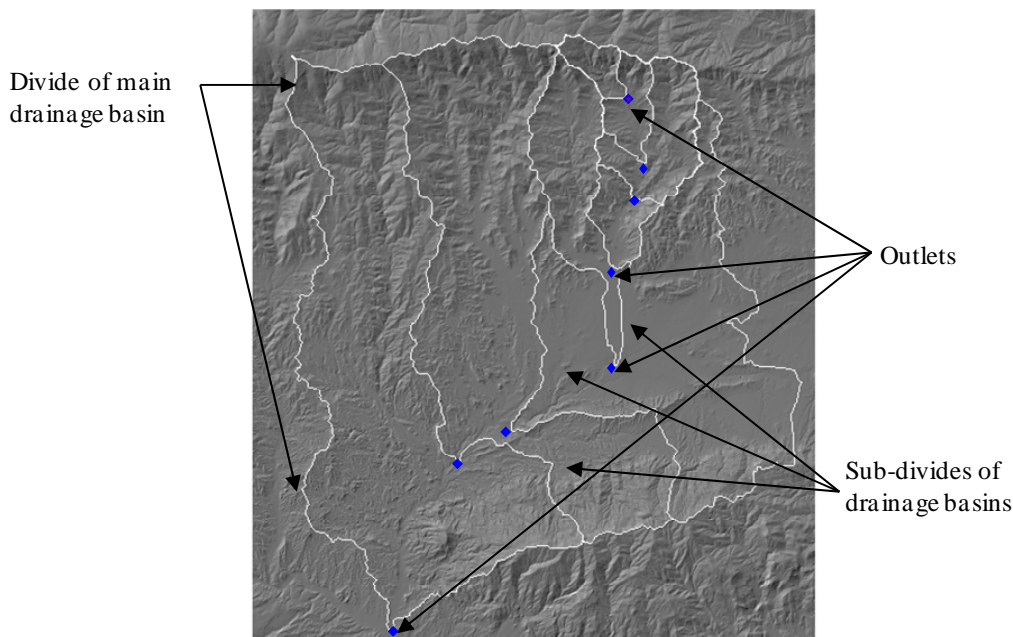


Figure 3.2 Watershed areas of different outlets and hence different sizes within Tabernas Basin.

The drainage catchment is compound of two interrelated systems: the drainage networks and the hillslopes. The hillslope control the production of rainfall water runoff, which, in turn, is transported through the channel network toward the basin outlet (Chorley et al., 1984). The runoff-contributing areas of the hillslope are both a cause and effect of the drainage network's growth and development (Rodríguez-Iturbe & Rinaldo, 1997). According to runoff-production mechanisms (saturated or overland flow), drainage networks can be classified, or even identified, according to these mechanisms. In studying river basin, it is essential to understand the circuit of reciprocal control between the systems of hillslopes and the drainage network of a basin. Since channel networks evolution and formation are related to the hillslope processes and the dominant materials (i.e. dominant lithology) that compound these sites. For so, scientists placed the reciprocal control

processes between parts of drainage basins at the heart of hydrology. Drainage networks identify organized transport system in space and also operate as dynamic space-filling systems in temporal landscape evolution (Willgoose et al., 1991). The drainage network defines a drainage basin, and thus provides both a framework for integrating spatial elements of the land surface, and also structure for dissecting sampling space into functional areas. These functional areas are units amenable to statistical treatment as sample replicates, and serve as spatial models for physical system analysis of fluvial landscape (Jarvis, 1977). Smart (1972a) appointed out that in a qualitative analysis of channel network, it is convenient to chose as a basic unit for study the set of all channels above a given point (outlet) in the network (i.e. all channel that contribute to the discharge at that point).

It is obvious that the drainage network system should be seen as the pattern that connects the different parts of the catchment to each other (i.e. connectivity of tributaries). The patterns formed by stream channels are thought to reflect regional tectonics (Cox, 1989) and local geologic structure (Abrahams & Flint, 1983), as well as prevailing erosional mechanisms (Dunne, 1980) and climate (Tucker & Slingerland, 1997). Herein, it is important to mention that channel network system as a whole, and together with hillslope system, relates the precipitation input into the basin to the surface runoff at the outlet. Such concept has formed the core discipline in hydrology and geomorphology in order to achieve better understanding and high efficiency in watershed management (e.g. Viessman & Lewis, 1997).

3.3.2. Drainage basins and channel networks classification

In order to understand the interaction between fields of physical science that govern watersheds and corresponding drainage networks, it is necessary to define their terms and functions. Streams may be classified generally, based upon physical characteristics, or formally, according to stream classification system (DeBarry, 2004). Watersheds are typically classified based on stream characteristics, and for that reason, classification names are often interchanged between streams and watersheds. In general, streams (or watersheds) are classified based upon their form and patterns or networks they create (figure 3.3). Drainage patterns are primarily controlled by the overall topography (e.g. slope) and underlying geologic structure (e.g. soil and rock properties) of the watershed. Based on their stream pattern system, channel networks are classified into the following:

- i) Dendritic pattern: these patterns are related to streams showing a dendritic pattern from a treelike, or dendritic, arrangement of small streams or tributaries in the headwaters (branches) that flow in a variety of directions and continually join to eventually form the “major” stream of the channel network. It is the type of stream one expects to find in a region that has adequate rainfall and no unusual geologic features.
- ii) Parallel pattern: the parallel patterns are those in which tributary streams flow in the same general direction and usually join at small angles, is essentially an elongated variant of the dendritic pattern.

Parallel drainage occurs in areas with a regional slope, prevailing wind, or some other factor that causes streams to flow unusually far in one direction before merging with another.

iii) Trellis pattern: a squared off drainage pattern in which streams often flow directly toward each other from opposite directions and then make right angle turns when they meet. Trellis patterns are common in places where layered sedimentary rocks are tilted up from the horizontal.

iv) Radial pattern: a circular arrangement of streams that flow outward in all directions away from a central high area. Radial drainage patterns are common in the vicinity of volcanic cones, salt domes, granite intrusions, and other localized uplifts.

v) Centripetal pattern: a circular arrangement of streams, where water flows inward from all directions toward the centre of the area. Centripetal drainage is likely in karst topography and in deserts where intermittent streams flow toward a temporary salt lake or basin.

vi) Deranged pattern: in areas recently disturbed by events such as volcanic deposition or glacial activity, the first stream pattern to emerge are called deranged stream patterns. These form by the water following the path of least resistance. As sediments get transported, the stream adjusts its course accordingly over time.

vii) Rectangular pattern: in a rectangular or grid-like drainage pattern, streams form angularly, near 90-degree turns, due primarily to following the fissure, tectonic faults, or joints in the bed rock.

viii) Annular pattern: can be considered to represent a bent trellis; they are common on deeply eroded domes such as eroded volcanoes or uplifted sedimentary domes.

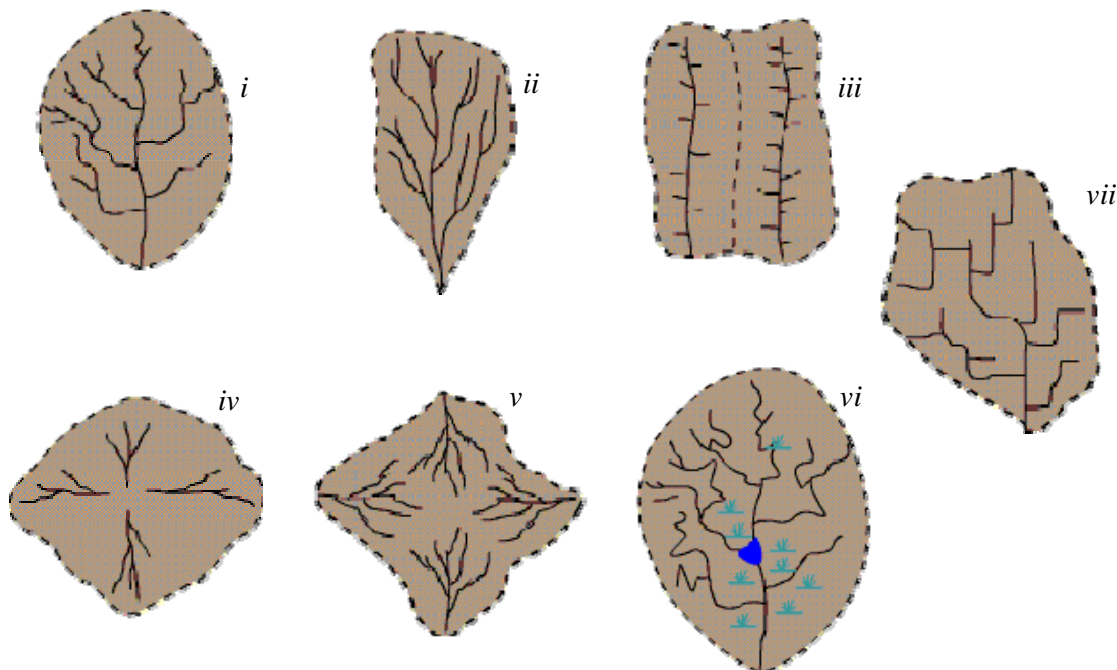


Figure 3.3 Watershed classification based on dominates channel patterns. i) dendritic pattern; ii) Parallel pattern; iii) Trellis pattern; iv) Radial pattern; v) Centripetal pattern; vi) Deranged pattern; and vii) Rectangular pattern.

In order to understand pattern factor analysis of channel networks, two important concepts related to channel characteristics should be clarified, that is sinuosity of channel network and stream longitudinal profile.

Sinuosity is a commonly used parameter to describe the degree of meander activity in a stream, which is the amount of stream curvature. Sinuosity is defined as the ratio of the distance along the channel (channel length) to the distance along the valley (valley length). In pattern factor definition, sinuosity is the most highlighted and widely used for pattern definition of streams and channels (figure 3.4). This factor is represented quantitatively by the sinuosity ratio computed by dividing the centreline of the channel reach or segment by the length of the valley centreline. In figure 3.1 the sinuosity ratio is the distance between two points on the stream measured along the channel divided by the straight line distance between the two points. If the sinuosity ratio is 1.5 or greater the channel is considered to be a meandering one.

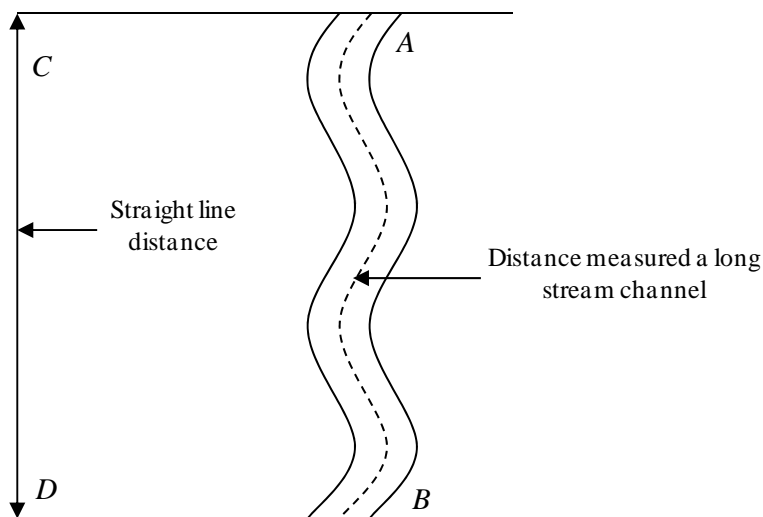


Figure 3.4 Illustration of sinuosity concept. Sinuosity ratio = distance measured along stream (A, B) / straight line distance (C,D).

Whereas, the longitudinal profile is a depiction of the down slope gradient of a stream with elevation (figure 3.5). The longitudinal profile of a stream can reveal whether a stream has achieved a graded state, over only a part or the entire stream. The curved profile of a graded stream exhibits a steeper slope upstream giving way to a gentle slope in the down valley direction. Initially stream profiles may be irregular with the stream gradient interrupted by “knickpoints” where waterfalls are found. Knickpoints form where the stream flows over an exposure of resistant bedrock or from tectonic uplift. The knickpoints slowly wear down and migrate upstream as water spills over them. Through time the profile is smoothed to a gentle concave shape. Profile factors or longitudinal profiles are used mainly to examine disturbance locations in stream networks. Often, therefore, it is relevant to construct a stream profile, or the longitudinal plot of elevation change versus horizontal distance (Leopold & Maddock, 1953; Hack, 1957).

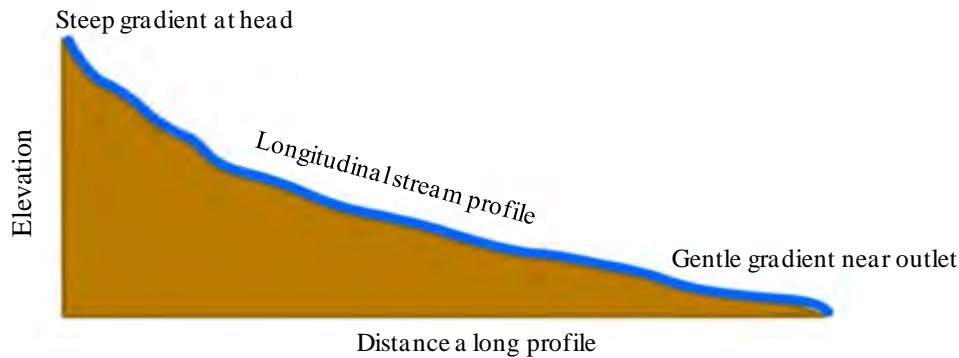


Figure 3.5 A schematic illustration of a longitudinal stream profile.

To the contrary of watershed classification, stream classification is not limited to the patterns of channel networks that they produce; it extends to several categories and forms. Scientists classified streams to two major categories: generalized stream classifications and formal stream classifications.

1. Generalized stream classifications are mainly related to the interaction between local conditions and physical features that comprise them (i.e. climate, hydrology, geology, soils, relief and landforms, etc.). It can be described as, under natural conditions, the feedback and readjustment processes (i.e. natural variation in channel geometry and shape) of channels and streams to reach stability conditions (DeBarry, 2004). Streams balance erosion, sediment transport, and sedimentation to reach their equilibrium state (Kelley et al., 1988; Myers et al., 2007). If one or more of these factors is altered, the stream will adjust to accommodate this change. Under this classification system, streams or channels can be classified to the following:

a) Alluvial versus nonalluvial channels: alluvial channels are those that flow on deposited alluvial materials, and most continually shift in horizontal and vertical location. Whereas, non-alluvial channels are those running through nondeposited materials such as bedrock, and are more constant in their flow path.

b) Channel morphology: according to its morphology channels can be classified as straight, meandering, braided, and anabranching. Predominantly single-thread streams are described as either straight, sinuous (gently meandering), or meandering by their sinuosity ratio.

i- Straight segments in alluvial streams are rare, but common to bedrock-controlled channels and steep mountain slopes, such as those in a parallel drainage.

ii- Meanders are common where terrain is flat enough to allow a river to move sideways, undercutting its bank on the inside of the curve.

iii- Braided pattern are a rope-like pattern of twisting channels that separate and then join again all along the stream. Stream braiding is common in semi-arid regions, where floods bring more sediment into the channel than the normal flow of the stream is capable of carrying. A maze of sandbars and low islands may form during periods of low water and then be destroyed when floodwaters carry the

material farther downstream (Zwolinski, 2003). Braided channels typically have high bedload, variable discharge, and poorly vegetated, easily eroded banks. A meandering stream can become locally braided in reaction to a sudden influx of sediment from a bank or tributary.

iv- Anabranching or multichannelled are streams that appear superficially similar to braided streams except the bars or islands are not formed by contemporaneous deposition but by erosion. Anabranching streams have more than one channel separated by stable vegetated islands that are rarely covered during floods.

c) Constancy of flow: It is related to the time and amount of flow carried by the streams and include the following: perennial, intermittent, and ephemeral. Perennial stream carries some flow at all times (i.e. flows continuously). Intermittent streams appear to dry up when the flow has the potential of being totally absorbed by the bed and underlying materials. Ephemeral streams flow only or during or shortly after a rainfall event and are often referred as channels (Leopold & Miller, 1956). Accordingly, changes in climate conditions may leads to a dramatic shift from one type to another, e.g. in wet years intermittent streams may flow continuously.

d) Contributing to or from the ground table: include two categories Influent versus effluent. Effluent streams are those that are recharged by base flow; they are also referred to as “gaining streams”. While, influent streams are those that recharged the aquifer, also referred to as “losing streams”.

e) Genetic classification: this type of classification includes consequent, subsequent, resquent, insequent, and obsequent. Based upon their formation or origin streams are classified to five generic classes. “*Consequent*” streams are those whose course is a direct consequence of the original slope of the surface upon which it developed, i.e., streams that follow slope of the original land. “*Subsequent*” streams are those whose course has been determined by selective headward erosion along weak strata. These streams have generally developed after the original stream. “*Resequent*” streams are streams whose course follows the original relief, but at a lower level than the original slope (e.g., flows down a course determined by the underlying strata in the same direction). “*Obsequent*” streams are streams flowing in the opposite direction of the consequent drainage. “*Insequent*” streams have an almost random drainage often forming dendritic patterns, are typically tributaries that have developed by headward erosion on a horizontally stratified belt or on homogeneous rocks.

f) Channel composition: Alluvial channels can be classified by the type of load composing their channel. I) Suspended-load channel: <3% of particle load is bedload. II) Mixed-load channel: 3-11% is bedload. III) Bed-load channel: >11% is bedload.

g) Depositional or erosional regime: channels can be classified to aggradational (depositional) or degradational (erosional) in relation to available energy for initiate erosion process. If the total stream

energy is greater than that required to transport the sediment provided it, then the stream will erode. If the energy is less than that required, the stream will aggrade.

h) Equilibrium conditions: herein, streams can be divided into graded and non-graded streams. Graded streams, also known as steady state or balances, are channels which have regulated its various parameters (depth, width, slope, velocity, etc.) to obtain the most efficient conditions for flow and sediment transport. A graded stream is capable of maintaining a steady-state condition. The general characteristics of such streams are: i) slope of the longitudinal profile is concave upward, increasing exponentially upstream; ii) no falls or basins exist within the channel profile; iii) no net erosion or deposition occurs along its channel; and iv) The stream is capable of handling all sediment introduced to it from its tributaries. Non-graded streams are channels of high potential energy that is, within the system, not evenly distributed along the profile; contains falls and basins.

2. Formal stream classification: in this case stream classification arises out of a particular disciplines needed to standardized analytical procedures (DeBarry, 2004). Every discipline looks at stream classifications in different ways, each to meet the specific purpose at hand. The major groups of stream classifications (i.e. ordering) are based on stream order (e.g. Horton, 1945; Strahler, 1957) or stream magnitude (Shreve, 1966, 1967) and fluvial geomorphology (e.g. Rosgen, 1994). Since the ordering system is widely used throughout the current study in particular y in geomorphometrical description of channel network in general, it's worthy to highlight the major concepts and structures of this approach. Herein, we consider Rosgen's classification is highly generalized, and hence, that extends beyond the aims of our work. So, we are going to detach the ordering streams based on order and magnitude, and dropped out the Rosgen's method.

3.3.2.1 Ordering system

Ordering systems are used to group or characterize the parts that constitute the drainage network. Horton (1945) proposed the first approach for channel ordering based on order concept. Later on, Strahler (1952a) revised Horton's scheme and proposed some modification to avoid ambiguities, difficulties and restrictions related to subjective decisions (Smart, 1972a). Nowadays, the so-called Strahler system or Strahler-Horton ordering system is the wide common used in hydrogeomorphology. Before describing the Strahler-ordering system, it's important to verify some related terminologies that will outline the basic notion for all coming concepts. The terminology used here is wide spread in geomorphic literature, which used firstly by Shreve (1966, 1967). Herein, "*Sources*" are the points farthest upstream in a channel network, and the outlet is the point farthest downstream. The point at which tow channels are combine to form one is called a "*junction or node*" (i.e. it is assumed that for an idealized channel networks multiple junctions do not occur; apparent exceptions must be resolved by more detailed mapping or by an arbitrary decision). "*Links*" are the channel segments between a source and the first junction downstream, between two successive junctions, or between the outlet and

the first junction upstream. Links may be classified as “*exterior*” or “*interior*” depending on whether they have a source or a junction at the upstream end. Each link has certain properties: “*length*”, the distance along the stream; “*geometric length*”, the distance between end points; “*height*” or “*drop*”, the elevation difference between upstream and downstream junctions; “*average slope*”, height divided by length; “*contributing area*”, the total area draining through the link measured at the downstream end; and “*local or directly contributing area*”, the area draining directly into a link and not through any other link. A channel with n sources has $2n-1$ links, from which n exterior links (l_e), $n-1$ interior links (l_i), and $n-1$ junctions. The magnitude (μ) of a link is the number of sources upstream; thus an exterior link has magnitude unity and an interior link has a magnitude that is the sum of the magnitudes of the two links joining at its upstream end. The magnitude of the channel network in the total number of sources in the network or, what is equivalent, the magnitude of the outlet link. The “*link distance*” of a link is the number of links between the upstream node of the link and the outlet of the network, following the direct downstream flow route (Jarvis, 1972). The “*diameter*” of the network is the maximum link distance in the network (Werner & Smart, 1973).

Accordingly, Horton-Strahler ordering system procedure analyses networks could be described as follows:

- i. Channels that originate at a source, and have no tributaries are defined to be first-order streams;
- ii. When two streams of order ω join, a stream of order $\omega + 1$ is created;
- iii. When two streams of different order join, the channel segment immediately downstream has the higher order of the two combining streams (figure 3.6a)

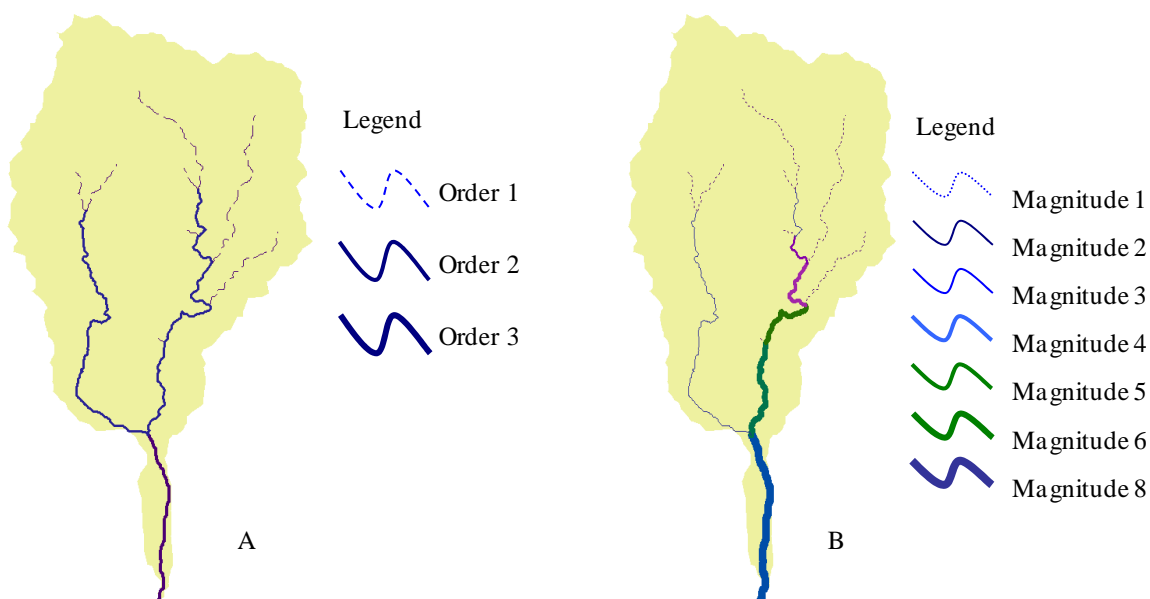


Figure 3.6 Two ordering systems of stream channel networks. A) Horton-Strahler ordering system. B) Shreve ordering system.

Rodriguez-Iturbe and Rinaldo (1997) appointed out that the resulted whole network embodies a deep sense of regularity, not the trivial regularity of size, but the much deeper regularity of formal relations between the parts. This deeper regularity was first observed by Horton (1945) in the planner projection of the drainage network. Completely contrary to the regularity approach, Shreve (1966, 1967) proposed the random topology model that based upon the concept that networks of given magnitude, under the absence of geologic control, are comparable in topological complexity, that is chance is the only criteria operating on the organization of the drainage network. Accordingly, Shreve proposed the link magnitude system for ordering channel networks. In this system, channel networks are ordered based on its magnitude or the magnitude of the outlet stream link (figure 3.6b).

3.3.3. Geometry of stream networks

In geomorphology, quantification of channel network geometry aims to study system complexity and physical-evolution processes. The relationships between physical processes and the geometry of natural structures basically requires the testing of elementary organization models, such as random and nonrandom organization and the range of scale for which distinct organizations are valid (Crave & Davy, 1997). Since the early work of Horton (1945), many experimental measures have shown that channel geometries follow empirical lows.

Horton (1945), with the use of his ordering procedure, was able to state his famous laws of drainage composition, widely named “*Horton Laws*”. Qualitatively, the essence of these laws is that, for a given channel network, the number of streams of successive orders and the mean lengths of streams of successive orders both can be approximately represented by simple geometric progressions. Quantitatively, law of stream number or “*bifurcation ratio*” is expressed as

$$N_{\omega-1}/N_{\omega} \approx R_B \quad \omega = 2, 3, \dots, \Omega \quad 3.1$$

where N_{ω} is the number of streams of order ω , and Ω is the total network order

Horton law of stream length or “*length ratio*” is expressed as

$$\bar{L}_{\omega}/\bar{L}_{\omega-1} \approx R_L \quad \omega = 2, 3, \dots, \Omega \quad 3.2$$

where \bar{L}_{ω} is the arithmetic average of the length of streams of order ω

The two laws are often represented graphically as Horton diagrams (Smart, 1972a), in which $\ln N_{\omega}$ and $\ln \bar{L}_{\omega}$ are plotted against ω , and the values of R_B and R_L is obtained from the slope of the straight line fit to such plots; the procedure is called the Horton analysis. Smart (1972a) a noted that Eq. 3.1 is a statement about the topologic structure of the networks and equation 3.2 is a statement about the geometric structure.

Similarly, Horton (1945) also proposed a slope law of stream network “*slope ratio*”, which is expressed as

$$\bar{S}_{\omega-1}/\bar{S}_{\omega} \approx R_S \quad \omega = 2, 3, \dots, \Omega \quad 3.3$$

where \bar{S}_{ω} is the arithmetic average slope of streams of order ω

Schumm (1956) introduced a Horton-type law for the drainage area or “*area ratio*” expressed as

$$\bar{A}_{\omega}/\bar{A}_{\omega-1} \approx R_{Aw} \quad \omega = 2, 3, \dots, \Omega \quad 3.4$$

where \bar{A}_{ω} is the total area of basin of order ω

Observations on natural networks indicate that value of R_B , R_L , R_S and R_{Aw} are usually falls in the range between 3-5, 1.5-3.5, 1.5-3.5, and 3-6, respectively. These values are more related to homogeneous rocks, mainly the R_B , but could reach 10 where pronounced structural control encourages the development of elongated narrow drainage basin (Chorley et al., 1984).

The importance of the above mentioned relationships that it have permitted the study of network components (Horton, 1945), which have lead to establish relations between stream order and the frequency or number of streams of each order and the lengths, gradients and drainage areas of streams of each order (Chorley et al., 1984). Moreover, it has been demonstrated that stream discharge increases systematically (Leopold & Miller, 1956) with order. Such findings indicate that the drainage network has developed in response to the erosive forces acting on the erodible materials that comprise the drainage basin (Calver, 1978). The result is a drainage pattern with characteristics that can be related to the erodibility of the material comprising the drainage basin as well as the climatic and hydrologic controls (Chorley et al., 1984). Although, some voices (Kirchner, 1993) appointed out to the statistical inevitability of Horton’s laws, and concluded that regular geometric properties of Horton compel no particular conclusion about the origin or structure of stream networks.

Several geomorphometrical basin measurements have been used throughout the literature of geomorphology, each of which describes the drainage catchment and channel network properties according to intrinsic characteristics, related mainly to composition and formation of the channel network. From one hand, various scientists (e.g. Strahler, 1958; Abrahams, 1984a) tried to reorganize and order these measurements in relation to planimetric and randomness properties of stream network formation. On the other hand, others (e.g. Smart, 1972a & b; Werner & Smart, 1973) used statistical concepts, such as geometric similarities in order to derive, approve and organize channel network properties. It is important mention that all geomorphometrical properties are interrelated in more or less manner, since the majority, directly or indirectly, is related to the Horton-Strahler and Shreve works.

Throughout the coming paragraph, we shall try to explain these procedures and highlight the most important in relation to the present work. Although reiteration is evident between procedures, we believe it is the most convenient to mention the procedures in separated context. Subsequently, the rest of properties, which are not mentioned in the above procedures and have been used in the analysis test, will be fulfilled separately in agreement with its importance in the analysis of the channel network.

A- Strahler's procedure:

In quantitative geomorphology, the dimensional analysis forms an operational basis in defining geometric, kinematic, and dynamic properties of fluvial landforms (Strahler, 1958). Within geomorphic parameters, correlations and regressions, and hence statistical analysis, between sets of observed dimensional data must be estimated, in order to define empirical laws of behaviour of natural phenomena. Strahler (1958) appointed out that all geometrical properties that describe form, or morphology, can be reduced to length dimensions, designated by the symbol (L). Accordingly, he ordered the geometric properties of a drainage catchment and its channel network according to the dimensions they produce. From which, three main categories were identified (table 3.1):

- i. Properties measured or counted solely from channel network and basin outline reduced to horizontal plane.
- ii. Properties required areal measures (planimetric): Areal measures and volumes have the dimensions of length squared L^2 and length cubed L^3 , respectively.
- iii. Properties involving elevation references.

Dimensionless parameters include stream-order number, stream azimuth, ground-slope angle, and channel gradient. Combinations of dimensional elements of the same unit produce dimensionless numbers, such as stream-length ratio, basin circulatory ratio, ruggedness number, and hypsometric integral, which provide descriptive indices of the terrain, irrespective of scale.

B- Chorley procedure:

Chorley et al., (1984) divided the geomorphological properties in relation to the morphology of the drainage network catchment; that is length, area, slope and relief character of the studied property. In this classification they highlighted the followings:

1. Basin length measurements: which include parts of the properties measured to horizontal plane of Strahler, such as L_w , L_t , L_a , L_g and P . In addition, they added followings:

1. Properties measured reduced to horizontal plane:				
Property	Symbol	Reference	Unit	Dimensions
Stream order	ω	Horton, 1945; Strahler, 1956	Enumerative	0
Order of the drainage network*	Ω	Horton, 1945; Strahler, 1956	Enumerative	0
Number of streams or basins of order ω	N_{ω}	Horton, 1945; Strahler, 1956	Enumerative	0
Entrance angle	ξ	Horton, 1945; Strahler, 1954; Schumm, 1956	Degree	0
Stream azimuth	ζ	Melton 1957; Strahler, 1954	Degree	0
Stream length (total channel length)	L_t	Horton, 1945	Meters	L
length of stream segment of order ω	L_{ω}	Horton, 1945	Meters	L
Mean stream length (mean length of segment of order ω)	\bar{L}_{ω}	Horton, 1945; Strahler, 1952a, 1954, 1957; Miller, 1953	Meters	L
longest stream in the channel network*	L_a	Hack, 1957	Meters	L
Total length of stream of order ω	$\sum L_{\omega}$	Horton 1945; Strahler, 1957	Meters	L
length of overland flow, slope length	L_g	Horton, 1945	Meters	L
Ratio of stream length ratio to bifurcation ratio	R_{Lb}	Horton, 1945		0
Basin perimeter	P	Smith, 1950	Meters	L
Basin length	L_b	Schumm, 1956	Meters	L
2. Properties required areal measures (planimetric):				
Total area of basin	A	Horton, 1932, 1945	m^2	L^2
Area of basin of order ω	A_{ω}	Horton, 1945	m^2	L^2
Inter basin area	A_i	Schumm, 1956	m^2	L^2
Drainage density*	Dd	Horton, 1945	m per m^2	L^{-1}
Constant of channel maintenance	C	Schumm, 1956; Strahler, 1957	m^2 per m	L

Stream frequency*	F_S	Horton, 1945	Number per m ²	L^{-2}
Texture ratio (drainage texture)	T	Smith, 1950	Number per m	L^{-1}
Basin circularity index	R_c	Miller, 1953; Strahler, 1964		0
Basin elongation ratio	R_e	Schumm, 1956		0
3. Properties involving elevation references:				
Total stream channel slope	θ_c	Horton, 1945; Strahler, 1952a; Schumm, 1956	Degrees or m/m or %	0
Stream segment slope of order ω	θ_ω	Horton, 1945	Degrees or m/m or %	0
Relief	H	Strahler, 1952b; Schumm, 1956; Melton, 1957		0
Relief ratio	R_H	Schumm, 1956; Melton, 1957		0
Relative relief	R_r	Melton, 1957		0
Available relief	H_a	Johnson, 1933		0
Drainage relief	H_d	Johnson, 1933		0
Relative basin area (in hypsometry)	x	Strahler, 1952b		0
Hypsometry integral	\int	Strahler, 1952b		0
Volume of landmass	V	Strahler, 195b	m ³	L^3
Curvature of slope profile	K	Speitht, 1980; Evans, 1980	Degrees per m	L^{-1}

Table 3.1 channel network properties adapted from Strahler (1958). (*) Indicates to properties that have been used as geomorphometric indices in the model approval.

i) X_c defined as the belt of no sheet erosion. The width from the divide of the convex upper slope to the point where there is evidence of erosion by surface flow (e.g. rill or stream channel head).

ii) L_g the length of overland flow. This is the distance from a point on a divide orthogonally (i.e. down the direction of steepest land slope) to the adjacent stream channel. The mean value of the length of overland flow \bar{L}_g gives a measure of regional stream spacing and is approximately equal to the reciprocal of twice of the drainage density.

iii) L_B defined as the overall maximum basin length measured from the outlet.

2. Areal variables: almost approximate to Strahler's planimetric measures, which include the following main properties: A , A_w , Dd , F_S , R_S and R_e .

3. Gradient measures: contain three measures defined as follows:

- θ_ω the average slope of segment link of order ω
- S_g the maximum slope of the ground surface at a given point
- θ_{\max} the maximum angle of a given valley-side slope profile

4. Relief properties: which include H , R_H , and \int , in addition to the ruggedness number (HD)

Chorley et al., (1984) appointed that H , Dd , and X_c which, in the common absence of pronounced basal slope concavities, together define the major diagnostic features of the geometry of fluvial eroded terrains.

It is obvious that, the above procedures excluded the topologic properties of the channel networks, which is considered as an indispensable factor to explain channel network properties and evolution in natural landscapes. So, we believe that any procedure that does not include the randomness properties is regarded as a shaky process.

In the same direction and in addition to the above planimetric procedures, James and krumbein (1969) proposed a classification of links that emphasizes the arrangements of main channel and tributaries. They proposed to classify links according to its orientation (measured either in terms of entrance angles or by absolute azimuth) to sis or tans streams, which seems to be a more sensitive expression for the effect of faults, joints, banding, etc. on the structure of stream networks (Abrahams, 1977, 1984b). Chorley et al., (1984) recognized that the orientation of channel link is not wholly controlled by structural trends, but is also inversely related to local relief and tends to increase as the order of the receiving stream segment increases. For that reason, James and krumbein's procedure have received little attention, and all the efforts in that direction were oriented to interpret geologic structure and related effect on channel network patterns.

C- Abraham's procedure:

Abrahams (1984a) studied factors that control planimetric properties of channel networks, in which he concluded that morphology of most channel networks is largely inherited from the past or strongly influenced by inherited forms. Accordingly, he described channel network properties according to the following characteristics:

1. topological properties:

With the introduction of random topology model concept by Shreve (1966), channel network properties underwent a dramatic change. Rodríguez-Iturbe and Rinaldo (1997) appointed that two basis postulates constitute the foundation of this model:

- A. In the absence of environmental controls, a natural population of channel network will be topologically random. Shreve equated the notion of “randomly merging stream channels” with a topologically random population within which all topological distinct channel networks (*TDCN*) with a given number of sources are equally likely.
- B. For drainage basins developed under comparable environmental conditions, the exterior and interior link lengths and their associated areas are independent random variables with separate statistical distributions that are independent of location within the basin (Smart, 1968, 1974, 1978; Shreve, 1967, 1969, 1975).

Starting with these two postulates, many observed features of drainage basin composition relating to topology and channel lengths can be adequately reproduced. Shreve (1966) demonstrated that in a topologically random population of networks in which each network has N_1 first order streams, the number of *TDCN* $W(N_1)$ is given by Cayley's (1859) expression

$$W(N_1) = \frac{1}{2N_1 - 1} \binom{2N_1 - 1}{N_1} \quad 3.5$$

And the number of *TDCN* of order Ω having $N_1, N_2, \dots, N_{\Omega-1}, 1$ streams of order 1, 2, ..., $\Omega-1, \Omega$, respectively, is equal to

$$W(N_1, N_2, \dots, N_{\Omega-1}, 1) = \prod_{\omega=1}^{\Omega-1} 2^{T_\omega} \binom{N_{\omega-2}}{T_\omega} \quad 3.6$$

where N is the number of sources in the channel network, and $T_\omega = N_\omega - 2N_{\omega+1}$.

The general term of the product in Eq. (3.6) is the number of topologically distinct ways in which the N_ω streams of order ω may be arranged as tributaries to the streams of higher order in the network.

Recognizing that natural channel networks are ordinarily embedded in much larger networks that for practical purposes may be considered infinite in extent (Abrahams, 1984a), Shreve (1966, 1967) derived the properties of infinite topologically random channel networks. From which we detached the following:

- i. The probability of drawing a link of magnitude μ

$$p(\mu) = \frac{2^{-(2\mu-1)}}{2\mu-1} \binom{2\mu-1}{\mu} \quad \mu=1, 2, \dots \quad 3.7$$

- ii. 2) The probability of drawing a link, sub-network, or basin of order ω is $1/2^\omega$
 iii. 3) The probability of drawing a stream of order ω from a population of streams is $3/4^\omega$
 iv. 4) The average number of links in streams of order ω is $2^{\omega-1}$
 v. 5) The average number of tributaries to streams of order ω is $2^{\Omega-1} - 1$, and the average number of these tributaries that are order ω is $2^{\Omega-\omega-1}$

Because of the large values of $W(N)$, for even relatively small N , several grouping methods of *TDCN* was proposed achieve more effective and efficient application in randomness applications. For so, Werner and Smart (1973) proposed two new methods for channel network classification: the first is related to topologic path length and the second is related to channel network diameter.

I) Werner and Smart introduced the concept of “*topologic path length*” that is the number of links traversed a path and diameter of channel network. A path is the shortest route between the outlet of a channel network and a source or a junction; thus, a network of n magnitude has $2n-1$ paths. Accordingly they introduced the following properties:

- a) Number of different path-length classes ($N_p(\mu)$)

$$N_p(\mu) = \frac{1}{2}(\mu^2 + 3\mu) - \mu(q+1) + 2^{q-1} \quad 3.8$$

$$q = \lfloor \log_2(\mu-1) \rfloor + 2 \quad 3.9$$

where $\lfloor x \rfloor$ means the integer part of x

- b) Total path length classes *TPLC*

$$TPLC = 2\mu - 1 \quad 3.10$$

II) The “*Network diameter*”, symbolized here as d , is defined as the maximum length distance with maximum number of paths in the channel network, that is the largest path length channel in a network. As such the diameter provides a measure of the number of links forming the trunk channel or largest path length through which a basin outflows, thus considered as a means of expressing basin elongation

(Flint & Proctor, 1979). Werner and Smart classified channel network based on the number of network diameter classes, using the following equation

$$N_d(\mu) = \mu - q + 1 \quad 3.11$$

Channel network diameter will be calculated in two different ways; the first is directly by counting the number of paths as defined above. The second is by the Werner & Smart, (1973) approach, who proposed the following equation in order to calculate the diameter based on the magnitude of the network

$$d_{cal} = 2 * \sqrt{\pi * \mu} \quad 3.12$$

Several scientists (e.g. Smart, 1974; Shreve, 1975) appointed out that the unlimited geomorphological observations, well predicted by the random model, provides convincing evidence of the usefulness of the random model, mainly in tree theory (Werner & Smart, 1973), in predicting the orientation free planimetric properties of channel networks and their drainage basins in uniform environments.

1. link properties

Schumm (1956) studied and introduced the concepts of average link lengths:

- i. Average exterior link length (\bar{l}_e): average length of exterior streams
- ii. Average interior link length (\bar{l}_i): average length of interior streams
- iii. The ratio length link (inR_A): expressed as

$$\bar{l}_e / \bar{l}_i = inR_A \quad 3.13$$

Between topologic and link properties, Jarvis (1972) introduced a potential geomorphometric index that describe the drainage network structure in relation to magnitude and average interior and exterior links. The Jarvis index of structure (E) is defined by

$$E = \sum \mu \cdot l_i / \sum \mu \cdot l_e \quad 3.14$$

where μ is the magnitude of a given point and l is its link distance. The subscripts i and e denote summation over the interior points and over the exterior points (sources), respectively.

The potential of the E index resides in its precise structural model, which incorporates all the topologic information contained in the network graph at the ambilateral class level. Herein, the magnitude parameter summarizes the amount of drainage development headward of a given link, and the link distance parameter summarizes the structural configuration of the network downstream from the link.

2. basin area properties

In this direction, Smart defines the following properties:

- i. Average area of exterior link (\bar{a}_e): the area that drains directly to the exterior links.
- ii. Average area of interior link (\bar{a}_i): defined as the area that drains to the interior links in the channel networks
- iii. The ratio of area density (α_t) (Smart, 1972b): defined as

$$\bar{a}_e / \bar{a}_i = \alpha_t \quad 3.15$$

3. density properties

Abrahams (1984a), in defining channel network properties, highlighted three types of densities that could be used as geomorphometrical indices: drainage density, relative density, and link density.

i) *Drainage density:*

The drainage density (Dd), which is L_t/A , expresses the texture of fluvial dissection in terms of the total length of stream channel network per unit area (Horton, 1945), represents a very important geomorphometric parameter. It is considered as a useful measure of topographic texture or linear scale of landforms in fluvial eroded landscapes. As such it has been widely employed to characterize landscape (i.e. index of landscape dissection) and to predict runoff characteristics. Mather (1972) described another parameter considered to be very closely related to Dd , the source density (Ds) defined as the number of sources per unit area. However, this parameter is very sensitive to possible map-to-map inconsistencies in the portrayal of the drainage network from topographic maps (Mark, 1975), for so little attention have been made to this parameter.

Values of Dd vary widely (Chorley et al., 1984), being about 3 (mile/sq. mile) for chalk terrain, 4-5 for permeable sandstone, 20-30 for metamorphic terrain, 50-100 for the dryer areas of American West, 200-400 for shale badlands and > 1000 for unvegetated clay badlands. It is clear that Dd is highly influenced by environmental (e.g. climate and rock type) and local factors, e.g. relief and ground slope (Horton, 1945). In addition, it has been approved that relation between Dd and controlling factor is scale dependent, that is the relative importance of these factors is scale dependent (Rodriguez-Iturbe & Escobar, 1982). At the macro-scale, climate is the major control of Dd (e.g. Wharton, 1994). Whereas at the meso-scale, relief, lithology and stage of drainage network development are the major controlling factors. Finally, at the micro-scale, space filling seems to be the major control of Dd (Marcus, 1980).

ii) *Relative density:*

Compound of two basic properties, the first is Melton's ratio and the second is Shreve's ratio.

Melton's ratio is related directly to the Melton's law, in which he derived a relationship between drainage density (Dd) and channel frequency (Fs). Relative density (Dr) is a dimensionless ratio expressed as

$$Fs/Dd^2 = Dr \quad 3.16$$

Melton (1958b) describe (Dr) as a scale-free measure of the -in-completeness with which the channel network fills the basin outline for a given number of channel segments. Whereas, Shreve's ratio (1967) is a kind of morphological simplification of Melton's ratio, expressed as

$$k = \bar{a}/\bar{l}^2 \quad 3.17$$

where \bar{a} is the mean link area, and \bar{l} is the mean link length

iii) *Link density:*

Smart (1972b) defined link density as

$$K = \bar{l}^2/\bar{a} \quad 3.18$$

Which is the reciprocal of Shreve's ratio k . Abrahams (1980) termed K the macroscopic link density because it pertains to an entire drainage basin. The microscopic analogy of K , that is, the equivalent property for an individual link and its drainage area, is

$$\phi = l^2/a \quad 3.19$$

Abrahams (1984a) mentioned that values of k , K , and ϕ are dimensionless and typically have values of close to unity in mature landscapes.

4. angular properties

Stream junction angles are important morphometric property of channel network (e.g. Horton, 1945; Howard, 1971a; Abrahams, 1980b, 1984b). The first quantitative application of junction angles was by Horton (1945), who proposed that a simple geometric model could be applied to the angle at which a tributary enters a main stream. Howard (1971a) modified Horton's model to adapt streams of equal declivity, since in reality such streams and their junction angles are rarely close to 0° (predicted by the Horton's model).

5. orientation properties

Stream orientations are a basic feature of the drainage pattern that is widely employed by geologist to interpret the underlying geological structure (Abrahams, 1984a). For so, much of the research have focused on the alignment of streams with lineation in underlying bedrocks (Strahler, 1954; Jarvis, 1976a).

Herein, throughout the present work we dropped down all geomorphometric properties related to stream junction and orientation, since deriving such properties was so exhaustive and time consuming. Another important factor, that is, such properties were heavily controlled by external factors related to geology and environment prevailing conditions. Dimensionless parameters, and hence ratio properties, are considered to be more effective in detecting differences due to varying lithology and degree of maturity (Smart, 1972a)

E- Geometrical similarity:

The concept of geometrical similarities was first introduced into drainage basin geomorphology by (Strahler, 1958), who appointed that “*systems of landforms involving the same geologic processes and materials are generally recognized to possess considerable degree of similarity*”. According to this definition, two channel networks have exact geometric similarity if all pairs of corresponding dimensionless variables are numerically equal (Smart, 1972b). Strahler noted that although exact geometric similarity of course does not actually occur in nature, approximate similarity may exist. Smart and Moruzzi (1971a) made the concept somewhat more precise by proposing that two drainage networks have statistical geometrical similarities if all corresponding dimensionless variables have the same distribution function. Smart (1972a & b) appointed out that Horton’s laws (bifurcation, stream length, area and slope ratios) are the kind of dimensionless variables expected to be used under statistical geometric similarity consideration.

This is because these quantities do not provide any effective discrimination in the classification of the network structure (Kirchner, 1993), Smart (1972a) considered dimensionless variables related to link lengths and their associated drainage area to be the elementary units from which drainage basin are constructed.

In this direction, and based on infinite topologically random model in which all links have length l and drain a region of area a , Smart (1972 a & b) defined several useful statistics, from which:

i) The approving of the Melton’s law in relation to the topological random model

$$F_s / Dd^2 \approx 2/3 \quad 3.20$$

in excellent agreement with Melton’s observed value of 0.69.

ii) The microscopic drainage density (δ_j) is given by expression

$$\delta_j = l_j / a_j \quad j = 1, 2, 3, \dots, N \quad 3.21$$

And mean microscopic drainage density is then defined by

$$\bar{\delta} = \frac{1}{N} \sum_{j=1}^N \frac{l_j}{a_j} \quad 3.22$$

The macroscopic drainage density, which is the commonly used parameter in geomorphic analysis, is given by

$$D = L/A = \sum_j l_j / \sum_j a_j = \bar{l}_j / \bar{a}_j \quad 3.23$$

where L is the total length and A the total area of the set of N links.

iii) Under a uniform drainage density, Smart introduced the concept ϕ to represent drainage densities, expressed by

$$\phi_j = l_j^2 / a_j = \delta_j l_j = \delta_j^2 a_j \quad j = 1, 2, 3, \dots, N \quad 3.24$$

$$\bar{\phi} = (1/N) \sum_j (l_j^2 / a_j) \quad 3.25$$

The macroscopic analogue of ϕ is expressed by

$$K = \frac{1}{N} \frac{L^2}{A} = \frac{1}{N} \frac{(\sum_j l_j)^2}{\sum_j a_j} = D \bar{l}_j = D^2 \bar{a}_j = \bar{l}_j^2 / \bar{a}_j \quad 3.26$$

Under uniform drainage density conditions, $\phi=K$.

iv) Based on the well-established property of channel network, that is the exterior and interior link lengths have different distributions, Smart (1972b) suggests the following properties for characterizing and distinguishing channel network structure:

$$\lambda = \bar{l}_e / \bar{l}_i \quad 3.27a$$

$$\alpha = \bar{a}_e / \bar{a}_i \quad 3.27b$$

$$K_e = \bar{l}_e^2 / \bar{a}_e \quad 3.27c$$

$$K_i = \bar{l}_i^2 / \bar{a}_i \quad 3.27d$$

where the subscripts e and i refer to exterior and interior links, respectively.

v) Dissimilarity index: Smart (1972b) introduced a more comprehensive quantitative test to compare different channel networks, in which he proposed to use the dimensionless properties of λ , α and k_e as orthogonal coordinates in a three-dimensional space; then each network is represented by a point in this space, and the Euclidean distance (d_{mn}) between pairs of points can be used as a measure of similarity or dissimilarity, expressed as

$$d_{mn} = [(\lambda_m - \lambda_n)^2 + (\alpha_m - \alpha_n)^2 + (K_{em} - K_{en})^2]^{0.5} \quad 3.28$$

where m and n refers to the pair compared channel networks.

It is obvious that the Eq. 3.22 is the sum products of the subtract values of Eq. 3.21a, b, and c. Eq. 3.21d have been dropped off because it is not an independent quantity, since

$$\lambda^2/\alpha = K_e/K_i \quad 3.29$$

The above planimetric properties, mainly ϕ_e , varies in their relations with dominant landscape processes (Abrahams, 1980). The efficiency of these relations (i.e. ground slope control of planimetric properties) depends on the character of the geomorphic processes (Hortonian overland flow versus saturation overland flow) controlling the location of the channel initiation.

The Shreve (1966) model approach of randomness has provided a fundamental probabilistic basis for statistically evaluating the topologic properties of stream network. As a result, several procedures for channel network classification have been proposed, in addition to the geometrical similarity, Mock (1971) proposed a classification procedures based on link magnitude. He classified channel link by types according to their numerical relationships with their upstream and downstream neighbours. Accordingly, six types of channel links have been identified: i) source links, ii) tributary source links, iii) bifurcating links, iv) tributary bifurcating links, v) cis-trans links, and vi) tributary links. Mock (1971) indicated that each link type may have different length properties, and hence different types of stream networks.

3.3.4. Relief characteristics

The term relief is used to describe the vertical dimension or amplitude of topography (Mark, 1975). Strahler (1958) defined relief as difference of elevation between summit and valley floor. Relief is a dimensionless measure, usually used to quantify two different points in the landscape in terms of rate of change (i.e. ratio). In literature, definitions of relief measures are slightly fuzzy; that is, the same terminology has been used for different concepts, and vice versa. For so carefulness is needed in terminology designation. Accordingly, the most recent terminology for relief concept and measurements adapted are detached as follows:

- a. Basin relief (H): also known as local relief, and defined as, for any finite area of a surface, the difference between the highest and the lowest elevations occurring within basin area (Mark, 1975).
- b. Relief ratio (R_H): in general terms Shaw (1984) defined relief ratio or stream gradient as a number calculated to describe the slope of a river or stream. The calculation is just the difference in elevation between the river's source and the river's confluence or outlet divided by the total length of the river or stream. This gives the average drop in elevation per unit length of river. Whereas, Lindsay (2005) defined R_H as a dimensionless measure that describes the relief of a surface area in relation to the main stream channel.

$$R_H = H/LFp \quad 3.30$$

where LFp is the longest flowpath length from a cell to the catchment divide, which is usually the longest stream channel.

c. Relative relief (R_r): since the size of the drainage basin varies, many workers have determined a dimensionless relative relief number by dividing the relief by some other linear dimension of the basin. This number have included basin diameter (Maxwell, 1960), basin perimeter and square root of basin area (Melton, 1957). Herein, basin perimeter (P) has been adapted in defining the R_r .

$$R_r = H/P \quad 3.31$$

d. Available relief (H_a): defined as the vertical distance from the former position of an upland surface down to the position of adjacent graded stream (Johnson, 1933).

e. Drainage relief (H_d): defined as the vertical distance between adjacent divides and streams (Johnson, 1933).

Hypsometry:

Hypsometry is defined as the science dealing with the measurement of height relative to sea level. Hypsometry was first introduced in geomorphological studies by Clarke (1966), where he defined hypsometry as “the measurement of the interrelationships of area and altitude”. Most of hypsometric measurements that describe aspects of the distribution of landmass with elevation are based upon the hypsometric curve. The most widely used form of curve is the relative or percentage hypsometric curve, generally known as “hypsometric curve” (Mark, 1975). Accordingly, a hypsometric curve (HC) could be defined as an empirical cumulative distribution function of elevations in a catchment; that is, a non-dimensional area-elevation curve that allows a ready comparison of catchments with different area and steepness, and has been used as an indicator of the geomorphic maturity of catchments and landforms (Strahler, 1952b, 1956). It plots relative area above a height against relative height, and is the graph of the hypsometric function, here termed as $f(h)$, where h (the relative height) is defined as:

$$h = \frac{z - z_{\min}}{z_{\max} - z_{\min}} \quad 3.32$$

where z is the actual elevation, and Z_{\max} and Z_{\min} are the highest and lowest elevations, respectively, within the study area.

Geometrically speaking, Strahler appointed out that this value is equal to the ratio of the volume between the land surface and a plan passing through Z_{\min} to the volume of a reference solid bounded by the perimeter of the area and planes through Z_{\max} and Z_{\min} .

The Hypsometric Integral (HI), a derived index of the HC and the most widely used parameter in hypsometry, is given by the following (Strahler, 1952b):

$$HI = \int_0^1 a(h)dh \quad 3.33$$

where h is the elevation and a is the area curve

Graphically, HI can be determined by measuring the area under the relative hypsometric curve (Mark, 1984). HI expresses the unconsumed volume of a drainage basin as a percentage of that delimited by the summit plane, base plane, and perimeter. Chorley et al., (1984) appointed that where a particular resistant geological outcrop maintains a proportion of the summit plane during considerable erosion of the rest of the basin, HI may reach low values (figure 3.7D). However, in uniformly erodible material the continued erosion of the basin high point may stabilize HI in a middle range of values between 0.4-0.6 (figure 3.7B & C). Figure 3.7 describe the HI in four sub catchments within Tabernas basin characterized by different relief and lithologic formations. In general, the lesser the basin size the higher the homogeneity is in the prevailing structure relief and dominant processes within these formations. Hence, differences in hypsometric curves between landscapes arise because the geomorphic processes that shape the landscape may be different. It is this form of the hypsometric curve and function upon which some important terrain parameters are based on, e.g. similarities between catchments.

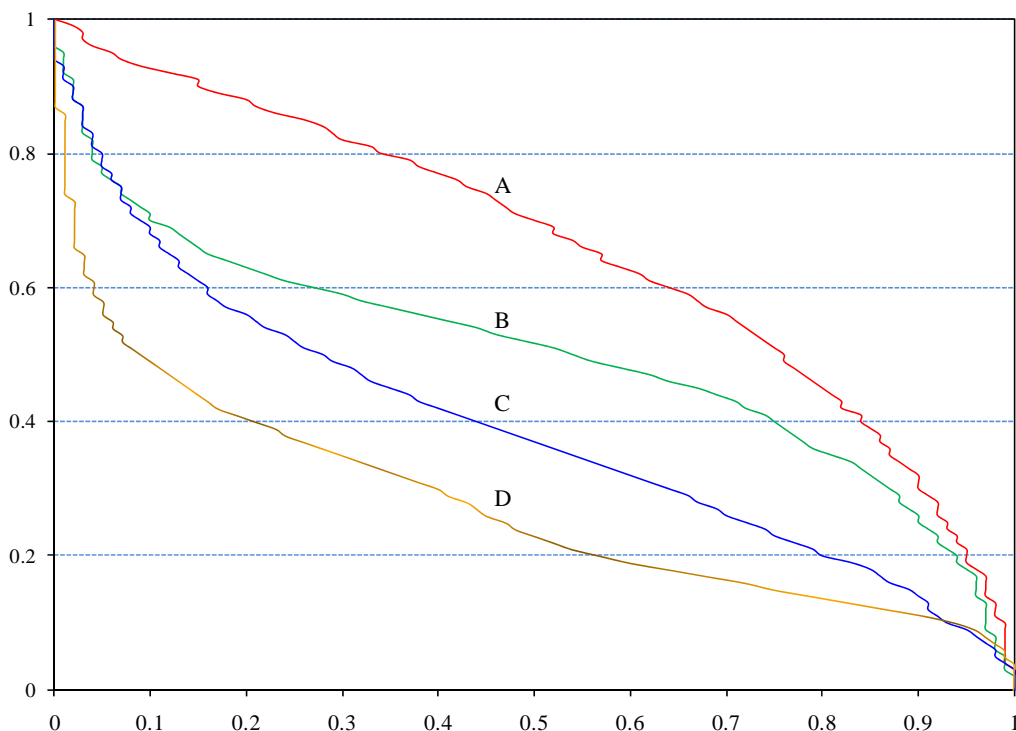


Figure 3.7 The HI curves of different sub-catchments of Tabernas Basin. A) $HI = 65.9$ with catchment basin = 0.468 km^2 ; B) $HI = 50.04$ and catchment size = 5.29 km^2 ; C) $HI = 39.08$ and catchment size = 37.2 km^2 ; and D) $HI = 27.6$ with catchment size = 252.48 km^2 .

One of the principle applications of the HI in geomorphic processes is the revelation stage of landscape development. In general, those areas having HI values above 0.60 were considered to be in a youthful or in-equilibrium phase, values of HI between 0.35-0.60 indicated equilibrium drainage

basins, while value below 0.35 were thought to characterize a transitory mandknock phase in landscape development (Strahler, 1952b; Mark, 1984). The stage of landscape development, widely known as landscape evolution, was firstly proposed by Davis (1909), whom developed several theories of landscape evolution including the fluvial cycle where he envisioned the progressive evolution of streams from youthful to old age. Each stage (i.e. age) was defined by particular morphologic elements. These ages could be summarized as follows:

1. Youthful (initial): Narrow v-shaped valley, no floodplain, steep gradient
2. Mature (intermediate): broad valley with flood plain, meandering stream, lower gradient
3. Old Age (terminal): river meanders over a broad plain with oxbow lakes, stream gradient of very low
4. Rejuvenation: change in base level renews youthful conditions

Distinction between age classifications is not straightforward as the boundaries are diffuse between the classes, for which qualitative and quantitative bases had been proposed to achieve more simple and direct classification. Accordingly, geomorphologists introduced different classification patterns of river and streams based on alternative approaches, e.g. geomorphological aspects. In the same direction, Leopold and Miller (1956) define channels streams (mainly ephemeral ones) in relation to its physical characteristics. These characteristics can be grouped into dimension factors, profile factors and patterns factors (DeParry, 2004). From dimension factors, the bankfull discharge in relation to area can be detached.

3.3.5. Fractal and scaling laws in channel networks

Since Mandelbrot (1977) introduced the concept of fractal object to describe irregular shapes that exhibit similar patterns (in a deterministic or statistical sense) at different scales in nature, many researchers studied the fractal structure of river networks (e.g., Hemlinger et al., 1993). Early documentation of power laws or scaling behaviour led to the recognition that processes at fine scales propagate over vast distances, thereby creating new patterns and complexity (Mandelbrot 1982). In general, fractals provide a mathematical framework for treatment of irregular, apparently complex shapes that display similar patterns or geometric characteristics over a range of scales. In river basins, since we deal with statistical description of components, the fractal scaling property refers to the invariance of the probability distributions describing the object's composition under geometric transformations or change of scale (Gupta & Waymire, 1989). Accordingly, it's important to highlight two important concepts that are widely used in fractal geometry, that is, "*self-similarity*" and "*self-affine*".

Self-similarity is a concept that refers to invariance of phenomena with scale, not with additive translation but rather to multiplicative change. A self-similar object appears unchanged after changing

its size; whatever the direction was (increasing or decreasing) objects hold the same structure. This similarity of the parts to the whole is called *self-similarity*, generally known as scaling (Rodríguez-Iturbe & Rinaldo, 1997). Whereas, *self-affinity* is referred to objects or processes that are indistinguishable at different scales of observation but that need to be scales in different directions with different factors (i.e. different geometrical directions are scaled differently to preserve shape or statistical moments). Therefore, topographic contours are described as self-similar (e.g. Mandelbrot, 1985; Gilbert, 1989), while vertical topographic relief may be considered self-affine (e.g. Turcotte, 1999).

Mathematically, to understand scaling we will consider the functional equation $f(xy) = f(x)f(y)$, where $f(\cdot)$ is a function of variables x and y . It is well known that a general solution to this equation is a power law given by

$$f(x) = cx^\varepsilon \tag{3.34}$$

where c is a scale parameter, typical for the fractal geometry, which should be evaluated for each specific curve, and ε is a scaling exponent or the fractal dimension.

Thus, if a system is known at some reference scale x then the behaviour is known at any multiple of x within the valid domain. That is, the set f is said to scale and the property of obeying a power law is referred to as scaling. The term scale invariance applies when the scaling exponent is constant across a wide range of x (Milne et al., 2002).

Empirical scaling relations have been known for decades in biology and hydrology. For example, in the “downstream” hydraulic geometry of river networks, velocity, depth, width, slope, and friction vary as powers of stream discharge (m³/s; Leopold, et al., 1964). Such relations hold across the multiple spatial scales of a river network (Milne et al., 2002). In general, the topology of river basins, the hydraulic geometry and even hydrologic response of basins to different kinds of input (e.g. rainfall) are characterized by power law relationships between the variable involved in their description (Rodríguez-Iturbe & Rinaldo, 1997). Moreover, great efforts have been made by geomorphologists to interpret the physical processes that might be related to the various power laws (fractals) and their exponent parameters (i.e. fractal dimensions) (e.g. Phillips, 1993). Although there have been observed departures from the random topology model of Shreve (1966, 1967), careful interpretation of the fractal measures (dimensions) estimated from traditional morphometric parameters might provide useful information for understanding the evolution of landforms and the relationship to the underlying geological constraints.

From these relations we will pick up two scale relations that have been used in the analysis process as geomorphometrical indices, they are Hack’s and Melton’s laws.

i. Hack's law

Hack (1957) has demonstrated the applicability of a power scaling function relates main stream channel of the network with its corresponding drainage area, by the following expression

$$La \propto A^h \quad 3.35$$

where La is the length on the main stream or largest channel measured to the drainage divide and A is the area of the basin, and h is the exponent of Hack.

Hack found the value of h approximates 0.6, for which he concluded that basins tend to be more elongated as they increase in size. Later, he extended the results to all rivers of the world, finding that the exponent of Eq. 3.25 remains close to 0.6. Gray (1961) later refined the analysis of Hack, finding a difference in the exponent from 0.568 to 0.6. Actually, several authors appointed out that Hack's exponent could oscillate between 0.4-0.6 for large and small catchments, respectively (e.g. Mesa & Gupta, 1987; Robert & Roy, 1990).

Researchers provided several theories to explain the previous results. The first explanation (i.e. classical) for the change in h values was to conjecture that basins have anisotropic shapes and tend to become narrower as they enlarge or elongate (i.e. small catchments contain a circular form while large catchments have elongated form). The second theory explains the results in relation to the fractal character of the main channel with growing sinuosity with drainage area (Robert & Roy, 1990). The third theory interpret the Hack's law under the framework of the optimal channel networks (OCNs), in which h value variations is the result of the consequence of competition and minimization of energy expenditure (Ijjasz-Vasquez et al., 1993a). Whereas, Rigon et al., (1996) found that h value, elongation and fractal characters are closely related, suggesting that Hack's law to be viewed within a statistical framework and not necessarily in connection with arbitrary definitions of suitable basins or sub-basins, for example, at predefined outlet. The truthful explanation of the Hack's incongruent exponent still to be an open problem in hydrology, and the question if the causes of this variation is of topologic or geometric or morphologic origin, open the gate for diverse and unlimited types of studies in that direction.

Mesa and Gupta (1987) derived the theoretical value of Hack law (h) based on the random topology model of channel network, in which they expressed it as

$$h_{\mu} = 1/2 \left(\frac{\pi + \pi^{0.5} * \mu^{-0.5}}{\pi - \mu^{-1}} \right) \quad 3.36$$

where μ is the magnitude of the channel network

ii. Melton's law

As mentioned earlier, Horton (1945) introduced the concept of channel frequency (F_s), which relates Strahler-Hortons' stream numbers to its drainage area. Scientists revealed that it is possible to construct two hypothetical basins having the same drainage density but with different stream

frequency, and vice versa. Melton (1958a) demonstrated that F_s is highly correlated with Dd by a log-linear regression for mature basins covering a vast range conditions (scale, climate, relief, surface cover and geology type). Melton's law is expressed by

$$F_s = 0.694 Dd^\theta \quad 3.37$$

where $\theta \approx 2$

Melton's expression was revisited by Shreve (1967), who produced a related term k based on the length, frequency and drainage area of individual channel links (mentioned earlier), rather than the channel system as a whole. Possible perturbation related to Eq. 3.25, mentioned by Melton is related to source definition, which is directly related to F_s value. Moreover, Melton studies Eq. 3.25 in relation to basin's relief, perimeter, area and length, in which he argued for considering these relations to be 'growth models'. This argument is predicated upon the assumption that a collection of basins measured at a particular point in time can be considered equivalent to the behaviour of a single basin over time (Keylock, 2003).

3.3.6. Multifractal approach

Multifractal concept have been defined as geometric objects that exhibit different local fractal dimensions in different regions within a geometrical support; thus, multifractal measures concern the study of the distribution of a physical quantity on a geometric support (e.g. ordinary plane, a surface, a volume, or a fractal itself). Multifractals require that the fractal concept is generalized to include complex structures with more than one scaling exponent, that is, a spectrum of exponents (Rodríguez-Iturbe & Rinaldo, 1997). In general, multifractals are infinite sets exponents, which describe the scaling (power law) of all the moments of a distribution of some quantities which are defined on a fractal structure (De Bartolo et al., 2000). For which, in many cases, specific members of these sets of exponents coincide with the fractal dimensionalities of geometrical substructure of the underlying fractal (De Bartolo et al., 2004).

Recent studies (Ijjasz-Vasquez et al., 1992; Rinaldo et al., 1992; De Bartolo et al., 2000, 2004, 2006) have approved that the monofractal analysis of the river networks can be generalized through the use of multifractals. For example, the spatial distribution and the scaling properties of some important hydrological properties, such as contributing drainage area, slopes, dissipation energy, channel initiation function and the width function, can be characterized through the formulism of the multifractal spectrum, $f(x)$ introduced by Halsey et al., (1986). In particular, fluvial network may be considered intricate spatial self-organized structures (Rodríguez-Iturbe & Rinaldo, 1997). In such processes, scientists showed that multifractality is concerned to multiscaling properties (Coniglio & Zannetti, 1989).

Multifractal concept has been evolved throughout the last decades and several algorithms (e.g. box-counting, sandbox algorithm, etc.) have been proposed to define the optimum fractal dimension

for the channel networks (e.g. De Bartolo et al., 2000, 2006). In these studies river networks are usually represented by discrete distributions of ‘net-points’, and by analyzing such sets of points a spectrum of generalized fractal dimensions is achieved. Such a spectrum is fully representative of all the fractal dimensions associated to each single substructure of the network or a portion of it, each one being characterized by its own scale exponent (De Bartolo, 2004).

The idea of multifractality and the ability to describe phenomena with different scaling exponents has open entire new fields because of the capability of this type of analysis for describing the geometry of physical systems. Ijjasz-Vasquez et al., (1992) affirmed that the multifractal formalism is a useful tool to describe the spatial distribution and scaling properties in river basins. In which, multifractal description of the spatial organization of variables in river basins goes one step beyond the topological and fractal analysis of the form of river networks and provides a tool to understand not only the form of the network but also the distribution and scaling of more physical variables in river basins. Rodriguez-Iturbe and Rinaldo (1997) affirmed that multifractal descriptors enlarge our ability to describe nature, as well bear a more precise and realistic resemblance to real river networks. Accordingly, they concluded that “if geographic and geophysical fields are generally multifractal, that is, characterized by a hierarchy of fractal dimensions, then inconsistencies are inevitable when the fields are forced into geometric framework involving single fractal dimension”.

For all the above, we believe that the multifractality approach is more consistent than monofractal one in describing data from the elevation field of real rivers. In relation to such considerations, and in order to achieve the best approximation to natural channel networks, it is acceptable that multifractality, and hence multiscaling, concept should be considered in whatever approach used to derive landscape structure.

3.3.7. Channel network evolution

Smith et al., (1997) appointed out that advances in our understanding of the evolution of fluvial landscapes may be classified in terms of three distinct approaches to the problem. These approaches include (i) deterministic modelling that is continuous in space and time and based on conservation principles, (ii) stochastic modelling that is discrete in space and time and based on conservation principles, and (iii) deterministic modelling that is based on the search for variational principles that characterize self-organizing drainage surfaces in terms of the minimization or maximization of some aggregate quantity. Whereas each approach has contributed significantly to our understanding of drainage basin phenomena, each possesses its own advantages and limitations, and there is no current theoretical basis that unifies all three approaches.

It seems to be highly doubtful to emphasize one approach over the rest, for which we believe that it's more convenient to highlight all approaches, and then detach the last advances on evolution theories of fluvial systems. Accordingly, conceptual models, mainly based on physical mechanisms,

will be detached as major line to understand channel network evolution. Such models explain channel network evolution and growth under different initial conditions. Three broad physical mechanisms have been proposed for channel network growth (Abrahams, 1984a; Schumm et al., 1984); these are the Hortonian, the headward growth and branching, and finally the Glockian evolution.

(A) Horton's model:

The rational model of channel network evolution proposed by Horton (1945) assumes deterministic processes. Horton described growth process in which a thin sheet of water in a uniform flow conditions exceeds a "*critical shear stress*" at a distance x downstream from the divide. The critical shear stress is thought of as a threshold for mobilizing bottom material, and thus a system of parallel rills is developed, which rapidly propagates over the entire surface. Divide migration through competition and transverse grading subsequently generate a dendritic pattern. Divide migration refers to the capture of small rills by slopes, which drain toward the dominant rill through drainage directions established by the maximum gradients. Horton's scheme has the essential ingredients for large-scale network growth but lacks the ability to describe the effects of heterogeneities in the surface structure on the development of the network (Leopold et al., 1964; Abrahams, 1984a).

(B) Headward growth model

The most widespread and acceptable between researchers was first proposed by (Schumm, 1956) and later developed by Howard (1971a, b, & c) and Smart and Moruzzi (1971a & b). According to this model, a network is formed as a wave of dissections progressing from the outlet into an unchanneled landscape. Thus channels grow upstream and bifurcate, filling the available drainage area. Whatever the rule of branching, growing networks may be subjected to processes of stream capture through which large streams migrate sideways, capturing smaller ones (Rodriguez-Iturbe & Rinaldo, 1997).

(C) Glockian model

In this approach, Glock (1931) proposed a different conceptual picture for network growth, based on stages in the growth process. These stages are classified as follows: *i*) network initiation through the rapid carving of a skeletal pattern; *ii*) network elongation by headward growth up to maximum extension; *iii*) network elaboration through the development of tributaries; and, *iv*) a stage of simplification where tributaries disappear owing to the reduced relief.

In channel network evolution, it is highly plausible that no general rule can be inferred from simple conceptual models (Howard, 1994). Network growth is instead produced by complex interactions that seldom yield to a simplified description. Accordingly, important processes can affect the planimetric and elevation structure of drainage basins. From which, several can be detached, such as *i*) the interplay of the prevailing erosional processes of dispersive and concentrative nature; *ii*) the spatial and temporal development of channel links; headward growth and branching; *iii*) the large

scale migration of valleys and divides and the related capture processes; and iv) the progressive adjustments of junction angles of confluent streams (Howard, 1971a, 1990). Rodriguez-Iturbe and Rinaldo (1997) appointed out that many models have been developed in the past to provide realistic simulation of the temporal evolution of the landforms based on a deterministic description of the effects of the chief geomorphic agents. However, several questions rose on the importance of these models; the most important is what should be the effects of initial conditions and inheritance on basin form and evolution?

The development of drainage basins requires at least two superimposed processes (Rigon et al., 1994), dispersive and concentrative. The first is a diffusional, creep-like mass-wasting process capable of eroding the land surface with finite gradients, even for vanishingly small contributing areas A . such a process must be characterized by a progressive loss of efficiency as A increases so that in the average the gradient of land surface increases downslope if rates of surface lowering are essentially uniform in space. The second is a concentrative fluvial process that increases its efficiency with contributing area, that is, with flow rates, but requires large gradients for small values of A (Rodriguez-Iturbe & Rinaldo, 1997). The resulting combination of processes and the embedded spatial transition from slope-dependent mass-wasting to concentrative runoff processes in channels justifies the essentials of the morphology of river basin, as recognized by Gilbert (1909) and Howard (1994):

“... On the upper slopes, where water currents are weak, soil creep dominates and the profiles are convex. On lower slopes water flow dominates and profiles are concave.”

Finally, it worth's to mention that Smith et al., (1997) have produced a family of continuous models, based on stability model of Smith and Bretherton (1972), that provide an elementary theory of evolution of fluvial landscapes in terms of (1) the emergence of channelized flows; (2) the development of stable surfaces with ridges and valleys; (3) the decline of the surfaces; (4) relationships between surface forms and surface flows; and (5) environmentally caused landform variability.

3.3.8. Geomorphic concept of landscape change

Geomorphologists recognize that the interface between the atmosphere and the solid earth, the landscape, is dynamic. Drainage basins and their components, slope and channels, are either adjusting rapidly to altered conditions (instability), or they are in dynamic equilibrium with present conditions (Schumm et al., 1984). From a physical process understanding, the fluvial system may best be described as an open dissipative process-response system, which self-adjusts (self-organizes) in response to external forcing (Molnar, 2006). Several geomorphic concepts of landscape change have been introduced, for the understanding of the adjustment of fluvial systems. Such concepts are not mutually exclusive and many coexist and explain each other. The first four are traditional concepts of geomorphology (Schumm, 1977), whereas the rest are related to physical relations.

i. Uniformity

In natural landscapes, uniformity implies that past, present and future erosional and depositional processes occur under the same physical laws; that is, the nature of the process does not change. It does not mean that a uniform (constant) erosion/deposition process rate occurs but that events leading to landscape change of different magnitude will continue to occur.

ii. Thresholds

This concept states that the response of fluvial systems may be strongly influenced by geomorphic thresholds. Schumm (1977) stated that fluvial system does not respond to change until some threshold is exceeded. Threshold may be extrinsic (external), where the system responds to external influences, such as climate, base-level or land use changes, or intrinsic (internal), where the system adjusts by its own dynamics to a condition of incipient stability (Schumm et al., 1984). The later type, changes occur with no need in external variable (e.g. long-term progressive weathering that reduced the strength of the slope materials) until eventually there is slope adjustment and mass movement (Kirkby, 1971). In semi-arid regions, the dominant is the intrinsic threshold where sediment storage progressively increases the slope of the valley floor until failure occurs by gullying. In general, and from a geomorphic point of view, thresholds can be of two types (Schumm et al., 1984). Herein, a threshold of landform stability is exceeded either by intrinsic change of the landform itself (i.e. intrinsic threshold) or by a change of an external variable (i.e. extrinsic threshold).

iii. Landscape evolution

This concept states that within geological constraints there is a deterministic sequence of landscape evolution through time (Schumm, 1977). After a period of uplift $U(t)$, erosion $e(t)$ acts on the landscape (in fact they always acts together), in which the present river (landscape) state reflects a balance of these factors. Chorley et al., (1984) explained this process in relation to feedback process. They stated that the output of a geomorphic system can be expressed in two ways: first, by the rate at which mass (i.e. sediment) are evacuated from it, and second, the energy which has been expended in sustaining and transforming it. This leads to the important concept of system state termed “*equilibrium*”. A graded stream is in equilibrium with a balance between sediment supply and transporting capacity. An event which disturbs this balance will result in channel change which will attempt to re-establish this balance and return to equilibrium. Paradoxically equilibrium can only be expressed with reference to directions of changes (Chorley & Beckinsale, 1980), illustrated by the followings:

- a. A quasi-equilibrium state: A condition when the rate of change of forms declines through time to a state of relatively slow change. The late-stage surface of low relief of the cycle of erosion.
- b. A steady state equilibrium: A condition wherein form oscillates around a stable average value due to the operation of interacting feedback loops in the system, which will be referred to shortly.

- c. Dynamic equilibrium state: a condition of oscillation about a mean value which is, itself, trending continuously through time.
- d. Dynamic metastable equilibrium: a condition of oscillation about mean value of form which is trending through time and, at the same time, is subjected to step-like discontinuities as a threshold effect operates to promote a sudden change of form

It is thus clear that true equilibrium is a theoretical state towards which the system behaviour is trending with greater or lesser rapidity, by attempting to absorb the successive effects of a sequence of process inputs of differing magnitude and frequency (Chorley et al., 1984).

iv. Complexity

The concept accepts that the fluvial system is a complex system and that deterministic predictability of its behaviour (locally) is impossible (Schumm, 1977). In this direction it is contradictory with previous concept, since complexity in processes is related to complex history in the landscape. For example, many fluvial successions will display characteristics of more than one type of river, which is attributed to recognition of the complexity and variability of fluvial systems in space and time (Gupta & Waymire, 1989). Two types of diversity and complexity can be identified in fluvial systems (Rayburg & Neave, 2008): (1) the variety of morphologic structures found within the system (external variability); and (2) the variety of forms within each type of morphologic structure (internal variability). Both types of complexity can have a profound impact on the morphologic, hydraulic and ecologic diversity of fluvial systems.

The complex response is an inherent property of the fluvial system that is attributed to the followings: I) processes operate together over many timescales are involved; II) adjustment process in the fluvial systems takes long time and different adjustments are overlapped; and, III) it is not only the external forces but also the system itself causes adjustment.

v. Optimality (efficiency)

Regularity in the topological structure of river networks and in the distribution of their channel properties is an intriguing display of self-organization in nature (Molnar, 2002). Efficiency and optimality in energy expenditure have been used to explain the regularity in hydraulic geometry (Leopold & Maddock, 1953; Leopold & Langbein, 1962), channel pattern (Bull, 1979), and river network structure (Howard, 1990; Rigon et al., 1993), and Hack's relationship (Ijjasz-Vasquez et al., 1993a). The concept of optimal channel energy was first introduced by Rodriguez-Iturbe et al., (1992) who suggested that the fluvial system adjusts its river network structure and channel geometry in such a way that it is most efficient in transporting water and sediment. They postulated three principles that define the optimal topological structure: (1) minimum energy expenditure in a river link, (2) constant energy expenditure per unit channel bed area, and (3) minimum energy expenditure in the whole network. A combination of these principles led to the definition and modelling of optimal channel

networks (*OCNs*) that exhibit remarkable similarities with natural river networks in their fractal aggregation structure, as well as other empirical geomorphological properties (e.g. Ijjasz-Vasquez et al., 1993b). The total energy expenditure can be expressed as:

$$OCN = \sum_i^N l_i A_i^{0.5} \quad 3.38$$

where i is the link index, N the number of links, and l and A are the length and the area of each link.

vi. Self-organized criticality (*SOC*)

The concept of *SOC* was originated with reference to the search for dynamic explanation for the behaviour of many spatial extended dynamic systems with both spatial and temporal degrees of freedom. Self-organized criticality (or self-organized spatial structure in river networks) was first introduced by Bak et al., (1987), in which they defined *SOC* as the tendency of large dissipative systems with many degrees of freedom to build up a state poised at criticality that is characterized by a wide range of length and time scale (i.e. complexity of physical systems). According to this theory, complexity originates from the tendency of an open dynamic system to organize itself into a critical state. At the critical states events of all sizes may occur, interaction (correlation) goes to infinity, and predictability is possible only in a mean statistical sense, not for individual events (Bak et al., 1988; Bak & Paczuski, 1995).

The *SOC* model reveals that a system with very simple rules may organize itself into a critical state in which events of all sizes occur, a state which is characterized by local instability but global stability. This means that locally every site is sensitive to the initial conditions, every change in local conditions will result in a different outcome locally (Turcotte, 1999). However, on a global scale, the system will go to a critical state regardless of which initial conditions were chosen. The critical state is achieved by self-organization independently of initial conditions (Rodríguez-Iturbe & Rinaldo, 1997). At the critical state one simple disturbance may lead to a small response (avalanche) or to huge one (spanning the entire system). In this case, criticality is manifested in a consistent power law distribution for avalanche sizes across a wide range of scales. The relevance of the *SOC* concept to natural fluvial systems is that landscape models developed on the basis of *SOC* concepts have statistical properties remarkably similar to natural river basins (Rigon et al., 1994). Examples of this are the probability distributions of accumulated area, distributions of link lengths, slope, etc.

The question that may be raised when applying the *SOC* and optimality concept to landscape change is that of inference. The inference is made that because *SOC* and *OCN* models lead to properties that are remarkably similar to natural fluvial systems, which means that nature follows these concepts in landscape development (Turcotte, 1999). Rodríguez-Iturbe and Rinaldo (1997) appointed out that *OCNs* are case spatial model of *SOC*, which reinforces the suggestion that natural fractal structures like river networks may indeed arise as a joint consequence of optimality and randomness.

Specifically, natural fractal structures in the fluvial landscape are dynamically accessible optimal states, corresponding to local optimal niches of a complex fitness landscape where evolution can settle in a stable manner. Such relative stability is achieved with respect to perturbations and is nonetheless reminiscent of its dynamic history, including an imprinting of its initial conditions and long live signatures of boundary conditions, here surrogating geologic constraints.

3.4. A reduced quantitative approach for channel networks properties

3.4.1. Introduction

The previous paragraphs provided a comprehensive introduction to geomorphometrical parameters widely used in characterizing variations in channel network morphology. In the present work, we will try to pick out a representative set of these indices that cover all possible variations in stream network properties. This is because river basins and embedded stream networks are characterized by complex morphology that cannot be adequately expressed by a single descriptor; therefore, a combination of parameters is the most powerful approach for a justifiable morphometric classification of the landscape.

The basic objective of such procedure is to achieve the best representation (i.e. quantitative) of stream characteristics without any loss of considerable information. Herein, and for simplicity, the terminologies parameters, descriptors, attributes and indices will be used as synonymous, in order to represent the quantitative geomorphometrical characteristics of the drainage network system. Since delineating stream networks is the general aim of the present study, all parameters related to pure area description will be excluded, while those that incorporate mixture parameters of channel network and basin area will be included. Accordingly, a formulated group of parameters (geomorphometrical indices) have been selected to represent the main geomorphometric characteristics of the channel networks. As a result, a group of 29 indices have been defined and listed in table (3.2). It is important to underline that the last two indices were dropped down from the current stage of analysis. This is because the definition of these indices are not direct and require the construction of linear regression model, which make it impossible to be calculated within catchments of first and second order streams.

No.	Geomorphometrical indices	Reference	Symbol	Expression
1	Order of the channel network	Horton 1945; Strahler 1957	Ω	
2	Longest stream in the channel network	Hack 1957	La	
3	Drainage network density	Horton 1945	Dd	$Dd = L_t / A$
4	Magnitude of the channel network	Shreve 1966	μ	
5	Ratio of average stream length	Schumm 1956	inR_A	$inR_A = \bar{l}_e / \bar{l}_i$
6	General area ratio	Smart 1972	a_t	$\bar{a}_e / \bar{a}_i = a_t$
7	Macroscopic exterior link density	Abraham 1980	K_e	$\bar{l}_e / \bar{a}_e = k_e$
8	Macroscopic interior link density	Abraham 1980	K_i	$\bar{l}_i / \bar{a}_i = k_i$
9	Link density	Smart 1972	ϕ_k	$\phi_k = \bar{l}^2 / \bar{a}$
10	Horton Bifurcation ratio	Horton 1945	R_B	$N_{\omega-1} / N_{\omega} \approx R_B$
11	Horton Length ratio	Horton 1945	R_L	$\bar{L}_{\omega} / \bar{L}_{\omega-1} \approx R_L$
12	Horton Area ratio	Horton 1945	R_{Aw}	$\bar{A}_{\omega} / \bar{A}_{\omega-1} \approx R_{Aw}$
13	Channel frequency	Horton 1945	F_S	$F_S = N / A$
14	Exceedence probability slope of stream length	Tarboton et al. 1988	P_S	$P_S = m/n + 1$ *
15	Optimal channel network or catchment energy	Rodriguez-Iturbe et al. 1992	OCN	$OCN = \sum_i^N liAi^{0.5}$
16	Number of different path-length classes	Werner & Smart 1973	$N_p(\mu)$	$N_p(\mu) = \frac{1}{2}(\mu^2 + 3\mu) - \mu(q+1) + 2^{q-1}$ $q = \lceil \log_2(\mu-1) \rceil + 2$
17	Stream network diameter	Werner & Smart 1973	D_{obs}	
18	Theoretical stream network diameter	Werner & Smart 1973	D_{ocal}	$D_{cal} = 2 * \sqrt{\pi * \mu}$
19	Number of network diameter classes	Werner & Smart 1973	$N_d(\mu)$	$N_d(\mu) = \mu - q + 1$
20	Total path length classes	Werner & Smart 1973	$TPLC$	$TPLC = 2\mu - 1$

21	Topographically distinct channel network	Shreve 1966	<i>TDCN</i>	$W(N1) = \frac{1}{2N_1 - 1} \binom{2N_1 - 1}{N_1}$ $W(N_1, N_2, \dots, N_{\Omega-1}) = \prod_{\omega=1}^{\Omega-1} 2^{T_{\omega}} \binom{N_{\omega-2}}{T_{\omega}}$
22	Probability of drawing a link of magnitude μ	Shreve 1966	$p(\mu)$	$p(\mu) = \frac{2^{-(2\mu-1)}}{2\mu-1} \binom{2\mu-1}{\mu}$
23	Jarvis index	Jarvis 1972	E	$E = \sum \mu \cdot \bar{li} / \sum \mu \cdot \bar{le}$
24	Stream network development index	Strahler 1957	Isd	$Isd = L/P$
25	Fractal dimension of the channel network	Tarboton et al. 1988	ε	
26	Hack theory value	Mesa & Gupta 1987	$H\mu$	$H_{\mu} = 1/2 \left(\frac{\pi + \pi^{0.5} * \mu^{-0.5}}{\pi - \mu^{-1}} \right)$
27	Melton Ratio	Shreve 1967	K	$K = (2\mu - 1)/LDd$
28	Fractal dimension of Hack's law	Hack 1957	h	$La = \beta A^h$
29	Fractal dimension of Melton's law	Melton 1958a	θ	$Fs = \beta Dd^{\theta}$

Table 3.2 Geomorphometrical indices proposed for the comparison and validation procedure between different drainage networks.

* where m is the ranking from longest to shortest stream length and n is the number of streams in the sample dataset (Tarboton et al., 1988)

3.4.2. Treatment for methodological comparison

In general, the mentioned parameters are founded between the most widely used by researchers in the field of quantitative geomorphology for river basin analysis. The resulting proliferation of these quantitative descriptors has created problems for workers in the field of fluvial geomorphology and hydrology, since various parameters measure the same element but in different ways or contains common dimensions (Ebisemiju, 1979a). A quick inspection to the selected indices highlighted the presence of a considerable amount of redundancy in the defined matrix, because many of the morphometric parameters are strongly inter-correlated, e.g. (μ) and the majority of topological indices. Thus, a clear need to reduce the number of parameters to a few that adequately simulate drainage network morphology is needed.

The filtering process of such large number of interrelated variables for their underlying dimensions is best achieved by the multivariate statistical techniques of factor analysis or principle component analysis (Mather & Doornkamp, 1970; Mark, 1975). Although the use of principal component analysis (*PCA*), factor analysis and rotations in geographical investigations has been the subject of debate for many years (e.g. Armstrong, 1969; Mark & Church, 1977), its suitability for examining the inter-correlations structure of geographical parameters and the intensity of their interaction has been widely demonstrated (Mather & Doornkamp, 1970; Abrahams, 1972; Ebisemiju, 1979a & b; Castillo, 1986; Romero & López, 1987). The main applications of factor analytic techniques are: *i*) to reduce the number of variables, and *ii*) to detect structure in the relationships between variables, that is, to classify variables. Therefore, the factor analytic technique is applied as a data reduction or structure detection method.

Herein, a modified approach of Ebisemiju (1979a) has been proposed that combines between multivariate statistical technique and a complementary correlation test. The first determines the major factors that each parameter belong to, whereas the latter define the degree of inter-correlation among parameters in the same factor. This is somewhat different to the Ebisemiju (1979a) work, where he defined a representative parameter based on loading degree in each factor of the multivariate approach. He argued that if several variables have high loadings on a factor, then they should represent the same character, in which case some may be deleted. But, and as mentioned earlier, the geomorphometric indices are highly specialized attributes that could be formed by one or more parameters that describe general or particular stream network properties, e.g. topologic vs. geometric. Such properties are complementary ones and the exclusion of parameters based on loading degree may cut down the strengthen property of these indices in the final comparison process. Herein, two important points must be accentuated. First, all stream network properties (i.e. geometry, topology, optimality, fractality) should be included in the final test, as well as the mixture (or the combination) of these attributes since they are, in many cases, more powerful than original ones. So, at least one representative parameter of these characteristics is necessary for a justifiable representation of

drainage network properties. Second, inert-correlation was carried out between indices that describe the same property. For example, if a factor includes 4 indices, one describes the geometry and the other three describe the topology, then the geometric indices are included directly and the correlation is carried between the topological attributes.

The geomorphometrical indices were defined from the digitized blue lines of Tabernas Basin (figure 2.5, Chapter 2), which was extracted by digitizing process on topographic maps at 1:50000 scale, corresponding to 16 sheets of the *L* series of the Spanish Military Centre of Geography. The digitalization process was realized by the Cartalinx software, and the corresponding geomorphometric values for each segments was also integrated to the original dataset provided by the software itself. Since several unrealistic segments were observed mainly in smooth flat areas, a refining process has been concluded in comparison to the orthophotographs of the area. Later on, a group of 389 sub-catchments of varying orders were selected and used in the matrix analysis. These range in size from approximately 572 km² to 0.1 km². In each sub-catchment, the 27 geomorphometric indices were calculated and defined. The produced data matrix was then subjected to the *PCA* for factor definition.

3.4.3. Selection of parameters

As we are looking for indices that have low inter-correlation, and since we need an analysis that allows considering some variables in relation to their effects, the principle component analysis (*PCA*) will be used to achieve these aims. Application of *PCA* on the data matrix outlined by all sub-catchments values have formed a group of factors, each of which describes the weight of the descriptor in the factor, and the degree of correlation between others (table 3.3). The eigenvalues correlation matrix of the *PCA* analysis shows that 5 factors explain almost 80.5 % of the total variance in the analysis test. In same direction, plotting of factor coordinates for variable representation (figure 3.8a) revealed that not all the variables are well presented by these two factors indicating the presence of extreme variability between factors. In order to explain such behaviour, variability between cases was study by the projection of cases coordinates (figure 3.8b). Herein, a clear clustering is observed between two groups: the first group is clustered to the right hand of the coordinate and highlighted by an ellipse and the second is extended out of this range. In addition, a clear inverse curve relationship confirms such clustering and the presence of two major groups between cases. These clusters are widely related to catchment size giving rise to a kind of particularity to the drainage network properties under these dimensions. These observations bear a kind of rationality since the majority of these catchments are first order basins, where ratio indices are disappeared and several topologic and geometric characteristics are somewhat similar.

No.	Index	Factor1	Factor2	Factor3	Factor4	Factor5
1	Ω	-0.8889	-0.2243	0.0915	-0.3143	-0.0562
2	La	-0.9356	0.0634	-0.0988	-0.0439	-0.1679
3	Dd	0.2094	0.6024	0.2093	-0.7009	0.0685
4	μ	-0.9414	0.2367	0.1547	0.1339	0.0502
5	inR_A	0.1292	-0.2609	0.7283	0.0281	-0.1247
6	a_t	0.4676	-0.2505	0.7193	-0.0372	-0.1055
7	K_e	0.1108	0.5843	0.1447	-0.7328	0.0665
8	K_i	0.5414	0.7734	0.0205	-0.0333	0.0711
9	ϕ_k	0.4590	0.6689	-0.0051	-0.0207	-0.4938
10	R_B	-0.2625	0.1889	0.2632	0.2097	-0.0793
11	R_L	-0.0395	0.2191	-0.5632	0.0644	-0.0009
12	R_{AR}	-0.2046	0.1122	-0.6851	-0.0028	0.1140
13	Fs	0.1022	0.2247	0.3013	-0.5756	0.6705
14	$H\mu$	0.7462	0.4150	0.0492	0.4879	0.0497
15	K	-0.2369	-0.5449	0.0509	0.2598	0.6519
16	P_S	-0.0465	-0.1479	0.2901	0.1556	-0.1276
17	OCN	-0.8675	0.2302	0.1358	0.1218	-0.0011
18	$N_p(\mu)$	-0.6715	0.4657	0.3003	0.3995	0.1011
19	D_{obs}	-0.9496	0.0631	-0.0149	-0.0440	0.0249
20	D_{cal}	-0.9871	0.0487	0.0319	-0.0607	0.0189
21	$N_d(\mu)$	-0.7695	0.4551	0.1804	0.3645	0.0829
22	$TPLC$	-0.9414	0.2367	0.1547	0.1339	0.0502
23	$TDCN$	-0.5292	0.3485	0.3474	0.3208	0.1021
24	$p(\mu)$	0.6592	0.4721	0.0136	0.5319	0.0625
25	E	0.3577	-0.2755	0.6671	-0.0543	-0.1895
26	Isd	-0.9200	0.0748	0.0712	-0.1980	-0.1013
27	ε	-0.8086	-0.2021	-0.1525	-0.2852	-0.4022

Table 3.3 Main factor coordinates (representing 80% of the accumulative eigenvalues) of the 27 geomorphometrical indices used in the principle component analysis (PCA) analysis. Shaded values describe the highest weight effect of parameters within each factor.

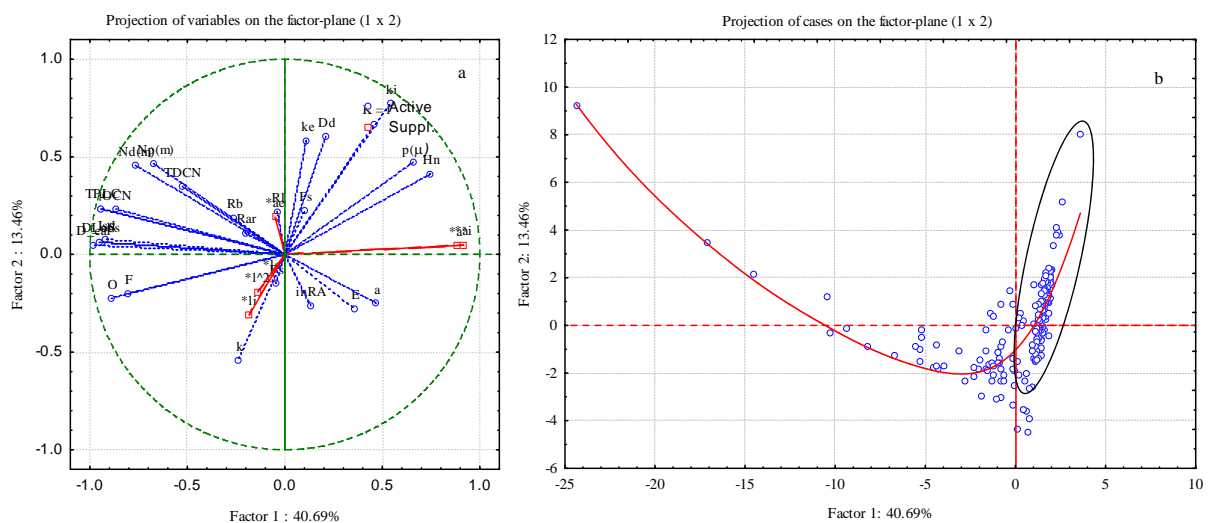


Figure 3.8 Projection of factor coordinates (1 & 2) in relation to a) variables and b) cases.

Thus, results of the *PCA* realized for basin catchments above and below 1 km^2 (more than 93% of these scales are one order drainage networks) revealed different distributions for case coordinates (figure 3.9). Figure 3.9 underline two aspects in relation to catchment size: first, the distribution of cases in small basins (i.e. catchments $< 1 \text{ km}^2$) is homogeneous between coordinates (figure 3.9a) indicating equal effect between factors; second, in large basins (i.e. $> 1 \text{ km}^2$) a cluster representation is still found between cases with convex fit curve model (figure 3.9b). This is exactly the contrary to the *PCA* where cases are not separated in relation to scale and concave relationship fit is detached (figure 3.8b). Not only cases variability is altered, but also loading weight of indices in each factor is changed in relation to basin size (table 3.4). The direct comparison between results of *PCA* carried out based on basin size (tables 3.3 & 3.4) shows that not only the weight of the parameter is changed within the factor itself, but also is moved from one factor to another (e.g. R_B , k_e , and k_i). Such findings confirm the useless of using the highest loading parameter on the factor as a representative index. These results underline the importance of scale dimension on the form and type in which the geomorphometric properties are applied in the comparison between catchments.

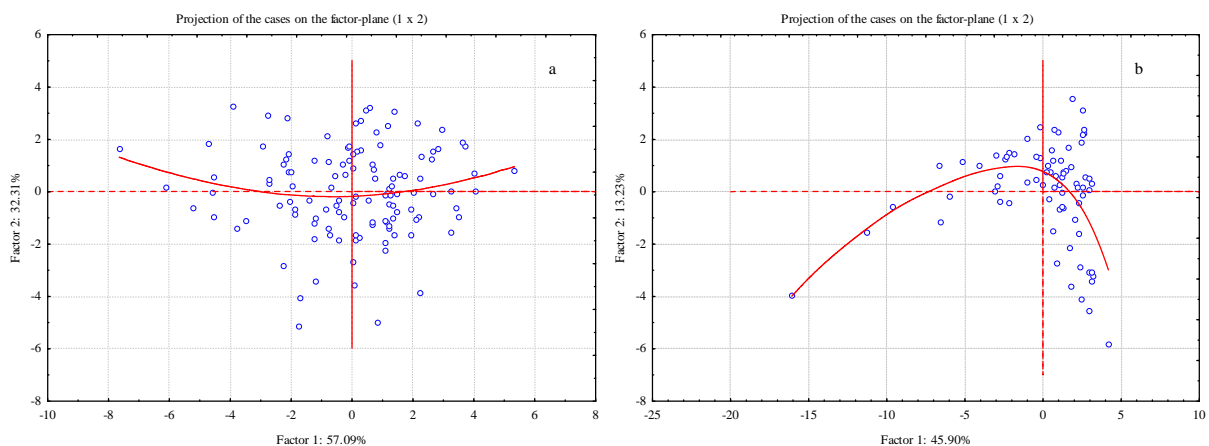


Figure 3.9 Projection of factor coordinates (1 & 2) in relation to cases, a) below 1 km^2 ; and c) above 1 km^2 .

A close inspection to the factors of the eigenvalues matrix underlines a great influence of the geometric, topologic and fractal parameters in the first factor indicating similarity effect in the final drainage network structure. The importance of such effect should not be ignored, for which representative parameters of each property must be included in order to ensure a subjective representation of the drainage network characteristics. The second factor characterizes parts of density properties, K_i and ϕ_k . The third factor describes Horton ratios, average link length and area ratios, Exceedence probability slope and E index. All these index, in general describe the complex structure formation of the stream system in relation to link and area properties. The fourth factor describes drainage network density properties, both general and macroscopic of exterior links. The fifth is related to stream frequency and Melton ratio; both are inter-related in the formation of Melton's law.

No.	Index	Factor1	Factor2	Factor3	Factor4	Factor5
1	Ω	-0.9156	0.2610	0.0561	0.0264	0.1806
2	La	-0.9109	-0.1666	-0.1013	-0.0124	-0.1489
3	Dd	-0.0923	0.5670	-0.3112	0.7269	-0.0503
4	μ	-0.9353	-0.2790	0.1205	0.1190	-0.0426
5	inR_A	0.1137	0.2176	0.7449	0.1598	-0.3345
6	a_t	0.4901	0.2294	0.6634	0.3073	0.2235
7	K_e	-0.1951	0.5763	-0.3756	0.6122	-0.0979
8	K_i	0.5968	-0.5823	-0.3008	0.3793	-0.0491
9	ϕ_k	0.5222	-0.4995	-0.2003	0.4885	-0.1923
10	R_B	-0.2890	-0.2684	0.2132	0.1677	0.5527
11	R_L	0.0010	-0.2610	-0.5510	-0.0533	0.4993
12	R_{AR}	-0.1800	-0.0906	-0.6063	-0.3582	-0.3498
13	F_s	-0.2905	0.7569	-0.0713	0.3152	-0.0209
14	$H\mu$	0.7495	-0.6028	0.0979	0.1296	-0.0899
15	K	-0.3079	0.1874	0.3445	-0.6727	0.1415
16	P_s	-0.0473	-0.0385	0.3809	-0.2008	-0.3689
17	OCN	-0.8564	-0.2700	0.0981	0.1256	-0.0094
18	$N_p(\mu)$	-0.7022	-0.5098	0.2388	0.2768	0.0420
19	D_{obs}	-0.9436	-0.0930	-0.0173	-0.0592	-0.1885
20	D_{cal}	-0.9878	-0.0720	0.0167	-0.0052	-0.0729
21	$N_d(\mu)$	-0.8092	-0.5075	0.1492	0.1636	-0.0879
22	$TPLC$	-0.9353	-0.2790	0.1205	0.1190	-0.0426
23	$TDCN$	-0.5310	-0.3723	0.2724	0.3132	0.2116
24	$p(\mu)$	0.6302	-0.7036	0.0672	0.0999	-0.1562
25	E	0.3768	0.2530	0.6573	0.2190	-0.0507
26	Isd	-0.9247	0.0181	-0.0048	0.1314	-0.0430
27	ε	-0.8755	0.1786	-0.1855	-0.0561	-0.0672

Table 3.4 Main factor coordinates (representing 82.3% of the accumulative eigenvalues) of the 27 geomorphometrical indices used in the principle component analysis (PCA) analysis with basin size > 1km². Shaded values describe the highest weight effect of parameters within each factor.

In view of that, factor coordinates were used as a classificatory line between the geomorphometrical parameters. From one hand, for factors that explain one loading parameter, the geomorphometric index was used directly as representative of particular property. On the other hand, factors that contain more than one descriptor, similar geomorphometrical descriptors were grouped in relation to their property (e.g. geometric, topologic, etc.), for which selection of the representative index was determined by Kendall tau correlation coefficient. Thus, highly correlated indices have been grouped and one representing parameter is selected.

Applying such procedure to the resulted factors of table (3.3), the following interpretations are achieved. In the first factor, the different properties are grouped and tested. First, the topologic properties showed high significant correlation (table 3.5) between all indices. All correlations are positive with the exception of $p(\mu)$, which indicates a negative correlation coefficient with all

parameters. Hence, u and $p(\mu)$ were selected to represent this category. Second, geometric properties of Ω and La maintained non significant correlation (i.e. with $p = 0.0263$), for which both are selected. Third, the rest of indices were selected directly since they describe different properties of the stream network.

μ	$N_p(\mu)$	D_{obs}	D_{cal}	$N_d(\mu)$	$TPLC$	$TDCN$	$p(\mu)$
1.0000	0.5964	0.9969	1.0000	0.8934	1.0000	0.8620	-0.9997
	1.0000	0.5878	0.5964	0.8934	0.5964	0.5898	-0.5955
		1.0000	0.9969	0.8803	0.9969	0.8583	-0.9966
			1.0000	0.8934	1.0000	0.8620	-0.9997
				1.0000	0.8934	0.8706	-0.8921
					1.0000	0.8620	-0.9997
						1.0000	-0.8617
							1.0000

Figure 3.5 Correlation matrix for the topologic properties in the first factor. Shaded values indicated significance at $p < 0.01$.

The second factor includes density properties of K_i and ϕ_k , from which the first attribute has been selected as representative one. In the third factor, E and P_S were selected directly, whereas the rest was tested with the correlation coefficient (table 3.6). This factor includes Horton laws, as well as ratios of average exterior and interior link lengths and areas (inR_A , a_t , respectively). Length, area and general area ratios are significantly correlated with the rest of the parameters, and hence were dropped down from the matrix analysis. In the fourth factor general drainage density was privileged over the macroscopic interior link density. Factor five describes different properties and hence both parameters are included directly. Finally, the independent parameters and low correlated ones were selected and organized (table 3.7), which cover a broad range of stream network structure properties.

inR_A	a_t	R_B	R_L	R_{AR}
1.0000	0.3988	0.0648	-0.7838	-0.3144
	1.0000	0.2503	-0.2888	-0.7505
		1.0000	0.0172	-0.3819
			1.0000	0.3036
				1.0000

Figure 3.6 Correlation matrix between attributes of the third factor. Shaded values indicated significance at $p < 0.01$.

Thus by using the above approach, it has been possible to reduce the battery of geomorphometric indices to 16 representative parameters, which completely describe the main drainage network properties. In particular, the 5 factors of the *PCA* may be considered as an objective summarization of the underlying dimensions of stream network characterization. Of course, the attributes included in any analysis depends on the nature of the problem under investigation. Herein, and since the general aim of the present study is delineation of stream network from DEMs, such matrix will be used mainly for the comparison between different streams of varying structures and origin.

No.	Geomorphometrical Index	Symbol
1	Drainage network order	Ω
2	Drainage density	Dd
3	Longest stream network	La
4	Magnitude of the drainage network	μ
5	Ratio of average stream length	inR_A
6	Macroscopic interior link density	K_i
7	Bifurcation ratio	R_B
8	Channel network frequency	F_S
9	Hack theory value	H_μ
10	Melton ratio	k
11	Exceedence probability slope	P_S
12	Optimal channel network or catchment energy	OCN
13	Probability of drawing a link of magnitude μ	$p(\mu)$
14	Jarvis index	E
15	Stream network development index	Isd
16	Fractal value of the channel network	ε

Table 3.7 Indices used in the comparison test between *BLs* and channel networks defined from DEMs.

3.4.4. Conclusions

This work shows that there is a clear need for a methodological approach for quantitative description and analysis of drainage basin morphology. This is usually has been achieved by using the geomorphometrical attributes that describe parts or total characteristics of the drainage network system. In general, these indices have been characterized by a considerable amount of redundancy and strong autocorrelation, because they describe similar properties. Hence, and in order to simplify the complex inter-relationships between these parameters, scientists used factorial analytical approach to identify the basic underlying dimensions. Mainly, they selected the highest loading parameter on the factor as a representing parameter. This study has demonstrated that this approach is somewhat erratic and unreliable, because parameters weight and presence in each factor is highly sensitive to scale dimensions of the catchment basin. This is attributed mainly to first order streams, which provides similar variability between various properties (e.g. order and magnitude).

In order to avoid such inconveniences, this study propose a new approach for geomorphometric index selection based on the combination of multivariate statistical technique and a complementary correlation test. The selection of the indices in this approach includes a purely objective procedure and some subjectivity. First, a principle component analysis (*PCA*) is used to define the major line variability that characterizes the drainage network under study, herein the factors of the *PCA*. Second, in each factor similar morphometric properties are grouped and tested by a correlation analysis, whereas single variables was included directly in the final parameter matrix. By

doing this, the geomorphometric properties maintain a more coherent approach for drainage networks comparison and analysis. In addition, this study underlines the need for deeper understanding on scale effect and mode of comparison between hydrological units.

In general, the results of this approach indicate that drainage network morphology can be quite fully described and simulated by measurement and analysis of reduced number of indices. The parameters in table (3.7) describe the main structure properties of the drainage networks, which include geometric, topologic, fractality, optimality, and self organization. The hydrologic and geomorphic relevance of these parameters are well documented. While in some cases few parameters may achieve significant conclusions, a wide range of descriptors is desirable in fluvial systems description, because the geomorphometric indices are specialized direct parameters that describe one structure property.

Chapter 4

AUTOMATIC STREAM NETWORK DELINEATION FROM DEMS

4.1. General revision

Advents in the last decades, mainly digital interpretation of cartographic data, have provided new tools and devices for channel network extraction and delineation, which opened the gates for a more efficient research and results with new dimensions and concepts. The widespread of digital representation of surface relief, mainly Digital Elevation Models (DEMs), has made it possible objectively extract, calculate and store geomorphological parameters for hydrological modelling at several scales (Gyasi-Agyei et al., 1995). Their utilities are not limited to the explicit information that they contain (i.e. elevation), but it extends to the spatial relations between their datasets (i.e. implicit information), giving rise to unlimited use in almost all landscape disciplines (Felicísimo, 1996). For channel networks, deeper insight into the structure, both planar and three-dimensional, of large channel networks, and hence corresponding catchment areas, has been gained after the introduction of DEMs (Rodríguez-Iturbe & Rinaldo, 1997). In particular, the analysis of large river networks obtained from DEMs has made it possible to acquire a completely new set of statistical analysis aimed at the determination of scaling properties of the observation made in the field (e.g. Grayson & Blöschl, 2000).

Defining topographic and geomorphic information has evolved from manual methods to automatic ones with the availability of DEMs (e.g. Gandolfi & Bischetti, 1997). Topography defines the effects of gravity on the movement of water and sediments in hydrological basins, for so DEMs play a considerable role in hydrologic simulation, soil erosion and landscape-evolution modelling (Zhang et al., 1999). Principle uses of DEMs in hydrology include the quantitative description of geomorphological characteristics of catchments (e.g. drainage density, runoff areas, etc.), identification of topographic variables, enhancement of hydrological models, and the integration of geomorphological parameters in landscape evolution models at different scales (Quinn et al., 1991; Tarboton et al., 1991, 1992; Montgomery & Dietrich, 1992; Gyasi-Agyei et al., 1995; Da Ros & Borga, 1997; Tarboton & Ames, 2001).

Among researchers, it is widely acceptable to distinguish two distinct periods in relation to channel network delineation: they are before and after DEMs application. The first period corresponds to the use of traditional methods and based on the manual derivation of topographic structures. Channel and streams networks are not an exception and always represented in this approach by continued lines, known as “blue lines (*BLs*)”. The second age is attributed to the digital representation of surface landforms and cartographic data, which is culminated by the invention and construction of

DEMs. The earliest ideas on using DEMs data to delineate channel network were based upon using local surface properties to look for a part of the topographic surface that is locally concave upward, and mark this position as a valley or drainage network, presuming that it is where surface water runoff is likely to be concentrated (e.g. Peucker & Douglas, 1975). At the beginnings of the eighties of the past century a more physically nature-justifiable method had been introduced to the studies of channel networks definitions (e.g. O'Callaghan & Mark, 1984, Jenson & Domingue, 1988). Both approaches have extended to comprise the vast majority of today published works that deals with automatic derivation and delineation of channel and stream networks.

Herein, and throughout the coming paragraphs we will provide a comprehensive description for channel network delineation, both automatic and manual ones, as well as principle algorithms used to define channel network limits and extensions. Currently, and as mentioned earlier, streams and channel networks may be derived in two basic forms: the traditional approach (manual derivation) and the objective approach (automatic derivation).

4.2. Manual derivation of channel networks

In earliest approaches for channel network delineation, features would either have to be measured directly in the field or derived from secondary sources, e.g. digitizing from topographic map or aerial photographs and stereo images. Nearly, most of the hydrological and geomorphological aspects of channel and stream network studies (e.g. patterns and forms, evolution, morphometry, etc.) are based upon such extraction (Abrahams, 1984a).

When using topographic maps, channel network can be derived from the *BLs* or inferred from contour line crenulations in the convergent topography. The accuracy of the drainage network derived from the *BLs* depends on different factors, which includes the scale of the map source and the quality of original surveying, the dynamism of the network itself, landform/relieve contrasts, and finally to large extent on the subjectivity of the cartographer. Wood (1996a) highlighted the temporality of ephemeral streams, where networks with such channels may have particular symbolic representations (e.g. USGS 1:24000 topographic maps), or they may not be distinguished from permanent streams (e.g. Ordnance Survey 1:50000). If an alternative measure of drainage density is required, contour data may be examined so that channel form may be extracted. Moreover, the accuracy of contour maps as sources of detailed channel networks information, mainly external streams, has been questioned either because the accuracy of the contours themselves may be questionable (Wood, 1993) or because there can be varying interpretations of the same contour data (Horton, 1945; Strahler, 1952a; Shreve, 1966; etc.), and whether or not contour crenulations should be included in the network is a visual interpretation and a pure subjective judgment that has no quantitative rules (Mark, 1983).

Different authors (Melton, 1957; Lubowe, 1964; Coffman et al., 1972; Shreve, 1974; Mark, 1983) have proposed quantitative approaches for *BLs* definition from contour-line crenulations, and

the expected results were not fruitful since the general extracted models were rather more appropriate to specific locations or areas (e.g. Mark's model for the Appalachian Plateau in USA). Nowadays, the subjectivity and the experience of the cartographer still play a significant role in the definition of the *BLs*, regardless of the advances in auxiliary tools and materials (e.g. highly resolution aerial photographs, 3D and GIS programs). Several studies have demonstrated that *BLs* networks from topographic maps miss a substantial proportion of first-, second, or even third-order streams (Morisawa, 1957; Coates, 1958; Montgomery & Foulfoula-Georgiou, 1993). Moreover, two or three topographic maps of different scales may be available for a particular catchment and the geomorphological parameters estimated from these maps may lead to an erroneous conclusion about the scale effects on these parameters (Gyasi-Agyei et al., 1995). Hence, the use of *BLs* as a unique source of information over available drainage network properties implies a certain risk that should be taken into account and handled by the use of complementary information (e.g. field studies, stereo images, etc.).

4.3. Automatic derivation of channel networks

Limitations and subjectivity of manual procedures in stream network definition highlighted the need for a more precise and efficient approach in depicting landscape dissection. The widespread of digital data (e.g. DEMs, Radar, Stereo photogrammetry, LiDER, etc.) has opened new gates for a more objective approaches for channel network delineation. In the present work, efforts are highlighted on DEMs as the basic unit for drainage network definition since it forms the overwhelming majority used data in GIS packages. In this direction, advents in DEMs have allowed a systematic definition of channel networks using different techniques and methods. These approaches are based on basic knowledge of water redistribution in natural landscapes. Also, we believe that DEMs could provide more information upon landscape dissection than what we have today, as one of the core principles of science is to obtain the maximum advantage of the available information. This is because all the topographic information is implicitly contained by the DEM matrix itself. Furthermore, the accomplished studies by such approach provide a complete explicit assumptions and methods and, therefore are, less subjective and closer to the scientific methodology.

From the multitude of literature on automatic channel network extraction, it is possible to characterize all the methods according to five general approaches (Wood, 1990).

I- Topological/geometrical

In this approach the feature extraction techniques are analogous of Lam's (1983) point/area interpolation procedure. Both define the metric used for the source and target, in which interpolation the source and target are either 0-dimensional point space or 2-dimensional surface space (Wood, 1996a). Accordingly, in channel network extraction the target is either n-dimensional space or a more abstract topological 'space'. Early topographers (e.g. Cayley, 1859; Maxwell, 1870) recognized that

surface model contains important topological information that could characterize a surface. They reported how any contour map describing surface forms contain a set of important topological relationships between summits (local maxima), immits (local minima), bars (lowest point dividing two immits) and passes (lowest two points dividing two summits). From the topological connectivity of these point locations, the line features of water-courses and watersheds, as well as the area features of hills and dales could all be delimited. Wolf (1991) used the more standard classification of surface topology by modelling connectivity relationships of topological forms using graph theory. Thus the topology of any surface could be described using a weighted surface network of pits, peaks and passes connected by ridges and channels (Mackness & Beard, 1993).

The drawback of this approach resides in the difficulties in the conversion between topological and geomorphological representation of channel networks (Wood, 1990). Hence, the fragmentation of the networks produced by many of the geomorphic techniques (e.g. Peucker & Douglas, 1974; Toriwaki & Fukumura, 1978; Band, 1986) makes the identification of topological relationships difficult (Wood, 1996b). Two categories of solution to this problem have been adapted. Hutchinson (1989) described a method of interpolating elevation using a drainage enforcement algorithm to force hydrological connectivity. This is done by identifying peaks and passes and forcing topological connectivity via channels that contains no pit. The other category adapted by many more researchers (e.g. Band, 1986) is to force topological connectivity after the process-deriving channel network. This may be in the form of line thinning (Skidmore, 1990), line joining and elimination (Wood, 1990), or/and the combination of external data sources (Vogt et al., 2003).

II- Local/global

The classification is made between three levels of operation. First, local extraction routines are realized by using a fixed window size that is less than the size of the entire surface mode (e.g. Band, 1986). Second, a quasi-local approach uses an adaptive local window size, which may be changed according to the characteristics of the surface mode (e.g. Jensen & Domingue, 1988; Skidmore, 1990). Third, a global routine approach is applied that uses information from the entire surface model for the extraction of terrain landforms (e.g. Band & Wood, 1988; Band, 1989).

III- Approximation/exact

Such approach is realized through distinct interpolation processes to the different parts of the terrain. The exact interpolation will emphasize all source values such that spatially coincident source and targets will have identical values. Approximate interpolation may result in deviation between the source and the target. In hydrological feature extraction, all methods use some kind of morphometric characterization, where it is possible to distinguish between approximate and exact interpolators (e.g. Evans, 1979).

IV- *Indirect/direct*

In this approach, hydrological feature extraction from DEMs is realized by two procedures. The first one comprises the identification and measurements (e.g. channel cross-section) of the target-morphometry. The second consists of the association of target features with some other set of properties, which can be in turn related to morphometry. Wood (1996a) detected a probable loss of analogy in this approach that emerges with the distinction between deterministic and stochastic interpolation method. If the source and target values are both morphometric, it is possible to invoke a deterministic relationship between the two.

In drainage channel network fluvial convergent processes are dominated over hillslope divergent processes. Indeed, if it is possible to determine fluvial and hillslope processes then drainage channel networks can be (indirectly) identified (e.g. Montgomery & Dietrich 1988, 1989, 1992). Such methods are desirable when morphometry alone is not sufficient to characterize hydrology because other factors, which may vary spatially, have significant importance in hydrological modelling (Beven, 1995). The morphometric definition of relieve landforms could play a noteworthy role in this case. For example, if drainage divides are relatively unambiguous in terms of their hydrological function, but may not be well expressed as morphometric ridge features (Wood, 1996a). Conversely, channel networks may have a strong morphometric expression but have a widely varying hydrological role (e.g. heavily dissected badlands in semi arid environment).

V- *Recursive/systematic*

This approach may be described as a way in which the feature extraction is applied spatially over the surface model (Wood, 1996a). Systematic approach proceeds in some orderly way that is entirely independent of the characteristics of the source. Recursive ones are those which traverse the source in a pattern determined by the source itself. The parallel in the recursive approach can be drawn with the gradual/abrupt distinction of Lam (1983). So, gradual interpolation applies the same rules over the entire source whereas abrupt interpolation can involve the application of different points determined by barriers in the source (e.g. Band, 1989).

The above mentioned approaches summarize almost all methods and procedures employed in determining channel and valley positions in the landscape. From which, attention will be paid to the global/local approaches, mainly Band's (1986) and O'Callaghan and Mark's (1984) methods, given that the vast majority of the subsequent proposed algorithms are considered as derivatives or enhancement of these two methods (e.g. Tribe, 1992; Bischeltti et al., 1998).

It is important to underline that the global/local approaches, represented by Band's and O'Callaghan and Mark's methods, verify channel network and valley location in relation to water concentration in the topographic surface. However, streams and channel network limits are defined by a threshold point that determine where channels begin in the landscape, widely known as the "*specific*

threshold area or threshold support area” and will be symbolized as (A_S). It is the essence of this work the selection of the appropriate A_S . The selection of the optimum A_S has been the battlefield between scientists, since A_S value affects directly the final results of predicted hydrologic and geomorphologic models (e.g. Hancock, 2005). The majority of the proposed methods assume A_S as a constant value, and evaluated its validity in a qualitative and quantitative form in judgment to the *BLs* generated from topographic maps (Zevenberguen & Thorn, 1987; Jenson & Domingue, 1988; Band, 1989). The accuracy of *BLs*, although form a basic reference for hydrologists and geomorphologists, depends a lot on personal judgments (Gandolfi & Bischetti, 1997) and shows significant discrepancies from field observed networks when compared with high- and medium-scale maps (Mark, 1983). The choice of the appropriate A_S used to define the optimum channel network is highly related to the scale and resolution of the original data (e.g. Walker & Willgoose, 1999; Thompson et al., 2001).

Fever for optimum A_S extraction has led researchers to improve the automatic approaches for landscape dissection, in relation to usefulness and availability of environmental conditions (i.e. local factors). Thus, two main branches for the automatic delineation of channel networks from DEMs have been evolved: The first group uses DEMs data with no reference to local factors (e.g. Band, 1986; O’Callaghan & Mark 1984; Skidmore, 1990; Tribe 1991, 1992; Tarboton et al., 1991, 1992; Bischetti et al., 1998). The second group incorporates local factors as correction parameters in the delineation process (Abrahams, 1984a; Montgomery & Dietrich, 1989, 1991; Dietrich et al., 1992, 1993; Tucker & Slingerland, 1996; Tucker & Bars, 1998; Vogt et al., 2003). The above approaches correspond to the following hypothetical concerns: first, if DEMs own sufficient information to represent landform structure, and hence channel networks; and, the second is the availability of data that allows for local-factors definition (i.e. climate, runoff and soil erosion, vegetation cover, relief, etc.). The first concern is related to the scale and resolution of the DEM, that is, the availability of the appropriate resolution that describes available features and hence dominant processes in the landscape (e.g. badlands landscapes, plains or deserted landscapes). The second concern is the most common, since in many cases availability of preceding data is limited to concrete sites and locations (i.e. experimental field sites), as well as large scale studies over vast areas delimit the accessibility of local data. For so, it is important to keep in mind the dimension, type and availability of data in the model approach, in order to achieve the best approximation to natural rivers and streams. In the two approaches, the way of using the DEM-data consists of four main steps:

- i. Data training (DEM filling depressions)
- ii. Determining flow direction
- iii. Valley and drainage network delineation, i.e. verify channel network and valley location in the landscape;
- iv. Finally, definition of the appropriate A_S that determines where channels begin in the landscape.

Generally, the above mentioned steps are the most widely used in hydrological and geomorphological studies, and are the basic procedure to follow for automatic delineation of stream and channel networks. In the next paragraphs, these steps will be highlighted and explained in relation to the main approaches of O'Callaghan and Mark and Band.

4.3.1. O'Callaghan and Mark's method

O'Callaghan and Mark (1984) have described a simple physically-foremost algorithm for ridge and channel network delineation from digital-gridded data of DEMs. In which, the proposed algorithm quantifies the drainage accumulation (which can be thought of as the approximate volume of surface and subsurface water flow) at each grid cell in the DEM. Cells which had a drainage accumulation above a user-specific threshold (A_S) were considered to be on a drainage channel. Jenson and Domingue (1988) enhanced O'Callaghan and Mark's method in order to achieve faster and more operational viability in drainage basins and channel networks definition. Mathematically speaking, stream channel can be determined by using a simple Boolean operator such as:

$$\text{Streams} = \text{if (upstream elements} \geq N \text{ then 1 else 0)} \quad 4.1$$

where N is the number of upstream cells

This method has been widely used between scientists because of its simplicity and efficiency. However, one of its main inconveniences is the high susceptibility of the method used to define flow direction, which may influence the final channel network structure form and properties. In general, the main lines of this method consist of five main steps that are of general utility for all subsequent steps. These are, in the order that they are produced, a depressionless DEM, a data set indicating the flow direction for each cell, a flow accumulation dataset in which each cell receives a value equal to the total number of cells that drain to it, and finally stream limits delineation based on A_S value.

- *Pit removal (filling depressions):* A pit is defined as a point (e.g. cell) or set of adjacent points surrounded by neighbours that have higher elevations, and acts as sinks to overland flow. In general, DEMs almost always contain depressions that hinder flow direction (Jenson & Domingue, 1988). Some depressions are attributed to natural features, e.g. recently glaciated or karst landscape (Band, 1989) or excavations (Jenson & Domingue, 1988; Hutchinson 1989), but more often artefacts that arise from input data errors, interpolation procedures and the limited horizontal and vertical resolution of the DEM (e.g. Mark, 1984; Jenson & Domingue, 1988; Tribe, 1992; Felicísimo, 1994). Several algorithms have been proposed to solve depression-artefact areas that differ slightly in the applied algorithms (Tribe, 1991); for example Band (1989) used recursive algorithms, whereas O'Callaghan & Mark (1984) used iterative ones.

Pit definition and treatment aims to generate a depressionless DEM that allows for hydrological connectivity in the data matrix, in which the cells contained in depressions are raised to the lowest elevation value on the rim of the depression. Accordingly, in the special case where flow

route is of interest within a depression, the original DEM values would be used rather than the depressionless DEM, and the flow paths with the depression would terminate at the bottom of the depression rather than at the basin outlet (Jenson & Domingue, 1988). The same problem arises in flat areas (depression areas), also considered as spurious features and attributed to data errors and limitations of DEM resolution (Martz & Garbrecht, 1998). Several algorithms have been proposed to treat this problem (Mark, 1983; Jenson & Domingue, 1988; Martz & Garbrecht, 1992). In our work, depressions and flat areas were treated using the method of Martz and Garbrecht (1998), because it provides a more realistic approximation of depressions and flat area treatment. This method combines depression breaching and filling to remove spurious sinks from a DEM. The breaching is used to eliminate or reduce depressions that can reasonably be expected to have resulted from elevation over estimation. While, for drainage direction over flat areas, the method uses information on the surrounding topography and allows flow convergence within such area.

- *Definition of drainage direction matrix (flow directions):* Flow direction is one of the basic hydrology-related parameter. A drainage direction matrix is a set of pointers that assign flow from each grid cell or pixel to one of its eight nearest neighbours, either adjacent or diagonally, in the direction with steepest downward slope. This method, designated (*D8*) algorithm, was early introduced by O'Callaghan and Mark (1984) and has been widely used in hydrology to determine the paths of water, sediment and contaminant movement. The algorithm is based on the flow of water over the terrain in the direction of steepest slope and is a computed version of the catchment area measurement (Speight, 1974). Problems of this approach arise from the discretization mode of flow into only one of eight possible directions (e.g. Quinn et al., 1991) and it's tend to produce parallel lines along preferred directions (Moore et al., 1993). A number of other single-neighbour algorithms have been published. *Rho8* (Fairfield & Leymarie, 1991) is a stochastic extension of *D8* in which a degree of randomness is introduced into the assignment of flow directions in order to reduce the grid bias. The drawback of this method is that, especially for small catchments, it produces different results if applied several times (Gruber & Peckham, 2009). The aspect-driven *kinematic routing algorithm* (Lea, 1992) specifies flow direction continuously and assigns flow to cardinal cells in a way that traces longer flow lines with less grid bias than *D8*.

To overcome this problem a multiple flow direction (*D ∞*) approach has been proposed (e.g. Quinn et al., 1991; Freeman, 1991; Lea 1992; Costa-Cabral & Burges, 1994, Tarboton, 1997) that allows flow divergence to be presented. These algorithms allocate flow fractionally to multiple nearest-neighbour node (Gallant & Wilson, 2000) in proportion to the slope (Quinn et al., 1995), or to the aspect associated to each cell (Lea 1992), or to the dimensional proportion originating uniformly over the pixel area (Costa-Cabral & Burges, 1994), or to the triangular facet (Tarboton, 1997). In this work, the focus is channel networks, where splitting, braiding or dispersing is not admitted, so the *D8* method was used.

- *Flow accumulation dataset:* This procedure makes use of the flow direction dataset to create the flow accumulation matrix, where each cell is assigned a value equal to the number of cells that drain to it. Moore et al., (1991) assigned it as upslope area which he defined as the total catchment area (contributing area) above a point or short length of contour. Contributing area, also known as *basin area*, is a planar area and not a surface area. It describes the spatial extent of a collecting area as seen from the sky. Cells having a flow accumulation value of zero (to which no other cells flow) generally correspond to ridge and divide formations (Jenson & Domingue, 1988).
- *Defining a constant threshold area (A_s):* A pixel or a value, at the flow accumulation matrix above which, the terrain is slope-dominated processes (hillslope) and down which fluvial-dominated processes (channel). In other words, the threshold area is the minimum drainage area required to drain to appoint for a channel to form. Neither O'Callaghan and Mark nor Jenson and Domingue provided an objective methodology for A_s selection rather they selected arbitrary values to define different stream limits.

4.3.2. Band's method

Band (1986) suggested the use of a non-constant specific threshold for the definition of ridge and channel network using the Peucker and Douglas (1975) algorithm, which consists of employing a set of local-parallel processing operators to flag upward concave and convex cells as potential stream and ridge points. This algorithm is related to the basic notion that convex pixels in the terrain are related to divergent processes and hence hillslope features, whereas concave ones are related to convergent processes and hence valleys and channel network formations (Kirkby & Chorley, 1967). The method of Band can be resumed in the following:

- *Cell nomination:* The first step in network construction is the applying of Peucker and Douglas' (1975) for marking convex and concave upward points as ridge and streams, respectively. The purpose of this step is to extract a set of segments that may serve as a basis to grow and connect the rest of the drainage system.
- *Thinning process:* The resulting cells of Peucker and Douglas' algorithm are a group of segments that categorize the relief forms to concave or convex forms. These segments could be found as fragmented, connected or forming more than one parallel line of cells. For so, thinning processes (i.e. operations refer to a set of topologic techniques in which parallel cells are eliminated if their deletion does not disconnect adjacent ones) are required. This is done to reduce the digital line to a connected, one-pixel wide chain of raster cells. The nominated segments and thinning to one-pixel-wide line using an iterative local-parallel processor preserving 8-connectedness, in which each iteration alternately considers only north, south, east, or west border point to deletion. Pixels are removed if and only if they are not end points and their removal will not disconnect a contiguous path of pixels.

- *Channel segment connection:* The next step searches for segment ends within the stream lines and labelled them as downstream or upstream nodes. This is done by starting at the segment end and moving along the segment until either another node is reached or a set number of cells have been traversed and then comparing elevations. Downstream nodes are then activated to begin draining successive lower cells until another stream segment is encountered. Differences in elevation of the neighbouring pixels are first adjusted for the variable distances to the centre cell based on position in the 3 x 3 kernel window and the variable cell dimensions of the digital elevation data, which is registered to geodetic, rather than rectangular grid.
- *Pit removal and fine cell thinning:* Pit removal is an essential process in hydrological connectivity and in Bands' method is realized during the preceding step. After that a second and fine thinning process is repeated again to the final, cell-wide-line representation of the stream network, in order to maintain the drainage line in the valley bottom.
- *Defining a threshold (A_S):* In Band's method the threshold point is more robust than the case of O'Callaghan and Mark's procedure, and can be defined as the point at which distinct runoff producing source areas must be explicitly located relative to the drainage network (Band, 1986). Indeed, this value is used to connect upstream grid cells resulted from the thinning process, which correspond to number of cells rather than accumulation area. Hence, the accumulation threshold in O'Callaghan and mark is constant and represent accumulation drainage area, whereas the Band's is variable and represents the number of grid cells that allows for a connection with adjacent segments and above which no connection is performed. Again, Band did not provide a methodological procedure for the definition of the appropriate A_S . Although, Band's method has shown good results in the majority of the studied sites (Band, 1986; Tarboton et al., 1991) mainly in abrupt terrains of high relief and slope, nonetheless in flat and smooth areas the algorithm is less efficient because the connection between segments relies heavily on the comparison of the maximum slope.

It is important to underline that the above two methods (Band and O'Colloghan and Mark) are in highly concurrence in defining the main channels and valleys in the drainage network, but with well inconsistency on lateral streams that connect hillslopes to major valleys. So, answering where channels begin in the landscape opened the debate between researchers on aptness of algorithms and procedures that best describe lateral streams (e.g. rills and gullies). Accordingly, researcher's efforts have been directed into the quantitative derivation of a suitable A_S value that best describes stream network limits in the landscape.

4.4. Threshold definition mode (Channel initiation)

Representation of stream sources or channel heads is of obvious importance and highlights the urgent need for procedures that replaces traditional and manual methods. The persistent problem of defining where channels begin on the hillslope and determining the physical extent of the drainage

network has shaped the appropriate mode for A_s definition. In general, using a constant A_s value for stream network delineation is a general accepted means of determining where channel begin in the landscape (e.g. O'Callaghan & Mark, 1984; Band, 1986; Montgomery & Dietrich, 1992). However, drainage density has been shown to vary between regions due to different climatic regimes, natural landscape characteristics, and land-use impacts (e.g. Gandolfi & Bischetti, 1997; Tucker & Bras, 1998). As mentioned earlier, identifying the headward extent of a drainage network by field methods is costly in terms of economics, time, and physical labour. In addition, assigning a constant critical support area disregards the spatial variability of headwater source areas may lead to significant differences between field observations and predicted conditions (Barling et al., 1994; Western et al., 1999; Willgoose & Perera, 2001).

The channel head represents the start of the drainage network and its location is influenced by the geomorphic processes and local factors of underlying bedrock, soil properties, climate regime, surface cover, slope characteristics, ground water interactions, and land use (Kirkby, 1976; Montgomery & Dietrich 1988, 1989; Martz & Garbrecht, 1992; Moore et al., 1993). These factors, in turn determine shape, form and structure of the prevailing drainage network system. Hence, meeting the challenge of locating channel heads is thus the key to accurate mapping of stream network (Heine et al., 2004). Thus, small errors in source area definition could lead to major modifications in the final stream network structure properties. Two general approaches have been proposed to explain landscape dissection, often expressed in terms of drainage density, in which channel network initiation and channel head locations can be mathematically described:

I- *Stability/instability approach:*

This concept is based on the transition from straight or convex hillslopes to concave valley forms, which represents a transition in process dominant. The constant critical support area was first proposed by Gilbert (1909) who argued that slope-dependent sediment transport on hillslopes gives rise to convex slopes, whereas discharge- and slope-dependant sediment transport in channels gives rise to concave profiles. The Gilbert's model was quantified in terms of linear stability analysis (Smith & Bretherton, 1972), and is based on the view that valleys form where convergence processes cause rill flow or gully excavation by runoff erosion to outpace infilling by diffusive processes such as rain splash. The instability model has been extended to include finite-scale effects (Loewenherz, 1991), length scale effect (Tarboton et al., 1992), and more general process laws (kirkby, 1993).

II- *Geomorphic threshold:*

Based on the concept that valley and channel formation is controlled by geomorphic thresholds (Schumm, 1973, 1977; Schumm et al., 1984). Process thresholds, mainly geomorphic ones that control landscape structure and drainage density may alternate between runoff-generation thresholds (e.g. Horton, 1945; Ijjász-Vásquez et al., 1992; Dietrich et al., 1993) or slope-stability

thresholds (Montgomery & Deitrich, 1989; Willgoose et al., 1991; Tarboton et al., 1992; Howard, 1994). This is based on the concept that channel heads is associated with a change in the sediment transport processes at a critical contributing area (A_s). The change essentially distinguishes between slope-dependent processes upslope of the channel head and discharge- and fluvial-dependent processes downslope of the channel head (Rodriguez-Iturbe & Rinaldo, 1997).

Herein, it is important to underline that geomorphic and stability theories need not be mutually exclusive (Tucker & Bras, 1998); rather, the two models constitute end-member cases, and any given landscape may be instability-dominated or threshold-dominated, depending on the climate, relief, geology, and stage of evolution (Kirkby, 1993). Both approaches highlight the existence of a critical point at which dominant transition processes are interchanged from convex hillslopes to concave valleys, and vice versa. But, application of these approaches implies differences in incorporating the local factors (e.g. climate, tectonics, lithology, relief, vegetation cover, land use) to the model approach. Accordingly, two general approaches have been used to simulate stream network sources from DEMs data: the first is represented by the slope-dependent critical support area (e.g. Dietrich et al., 1992, 1993), whereas the second is given by the constant threshold area (e.g. Tarboton et al., 1991). The former incorporates local factors and assumes that channel heads represent an erosional threshold area (Montgomery & Foulfoula-Georgiou, 1993), whereas the latter uses DEMs data solely and assumes that channel heads represent a transition in scale characteristics.

4.4.1. Automatic thresholds with local factors (indirect models)

This approach includes all mechanisms that relates soil erosion and runoff type to channel initiation as well as methods that incorporate distinct local and environmental factors, e.g. tectonics, lithology, relief, climates, etc. One of the main examples of such approaches is the slope-dependent critical support area method. Several researchers (e.g. Dietrich & Dune 1993; Dietrich et al., 1993) have shown that at the channel heads, there is typically a process change, upslope of which mass wasting and diffusive processes predominate and downslope of which runoff-driven incision occurs. Therefore, there appear to be a threshold of erosion resistance which sets the location of the channel head at a specific drainage area and local slope, and hence determines the extent of the channel network in the drainage basin (Willgoose et al., 1991). Such erosion threshold is specific to the particular mechanism controlling channel-initiation (e.g. overland flow, shallow landsliding, and seepage erosion) and is expressed in terms of the contributing drainage area and local ground surface slope.

For example, Montgomery and Foulfoula-Georgiou (1993) proposed two distinct models for channel initiation, based on Flint's power law relationship (1974), parameterized according to local dominant factors (e.g. runoff and erosion type, basal shear stress of the flow or critical shear stress of the ground surface, soil transmissivity, and bulk density of water and soil, etc.). For overland flow,

channel initiation may be assumed to occur where the basal shear stress of the flow (τ_b) exceeds the critical shear stress of the ground surface (τ_{cr}). In the case of a steady state rainfall intensity (q_r) and laminar flow model, the critical contributing area (A_{cr}) required for $\tau_b > \tau_{cr}$ is given by

$$A_{cr} = C / (\tan \theta)^2 \quad 4.2$$

where $C = f(\tau_{cr}^3, q_r^{-1})$, and θ is the local slope (Dietrich et al., 1993)

In consequence, channels may be defined using the criterion of $A(\tan \theta)^2 \geq C$, from Eq. (4.2). This means that channels on deeper slopes initiated with relatively smaller drainage areas. Likewise, channel initiation by shallow landsliding is derived from combining a model for shallow through-flow and the infinite slope stability model, in which (A_{cr}) is defined as

$$A_{cr} = (T / q_r) \sin \theta (\rho_s / \rho_w) [1 - (\tan \phi / \tan \theta)] \quad 4.3$$

where T is soil transmissivity, ρ_s and ρ_w are the bulk density of the soil and water, respectively. ϕ is the friction angle of the soil (Montgomery & Dietrich, 1994).

These threshold models predict systematic source area-slope relationships as presented in Figure 4.1.

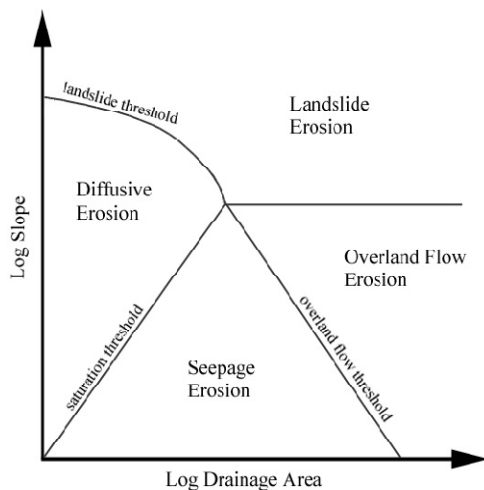


Figure 4.1 A Schematic representation of landscape dominant channel initiation processes in relation to source area-slope relationship (Montgomery & Dietrich, 1994).

Analytical models that couple steady-state hydrologic runoff with slope-stability laws predict area-slope relationships that reasonably correspond to field-based studies where landsliding and overland flow are the dominant controls on channel head locations (Dietrich et al. 1993; Bischetti et al. 1998; Vandekerckhove et al. 2000). Such threshold models, calibrated with field data, can be used to extract drainage networks from digital elevation data that reflect real landscape conditions (Gandolfi & Bischetti, 1997). Nevertheless, Montgomery & Foulfoula-Georgiou (1993) recognized that identification of an appropriate value for C is a major impediment to implement the overland flow model for channel network extraction from DEMs, as this parameter should vary with both rainfall and critical shear stress of the ground surface; the latter reflects both soil properties and vegetation-cover type and density. In addition, these algorithms provide reasonable estimates of hillslope lengths when

used with sufficient resolution, finer than 30 m. Moreover, even when best fit parameters for field observed channel heads were used to define slope dependent thresholds in the DEM algorithms the resulting drainage densities were too high (Bischetti et al., 1998). This is attributed to the highly spatial varying character of the critical shear stress of the ground surface.

Models of channel-initiation by the processes discussed above are expressed in terms of drainage area because this parameter serves as a surrogate for discharge under the assumption that flowpaths follow the ground-surface topography. However, there is a potential that the dominant hillslope flowpaths responsible for channel-initiation are not a function of the surface topography but instead are dependent on the topography of the underlying bedrock or are occurring within the bedrock itself (e.g. Beven & Kirkby, 1979; Montgomery et al., 1997; Freer et al., 2002). In cases of bedrock-controlled flowpaths, the discharge may not scale with the topographically defined drainage area, which would imply that an area-slope relationship may not exist for channel head locations. Consequently, an erosion threshold model cast in terms of drainage area to predict channel-initiation may be inappropriate in areas where the nature of the underlying bedrock controls flowpaths and strongly influences channel head locations (Jaeger, 2004).

Selecting the optimum A_S is a complicated task, since drainage channel formation is the final result of different physical-environment factors, such as climate, relief, tectonics, lithology, vegetation, land use, and stage of landscape evolution (Kirkby, 1993; Da Ros & Borga, 1997; Gandolfi & Bischetti, 1997; Vogt et al., 2003) and the capacity of the defined models to obtain an adequate A_S value that permits the extraction of the optimum channel network from the available scale and resolution. Thus, a unique A_S value in a widely varying landscape conditions could be of low suitability to reflect natural variability of drainage density. So, for a more precise delineation of stream limits, several researchers proposed complex models that integrate most local or physical factors to represent relief and climate variation. Such approaches could be viewed in two parallel forms: either by dividing the landscape according to available environmental conditions and then applying different A_S values, or integrating these conditions in the model approach (i.e. algorithm) as mentioned earlier in Eq. 4.2 and 4.3. For instance, Vogt et al. (2003) integrated 7 environmental factors in their model in order to extract the optimum channel network on a regional scale. They revealed that valley development (V) is the result of a functional relationship between environmental factors, expressed as the following:

$$V = f(C, R, Ve, I, S, P, T) \quad 4.4$$

where C stands for climate, R for relief factors, Ve vegetation cover, I for lithology and rock structure, S for the soil characteristics, P for the type of hillslope processes, and T for time.

Nevertheless, drainage network definition is still needed as a prior step in a lot of geomorphological and hydrological studies, for which such information is scarce or even not available. In other cases identifying erosion types or sediment transport processes is a tedious task,

mainly in heterogeneous landscapes, and its performance from the available models require the division of the area to different lithological classes, especially when using DEMs of high resolutions (e.g. <10m). Hence, the basic aim of the current work is the affirmation of the need for the automatic definition of channel headward extent a priori to landscape studies. Under this approach, local factors will be ignored and model improvement will be limited to DEM data solely.

4.4.2. Automatic thresholds without local factors (direct models)

The assumption of no priori information is available for landscape dissection would prompt on the adoption of direct models over indirect approaches, and hence accentuate all efforts on algorithms that use DEM data solely. The constant slope-area relationship is the widely common algorithm applied to define channel network limits in the landscape. As mentioned earlier, constant threshold area or constant critical support area (A_s) comes from early Gilbert (1909) notions that slope-dependent sediment transport on hillslopes gives rise to convex slopes, whereas discharge- and slope-dependent sediment transport in channels gives rise to concave slope profile. This hypothesis has been transformed into the proposition that channel heads correspond to the transition from convex to concave profile. Such theory predicts that channel heads is associated with a change in the relation between local slope and drainage area or discharge (e.g. Kirkby, 1971, 1986; Smith & Bretherton, 1972; Willgoose et al., 1991). Mathematically, the hypothesis consists of deriving an adjusted algorithm between the average slope of the fluvial segments and the draining area to these segments in the channel network extracted from arbitrary small threshold. The result of this relationship is a straight line revealing the consistency of scale variation between slope and corresponding drainage area (Tarboton et al., 1991, 1992). This variation can be expressed in a power-law relationship (e.g. Hack, 1957; Flint, 1974; Tarboton et al., 1989; Willgoose et al., 1991; Ibbitt et al., 1999) that relates local slope at any point along the channel (S) with its corresponding contributing area (A).

$$S = cA^{-\theta} \quad 4.5$$

where c is a constant and θ is a scaling coefficient

In a log-log plot of S against A , the transition from convex hillslopes to concave valleys is expressed by a characteristic change from a positive to negative trend. Tarboton et al., (1991) proposed to use the value of the A at this break as the critical contributing area (A_s). Tarboton and co-workers proposal depends on the fact that there is a basic scale where the slope-area breaks suggesting different processes above and below this break. They interpreted the break as the scale at which stability changes and hence can be used to determine drainage density threshold. Their model was basically to extract the highest resolution network that satisfies scaling laws that have been found to hold constant for channel networks (Horton, 1945; Schumm, 1956; Broscio, 1959; Flint, 1974; Gupta & Waymire, 1989; Tarboton et al., 1989, 1992). Such model corresponds at using the smallest A_s as the rational support area for which elevation related properties hold constant. To achieve this aim they

applied two techniques: the first is the power law scaling of Eq. 4.5; and the second is a constant drop analysis (*CDA*). The final results were almost similar for which they concluded that the two techniques are complements.

The first technique consists of the following operations: first, an arbitrary critical support area (A_S) is assumed, and a channel network is extracted from a DEM. Second, a plot of average slope is generated versus the drainage area at the downstream end of the link in the extracted channel networks. Finally, the individual values are averaged and the appropriate critical support area is determined from the inflection in the composite slope-drainage area relationship for the averaged data. The change of the direction in the curve relationship will indicate the change in scale properties. In order to objectively check for the breaking in scale Tarboton et al., used a two phase regression model (figure 4.2). Herein, the slope-area relationship maybe constructed either based on single channel profile, or based on the catchments. In the first case, the link of each segment en the channel network is analyzed (i.e. slope of the segment versus its drainage area). In the second case, the contributing area at each cell in the catchment is compared to its corresponding slope. Such knowledge was applied to the 30 m DEM of Tabernas basin and the results of the breaking points determined a threshold drainage area of 128 m², which clearly produce a drainage network of completely feathering aspect.

The second technique consists of choosing distinct A_S values objectively using the constant drop property (*CDP*) of Strahler streams. The basic concept of *CDP* law is based on that average drop of links along Strahler streams of order ω is approximately constant; that is, independent of order (Broscoe, 1959). In the constant drop analysis (*CDA*), the supported area threshold used to map channels is chosen objectively. The smallest support area threshold that produces a channel network where the mean drop in first order streams is not statistically different from the mean drop in higher order streams is selected. Stream drop is defined as the difference in elevation between the beginning and end of Strahler streams. The *CDP* is an empirical geomorphological attribute of properly graded drainage networks that has a physical basis in terms of geomorphological laws governing drainage network evolution (Strahler, 1956). Tarboton et al., (1991) argued that by using the smallest weighted support area that produces networks consistent with this property we are extracting the highest resolution drainage network statistically consistent with geomorphological laws. In order to find out if the drop of channel segments (highly variable) is independent of channel order, for which it coincides with the smallest A_S searched, Tarboton et al., (1991) used the t statistics (Eq. 4.6) for the comparison of means of different populations (Bayer, 1984) to compare the mean drop of streams of different orders (i.e. the difference in mean stream drop between the first and higher order streams). Accordingly, a random number of thresholds are used, and the smallest t value is selected between the significant values.

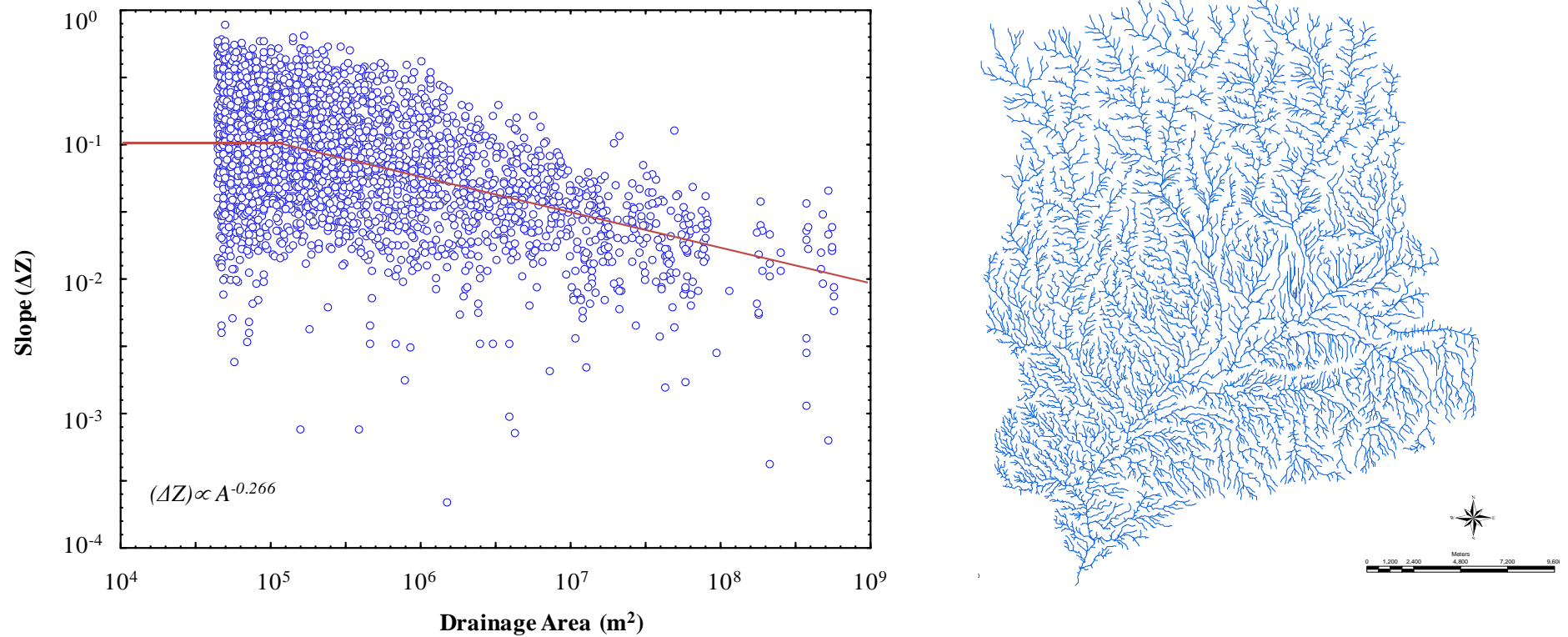


Figure 4.2 Slope-area relationship approach for stream network delineation; a) logarithmic Slope versus drainage area and two phase regression plot from all cells on 30 m DEM in Tabernas Basin; and b) drainage network extracted by a breaking point of 128 m (i.e. ≈ 6 cells).

$$t = \frac{\bar{x} - \bar{y}}{\sqrt{\frac{(n_x - 1)s_x^2 + (n_y - 1)s_y^2}{n_x + n_y - 2} \left(\frac{1}{n_x} + \frac{1}{n_y} \right)}} \quad 4.6$$

where \bar{x} and \bar{y} are the sample means, s_x and s_y are the sample variances, and n_x and n_y are the sample sizes of the two populations x and y .

Again, the CDA was applied to the 30 m DEM of Tabernas basin and the results of the breaking points determined a threshold drainage area of 128 m², which produce a drainage network of the main valley system (figure 4.3).

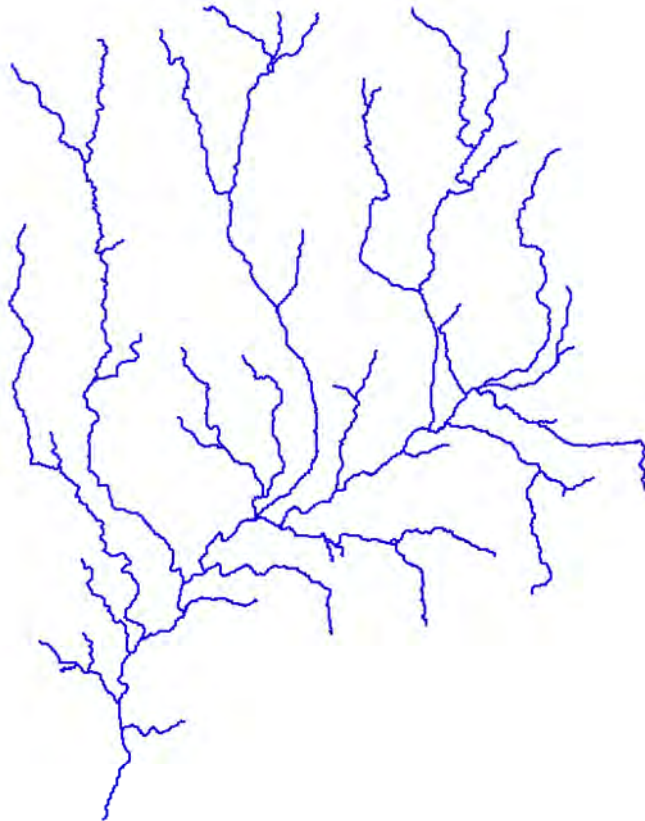


Figure 4.3 Channel networks extracted by the O'Callaghan and Mark's and delineated by the Constant Drop Analysis (CDA) approach in a 30 m DEM with a support area of 4000 cells.

The capacity of Tarboton's model has been widely criticized by researchers, e.g. Montgomery and Foufoula-Georgiou (1993) and Helmlinger et al., (1993), in which they demonstrated that A_S value defined by the above approaches is more appropriate for depicting hillslope/valley transition than for identifying channel heads; that is, the extent of divergent topography, or the hillslope scale. Moreover, the inflection in the drainage area-slope relation that one can infer from low-resolution DEM data is related to smoothing rather than the hillslope/valley transition (Dietrich et al., 1993). However, the implementation of this method to DEM-extracted channel networks has been inconclusive (Helmlinger et al., 1993) since, as Tarboton et al., (1989) pointed out, the slope-area scaling break was usually just a steepening of a negative slope and not a change from positive to negative slope as required by the theoretical stability analysis. Moreover, Garbrecht and Martz (2000) appointed out that an accurate estimation of local slope requires either a high-resolution DEM or field measurements,

since low-resolution DEMs (e.g. < 30 m) produces biased local slopes of approximately zero or increments thereof. Likewise, the *CDP* analysis endures the above critics and also undergoes additional involvements, where, in some cases, the selection of the smallest t between significant values were difficult, or even impossible, to achieve, mainly in small catchment, because small A_S values may generate streams of false extensions (feathering) that hamper the t value. Such result has been confirmed earlier by Peckham (1995) who found that *CDP* law only holds for regions with very homogeneous physiographic and humid climates. Indeed, the work of Tarboton and co-workers (1991, 1992, & 2001) in channel network delineation represents the best to data both for their geomorphic justification of stream initiation and for their improvements in predicting, and thus mapping, channel extensions and drainage channel networks. As well as facility to use and incorporation in GIS packages (ArcGIS, MapWindow, SAGA, RiverTools, etc).

In the same direction, researchers (e.g. Montgomery & Dietrich, 1988, 1992; Dietrich et al., 1992) have underlined the importance and the need for field calibration parameters in order to define the correlation between slope and drainage area in channel heads. They pointed out a dependence of A_S on the slope immediately upstream from the channel source (local slope) and proposed a power law relationship to determine the value of the threshold area as a function of the local slope in relation to climate, tectonics and lithology. They concluded that local parameters (climate, tectonics, vegetation, etc.) are important and necessary in determining the perfect power law relationship and corresponding scale dimension. In addition, and most important, evidence of their studies has suggested that A_S is not constant in a basin but is a function of the local valley slope (the slope immediately upstream of the channel source in the unchanneled valley) and therefore may vary within a basin. Furthermore, the fractal implication of the scaling structure of Eq. 4.5 that varies from basin to basin (where θ is observed in the range of 0.4-0.78; Tarboton et al., 1989) has important theoretical implications because it impairs simple scaling models of slope versus area. Such premise suggests that instead the behaviour is multiscaling because different moments scale with different laws (Rodríguez-Iturbe & Rinaldo, 1997). For so, we believe that any model or procedure used to define channel network extents should consider landscape heterogeneity and dominant processes, as well as the resolution of the DEM-data applied.

Later works of Montgomery and Georgiou-Foufoula (1993) over the hillslope scale and the drainage area-slope relationship using high-resolution DEMs underlined the presence of two transition points (figure 4.4): *i*) A reversal at very small drainage area; and, *ii*) An inflection at local slopes. They appointed out that the reversal point approximates to the hillslope length scale whereas the inflection is more appropriate to describe hillslope/valley transition mentioned earlier. The above findings not only verify hillslope length scale but also underline the importance of the flow direction method ($D8$ or $D\infty$) used to delineate the channel network. The former does not allow for the best representation of flow in divergent topography, which matters at small scale (Cabral & Burges, 1994); rather it

simulates more the convergent topography of the valleys features in the landscape (Rodríguez-Iturbe & Rinaldo, 1997). Hence, the appreciation of the reverse trend in the slope-drainage area relationship is dependent on: *i*) the DEM capacity to resolve hillslope processes, i.e. resolution effect (Tarolli & Fontana, 2009); *ii*) the presence of only a single inflection point in the longitudinal profile near the stream channel (McMaster, 2002); and, *iii*) the slope and accumulated runoff being relatively constant between streams (Peckham, 1998).

In the above example, with 30-m DEM grid resolution corresponding to Tabernas Basin, the reversal is about 5.6 cells, corresponding to hillslope scale of about 128 m, with good agreement with hillslope lengths of the area. Whereas, the inflection point in the link slope plot (figure 4.4) reaches 1760 cells that is too large to define first order streams of the area, but approximates well to main valleys and high order stream networks of the catchment area. In this example, slope values were averaged for each 0.04 log interval of drainage area. Tarolli and Fontana (2009) underlined that, although such process may produce trends and transitions, but it removes uncertainties related to the selection of the individual profiles.

Montgomery and Georgiou-Foufoula (1993) underlined the inefficiency of the drainage area-slope relationship to delineate channel networks limits, and appointed to the usefulness of the slope-dependent area threshold for stream source area definition. Accordingly, they insisted in the appropriateness of the Eq. 4.2 and reported that the proper identification of the channel network from DEMs depends on the value of C that controls the spatially varying A_S . For which, and in the case of prior-data deficiency, they proposed using as C the smallest value that does not result in a significant feathering. Again, such approach implies a lot of inconveniences in defining the optimum A_S value and hence channel network limits. First, the optical feathering definition implies highly subjective procedure that is inappropriate for automatic modelling approaches (mathematical), so as to be incorporated to programmable software (GIS packages). Second, the scale and the size of the study area involve not only objectivity but also time and effort consuming. In small size areas, it is possible to verify feathering streams and other possible problems in the defined drainage network (e.g. more than two effluents in the one junction). While, in large scale areas the optical definition is of high complexity and entails a vast amount of efforts in order to achieve a rational C value. Finally, C value should represent a spatially varying A_S that characterizes a heterogeneous landscape, that is, impossible to obtain with the optical definition of feathering in the channel network.

Another important problem associated to the use of area-slope relationship is its limited application to the O'Collaghan and Mark's method for A_S definition. Since the slope-area relationship relates accumulated drainage area at any location in the channel network with the corresponding slope, which is possible to identify by the O'Collaghan and Mark's approach. Whereas, the Band's method define streams and channels in relation to Gilbert's model of convex hillslope features and concave channel features. Hence, the constant approach of area-slope relationship needs the accumulation

drainage matrix for both stream-routing and A_S definition, while the *CDA* is applicable to both methods and uses the flow accumulation dataset for stream and channel lines definition.

However, Tarboton (2003) recognized the limitation of the constant approach (i.e. A_S definition based on area-slope relationship or *CDA*) since drainage density of the channel network extracted is spatially uniform. So, they proposed an objective model to delineate channel network from DEMs based on correct-scale identification associated with the terrain. In order to smooth landscape-heterogeneity effect on the optimum A_S , they suggested local-curvature identification as a method to account for spatially variable drainage density, so that network is adjusted in order to match the nature structure of the topography. The procedure consists of using Peucker and Douglas's algorithm to define drainage courses. Next, compensative parameters for spatial heterogeneity are used to enhance course line connection in the channel network. Compensation parameters are defined based on the second derivatives of the surface, proposed by Wilson and Gallant (2000). Finally, the application of the *CDA* method to define channel network limits in the landscape. The general premise of the origin work of Tarboton and Ames (2001) was that the drainage density of extracted channel networks should be adjusted to match the natural texture of the topography, so that the drainage network provides a good approximation of the domain over which channel processes, totally distinct from hillslopes processes events.

Finally, Heine et al., (2004) revised approximately all the above methods for stream network delineation and proposed 2 new approaches. The first is an analytical approach, based on using logistic regression model, which predicts the probability that a cell contains a stream. The second is extracting the stream channel head locations from digital orthophotoquads (DOQs). From which they concluded that, *i*) the DOQs is the most precise, but is labour intensive and is applicable only in a small limited catchments where vegetation cover does not obscure channel head location; and *ii*) the logistic regression has the broadest applicability because it can be implemented in an automated fashion using only DEMs while still achieving accuracies for mapping streams of low order that are far superior to existing USGS maps. Indeed, the work of Tarboton and co-workers (1991, 1992 & 2001) in channel network delineation represents the best to data both for their geomorphic justification of stream initiation and for their improvements in predicting, and thus mapping, channel extensions and drainage channel networks. As well as facility to use and incorporation in GIS packages.

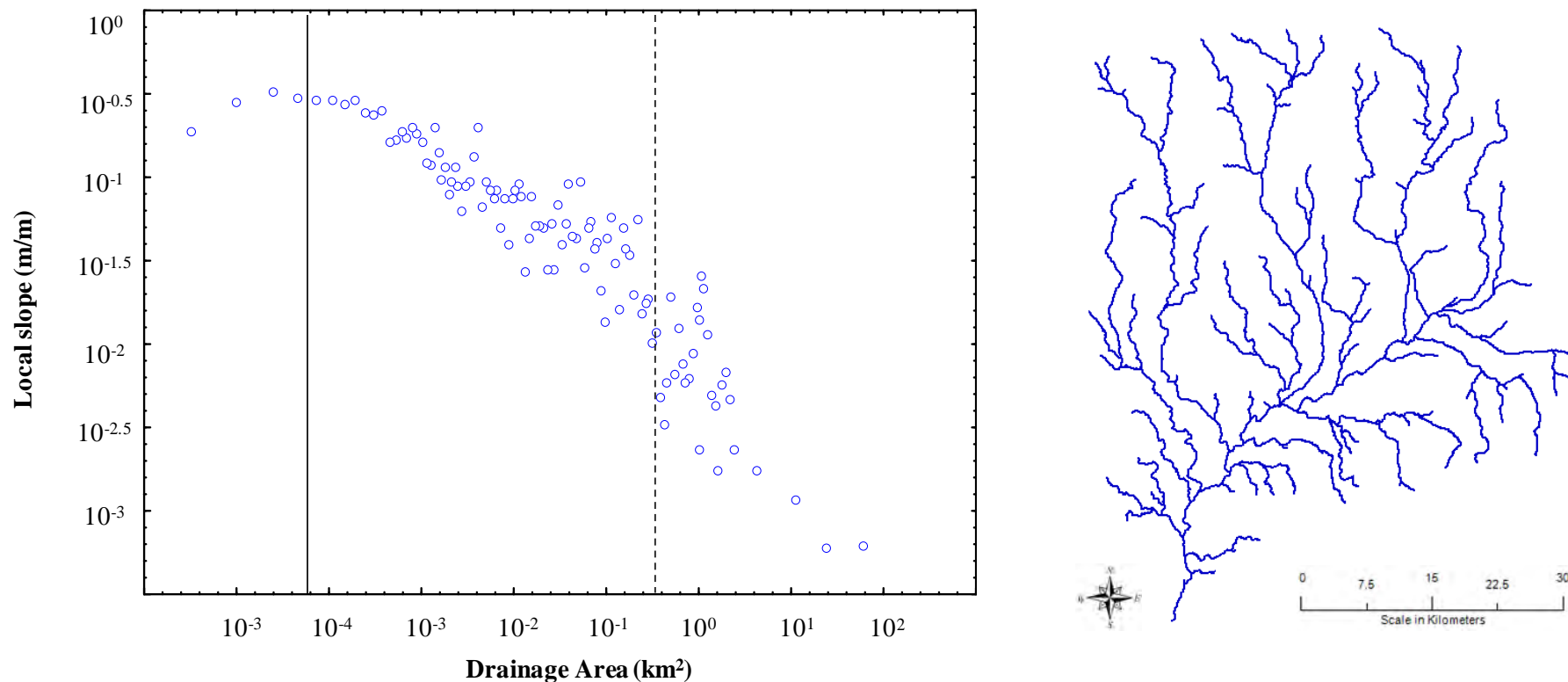


Figure 4.4 Slope-area relationship approach for stream network delineation; a) logarithmic diagrams of local slope versus drainage area for averaged data of individual links from 30 m DEM with support area of 50 cells used to extract the drainage network in Tabernas Basin (the vertical black and dashed lines show the slope-area reversal and inflection points at the hillslope-valley transition, respectively); b) the drainage network delineated by the inflection point with a drainage area of 1.58 km² (i.e. \approx 1760 cells).

Whilst several GIS software packages have been constructed and developed in order to achieve the best approximation for automatic representation of natural landscape dissection (table 4.1). Such software form one of the main tools for terrain management, which could be either dedicated on the direct definition and delineation of river basins and related drainage networks, e.g. Watershed and Stream Delineation Tools (WSDT) (Olivera, 2001), or incorporate topographic and geomorphic functions, e.g. Terrain Analysis Using Digital Elevation Models (TAUDEM) (Tarboton, 2001). In this case, both approaches are modelled under general GIS packages, such as ARCGIS, MapWindow, SAGA, etc. Whilst, other GIS packages have been dedicated just only for distributed hydrological analysis and watershed delineation, e.g. StarHydro.

4.5. Multifractal approach in stream network delineation

In the last decades researchers (e.g. Mandelbort, 1982; Ijjasz-Vasquez et al. 1992; Rinaldo et al. 1992; Cheng et al., 2001; De Bartolo et al., 2000, 2004, 2006) appointed out to the appropriateness of the multiple fractal approach over the simple one in depicting landscape dissection. In which, they asserted that complex heterogeneous landscapes are best described under the multiple dimension approach. In general, using a single A_S value over extending area of heterogeneous landforms is usually applied due to the lack of necessary information (Hutchinson & Dowling, 1991; Verdin & Jenson, 1996; Graham et al., 1999). Theoretically, the use of a single A_S is applicable only under landscape homogeneous conditions (Gandolfi & Bischetti, 1997; Bischetti et al., 1998; Colombo et al., 2001; Vogt et al., 2003), which is often limited to small-scale size catchments. This coincides with the findings of Schertzer and Lovejoy (1989) and Lavallée et al., (1993) who argued that a monofractal dimension (or, simple scale) do not seem entirely consistent with the properties of measured field data. They interpreted fractal characters observed in real topographies as multi-dimensional geometric framework (i.e. multifractal approach). Rodriguez-Iturbe and Rinaldo (1997) revealed that if geographic fields are characterized by a hierarchy of fractal dimensions then inconsistencies are inevitable when the fields are forced into single fractal dimensions. So, whatever the approach used, it should describe the existing landforms, irrespective of terrain heterogeneity. Thus, an adequate solution, according to our judgment, could be achieved by using algorithms that best simulate landscape spatial heterogeneity, represent dominant processes, and make use of available data. These conditions are limiting factors for the best approximation of landscape dissection, which should be defeated or even minimized for whatever procedure employed. Thus, a unique A_S value in a widely varying landscape conditions could be of slight suitability to reflect natural variability of drainage density.

GIS Package	Source & Author	Direction	Applications
Watershed and Stream Delineation Tools (WSDT)	Hydrologic Engineering Centre of the US Army Corps of Engineers.	https://ceprofs.civil.tamu.edu/folivera/GISTools/wsdtd/home.htm	Hydrological applications
Hydrologic Modelling System (CRWR-PrePro. HEC-HMS)	Francisco Olivera.	http://www.crwr.utexas.edu/gis/gishyd98/class/prepro/webfiles/prepro.htm	Hydrological applications
Terrain Analysis Using Digital Elevation Models (TAUDEM)	Tarboton, 2001	http://hydrology.usu.edu/taudem/taudem5.0/index.html	Hydrological applications
StarHydro	Software Tools for Academics and Researchers	http://web.mit.edu/star/hydro/	Hydrological applications
River tools	Rivix, LLC	http://www.rivertools.com/	digital terrain analysis Hydrological applications
Geospatial Analysis Tool (Whitebox GAT)	John Lindsay, 2007	http://www.uoguelph.ca/~hydrogeo/Whitebox/index.html	Geospatial analysis Hydrological applications Land surface Terrain analysis
ILWIS	World Institute for Conservation and Environment (WICE)	http://www.ilwis.org/	General GIS System
System for Automated Geoscientific Analysis (SAGA)	SAGA user group association	http://www.saga-gis.org	General GIS System
ARCGIS	ESRI	http://www.esri.com/	General GIS System
IDRISI	Clark Labs	http://www.clarklabs.org/	General GIS System
Geographic Resources Analysis Support System (GRASS)	U.S. Army Construction Engineering Research Laboratories	http://www.phygeo.uni-hannover.de/grass/index.php	General GIS System

Table 4.1 Main GIS systems that treat directly or incorporate basic models for channel network delineation and extraction.

4.6. Validation procedures in channel networks

Drainage network validation is another battlefield in the studies of landscape dissection. Herein, it is highly acceptable that whatever procedure used to delineate stream limits, it should meet the challenge of landscape dissection under varying environmental conditions. While delineation of stream limits has received a considerable attention from scientists, validation of the achieved results is still in lagging behind. How and what to validate were between the several questions that opened the debates between researchers. The complex structure of natural stream system (i.e. geometric, topologic, fractality, self organization and optimality) makes it somewhat complicated to adapt a particular approach over the others. In general, two main approaches for stream network validation are the widespread between geomorphologists: quantitative and qualitative methods. The former includes a group of geomorphometrical indices (i.e. parameters) that describe stream network structure properties, extracted from different sources (e.g. *BLs*, automated drainage networks, etc.) and statistically compared. The latter include field visit and visual interpretation of the resulted data and the post comparison with other sources of data (e.g. orthophotographs, *3D* structures, etc.). In the current work, emphasis will be added to the quantitative approach, mainly geomorphometrical parameters, because of their direct effect on hydrological and geomorphological models. Field visit field work is still form one of the most precise approaches for channel network validations. The ‘relatively exact’ drainage network can be observed directly in the field, but time and efforts make it impractical to check for stream validity, mainly in large scale catchments. In addition, the limits between hillslopes and channels are a purely subjective judgment of the researcher (e.g. Leopold & Miller, 1956). Nevertheless, scientists deem that field survey, or the integration of any proposed approach with field observation, is still one of the most reliable methods for network identification (Gandolfi & Bischatti, 1997), and therefore should be used to validate other techniques and approaches. Stream lines or channel networks from topographic maps, i.e. *BLs*, of different scales have formed the primary validation procedure approaches. A constant critical support area may be determined by matching predicted stream networks to the *BLs* on topographic maps. This method has several recognized limitations including the errors present in mapped stream networks and the theory behind choosing a constant critical source area. *BLs* origin and construction are of great importance. In general, all cartographic representations are a simplified abstraction of the reality, in which the cartographer judgment and experience are the unique qualitative parameter. Moreover, high detailed maps (e.g. 1:2500 and 1:5000) seem to be a valid source for drainage network validation but in some cases is not completely; as such validation should be made only in the limited range of scales shared by the simulated network and the validating dataset. The incapacity of the *BLs* in middle-scale measures to get an ideal and/or optimal description of the natural channel network had forced researchers to use a more sophisticated powerful means (e.g. aerial photographs) in order to get more enhanced and precise descriptions of watersheds and related drainage networks. The Photo-

interpretation has been widely used to validate automatic extraction procedures of landforms (Chorowicz et al., 1992; Miller et al., 2005; Lejot et al., 2007). It's obvious that channel network detection from aerial images obviates some of the shortfalls of the *BLs* (Gandolfi & Bischetti, 1997), but it still suffer concrete limitations, related to the obscuration and misleading effect of canopy, the scale of the image, the contrast of the relieve (e.g. shadows and distortions), and finally the subjectivity of the photo-interpreter (Morisawa, 1957; Coates, 1958; Coffman et al., 1972; Mark, 1984; Montgomery & Fournelle-Georgiou, 1993). In addition, aerial photograph interpreters are given the discretion as to which first-order or intermittent streams are included in the network, and their interpretation is highly dependent on the season or climate conditions when photographs were taken (e.g. Chorley & Dale, 1972; Mark, 1983).

Visualization approaches as a validation process have received little attention in geomorphological studies, whereas the majority of scientists tried to explain the results in relation to field observations. Visual processes provide an important methodological approach that is necessary for the development of interpretation tools. However, in the last years more attention has been paid to this discipline (e.g. Wood, 1996b, 1998, 2002; Pajarola, 1998, Pike, 2000; Bastin et al., 2002, Fisher et al., 2004; Voudouris et al., 2005; Wood et al., 2007). Nevertheless, the interpretation of the visualized objects serve as a preliminary step but not the final one, mainly when using objects of different resolutions and scales. In addition, judgment is still subjective and depends in the cartographer to decide where channels begin.

Finally, the quantitative geomorphology, mainly geomorphometrical indices, has formed an efficient approach to validate channel network-extraction and -delineation techniques (e.g. Horton, 1945; Strahler, 1956; Schumm, 1956; Hack, 1957; Melton, 1957; Shreve, 1966, Smart, 1968, Rodríguez-Iturbe & Valdes, 1972). Here, it is important to detach that in spite of its efficiency as a powerful tool in landscape disciplines, geomorphometric indices could bear some deficiencies, mainly in marginal modifications (Beauvais & Montgomery, 1997). Furthermore, the link between the geometry and the hydrological response of drainage networks suggest further criteria that can be used to evaluate the effect of the network identification method from the hydrological standpoint (Snell & Sivapalan, 1994; Gandolfi & Bischetti, 1997). Moreover, several geomorphometric indices (e.g. Horton's laws, Hack's law, Melton law, etc.) exist in most possible networks and thus their observance does not say much about the processes that control network growth and development, and hence drainage network limits (Rodríguez-Iturbe & Rinaldo, 1997).

In the last decade the technology of LiDAR (Light Detection and Ranging) has been widely used in environmental applications, mainly in topographic data and surface features (e.g. Brzank et al., 2008; Aguilar et al., 2009). Because of their extreme accuracy, main valleys and channels as well as fine streams and gullies are widely detected and identified by such technology. Accurate characterization of these features is directly impacted in the precise definition of hydrologic and

geomorphic parameters widely used in landscape modelling (e.g. runoff, erosion, sediment transport, etc.). Such characteristics of LiDAR data make it an outstanding and potential validation approach for stream network definition, both automatic and manual ones. In addition, the high detailed data of LiDAR (i.e. centmetric grid spacing) add new dimensions to the validation approach: the first is the 3D surface relief as an idealized visualization structures; and, the second is the application of the geoespacial analysis for a quantitative description of these features. So, a comprehensive approach for stream network delineation should incorporate, in addition to powerful algorithms, a powerful validation procedure that allows for a complete definition of the basin system and the embedded drainage network structure, a key issue that was taken into account in the presented study.

4.7. Conclusions

Automated delineation of channel network from DEMs is achieved by a threshold value (A_S) that determines where stream begins in the landscape. This value may describe area contributing to stream initiation (i.e. designated as threshold contributing area) or number of cells in a fragmented channel network (i.e. designated as connecting threshold value). The use of one approach over the other is related to the method of channel network extraction (e.g. Band's or O'Callaghan and Mark's). Whatever A_S value used, it should define stream limits in relation landscape complexity (i.e. homogeneity or heterogeneity) and data availability (i.e. DEMs data solely).

The present analysis of stream network delineation demonstrated that the available approaches fail to define an optimum A_S value, mainly under limited conditions of data availability and heterogeneous landforms. First, the constant threshold value extracted by the slope-area relationship or the constant drop analysis (CDA) showed a highly feathering and extremely smooth drainage networks, respectively. Such inconsistency is attributed to the use of single A_S value over a heterogeneous landscape, where a multifractal approach should be applied. Moreover, the above methods overlook the effect of local factor (e.g. runoff, vegetation, tectonics, etc.) leading to biased results of the depicted landscape. Secondly, validation of stream network should integrate both quantitative and qualitative procedures in order to achieve the best similarity between compared streams. What and how to compare is the scientist decision, but it also should form part of an integrated strategy for stream network validation.

Chapter 5

INTRINSIC HIERARCHICAL STRATIFICATION OF LANDSCAPE AND THE ADAPTIVE MODEL

5.1. Introduction

5.1.1. General revision

In landscape studies, delineation of channel networks is a major problem. Its effect goes farther than the edge of one discipline and restricts not only the results expected but also the methodologies used in the desired studies. Identification of channel networks, both permanent and ephemeral, are important from both a theoretical and practical perspective in geomorphologic and hydrologic disciplines, since it defines the relative extent of hillslope and channel processes in a catchment which, in turn, have important influences on watershed hydrological responses (Bischetti et al., 1998). Moreover, it can be used in various applications, such as studies of stream flow hydraulics (Wang & Yin, 1998), prediction of flooding and modelling of chemical transportation and deposition of pollutants in surface waterways (Breilinger et al., 1993; Pitlick, 1994; DeParry, 2004). Furthermore, characteristics of stream network can provide insight into surface and subsurface dominant processes (Horton, 1945; Leopold & Miller, 1956; Strahler, 1957, 1958, 1964; Kirkby, 1976; Beven, 1989) in landscape. Lately, incorporating the effects of three-dimensional terrain has become essential in surface hydrological modelling processes (Moore et al., 1991).

The early procedures for describing channel network from DEMs were based on the early work of Peucker and Douglas (1975), revised later by Band (1986), and O'Callaghan and Mark (1984). The first is related to the basic notion that convex pixels in the terrain are related to divergent processes and hence hillslope formation, whereas concave ones are related to convergent processes and hence valleys and channel network formations. The second is related to the threshold concept of Schumm (1973, 1977), that is, quantifying the drainage accumulation (i.e. the approximate surface and subsurface water flow) at each cell in the DEM. Consequently, and for both cases, cells which had a specific-user threshold (A_s) were considered to be on a drainage channel. Both procedures provide an approximately comparable main valley system, but define different lateral streams (i.e. first and second order links) that play a major role in modelling river basin system. This implies that it is possible to use both methods to define the same channel network, but not the same threshold value. Each method requires its own threshold since defining stream limits in both cases are different. So,

threshold definition is not only related to local conditions and DEM resolution, but also to the procedure used to derive the channel network.

In a reviewing literature, the automatic definition of channel network limits from DEMs can be derived using two broad approaches. The constant threshold approach assumes a unique and static value for defining channel network initiation. In this direction, the constant drop analysis (*CDA*) assumes similar principle bases with the constant threshold approach, that is, the presence of breaking scale for landscape dissection (Tarboton et al., 1991, 1992). Alternatively, the variant threshold approach assumes different values for drainage network extraction. This method define stream limits in relation to dominant sediment transport process or dominant erosion process, and uses a weighted threshold value of weighted accumulation area. However, the problem is raised when there are no previous data on the terrain or when definition is realized over large scale terrain, or even at extremely limited terrain of high details when available topographic maps of highest available scale does not cover such limits. In this case, DEMs will be the unique available information to define channel networks, and other landform structures. So, answering where channels begin in the landscape opened the debate between researchers on aptness of algorithms and procedures that best describe lateral streams (e.g. rills and gullies). The selection of the appropriate approach is of relative importance because current used methods ignore landscape heterogeneity and local factors. Adapting or imposing one approach over the other is justified in the local environment of the work and researcher experience. Both, the *CDA* and drainage area-slope relationship are inappropriate to assign stream networks initiation since several drawbacks are emerged when used under heterogeneous landscape conditions (e.g. resolution effect, local factors effect, multifractal characteristics of basin river systems, etc).

5.1.2. Importance of selecting the optimum threshold

Representation of stream sources or channel heads is of obvious importance and highlights the urgent need to an alternative procedure that replaces traditional and manual methods. The persistent problem of defining where channels begin on the hillslope and determining the physical extent of the drainage network has shaped the appropriate mode for A_S definition. Channel head represents the start of the drainage network, and its location is influenced by the geomorphic processes and local factors, which in turn determine shape, form and structure of the prevailing drainage network system. Hence, meeting the challenge of locating channel heads is thus the key to accurate mapping of stream network (Heine et al. 2004). Small errors in source area definition could lead to major modifications in the final stream network structure properties.

The choice of the appropriate A_S used to define the optimum channel network is highly related to the scale of the study area and the resolution of the original data (e.g. Walker & Willgoose 1999; Thompson et al. 2001; Hancock, 2005). Although it is true that DEMs may cloud the correct scale of

channel initiation (Montgomery & Dietrich, 1988), at large enough sizes of the basin such features may lose relevance (Rodríguez-Iturbe & Rinaldo, 1997). This implies that natural channel networks are scale invariants whereas streams derived from DEMs are self-affine structures (e.g. Tarboton et al. 1989, 1991; Mantilla et al., 2006). Such problems should be handled by the used model and the dimension of scale dependency should be defined in order to determine the appropriate resolution for the corresponding scale.

Source areas contributing to channel heads represent a transitional stage between convergent and divergent prevailing processes, giving rise to quantitative theories of channel and hillslope evolution (Montgomery & Dietrich, 1989). Physically based theories for predicting source areas contributing to channel heads will consequently contribute to network models and provide a linkage between hillslope processes and network properties (Montgomery & Dietrich, 1989), as well as it may consider as a key feature in quantifying drainage density (Moglen et al., 1998). Debates over the precise location of channel heads have occupied a considerable attention, both in field-survey data (e.g. Leopold & Miller, 1956) or DEM data (e.g. Montgomery & Dietrich 1988, 1989; Tarboton 1989; Tarboton et al. 1991, 1992; Montgomery & Foulfoula-Georgiou, 1993; Dietrich et al. 1993; Tucker & Bras, 1998). Several questions have occupied the core discussion between scientists, such as; does one consider intermittent or ephemeral streams? Or if DEMs are appropriate tools for drainage network definition, and if so what is the appropriate scale and resolution? Does valleys constitute stream network, or vice versa?

The debate over the optimality of A_S and if it is sufficient to determine channel initiation (Montgomery & Dietrich, 1988, 1989) is of great importance, since several geomorphometrical indices and topographic attributes depend on (e.g. Wilson et al., 2000). In river basin and corresponding drainage networks characteristics, special emphasis has been added to the direct and indirect effect of the appropriate A_S value derivation. First, accurate estimation of stream network limits is important as they determines (i) the hillslope travel distance and times, which in turn govern an accurate runoff prediction (e.g. Rodríguez-Iturbe & Valdes, 1979; Quinn et al., 1991; Moore et al., 1991; Montgomery & Foulfoula-georgiou, 1993;) and (ii) the essential component of quantitative theories for hillslope- and drainage network-evolution. Second, main relationships of catchment geomorphology (e.g. time of concentration of a basin, mean annual flood, geomorphologic unit hydrograph, optimal channel network, etc.) are often related to drainage area of the basin or drainage network density (Helmlinger et al., 1993; Ibbitt et al., 1999). Not only hydrological and geomorphological modelling is influenced by A_S values, but also general conservation and management planning are widely affected and altered. For example, agricultural strategies and urbanization planning are directly evaluated in relation to drainage density (low or high), where high peaked hydrograph resulted from high drainage density tend to have higher sediment production, and hence can present greater difficulties in development planning (Dunne & Leopold, 1978). The sound

separation between permanent and ephemeral streams may aid watershed planners in targeting and conservation planning (Heine et al., 2004).

In the same direction, scientists (e.g. Gandolfi & Bischetti, 1997; Da Ros & Borga, 1997) appointed out that the effect of A_s is extremely significant, and both scale properties as well as hydrological response are altered constantly. First, network properties when expressed in terms of Strahler ordering system are heavily influenced by the threshold area selection, whereas the width function approach (Gupta et al., 1986) seems to reduce the variability, as its function is linked with global characteristics of the network which exhibit more stable behaviour with the threshold area variation. Furthermore, varying the threshold area within a reasonable wide range of values, the influence of A_s on the hydrological response seems to be more crucial in small catchments, where the hillslope travel times are predominant, than in large basins where stream network properties are smoothly altered.

In relation to DEMs use in fluvial geomorphology, the great challenged to face was the ability of the scientific community in deriving models capable to describe the optimum channel networks under diverse conditions of local-data availability, scale dependency, and landscape heterogeneity (i.e. limited conditions). In this direction, several algorithms have been proposed, such as threshold connection (Band, 1986), constant threshold area (Tribe, 1992), and slope threshold (Montgomery & Dietrich, 1992), grid order threshold (Peckham, 1995), and constant drop analysis (Tarboton et al., 1991, 1992; Tarboton & Ames, 2001). The majority of these models failed to depict landscape dissection under varied-diverse conditions, and succeeded under particular conditions of diversity, such as limits between valleys and hillslopes or channelize and non-channelized areas in the landscape. Under these conditions, we believe that defining the optimum channel network using DEM-data under limited conditions of data availability and scale variability is still a basic requirement for hydrologic and geomorphologic studies.

In general, an adequate solution, according to our judgment, could be achieved by using algorithms that best simulate landscape spatial heterogeneity, represent landscape dominant processes, and make use of available data. These conditions are limiting factors for the best approximation of landscape dissection, which should be defeated or even minimized for whatever procedures employed. So, in order to achieve the adequate solution, three important requirements should be taken in mind in the proposed objectives and hence in the procedure applied for the optimum solution:

- DEM resolution is important to compensate spatial heterogeneity of the terrain, but not enough to capture all landscape details. Dietrich et al. (1993) detached that DEMs, even at very high resolution (e.g. 1m) are so sparse to capture the local topography around typical small channel heads, which often are only decimeters in size at their tips. For so, an equilibrium-conformity state is needed between proposed objectives and data used to achieve such objectives.

- Each landscape-dominant process requires a particular A_S value, for which more than one dominant process implies the need for more than A_S value. Bischetti et al., (1998) affirmed that a constant contributing area is not a realistic assumption.
- DEMs are the only available data beforehand in numerous occasions for hydrological and geomorphological studies. Thus, DEMs will be used solely as available data to use in the optimum definition of landscape dissection, and local parameters will be compensated by the intrinsic information provided by the DEM itself.

Accordingly, we propose a new compound model that defines channel networks in relations to the intrinsic-landscape information. Such approach attains to depict landscape dissection in relation to data availability (DEM resolution), presented heterogeneity (scale extension) and intrinsic information of landscape structure (landscape classification), and allows for terrain simplification (a simple model approach) instead of multiple complex approach (heterogeneous landscape). Indeed, the DEM reflects a set of processes characterized by similar scale properties with the DEM matrix itself, which may be used to extract as much information as possible.

5.2. Aims and objectives

In summary, the general objective of this work is to define the optimal channel network that best describe landscape dissection in order to verify hydrological, geomorphological and topological processes at a determined scale and resolution. Such objective highlights the need to a recursive examination of scale properties of the landscape, mainly hillslope channel relationships. Another associated objective is the generalized analysis of network complexity to other areas of distinct scale and resolution in order to obtain the best approach for channel networks depiction. In order to achieve these objectives, a new procedure has been proposed, based on the analysis of intrinsic information provided by the gridded-DEM data. Accordingly, the following hypothesis has been formulated; that is, “DEMs are appropriate tools for channel network description and the optimum A_S value is highly related to homogenous structures of the landscape”. In order to test this hypothesis, two sub-objectives have been formulated: i) Determining DEMs capacity and its contained information in the definition of the geomorphometry of the landscape (i.e. basin and stream network structure); and, ii) determining landform classification effect according to internal factors (intrinsic properties) concerning DEM capacity for terrain recognition. Throughout the present work, the proposed procedure for stream-limits definition was directly compared with the widely spread used procedure of *CDA*, both in relation to *BLs* as an acceptable and relatively suitable representative for natural channel networks.

In order to achieve these objectives, a new procedure has been proposed based on the analysis of intrinsic properties of channel network structure provided by the information extracted directly from DEM-data. At the same time, it should answer the basic question of, what part of the drainage network is the matter of interest for the research in order achieve the aimed goals of the study? Hence,

defining the optimum landscape dissection is widely related to a group of extrinsic and intrinsic factors that should be taken into account in the delineation of the drainage network that best simulate natural stream networks. The former is related to local factors and surrounding environment while the latter is related to dimension and uncertainties in the input data (i.e. DEM), scale of observation, and the model used to define the appropriate A_S value.

5.3. Methodology

5.3.1. Introduction

As mentioned earlier, the principle aim of the current work was to define stream networks that best describe landscape dissection, using DEM, solely. To reach such objective, it is necessary to use methods capable to obtain the best results from available data. At this level, and in order to avoid misleading in concepts and terminologies, two concepts should be separated for more accuracy in theory and model building. From now on, the term method will refer to the process of extraction and delineation of the possible stream and valley lines of the channel network in the catchment, whereas technique to the process of selecting and defining the optimum threshold or the critical support area (A_S). Throughout this work, neither we will accept or reject the most appropriate approaches (topological to geometrical, local to global, etc.) for channel network definition, nor the best method (Band or O'Callaghan and Mark) for drainage network extraction, since they are beyond the aim of this work. Rather we will concentrate all our efforts in the derivation of a new technique for the selection of the optimum A_S that best describe stream networks extracted from DEMs at a certain scale and resolution.

Herein, several questions are emerged in relation to DEMs capacities for channel network definition under both complex-heterogeneous as well homogeneous landscapes, such as, where do channels begin under such conditions? Is it sufficient to use a simple A_S value under homogeneous and heterogeneous landscape approaches? Do DEMs contain sufficient information to define the optimum channel network? And if so, what is the appropriate scale and resolution to be used? The effectiveness of answering such questions is directly influence and affects the success or failure of hydrological models, since several geomorphological and hydrologic parameters would be altered in relation to the defined channel networks, mainly first order streams and lateral channels. For example, hydrological properties of basin's response, as well scale effects on basin topology and on relationships between the basin morphometric properties and the hydrologic response are between the direct effects on defining optimum channel networks (Beven, 1989, 1995).

Given that our reference material will be the DEMs, it's necessary to recall two essential points from previous chapters:

- *DEM accuracy and certainty*

The accuracy of a DEM is dependent upon its source and the spatial resolution (i.e. grid spacing) of the data profiles. Another important factor influencing DEM accuracy is the horizontal and vertical dimension of the DEM. Horizontal accuracy of DEM data is dependent upon the horizontal spacing of the elevation matrix. Vertical accuracy of the DEM data is dependent upon the spatial resolution (horizontal grid spacing), quality of the source data, collection and processing procedures, and digitizing systems. As with horizontal accuracy, the entire process, beginning with project authorization, compilation of the source data sets, and the final girding process, must satisfy accuracy criteria usually applied to each system. Each source data set must qualify to be used in the next step of the process. Errors have the effect of compounding for each step of the process. Both vertical and horizontal accuracy of DEMs can be evaluated by different approach, such as the RMSE, Monte Carlo approach (Stochastic simulation), etc.

- *DEM resolution*

DEM's are considered as potential models for the representation of land surface forms. The fidelity with which the DEM models the true surface will depend on surface roughness and DEM resolution. As mentioned earlier, fractality of surfaces derived from DEMs suggest that there will always be detail at a finer scale than that measured at the DEM resolution, suggesting that all DEMs implicitly model at a certain scale involved by the grid cell resolution. Determination of the appropriate resolution of an interpolated or filtered DEM is usually a compromise between achieving fidelity to the true surface and respecting practical limits related to the density and accuracy of the source data (Hutchinson & Gallant, 2000). Since the capacity to understand catchment processes is reliant on DEM resolution and landscape input data, modeling grid size used in landscape quantification is of considerable importance. In general, the objectives of the research and the type of the indices and variable used will determine the appropriate grid resolution used to derive geomorphological input parameters for hydrological applications. The fractal properties of channel network highlight the convoluted problem of DEM resolution for stream source definition. For so, DEM-resolution suitability is more related to final goals and objectives rather than the appropriateness of high-resolution DEMs (e.g. 1 m grid size) over low-resolution ones (e.g. > 30 m grid size).

The study of channel networks in two sub-basins of Tabernas catchment (i.e. Rambla Honda and Cautivo) at 1 m grid dimension by the available techniques have shown little coincidence and irregular variation with the *BLs* and the orthophotographs of the catchments. The irregularity is shown in form of redundancy or feathering in the generated networks. For so, a new technique has been developed in order to avoid the anterior inconveniences and to select an adequate A_s value through a more objective criterion.

5.3.2. Origin of the model approach

Starting with the assumption that a DEM is the only available information to delineate a catchment and its related drainage network, we propose a new technique to select the optimum A_S for a specific location based on the intrinsic properties of the channel network. In this approach we assume that DEMs are self-contained structures, capable to determine its internal formation, and that channel complexity is best reflected by its corresponding intrinsic properties. This complexity is best revealed by the combination of structure regularity framework (i.e. bifurcation and length ratios of Horton) with topological random approach (i.e. topological link lengths properties of Shreve). The sharing point between the two approaches is reflected in the ratio between interior and exterior link length, known widely as the R_A (Schumm, 1956).

R_A is calculated as follows:

$$\bar{l}_i / \bar{l}_e = R_A \quad 5.1$$

where \bar{l}_i and \bar{l}_e is the average link lengths of interior and exterior links, respectively.

Herein, we believe that R_A bears direct and indirect information on channel network characteristics and age, which could be used to reveal basin dissection and maturity. The former is related to the processes dominant in the landscape, whereas the latter is the result of landscape evolution. The new technique consists of examining the curve relationship between the R_A ratio and the corresponding thresholds that generates these ratios. The resulting ratio changes throughout the axis of threshold values generating a varying-tendency curve. The rate of change of R_A , i.e. tendency curve, throughout the x axis of A_S represents several stages of catchment and channel network evolution. A_S is the threshold value that reflects drainage density and hence landscape dissection, for which we believe that it reflects, on the one hand drainage evolution and hence basin age, and on the other hand landscape complexity since different R_A values reflects distinct geometric and topologic information. Accordingly, we propose the following starting hypothesis; that is, R_A tendency curve is regular and steady in youth and homogeneous landscape, and unsteady-irregular in mature and heterogeneous landscapes.

5.3.3. A conceptual framework

The ratio of R_A was first studied by Schumm (1956), who in reality studied the inverse relationship of R_A ($\bar{l}_e / \bar{l}_i = inR_A$). Schumm tried to investigate the change of inR_A for distinct streams of different magnitudes, and found it to oscillate between 1.15-1.96. Likewise, for different-orders channel networks of different regions Smart (1972a) calculated the mean values of inR_A to be between 1.46 and 1.54. Shreve (1967) recognized that exterior and interior link lengths generally have different length properties. In a more detailed work, Smart (1972b) found that inR_A to range between 0.88-2.60, for which he concluded that inR_A ratio varies considerably between regions of different environment.

Furthermore, in consequent studies Jarvis (1976b, 1977) suggested that inR_A value also varies appreciably within regions of uniform environments. This discrepancy is ascribed to the strong distinctions between the digitized lines of river networks on topographic maps and the valley networks inferred by contour crenulations seem too large to be dismissed as mapping bias in source identification. Smart (1972b) used inR_A directly as a dimensionless parameter in order to describe quantitative characterization of channel network structure (i.e. dissimilarities between networks), mainly with varying lithology and degree of maturity.

On a further step, researchers tried to study R_A components separately in order to understand its distribution, relation and controlling factors. Comparing the mean interior links length (\bar{l}_i) with mean exterior links length (\bar{l}_e) yielded a variety of results (Jarvis, 1977). In their works, several authors (Melton, 1957; Smart, 1972a) appointed out that $\bar{l}_e > \bar{l}_i$, whereas Morisawa (1962) found \bar{l}_i to be greater than \bar{l}_e in all streams in the studied region. Whether exterior and interior link lengths covary was investigated by Jarvis (1976b) and positive correlations have been found, if and only \bar{l}_i and \bar{l}_e are grouped according to the corresponding diameter of the channel network. The interesting characteristics of these correlations is that they are low for small networks and tend to increase as network diameter increases, since diameter is the grouping factor. The positive correlations between \bar{l}_i and \bar{l}_e imply that the factors giving rise to the systematic variations in drainage density and link lengths within a particular region affect exterior and interior links in a similar way. Controlling factors that govern variations in link lengths properties are concern to climate, geology, relief, or space-filling constraints (Abrahams, 1984a). Abrahams (1972, 1977) studied the effect of differences in relief and ground slope over length links properties and found that in mature fluvial eroded landscapes with uniform environments exterior and interior link lengths vary inversely with relief (and slope) over space as well as through time, irrespective to the erosional history of the landscape. Space filling is another important factor for controlling link lengths properties that affect exterior and interior link lengths separately or jointly. On the one hand, it appears that the availability of space for link development is a major control for exterior link lengths and that the availability of space is conditioned by the geometrical requirements of fitting drainage basins together in space (Jarvis, 1976a). On the other hand, interior link lengths in uniform environments are governed by two space-filling considerations: (1) the tendency of channel networks to develop a uniform drainage density; and (2) the requirement that their drainage basins fit together in space (Abrahams, 1984a). Finally, Smart (1981) found a positive relation between exterior and interior link lengths and the magnitude of the link joined downstream (μ_D). This positive correlation is seen to be the expectable outcome in the way in which basins fit together in space and the tendency of interior links with different divide angles to maintain a constant drainage density (Abrahams, 1984a).

It's obvious that link length properties of stream networks bear a considerable amount of information that explains channel network evolution and behavior. Since the early work of Horton over channel network geometry (i.e. Horton's Laws that explains the regularity of formal relations between the parts of a channel network), authors tried to enhance and demonstrate the applicability of these characteristics in nature, mainly bifurcation and lengths link ratios. For instance, Strahler (1958) used the dimensionless parameter $\bar{L}\omega$ (i.e. mean length of segments of order ω) between others in order to describe the geometrical similarities of landforms in different regions. Shreve (1969) used link lengths of exterior and interior links as separated variables and study their distribution and relation with topologically random channel network model. Jarvis (1972) in order to describe the topological structure of the network used a sophisticated topologic measure (E) (equation 3.14) that uses R_A in relation to magnitude (μ) in order to escape the difficult interpretation of standard analysis of bifurcation ratio.

The first attempt of determining channel limits with R_A components has been realized by Shreve (1974), where he used exterior and interior link lengths as separated variables and associated them with area in order to define source of channel heads (A_S). In a general revision of previous studies on network structure and properties, Abrahams (1984a) concluded that R_A was approximately equal to unity. Nevertheless, Montgomery and Foulfoula-Georgiou (1993) tried to use R_A of different thresholds to examine whether statistical properties of channel networks are useful for estimating parameters of slope-area relationship. In their work they studied the change of R_A from networks defined with different threshold areas, and concluded that these properties do not change systematically with the imposed A_S . They interpreted the results as follows: *"Although the ratio of R_A varies, it remains generally close to unity. This reflects the interdependence of the number and lengths of network links. A smaller source area results in an almost equal increase in the number of interior and exterior links and decreases the mean length of both populations. Consequently, this ratio is rather insensitive to the source area used to defined the network and therefore does not provide useful constraints on network extent"*. In their interpretation of their results it seems that Montgomery and Foulfoula-Georgiou anticipated a significant statistical relationship for the varying ratios of R_A , which seems to be improbable. In addition, they disregard the local and environmental effect over channel network formation and evolution, for which the resulted curve should be interpreted in changing phases rather than the totality.

The resulted drainage network proposed by Horton embodies a deep sense of regularity, not the trivial regularity of size, but the much deeper regularity of formal relations between the parts (Rodriguez-Iturbe & Rinaldo, 1997). The structure regularity framework is widely represented by 'Horton ratios or laws'. The ratio of number of streams (i.e. bifurcation ratio) and length of streams (i.e. length ratio) between successive orders is approximately constant. Mathematically the ratios are

$$N_{\omega-1}/N_{\omega} \approx R_B \quad 5.3$$

$$\bar{L}_\omega / \bar{L}_{\omega-1} \approx R_L \quad 5.4$$

where N_ω is the number of streams of order ω and L_ω is the mean length of streams of order ω . The R_B and R_L are bifurcation and length ratios, respectively.

Completely contrary to the regularity approach, Shreve (1966, 1967) proposed the random topology model that based upon the concept that networks of given magnitude, under the absence of geologic control, are comparable in topological complexity, that is chance is the only criteria operating on the organization of the drainage network. Accordingly, Shreve proposed the link magnitude system for ordering channel networks. In this system, channel networks are ordered based on its magnitude or the magnitude of the outlet stream link. The topologic properties of drainage networks have played a fundamental role in the formulation of drainage network models (e.g. Shreve, 1966, 1967; Smart, 1972a; Jarvis, 1977; Abrahams, 1984a). Both of the major models that have been used to study drainage networks, Horton-Strahler and Shreve-Smart, are mainly based on network planimetric and topologic structure properties. According to Shreve (1975) it has been clear that topologic properties dominate the orientation-free planimetric aspects of river basin geomorphology. Both approaches of structure regularity (i.e. Horton's laws) and randomness (i.e. Shreve's random topology model) have been widely confirmed by observation on natural channel networks (Jarvis, 1977). The dilemma arises of how can natural network simultaneously satisfy two distinct contradictory approaches, the deterministic model approach (structure regularity) of Horton and the topologic random model of Shreve? Researchers (e.g. Shreve, 1966, 1967, 1969; Smart, 1972a, 1974) appointed out that, although random topology model seemingly implies the absence of structural regularity, the regularity of Horton's laws are completely and efficiently explained by the random topology model, which consider the Hortonian analysis as a consequence of the topologic randomness and not an alternative one. These foundations are of great harmony with famous chaos theory in organizational development, directly speaking concepts such as self-organization, bifurcation, self-affine and self similarity (Rodriguez-Iturbe & Rinaldo, 1997).

Nevertheless, the supposedly characteristic network parameters generated by the Horton-Strahler approach, the stream length ratio and the bifurcation ratio, are rather highly correlated (Melton, 1958a; Ghose et al., 1967; Smart 1968). This suggests that just as bifurcation ratios may be explained by the random topology model and generally fails to convey much geomorphic information, so stream length ratios are largely redundant artefacts of the ordering method (Jarvis, 1977). A relationship between the stream length ratio and the standardized structural measures of $d / N_1^{0.5}$ and $\bar{p}_e / N_1^{0.5}$ (where d is the diameter, \bar{p}_e is the mean source height of exterior lengths, and N is the number of streams) reveals a clear indication of the topologic influence upon stream lengths (Jarvis, 1975). In general, the above mentioned observations of link lengths properties of channel networks

confirm R_A is an independent geomorphometrical parameter, which is related to the intrinsic properties of the dominated channel network, for which each landscape has its own specific R_A value.

5.3.4. Model derivation

The current synthesis on model derivation is an essential step in the formulation of the working hypothesis, which is mainly proceeded from earlier discussions. The R_A ratio represents a simple case in a dynamic complex landscape, in which the applicability of this dimensionless index is limited to catchments of homogeneous landforms and processes. In addition, R_A confirms more to the Horton's law of stream lengths link rather than the Shreve's random topology model. Whereas, in reality, formation of channel network in natural landscapes is the result of a complex evolutionary process throughout the time in relation to different local and environmental factors (e.g. tectonics, landforms, lithology, etc.), which in turns implies the need to a more sophisticated model capable to adapt to natural formation and, most important, integrates random and regularity concepts in stream delineation. It seems reasonable to accept differences in interior and exterior lengths due to different growth processes of headwater extension, bifurcation and tributary ramification. However, the network is an organized spatial system and this surely implies some kind of coordination or adjustment between interior and exterior links (Jarvis, 1977).

Smart (1968, 1972a), and in order to explain the topologic behaviour of ordered stream lengths in a random length link model, developed an alternative model based on two assumptions, 1) that channel network are topologically random, and 2) that the lengths of interior link lengths in a given network are independent random variables drawn from a common population. Smart deduced that the mean stream length of order ω is given by:

$$\bar{L}_\omega = \bar{l}_i \prod_{a=2}^{\omega} (N_{a-1} - 1) / (2N_a - 1) \quad \omega = 2, 3, \dots, \Omega \quad 5.5$$

where N_a is the number of streams of order a, and Ω is the network order.

Whereas, the individual stream length ratios are given by:

$$\lambda_2 = \bar{L}_2 / \bar{L}_1 = R_A (N_1 - 1) / (2N_2 - 1) \quad 5.6$$

$$\lambda_{\omega'} = \bar{L}_{\omega'} / \bar{L}_{\omega'-1} = (N_{\omega'-1} - 1) / (2N_{\omega'} - 1) \quad \omega' = 3, 4, \dots, \Omega \quad 5.7$$

And hence, the total mean stream length can be expresses again as

$$\lambda_\omega = \lambda_2 + \lambda_{\omega'} = \bar{L}_\omega \quad 5.8$$

The ratio R_A is required for λ_2 because generally $\bar{l}_e \neq \bar{l}_i$, and there is no theoretical model for relating \bar{l}_i and \bar{l}_e (Abrahams, 1984a). Getting back to the Horton's laws of stream number and stream lengths, it is accepted that the number of streams N_ω of order ω decreases as a geometric series with R_B

(Eq. 5.3), and mean length of streams \bar{L}_ω of order ω increases as a geometric series with R_L (Eq.5.4). Accordingly, the individual stream length ratio of equation (5.4) could be reorganized by

$$\lambda_\omega = \bar{L}_\omega / \bar{L}_{\omega-1} = \bar{L}_\omega \sim R_L \quad \omega = 2, 3, \dots, \Omega \quad 5.9$$

Smart (1972a) noted that if N_ω is moderately large then $\lambda_\omega \sim R_B / 2$. Thus, if R_B is close to the model value of 4 for topologically random network, $\lambda_\omega \sim 2$.

In fact, the complexity of Smart's model is of great importance since it describes, explains and adapts more to natural channel networks than Horton's model. Such importance is reflected in two points: first, researches have indicated that Smart's model is superior to Horton's law of stream lengths in that it permits the individual stream length ratios to vary within a single network, whereas Horton's law assumes that they are constant (Abrahams, 1984a). Of course, the success of Smart's stream length model is conditioned to the validity of its two previous assumptions; and second, models explaining frequency distributions of R_A in most, if not all, natural landscapes represent a mixture of link length subpopulations from different parts of the landscape characterized by dissimilar ground slope and/or environmental conditions (Abrahams & Miller, 1982).

If we assume that channel networks are space-filling with a fractal dimension of 2 in the plane (Mandelbrot, 1989), where Hortonian's laws holds exactly at all scales in the network, we can accept the assumption of Smart, in the case of moderately large N_ω , that

$$\lambda_\omega \sim R_B / 2 \approx R_B = 2\lambda_\omega \quad 5.10$$

Reorganizing equations 5.6, 5.7 and 5.8 in 5.3 and 5.9, and substituting in 5.10 we can get a modified value of R_A given by:

$$R'_A = [2 * (\Delta + (\Lambda * R_A))] / \Gamma \quad 5.11$$

$$\text{where} \quad \Delta = (N_1 - 1) / (2N_2 - 1),$$

$$\Lambda = \sum_{\omega=3}^{\Omega} (N_{\omega-1} - 1) / (2N_\omega - 1) = \lambda_3$$

$$\Gamma = \sum_{\omega=2}^{\Omega} (N_{\omega-1} / N_\omega)$$

The new value of Eq. 5.11 describes better natural channel networks than R_A does, since R'_A integrates Horton's structure-regularity approach and the random topology model of Shreve, both widely confirmed by observations on natural channel networks and best adapt to natural complex landscapes. The previous theory of modified link proportion (i.e. R'_A) is a valid assumption in all types of drainage networks, independently of landscape structure, i.e. homogeneity or heterogeneity. Moreover, equation 5.11 of R'_A implies that bifurcation and length properties are related to channel network complexity, which is directly linked to landscape structure and composition (Smart, 1978).

According to the degree of complexity in the drainage basin, R'_A reorganizes its value to adapt to the channel network evolution, which is represented by the total order of the drainage basin (i.e. Ω) and the sub-orders (i.e. ω) in the drainage network.

A general conceptual framework that covers R'_A behaviour is given in that, in a homogeneous landscape with similar environmental and local conditions, R'_A holds a constant-tendency change within the same order in the channel network and varying tendencies between orders (figure 5.1a). Such behaviour is quite similar to Schumm (1973, 1977) experimental model for stream initiation. Conversely, in heterogeneous structure formations, R'_A holds unsteady-tendency change through order change (figure 5.1b). Such oscillation is maintained till a stabilization stage is reached, where the model is capable to recognize all the existing relief forms. So, R'_A curve is steady in homogenous landforms and unsteady in heterogeneous relief leading to variable rates of change depending on DEM capacity to convey the finest terrain forms at the working resolution.

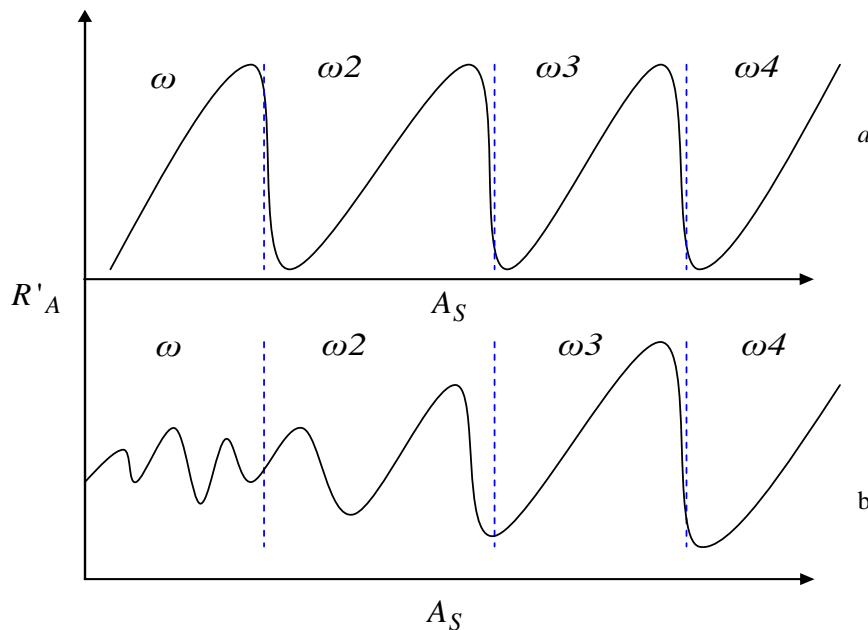


Figure 5.1 A conceptual framework for R'_A behaviour in, a) a hypothetical homogeneous landscape, and b) a hypothetical heterogeneous landscape.

5.3.5. The concept of stability zone and the hierarchical stratification approach

To achieve the general objective (i.e. define a channel network that best describe landscape complexity with least possible feathering) of the present work R'_A will be applied in a successive way, in which an arbitrary number of growing A_S values will be used. So, a changeable relationship will be constructed between growing A_S and their corresponding R'_A values, in which each R'_A is plotted against its related threshold leading to a varying-tendency curve relationship in the scatterplot (figure 5.1). The constructed curve contains several geomorphologic information that can be used in drainage network interpretation, among which the breaking scale point that describes change in dominant

processes from hillslope to fluvial ones (Tarboton et al., 1989, 1991). Taking into account that more than one threshold value could provide nearly similar geomorphometric properties, and in contrary to Tarboton proposal of a constant threshold value of one breaking scale point, it is highly probable that more than one A_S value (i.e. range of A_S values) can serve as the optimum threshold for stream source extraction in the landscape. The curve relationship between R'_A and A_S will form stages of tendencies or rate of changes (RC) each of which will be examined and interpreted separately. Indeed, these change-stages reflect the algorithm response to the degree of landscape complexity. Each stage in the curve represents the model capacity to define landscape composition in relation to DEM-grid dimension.

Herein, the maximum rate of change (MRC) in the curve relationship will represent a range of threshold values that best define channel network limits in the landscape, and where the model is able to define the best A_S value for the available grid dimension. First, under similar tectonic and environmental conditions, each stage represents a change in channel network dimensions, and hence a change in the order of the stream network. In this case the MRC will be the first one observed in the curve relationship. Whereas, under heterogeneous environmental and local conditions the generated curve is irregular and the changes are not related to changes in order, rather to model capacity to interpret landforms features. In this case, the MRC , i.e. later on will be referred to as stability zone (SZ), is the highest in the curve, in which the model best define the terrain and detect the possible optimum landscape dissection.

It's obvious that each RC area bears a range of thresholds, from which the local minima (i.e. minimum rate of change), the local maxima (i.e. maximum rate of change) and the average of both are detached. These locals are connected, in one way or another to catchment complexity. In this context and according to landscape heterogeneity, we believe that local minima represents the maximum complexity of the generated drainage network with minimum possible feathering in a heterogeneous complex landscape, whereas the local maxima represent the minimum complexity with the minimum possible feathering in a homogeneous simple landscape. Accordingly, local minima will be applied to heterogeneous landforms and local maxima to homogeneous terrain features. Of course, these points are related to other controlling factors such as DEM resolution and local factors. Throughout the present work, the minimum or maximum threshold interpretation will be delimited to some local-factor effects (e.g. geology, soil erosion, and runoff type), since environmental factors effects goes beyond the scope of this work.

Indeed, the stability-zone theory seems to work better under homogeneous landform than heterogeneous relief settings. Thus, if it is possible to identify these conditions, stability-zone model will fairly approximate to the optimum conditions necessary for defining the optimum range of A_S values. In this direction, scientists have related landform structure and/or geomorphic form of

catchments to the evolution stage of its channel network (Strahler, 1952a; Abrahams, 1977, 1984a; Mark, 1984; Willgoose & Hancock, 1998; Hancock & Willgoose, 2002; Hancock, 2005). For instance, Strahler (1952b, 1964) divided landforms into youth, mature (early and late ones) and monadnock characteristic shapes, reflecting increasing catchment age. These characteristic shapes are also consistent with different catchment erosion processes, catchment geometry and network forms (Abrahams, 1977; Willgoose & Hancock, 1998). The youth, mature, and old classifications generally equate to the headwaters, transfer, and depositional zones, respectively (DeBarry, 2004). In the present work, we will assume a direct linkage between homogeneity of landforms and age evolution, for which youthful drainage basins will reflect homogeneous relief, mature catchments will reflect a moderate heterogeneity, and finally old river basins will be represented by strong and complex heterogeneous structures.

In conclusion, the complexity of the curve, and hence the tendencies, depends on two important points: a) DEM resolution: DEMs of fine grid resolution are more realistic representation of real-world structure and process than coarse grid ones (Schoorl et al., 2000). So, for catchments of the same size area, in high resolution DEMs more terrain forms will be detected and more heterogeneous landscape is appreciated than low resolutions, and hence a complex-tendency curve (as observed in figure 5.1b) may be observed; and, b) Landform heterogeneity: mature basins occupy large areas, and hence more landforms and relief types, which is reflected by an unsteady tendency-curve relationship, whereas youth basins occupy relatively small areas and, hence, are generally characterized by similar local and environmental conditions. These small areas, usually represented by first order streams of the channel network, are highly homogeneous and are formed by small number of similar relief forms that generate a steadier tendency-curve relationship and clearer dominant stability zone than larger areas.

It is obvious that the curve tendency relationship formed by A_S and R'_A is steadier in homogeneous relief than heterogeneous landforms. Indeed, application of a constant threshold value in heterogeneous structures could lead to error propagation in form of data losing (i.e. poor defined drainage networks) or data exaggeration (i.e. feathering in channel network). On the contrary, a single or a constant A_S value defines better stream limits in homogeneous landscapes, highlighting the need for a simple landscape classification approach. So, in order to define landform heterogeneity, a group of relief indices (i.e. described earlier in chapter three) formed by the hypsometric integral (HI), relief ratio (R_H), Basin relief (H), and relative relief (R_r) have been evaluated in relation to catchment size. The HI has been selected between the remainder of indices, as a good descriptor of homogeneity-heterogeneity, for the followings:

- i) the HI describes implicitly the relationships between landform–evolution stage and dominant process in the landscape, whereas the rest of indices have been used in a simple descriptive sense for physiographic classification (e.g. catchment shape);

ii) the high correlation between the catchment area (A) and the relief indices (table 5.1) could lead to bias and misinterpretation in results and hence wrong conclusions; and,

iii) finally, the availability of different and vast amount of bibliography and studies enables a valid conclusions and interpretations of the HI effect (e.g. Strahler, 1952b, 1958; Leopold & Miller, 1956; Abrahams, 1977, Chorley et al., 1984; Mark, 1984).

variable	HI	H	R_H	R_r
$A-Di-1^*$	-0.1081	0.6709	-0.7221	-0.8033
$A-Di-2^{**}$	-0.3619	0.5338	-0.7814	-0.7237
$A-Di-3^{**}$	-0.4249	0.5739	-0.7296	-0.8993

Table 5.1 Rank order correlation index of Spearman (R) between relief indices (HI , H , R_H , and R_r) and catchment area (A) in Tabernas Basin. A is classified according to channel network diameter (Di) value (i.e. $Di-1 \leq 3$, $4 \leq Di-2 \leq 9$, $Di-3 \geq 10$). (*) Marked correlations are significant at $p < 0.05$. (**) Marked correlations are significant at $p < 0.01$.

In order to verify landscape units of similar characteristic properties (i.e. possible homogeneous parts of the catchment area), a hierarchical stratification procedure (HSP) has been integrated in the above approach. In this process, the intrinsic properties of the channel network will control the classification process of catchment units, which allows for a simple reclassification of the generated sub-catchments of decreasing orders. Such classification provides as much as A_S values in relation to the classified sub-basins, which usually approximates to homogenous relief forms identified by a user-defined value.

Concisely, the procedure to use in order to define the optimum drainage network in the studied landscape can be summarized as follows:

- 1) Definition of the MSZ for all the catchment from the A_S and R'_A relationship
- 2) Definition of the optimum A_S : selection of local minimum or maximum, in order to define the degree of heterogeneity/homogeneity in the landscape, as the optimum A_S will depend at the following conditions (primary cases):
 - If the study area forms a unique stability zone (SZ): such condition indicates a highly homogeneous terrain dominated by one erosional process;
 - If the MSZ starts from a saddle or a watershed divide: herein, we will assume that a divide or a saddle is not only a fine vector line that is represented by one pixel, rather a coarse line of 3 pixels as maximum, i.e. $A_S \leq 3$. In addition, the curve under these values is meaningless and unreliable; and,
 - If HI value ≥ 0.60 : several authors (e.g. Strahler, 1952b; Chorley et al., 1984; Willgoose & Hancock, 1998; Hurtrez et al., 1999) have appointed out that above such value uniformity of erodible materials are the dominant aspect in the landscape. Under these conditions the majority of

the constructed curve relationships are formed by either only one stability zone (*SZ*) or several ones but with equal stage tendencies, which confirms previous conclusions of homogeneity in relation to *HI* values.

3) The *HSP* or terrain classification: The *HSP* consists of the following:

- Applying the selected A_S from the defined *MSZ* at the studied catchment.
- In the generated drainage network, we define the catchment order or the order of the stream network (Ω).
- All the sub-catchments of order $\Omega-1$ are selected and the *MSZ* of each one is re-defined, and the corresponding drainage network is extracted.
- The process of *HSP* is repeated until the classified sub-catchments reached one of the primary conditions mentioned earlier in step 2.
- Again, the *HSP* is repeated with sub-catchments of order $\Omega-2$ and the *MSZ* is defined until the sub-catchments reach the conditions mentioned in point *d*.
- The process is repeated as necessary to all sub-catchments of successive descending order until all the catchment basin have been classified and corresponding channel networks are defined.

4) Finally, the sub-classified catchments are reconnected in order to build the final drainage network structure.

It's important to underline that *MRC* and *HSP* processes are successive and complementary steps in the present methodology approach, and, in our opinion, the two processes promise a good approximation to drainage networks that are well adapt to complex heterogeneous landscape. Hereafter, the combination of R'_A and *HSP* will be symbolized and designated as the $R'_A t$ approach, whereas R'_A algorithm will be assigned as the “*adaptive model*”. Figure 5.2 illustrates a schematic representation for the $R'_A t$ approach that reveals flow direction for the procedure execution.

5.3.6. Quantitative characterization of channel network

The quantitative analysis of drainage basins is the main procedure for characterizing variations, mainly small ones, in channel network structure. In chapter three, emphasis had been drawn on the definition and selection of the geomorphometric attributes that best describe general and particular property variation in stream networks. Previous results in chapter three led to the identification of 16 geomorphometric attributes (table 3.7) that enables for a direct comparison between different channel networks and among streams of the same system. Herein, and for simplicity, the terms parameter, descriptor, attribute and index will be used interchangeably throughout the work in order to represent the quantitative geomorphometric characteristics of the drainage network system.

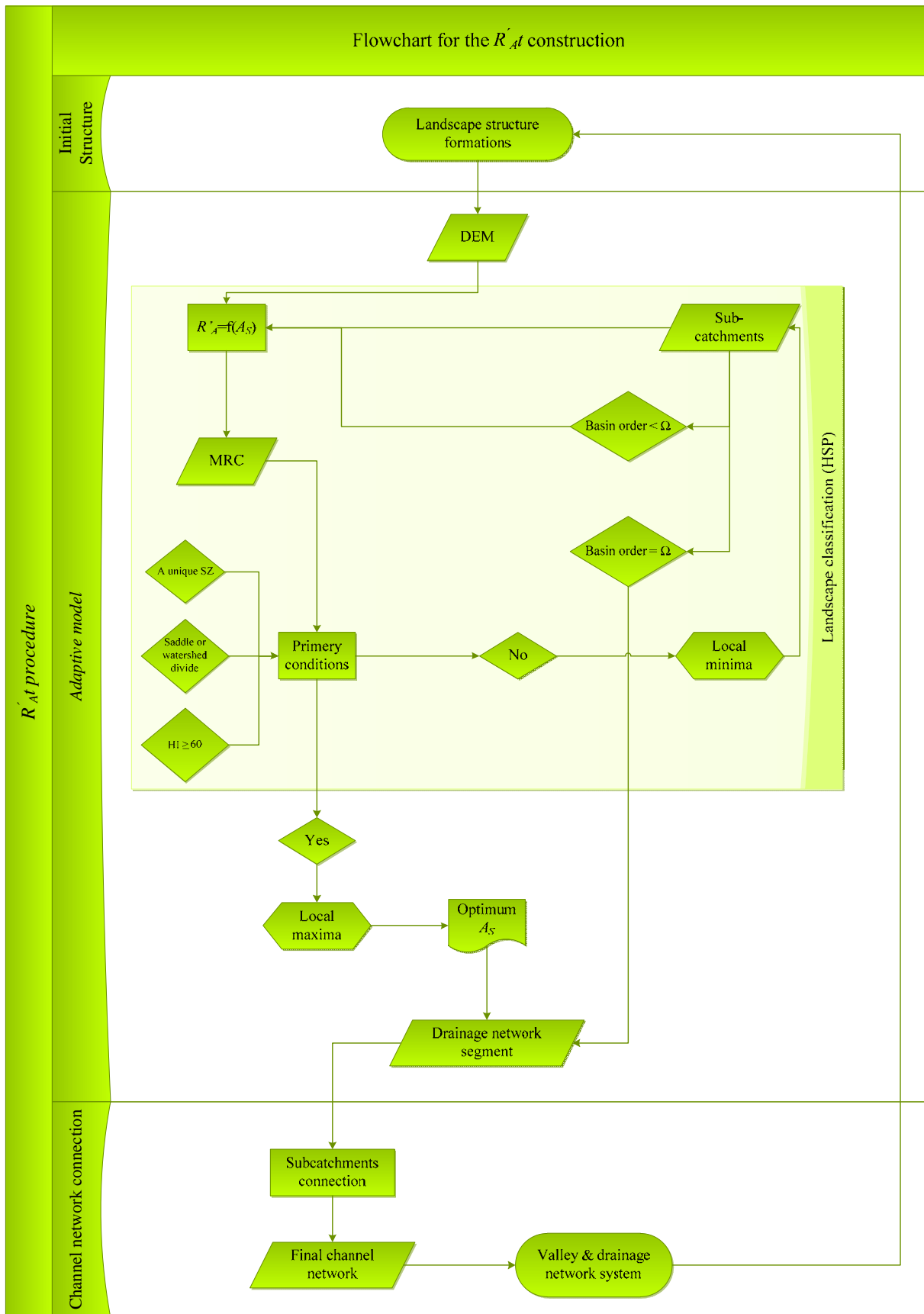


Figure 5.2 A schematic flowchart representing the $R'_A t$ approach and related processes.

Mode and type of comparison are between the several factors that limit validation procedures between DEM-generated channel networks and the natural streams represented by the blue lines (*BLs*). Herein, we need to compare two drainage network values that have the same influence on the association, regardless of the absolute size of the values (i.e. degree of similarity between two point values). In addition, traditional measures of correlation, such as Pearson or Spearman test, need more than two data points (i.e. minimum of three values) in order to achieve a degree of significance. Moreover, the comparison measure between sample points is direct and should be validated whether or not there is a data, since presence or absence of data (i.e. streams) is counted in the analysis process and not considered as a missing value; that is, one-to one comparison test. For so, the Gower Metric (*GM*) test of association (Gower, 1971) has been used in order to determine the degree of similarities between pair-association values of selected indices. The *GM* quantitative formula is given by:

$$D = \frac{1}{m} * |D_{ik} - D_{jk}| / k_n \quad k=1, m \quad 5.12$$

where D_{ik} is the data value of row i and column k , m is the number of variables, and n is the range of k .

The *GM* measure the similarity between pairs of sampling units, and the resulting matrix of similarities, has always direct positive values. This is important for the multidimensional Euclidean representation of the sample that also establishes some inequalities among the similarities relating three individuals, which cope directly with our search. Moreover, the *GM* test considers all compared factors as equivalent in a pool and thus is suitable for global comparisons.

In order to add more validity to the comparison model, the dissimilarity index (d_{mn}) (Eq. 3.22) of Smart (1972b) has been used as a complementary analysis after the *GM* test. The dissimilarity index of Smart is an effective parameter in detecting differences due to varying lithology and degree of maturity in drainage basins. The efficiency of the index is such that it can easily detect differences due to operator variation (Smart, 1972b) when comparing river basins of the same environmental conditions.

5.3.7. Model validation and auxiliary interpretations

In all above mentioned steps, the general idea was to prepare a conceptual framework for defining channel networks from DEMs based on the intrinsic properties of stream network structure. Both, deterministic and random approaches for channel networks, have explained major natural stream network distribution, behaviour, and evolution models. The proposed model of R'_A is the integrated form of regularity/randomness assumptions, which explains drainage network limits in relation to intrinsic stream network information provided by the dataset structure (i.e. DEM). Indeed, the intrinsic information is the final result of the model interpretation to the grid DEM resolution. The internal structure of the landscape interpreted by DEMs are scale dependent, in contrary to natural landform

structures (e.g. Mandelbrot, 1982; Tarboton et al., 1988), where river basins and drainage networks are not an exception.

In order to accept the model capacity in defining drainage networks limits, in addition to the quantitative analysis of geomorphometric indices mentioned earlier, two types of dataset structure have been used to represent natural landscapes: 1) first, a real-type dataset obtained from “Laser Scanning” that represents the finest-landscape structure; and 2) second, a virtual data structure extracted from DEMs of several resolutions, mainly 1- and 30-m DEMs, as well as highly defined orthophotographs of 0.5 m resolution.

The first dataset represents the last generation of available data types used in landscape studies, which consists of thousands of points that represents the finest relief forms of the landscape. The data is obtained from a hypsometric laser scanner that captures a digital 3D picture of the relief forms. Landscape studies and relief forms definition by means of laser scanning is relatively new discipline, which is reflected in the limited amount of available publications and bibliography. In addition, and due to the real time representation of the data, the constructed DTMs from these devices will serve as a validation tool for the model capacity in detecting process-dominant change, i.e. hillslopes to alluvial ones. Therefore, the treatment of data and generation of channel networks will be handled in a separated chapter. The second dataset are a group of DEMs of different resolutions; from which we detach the 1- and 30-m resolution that represent two different types of landscapes, heterogeneous and homogenous ones. The orthophotographs were used as a reference background for the different extracted or generated channel networks in order to highlight or even detach dissected from un-dissected terrains.

Results and model validation will be controlled by the data type used in channel network extraction. In the case of laser scanners data, geospatial analysis methods will be used to define channel limits, whereas in traditional gridded DEMs, *BLs* and auxiliary datasets of fieldwork will be used as a reference point for model validation. Although, *BLs* have been widely criticized by scientists, for the related errors produced by several factors (e.g. scale effect, worker judgments, etc.), their use is still the major reference for channel networks validation. Herein, *BLs* efficiency and accuracy will not be handled in this work, as it is out of the scope of this work; rather we will accept the available data as received from its sources. Accordingly, the general aspects of the validation process will include the following:

1. A *quantitative validation*: the main validation process, which consists of the extraction of the drainage networks and the definition of the optimum A_S for each drainage basin. Consequently, two types of indices are calculated, the geomorphometrical indices and the fractal values. For each-type indices, the values will be compared as observed for the automated networks and as expected for the *BLs*, for the same catchment.

2. A *qualitative interpretation*: a complementary validation process but of significant importance, since quantitative analysis needs to be validated in nature. In this case, the interpretation process includes visual validation and field visits: the former consists of a validation process that incorporates a series of orthophotographs at 0.5 m resolution, which permits a superimposition of the generated drainage networks over the terrain landforms and to realize a direct comparison between the channel network limits and natural terrain. The latter comprises a localization of channel limits through a direct visit to the study area. Fields visit is of great importance since it permits localizing the limits of stream networks in nature at the present moment, but is also of considerable complexity since definition of channel limits at low resolutions (i.e. <50m) is subjective and lack to any practical definition.

It worth to underline that the study was carried out on the Tabernas Basin area, which consists of several landscape units associated to various lithologic and tectonic formations more or less affected by different tectonic events of the Miocene, as well as different hydrologic and geomorphic processes underlined by varying climatic conditions. In Tabernas, the model testing and validation was carried out upon two major level scales. First, the Tabernas basin as a whole representing a highly heterogeneous landscape and is verified by the DEM at 30 m grid resolution. Second, two limited units of well homogeneous landscapes but of distinct relief formations represented by El Cautivo and La Rambla Honda catchments and verified by the DEMs at 1 m grid dimensions. The reason for selecting two landscape units was that the relative homogeneity of each one facilitates the examination of hillslope–stream limits, and both units, which are different from each other, enables comparing the robustness of the applied procedure. In addition, the model application at Tabernas Basin level allows for testing model flexibility.

5.4. Analysis and Results

5.4.1. Introduction

The application of the methodology proposed in this work consists of using R'_A algorithm in harmony with the *MRC* and *HSP* methods, named R'_{At} approach. As mentioned earlier, and in order to achieve a broad cover of different relief formations, two-level scale analyses have been realized. The first includes all Tabernas Basin at 30 m DEM resolution, a perfect example of broadly wide-range of heterogeneous landscape of about 560 km². The second level of analysis includes two catchments of relatively homogeneous relief forms at 1 m grid DEM resolution, but with different erosional processes. Tarboton and Ames method (2001) was used throughout the work for skeleton channel network definition, because we believe that it approximates well to natural drainage network formations than other methods.

During the work, two categories of channel networks will be developed and constructed. The first is the digitalized *BLs* from topographic maps at 1:50000 and 1:500 scale, equivalent to 30 and 1 m grid resolutions, respectively. So, the geomorphometrical characteristics derived from these

formations will be referred to as observed values. The second is the automated channel networks defined from DEMs with two different techniques for A_S definition: the $R'_A t$ methodology proposed in this thesis, and the Constant Drop Analysis (*CDA*) as an example of equivalent results generated by an established approach, which will be used for benchmark comparisons. Both resulting drainage networks calculated from these automated techniques will be referred to as expected values.

5.4.2. The analysis of Tabernas Basin at 30 m

5.4.2.1. Drainage network delineation

In Tabernas Basin, all related channel networks have been delineated and prepared for the test-comparison process, i.e. observed structures represented by *BLs* versus expected ones derived from automatic techniques. First, the *CDA* technique was applied directly to the channel network, which was extracted by the local-curvature method. A slightly smooth drainage network has been verified (corresponding to $A_S = 500$ cells), which, in clear evidence, represents the main channels and valleys of the area and not the complete drainage network system (figure 5.3). Second, the $R'_A t$ procedure has been applied to Tabernas Basin and a third channel network was extracted and defined, giving way to a compound iterative process that will be highlighted step-by-step in the coming paragraphs.

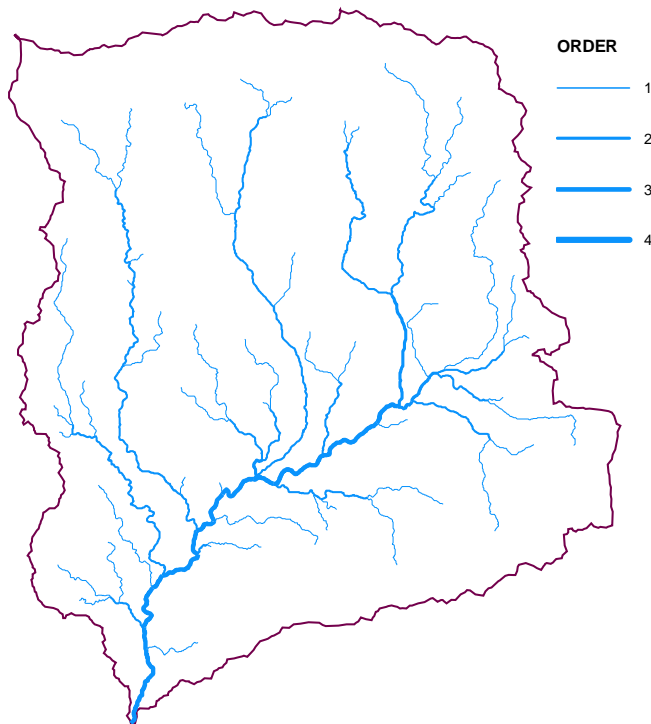


Figure 5.3 Channel networks delineated by the constant drop analysis (*CDA*) procedure with $A_S = 500$ cells.

On the other hand, The application of R'_A algorithm in Tabernas Basin provided a curve relationship of varying rate of changes, with a clear stability zone (*SZ*) at the final part of the curve relationship (figure 5.4) with $R'_A = 7.703$. At the working resolution, the *SZ* of Tabernas Basin extends

over a high range of A_S values that oscillate between 4650-11700 cells, representing local minimum and maximum, respectively.

The curve relationship in figure 5.4 reveals a clear positive tendency in the values of R'_A between thresholds of 4650-11700. The constructed *MRC* or the stability zone bears several indicating geomorphological information, from which we detach the points of local minimum and maximum. These locals will form the basic reference points in defining the appropriate A_S , in order to extract the optimum channel network. According to the proposed $R'_A t$ procedure, the local minimum should represent the appropriate A_S value to extract the optimum channel network at the available scale and resolution, since none of the primary conditions of the $R'_A t$ approach have been occurred. These conditions are formed by a hypsometric integral (*HI*) value for Tabernas basin of about 31.41% (Figure 5.5), more than one *SZ* is detected, and finally the *MRC* starts from A_S value of 4650, which is neither a saddle nor a watershed divide.

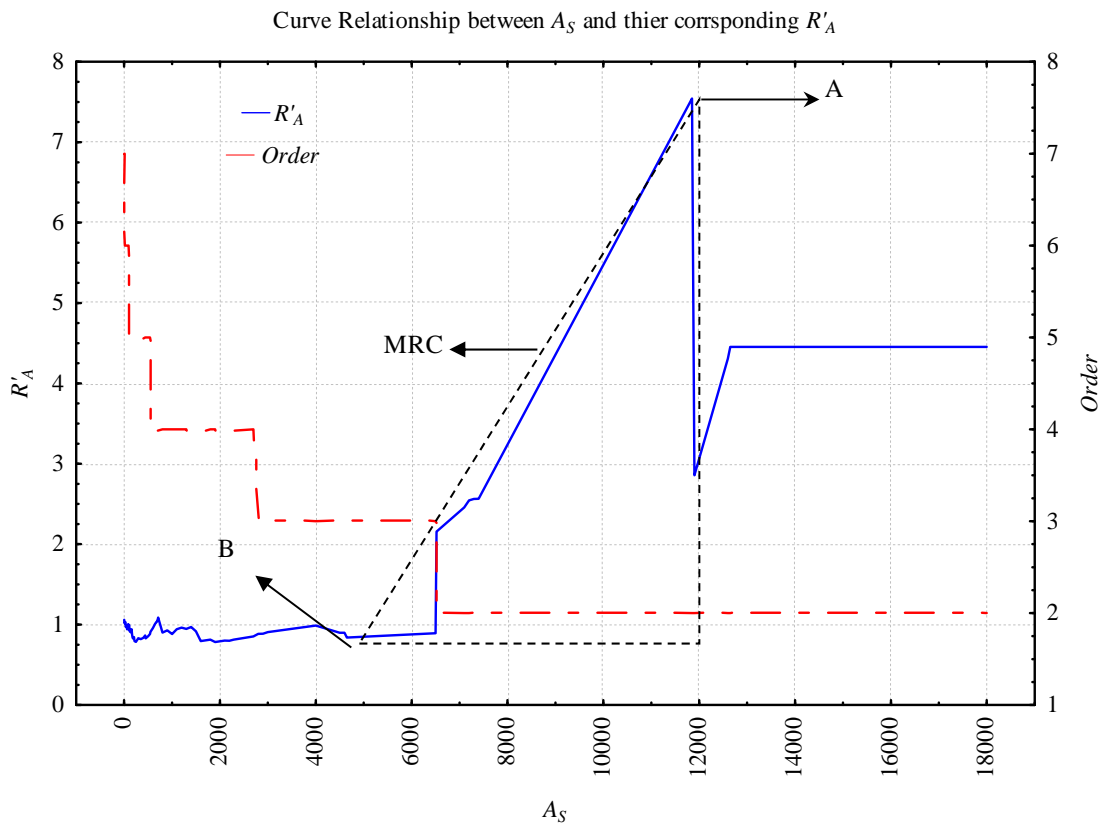


Figure 5.4 The curve relationship between R'_A and its corresponding A_S values for Tabernas Basin. A) Local maximum. B) Local minimum. The shaded area explains the concept of Maximum Rate of Change (*MRC*) or “*Stability Zone (SZ)*” in the curve relationship.

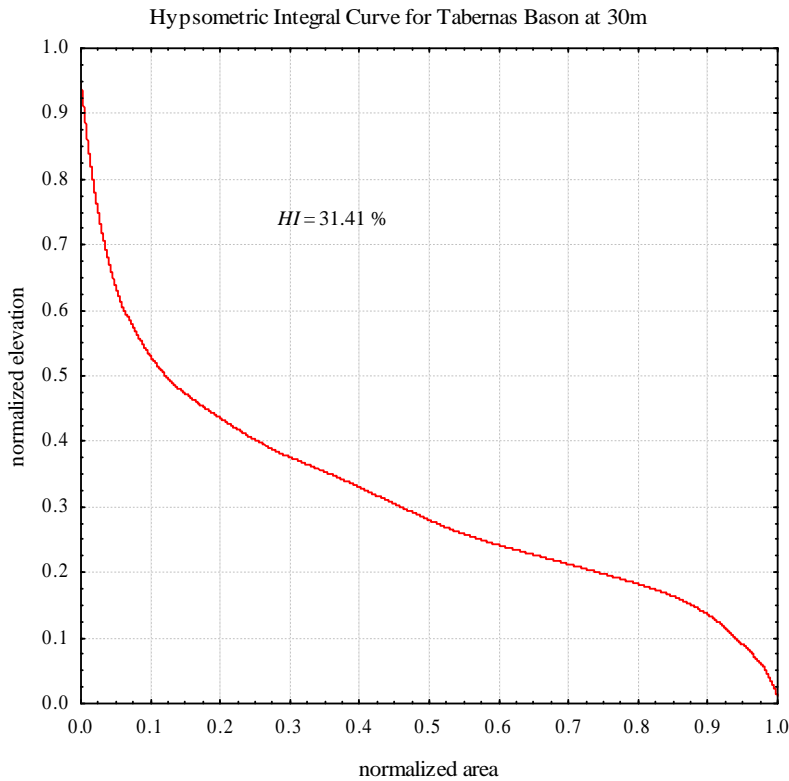


Figure 5.5 Hypsometric integral (*HI*) curve for Tabernas Basin DEM at 30 m resolution

The constructed drainage network with A_S of 4650 is slightly branched and describes the main valleys of the study area (figure 5.4). One of the principle advantages of the *HSP* process is that it classifies the catchment basin area in sub hierarchical classes according to the general order of the generated channel network, that is Ω , i.e. herein $\Omega = 3$. Hence and according to the *HSP* method, the Ω part of the catchment will be accepted as it is, whereas the sub-catchments will be treated in a hierarchical sequence; that is repeating the above process over sub-basins of order $\Omega-1$, $\Omega-2$, ..., $\Omega-n$, i.e. $n = \Omega - (\Omega - 1)$, respectively. Each of the following order sequence will be treated separately and the $R'_A t$ procedure will be applied to each level order, until the whole catchment area is classified (table 5.2, and figure 5.6). Finally, the channel networks of the reclassified sub-catchments are reconnected and the constructed channel network is considered as the appropriate drainage network for the present landscape at the available scale and resolution (Figure 5.7).

Cuenca	Area (km ²)	(Ω)	(Dd)	(μ)
$\Omega-2^*$	36.222	1	0.2717	1
$\Omega-2^{**}$	76.386	1	0.2099	1
$\Omega-1^*$	113.987	2	0.1363	2
$\Omega-1^{**}$	252.489	2	0.1019	2
Ω	567.265	3	0.3336	7

Table 5.2 Tabernas Basin and the main sub-catchments presented in figure 5.6

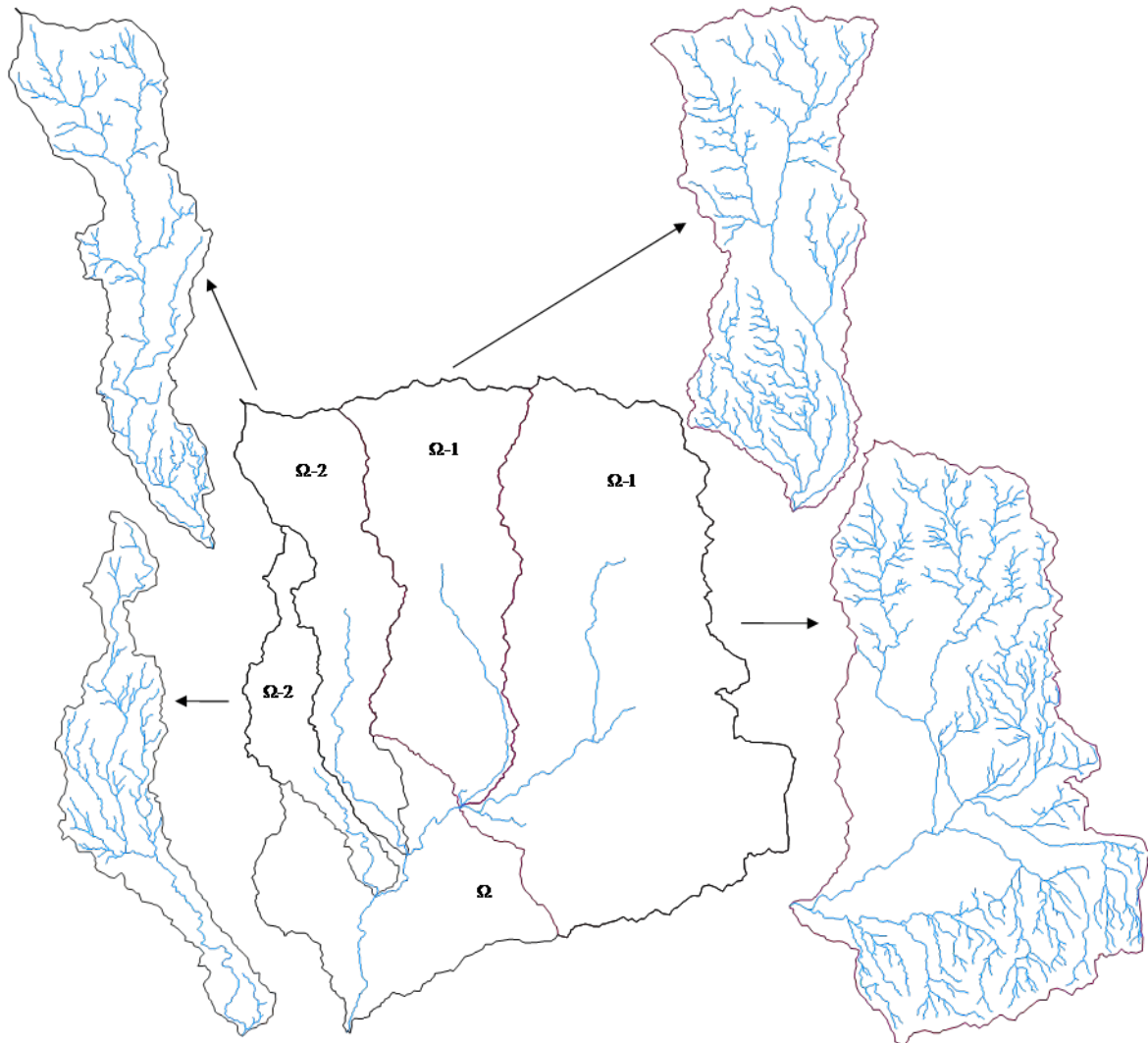


Figure 5.6 Order and classification of Tabernas Basin are defined by the maximum rate of change (*MRC*) from the curve relationship of R'_A and A_S . Herein, $\Omega=3$ represented by the white colour in the catchment, the yellow and green colours represents the sub-catchments of the following order (i.e. $\Omega=2$), and the dark gray colours represents sub-catchments of order 1.

In a general sense, the resulted classified sub-catchments of Tabernas Basin bear not as much information as the whole catchment or at least similar structure formations. Such conditions may imply a kind of simplicity to the terrain and hence more homogeneity, since the smaller the terrain is the lesser the amount of landform types are in the landscape. A simple comparison between the main sub-catchments of Tabernas Basin according to different landform classes confirms that homogeneity is more appreciated in small terrains than large ones (figure 5.8). It is highly feasible to find contradictory conditions to the above case, such as large deserts and great plains that are characterized by a clear homogeneous landform classes in vast extended areas. However, under such conditions the behaviour of the R'_A algorithm, and hence the curve relationship, will be applied to such formations.

The final result of applying the $R'_A t$ procedure is a highly-dissected branched channel network, that divides the landscape and hence the total basin to different levels of details. The degree in which

the generated drainage network with $R'_A t$ technique simulate natural streams is evident, mainly in the higher parts of the basin (figure 5.7), which reflects landform age and hence levels of complex properties in source areas or homogeneous terrains. Whereas, the low parts of the basin (e.g. near the outlet) have demonstrated a lesser degree of details than other parts of the catchment. The unlike approximation form in the low parts could be attributed to several factors, from which DEM resolution, terrain complexity and $R'_A t$ efficiency are detached.

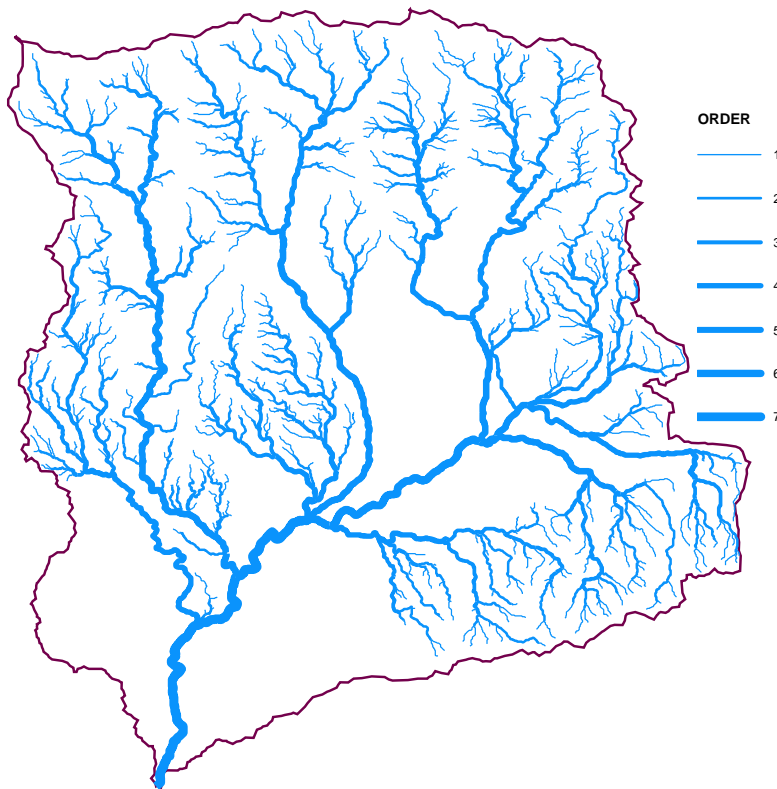


Figure 5.7 Channel networks in Tabernas Basin after reconnecting the reconstructed parts. Herein, the channel network is classified according to its order

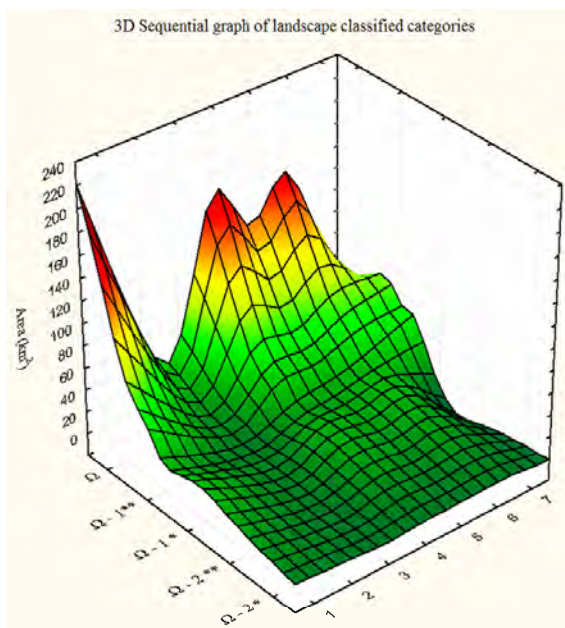


Figure 5.8 Tabernas sub-basins mentioned earlier in table 5.4 classified according to Pennock, Zebarth, and deJong (1987) landform classification scheme. This scheme classifies individual cells based on local (3x3 moving window) measures of slope and curvature. The output of this model is the following landform classes: 1) Convergent Footslope 2) Divergent Footslope 3) Convergent Shoulder 4) Divergent Shoulder 5) Convergent Backslope 6) Divergent Backslope 7) Level & smooth plane.

5.4.2.2. The comparison mode between techniques

As mentioned in previous chapters, geomorphometrical indices will be used throughout the present work as a comparing mode and consistent validating tool between natural channel network, represented by *BLs*, and automatic-generated drainage networks, delineated by *CDA* and *R'_At* techniques. Accordingly, three groups of datasets have been constructed that cover all data aspects necessary for result validation. The first group represents the geomorphometrical indices of the *BLs*, which, herein, will be referred to as expected or reference values to compare with. The second and the third groups are formed by the geomorphometric indices corresponding to the drainage network delineated by *R'_At* and *CDA* techniques. The last two datasets of indices will be considered as the observed value in the analysis tests.

In order to realize the comparison process, each of the sub-catchments generated by the *HSP* method has been used. In Tabernas basin, 389 sub-catchments had been constructed, from which 59 sub-catchments have been eliminated since no blue-line segments have been detected within the catchment boundaries, or in relation to other type of difficulties in definition and calculation process, mainly with first order streams in the channel networks. In the 330 remained sub-catchments, three replicates of datasets have been constructed, corresponding to the *BLs* and to the automated techniques used in channel network definition. 16 geomorphometrical indices have been selected, representing a wide range of drainage network properties (i.e. geometric, topologic, fractal, optimality, etc.) and usually used in stream and river basin analysis (table 3.7). It's important to mention that Hack's and Melton's fractal values have been used separately in the comparison analysis, because their definition require a linear relationship, a basic requisite that is not necessary for the rest of the parameters. Thus, they have been used in a posterior step of the analysis rather than the initial one.

Thus, the mode of comparison between the generated datasets is of considerable importance, since in one way or another all final results will depends on. Herein, two modes of comparisons have been applied:

1. An *Overall comparison* will be applied in which the geomorphometrical indices defined in table 3.7 will be used as descriptive parameters. The application area will be the catchment and sub-catchments of Tabernas Basin. The terminology of overall comparison is referred to the amount of parameters used in the comparison process; that is, all the indices with exception to fractal ones. The comparison process was performed using the Gower metric (*GM*) test of association because it performs overall comparisons based on the total dissimilarity associated with the set of geomorphometric indices. The final result will be a percentage of enhancements (%) in the comparison between automatic and digitized channel networks for each geomorphometric index.

2. A *Partial comparison* will be performed in which the fractal dimensions of Hack and Melton (α and θ , respectively) will be used as comparing parameters between channel networks. In each

studied drainage networks, α and θ are calculated and the results are compared with the digitalized network as well as with empirical-defined values for both parameters. Experimentally, α value reflects catchment shape and oscillates between 0.4 for large catchments to 0.6 for small catchments. Likewise, θ value tends to conserve constant in nature and approximates 2.

In both cases of comparisons (overall and partial) there will be two levels of analysis. The first one is before applying the *HSP*, which consists of applying the R'_A algorithm over the classified catchments of Tabernas basin without any consideration to the hierarchical stratification; that is, considering each sub catchment as independent one. The second level consists of using the $R'_A t$ procedure completely in all Tabernas Basin. The aim of the level comparison, i.e. before and after, is to check over the integrity and functionality of R'_A model and, in general, potentiality of $R'_A t$ technique in delineating channel network at varying scales.

I. The comparison without applying the HSP

1.1. The overall comparison analysis

A dataset matrix of 330 sub-catchments of different sizes has been selected to be used in the analysis of model efficiency in channel network delineation. The dataset comprises a group of catchments of different sizes that oscillate between 0.21-567.265 km² of different tectonics and environmental conditions, all are located within the Tabernas Basin. The overall comparison mode between datasets of the drainage networks for the sub-catchments of Tabernas Basin demonstrates a clear advantage for the R'_A model over the *CDA*, in 13 of the 16 indices used in the comparison process (table 5.3). Whereas, if Tabernas Basin was selected as a whole and the comparison are realized between the two techniques, a clear advantage is observed for the *CDA* over the R'_A (table 5.4). Failing in result enhancement of the R'_A technique at Tabernas Basin-level size is contradictory to what we have obtained earlier in table 5.3. In order to understand such failure, a direct comparison between stream network delineated by R'_A technique and the *BLs* using the drainage density parameter reveals a clear enhancement at basins of small size scale, i.e. less than 5 Km², and a parent decline over that scale (figure 5.9). In order to counteract this gap failure, the *HSP* was introduced in the R'_A technique as a compensator factor in heterogeneous landscapes, in order to achieve more appropriate adaptation to natural channel networks, herein represented by the *BLs*.

Degree of enhancement %				
No.	Index	CDA	R_A^t	similar
1	Ω	9.16666	77.5	13.333
2	La	38.9743	58.9744	2.0513
3	Dd	20.5128	78.9743	0.5128
4	μ	12.3967	84.2975	3.3057
5	inR_A	54.1666	45	0.8333
6	K_i	26.6666	72.8205	0.5128
7	R_B	38.9831	55.9322	5.0847
8	F_S	42.5641	51.7948	5.6411
9	H_μ	12.5	81.6666	5.8333
10	k	57.7319	41.7525	0.5155
11	P_S	44.0678	55.0847	0.8475
12	OCN	11.2821	88.2051	0.5128
13	$p(\mu)$	44.56	53.68	1.76
14	E	51.6949	47.4576	0.8475
15	Isd	19.4872	80	0.5128
16	ε	19.4872	79.4872	1.0256

Table 5.3 Degrees of result enhancement (%) in comparison between geomorphometrical parameters of the *BLs* and automated channel networks using the *GM* test before using the *HSP*. Shaded values indicate the best values.

	Index	<i>BLs</i>	CDA	R_A^t	<i>BLs-CDA</i>	<i>BLs-R_A^t</i>
1	Ω	6	5	3	0.0029	0.0088
2	La	46.041	44.57	35.429	0.0043	0.0310
3	Dd	1.7625	0.5348	0.1462	0.0036	0.0047
4	μ	407	51	7	1.0409	1.1696
5	inR_A	1.504	1.2353	2.0196	0.0007	0.0015
6	K_i	0.0492	0.0190	0.0122	$8.8*10^{-5}$	0.0001
7	R_B	2.5809	1.9303	1.6666	0.0019	0.0027
8	F_S	1.4332	0.1780	0.0229	0.0036	0.0041
	H_μ	0.5143	0.5429	0.7416	$8.3*10^{-5}$	0.00066
9	k	0.4614	0.6223	1.0714	0.0004	0.0017
10	P_S	-0.9431	-0.9202	-0.4792	$6.6*10^{-5}$	0.0014
11	OCN	1358.67	949.31	361.92	1.1969	2.9145
12	$p(\mu)$	$3.4*10^{-5}$	0.00078	0.0161	$2.1*10^{-6}$	$4.4*10^{-5}$
13	E	0.6649	0.8097	0.4951	0.00042	0.00049
14	Isd	6.514	1.9769	0.5405	0.0132	0.0175
15	ε	1.5518	1.5271	1.486	$7.2*10^{-5}$	0.0002

Table 5.4 Direct comparison values for Tabernas Basin without using *HSP*. Again, shaded values indicate best results.

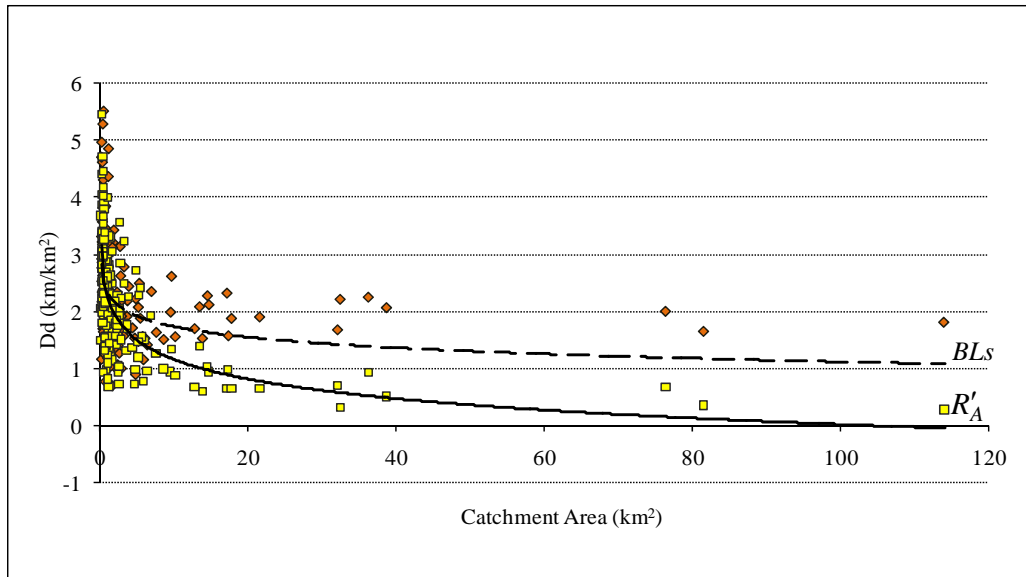


Figure 5.9 Curve relationships between catchment area (A) and corresponding drainage density (Dd), for both BLs and automated channel network delineated by the $R'_A t$ technique without the hierarchical stratification procedure (HSP).

1.2. The partial comparison analysis

As in the previous section and in order to continue with same methodology, empirical values of Hack's and Melton's laws, i.e. 0.4-0.6 for α and 2 for θ , were substituted with calculated values of the BLs of the studied area. In this context, and under the present scale and resolution, α value of Hack's law for the digitized drainage network in Tabernas Basin approximates to the empirical one with a value of about 0.6128 (figure 5.10a). While, Melton's θ shows anomalous value of 1.0877 (figure 5.10b), which doesn't approximate to the empirical one, i.e. ≈ 2 , but again will be accepted as it is and its deviation will be explained later.

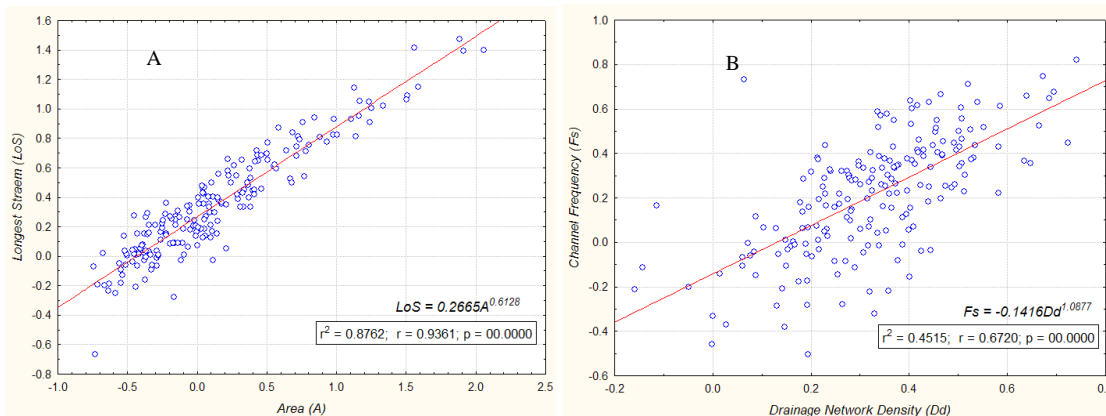


Figure 5.10 Fractal dimensions of Hack's and Melton's laws for the BLs in Tabernas Basin. A) Hack's α value of 0.6128 and highly r^2 that approximates to 0.88. B) Melton's θ value of 1.0877 with low r^2 that approximates to 0.4515. The two relationships are highly significant at 0.01 confidence level.

For the automated channel networks, the situation is completely different, where approximations to BLs and optimum values are somewhat contradictory. Values of α and θ with their corresponding level of significance are shown in table 5.5. It's obvious that with a simple observation

to table 5.5 results reveal a clear enhancement for $R'_A t$ technique over CDA since both values of r^2 is of irrelevant importance. Statistically, dissimilarity index of GM test for BLs is higher in the case of CDA than the $R'_A t$ technique (table 5.5) showing a good approximation to natural stream properties for the $R'_A t$ procedure. The two types of comparisons (overall and partial), for the first stage of the analysis, i.e. without HSP , have shown a clear evidence of the highly potential of the $R'_A t$ in simulating BLs characteristic properties. However, evidence for exhaustive comparison of some parameters, such as Dd in figure 5.9, indicates a gap failure at highly-scale sizes for catchment analysis, for which the HSP was adapted and introduced.

		Calculated values			GM test	
		CDA	$R'_A t$	BLs	$BLs-CDA$	$BLs-R'_A t$
α	Hack	0.5833	0.6049	0.6128	0.01475	0.01315
r^2		0.8815	0.8127	0.8762		
ϕ	Melton	1.9643	1.6656	1.0877	0.4383	0.28895
r^2		0.9119	0.7044	0.4515		

Table 5.5 Values of partial comparison between α and θ for the studied catchments in Tabernas Basin and the GM test values. All values are highly significant at 0.01 ($p < 0.00000$).

II. The Comparison with the HSP:

It's obvious that the constructed drainage network with $R'_A t$ technique and without the HSP procedure fails in the enhancement of landscape dissection in particular cases, mainly in large areas. Such failure could be attributed to high landform heterogeneity in some parts of the terrain; whereas, $R'_A t$ without the HSP succeeded more in small scale areas of homogeneous relief forms. In order to avoid this failure, the HSP was introduced to compensate model capacity in such terrains. As usual, the reference BLs are calculated, which will contain the same values for the two level of analysis and the same for the CDA since HSP forms part of the $R'_A t$ procedure and none of the previous techniques.

II.1. The overall comparison analysis

Again, the constructed drainage networks from CDA and $R'_A t$ techniques were compared with the BLs dataset and results again get back to confirm the high efficient capacity of the $R'_A t$ approach over the CDA technique (table 5.6). Once more, results confirm a noteworthy enhancement for $R'_A t$ over CDA technique, mainly in geometrical parameters such as Dd and ϵ . Such enhancements are translated in a more precise adjustment between curve relationship of Dd and its corresponding drainage area (figure 5.11), as seen earlier in figure 5.9. Although results have confirmed greater enhancement for the $R'_A t$ over the CDA in almost all studied parameters, in both cases before and after

using the *HSP* method, some indices revealed fairly decline in topological-parameters enhancement, such as Ω , μ , and $p(\mu)$. Such fall maintains the superiority of the $R'_A t$ approach but the degree of similarity has been reduced. These observations are confirmed a gain when compared with the delineated channel networks using the $R'_A t$ and *CDA* techniques at Tabernas Basin level (table 5.7).

Degree of enhancement %				
No.	Index	<i>CDA</i>	$R'_A t$	similar
1	Ω	6.7226	64.7059	29.4118
2	La	34.8717	64.1025	1.0256
3	Dd	9.7435	89.7435	0.5128
4	μ	13.5593	80.5085	5.9322
5	inR_A	45.3781	53.7815	0.8403
6	K_i	29.8969	69.5876	0.5154
7	R_B	38.9831	55.9322	5.0847
8	F_S	15.8333	78.3333	5.8333
9	H_u	8.3333	82.5	9.1666
10	k	53.6	45.6	0.8
11	P_S	41.5254	57.6271	0.8474
12	OCN	5.6410	93.84615	0.5128
13	$p(\mu)$	49.56	47.88	2.56
14	E	51.020	47.9591	1.0204
15	Isd	9.2307	90.2564	0.5128
16	ε	12.3076	86.6666	1.0256

Table 5.6 Degrees of result enhancement (%) in the overall comparison between geomorphometrical parameters of the *BLs* and automated channel networks using the *GM* test after using the *HSP*. Shaded values indicate the best values.

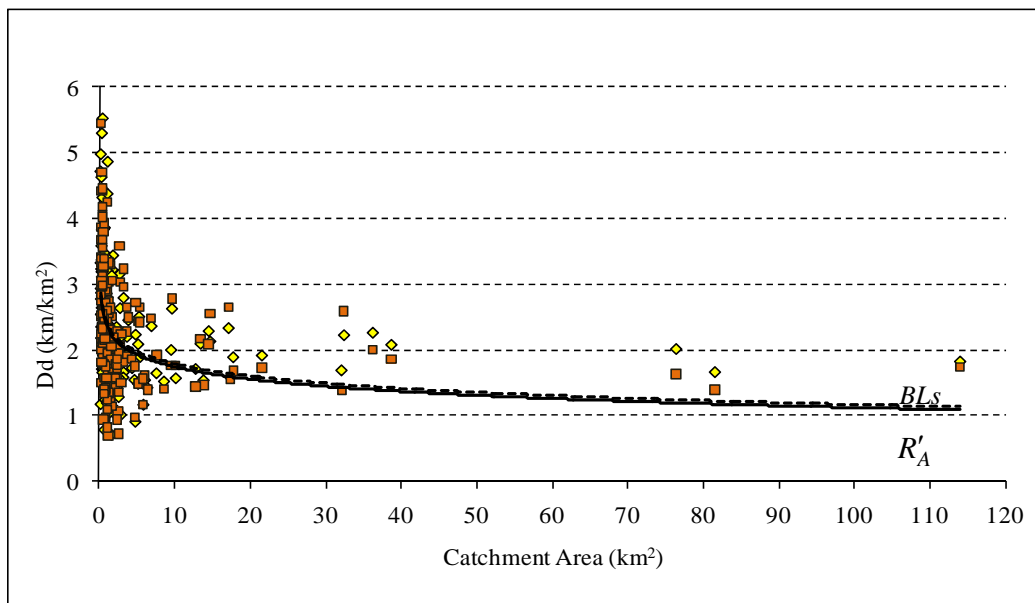


Figure 5.11. Curve relationships between Catchment Area (*A*) and corresponding drainage density (*Dd*), for both *BLs* and automated channel network delineated by the $R'_A t$ technique with the hierarchical stratification procedure (*HSP*).

In general, the constructed channel networks defined by $R'_A t$ procedure shows a considerable enhancement in geometrical parameters, a moderately improvement in topological ones, and a non-enhanced results with parameters that integrate drainage area with length parameters. This

inconsistency in parameters behaviour can be attributed to the following: 1) automated-technique capacity to delineate channel network from DEMs is different to that of *BLs* procedures; 2) Channel network delineation techniques integrate or/and define a specific catchments area (A_S) in order to define where channel begins, whereas *BLs* are a purely subjective decision of technicians; 3) finally, none of the proposed models used for automatic channel networks delineation is capable to define a channel network with a single stream; that is, a single stream in a small sub catchment, which could be considered as one of the main disadvantages of automatic models for stream delineation. For so, and in order to achieve similar geometrical properties in stream structures, models needed minimum three segments in the channel network, i.e. $\Omega = \mu = 2$. Thus, 1 exterior stream with λ_i length in the digitized *BLs*, i.e. $\Omega = \mu = 1$, is the same to λ_i length but with higher order and magnitude, i.e. minimum $\Omega = \mu = 2$, for automatic channel networks. As a result, similar geometric measurements of the same catchment, mainly exterior stream-links, calculated and defined with different techniques, but with different topological properties.

No.	Index	<i>BL</i>	<i>CDA</i>	R_A^t	<i>BL-CDA</i>	<i>BL-R_A^t</i>
1	Ω	6	5	7	0.0029	0.0029
2	La	46.041	44.57	46.748	0.0043	0.0021
3	Dd	1.76245	0.53488	1.448	0.0035	0.0009
4	μ	407	51	689	1.0409	0.8246
5	inR_A	1.504	1.235	0.577	0.0007	0.0027
6	K_i	0.0492	0.0190	0.0898	$8.8 \cdot 10^{-5}$	0.0001
7	R_B	2.5809	1.9303	2.7717	0.0019	0.0006
8	F_S	1.43319	0.17805	2.4274	0.0037	0.0029
9	H_u	0.5143	0.5429	0.5109	$8.3 \cdot 10^{-5}$	$9.9 \cdot 10^{-6}$
10	k	0.46139	0.62233	1.1577	0.0005	0.0020
11	P_S	-0.9431	-0.9202	-0.7993	$6.6 \cdot 10^{-5}$	0.0004
12	<i>OCN</i>	1358.67	949.317	1557.31	1.1969	0.5808
13	$p(\mu)$	$3.4 \cdot 10^{-5}$	0.00078	$2.4 \cdot 10^{-5}$	$2.1 \cdot 10^{-6}$	$2.2 \cdot 10^{-6}$
14	E	0.6530	2.1740	1.3157	0.0044	0.0019
15	Isd	6.514	1.9769	5.3518	0.0133	0.0034
16	ε	1.5518	1.5271	1.5532	$7.2 \cdot 10^{-5}$	$4 \cdot 10^{-6}$

Table 5.7 Direct comparison values for Tabernas Basin using *HSP*. Again, shaded values indicate best results.

For the overall comparison, figures 5.12 and 5.13 show that, visually speaking, the constructed channel network with R_A^t approximates the general aspect of natural drainage network and enhance landscape dissection better than *CDA*. In addition, mathematically speaking, the *GM* test reveals that enhancement in similarities have been reduced to the minimum in the case of R_A^t compared with *CDA* (table 5.7). Moreover, estimations for *CDA* technique reveal a clear deterioration in channel network aspect at different basin level scales. This deterioration can be measured as sub-estimation of the channel network (figure 5.12b), super-estimation or feathering for the drainage network (figure 5.13b), and hence failure in detecting a suitable A_S for almost 35% of the studied catchments, mainly in small ones, i.e. basin catchment area less than 0.6 km².

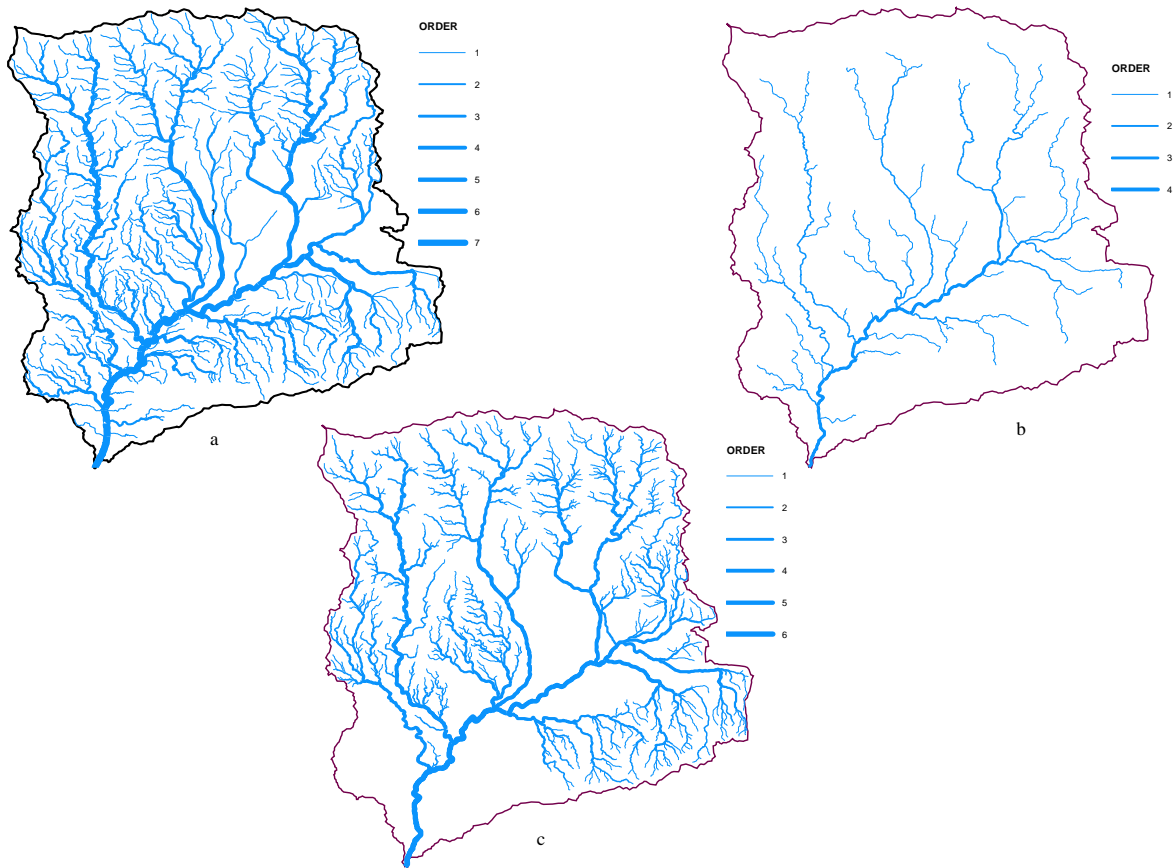


Figure 5.12 Comparison between channel networks in Tabernas Basin delineated by, a) the digitized blue lines (BLs); b) Channel networks extracted with CDA procedures with $A_S = 500$; and, c) channel network defined by the $R'_A t$ procedure.

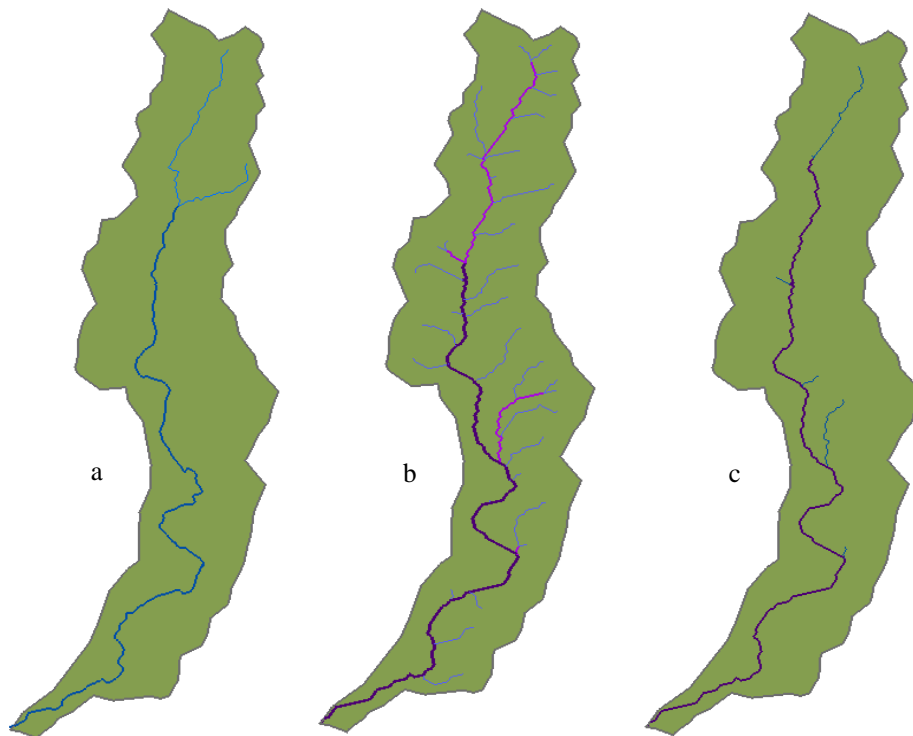


Figure 5.13 Observed sub-catchment within Tabernas Basin and its corresponding drainage networks defined by: a) Blue lines; b) the CDA with $A_S = 8$, and c) the $R'_A t$ with $A_S = 35$.

II.2. The partial comparison analysis

In the case of the partial comparison analysis, α and θ values have confirmed again the efficiency of $R'_A t$ in defining landscape dissection in comparison with extracted BLs over the CDA technique. Results for the partial comparison continue in the same line of previous results, and again demonstrated a reasonable enhancement in channel networks characteristics, mainly for Melton's dimension, where θ value of $R'_A t$ technique approximates BLs value (table 5.8). The GM test results in table 5.8 shows that dissimilarities between $BLs-CDA$ is higher for both values of α and θ than $R'_A t - BLs$. while the empirical Hack's values α oscillate in the margins of that suggested by scientists, θ values of Melton approximate to 1, which is nearly half of that proposed by researchers. These findings highlight the consistency of Hack's law at heterogeneous landscapes of varying environmental conditions, the contrary to Melton's law where it shows high deviation between different size scale values.

		Calculated values			GM test	
		CDA	$R'_A t$	BLs	$BLs-CDA$	$BLs-R'_A t$
α	Hack	0.5623	0.6224	0.6128	0.0169	0.0039
r^2		0.9088	0.9166	0.9040		
θ	Melton	2.0562	1.1008	1.1082	0.474	0.0037
r^2		0.9352	0.5264	0.4681		

Table 5.8 Comparison values of α and θ and their Gower Metric (GM) test of association for the total comparison with HSP in studied catchments of Tabernas sub-basins. All values are highly significant at 0.01 ($p < 0.00000$).

It seems that variations in α and θ values are completely inconsistent and could be attributed to local and environmental factors as well as dataset dimension. BLs dissection, and hence stream network frequency, is absolutely different in smooth terrain to that of abrupt relief, where the topographic contrast enhances visualization and interpretation of the landscape, thus highly branched BLs , which may lead to higher variations in Melton's value θ . In addition, it seems that the scale of the area plays a significant role in determining θ value. So, θ value was recalculated again for the same dataset of the BLs but in relation to catchment size and results revealed that θ value is readjusted considerably to approximate empirical values of 2 described by researchers for natural river basins as basin size is increased (figure 5.14). Furthermore, the coefficient of determination (R^2) takes the same tendency and tends to enhance as catchments sizes increase. The above mentioned analysis has been realized and the same tendencies and observations were detected in the channel networks defined by the automated utilized techniques (table 5.9).

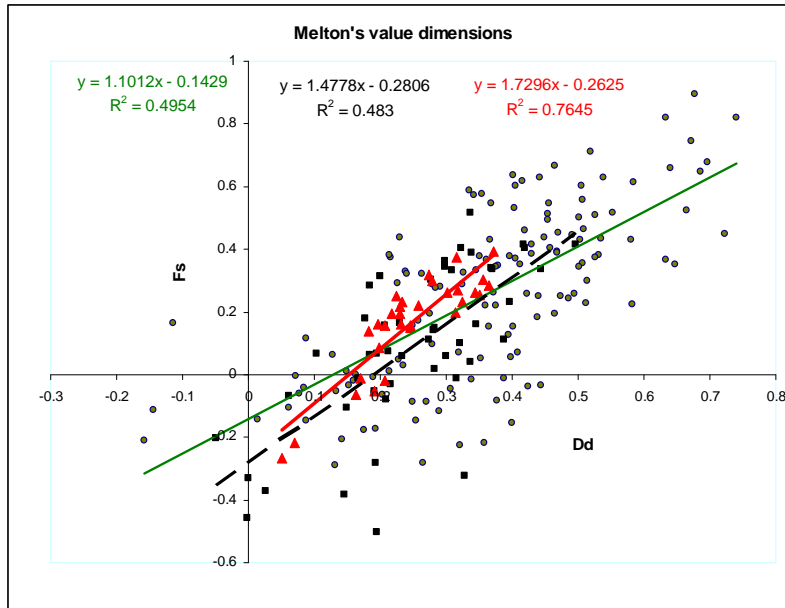


Figure 5.14 Estimation of Melton's value (θ) for the digitized-*BLs* in the sub-catchments of Tabernas Basin. Values are grouped according to their sizes, where circles and green line curve represents catchments between 0.1-2 km², squares and black line for catchment's size between 2-10km², and finally triangles and red line for catchments >10 km².

Catchment size (km ²)	<i>CDA</i>		<i>R'_At</i>	
	θ	R^2	θ	R^2
0.1-2	1.1826	0.5291	0.8854	0.3506
2-10	1.617	0.8536	0.9927	0.5385
<10	2.0853	0.922	1.2912	0.8919

Table 5.9 Dimensions of Melton's value (θ) for channel networks delineated by *CDA* and *R'_At* techniques in Tabernas sub-basins in relation to catchment size. Same tendencies and observations are detected for all constructed channels.

5.4.3. The analysis of El Cautivo and La Rambla Honda Basins

5.4.3.1. Introduction

The Cautivo and Rambla Honda basins are characterized by their relatively homogeneous lithology and tectonic origin, mainly concerning geological and soil erosion forms. For which, it is highly expected that results from applied techniques should perform better and to convey a higher capacity in simulating natural landscape dissection. The two catchments are constructed from high-resolution DEMs (i.e. 1 m grid), and limited size area that permits a comprehensive field visit for both sites. Hence, comparison mode will be modified to adapt the new condition of the studied catchments. The partial comparison mode needs a group of sub-catchments in order to define the fractal dimensions α and θ , a requisite that is not available in this case, for which it was dropped down from the comparison process. The overall comparison results using geomorphometrical indices will be sustained as the principle mode of comparison, and the total comparison will be compensated by a visual interpretation of the results, that is, the field visit and the in-situ interpretations of the delineated

channel networks. Visual interpretation, or scientific visualization, of landscape and hence channel networks, are not less important than other presented methods in providing methodological approaches (Wood, 1995) for drainage network delineation.

For the Cautivo catchment, and in order to have a uniform comparison mode, channel network has been constructed in a well-defined section of the total catchment, since available-DEM limits doesn't cover a complete hydrological catchment unit (figure 5.15). The overall comparison has been performed with the same methodology explained earlier. The visual interpretation was carried out with several visits to the studied catchments. Again subjectivity is recognized to form part of the applied methodology in defining where channels begin in the terrain or stream sources.

5.4.3.2. Drainage network delineation

Again, the R_A^t and *CDA* techniques were applied in order to define the optimal drainage network for the Cautivo and the Rambla Honda catchments. In the Cautivo catchment, the R_A^t technique provided an enhanced-like aspect to the drainage network over the *CDA* and even the digitized *BLs* (figure 5.15). While field visits have confirmed location and limits for all the defined streams by the R_A^t approach (figure 5.15c), presence or absence of some streams was quite obvious between the *BLs* and the *CDA* approaches (figure 5.15a and b). In general, the digitized-*BLs* shows high depiction for the stream network in the mid part of the basin and absence of clear streams in the upper and lower-mid parts of the catchment (figure 5.15a), whereas the *CDA* technique resulted with feathering in almost all parts of the basin (figure 5.15b). Finally, the R_A^t technique highlighted a well dissected landscape with a fairly distribution of first order streams in almost all section parts of the catchment (figure 5.15c). These observations, once again, confirms the capacity of the R_A^t model to adapt to landform structure whatever the complexity is, leading to a reasonably harmonized definition for the stream network limits.

In the case of the Rambla Honda, visualization of the 3D terrain forms and the delineated channel networks by the 3 techniques (figure 5.16) shows a relatively good improvement of landscape depiction by the R_A^t approach over the *CDA* technique, and even a better approximation to natural landscape dissection than the digitized *BLs* (figure 5.16a). Such enhancement is widely attributed to the highly smooth relief formation of the Rambla Honda field site, which makes it somewhat little complicated to be interpreted by cartographers. A completely different situation is achieved by applying the *CDA* technique, where the results revealed a channel network modified entirely in almost all the aspects compared with the *BLs* (figure 5.16c). In general, the *CDA* technique verified an extremely high dissected terrain, a property that does not form part of the Rambla Honda Landscape. Once again, the field visits have confirmed the above observations, in which the R_A^t technique and the *BLs* depict fairly the drainage network of the studied basin.

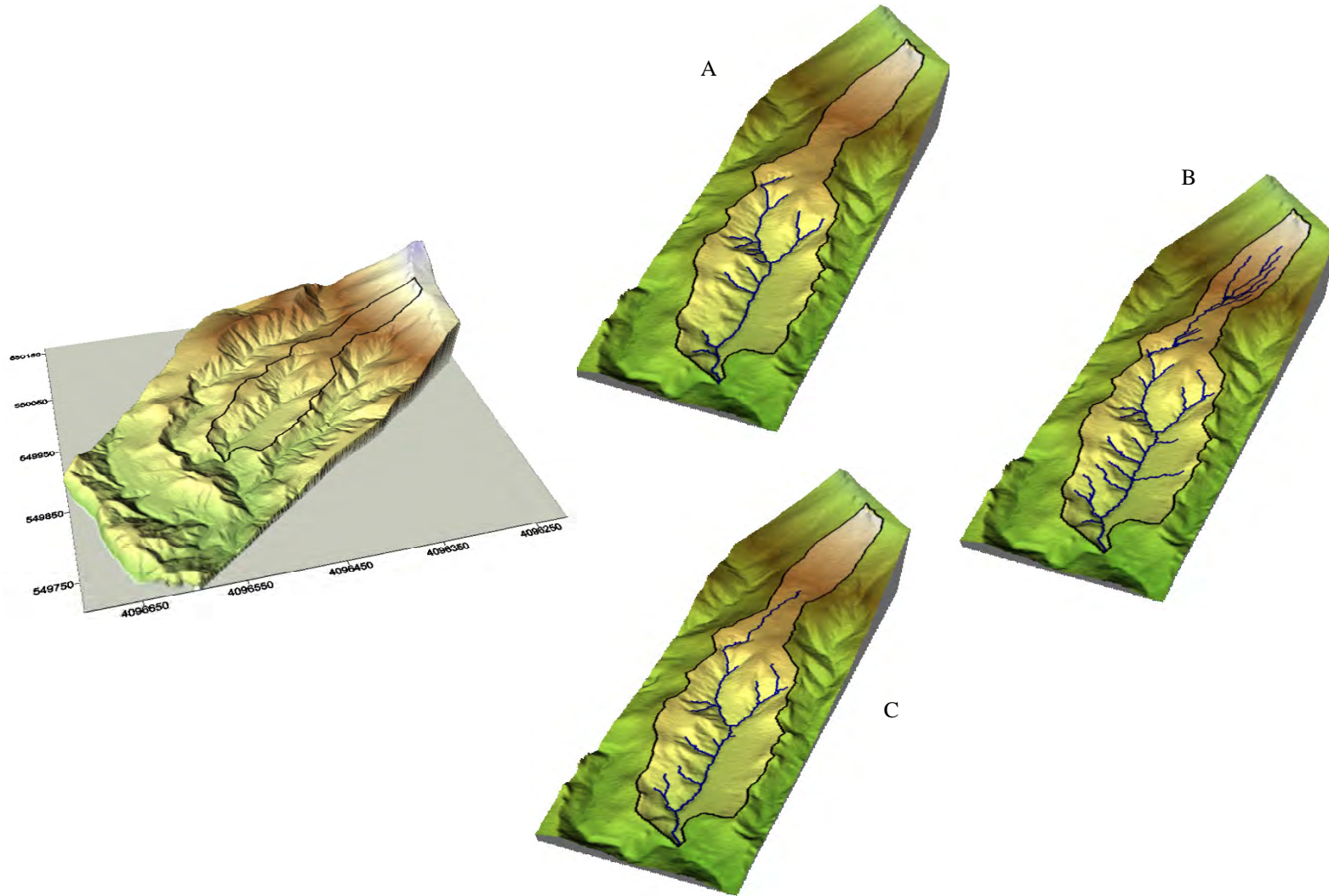


Figure 5.15 The Cautivo Basin field site with different channel networks defined by the *CDA* and $R'_A t$ techniques compared with *BLs*. A) Digitized channel network (*BLs*); B) Defined channel network by *CDA* technique with $A_S = 8$ cells; and, C) Delineated channel network by $R'_A t$ technique.

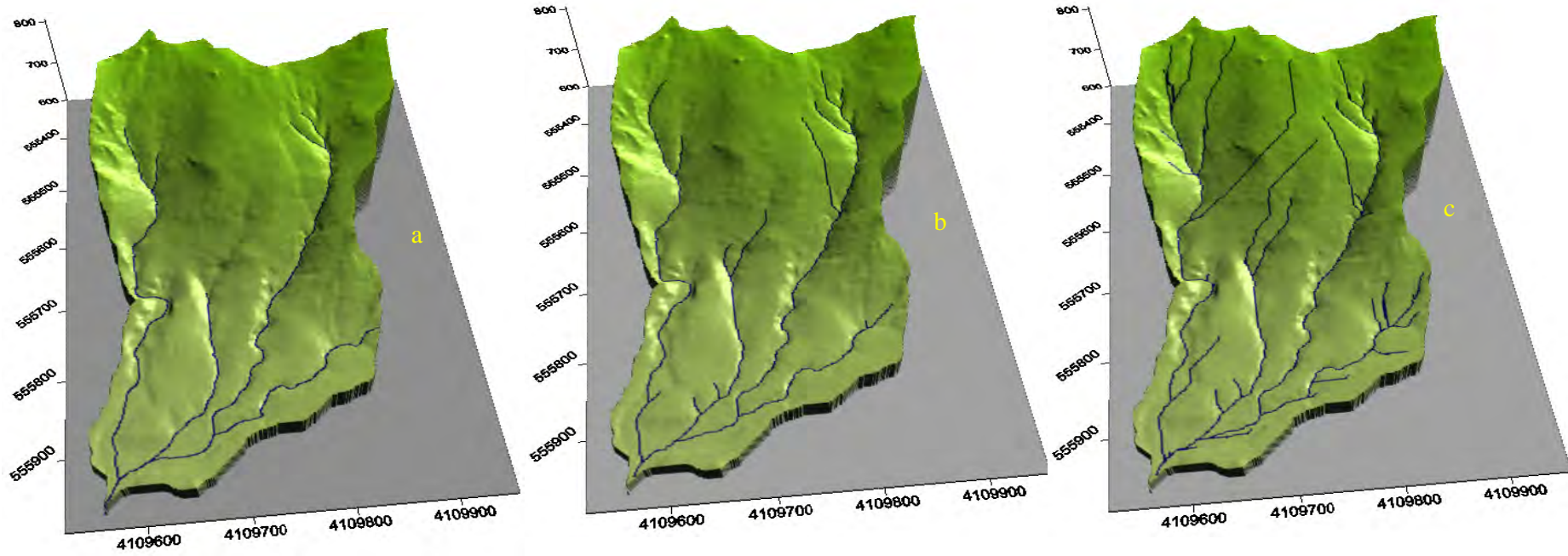


Figure 5.16 Rambla Honda Basin field site with different channel networks defined by the *CDA* and $R'_A t$ techniques compared with *BLs*. a) Digitized channel network (*BLs*); b) Delineated channel network by $R'_A t$ technique; and, c) Defined channel network by *CDA* technique with $A_S = 14$ cells.

It is worthy to mention here that under such terrain formations automated delineation of channel networks from high-resolution DEMs is more complicated than the case of low resolutions, which could be attributed to the high possibility of errors propagation, introduced both in source data, i.e. DEM data matrix, or in channel network extraction methods (e.g. pit filling, flow direction, accumulating area, etc.). Such errors may induce several unlike aspects in the extracted channel network such as the case of the Rambla Honda where channel floors are so wide that generate more than one line flow direction in the same valley link, even in first order links (figure 5.16c). Thus, with an imprecise technique the final results are represented by a highly undefined, i.e. high feathering, channel network. Nowadays, new approaches for channel network delineation in valley floor or thalweg formations are ascribed and approved (Madej, 1999; Tate et al., 2002; Vianello et al., 2009), which could be used in combination with the above models to achieve a best representation of watercourses in valley floors.

5.4.3.3. Geomorphometrical indices Analysis

The geomorphometrical indices for $R'_A t$ and CDA techniques were calculated using the same methodology employed before for Tabernas Basin, with the exclusion of α and θ . The obtained results confirmed the previous observations of the high similarity between $BLs-R'_A t$ over $BLs-CDA$ (tables 5.10 & 5.11). Once more, the geomorphometric descriptors have shown different behaviour according to its type. For example, in El Cautivo basin three geomorphometric attributes (inR_A , R_B and E) revealed better approximation between $BLs-CDA$, whereas the remainder underlined greater similarities between $BLs-R'_A t$. While in La Rambla Honda basin just only the (P_S) revealed a considerable similarity between the $BLs-CDA$ techniques. Such results underline the potential and the capacity of the geomorphometric attributes as a mode of comparison between stream networks.

No.	Index	BLs	CDA	$R'_A t$	$BLs-CDA$	$BLs-R'_A t$
1	Ω	3	3	3	0	0
2	La	235.4	377.9	312.9	0.41666	0.22661
3	Dd	0.0262	0.0569	0.0291	$8.9*10^{-05}$	$8.6*10^{-06}$
4	μ	13	35	13	0.06432	0
5	inR_A	1.0764	1.1363	0.8858	0.00018	0.00056
6	K_i	0.00178	0.00227	0.00224	$1.41*10^{-06}$	$1.35*10^{-06}$
7	R_B	2.33	1.93	2.77	0.00116	0.00129
8	F_S	0.0013	0.0034	0.0013	$6.1*10^{-06}$	0
9	H_μ	0.5927	0.5527	0.5927	0.00011	0
10	k	1.9209	1.1228	1.5513	0.00233	0.00108
11	P_S	-0.9685	-0.7763	-0.8797	0.00056	0.00025
12	OCN	6392.9	10559.3	6410.9	12.182	0.0526
13	$p(\mu)$	0.0061	0.0013	0.0061	$1.4*10^{-5}$	0
14	E	0.1589	0.1043	0.0709	0.00015	0.00025
15	Isd	0.5953	1.2953	0.6624	0.00204	0.00019
16	ε	1.847	1.8922	1.8707	0.00013	$6.9*10^{-05}$

Table 5.10 Direct comparison values for the Cautivo Basin. Shaded values indicate best results.

No.	Index	<i>BLs</i>	<i>CDA</i>	$R'_A t$	<i>BLs-CDA</i>	<i>BLs-$R'_A t$</i>
1	Ω	3	4	3	0.00292	0
2	<i>La</i>	622.4	688.9	619.9	0.19444	0.00731
3	<i>Dd</i>	0.01118	0.02484	0.01421	$3.9 \cdot 10^{-05}$	$8.9 \cdot 10^{-06}$
4	μ	6	60	15	0.157894	0.026315
5	<i>inR_A</i>	0.6271	0.9287	0.3329	0.00088	0.00086
6	<i>K_i</i>	0.00241	0.00117	0.00269	$3.6 \cdot 10^{-06}$	$8.1 \cdot 10^{-07}$
7	<i>R_B</i>	1.2	2.76	2.515	0.00456	0.000385
8	<i>F_s</i>	$7.1 \cdot 10^{-5}$	0.00076	0.00018	$2.02 \cdot 10^{-06}$	$3.4 \cdot 10^{-07}$
9	<i>H_u</i>	0.6496	0.53928	0.52528	0.000322	0.000188
10	<i>k</i>	0.56784	1.24633	0.92737	0.001983	0.001051
11	<i>P_s</i>	-0.7478	-0.6009	-0.4426	0.000429	0.000892
12	<i>OCN</i>	23235.1	53492.5	30159.4	88.4719	20.24649
13	<i>p(μ)</i>	0.02051	0.00061	0.00489	$5.8 \cdot 10^{-5}$	$4.5 \cdot 10^{-5}$
14	<i>E</i>	0.3287	0.0872	0.0988	0.000706	0.000669
15	<i>Isd</i>	0.9352	2.0764	1.1883	0.003336	0.000739
16	ε	1.8707	1.9236	1.9008	0.000154	$8.8 \cdot 10^{-05}$

Table 5.11 Direct comparison values for Rambla Honda Basin. Again, shaded values indicate best results.

It seems that the $R'_A t$ approach contains a clear capacity to improve channel network delineation over the *CDA* technique and simulates more *BLs* characteristics than *CDA* does. A quick observation to figures 5.15 and 5.16, as well tables 5.10 and 5.11 reveals with no doubt that drainage network delineated by $R'_A t$ is not only best imitates *BLs* but also improve automatic delineated channel networks to approximate natural drainage system, a matter that will be detailed and tested in the coming paragraphs.

5.4.4. Physical validation process

An independent set of analysis was used for the validation phase, which includes a local verification of the extent, size and limits for the studied channel networks. Such processes include a field visit, 3D visualization with DEM data and orthophotographs, and a combination of both named as experimental comparison. In spite of the vast advances in tools, devices and techniques of data capture for landforms depiction, field visit still play a major role in validation procedures of many earth science disciplines (e.g. Chorley et al., 1984; Montgomery & Dietrich, 1992). Yet, fieldwork is often tedious, time consuming and highly expensive, but there can be no substitute for it. In this study, fieldwork was considered indispensable and crucial since our reference point was always to represent natural landscape dissection with the digitized-*BLs*. Such assertion implies various undeniable errors related to the accuracy of the acquired data, for instance, the scale of the original data (i.e. scale of the topographic maps), time of data acquisition (i.e. time of flying for aerial photographs), cartographer experience and background, and finally texture and structure of depicted terrain. In a dynamic landscape and throughout the time, streams are altered by dominant extrinsic factors (e.g. runoff and soil erosion processes), which incites several modifications in the drainage network properties, such as channel heads extinction or/and change in channel location, mainly due to mass movements. For instance, El Cautivo Basin is characterized by highly erosive processes (Solé-Benet et al., 1997;

Cantón et al., 2001, 2004) that allows for continuous changes in relief form structure. Whereas, the Rambla Honda Catchment is developed on micaschists and formed by a more stable hillslopes of smooth gradients and insignificant erosional rates (Solé-Benet et al., 2009), induced by the scarce perturbation processes (Puigdefábregas et al., 1996) and leading to a well preserved sedimentary structure and a stable terrain morphology. Furthermore, DEMs and *BLs* construction had been realized since more than 10 years, a sufficient time for possible substantial alterations in the natural channel network in a dynamic and active landscape, mainly in the Cautivo field site (Harvey, 1987; Cantón, 1999). Hence, physical validation should be realized with care, mainly for channel extents and limits.

It's obvious that the channel networks in the two studied catchments are approximately estimating the same characteristics in the main stream channel, i.e. high order channels, and roughly differentiated in first order segments. So, efforts are concentrated upon the definition of first-order stream's location and head extension. Several field visits have been realized for both catchments, in which the digitized-*BLs* and the automatic-delineated channel network were validated in the terrain. In each defined channel network, first order streams were verified and studied, highlighting on presence, location, length, and extent of each segment. In both cases, first order streams of the *BLs* are registered and analyzed in relation to the other two techniques; next comments are added, if necessary, as auxiliary results in order to facilitate the interpretation process of each channel segment. The highly different lithology and relief contrast nature of the two sites implies different levels of difficulties in the form of separating, discerning and detecting rills or first order streams. In the Cautivo site, the highly contrast in relief formation make it less difficult to detect channel location and head extension than the Rambla Honda site, where highly eroded marls of the Cautivo Basin simulate better relief features than smooth-micasquite formations of the Rambla Honda does. A quick inspection to figure 5.15 permits, for any observer, an effortless detachment for the different types of channels, mainly first order streams, i.e. head and locations, or even deducing the existing of more streams and rills that are not detached by the used techniques. Whilst, the Rambla Honda field site offers a controversy different example, instead it is almost impossible to determine the presence of the streams and less more their head location and extinction (figure 5.16). So, in the Rambla Honda field site it was almost impossible to determine such information since in highly smooth rounded hillslopes eye observation seems to be useless and imply high subjectivity in decision making. So, field comparisons and observations were restricted to the Cautivo Basin, whereas the 3D analysis and the statistical comparisons were realized in the two catchments. As the DEM used in landform description is of 1m-grid size, we will accept the smallest hillslope extent as 1 m length from the channel to the nearest drainage divide. So, an exterior stream link is accepted as a channel if and only when both sides of the channel limits are ≥ 2 m length. Exterior streams have been numbered and then evaluated in relation to the previous mentioned criteria, first for the digitized-*BLs* (figure 5.17) and then for the automated drainage networks delineated by the *CDA* and the $R'_A t$ techniques (figures 12 & 13). Accordingly, two

main comparison-modes were realized, the first is experimental and the second concerns to visual interpretation of constructed 3D models and the available orthophotographs of 0.5 m resolution.

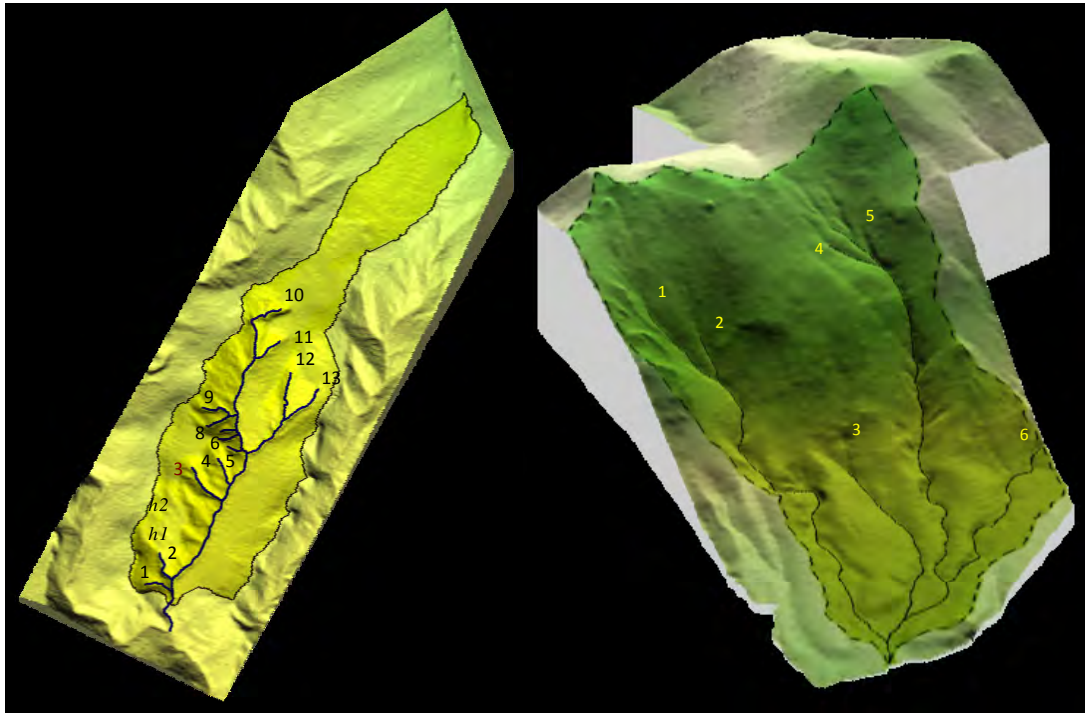


Figure 5.17 Quantification of first order streams of the digitized BLs in the Cautivo (a) and Rambla Honda (b) catchments.

5.4.4.1. Experimental comparison

In order to verify the degree of consistency between first-order streams in the digitized-BLs, a hypothetical quantification of these links has been performed, based on the following steps: *i*) first, in each exterior link, the contributing area value in the source segment was defined, which represents the (A_S^*) of this link stream; *ii*) second, the (A_S^*) value of each exterior link was used to define the drainage network, first for the basin unit corresponding to this link and second for the complete catchment; and *iii*) finally, from the resulted channel networks, the main geomorphometric properties (e.g. Ω , μ and L) and the new contributing area was defined and compared with initial ones (tables 5.12 & 5.13). In addition, the general statistical characteristics were compared for all studied channel networks in the two catchments (tables 5.14).

No.	A (m ²)	L (m)	Ω	μ	A _S [`] (m ²)	L* (m)	Ω *	μ *	Ω **	μ **
1	231	18.58	1	1	38	1.333	2	3	4	155
2	914	19.11			212	21.7	1	1	3	25
3	938	27.31			288	28.5	1	1	3	16
4	318	17			95	16.3	1	1	4	60
5	62	12.7			5	2.766	3	6	5	1256
6	45	13.85			6	14.2	1	1	5	1031
7	66	10.19			17	10.8	1	1	5	351
8	357	16.11			181	17.8	1	1	3	32
9	246	18.96			38	7.8	2	2	4	155
10	6220	43.34			5415	238.7	1	1	1	1
11	613	17.97			237	17.8	1	1	3	24
12	327	27.79			35	1.9	2	2	4	167
13	1152	27.3			114	14.8	2	3	3	52

Table 5.12 Direct comparison between first order streams of the digitized-BLs in El Cautivo Basin numbered according to figure (5.17). The first five columns correspond to the original data of the digitized-BLs and its main geomorphometric indices. A_S[`] define contributing area at channel initiation. (*) Values change after the use of the new A_S. (**) Total change in Ω and μ for the channel network, original values correspond to 3 and 13, respectively.

No.	A (m ²)	L (m)	Ω	μ	A _S [`] (m ²)	L* (m)	Ω *	μ *	Ω **	μ **
1	16918	248.9	1	1	3073	215.3	1	1	3	8
2	12975	59.4			1033	28.88	2	5	4	35
3	2123	55.22			1140	58.4	1	1	4	30
4	24686	237.2			7387	243.1	1	1	3	5
5	13461	51.2			7447	54.7	1	1	3	5
6	12391	94			6077	99.9	1	1	3	5

Table 5.13 Direct comparison between first order streams of the digitized-BLs in La Rambla Honda Basin numbered according to figure (5.17). The first five columns correspond to the original data of the digitized-BLs and its main geomorphometric indices. A_S[`] define contributing area at channel initiation. (*) Indicates values change after the use of the new A_S. (**) Modification in the total value of Ω and μ for the channel network, in which original values corresponds to 3 and 6, consecutively.

		BLs		R _A ^t		CDA	
		A _S	L	A _S	L	A _S	L
El Cautivo	Min.	5	19.19	74	2.4	14.9	1
	Max.	5415	43.34	976	28.97	300.7	48.9
	Mean	513.9	20.78	311.9	13.69	104.11	17.34
	Median	95	18.58	235	9.8	91.6	15.9
	St. Dev.	1475.6	8.77	247.19	9.24	56.11	11.77
Rambla Honda	Min.	1036	51.2	523	1	19	1
	Max.	7447	248.9	7160	127.2	1679	264.9
	Mean	4359.5	124.32	2108.1	38.6	384.8	31.3
	Median	4575	76.7	1386	23.1	297.5	10.4
	St. Dev.	3474.38	93.29	1858	41.1	367.2	50.2

Table 5.14 Description of the general statistics of length (L) and threshold value (A_S) of first order streams for the 3 compared channel networks in the two studied basins.

The above results reveal a variable and unpredictable shift in the channel network behaviour when using distinct A_S values. Delineated streams and channels networks defined by the new A_S values were completely or partially modified, in which aspect and corresponding parameters were readjusted to adapt the new formations. Geomorphometrical indices, of both individual streams and the total drainage network were altered drastically in the Cautivo Basin (table 5.12), whereas the Rambla Honda Catchment revealed a variable change, in which the first three A_S values underlined a severely modification and the rest a partially one (table 5.13). This change in the studied geomorphometric values, leads to a total adjustment in the channel network length scale characteristics. On the one hand, it can shift length-scale characteristics to highly exaggerated values that correspond to non-alluvial processes, i.e. valleys and streams, in the catchment area. For instance, in table 5.12, the magnitude (μ) in fifth link stream is shifted up from 1 to 6 for original sub-catchment and from 13 to 1256 for the whole basin, a non-reliable value that corresponds to a highly feathering aspect of the channel network and a diffuse border limits between hillslopes and channel networks (figure 5.18a). On the other hand, length scale characteristics may go down to just represent parts of the channel network or even the main stream channel, as observed in the tenth stream link, e.g. μ and Ω are shifted down from 13 to 1 and from 3 to 1 for the whole catchment, respectively (figure 5.18b). Likewise, the first value of upstream contributing area of the first order stream link registered in table 5.14, in Rambla Honda Basin, are so high that the generated drainage network from that threshold almost generates no hillslopes, rather a highly feathered drainage network that covers all the basin area (figure 5.19a). While the A_S value of the second and the three links (table 5.13) produce an extremely feathering channel network, the rest of the values generate a moderately dissected channel network that approximate to early-defined ones (figure 5.19b). Therefore, the constructed BLs seems to be highly subjective and depends, to more or less extend, on worker experience, relief contrasts and final aims of the work. Unpredictability of A_S values for digitized BLs and subjectivity of the topographer make it impossible to obtain similar length scale characteristics between BLs and automatic-delineated channel networks, i.e. obtained from DEMs. Nevertheless, it provides an approximated description of landscape dissection that is useful as a general initial step rather than a final absolute value, mainly for automatic-defined drainage networks described by mathematical models. Moreover, the general statistics of the A_S values of first order streams (table 5.14) reveal little about stream network properties. Comparison between values highlighted more similarity between the pairs $BLs-R'_A t$ than $BLs-CDA$, in both catchments. In the Cautivo basin, maximum, mean and standard deviation values of the $R'_A t$ approach approximate well to natural dissection, the minimum and median values give raise to CDA technique. However, the length characteristics reveal a differing situation where just only minimum and standard deviation produce better representation in the case of the $R'_A t$ approach. Again, the Rambla Honda basin reveals the same tendency, better similarity for the A_S values for the $R'_A t$ approach and enhance approximation for the length values for the CDA technique. In order to verify

such confusion, mean and median A_S values were used to generate different channel networks in each basin (figures 5.20 and 5.21).

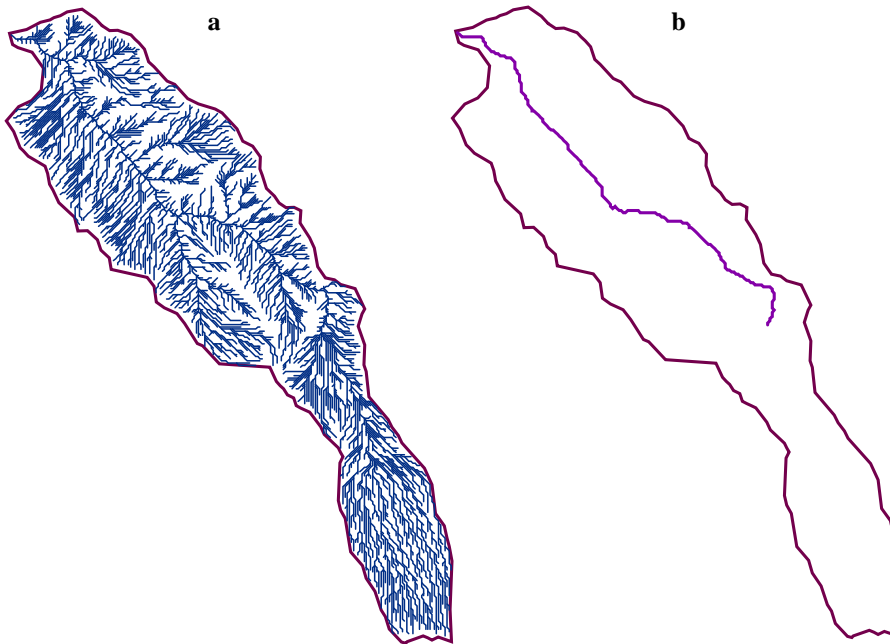


Figure 5.18 Two possible sketches for a modified channel network according to minimum and maximum average values defined from the BLs source area segments; a) Drainage network with A_S vale of 5 cells. b) Channel network with A_S value of 5415 cells.

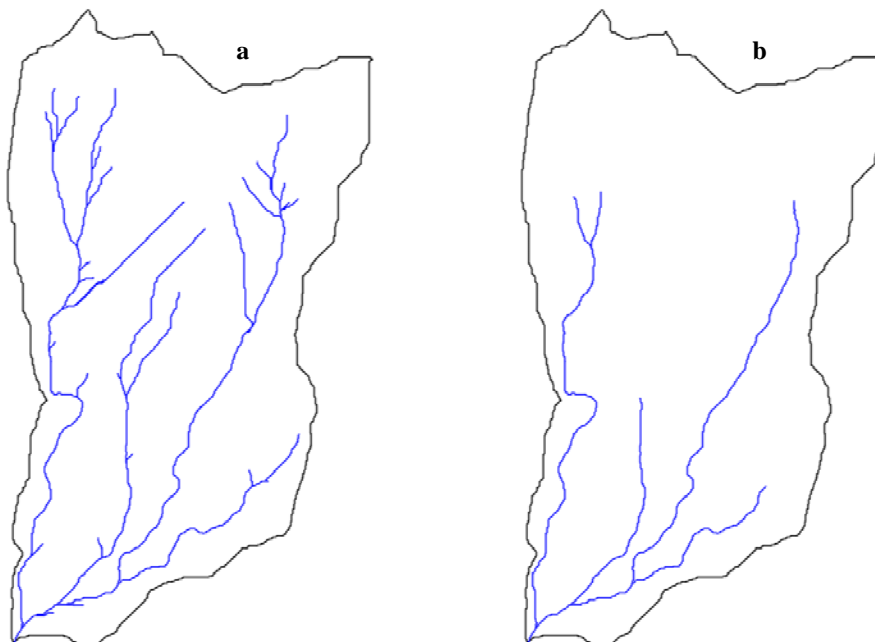


Figure 5.19 Two possible sketches for a modified channel network according to minimum and maximum average values defined from the BLs source area segments; a) Drainage network with A_S vale of 1033 cells. b) Channel network with A_S value of 7447 cells.

Drainage networks defined by means of general statistical values of available thresholds (A_S) highlight insignificant information about stream extents in nature, since none of the provided A_S values have presented a stream network that adapt to natural landscape dissection. Moreover, such results put in evidence the appropriateness of using a single A_S value, even in apparent homogeneous landscapes.

Figures 5.20 and 5.21 reveal a clear inconsistency and high variability in verifying the importance and significance of mean and median statistical values for the optimum A_S definition.

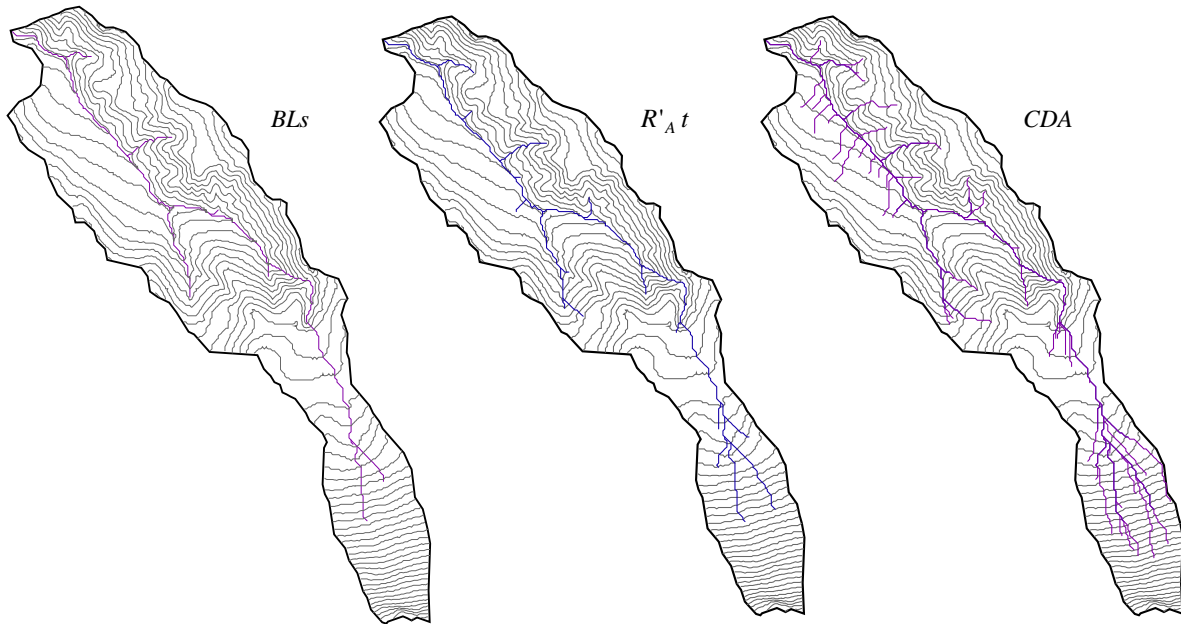


Figure 5.20a Channel networks of El Cautivo basin constructed by the mean A_S values of the three-type channel networks mentioned earlier in table 5.14.

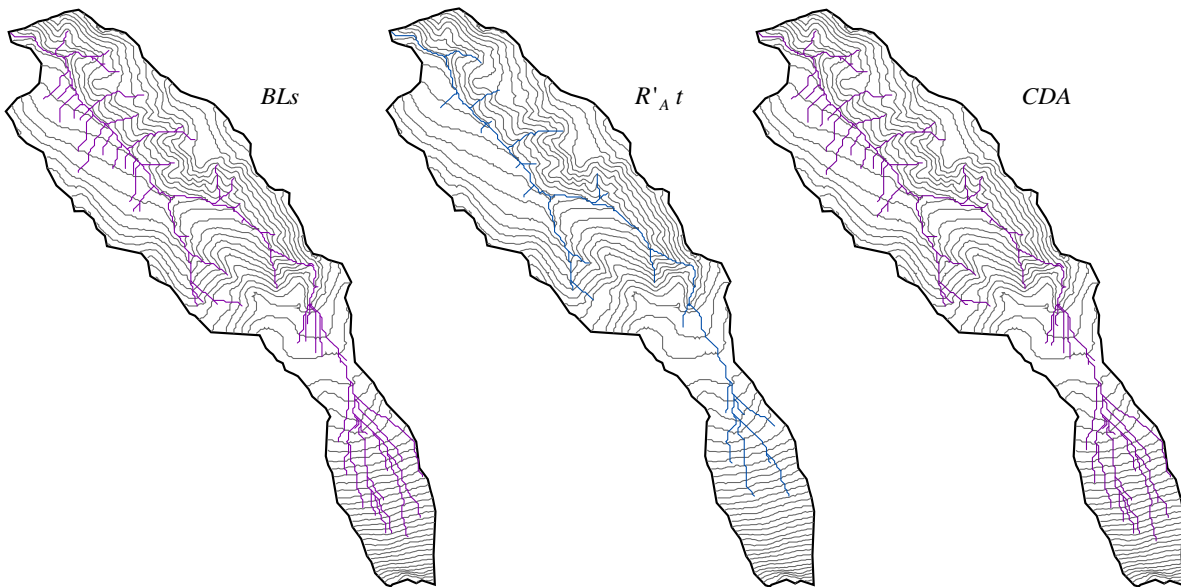


Figure 5.20b Channel networks of El Cautivo basin constructed by the median A_S values of the three-type channel networks mentioned earlier in table 5.14.

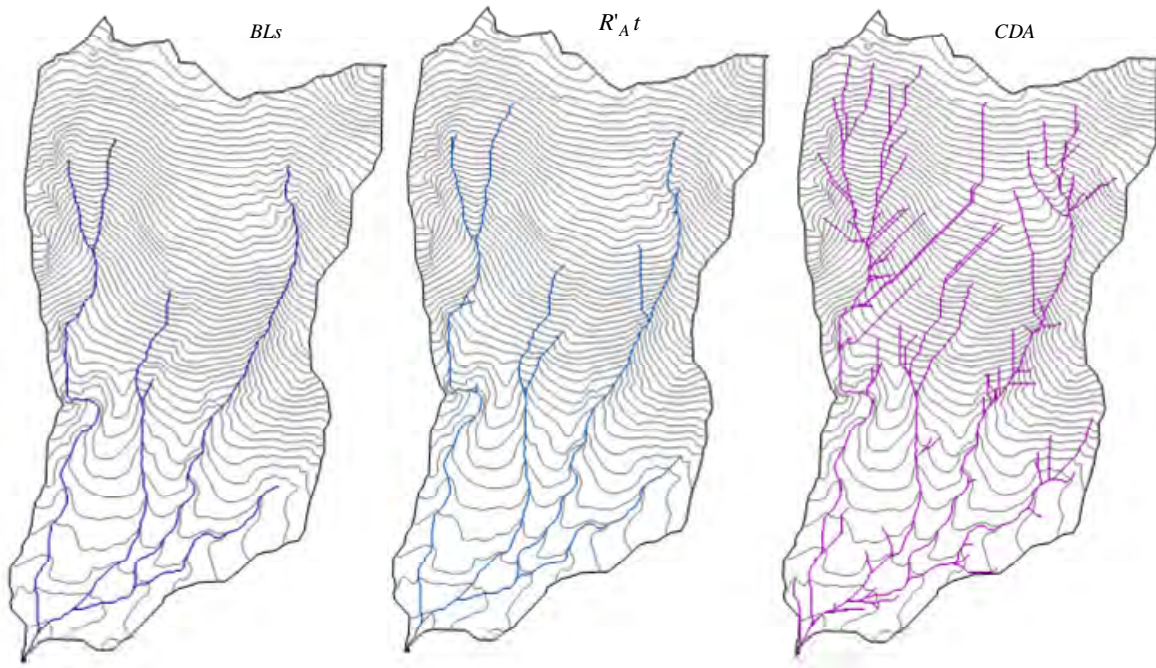


Figure 5.21a Channel networks of La Rambla Honda basin constructed by the mean A_S values of the three-type channel networks mentioned earlier in table 5.14.

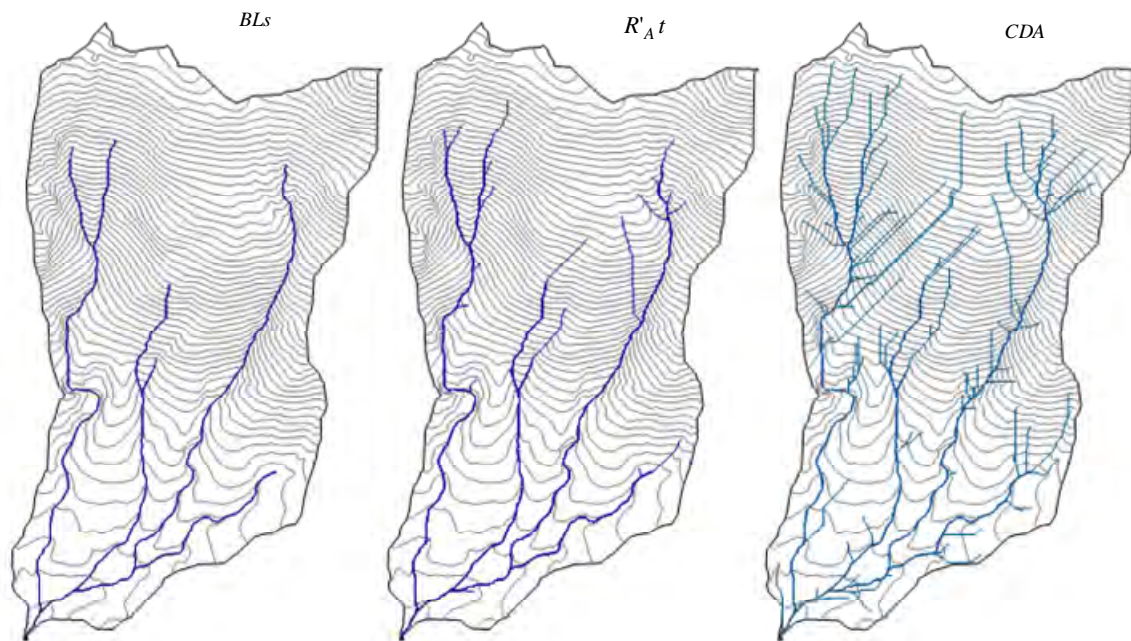


Figure 5.21b Channel networks of La Rambla Honda basin constructed by the median A_S values of the three-type channel networks mentioned earlier in table 5.14.

It appears that the mean statistical value derived from source areas of exterior streams seems to be more efficient for validating process than median ones, since it holds almost a constant and approximately similar representation of landscape dissection for the two studied catchments and for the BLs and $R'_A t$ techniques (figures 5.20 and 5.21). Such similarity is reflected in a fairly dissected drainage network that adapted roughly to convergence crenulations in the contour lines presented in

the delimited catchments. For instance, in the Cautivo catchment, the drainage network defined by the statistical mean value of source areas of the *BLs* appears to be too coarse relatively to contour crenulations, smoother one for the $R'_A t$ technique, and finally a highly feathering one for the *CDA* method (figure 5.20a). The same is observed in the Rambla Honda catchment (figure 5.21a).

In fact, stream adaptation to contour crenulations is somewhat subjective, and there is no clear efficient quantitative approach is available (Mark, 1983). Thus, the comparison between techniques will be encompassed in a detailed redefinition of the *BLs* in direct comparison to the resulted channel networks of the *CDA* and the $R'_A t$ techniques for both Cautivo and Rambla Honda catchments. For which the digitized *BLs* were fixed as a background and the drainage networks of both methods has overlaid above it (figure 5.22). The direct comparison emphasizes two important aspects of the channel network, locations and extend. Location is directly related to method used for the definition of channel network position, that is, flow direction, which is fairly adapted to that of the *BLs*. Whereas, extend is directly related to the stream source or the optimum A_S value used for stream delineation, which again confirms previous results of quantitative approaches. These results reveal the high approximation of the $R'_A t$ technique to the *BLs* in both catchments (figure 5.22a and c) and the coarse one in the *CDA* technique (figure 5.22b and d).

5.4.1.1. Visual interpretation

A kind of a subjective-weighted-eye validation for first order streams location and head extension. This type of interpretation has been limited to the smaller size catchments of Cautivo and Rambla Honda basins, because the size of Tabernas Basin (572 km²) and the large amount of first order streams, i.e. 407 streams, makes it impossible to compare and visit all presented exterior-link streams. In addition, a 30 m grid dimension implies a divergent source area of two borders that is 60 m wide, which is impossible to compare with the orthophotographs of 0.5 m resolution. Field visit for the two catchments have permitted an exhausted definition of first order streams in the channel network. While subjectivity is the essential criteria for channel definition, personal formation and experience are of significant importance to discern the limits between convergent and divergent topography, where in some cases three persons weren't able to agree upon the location of the head extinction or even the presence for some streams.

In order to enhance the visual interpretation of relief landforms, in general, and of smooth-terrain features, in particular, a highly detailed orthophotographs (Junta de Andalucía, 2007) have been used to enhance detection capacity. With the aid of the orthophotographs, the visualization process has introduced a real dimension in the detection and the definition of the stream lengths and extensions. The two catchment limits of the Cautivo and Rambla Honda, again, have been superimposed directly over the detailed terrain and a visualization inspection has been realized between first order streams for the studied channel networks (figures 5.23 & 5.24). In the Cautivo Catchment, the high detailed

channel network generated by the *CDA* technique reveals high feathering in the upper part of the catchment, and showing at the same time the emergence of some streams in a clear hillslope formation (figure 5.24c). While, the R'_{At} technique reveals a clear adjustment of the stream network to the smooth dissected terrain of the defined area, which highlighted a considerable enhancement in landscape dissection, even over the digitized *BLs* (figures 5.23a & b). The same was observed in the Rambla Honda Catchment (figure 5.24).

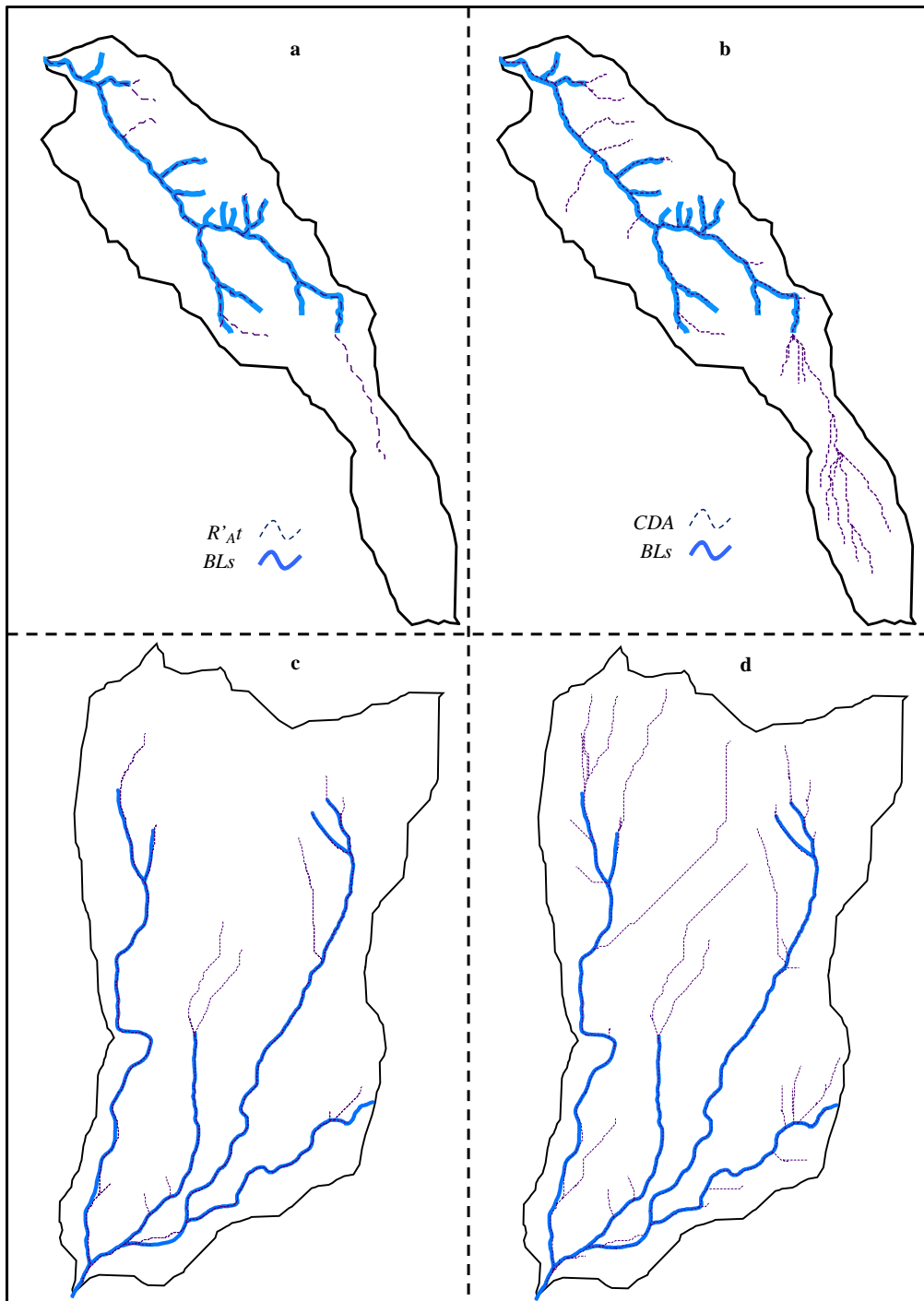


Figure 5.22 A direct comparison between the *BLs* and the automated channel networks for El Cautivo and Rambla Honda catchments; a) R'_{At} and *BLs* in El Cautivo basin. b) *CDA* and *BLs* in El Cautivo basin; c) R'_{At} and *BLs* in La Rambla Honda basin; d) *CDA* and *BLs* in La Rambla Honda basin.

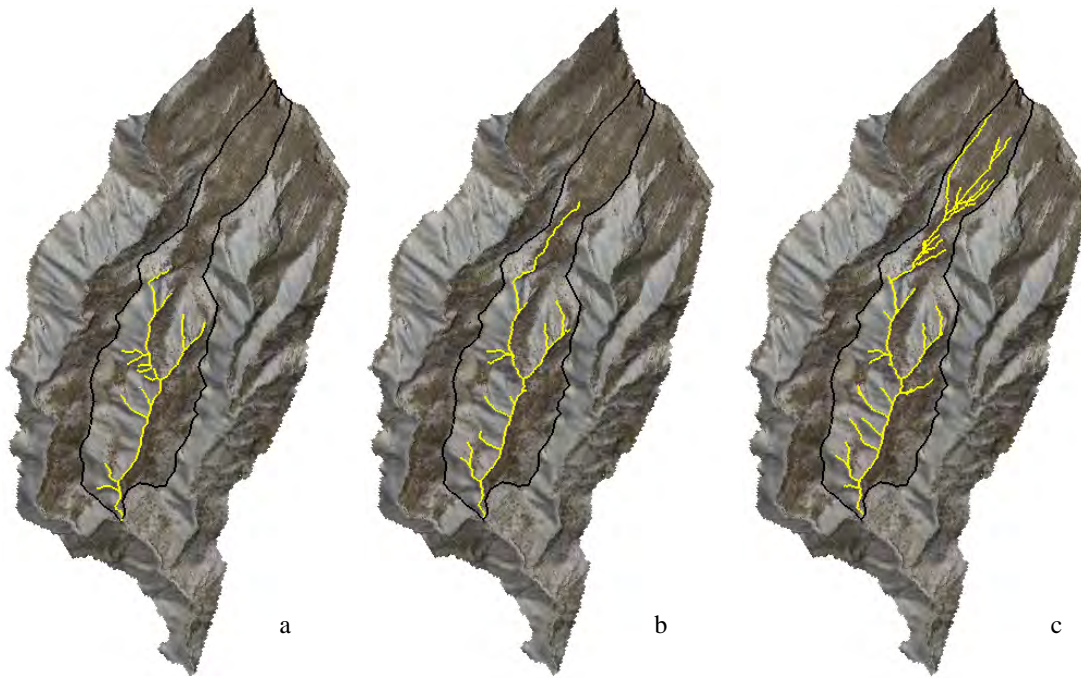


Figure 5.23 Visualized channel networks using orthophotographs for El Cautivo catchment; *a*) manual digitized BLs; *b*) channel network defined by the $R'_A t$ technique; and *c*) channel network defined by the *CDA* method.

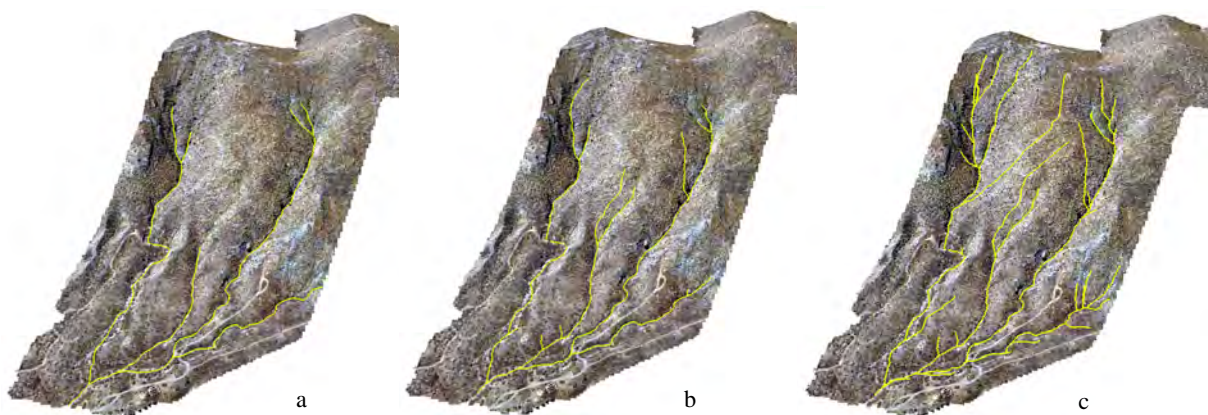


Figure 5.24 Visual validation for the studied channel networks using the orthophotographs of the Rambla Honda catchment; *a*) manual digitized BLs; *b*) channel network defined by the $R'_A t$ technique; and *c*) channel network defined by the *CDA* method

In general, the visual interpretation and field visits can be referred to as a kind of auxiliary data that helps in statistical results interpretation and validation, as well as abnormalities detachments and/or time-change effect in the primary datasets, i.e. DEMs. The two examples confirm a prevalent advantage of the $R'_A t$ technique over the *CDA* and even in some cases over the *BLs*, where objective models, i.e. proposed models, surpass subjectivity approach of digitized-*BLs*. Moreover, mainly in the case of the Rambla Honda site, failure of the *BLs* in defining first order streams makes it useless to use in the corresponding study at the appropriate scale, since comparison will be impossible between gridded datasets and field data.

5.5. Discussion and validation

5.5.1. Introduction

In channel network delineation, it is highly accepted that whatever the technique used, it should assure the general aims of the studied work. Within such a framework and under the automatic approach, the constructed drainage networks have shown to be greatly related to several direct and indirect factors, such as DEMs resolution, terrain complexity and heterogeneity, and availability of auxiliary data, as well as the model approach used to define channel network limits in the landscape. For so, it is well assumed that the best approach for channel network delineation that is capable to minimize the controlling-factors effect and at the same time makes use of available information. The previous affirmations over the adequate solution in defining stream limits are the major lines to take in mind in the delineation process, as the final aim to achieve. The adaptive model and the intrinsic hierarchical classification are the proposed approach to attain such objective, as well as to verify landscape features in relation to available scale and resolution.

5.5.2. The adaptive model and the *HSP* procedure

The adaptive model, based on geometrical and topological properties of the channel network, consists of, basically, achieving an equilibrium state between such properties, which is reflected in the *MRC* in the curve relationship between A_S and R'_A (figure 5.4). This curve tries to establish the optimum approximation of an equilibrium point between bifurcation and length properties as well R_A ratio, which best describe channel network structure. As mentioned earlier, a general conceptual framework that explains R'_A behaviour in a hypothetical landscape (completely homogeneous vs. heterogeneous) is the trenching process described in figure 5.1. Schumm et al., (1984) attributed such behaviour to extrinsic control factors (e.g. climate, tectonics, land use, etc) and other intrinsic ones of strong geomorphic controls.

In a laboratory experimental study of fan growth and basin formation, Schumm (1977) found out that precipitation when delivered to a sediment source area at a constant rate the resulting runoff and sediment moved out of the initial drainage basin to a piedmont area where a miniature fan was formed. During fan growth, the fan was trenched repeatedly, as the fan head oversteepened as a result of aggradation, and then it adjusted to this oversteepened condition by trenching (figure 5.1a). It is important to emphasize that fan-head trenching is not the result of changing extrinsic factors, rather is the exceeding of an intrinsic geomorphic threshold, that is, the oversteepening of the fan head. This is the case of a homogeneous landscape where all extrinsic factors are constant (figure 5.1a). Whereas, in nature this is not the case, where channel networks are the result of the integration of different extrinsic and intrinsic factors, that is, a heterogeneous landscape (figure 5.1b). It is important to highlight that the geomorphic threshold, as indicated in figure 5.1 will probably not be a single value;

rather there should be a range of thresholds (Schumm et al., 1984), which is related directly to variations of local factors of the source area. So, in a hypothetical homogeneous terrain, each change in the range of thresholds (i.e. from ω_1 to ω_2 , ω_2 to ω_3 , ..., ω_{n-1} to ω_n , respectively) will reflect a change in terrain properties (i.e. structure, form and shape, evolution, etc.) and hence possible changes in dominant processes. Of course, in nature, such approach is available under limited-scale size catchments that are probably reflected by one stability zone and hence one dominant process.

On the contrary and in a heterogeneous landscape, the curve tendency is completely different, where channel network is the final result of the integration of extrinsic and intrinsic factors over the landscape. In this case, the adaptive model tries to achieve an equilibrium point between the different dominant factors over that terrain. These are completely different in hillslopes than valleys and in first order streams or source areas than in higher order streams (i.e. $\geq \omega_2$). In relation to landscape features, divergent processes are dominant in hillslope structures whereas convergent processes are the dominant aspects in streams and valley formations. Moreover, source areas and first order streams are dominated by a more dynamic and active processes than higher order streams or main channels, in which incision process implies different effects upstream and downstream channel (e.g. Schumm, 1977; Bull & Kirkby, 2002). Herein, sediment generation, movement and deposition are the causing factor for such effects. The position of the channel head is controlled by the balance of sediment supply and sediment removal (Dietrich & Dunne, 1993). For instance, during discharge events channel heads may advance upslope, or retreat downslope if the hollow refills (Bull & Kirkby, 2002). Whereas, higher order streams usually act as deposition zones of smooth gradients and structures. Under such conditions, the landscape is highly complex in areas of generation, smoother in transitional zones, and poorly diverse in depositional areas. Hence, and in relation to DEM-data resolution, the adaptive model verifies each zone in relation to its complexity and interprets it in a degree of stability (i.e. rate of change) in the curve relationship (figure 5.1b); that is, the more the heterogeneity is the lesser the stability is in the curve relationship, and vice versa. Consequently, in a real heterogeneous terrain, changes in curve direction will reflect variations in terrain properties, but the most significant is the maximum one that reveals dominant processes and formations (e.g. large valleys) over insignificant ones (e.g. ephemeral streams, rills, etc.). So, it should be highly rational to look for the several parts of the terrain of similar structural formations that is widely dominant by one active process. Thus, several A_S values are needed to cover the landscape formations and to verify its units in relation to DEM-grid dimensions. Soon after, scientists have confirmed the suitability of multiple framework and multifractal approach over the simple one (e.g. Ijjász-Vasquez et al., 1992; Rinaldo et al., 1992; Rodríguez-Iturbe & Rinaldo, 1997; De Bartolo et al., 2004, 2006) and the non realistic assumption of one constant A_S value in case of multiple-dominant landscape processes.

The detection of the first range of thresholds does not depend only on the dominant process and terrain complexity, but also on the scale of the source data, herein DEM resolution. It is important

to underline that fine resolution DEMs are more appropriate to define local dominant process at source areas than coarse ones (Zhang & Montgomery, 1994; Wolok & price, 1994; Walker & Willgoose, 1999; Wilson et al., 2000; Artan et al., 2000; Thompson et al., 2001; Kienzle, 2004; Hancock, 2005). For example, Montgomery and Foufoula-Georgiou highlighted that a DEM resolution finer than 30 m grid size is required to accurately resolve the hillslope/valley transition. Whereas, Dietrich et al., (1993) detached that even 1 m DEM resolution are so sparse to capture the local topography around small channel heads. Thus, the capacity of the DEM data to detect the range of thresholds is highly related to the grid-data size; that is, the higher the grid resolution is the more the possibility to define the earlier rate of changes in the curve relationship (figure 5.25).

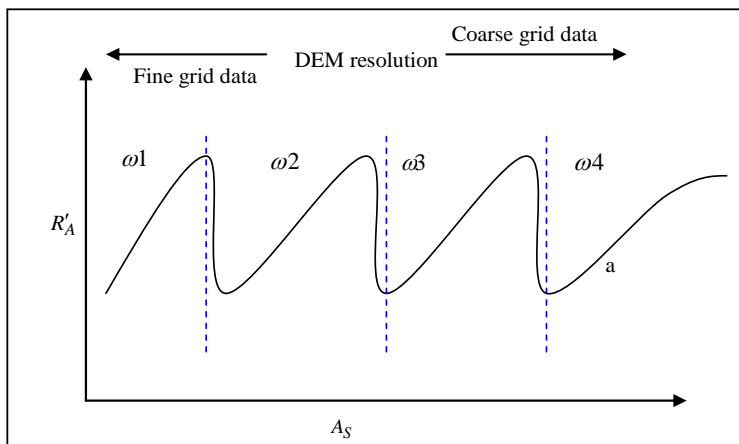


Figure 5.25 DEMs capacity in relation to its resolution in detection the range of the critical threshold.

Herein, understanding the adaptive-model function implies a closer inspection of the curve relationship of A_S and R'_A . Therefore, the Cautivo and Rambla Honda Basins have been selected since approving and inspection of model behaviour in high resolution data, i.e. 1 m, is relatively easier, a function that permits a comprehensive understanding of how the model acts in the terrain. Hence, the curves relationship of the Cautivo and the Rambla Honda field sites have been constructed and then segmented and visualized according to the change of order in the channel network.

For the Cautivo basin, a range of A_S values that extend between 3 and 135 was used in the constructed curve relationship (figure 5.26a), above which the channel network corresponds to divides, and down these values the adaptive model is not applicable, since at least 3 stream segments are needed so that a rate of change could be identified by the algorithm. As mentioned earlier, in a homogeneous landscape, the curve relationship takes a steady state of change (i.e. constant rate of change) with order change in the channel network evolution (figure 5.1a). In this case, the situation is completely different and coincides more with a non-steady rate of change (figure 5.1b), which represents a heterogeneous landscape of different features and processes.

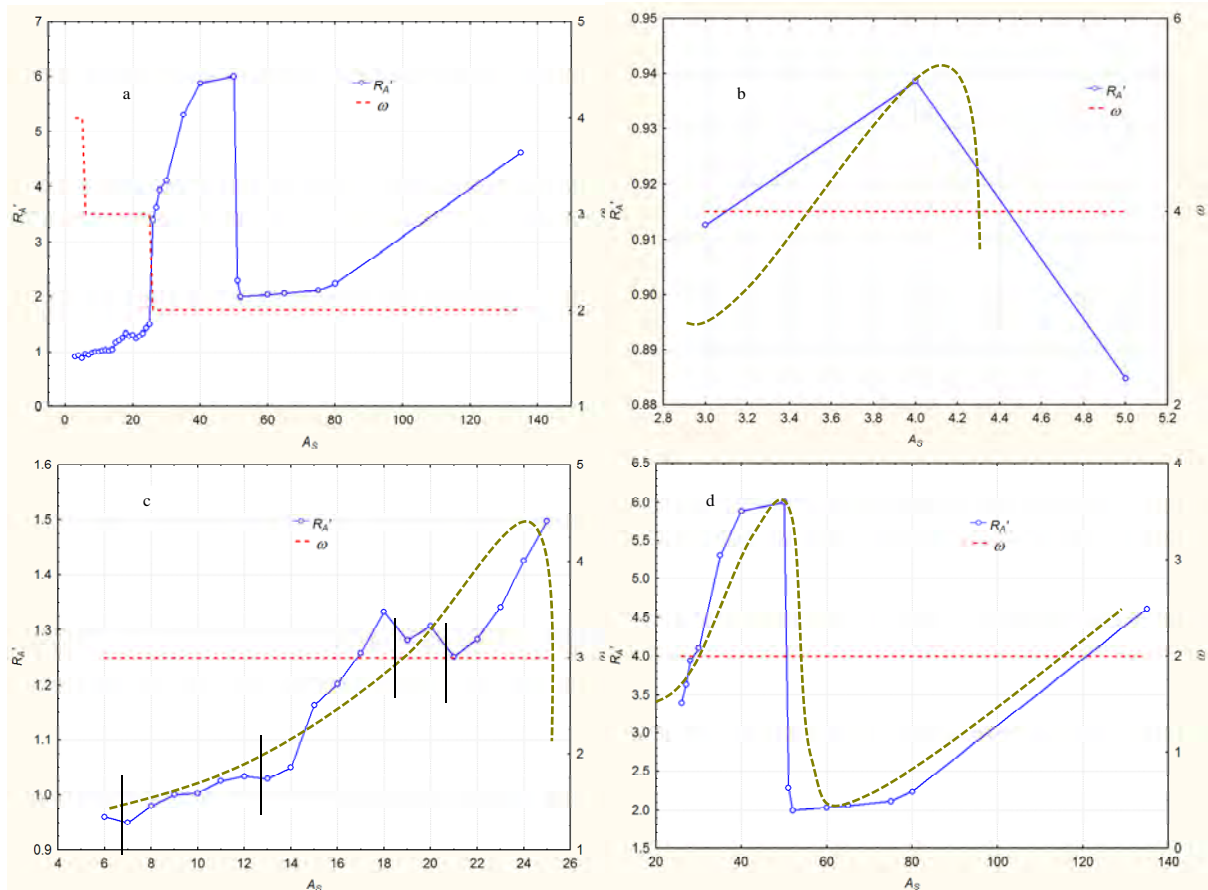


Figure 5.26 Curve relationships for the adaptive model in the Cautivo Catchment. Continued lines in c indicate the 3 rate of changes (RC) areas generated by the R'_A model.

It is obvious that the segmented curves of the Cautivo catchment reveal a clear coupling resemblance between theoretical curve tendencies (figure 5.1b) and the present ones (figure 5.26). The dotted green lines represent the proposed-curve stages in the optimum case of homogenous conditions, whereas the solid blue lines represent the curve stages under the real conditions of intrinsic and extrinsic factors for the Cautivo catchment. Herein, the curves in each segment are not steady ones; rather they are characterized by a continuous fluctuation throughout the curve tendency. Such fluctuations reflect local factors and environmental conditions in a way such that the major fluctuating is in the curve the higher is the effect of such factors, and vice versa. We believe that the capacity of the adaptive model to recognize such factors is clearly evident, in which as long as the model recognize such factors, the less the fluctuation produced and hence a clear stability zone (*SZ*) is formed. Therefore, the curve relationship of A_S and R'_A was segmented according to order-change in the constructed drainage network, providing 3 possible sections. The first segment is associated to A_S values between 3 and 5 (figure 5.26b) and corresponds to a channel network of $\Omega = 4$. In this case, no *SZ* was defined and the constructed drainage networks are highly diffused and contain a lot of parallel lines or feathering (figure 5.27). The second segment corresponds to channel networks of order 3 (figure 5.26c), which is related to a range of A_S values that extends from 6 to 25. In this case, the curve is fairly fluctuated with approximately 3 clear areas of *RC* indicating a moderate effect of local factors

and a limited number of prevailing processes (i.e. runoff and erosion) or even a moderate terrain structure reflected in a reduced amount of different landscape features. The channel networks generated in this range are characterized by a more acceptable visual structure and less feathering aspect (figure 5.28). Finally, the last segment stage corresponds to $\Omega = 2$ and a range of A_S values that oscillate between 26 and 135 (figure 5.26d).

Herein, two clear RC areas are identified. The first one extend from 21 to 50 with $RC = 124.96$, which corresponds to the size of the area under the curve relationship that extends between the minimum and maximum values. The second extends from 52 to 135 and curve-area size of about 46.15. It is important to underline that the first area is not limited to the third order level of the curve relationship, rather it extends to the anterior level ($\Omega = 3$). Such fact could be attributed to both extrinsic and intrinsic factors, where dominant processes and landforms are diffuse in the limiting zone between orders. So, in a heterogeneous terrain structure, formed stages may extend to anterior levels since limits and borders between order levels are not strict rather is gradual, which allows for a transitional change from one dominant process and structure to another. According to the $R'_A t$ approach, the SZ corresponds to the first SZ , that is 21-50, and the optimum A_S to use will be 21 corresponding to the minimum value in the MRC , since neither of the primary conditions has been observed. Such value concurs with the proposed goal of maximum complexity and minimum feathering in the constructed channel network, which is related directly to model capacity in delineating channel network limits under the current scale and resolution. Under these conditions, the resulted channel network is characterized by a moderately dissected aspect that adapts well to relief landforms of the Cautivo basin, as well as a completely vanishing of feathering features (figure 5.29). Order (Ω) and magnitude (μ) of the resulted channel network approximates fairly to those of the digitized BLs , with Ω value of 3 for both and μ value of 16 and 13, respectively.

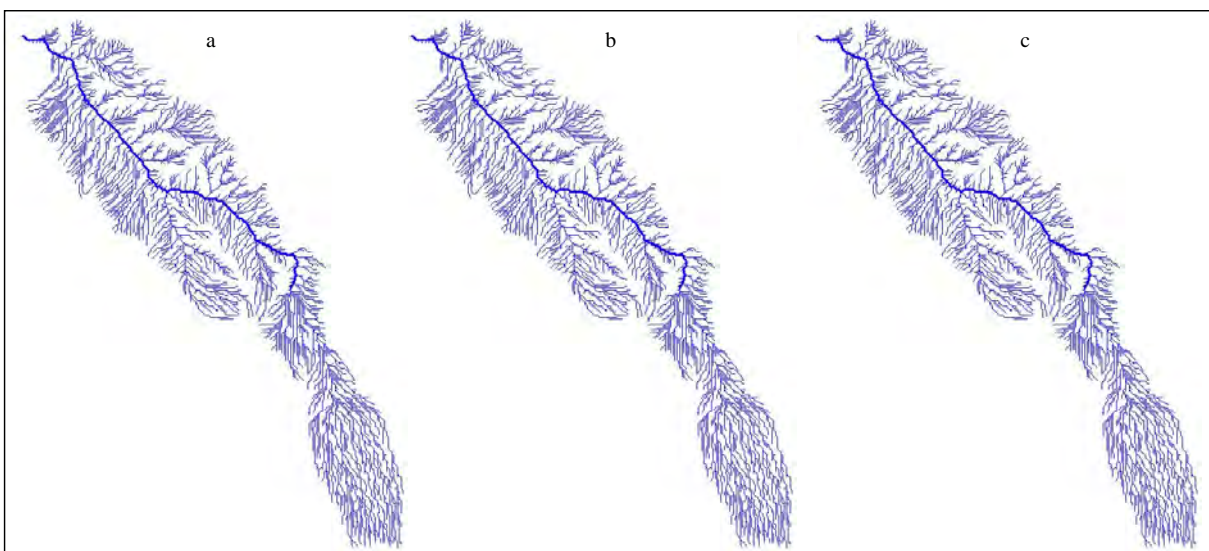


Figure 5.27 Channel networks delineated by different A_S values localized in the order level 4 ($\Omega = 4$) in the Cautivo catchment, a) $A_S = 3$; b) $A_S = 4$; and, c) $A_S = 5$.

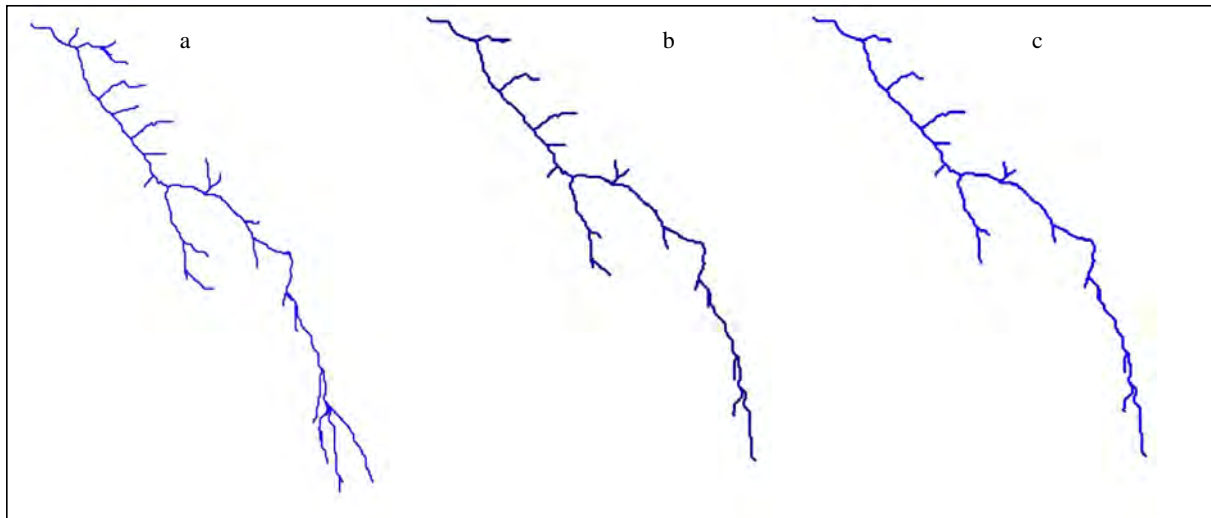


Figure 5.28 Generated channel network with different A_S values localized in the third order level ($\Omega = 3$). A) $A_S = 12$. B) $A_S = 18$. C) $A_S = 20$.

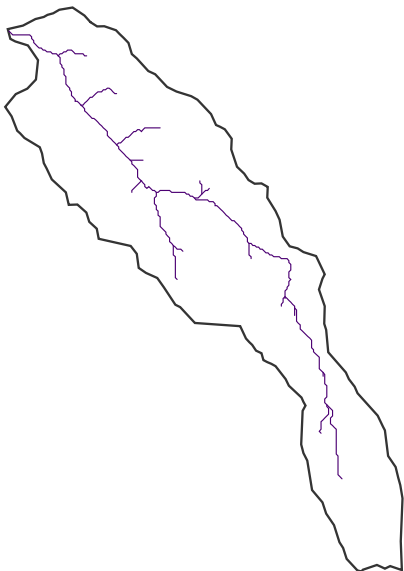


Figure 5.29 Channel stream network in the Cautivo catchment with $A_S = 21$.

The second step in the $R'_A t$ procedure involves the application of the hierarchical stratification procedure (*HSP*) in order to classify the drainage basin into different hierarchical classes of sub-catchments in relation to stream order. Such process delineates three sub catchments of $\Omega = 2$ and 5 sub-catchments with $\Omega = 1$ (figure 5.30). In relation to the first category (i.e. $\Omega = 2$) each sub-catchment has been treated independently and the optimum A_S value was selected after the construction of the A_S and R'_A curve relationship and the selection of the corresponding *SZ* for each one. Whereas, in the last category ($\Omega = 1$), just only one sub-catchment was possible to be reclassified (figure 5.30), and the rest has been left as it is, since one or more of the primary conditions of the $R'_A t$ procedure were achieved. Again, the *SZs* were defined and the optimum A_S values for each sub-catchment has been selected (table 5.15).

No.	SZ	Primary conditions	A_S	Incision process	Ω	μ	D_d (m/m ²)
1	3-35	The minimum is a divide	35	Sheet erosion and Piping	2	2	0.3064
2	8-18	None	8	Piping	2	2	0.3584
3	5-22	$HI = 62.1$	22	Rill erosion	2	3	0.3559
4	12-20	None	12	Rill erosion	2	3	0.3706

Table 5.15 The optimum A_S values defined according to the $R'_A t$ approach in El Cautivo Basin and the corresponding information of the reclassified sub-catchments.

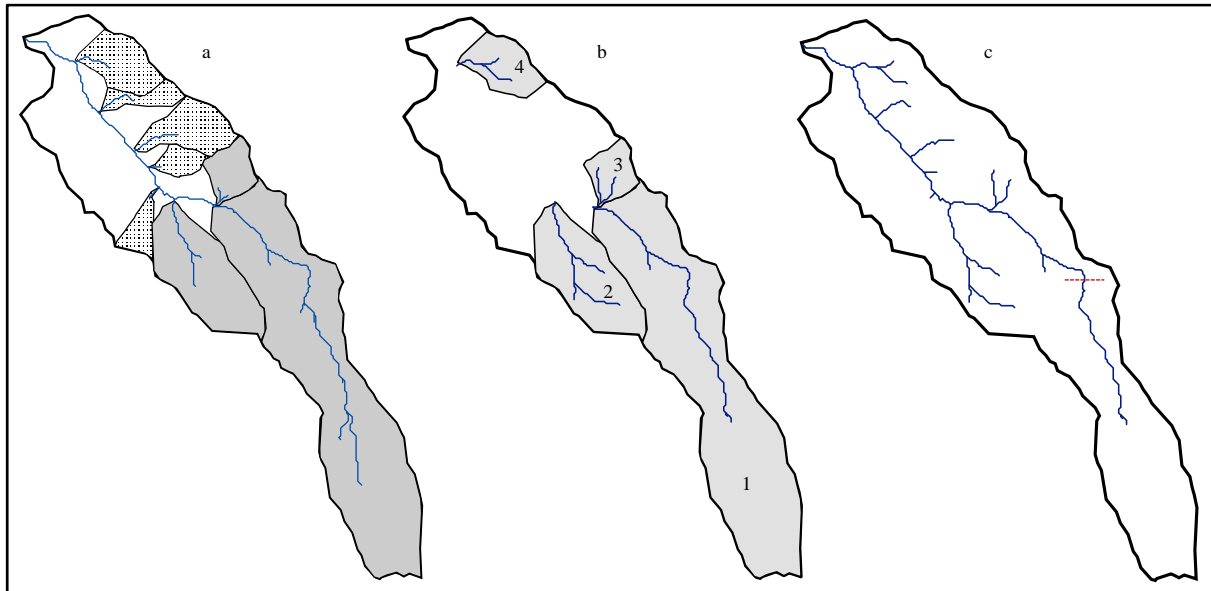


Figure 5.30 Generated sub-catchments in the Cautivo basin using the *HSP* procedure. Gray highlighted sub-catchments of first order streams ($\Omega = 1$) and uncoloured are second order streams ($\Omega = 2$). b) Amount of enhancement in the reclassified sub-catchments in the Cautivo basin. c) The final channel networks delineated by the $R'_A t$ procedure.

The final result of the $R'_A t$ procedure is an evident readjustment in the generated drainage network, which is reflected in an apparent enhancement (visual appearance) in depicting landscape dissection for the delineated sub-catchments of the Cautivo Basin. Such enhancement is expressed in two distinct forms: *i*) the first as an apparent increase in the length of the channel networks and hence landscape dissection, such as the cases in sub-basins 2, 3 and 4 (figure 5.30c); *ii*) whereas the second type shows a clear decrease in the dissected channel network, and hence a clear smoothing in relief form structure, such as the case of sub-basin 1 (figure 5.30c).

In order to explain the above results we should return to the Montgomery and Dietrich (1994) histogram for channel incision (figure 4.1). Processes controlling each channel-head-initiation mechanism are related to specific threshold, according to which Montgomery and Dietrich divided the landscape into process regimes by plotting erosional thresholds for different processes of channel incision. The schematic representation in figure 4.1 indicates that each erosional zone type needs a particular threshold value in order to define channel head location. A detailed inspection to the studied area reveals that the dominant erosional processes prevailed in the Cautivo area are rill, gully, splash

and piping erosion (Solè-Benet et al., 2009). According to the erosional curve limits, at least 3 threshold values are needed to represent prevailing erosional processes required to depict convergent and divergent processes and hence channel network limits. In view of that, a field visit for the channel heads in the studied site allowed for the definition of 3 basic types of prevailing soil erosion types: piping, sheet and rill erosion (table 5.15). It is important to underline that erosional processes are interrelated (e.g. Montgomery & Dietrich, 1994; Bull & Kirkby, 2002), in one way or another, where, for instance, in arid environments gully and pipe erosions are closely associated (e.g. Leopold et al., 1964; Bocco, 1991), whereas rainsplash (i.e. splash erosion) may protect a surface against incision by rillwash, and the relative intensities of diffusive rainsplash and incisive rillwash would determine the position of the channel head (Dunne, 1980). Herein, neither erosion-process type nor its causes are the goal of this work; rather only it will be used to highlight the functional capacity of the model over the terrain to determine stream limits and extensions in relation to intrinsic properties (i.e. in this case channel heads with different incision processes). Under these conditions, we will try to explain how the adaptive model is capable to verify and classify the terrain according to different regimes in relation to dominant erosion processes and type of terrain features.

First, the R'_A algorithm tries to define a rational balance state in the channel network, which is the rate of change of the first order streams (exterior links) in relation to the higher order streams (interior links). This is mainly related to the channel network evolution, since first order streams represent youth structures, whereas the outlet and the main streams represent the initial conditions of the channel network formation (i.e. mature structures). Moreover, both exterior and interior link lengths generally have different length properties (Shreve, 1967), and hence independent parameters that represent variations in local factors (e.g. dominant erosion processes, vegetation cover, slope gradient, etc.). It is important to underline that the R'_A algorithm consists of two basic parts, the ratio of the exterior and interior link lengths (i.e. $R_A = \bar{l}_i / \bar{l}_e$) and the topologic interpretation of this ratio (i.e. individual stream length ratios of Smart presented in Eq. 5.6 and 5.7). These equations relates lengths to segment number properties, and hence bifurcation properties of these links. In consequence, the evolution stage of the channel network is linked to bifurcation and length properties in order to interpret channel network structure and formation. Thus, the R'_A algorithm tries to establish a balance stage between terrain complexity and original dataset used to define such landform features. Herein, landscape complexity is related to the amount of features the algorithm is able to detect. Whereas, in relation to the forming parameters, the model only verifies convergent topography that is flow accumulation, thus it differentiates landscape features to divergent hillslope and convergent valley structures. Therefore, limits of divergent flow accumulation of the hillslopes are detached from the convergent flow processes in channels and valleys. However, a heterogeneous landscape is characterized by different erosion processes, which implies different forms and degrees of channel initiation, and hence more than one A_S value is needed for the same region. Such approximation forms

the basis for the multiple framework and multi-fractal dimension approaches in the channel network definition (e.g. Rodríguez-Iturbe & Rinaldo, 1997; De Bartolo et al., 2004). The balance stage, in absence of limiting factors, is conceptualized by the curve relationship of R'_A and A_S in figure (5.1a), where evolution of a channel network implies a positive steady rate of change in the R'_A value through A_S -value change. Herein, as A_S value increases, exterior link lengths (\bar{l}_e) decrease, whereas interior link lengths (\bar{l}_i) maintain constant in the denominator, and hence R'_A value increases. Such state continues till all or part of first order streams (the current exterior links) are disappeared then a change in the total order of the channel network (ω) is produced and all or parts of second order links become exterior streams. The change from ω to $\omega - 1$ produces a negative change in the curve direction (figure 5.1a) and a new steady state will be formed for the new order (i.e. $\omega - 1$). The process is repeated until ω value reaches 1, for which the algorithm is unable to define a rate of change or a ratio, since the algorithm needs minimum three segments to define a rational A_S value and hence no channel detection. Such inconvenience is related directly to the model structure; that is, bifurcation and length link ratios. This disadvantage is compensated by the efficiency and the capacity of the model to define homogeneous terrain structures in relation to dominant processes or/and landforms (i.e. hierarchical classification). Such classification allows for a more precise depiction of landscape dissection by the application of the algorithm over limited homogeneous parts of the terrain structure. The procedure of *MRC* and *HSP* continue till the entire channel network is re-segmented and the optimum dissection is achieved.

However, in natural landscapes the situation is completely different, since intrinsic and extrinsic factors (e.g. climate, tectonics, relief, vegetation, lithology, hydrologic character, space filling, etc.) interact permanently in the dynamic formation of the drainage network system (e.g. Leopold & Langbein, 1962, 1965; Abrahams, 1976, 1980a, 1984a; Jarvis, 1976a; Gregory & Gardiner, 1975; Schumm, 1977; Schumm et al., 1984; Howard, 1994). Such controlling factors have a multidirectional effect; that is, external and internal streams could be affected equally or independently depending on factors type (Abrahams, 1976, 1977; Marcus, 1980) and scale variation (Morgan, 1973; Gregory, 1976). Hence, it is highly acceptable that channel networks are the final results of a dynamic interaction between surface relief, defined by the DEM data, with the intrinsic and extrinsic surrounding factors. Thus, the dataset used to define such features is a highly limiting factor, which should be spaced enough to verify and interpret the effect of such factors over that surface. For instance, climate effect is well detached by low resolution DEMs, whereas vegetation or hydrologic character is poorly defined by such dimensions. Moreover, high resolutions (e.g. ≥ 1 m) identify perfectly gully and pipe erosion effects, but unlikely to define convergent processes of rill erosion. Under such heterogeneous conditions, the R'_A model recognizes the surface relief in relation to the degree of complexity of that terrain and the amount of intrinsic and extrinsic factors that interact in

that surface at this level. Such recognition is reflected in the amount of oscillation or steadiness in the curve relationship of R'_A and A_S , since high steady state reveals approximately complete recognition, and vice versa.

So, each order change in the channel network will encompass one or several RC areas in relation to the degree of heterogeneity (i.e. the interacted factors) and the dimension of the gridded-DEM data. Consequently, as A_S value decreases more first order streams will be defined, and hence the border limits between hillslopes and streams are more confused, which will lead to the formation of an undefined zone between the convergent and divergent topography (i.e. fuzzy area). Such area will produce an irresolute effect that leads to a vacillating direction in the curve relationship, and hence a clear unsteady tendency in the curve relationship (figures 5.1b and 5.26c). In contrast, as A_S increases the border limit area is reduced (the fuzzy area between hillslopes and streams) and the classified features, indeed, are more probable to be located within a stream than a divergent topography. The reduction of the fuzzy area (i.e. border limits) implies a continuous growth in convergent features and incessant decrease in the channelled area. In searching such equilibrium state between certain channels and probable changing fuzzy areas, the curve relationship takes the unsteady tendency and several RC areas are formed in relation to model capacity to define dominant topography at that point. The permanent oscillation continuo till the curve is stabilized when the algorithm recognizes certainly that all classified pixels are located within the convergent topography; that is, valley or a channel stream formation. Herein, both length and bifurcation properties play a significant role in determine the extent and location of the SZ in the curve relationship.

Montgomery and Dietrich (1992) suggested that a limit to the landscape dissection is defined by the size of the hillslope separating valleys, from which they noted that this apparent limit only corresponds to the extent of valley dissection. Nevertheless, landscape dissection into distinct valleys is limited by a threshold of channelization that set a finite scale to the landscape. Based on field data, Montgomery and Dietrich (1992) suggested that an empirically defined topographic threshold associated with channel head locations defines the boundary between essentially smooth and undissected slopes and the valley bottoms to which they drain. Figure (5.31) shows that channel heads are verified through a topographically defined threshold between channel and unchanneled region in the landscape. Results of Montgomery and Dietrich revealed three important points: the first is related to the general environmental controls on channel initiation and the form of the transition, which reflects the different channel initiation processes involved; the second, suggest that any reasonable model for channel initiation at the basin scale should include some degree of spatial heterogeneity; and, finally, such results contradict the early assertion that landscape dissection is scale-independent (e.g. Tarboton et al., 1989, 1992; Gupta & Waymire, 1989; Maritan et al., 1996; Rigon et al., 1996, etc), rather it depends on the corresponding changes in the threshold of channelization, that is scale-dependent (e.g. Beauvais & Montgomery, 1996; Mantilla et al., 2006). We believe that whatever the

approach used to define source-area threshold (constant threshold or slope-dependent critical support area), channel initiation is basically a random process that depends on several factors mainly slope and upstream supporting drainage area (Dietrich et al., 1992), and may include one or several erosion processes (e.g. seepage, piping, landsliding, etc), thus resulting in a spatially heterogeneous characterization (Rodríguez-Iturbe & Rinaldo, 1997).

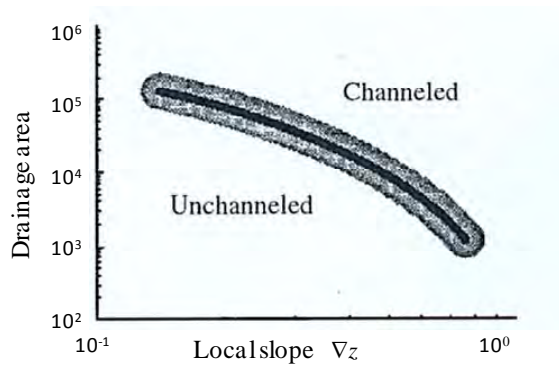


Figure 5.31 A schematic of the transition between channelled and unchanneled areas (after Montgomery & Dietrich, 1992).

Accordingly, limits between channelled and unchanneled valleys or the fuzzy area are controlled by inasmuch as processes involved in the channel initiation mechanisms (e.g. runoff and erosion processes). Such processes are scale-dependent, and hence each process implies a particular scale of channelization (i.e. degree of landscape dissection). More than one process implies more than one threshold and hence several scale features. Such processes are related to the intrinsic factors that are well integrated in the R'_A model approach. Therefore, changes in the curve relationship of R'_A and A_S are best described these processes and corresponding different related scales. Each SZ represents a particular scale of channelization that attributed to the evolution of the different natural processes contributing to the formation of the river basin and its embedded network. Hence, if more than one SZ is detected in one order level several channelization processes are interrelated at that scale, and the smaller the oscillation is in the level scale the greater the capacity of DEM data to distinguish such processes. Whilst the presence of a dominant stability zone between various should be attributed to a dominant process over the rest in the studied scale. In the same direction, a unique SZ is related directly to a distinctive particular channelization process. As a result, the MRC has been selected to represent the dominant process, and hence the optimum range of scales, in order to define the appropriate A_S value. However, given that the R'_A algorithm integrates both geometric and topologic properties the SZ is usually build on to include dominant as well as small and trivial processes for the channelization process. Hence, the MRC moves to the right or to the left in the curve relationship depending not only on the gridded-data resolution, as mentioned earlier (figure 5.25), but also on the number and importance of secondary trivial processes presented at that scale. Hence, the selection of the appropriate A_S value from the SZ is limited to a group of factors that permits a reasonable and

objective delineation of the drainage network. Such factors are established in relation to the controls embedded by local factors and environmental conditions.

In general, the local minimum (i.e. first value) in the *SZ* is selected to represent the optimum conditions for channelization and hence landscape dissection, except where the primary conditions for channelization are detected the local maximum is used. The primary conditions for channelization have been determined earlier in the methodology procedure for channel network delineation, as the following: The first primary condition is related to the formation of a unique stability zone in the curve relationship between A_S and R'_A . Such affirmation implies that the studied terrain is highly homogeneous and a unique channelization process has been detached. Under these conditions the fuzzy area is reduced to a fine-limited transitional process between convergent and divergent topography, which is located in the middle of the *SZ*. With a low A_S value, length properties, i.e. represented by R_A , approximates a unity (Montgomery & Foulfoula-Georgiou, 1993) whereas topologic properties varied strongly giving rise to an ordinary variation in R'_A value, which usually takes a form of an increasing positive change. Herein, a hillslope formation is the representative feature of such conditions. As A_S value increases length properties deviate from unity and topologic properties approximates to unity and terrain dominant processes begins to change from divergent features (i.e. hillslopes) to convergent processes (i.e. streams and channels). The midpoint between both processes is best represented by the fuzzy area mentioned earlier or the shaded area in figure 5.31 that reflects the general environmental controls on channel initiation (Montgomery & Dietrich, 1992). Thus, the optimum A_S value to use is located directly after the fuzzy zone. However, such value is so difficult to be isolated and defined since it is related to DEM-data resolution and local factors, for which another objective criterion should be used for A_S definition. Herein, as our hypothesis was formulated on the basis of defining a channel network that best describe landscape complexity with least possible feathering, we opted for the A_S value that guarantees dominant convergent processes, that is, the maximum value in the *SZ* area in the curve. The second primary condition is related to the initiation process of the *SZ*, which in some cases and under a particular conditions of channelization is initiated from a saddle or a watershed divide. So, the local maximum is selected as the optimum critical supporting area and the local minimum is neglected. The third condition is related to channel network age and evolution determined by the relief index of hypsometric integral (*HI*), which has been used earlier in similar cases. The *HI* reveals two important aspects of landscape-dissection form: the first is the uniformity of erodible materials in the basin (Chorley et al., 1984), since high *HI* values is related to high uniformity (homogeneity), and vice versa. The second is the landscape development and hence stage of evolution (Strahler, 1952b; Mark, 1984). Herein, threshold value for approximately completely homogeneous erodibility and evolution stage has been fixed to $HI \geq 55$, below this value will be accepted as a heterogeneous formation structure. Such value has been deduced in relation to early affirmations on landscape-development stage and erodibility (Davis, 1909; Strahler, 1952b,

1958; Leopold & Miller, 1956; Abrahams, 1977, 1984a; Willgoose & Hancock, 1998), for which they set $HI \leq 40$ and $40 < HI > 60$, for low and medium to high uniformly erodible materials, respectively.

In Table (5.15), results reveal two dominant erosion processes at the channel heads in the reclassified sub-catchments in the Cautivo Basin, which is reflected in different types of geomorphic channel head formations (Dietrich & Dunne, 1993). In the first two sub-catchments, piping is the dominant erosion process and channels incised directly by such effect. Thus, channel heads of small to moderate headcuts were observed in the two sub-basins. In addition, a gradual initiation in the first sub-catchment was observed followed by a clear headcut formation (highlighted by the red line in figure 5.30c), a peculiar and totally different feature to the rest of the basin formations that is attributed to the presence of a high concentration of overland flow and a rounded hillslope formation. Whereas in the other two sub-catchments (i.e. 3 and 4) rill erosion is the dominant process, and the gradual head channel form could be attributed directly to such processes. Herein, it is important to underline that the reclassification process (i.e. HSP) in the $R'_A t$ procedure could increase, decrease or in some cases maintain the drainage network properties in the classified sub-catchments. In addition, the maintenance in the drainage properties may be partial or complete, that is, part of the channel network properties are modified (table 5.16). In this case the topologic properties are usually maintained and the length properties are modified, for so care should be taken when using both properties in measuring the degree of enhancement in order to define landscape dissection. For instance, in the Cautivo sub-catchments (figure 5.30) in the first sub-basin all the indices are reduced with the new A_S value, whereas increased in the sub-catchments 2 and 4; and finally, the sub-basin 3 reveals a partial increment in length properties and unaffected change in topologic ones.

No. of Catchment	index	L_a	D_d	μ	F_S
1	Before	198.1	0.0291	7	0.0015
2		51.38	0.0257	3	0.0013
3		12.24	0.0287	2	0.0049
4		17.49	0.0193	1	0.0011
1	After	159.8	0.0199	3	0.0004
2		75.94	0.0339	5	0.0022
3		24.07	0.0689	3	0.0049
4		33.38	0.0503	5	0.0055

Table 5.16 Changes in geomorphometrical indices before and after applying the new A_S value according to the $R'_A t$ approach in the Cautivo Basin. Catchment number is related to figure 5.30.

The Rambla Honda Basin is another important example that can be used to verify and understand the form in which the $R'_A t$ approach, concretely the R'_A algorithm, treats and define landscape dissection under smooth homogeneous formations. Herein, the curve relationship and the tendencies are completely different, since several processes and formations are presented. Once more, the curve relationship between A_S and R'_A divides the studied catchment to three levels of complexity,

in relation to order change (figure 5.32a). The first corresponds to $\omega = 4$, which is characterized by a non-steady tendency form (figure 5.32b), and no clear *SZ* were detected in this level. In addition, whatever A_S value used at this level, the resulted channel networks are highly dissected and contain a lot of feathering (figure 5.33a). In the second sector of the curve (i.e. $\omega = 3$), the oscillation of R'_A values through A_S change is reduced and a clear *RC* area could be appreciated that extends between 25 and 60 (figure 5.32c). At this level scale, the constructed drainage network appreciates more a rational similarity with the natural landscape structure, but still very far from the real channel network or the digitized *BLs* (figure 5.33). Whereas, at the last level (i.e. $\omega = 2$), the situation is completely different where two clear *RC* zones are appreciated (figure 5.32d). The first range of the first *RC* zone extends from 120 to 650 and the second from 655 to 1200 with a rate of change of about 93.5 and 61.8, respectively. According to the $R'_A t$ procedure the optimum A_S value corresponds to the local minimum of the highest rate of change, that is, $A_S = 120$. Herein, it is well appreciated that the defined channel network approximates to the digitized streams and succeeded to describe all valleys and channels of the studied area. However, the *3D* terrain aspect presented in figure 5.16 suggests a higher dissected terrain than that proposed by the digitized-*BLs*. Such observation confirms again the futility of the digitized-*BLs* under particular scales and relief contrasts. Again, the $R'_A t$ procedure divides the basin to two main sub-catchments (figure 5.34a) of different degree of complexity. These are sub-classified and the process continuo until all the sub-basins has been divided and one of the primary conditions is achieved (figure 5.34b & c). The final result of the above procedure is a moderately dissected channel network that is adjusted to the smooth and low-contrasted relief of the Rambla Honda Basin (figure 5.16b). Furthermore, the constructed drainage network reveals a significant enhancement in the upper parts of the channel network in comparison to the *BLs* and *CDA* technique (figure 5.35), where first-order streams are so hazy to be detected and relief contrast is so smooth to be perceived by the topographer.

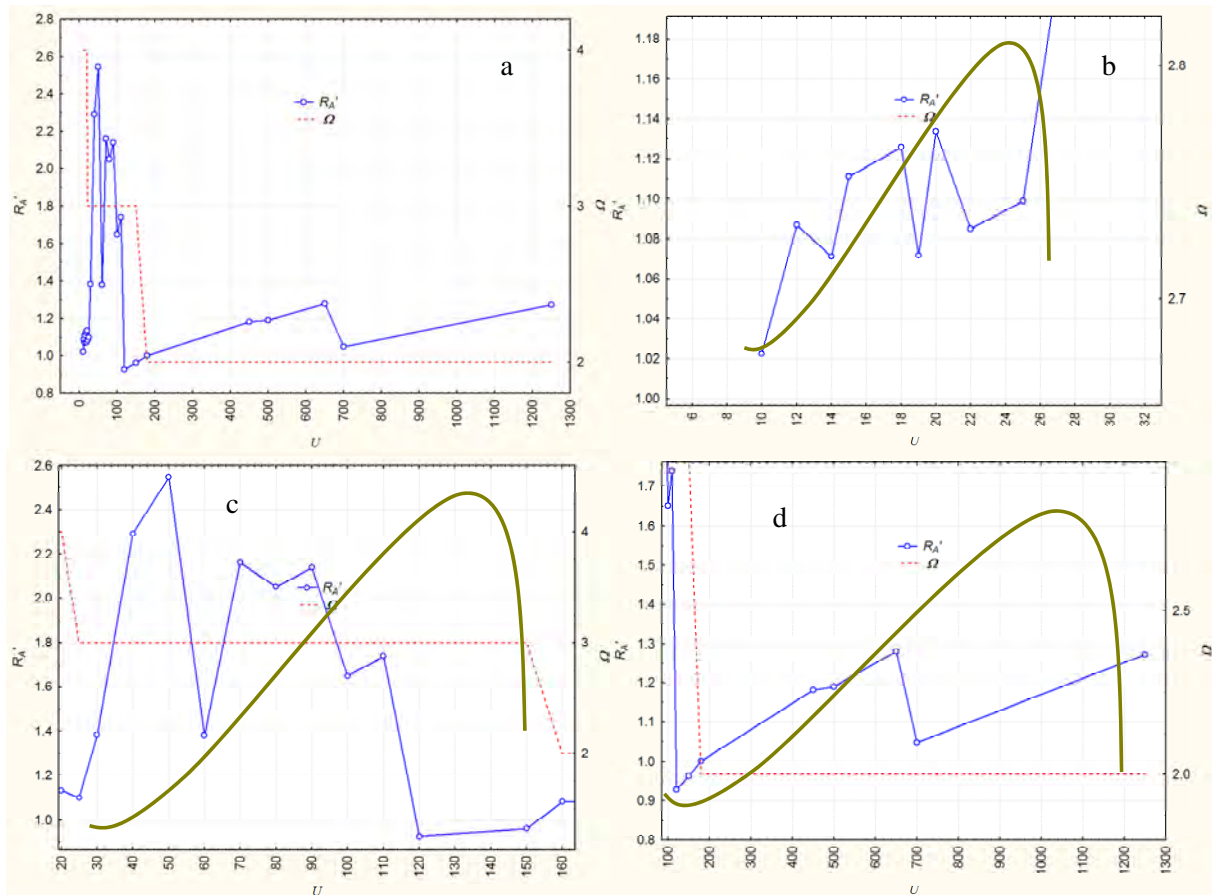


Figure 5.32 Curve relationships between A_S and R'_A in the Rambla Honda Basin and the theoretical and actual forms of change in each part in relation to order change. A) The total curve relationship in relation to order change. B) $\Omega = 4$. C) $\Omega = 3$. D) $\Omega = 2$.

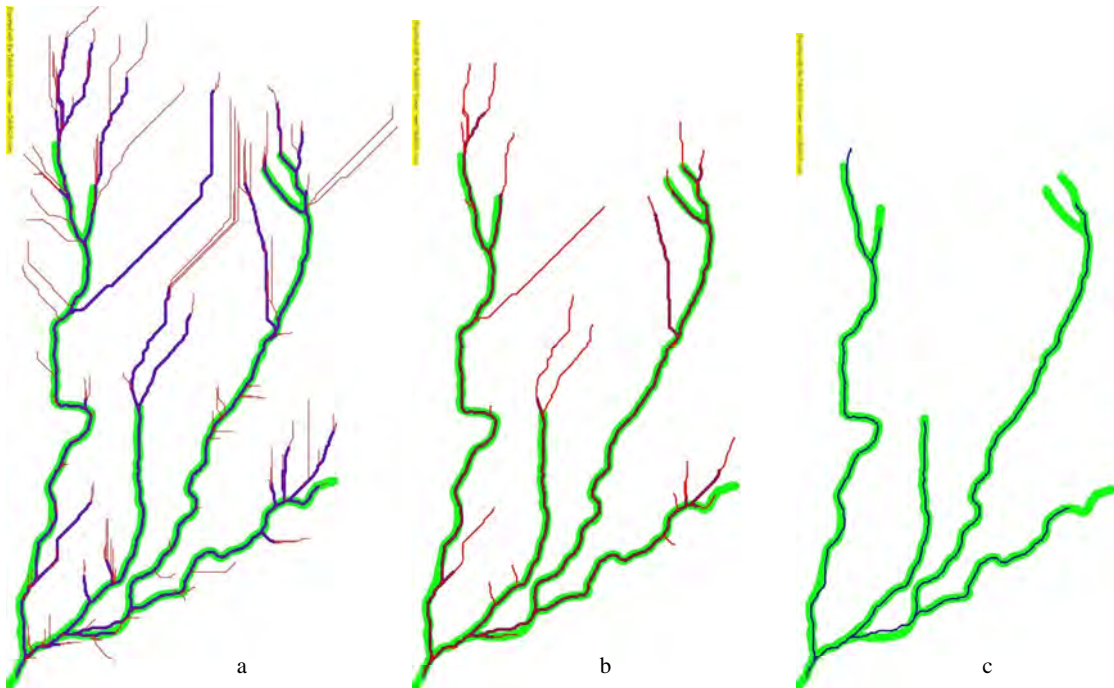


Figure 5.33 The digitized BLs in bold green and the channel network in the Cautivo delineated by different A_S values in relation to order change. a) $\Omega = 4$ and $A_S = 5$ and 20. b) $\Omega = 3$ and $A_S = 25$ and 60. c) $\Omega = 2$ and $A_S = 120$ and 700.

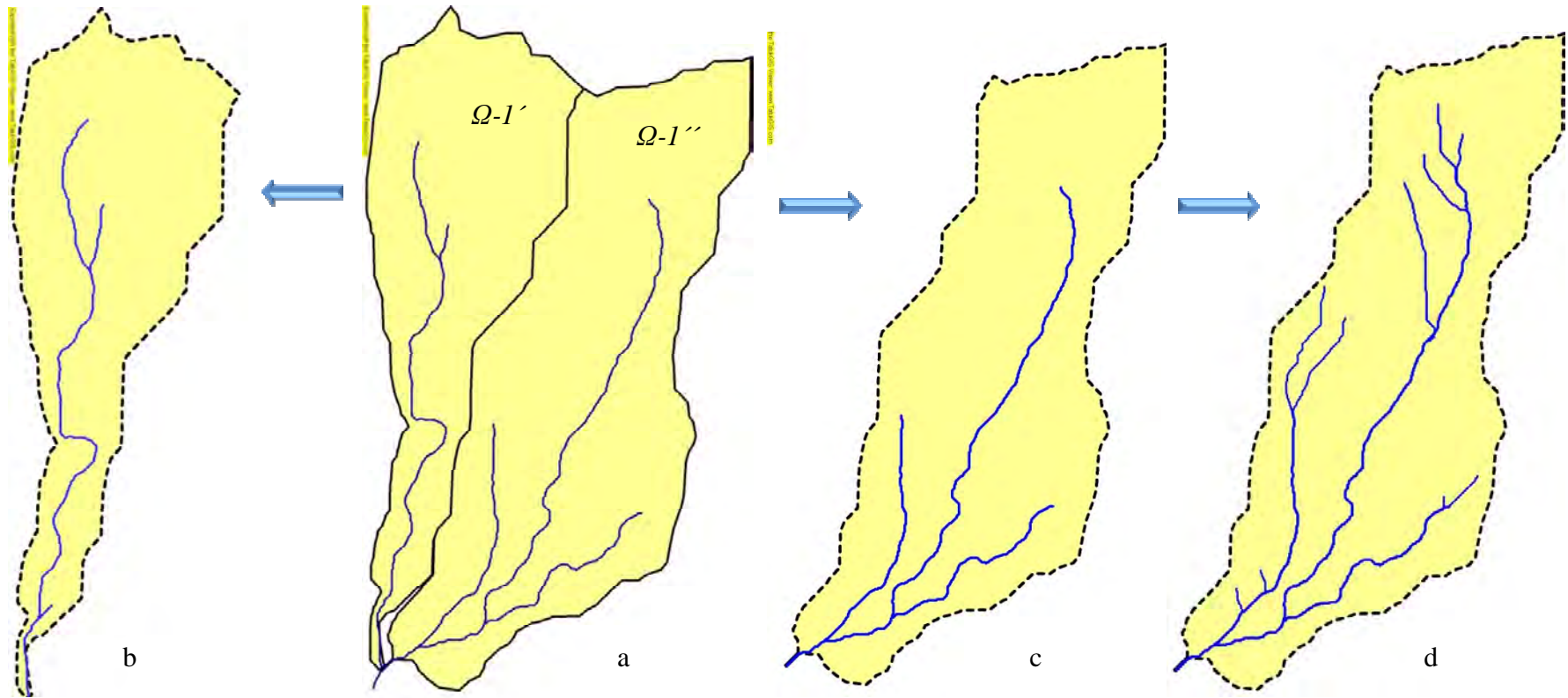


Figure 5.34 Main sub-basins of the Rambla Honda catchment resulted from the R_A^t procedure and the decent stratification method (*HSP*). a) The entire Rambla Honda Basin with $A_S = 120$. b) $\Omega-1'$ Sub-catchment of Rambla Honda that correspond the left part with an $A_S = 58$. c) $\Omega-1''$ Sub-catchment of Rambla Honda with $A_S = 120$. D) The final drainage network in the c catchment with the R_A^t procedure.

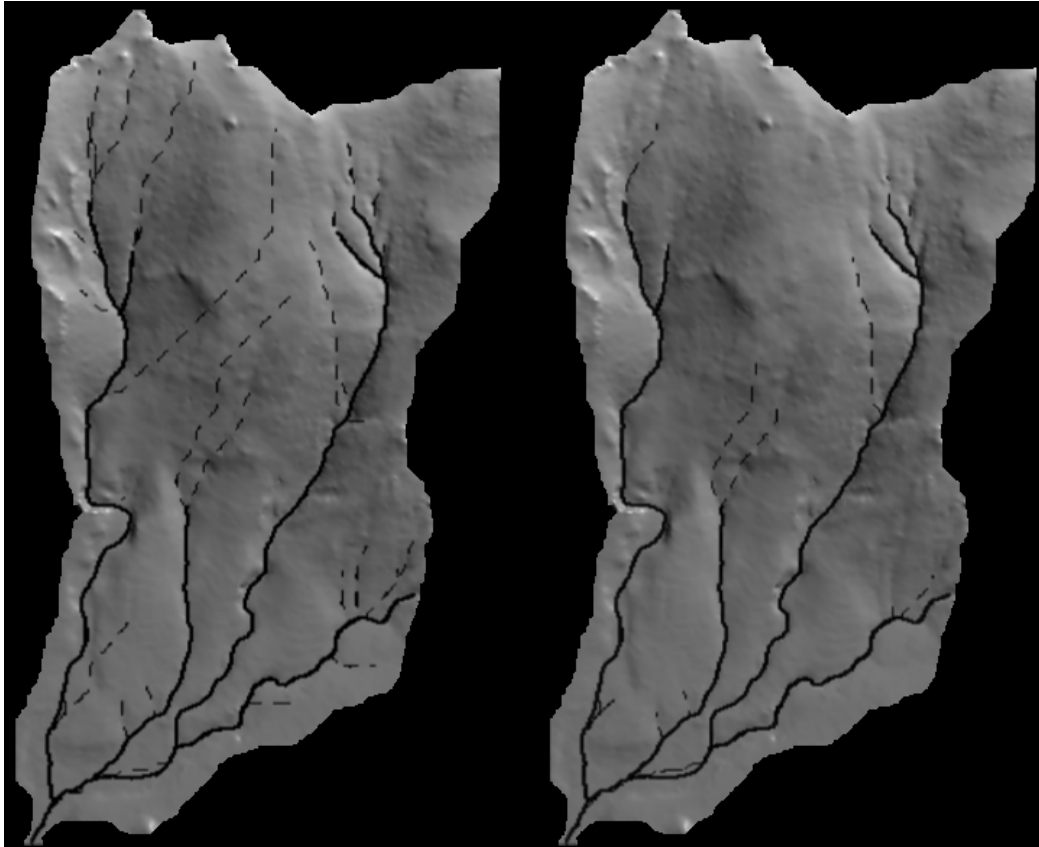


Figure 5.35. Direct comparison between channel network limits delineated by the (a) *CDA* technique and (b) the $R'_A t$ procedure and the *BLs* as a base for both marked as dotted lines.

It is important to underline that the Rambla Honda field site forms part of a large fan system, in which overland flow is the prevailing process for sediment and runoff generation. So, overland flow threshold should be adapted or used according to the curve of Montgomery and Dietrich (figure 4.1). However, since part of the primary data is unavailable and the model does not accept such information, the model behaviour could be substantially interpreted by the morphological features of the Rambla Honda Basin. Such features at a very detailed scale exhibit enough variations to count for their different hydrological behaviour (Puigdefábregas et al., 1996). These differences are referred to surface morphology as well as to their horizon layering. Stones on and within the surface are much larger in slope soils than in fan soils, which may influence surface runoff and infiltration at the hillslope scale; that is, higher infiltrations in fans system and higher runoff in hillslope features (Abrahams & Parsons, 1991; Puigdefábregas et al., 1996). These processes explain not only soil-water relationships under such conditions but also their morphological features. Such formations and processes give rise to a dominant dendritic drainage system conditioned by the local structure (i.e. sedimentary strata and fold axis) producing a main stream system formed by enlarged valleys, or named locally as Rambla, and a meandered thalweg aspect throughout the Rambla system that occupies the lower part of the basin. Conversely, a fine drainage system is verified in the upper part of the basin (figure 5.16), which is formed by a group of different stream formations related directly to the scale of surface morphology and the dominant hydrological behaviour. Therefore, the algorithm

recognizes the terrain complexity, which is, in this case, associated to dominant geomorphological features rather than erosional ones as seen before with the Cautivo Basin.

The main dominant features in the Rambla Honda basin include: *i*) upper hillslopes with a moderate steepness and soil profile thickness of 15-60 cm; *ii*) alluvial fan system characterized by smooth inclination and slope profile that could reach 10 m; and *iii*) the Rambla floor which forms the basic drainage system of the area, characterized mainly by a highly sediment profile of about 30m (Puigdefábregas et al., 1996, 1998b). In this case, the R'_A algorithm provides a value of $A_S = 120$ for the entire Rambla Honda Basin, and optimum A_S values of 58 and 120 for the sub-basins *b* and *c* (figure 5.34), respectively, that resulted from the *HSP*. Herein, the entire basin and the subsequent basin *c* coincide with the same A_S value of 120, whereas the sub-basin *b* shows a reasonably smaller A_S value of 58, giving rise to different conclusions. In the first case (the entire basin and the sub-basin *c*), the same A_S value indicates high similarity in geomorphological features and conditions for the two compared basins. Whereas, the sub-basin *b* approximates more to a catchment of idealized homogeneous formation; that is, similar hillslope formations (high similarity in geomorphological characteristics) that drains through a simple drainage network structure (figure 5.34b). Such idealized basin implies less heterogeneity and less complexity in the dominant features, for which the A_S value has decreased to the half value of the entire basin and a better tendency curve relationship is observed between A_S and corresponding R'_A values (figure 5.36). Herein, the *HSP* is stopped since all the generated first order streams have reached the primary conditions and the delineated channel network is accepted as the optimum one under the available conditions, i.e. heterogeneity and gridded–data dimension. Yet again, the *HSP* is applied to the sub-basin *c* and the optimum A_S value for each sub catchment is defined (figure 5.34d). Finally, the delineated channel networks for sub-basins *B* and *D* are reconnected to form the complete drainage system for the entire basin of the Rambla Honda Catchment (figure 5.16B). It is worth to underline that possible error in the border limits of the entire catchment, which corresponds to missing data, may be the responsible for a trivial fraction of some first order streams, mainly in the western and southern border of the basin. Even so, we believe that the generated channel network still the optimum possible alternative between *BLs* and the *CDA* technique.

Herein, the *BLs* and *CDA* techniques have provided different and contrasted aspects for the drainage network system in the Rambla Honda Basin. The digitized *BLs* of the Rambla Honda are poorly dissected and just represent the main valley system of the zone (figure 5.16A). In addition, first-order streams are disappeared and replaced by higher-order links. Such simplicity in the defined *BLs* is attributed to the smooth relief formations of reduced contrasts, which makes it so hard to be distinguished by the cartographer. On the contrary, the *CDA* technique provided an extremely dissected drainage network with a highly feathering aspect that goes through the unchannelized hillslopes (figure 5.16C). Such phenomenon causes erroneous results not only in the geometrical and

topological measures of the delineated drainage system but also in the hydrological response of the defined catchments (Montgomery & Foufoula-Georgiou, 1993; Miller & Burnett, 2007). So, qualitatively, none of the above techniques have estimated or provided an appropriate A_S to delineate the optimum channel networks in the Rambla Honda Basin.

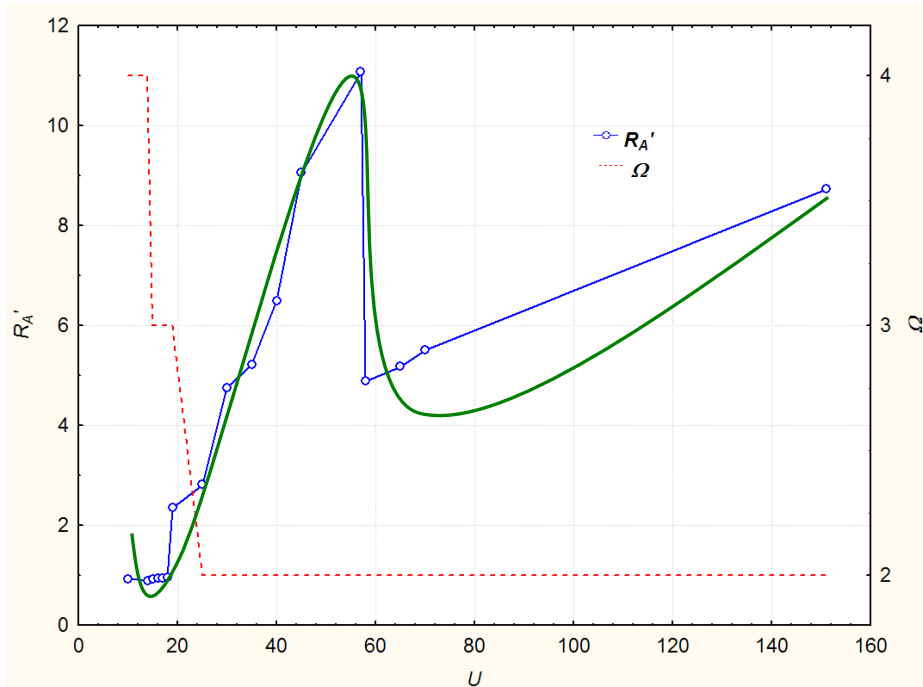


Figure 5.36 Form and type of the curve tendency relationship between A_S and R'_A in the sub-basin B of the Rambla Honda catchment.

The earlier comparison was carried under a qualitative approach of stream network validation, since surface-visualization technique forms and provides an important procedure for the dynamic interaction between user and computer (Wood, 1996a). This option is highly effective in small limited area with highly defined relief, such as the Cautivo and the Rambla Honda Basins. Whereas, in general, the majority of the case studies may include areas of different scale dimensions with diverse relief formations that makes it impossible for the visual comparison or even partial one, such as the Tabernas Basin. Figure (5.37a) provides the best approximation of a 3D construction of the surface relief forms in the Tabernas Basin with the digitized *BLs*. A quick inspection to the surface relief underlines that main channels and valleys are easily detached whereas first order streams are so difficult to be detected and compared, mainly between close ones. While figure (5.37b) provides the drainage network of the same area delineated by the *CDA* techniques, the visualization process still undergoes the expectations of detecting channels and valleys for the entire catchment area. So, quantitative validation approach is still the main and the direct process for results approval.

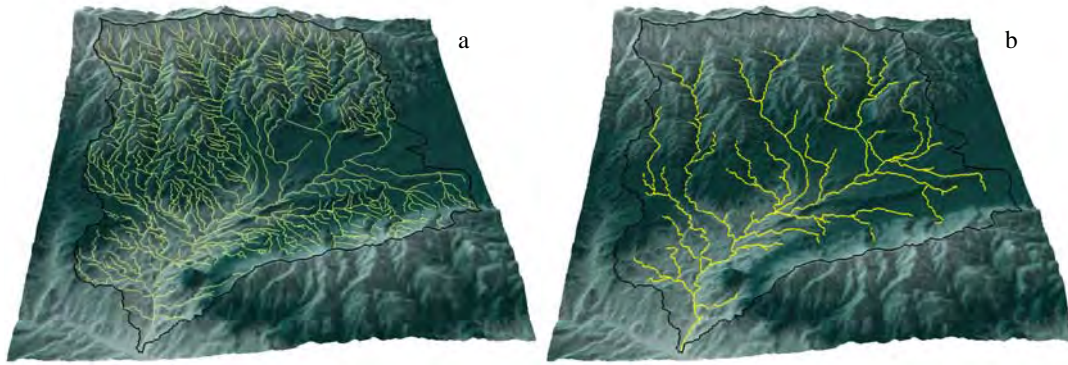


Figure 5.37 3D structure visualization of the drainage networks in Tabernas Basin, a) with *BLs* and b) with *CDA*.

As mentioned earlier, different geomorphometric indices were used to compare stream networks of different scales and local conditions. Throughout the work, the mode of comparison between techniques has been considered to be of vital importance, since several direct and indirect problems should be handled and faced. First, the problem of real surface or real data representation (i.e. natural streams) was handled by the use of the digitized-*BLs* from topographic maps. Whilst several studies have underlined the danger of attempting to use topographic maps alone for the study of river basin morphology (e.g. Chorley et al., 1984; Abrahams, 1984a), *BLs* still considered the best valid representation for landscape dissection. Second, types of parameters or indices to use in the comparison mode, in which four types of indices have been utilized: geometrical, topological, energy expenditure and fractal dimensions. These indices include the crucial majority of the parameters applied in geomorphological studies. Finally, the mode of comparison, i.e. type of test, between parameters, this problem was treated by the use of two global comparison approaches. The first tries to solve the direct comparison between pairs of observations (i.e. observed versus expected) and was called overall comparison. The Gower Metric (*GM*) test of association has been used to evade global effects in the matrix dataset and to measure the appropriateness of each technique in form of degrees of enhancement. The second comparison approach (i.e. partial comparison) deals with the values or indices that need more than three observations to be calculated. In this case, the comparison was realized in two levels, the first is with the *BLs* and the second is with empirical-defined values for each parameter.

5.5.3. Comparison between techniques

As mentioned earlier, the $R'_A t$ procedure consists of two essential parts, the R'_A algorithm and the *HSP* process. From one hand, both are considered as complementary procedures and are needed in order to achieve the optimum description of landscape dissection under changed conditions of homogeneity and heterogeneity. On the other hand, *CDA* is compounded of one step and search for the smallest weighted support area threshold where scaling laws break (Tarboton, et al., 1992). The comparison procedure was realized in two levels, the overall comparison using direct descriptors and the partial comparison using fractal dimensions of the delineated channel networks.

In Tabernas Basin, results of overall comparison between R'_A and CDA have demonstrated a contradictory enhancement at two distinct scales. With R'_A model, streams networks delineation was enhanced in 13 out of 16 parameters, i.e. approximately 81 %, used in the comparison process (table 5.3) in relation to the digitized *BLs*. Such comparison has been realized in a vast range of basins of different sizes that oscillate between 0.21-567.265 km². Whereas if the entire Tabernas Basin was used as the sole comparison unit (area size of 567.26 km²), the CDA technique reveals a completely better enhancement in the defined channel network (table 5.4) than the R'_A algorithm. Such contradiction in result enhancement was confirmed in relation to basin size scale, in which a direct comparison between the digitized-*BLs* and automatic delineated streams of R'_A revealed a breaking point in the relationship curve between drainage density and basin size (figure 5.9). These results show that improvement in channel network delineation was enhanced at basins size less than 5 Km² and above that scale the R'_A algorithm was less efficient than the CDA technique. These results are highly attributed to terrain complexity and hence the heterogeneity of the basin relief.

The algorithm in its pure form tries to verify the terrain in relation to data dimension (i.e. gridded-DEM resolution) and the degree of relief complexity; that is, the amount and type of landform features that occupy a particular landscape unit. DEM-resolution effect was greatly verified in geomorphological and hydrological studies (e.g. Zhang & Montgomery, 1994; Quinn et al., 1995; Wang & Yin, 1998; Wolock & MaCabe, 2000; Thompson et al., 2001; Hancock, 2005), whereas relief-complexity effect was generally included as a consequence in the combination of local-factors effect (e.g. Montgomery & Dietrich, 1992; Montgomery & Foufoula-Georgiou, 1993; Tucker et al., 2001b; Vogt et al., 2003). Other studies related drainage density (*Dd*) to relief or relative relief in combination with slope gradient (Strahler, 1964; Tucker & Bras, 1998) predicting different relationships in relation to dominant climatic conditions. Herein, it is important to underline that a landscape is a combination of a great number of individual geomorphologic forms (e.g. slopes, valleys, peaks, etc.), which gives the final shape to the terrestrial cover.

In this direction, Scheidegger (1991) argued that it is impossible to build a classification of landscapes on the basis of the morphology of their elements, as the latter could be combined to form systems characterized by extraordinary complexity. Rodríguez-Iturbe and Rinaldo (1997) underlined that attempts at such classification must therefore be based on features of a larger scales and of statistical character. If we assume that the R'_A algorithm recognizes the terrain in function of bifurcation and length properties, that is, channelled and unchannelled features, a simple landform classification scheme for terrain features will be adequate to represent terrain complexity. Herein, and for simplicity, we have proposed that the smaller the terrain is the higher the homogeneity is, and vice versa. Such assertion assumes that in small-basin units type and amount of prevailing topographic features are lesser than large ones, giving rise to homogeneous terrain structure. So, the Pennock et al.,

(1987) algorithm was applied to Tabernas Basin and its sub-catchments (figure 5.8), in which landform types are varied in relation to basin size. Figure 5.8 reveals a change in terrain complexity between sub-catchments of Tabernas Basin, where landform classes (i.e. type and amount) change from highly heterogeneous, in the case of Ω and $\Omega-I^{**}$, to moderately homogeneous, in the case of $\Omega-2^*$. So, inasmuch as the terrain is divided to smaller scale terrain units (i.e. sub-catchments) the higher the homogeneity is and the better the R'_A model proceeds or operates.

Contrary results have been detected in the *CDA* approach, where the efficiency of the technique is diminished as the basin size is reduced, mainly in sizes less than 0.5 km² (table 5.17). Results of table 5.17 reveal that the *CDA* approach loses efficiency as basin size decreases, where failure detection of an optimum A_S value is evident in catchments size < 5 km². Of course, such failure is higher in small catchments, e.g. between 0.1- 1 km², than larger ones, e.g. between 1.1-5 km². The limited efficiency of the *CDA* procedure in small scale catchments is attributed to the form in which the drop analysis is built, which is to look for statistical differences (comparison of means of different populations) in height drop in relation to order change (Tarboton et al., 1991). Such conditions are hard to achieve in small catchments since statistical variance is limited to two or three orders at maximum, which leads to failure detection of a significant differences between orders. So, homogeneity is not always a limiting factor for stream network delineation, but also an efficient technique is needed to achieve a more realistic landscape dissection. Hence, the *HSP*, which classifies a landscape to homogenous units, will not always promise a better efficiency of the algorithm used to select an appropriate A_S value; rather it may deteriorates such capacity leading in some cases to completely failure detection.

Basin size (km ²)	Total number catchments	Failed to be detected by <i>CDA</i>	<i>CDA</i> %	Failed to be detected by R'_A	R'_A %
0.1-0.49	92	87	94.56	1	1.08
0.5-1	51	29	56.86	1	1.96
1.1-4.9	77	15	19.4	0	0
5-567.2	45	0	0	0	0

Table 5.17 Number and percentage of catchments in which used techniques failed to detach a valid A_S value.

The *HSP* promises a systematic hierarchical classification for hydrological landscape units based on intrinsic properties of the channel network. From one hand, such intrinsic properties are best simulated and verified in a homogeneous landscape. On the other hand, the extent of the hierarchical classification process is limited to a general index of global homogeneity (i.e. either in landform features or dominant processes). Relief complexity and hence homogeneity is long recognized to have a direct and indirect effect on drainage network properties, both geometric and topologic ones (e.g. Abrahams, 1977; Willgoose & Hancock, 1998; Hurtrez et al., 1999). Several relief indices have been proposed to describe such characteristics, between which the hypsometric integral that have been used to define, in addition to basin maturity (Davis, 1909), the uniformity of dominant material and

processes in the landscape (e.g. Strahler, 1952b; Mark, 1984; Chorley et al., 1984). In the proposed methodology of the present study, the *HI* index was applied as a criterion condition, in addition to other two ones, in order to stop the hierarchical classification process in the $R'_A t$ procedure.

In general, the overall comparison analysis has shown greater enhancement in geomorphometrical properties for the R'_A model over the *CDA* technique. This improvement is reflected in 81 % in the cases of before and after the use of *HSP* approach (tables 5.3 and 5.6). In the first case (i.e. R'_A model without the *HSP*), and as mentioned earlier, if Tabernas basin is used as the unique unit of comparison, results confirmed the superiority of the *CDA* technique over the R'_A model for all the indices used in the comparison procedure (table 5.4). Whereas, when distinct catchments of different dimensions are used, the situation is completely different and the R'_A model reveals a clear enhancement over the *CDA* technique (table 5.3). Herein, 13 geomorphometrical indices have shown major similarity in relation to digitized-*BLs* and the defined channels by the R'_A technique. In the compared similarities, all indices showed a type of enhancement except the parameters inR_A , k , and E . These indices are not related to a particular property of channel network, rather they comprise different geometric and topologic characteristics. The inR_A is related to length properties, k is a complex index that is related to magnitude (μ), drainage density (Dd) and total length (L) of the channel network, and finally E is related to (μ) and average link length of both exterior and interior segments.

In the second case, where the R'_A model was used in combination with *HSP* for all sub-catchments, again 13 indices demonstrated greater similarity between the digitized-*BLs* and the $R'_A t$ procedure (table 5.6). In this case, k , $p(\mu)$ and E provided higher similarity for the *CDA* procedure and the digitized *BLs*. The E and k values have shown slightly enhancement for the $R'_A t$ procedure with respect to previous comparison, whereas the $p(\mu)$ value revealed a clear decline and higher dissimilarity value in relation to the first case of comparison of the $R'_A t$ procedure (table 5.3). Furthermore, the geomorphometric indices when compared in Tabernas Basin as a whole revealed a remarkable change, in which the enhancement is raised from 0 to 10 of the total descriptors used in the comparison process (table 5.7). Again, inR_A , ki , k in addition to P_s and $p(\mu)$ didn't remark any enhancement and appointed to higher dissimilarity between $R'_A t$ -*BLs* than *CDA*-*BLs*. Once more, these parameters do not pertain to a particular drainage network property; rather they underscore one or more aspects of the stream network characteristics. Such results underline the importance of the selected indices and the weight of each parameter in defining distinct properties in the delineated drainage network. For instance, and for Tabernas Basin, the parameters μ , Dd and L independently have shown positive enhancement whereas the combination of all, i.e. k index, did not.

Once again, the partial comparison analysis highlighted similar conclusions to the overall one. In the two cases (before and after using the *HSP*), Hack's (α) and Melton's (θ) values revealed a considerable enhancement for the $R'_A t$ approach over the *CDA* technique (tables 5.5 and 5.8). Moreover, the degree of enhancement is always greater when using the *HSP* approach, where the dissimilarity index values between the digitized-*BLs* and the defined streams from the $R'_A t$ approach are at minimum (table 5.4). The fractal dimensions α and θ have been widely used to describe various scale properties of stream and channel network system. The fractal value α describes the relation between the main stream length and its drainage area (e.g. Hack, 1957; Gray, 1961, Rigon et al., 1996), which extends from 0.4 to 0.6 for large and small catchments, respectively. Such results indicate a tendency toward elongation of the larger catchments; that is, basins tend to become longer and narrower as they enlarge (Rodríguez-Iturbe & Rinaldo, 1997). The θ value suggests that a direct relationship between channel frequency (F_S) versus drainage density (Dd) is conserved constant in nature with a value that approximates to 2 (Melton, 1958a). Researchers (e.g. Smart, 1978, 1981; Mark, 1984; Luo et al., 2007) have widely discussed that such values are highly related to the fundamental horizontal length scale associated with how the channel network dissects the landscape. Moreover, Montgomery and Dietrich (1992) observed that Hack-like relationships tend to also hold for unchanneled valleys, source areas, and low-order channels. Such affirmations underline that α and θ values are highly related to initial-data dimension, which is the scale of the topographic map in the case of the digitized-*BLs* and DEM resolution and A_S value for the automated channel networks.

For the three compared channel networks in Tabernas sub-basins, Hack's value approximates well to optimal one (tables 5.5 and 5.8) suggested by scientists. Whereas, Melton's dimension reveals a varying estimation to optimal values in relation to both catchment size scale and the procedure used to define channel network limits in the landscape (figure 5.14 and table 5.9). For instance, in Tabernas basin a set of about 250 sub-catchments have been used that oscillate between 0.18-567.2 km², from which 91% with a drainage area less than 10 km². It has been observed that α undergoes statistical fluctuation in relation to the basin size used in the constructed relationship (table 5.18) for the digitized-*BLs*. The significant fluctuation of α from the optimum values of Hack and Gray leads to a clear evidence on the fractal nature of river networks (Tarboton et al., 1988, 1989,; Rigon et al., 1996). Such results are in good agreement with previous conclusions of Maritan et al., (1996), in which they suggested that α is directly related to a suitable fractal dimension of the boundaries, to the elongation of the basin, and to the scaling exponent of mainstream length. The same results have been detached for θ , where fluctuations were observed in relation to scale boundaries in the digitized-*BLs* (figure 5.14) and for the automated channel networks of the *CDA* and $R'_A t$ techniques (table 5.13). But, with Melton's dimension the fluctuation goes beyond the range estimation of the optimal value, that is, θ approximates 2. Once more, such results confirm the importance of length scale properties used to derive the fundamental parameters associated to channel and stream network limits.

Basin size	0.1-0.59	0.6-4.9	5-19.9	20-567.2
α	0.66	0.62	0.57	0.44

Table 5.18 Fluctuations of Hack's value extracted from the digitized *BLs* in relation to the basin area size used in the relationship.

Again, the Cautivo and the Rambla Honda catchments have confirmed the previous results and emphasize on the efficiency of the $R'_A t$ approach over the *CDA* technique. The geomorphometric attributes used in the two areas revealed that the dissimilarity index is higher in the *BLs-CDA* combination than *BLs-R'_A t* one (tables 5.10 & 5.11). Almost the majority of the parameters underline a type of enhancement in result approximation to the digitized-*BLs* for the $R'_A t$ approach. In addition, the above results have put in evidence the capacity, efficiency and importance of the geomorphometric indices in describing the particular and general characteristics of the drainage network properties. Such description involves the geometric and topologic dimensions, as well as self organization optimality and criticality of natural landscapes. It is important to underline that these values have not been used to describe or determine the drainage network characteristics, rather they were used to compare the same basin scale under different A_S values defined by distinct delineation approaches. So, parameters interpretation, in a geomorphologic sense, provides no information on the appropriate A_S value used in stream network delineation. Nevertheless, the character of the drainage network is important because it can be used to interpret the geologic conditions responsible for certain patterns and, in addition, the texture of the pattern is controlled by, and in turn has an influence on, the hydrology of the drainage basin (Chorley et al., 1984).

5.5.4. Physical validation process

The quantitative approach (i.e. based on geomorphometrical indices evaluation and comparison) of stream and channel network validation is of great importance, as it provides a deep insight on the capacity of the techniques used in stream-limits definition. While such approach is valid under various limited conditions (e.g. scale and data resolution), its main disadvantage is related directly to the reference points for which automated drainage network ought to compare with, herein represented by the digitized-*BLs*. Although *BLs* are still widely used in the scientific and commercial works, several researchers (e.g. Chorley et al., 1984; Wood, 1996b) highlighted on a mixture of associated inconveniences, which is related mainly to cartographer background and experience, contrast of the terrain under study, original-data scale, and time of data acquisition. These considerations underline uncertainties on the validation process and make it useless without an auxiliary approach that minimizes such inconveniences. Hence, in situ validation is needed, which based on field visits as well as *3D* assessments with DEM data and orthophotographic images, in order to provide strengthen to the quantitative approach.

A simply quick inspection to the digitized-*BLs* revealed a clear subjectivity in range-value distribution of the upstream contributing area for exterior links of the *BLs* rather than a methodological one, in which the range and standard deviation is higher than that utilized in automated techniques (table 5.19). In general, the higher the range between minimum and maximum contributing source area for each upstream segment (i.e. A_S value) the lesser the possibility is to assign a unique A_S value for that region. Such variance implies high significant errors in the compared channel network, herein manual and automated ones. Of course, result interpretation in table (5.19) can be explained in distinct forms, in which the broad range of upstream source areas for Tabernas Basin may reflect the natural variability in the landscape characteristics that control channel-initiation. Whereas, in Rambla Honda and Cautivo Basins such results contemplate highly subjective judgment of the cartographer to the terrain-landforms contrasts. Such affirmation entails a varying conclusion in relation to the dominant relief formation: *i*) under homogeneous terrain structure, manual representation of stream networks is unpredictable and highly random, and the comparison process between manual and automated approaches is fairly doubtful; whereas, *ii*) under heterogeneous relief forms, the multifractal approach (i.e. multiscale dimension) is needed in order to estimate or even approximate the manual depiction of landscape dissection. Of course, the above confirmation is controlled and limited by several factors such as DEM resolution, scale of work, and dominant landscape processes.

	Standard deviation	Skewness	Min	Max	Range
Cautivo					
<i>BLs</i>	1643.484	3.3105	45.000	6220.00	6175.0
$R'_A t$	191.612	2.0990	208.20	933.000	724.80
<i>CDA</i>	159.501	1.9018	44.000	864.000	820.00
Rambla Honda					
<i>BLs</i>	7312.318	-0.1859	2123.0	24686.0	22563.0
$R'_A t$	1411.910	1.2980	887.00	5159.00	4272.00
<i>CDA</i>	1370.238	2.4192	26.000	6917.00	6891.00
Tabernas Basin					
<i>BLs</i>	188621.5	12.22	900	3126600	3125700
$R'_A t$	282261.5	22.61	8100	7155900	7147800
<i>CDA</i>	1262632	1.6137	1908000	8173800	6265800

Table 5.19 Descriptive statistics of contributing source area for first order streams of the *BLs* and the automatic drainage networks ($R'_A t$ and *CDA*) in Tabernas, El Cautivo and Rambla Honda catchments.

In the Cautivo catchment, field visits revealed a clear bias subjectivity in the delineated first order streams of the digitized *BLs*, which correspond to the choice of whether or not is a valid stream under the present scale and resolution. Moreover, the majority of the observed streams are presented with the exception to streams 5 and 6 of figure (5.17a), where their presence is highly doubtful under the mentioned criteria. Whereas, limit and extension of each segment is, with no doubt, the crucial divergence point in the comparison process. The majority of the segments should be larger than what

was registered and observed. The most evident case is the upper part of the catchment that drains directly to stream number 10 (figure 5.17a), where the stream should be extended more than twice than the present registered length. This failure in channel detection is attributed to the extreme change in relief contrast of smooth-inclined piedmont to an abrupt steep gradient valley caused by piping process. New streams should be incorporated to the digitized-*BLs* (such as the cases of sub-catchments *h1* and *h2* in figure 5.17a), while others should be bifurcated, reduced or even disappeared from the depicted terrain. It is important to underline that, under the current conditions of homogeneity and relief contrast, subjectivity is the main criteria in delineating channel limits, since in some cases change from divergent to convergent topography is vague and distinct opinion were collected between workers. So, it seems that fieldwork have provided some explanations over exterior-streams consistency, but also some uncertainties and doubts over the digitized-*BLs* as a unique mode for channels and stream validation. Hence, the above approach could be accepted as a convincing procedure if it is used as a partial assessment for stream network validation, and a complementary process should be introduced in order to achieve best equilibrium between manual and automated channel networks. While in the Rambla Honda catchment, the field visit provided scant information over the exterior limits of the digitized-*BLs*, a central problem that could be attributed to the highly smooth relief structure formed by soft rounded micascists formations, which makes it almost impossible to verify or localize the point inflection between convergent and divergent structure formations. So, in some cases, fieldwork should be planed, designed and prepared in order to achieve the best results that fit the proposed objects of the work.

Anterior results and observations underlined the highly subjective nature of the digitized-*BLs* that depends on several factors, but mainly on cartographer experience and relief contrast. Such observations are purely qualitative and give preliminary conclusions on manual stream definition. In order to reinforce such results, each exterior link was studied independently and the consistency of the A_S values for each link were approved in relation to the possible changes produced by the use of these values, for both the link as a part and the total drainage network as a whole (table 5.12 & 5.13). It seems that the final aspect of the channel network is drastically altered when using a changeable A_S value defined from each exterior link. Such change in channel network aspect and characteristics is highly unpredictable, which may shift up or down both qualitative and quantitative attributes of the equivalent automated-drainage and valley networks derived from DEMs. Results in tables 5.12 & 5.13 revealed a severe variability in the main geomorphometric indices used in the comparison process in relation to A_S values of exterior links, where changes in these values have been observed at both stream and catchment scale. As mentioned earlier, such variations imply an inconsistent increase and decrease, or even maintenance of the geomorphometric parameters, which gives new dimensions to the original characteristic length scale defined by the digitized-*BLs*. Again, these results highlight the risk of using digitized-*BLs* as a solely mode for the studying of drainage basin morphology. Such

foundations coincide with earlier works of several researchers (e.g. Mark, 1983), in which they appointed to the importance of the *BLs* but also on their risk and inconvenience. For instance, Chorley et al., (1984) mentioned that for some important geomorphometric descriptors, such as drainage density, subjectivity and differences of map and photograph scale may prevent a comparison of the results obtained by more than one investigator.

In the visual interpretation or the subjective-weighted-eye validation procedure, DEMs and orthophotographs have formed the basic unit in such inspection. DEMs were displayed for visual inspection as shaded relief models or 3D surface view, whereas orthophotographs of 0.5 m resolution were used directly because of their appropriateness on the recognition and interpretation of smooth as well as complex morphological features. The shaded relief models and 3D surface representation have been used throughout the work, not only for visual inspection but also in fieldwork and terrain classification. While, in the case of orthophotographs, both manual and automated drainage networks were superimposed directly over the corresponding landform structures (figure 5.23 & 5.24) and an exhaustive terrain inspection was realized mainly for first order stream links. Again, results confirm the previous stated conclusions over the high subjectivity of the digitized-*BLs*, the clear superiority of the $R'_A t$ approach over the *CDA* technique to depict landscape dissection, and finally the role of terrain contrasts and relief complexity on qualitative landform definition. Such conclusions emphasize two important points: First, the comparison between the *CDA* and $R'_A t$ techniques revealed the superiority of the latter approach over the former one, where all the comparison tests have shown a great enhancement in landscape depiction over the *CDA* technique and in some cases over the digitized-*BLs*, mainly in homogeneous terrain structure. Second, comparison tests, both qualitative and quantitative ones, employed in the analysis test have shown clear inconveniences that may deduce inadequacy or scantiness for depicting channel and stream limits. From one hand, the qualitative approach is highly subjective where cartographer experience and background, terrain complexity and original data scale are limiting factors. On the other hand, the quantitative approach is greatly susceptible to random errors generated in the original data or/and resulted from the algorithms used to delineate the channel networks, e.g. sink area, slope direction, contributing area, etc., (Tarboton et al., 1991).

Thus, a real data representation of fine relief forms is still needed in order to delineate the exact limits between convergent and divergent topography, as well as the validation of the model function under such landforms. Such representation should be realized to the finest scale units of terrain structure, where the dominant processes (hillslope or fluvial ones) is apparent and the limits between such functions are possible to be detected and handled by spatial analysis approaches. Real terrain representation has been achieved by means of Laser Scanner devices, which allows for a highly detailed inspection of the terrain structure at a sub-metric scale dimensions. Such approach will be handled and treated in a separated chapter, since spatial analysis for stream limits is fundamentally a

new methodology approach. Out of the debate if landscape dissection is or not scale independent, it is the goal of the new model approach to approximate such argument.

5.6. Conclusion and recommendations

The Digital Elevation Models (DEMs) have made it possible to objectively extract, calculate and store geomorphological parameters for hydrological modelling at several scales. Landscape depiction has been evolved from manual subjective methods to automated objective approaches, which, with the wide spread of DEMs, have facilitated and provided a reasonably acceptable description of river basins at different scales and resolutions. However, manual derivation of channel networks is widely limited to subjectivity of the topographer and the scale of topographic maps used to define such data. Hence, the automated techniques for channel network delineation from DEMs began to substitute manual ones because of its unlimited capacities and facilities to define terrain features all over the world. Although automated methods have provided objectively qualitative approaches based on mathematical algorithm, their efficiency under varying local and environmental conditions (e.g. tectonics, lithology, climate, vegetation, dominant runoff and sedimentation processes, etc.) is still a matter of debate between researchers. Whilst in several cases such information is scarce or even unavailable, for which DEM data is the solely available information for stream and channel network delineation.

In general, algorithms that uses DEM data only for stream delineation have demonstrated sever inconveniences and have been widely criticized in defining stream limits and channel heads, mainly in complex terrain conditions. Such approaches gave limited answers to source area depiction under varying local and environmental conditions in heterogeneous landscapes. Hence, we have proposed a new approach for stream network delineation that enhances landscape depiction and at the same time utilizes DEM data as the unique source of information. For which we proposed the following objectives: *i*) defining the optimal channel network that best describe landscape dissection; *ii*) the importance of validation-process type and form in drainage network studies; *iii*) verifying landform classification effect according to internal factors (intrinsic properties) concerning DEM capacity for terrain recognition; and, *iv*) Identifying scale variation effect over channel network extraction.

In this work, a new approach have been proposed to define an optimum threshold value (A_S) for stream network delineation based on the combination of the intrinsic properties of drainage network structure and a hierarchical stratification procedure (*HSP*). The first is based on the assumption that DEMs are self-contained structures to detect drainage networks, and that channel complexity is best reflected by its corresponding intrinsic properties. Basically, the model combines exterior and interior link lengths ratio (R_A) with length and bifurcation properties described in terms of structure regularity framework and topological random approach, in order to produce a varying ratio in

relation to changeable threshold values. The second is formed by an internal classification procedure, where the main basin units are stratified hierarchically to small sub units based on the intrinsic model. Such technique provides various critical thresholds in relation to DEM-data resolution and to the heterogeneity of the dominant landform structures. The new technique was designated as the $R'_A t$ procedure.

The above assumptions are attributed to the affirmation that the topography is a dynamic structure that reflects the processes, both temporal (e.g. erosion) and spatial (i.e. scale), that operate on it. Probably we can say that the temporal structure of the erosional processes (e.g. intensity and frequency) is reflected in the spatial structure of the topography. To reach this conclusion, the assumption of “a DEM is an adequate form to store and manage the topographic information” should be accomplished. In terms of information, a DEM is the syntax and the topography is the message. Hence, a perfect DEM should contain all the diversity without excessive redundancy. Indeed, the resolution handles such aspect: low resolution implies low diversity, which directly increases with the increasing of the resolution, but it reaches a level where the scale of the work (e.g. contour lines) do not provide further information, thereafter any kind of increasing resolution the DEM becomes redundant (del Barrio et al., 1993). Herein, the *HSP* allows adapting the best compromise between diversity (topographic heterogeneity) and redundancy (homogeneity that is achieved by the division toward excessively small catchments) for the discrete unites (sub-catchments) in the landscape.

In order to validate the $R'_A t$ approach, a new design was proposed based on a combination of direct and indirect comparison tests. The validation procedure was realized to check over and determine the algorithm capacity under varying terrain and environmental conditions. The procedure consists of a direct quantitative comparison procedure using the geomorphometric indices and extracted, first from digitized blue lines (*BLs*) and served as reference values, and second from the automatic techniques represented by the constant drop analysis (*CDA*) and the $R'_A t$ procedures. Afterward, a qualitative validation was realized based on field visit and orthophotographs visualization.

In general, results showed a clear enhancement in channel network depiction with the new approach over previous techniques. The $R'_A t$ procedure improved stream network delineation under varying landscape conditions (i.e. homogeneous vs. heterogeneous, micro- vs. macro-scale), with better approximation to natural stream networks. Both quantitative and qualitative comparisons confirmed a better performance of the $R'_A t$ technique over the *CDA* method. Moreover, the proposed procedure classifies landscape components to simplified hydrological units (i.e. basins and catchments) of reliable mono-fractal dimensions, which permits the use of a single A_S value in each hydrographic unit. Likewise, the current work and results underlined the importance, not only the algorithm used to delineate stream limits, but also the need to a complementary broad process of

comparison and validation. Since one of the major problem in the validation procedure is to answer two main questions: the first is what part of the drainage network should be validated? And the second is with what channel networks should be compare with?

In particular, the following conclusions are derived from the current work:

1) The $R'_A t$ approach has improved channel networks delineation and hence the assessment of landscape dissection, since its function depends on intrinsic properties of the drainage network, being at the same time objective and easy to implement. The comparison between the *CDA* and $R'_A t$ techniques revealed a prevalent advantage of the latter approach over the former, where all the comparison tests have shown greater enhancement in landscape depiction over the *CDA* technique and in some cases over the digitized-*BLs*, mainly in homogeneous terrain structure. This improvement is reflected qualitatively in an outstanding similarity in landscape depiction (i.e. dissection), or quantitatively in a wide resemblance between the geomorphometric attributes of the *BLs* and the $R'_A t$ procedure. The considerable improvement in stream limits detection of the $R'_A t$ over the *CDA* is attributed to two essential points: first, the $R'_A t$ technique recognizes the terrain in relation to its intrinsic properties and hence adapted well to prevailing landform structure; and, second, the *CDA* technique defines well main valley system but fails under particular conditions, mainly in small limited catchments of one or even two order system (i.e. $\Omega \leq 2$). Moreover, the above approach is less susceptible to effect of data errors than other studied approaches, where we were able to verify an acceptable drainage network system in all studied catchments. Accordingly, the fundamental basic of the model approach, i.e. the intrinsic properties, is practically detected in all channel network extracted from DEMs, which should form the basis for stream extraction in automated approaches. The procedure proposed has justification in terms of geomorphometrical network properties and evade deficiencies of slope-area or *CDA* techniques, and hence are more consistent in landscape depiction. It is important to underline that increasing or decreasing landscape dissection doesn't imply a real enhancement in channel network description, rather it should corresponds to an objective criteria that promises two important aspects: *i*) first, an optimum definition of landscape units, mainly convergent and divergent topography, at the available scale and resolution, i.e. data dimension, for the studied area; and *ii*) second, statistical or mathematical approximation of such model that promises an objective approach for subsequent validation and comparison procedures.

2) Not only landscape depiction, but also the degree of similarities between units of the terrain could be verified by the proposed approach. Since the *HSP* is based on the intrinsic properties of landscape components, classes or hydrological units of the same stability zone (*SZ*) or the same curve tendency are similar and may comprise the same prevailing features and processes. Such features are geomorphologically related either by the geometrical properties or by the topological characteristics; both features compound the R'_A model approach. Moreover, the curve relationship between R'_A and

A_S , as well as the corresponding SZ can reveal the degree of complexity in the studied catchment. From one hand, one stability zone in the curve relationship may indicate a clear dominant formation and/or process, which is usually found in idealized catchments (i.e. similar hillslope formations that drain through a simple drainage network structure). On the other hand, in homogeneous landscapes of more than one prevailing erosional process, the algorithm was able to verify the major hydrological units related to such processes, such as the case of El Cautivo and La Rambla Honda catchments.

3) The geomorphometric properties vary considerably with A_S values, and thus parameters reported without their associated A_S are meaningless and should be used in hydrological analysis with caution. In addition, the geomorphometric indices are sensitive attributes that could be formed by more than one geomorphometric parameter, i.e. compilation between geometry, topology, optimality, fractality, and landscape evolution. Hence, each geomorphometric index has variable dimensions, and their geomorphic and hydrologic importance is varied in relation to the parameters included in each index. So, in some cases the geomorphometric attributes could show contradictory results in drainage network comparison leading to erroneous conclusion. For instance, drainage density (i.e. geometric properties) may increase with A_S decreasing but at the same time magnitude (i.e. topologic properties) maintained constant, and vice versa. For so, care should be taken when using both properties in measuring similarities in stream and channel network systems. Such results underline the importance of the selected indices and the weight of each parameter in defining distinct properties in the delineated drainage network. Moreover, parameter interpretation, in a geomorphologic sense, provides no information on the appropriate A_S value to be use in stream network delineation. Although it is beyond the scope of the present work to dwell on explaining causes and types of indices change, caution must be exercised in interpreting parameter variations since susceptibility to the morphometric properties vary considerably with A_S .

4) The geomorphometrical indices should form part of any quantitative description and analysis of the channel network morphology. However, importance and significance of each attribute is to be evaluated by each scientist in relation to mode of validation and type of the test used in these processes. While in some cases few parameters may achieve significant conclusions, a wide range of descriptors is desirable in fluvial systems description, because the geomorphometric indices are specialized direct parameters that describe one structure property. Such description involves the geometric and topologic properties, as well as self organization, optimality and criticality of natural landscapes. On the other hand, this study clearly shows that there is a considerable amount of redundancy among the numerous geomorphometric parameters. Hence, a clear need is required to simplify the complex interrelationships of these parameters and identify their basic underlying dimensions. Results showed that a well design procedure analysis that includes a multivariate analysis technique (factorial or principle component analysis) could solve such a problem. Such procedure will not only reduced correlated indices, but also will provide criteria for an objective mutli-dimensional

morphological classification of the channel network systems. Moreover, this procedure will highlight the weight and the importance of these parameters in channel network definition. For instance, the fractal values (length scale properties of Hack and Melton) have shown no correlation with other parameters giving rise to unique characteristic description of stream network limits.

5) The digitized-*BLs* are an important source of information for hydrologic and geomorphologic studies, but also suffer extreme inconveniences that could lead to erroneous conclusions. These are the high subjectivity in which they depict landscape dissection in relation to several factors from which scale, relieve contrasts and cartographer experience are the most important, results that coincide with previous works of Morisawa (1957), Coates (1958), Coffman et al., (1972), Mark (1983), Chorley et al., (1984), Abrahams (1985), Tribe (1992), Montgomery and Foulfoula-Georgiou (1993), Wood (1996b), between others. So, in some case, it is therefore unlikely that a drainage network manually recognized from crenulations of contour lines will ever reflect exactly the network that exists in the field. Hence, this point should be borne in mind when considering the validation process or when using it as a solely mode for the studying of drainage basin morphology. Moreover, manual depicted drainage networks, represented by *BLs* at different scales, reflect subjective criteria for landscape dissection, whereas automated defined streams are the result of mathematical models that reproduce convergent topography in relation to measured attributes from DEMs matrix data. So, in some cases, such differences, produces noteworthy deviation between manual and automated procedures, and hence trivial values of the comparison processes. For which, validation methods that rely only on manual-depicted *BLs* are weakly efficient processes that generally give rise to un-interpretable values. Since channel networks are self-affine structures, and hence scale invariant, spatial analysis could be used to verify stream limits and hillslope structures.

6) In stream network validation, type and form of the designs and tests used are of great importance because of the various factors that control stream channel initiation and even definition. Types and amount as well as association between the geomorphometrical attributes used should be taken into account in the validation procedure. Moreover, the comparison between totally subjective structures (i.e. the digitized-*BLs*) with a completely objective formation (i.e. the automated drainage network) implies some errors or even contradictory results and conclusions between compared objects. In this case, topological properties are shifted up and down while link length properties maintained the same. For example, first order streams in the digitized-*BLs* do not maintain the same statistical distribution as automated channel networks, and where topological and geometrical properties varied considerably. So, the type and test analysis should be prepared in relation to such variations and care should be taken in the design of the validation procedures. The comparison tests, both qualitative and quantitative ones, employed in the analysis procedure have shown clear inconveniences that may deduce scantiness for depicting stream limits. From one hand, the qualitative approach is highly subjective where cartographer experience and background, terrain complexity and original data scale

are limiting factors. On the other hand, the quantitative approach is greatly susceptible to random errors generated in the original data or/and resulted from the algorithms used to delineate the channel networks, e.g. sink area, slope direction, contributing area, etc.

7) In a conceptual sense, where hillslope ends a stream channel should begin, but this is not always the case in the automated delineated channel networks. In general, mathematical models are able to verify convergent or divergent topography in relation to DEM-data dimension, as well as accuracy and uncertainties of the data matrix. However, a blurred-fuzzy zone may be defined in the delineation process, which makes definition of position and extension of stream limits a matter of not only a pure quantitative task but also a qualitative one. Hence, the comparison process is directly affected by these difficulties.

8) Once again, the delineation of channel network extent is readily derivable from DEM data, and the appropriate resolution is related to the general aims and objectives of the study. It is highly acceptable that higher DEM resolutions define better terrain complexity than lower ones, but self-affine structure and scale extend of landscapes make it useless in some cases to use high resolutions (i.e. > 5m). This is because any process is manifested in a concrete range of scales, and with high resolutions other processes may be detected. Moreover, terrain complexity and the degree of landscape diversity, redundancy and heterogeneity require the use of complex models of multiple approaches. Yet again, the objective of the work and the availability of the related parameters are highly considerable to achieve such approach.

9) The previous study highlights some evidence on the consistency of scaling values, such as Hack's (α) and Melton's (θ) laws, under varying environmental conditions. Hack's law of basin elongation revealed a more strictly concise variation with scaling up and down, giving rise to scale invariance property of streams and river network basins. On the contrary, Melton's value of stream frequency with drainage density highlighted a wide scattering in the relationship values under varying scales and resolutions, revealing a more widely range for the (θ) value stated early to conserve constant in nature with a value of 2 approximately. Indeed, such observations but in evidence the resemblance and similarity between manual and automated extracted drainage network, and hence comparison procedures should be planed and elaborated with care, since uncertainty is evident between both.

On the other hand, as any other approach, the present procedure of stream network delineation contains one or more drawbacks that may be summarized in the following:

1) The procedure itself is an iterative process of calculation, which is in some cases is time and effort consuming, mainly in broad scale size landscapes of heterogeneous landform structures defined by high resolution DEM data. For large scale landscapes, the process should include a complete verification of the terrain by using A_S value as much as possible to smooth the channel network to one

stream segment. Such process may include the using of dozens of A_S values to construct the curve tendency relationship and, hence, the definition of the *SZ*. We should observe that the rate of change in the curve relationship maybe extreme or moderate (i.e. differences between variations in the curve relationship) giving rise to different A_S values that should be used in the model construction. In the first case, any change in the A_S value may lead to a change in the *SZ* direction, while in the moderate case a high range of A_S values are needed to cause a change in the *SZ* direction. Such sensibility in the curve direction is in some cases more or less subtle to change in A_S value, and changes in the curve should be studied completely; that is, constructing a curve relationship between all possible A_S values that may generate a channel network of $\Omega \geq 2$.

2) The basic hydrological unit to verify by the model is a basin of $\Omega = 2$, which may induced some inconveniences in the comparison process. The basic algorithm relies on the definition of a ratio value between exterior and interior links in the channel network. Therefore, at minimum three segments are needed to form a ratio for the model construction, and under which the algorithm is unable to define a ratio value, which is needed to define a rational A_S value and hence no channel detection. Such inconvenience is related directly to the model structure; that is, bifurcation and length link ratios. This disadvantage is compensated by the efficiency and the capacity of the model to define homogeneous terrain structures in relation to dominant processes or/and landforms (i.e. hierarchical stratification). Such classification allows for a more precise depiction of landscape dissection by the application of the algorithm over limited homogeneous parts of the terrain structure. The procedure of *MRC* and *HSP* continue till the entire channel network is re-segmented and an optimum dissection is achieved.

3) In some cases, in small homogeneous catchments, uncertainties and errors in DEM data may affect the form of the *SZ* in the curve relationship of the R'_A model approach. It has been observed that the rate of change in the curve relationship of some catchments (e.g. small scale catchments of homogeneous landform structure with a well known prevailing erosional process) did not show the waiting tendency, and anomalous forms were observed. These odds may be attributed to the errors in the data matrix of the original DEM (i.e. vertical errors). So, uncertainties should be treated a priori to the model derivation, and hence stream network delineation. While this is true, the model may be used as a surrogate in the defining error propagation in the DEM-data matrix.

Chapter 6

SPATIAL ANALYSIS AND LANDFORM DEPICTION IN SIMULATED AND REAL LANDSCAPES

6.1. Introduction

In the previous chapters, stream delineation was revised in terms of modelling; that is, the algorithms that define stream limits in the landscape. While methods and techniques vary in their capacities to define these limits, validation of stream extents is still a pending task because of the fractality nature of landform structures. Questions of where channels begin and how to validate stream limits are still ambiguous and need to be clarified. The importance of such affirmations controls not only the capacity of the models used in defining landscape dissection but also in establishing qualitative procedures that integrate the fine scale dimension as a measure definition of landform structures. Herein, data obtained by laser scanning technology was used as an objective measure of natural data to validate landforms quantitatively using their anisotropic properties. In this approach, limits are established not only on the shape structures, but also on the prevailing processes within these formations. Thus, in chapter five stream limits were established and validated quantitatively and qualitatively based on length scale properties and visualization characteristics, respectively. In the present chapter, we will go further in stream limits definition by using the spatial structure properties of the terrain to establish a direct connection between forms and dominant processes as a potential validation approach.

In earth science, a landform or physical feature comprises a geomorphological unit, and is largely defined by its surface form and location in the landscape, as part of the terrain, and as such, is typically an element of topography. Bates and Jackson (2005) defined landform as “any physical feature of the earth’s surface having a characteristic, recognizable shape. While in relation to specific geomorphometry, landform is defined as “a terrain unit created by natural (or even artificial) processes in such a way that it may be recognized and described in terms of typical attributes where ever it may occur (Leighty, 2001). A geometrical definition of landforms, consistent with general geomorphometry, would focus on objective consideration of surface shape form only (MacMillan & Shary, 2009). Bolongaro-Crevenna et al., (2005) appointed out that the term “landform” as used by geoscientific modellers denotes a portion of the earth that unites the qualities of homogeneous and continuous relief due to the action of common geological and geomorphological processes. This concept of landform is essentially an idealized one; it follows then that the closer the study landform conforms to its definition, the greater the accuracy of the obtained model.

In general, a landform type may consist of a characteristic pattern of terrain that exhibits a defined variation in size, scale and shape of geomorphic features and occurs in a recognizable contextual position relative to adjacent geomorphic features (MacMillan & Shary, 2009). Examples of landform types include plains, mountains, hillslopes and valleys, which can be observed at multiple scales. Landform entities differ from one another in terms of characteristics, such as shape, size, orientation, relief and contextual position, dimensions (length, width and height), the statistical frequency of its principle geomorphic attributes (MacMillan & Shary, 2009), and by the physical processes that were involved in their formation (Etzelmuller & Sulebak, 2000). In earth science literature, a landform may be referred to in relation to its type, e.g. relief forms, landform patterns (Dikau et al., 1995) or by its elements, i.e. sub-component, mainly morphological ones (shape, steepness, orientation, moisture regime, relative position, etc.).

Definition and classification of landforms are greatly important since they define boundary conditions between processes operating on them. Size and shape of landform are interpreted as direct indicators of the processes understood to have produced the landform (del Barrio et al., 1993). Landform surface-shape has been widely used to infer hillslope forming processes, e.g. erosion and denudation, i.e. convexity surfaces with divergence processes, or geomorphic processes (e.g. alluvial), i.e. concave surfaces with convergence processes. Efforts in landform definition have been evolved with the use of DEMs, mainly automated procedures. Quantitative models have replaced qualitative approaches, and several procedures have been proposed. Procedures on quantitative description, i.e. derivation, of landform units can be carried out using various approaches, including classification of morphometric parameters, filter techniques, cluster analysis and multivariate statistics (Dikau et al., 1995; Sulebak et al., 1997; Dehn et al., 2001; Adediran et al., 2004; Bolongaro-Crevenna et al., 2005). Such description may involve the extraction of basic components of relief, e.g. elevation, slope, curvature, or the compound spatial derivatives of these descriptors, e.g. the compound topographic index (Beven & Kirkby, 1979), length slope factor (Moore et al., 1991), and stream power index (Moore et al., 1993). The extraction of ridge and channel patterns and subsequent catchment delimitation can be accomplished with pattern recognition, geometrical, and topological approaches (Brändli, 1996). In general, in most manual systems of landform classification, expert interprets available information about the land surface to partition it into spatial entities that separate and describe different landform classes. Herein, source data for manual classification may include stereo-photographs (Hengl & Rossiter, 2003), topographic maps (Hamond, 1965; Dikau, 1989), and more recently by digitizing on-screen 2D and 3D backdrops that use various combinations of derivatives of DEMs or digital imagery.

In the last few years the applications of GIS technologies have provided geomorphological research with a series of new possibilities for quantitative relief analysis (Dikau, 1989). Particular emphasis has been put on the geomorphometrical point attributes approach (Evans, 1980) and the

extraction of drainage basins variables from DEMs (e.g. Band, 1986). One of the main attributes related to landform classification is valley streams and hillslope formations. Automatic delineations of channel networks and stream extension have been widely treated in the previous chapter. Emphasis has been highlighted on methods and algorithm used in such classification and wide revision of literature was reviewed. In this direction, one of the key issues is channel network validation procedures. It is widely acceptable that comparing automated objective procedures of stream delineation with subjective one is highly doubtful and may lead to erroneous conclusions (Chorley et al., 1984), mainly with the study of drainage basin morphology. Indeed, validation of automatically derived catchment data sets is often performed through a comparison of the size of a sample of the derived catchments with the size as given in independent sources (Graham et al., 1999). Vogt et al., (2003) indicated that such comparison can give a first indication, but remains of limited value, especially with regard to river positions. In addition to field measures and photo-interpretation, the digitized-BLs have been widely used for stream network validation (e.g. Mark, 1983; Tarboton et al., 1989, 1991; Chorowicz et al., 1992; Tribe, 1992; Dietrich et al., 1993; Döll & Bernhard, 2002; Vogt et al., 2003; Heine et al., 2004). Scale, data of source map, cartographer experience and subjectivity between others are the main problems for BLs to be used as reference network for validation of automatic generated stream networks. Such problems may leads to some stream omissions or/and missing a substantial proportion of first-, second-, or even third-order streams (Coates, 1958; Montgomery & Foulfoula-Georgiou, 1993).

Aerial images or photo-interpretation and Satellite images have been considerably used to delineate fluvial drainage networks (e.g. Ichoku et al., 1996a; Gilvear & Bryant, 2003; Lejot et al., 2007), and to validate their extents (Chorowicz et al., 1992), or even to evaluate changes in their planform (Gurnell, 1997). From one hand, network detection from aerial photographs obviates some of the limits of the *BLs*, but on the other hand, there are some problems, related to the obscuration and misleading effect of canopy (Coates, 1958), the scale of image, the presence of distortions and shadows due to the difference in elevation when the terrain is rugged, and the subjectivity of the photo-interpreter (Gandolfi & Bischetti, 1997). Field work seems to be of great importance for channel network definition, but time, human resources and scale largely limit the practical applicability of this approach. Furthermore, even in high detailed terrain contrasts, subjectivity background and experience of the operator may play a significant role.

So, as far as the criteria used to compare the networks are concerned, visual judgment or qualitative comparison procedures introduce unnecessary element of subjectivity that should be avoided. Quantitative geomorphology provides a set of descriptors that can be used for this purpose, although some of them were found to be extremely sensitive to marginal modifications of the network geometry (Snell & Sivapalan, 1994) and the initial A_s value used for channel network extraction (e.g. Da Ros & Borga, 1997). But the problem of the real drainage network representation still persists,

since neither *BLs* nor field visit and visual interpretation have provided a strict quantitative mode for convergent/divergent hillslope depiction. Adding the scaling invariant and fractal characteristic properties of channel networks (e.g. De Bartolo et al., 2004) to the previous limitations, a more realistic criterion for channel network comparison and detection is still needed.

Geostatistical methods have been widely used in landforms detection and delineation (e.g. Wood, 1996a; Burrough & McDonnell, 1998). In this direction, the central tool for geostatistics is the (semi)variogram, which expresses quantitatively and succinctly spatially correlated variation (Oliver et al., 1989a; Burrough, 2001). The semivariograms have occupied a central part in the geospatial analysis approaches and its uses have been extended to include hydrological, topographical and geomorphological applications (e.g. Oliver & Webster, 1986; Meisel & Turner, 1998; Wu et al., 2000; Drăguț & Blaschke, 2006). Indeed, geostatistics provides as much as possible of enhanced and attractive tools for interpolation from point data and estimates of error bounds, estimates of error propagation and uncertainty ranges for spatial and temporal modelling, and data reduction and generalization (Burrough, 2001). So, it is widely observed that geostatistics is a powerful tool for spatial-variation detection of environmental patterns. Definition and measurements of spatial patterns in geomorphological studies is the first step in understanding dominant processes over terrain features. Grayson and Blöschl (2000) highlighted over the importance of probably defining spatial organization where it exists, and the importance of a careful interpretation and, hence, thoughtful representation of spatial characteristics.

Geostatistics has been widely used in elucidating spatial variations in several earth sciences and environmental applications, e.g. remote sensing (Atkinson et al., 1994; Chappell, 1998; Chappell et al., 2001), soil property variation and erosion (McBratney & Webster, 1983; Oliver, 1987; Bourennane et al., 1996; Chappell & Oliver, 2000), rainfall (e.g. Chappell & Agnew, 2001) and digital elevation modelling (Leenaers et al., 1990; Odeh et al., 1994; Chappell, 1996). While in fluvial geomorphology, geostatistics is new and deeper investigation is still needed. In the context of fluvial systems, geostatistical applications range from stochastic simulation of buried channels (Deutsch & Wang, 1996), detailed investigations of stage dependent flow structure (Legleiter et al., 2007), to spatial prediction of river channel topography (Legleiter & Kyriakidis, 2008). Geostatistics is much more than a method of interpolating data; rather it is a suite of tools for detailed structural spatial analysis (Olea, 1975; Chappell et al., 1996; Oliver et al., 2000). At its simplest, geostatistics is based on the derivation of a spatial model of the variation in sampled data (variogram) (Oliver et al., 1989b). Parameterizing the experimental variogram and evaluating its change over time has provided considerable information on processes and their controlling factors (e.g. Stein, 1998; Sun et al., 2003).

Deterministic single patterns, such as landform features, could be directly observed and represented by structural models such as DEMs. While such models are fraught of errors of sampling, measurement and interpolation, pattern representation is highly related to the scale, dimension and

accuracy of the data structure. The spatial variability or heterogeneity representation of landform structure is to be determined in relation to whether the dominant processes (convergent or divergent) are scale invariant or scale dependent. For example, surface flow representation at landscape scale could be achieved by available DEMs of ≥ 1 m grid dimension. While for detailed-surface micro-topography, such as rills or even micro-streams, highly detailed DEMs are needed. On the other hand, accuracy measurements are highly dependent on the measurement techniques, e.g. topographic maps, stereoscopic, etc. Channel networks and hillslope formations are the basic units to identify in real landscape structure. Streams and valley systems are the most complex patterns to identify, mainly in digital data structures. As shown in the previous chapter, stream delineation from DEMs is possible but is subjected to a set of limitation and uncertainties, such as type and capacity of the models used to define channel threshold area, scale and resolution of the initial data, DEMs errors and uncertainties, heterogeneity of the studied area, flow direction algorithm (D8 or D ∞). Such limitations underline the importance of a real validation procedure that permits the description of the stream limits under real landscape representation. In view of that, two essential procedures have been performed: *i*) a real landscape was defined by laser scanning techniques, which permits the detection of the finest landform element in the terrain; and, *ii*) a geostatistical analysis has been realized on the real data in order to obtain the best approximation for spatial-patterns discretization. Such approach allows for the precise identification of landscape features in relation to the dominant process at that scale. Properties of landform features and buried structures as well as river network systems can be quite properly treated as random variables and that their variation can be modelled using the semivariogram of regionalized variable theory (Oliver & Webster, 1986).

DEMs are the final result of a complex data matrix that describe not only direct information of surface and landform structure but also embedded information related to such features (e.g. surface curvature, flow accumulation, slope and aspect, etc.). Because of their susceptibility to error propagation at all level of treatment, real data captured directly from the terrain surface may comprises a good approximation to least biased measures for a real representation of landscape features. Hence, the surface real data captured directly from laser scanners will be applied in order to avoid earlier mentioned limitations in DEMs-matrix building. Herein, real terrain representation will be designated as digital land surface models (DLSMs).

Light Detection and Ranging (LiDAR) is a powerful remote sensing tool of remarkable impact on environmental science sector. Its noteworthy success is widely related to its ability to enable the creation of 3D landscape models and their surface features from different platforms, either ground-based or airborne devices (Devereux & Amable, 2009). In particular, LiDAR sensors are characterized by a huge ability to generate very accurate data at high spatial resolution (e.g. > 1 mm in the case of ground-based platforms). In principle, the main measurements of LiDAR data is the visual surface or digital surface model (DSM) showing the heights of all surface objects, from which the above DLSM

concept has been inferred. DLSDMs are natural data structures characterized by their extreme accuracy (i.e. < 1mm), mainly when features are captured directly with minimum filtering or interpolating procedures. Principle derivative of such structures may include DEMs, DTMs, models of terrain morphology, vegetation structure and dynamics, etc. Hence, highly accurate measurements are available for any surface structures that may include 2D and 3D representations of vary high complex terrain surfaces. Herein, the approach to data acquisition for any given purpose should be driven by the size and complexity of the subject scene or object, and what level of measurement detail and representivity is required over the area in question (Hetherington, 2009). For which, the nature of the scene or object and main goals and requirement of the study will thus define what level of measurements and accuracy can be classed as good quality.

The purpose of this experiment is, therefore, to investigate the exact geometrical limits and borders between landform elements using the semivariogram techniques. Such experiment allows characterizing stochastic properties of hillslope and stream features, obtaining reliable measures of border limits between landform elements, and validating some of the techniques used to define the optimum threshold area for stream-limits delineation (e.g. *CDA* and the $R'_A t$ techniques). An associated purpose is to describe the practical application of the semivariogram for representing spatial geomorphic variation quantitatively, in order to represent physical landform variations and limits, underlying special emphasis on hillslope and stream valley formations and the transitional zone between them (i.e. channel initiation zone). To achieve these objectives, high-detailed topography was captured by *TLS* to produce a DLSDM and DEM of high accuracy and resolutions.

6.2. Background

6.2.1. Introduction

Reliable measures of landform-structure geometry are important for the precise adaptation of hydrological response to real one. Extracting accurate stream network formation from DEMs tends to be challenging in both homogeneous as well as heterogeneous landscapes where fluvial systems are open dissipative process-response system and complex structure properties of highly related inter-relationships. Uniformity, complexity, optimality and Self-organized criticality, between others, are prevailing concepts in fluvial systems (e.g. Philips, 1998). Fractality and scale-invariance properties govern drainage network structures and river basin evolution, leading to complexity and variability of fluvial systems in space and time (Miall, 1996). All such characteristics make channel network definition a hardly complicated task of unlimited changeable interactions between such attributes. Furthermore, the type of DEMs used may encompass a considerable impact on the extraction of watershed hydrological features. For example, Creed et al. (2003) compared the ability to automatically extract wetland features from independent DEM data sources that were based on publicly available contour vectors, aerial photography and airborne LiDAR. Results differed markedly

between DEM types suggesting that both the resolution of the raw data and the method of DEM extraction acquisition and generation have a marked impact on the ability to extract features of hydrological significance (Hopkinson et al., 2009). So, and in order to avoid such restrictions, the landforms of the studied landscape were registered and defined using laser scanning techniques at a highly detailed resolution (i.e. approximately 6 cm). Benefits of laser scanning techniques over traditional methods for landform definition, and hence drainage networks derivation, are that it can be used to generate DEMs at resolution approaching sub-centimetre point spacing. Therefore, it can offer the potential to identify zero- (Tsukamoto et al., 1982) and first- (Strahler, 1957) order drainage features (e.g. hillslope depressions and alpine gullies) that control runoff generation and flow routing processes in headwater environments (Hopkinson et al., 2009). Finally, the detailed-relief extracted information was subjected to a thorough and exhaustive spatial analysis of semivariograms in two forms, to the raw data in form of Digital Land Surface Model (*DLSM*) and to the interpolated data in form of DEM.

6.2.2. The Spatial analysis and semivariogram approach

Geostatistics is a theoretically grounded collection of tools for spatial data analysis that is increasingly applied in diverse areas of environmental science (Goovaerts, 1997). In geostatistics the variogram is a central domain, in which it is essential for optimal estimation and interpolation by kriging (Burrough & McDonnell, 1998), as well as summarizes the spatial variance in the region of interest provided by the intrinsic hypothesis holds (Oliver et al., 1989a). Olea (1977) appointed out that the semivariogram is the key to the theory of the regionalized variable (Matheron, 1963).

Variograms or semivariograms, which is as intended comprises half value of the original variogram, were developed for the analysis of spatially dependent random variables, as opposed to the correlogram (i.e. autocorrelation plot), which originated with time series analysis (Robert & Richards, 1988). In addition to be the main instrument of the theory of regionalized variables, it quantifies and describes the magnitude, scale and intensity, general form of the spatial variation, provides basis for an optimum interpolation procedures, and assists applications to optimize sampling planes (e.g. Oliver et al., 1989b; Vendrusculo et al., 2004). In this direction, for instance, Richards (1976) used spatial series analysis to measure riffle wavelength, bed-profile oscillation, and to analyze the effect of riffle-pool sequences on channel morphometry. Robert and Richards (1988) confirmed the usefulness of the semivariograms in modelling sand ripples created by water flows of varied flows intensity. Likewise, Robert (1988) used the semivariograms to define micro-scale bed relief in gravel bed stream. Oliver and Webster (1986) promoted the use of the semivariogram techniques in place of the correlogram for the modelling and analysis of spatially-dependent geomorphic variables. Such assertion is based on the affirmation that the terrain is formed by an unbounded variation (i.e. properties of soil, landforms and buried structures can be quite properly treated as random variables) and hence can be modelled using the semivariogram of regionalized variable theory (Matheron, 1963). Moffat et al., (1986) used sample

variograms and kriging procedures to reveal local structures, mainly river valley position, on the Chiltern area. Fisher (1998) used the semivariograms in order to study error distribution in DEMs. Madej (1999) used spatial autocorrelation to quantify changes in morphological diversity and spatial structure in thalweg profiles in gravel-bed rivers. Chappell et al., (2003) studied channel network features modification after flood regimes using semivariograms and concluded that both channel morphology (i.e. spatial structure) and dynamic behaviour are well explained by geostatistics. Lark and Webster (2006) repeated Moffat et al., results and introduces some modifications to avoid trend and residual effects in the collected sample data, in order to enhance surface description. Merwade et al., (2006) uses directional semivariograms to infer the best kriging approach to interpolate river channel bathymetry. On the other hand, Curran (1988) has provided a broad functional introduction on employment of semivariograms in remote sensing, such as selection of a sampling unit (spatial resolution) and sample numbers for ground data collection (sampling scheme).

Basically, the semivariance of a random function is defined as half the variance of the increment $\{Z(x_i)-Z(x_i+h)\}$, where $Z(x_i)$ is the random variable of interest of the value (x_i) and h is the lag or distance, defined as

$$\gamma(h) = 1/2 E\{Z(x_i) - Z(x_i + h)\}^2 \quad (6.1)$$

that is, half of the mathematical expectation (E) of the squared of the difference between the values of the measured points, separated by the distance lag h . So, the equation for the estimation of the semivariance (γ) is given by:

$$\gamma(h) = \frac{1}{2N(h)} \sum_{i=1}^{N(h)} [Z(x_i) - Z(x_i + h)]^2 \quad (6.2)$$

where $N(h)$ is the number of pairs of measured values $Z(x_i)$ and $Z(x_i+h)$ separated by the vector lag h ; $Z(x_i)$ and $Z(x_i+h)$ are values of observations of the regionalized variable sampled at the points x_i and x_i+h .

A plot of $\gamma(h)$ against h is known as the experimental variogram (figure 6.1), which is the first step towards a quantitative description of the regionalized variation. Helpful information for interpolation, optimizing sampling and determining spatial patterns is all well described by experimental variograms (e.g. Isaaks & Srivastava, 1989; Burrough & McDonnell, 1998; Webster & Oliver; 2001).

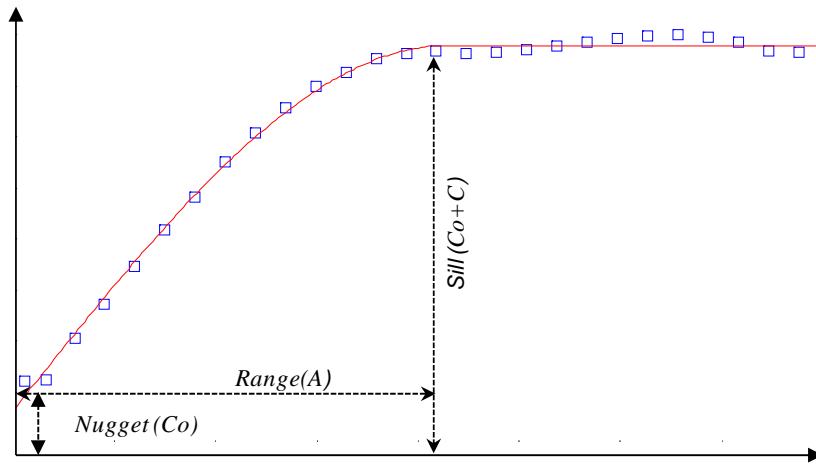


Figure 6.1 Experimental variogram with basic characteristics

Figure 6.1 reveals three basic and essential parameters in a semivariogram, which includes the followings:

- i) **Nugget variance (C_0):** when a semivariogram tends to zero ($\gamma(h) = 0$) a C_0 value is observed, but in practice the extrapolated semivariogram usually intercepts the ordinate at a positive value, that is C_0 . Such value reveals the discontinuity of the phenomenon for values smaller than the least distance between samples, which can arise from measurement error, discrete random variation and physically dependent variation occurring over distances much less than the sampling interval (Oliver & Webster, 1986; Vendrusculo et al., 2004).
- ii) **Range (A):** the separation distance over which spatial dependence is apparent, or within which the sample is spatially correlated and beyond which there is no longer spatial dependence. This is sometimes called Effective Range in order to distinguish range (A) from a model's range parameter (A_0). The important part of the variogram because it describes how inter-site differences are spatially dependent. Likewise, in interpolation processes, it gives an answer to the question posed in weighted movement average interpolation about how large the window should be (Burrough & McDonnell, 1998).
- iii) **Sill (C_0+C):** the model asymptote or the value of $\gamma(h)$ which corresponds to the range A . it implies that at (beyond) these values of the lag h there is no spatial dependence between the data points because all estimates of variances of differences will be invariant with sample separation distance.

A semivariogram may be, practically, uniform for all directions of the vector lag h and hence denotes the presence of isotropic effect within the spatial variability (all the directional sample variogram will be the same), or conversely exercise a directional effect and hence characterize an anisotropic distribution. Hence, anisotropy or directional variograms imply changes in the range or sill as the direction changes. In surface analysis, mainly terrain structure, the anisotropy may imply changes in range with direction, while the sill remains constant. This type of anisotropy is known as “*geometric (affine) anisotropy*”. Whereas, if the sill changes with direction while the range remains

constant the case is known as “zonal anisotropy”. In practice, it is rarely to find a pure zonal or geometric anisotropy; it is more common to find a mixture of the both anisotropies together (Isaaks & Srivastava, 1989). Such anisotropy can be taken into account by a simple linear transformation of the rectangular coordinates. It is perhaps best envisaged for a process with a spherical variogram in which the range, instead of being a constant, describes an ellipse in the plan of the lag (Webster & Oliver, 2000). This is shown in figure (6.2), where A is the maximum diameter of the ellipse (i.e. the range in the direction of greatest continuity, or least change with separation distance), and B is the minimum diameter, perpendicular to the first, and is the range in the direction of the least continuity (greatest change with separation distance). The angle φ is the direction in which the continuity is greatest.

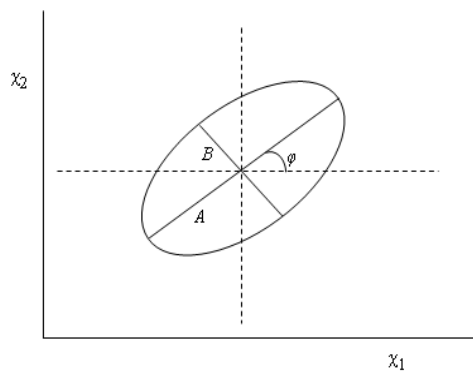


Figure 6.2 A representation of a geometric anisotropy in which the ellipse describes the range of a spherical variogram in two dimensions. The diameter A is the maximum range of the model, B is the minimum range, φ is the direction of the maximum range (after Webster & Oliver, 2001).

Several scientists (e.g. Cressie, 1985; McBratney & Webster, 1986; Robert & Richards, 1988; Oliver et al., 1989a) highlighted two main difficulties in using semivariograms. The first is related to the complexity of determining confidence levels analytically, and the second concerns the fitting of models to sample semivariograms. In general, there are a number of standard mathematical functions (i.e. models) that can be fitted to sample a semivariogram (Oliver & Webster, 1986), either single or in combination (McBratney & Webster, 1986). Moreover, this task may be performed either mechanically if the semivariogram is simply to be used as a tool for kriging or intentionally if the data under study are used to represent the natural world or to describe a specific phenomenon (Oliver & Webster, 1986). Models that best represents the configuration of the curve of the experimental semivariogram can be fall into two main groups: bounded (i.e. second-order stationary variation) and unbounded (i.e. non-stationary process variation) models. In the former, known also as transitive variograms, the curve line approaches the sill asymptotically at a finite lag. Such models may indicate the occurrence of transition structures, e.g. structures that are independent of each other but within which the values are highly correlated. While unbounded models (or non-transitive) have no finite a priori variance, where the curve increases indefinitely and the intrinsic hypothesis only hold (Oliver et al., 1989a); that is, have no sill within the area sample. These are models with no sill, which correspond to the possibility of infinite dispersion of the phenomenon (Vendrusculo et al., 2004).

So, the next step is to adjust a mathematical model that best represents the configuration of the curve of the experimental semivariogram. The simplest models for unbounded variation are power functions, which can be defined under isotropic variation by

$$\gamma(h) = wh^a \quad \text{for } 0 < a < 2 \quad (6.3)$$

where w is a linear parameter describing the intensity of the spatial variation, and $h = |h|$ is the lag distance.

The powerful parameter a determines the shape of the curve variogram. Where $a = 1$ indicates linear form, $a < 1$ the curve is convex upward, and conversely $a > 1$ the curve is concave upward. Such model approaches have been linked with the theory of fractals (Burrough, 1981, 1983; Burrough & McDonnell, 1998).

On the other hand, variations with the bounded models are mainly represented by three basic functions: spherical, exponential and gaussian models (figure 6.3). For the isotropic type variance, the models are typically represented by:

1. The spherical function is very common in earth sciences, and mathematically is given by

$$\gamma(h) = Co + C [1.5(h / A) - 0.5(h / A)^3] \quad \text{for } h \leq A \quad (6.4)$$

$$\gamma(h) = Co + C \quad \text{for } h \leq A \quad (6.5)$$

2. The exponential model rises solely from the origin and never quite reaches its sill, and mathematically is given by

$$\gamma(h) = Co + C[1 - \exp(-3h / A)] \quad (6.6)$$

3. The Gaussian or hyperbolic isotropic model is similar to the exponential model but assumes a gradual rise for the Co , and often used to model extremely continuous phenomena. It is equation is given by

$$\gamma(h) = C[1 - \exp(-3h^2/A^2)] \quad (6.7)$$

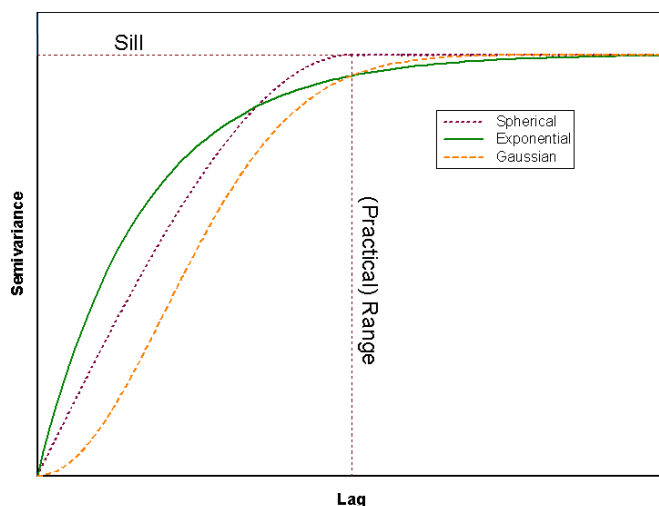


Figure 6.3 The three most commonly used transition models (spherical, exponential, and Gaussian) shown here with the same sill and range.

As mentioned earlier, anisotropic variogram models are similar to those for isotropic variograms but include directional information in the range parameter. This is verified in each model

fit by a linear transformation of the co-ordinates of the major and minor axis of variation (i.e. A , B and ϕ presented in figure 6.2) (Webster & Oliver, 2001). The formula for such transformation is

$$\Omega(\theta) = \{A^2 \cos^2(\theta - \phi) + B^2 \sin^2(\theta - \phi)\}^{1/2} \quad (6.8)$$

where Ω defines the anisotropy, ϕ is the direction in which the continuity is greatest, and ϕ is the direction of the lag, A is the distance parameter in the direction of maximum range, B is the distance parameter in the direction of minimum range (figure 6.2) in the bounded models above (Equations 6.5, 6.6 and 6.7).

The proportion $A:B$ is the anisotropic ratio, a measure that have been used widely for structure definition and variation in environmental science (e.g. Chappell et al., 2003; Legleiter et al., 2007; Zaluski & Moe, 2008). Throughout the present work, general anisotropic parameters and ratio will be used systematically for structure landform definition.

The importance of the model function used to fit the analyzed data in spatial analysis is determinant in later resulting estimates. Isaaks and Srivastava (1989) appointed out that “*the need for a particular model comes from the fact that we may need a variogram value for some distance or direction for which we do not have a sample variogram*”. The choice of a particular variogram model directly implies a belief in a certain type of spatial continuity; that is, the pattern of the spatial continuity (ordinary kriging). Thus, the parameters of these models will give insight into the nature of the variation, as well as its scale and magnitude (Robert & Richards, 1988). In general, a Gaussian-model variogram indicates a smoothly varying pattern, such as often occurs with elevation data. Whereas a spherical variogram model has a clear transition point, which implies one pattern is dominant. An exponential variogram model may suggest that the pattern of variation shows a gradual transition over a spread of ranges or that several patterns interfere (Burrough & McDonnell, 1998).

In sample datasets where a random process is a combination of several independent processes, one nested within another and acting at different characteristic spatial scale (Oliver, 2001), a nested variogram is needed to detect variations within these processes (Miessch, 1975). In this case, there would be both long- and short-range variation present. Thus the variogram of the regionalized variable $Z(x)$ can itself be a nested combination of two or more, Say S , individual variograms:

$$\gamma(h) = \gamma^1(h) + \gamma^2(h) + \dots + \gamma^S(h) \quad (6.9)$$

where the superscripts refer to the separate variograms.

If we assume that the processes are uncorrelated then we can represent this by the sum of S basic variograms (designated as reconnaissance variogram):

$$\gamma(h) = \sum_{k=1}^S b^k g^k(h) \quad (6.10)$$

where g^k is the k th basic variogram function, and b^k is a coefficient that measures the relative combination of the variances of the g^k to the sum.

Herein, the linear model of regionalization represents the real world in which factors such as relief, geology, tree-throw, fauna, and artificial divisions into field and farms, operate on their own characteristic spatial scale(s), and each with its particular form and parameters, b^k , for $k = 1, 2, \dots, S$ (Oliver, 2001).

6.2.3. Laser Scanning techniques

The last 20 years have promised new revolutionary techniques for real data acquisition, collection and measurements, mainly fieldwork and surveying processes. Scientists (e.g. McCaffrey et al., 2005; Buckley et al., 2008) appointed out to a revolutionary enhancement in technologies used to collect, process, analyze and model quantitative digital data. From the early use of radar and satellite imagery, passing through photogrammetry and laser scanning techniques, depiction of terrain, both processes and features, is accessible at different scale levels and resolutions. For instance, satellite images and digital photogrammetry allows very large samples to be generated and provides efficient means for deriving DEMs (e.g. Stojic et al., 1998; Toutin & Gray, 2000; Hirano et al., 2003;), while at macro-scales synthetic aperture radar (*SAR*) suggests potential (e.g. Wimmer et al., 2000; Niedermeier et al., 2005). Lately, laser scanning technique introduces significant development for meso-, and micro-scale studies for almost all science disciplines.

Light detection and ranging (LiDAR), also known as laser scanning, is a technique that has come to the forefront of surveying in the last 10 years. This laser-based measurement system allows for the rapid acquisition of detailed point data describing a terrain surface, from both aerial and/or terrestrial platforms (Buckley et al., 2008). Whilst in the last 2 decades, the aerial laser scanning has matured sufficiently that is considered nowadays one of the principle tools used in many environmental science applications, e.g. DTMs generation, surface and landform detection, topographic variables, channel network extraction, national mapping, erosion monitoring, flood modelling and control, and storm water quality treatment (Kraus & Pfeifer, 1998; Wehr & Lohr 1999; Mason et al., 2007; Brzank et al., 2008; Liu & Wang, 2008; Hopkinson et al., 2009; Vianello et al., 2009). Now, however, with the development curve levelling off, terrestrial LiDAR is opening up into many fields in the same way that photogrammetry it did before (Buckley et al., 2008). The terrestrial platforms or Terrestrial Laser Scanners (*TLSs*) have recently received a considerable attention due to the number of measurement benefits including three-dimensional (*3D*), fast and dense data capture, operation without the mandatory use of targets, and permanent visual record (Tsakiri et al., 2006). Indeed, in the last ten years terrestrial scanning has become a wide spread technology in several field survey applications because of the enhanced development in both devices and software used to deal and control such complex data. Traditionally, photogrammetry has been the most commonly used approach to collect *3D* elevation data (Carbonneau et al., 2003), in order to be applied for landform representation and detecting morphological changes in the micro-, meso-, and macro-scales (Chandler, 1999). With *TLS* several disadvantages of photogrammetric images (e.g. need for external control,

necessity of line-of-sight from two positions, reliance on indirect elevation measurement) have been defeated by the registering scans acquired from multiple scanner positions (Carbonneau et al., 2003).

The recent developments of *TLS* open a wide variety of applications and therefore the adaptation of laser scanners is increasing in most discipline applications (Fröhlich & Mettenleiter, 2004). *TLS* was originally developed for structural engineering applications, but is now increasingly being applied in environmental research due to its ability to collect remotely high precision and high-resolution data (Hodge et al., 2009). Geology, geomorphology, soil and engineering industries are between others that have got great benefits of laser scanning techniques. Example applications include detection, modelling and monitoring landslide features (Bitelli et al., 2004; Bauer et al., 2005; Biasion et al., 2005; Heritage & Hetherington, 2007; Oppikofer et al., 2008; Dunning et al., 2009) deformation monitoring (Tsakiri et al., 2006; Abellán et al., 2009), geological sedimentary outcrops (Bellian et al., 2005; Buckley et al., 2008), geological engineering (Slob & Hack, 2004), mapping rock mass fractures (Slob et al., 2005), cliff-retreat monitoring (Rosser et al., 2005), measuring volcanic forms (Pesci et al., 2007), measuring slope movement and rockfalls (Abellán et al., 2006), and fluvial morphology (Heritage & Hetherington, 2007; Brzank et al., 2008). For example, laser scanning techniques can produce high resolution DEMs with sufficient precision for microtopographic analysis (Aguilar et al., 2009), to extract and monitor local gully morphologic information (Betts & DeRose, 1999; James et al., 2007), volumetric assessments of geomorphic change (Thoma et al., 2005), morphological changes in barrier islands (White & Wang, 2003), flood modelling (Mason, et al., 2007; Schumann et al., 2008), mapping detention basins (Liu & Wang, 2008), geomorphological mapping (Jones et al., 2007), detection of channel bed morphology (Cavalli et al., 2008) modelling stream networks (Murphy et al., 2008), and to improve base map information such as slope and drainage network density (Vianello et al., 2009). Finally, Dunning et al., (2009) used *TLS* to both quantify the geometry and volume, and inform qualitative interpretations such as landslide processes, for which they concluded that such data has the potential to quantify and inform what primarily conceptual models of valley development area.

Laser scanners consist normally of a range measurement system (i.e. laser diode) in combination with a deflection tool for the laser beam, directing the laser beam into the direction to be measured. The deflection system points the laser beam into the direction to be measured, the laser beam is emitted and the reflected laser light is detected. The time that light needs to travel from the laser diode to the object surface and return is very precisely measured. Knowing the speed of light, the distance from the scanner to the object and the azimuth and angle of the beam, the position of each point where the beam is reflected can be calculated. The process yields a digital dataset, which is essentially a dense “point cloud”, where each point is represented by a coordinate *xyz* (relatively to the laser scanner device) in *3D* space. The final resulting data from the *TLS* is a raw *3D* point cloud constructed from individual point measurements. Geometric elements can be fitted during the post-processing and analysis, and the planar or spatial model of the object can therefore be generated. In

many situations, multiple scans are required from different locations to cover the whole object. So, the first task associated with building 3D models from laser scanner data is to transform the local *xyz* coordinates from each *TLS* station into a common reference frame (Al-Manasir & Fraser 2006), a process commonly known as “point cloud registration”. If only the object itself is of interest, it is sufficient to determine the relative orientation of the scans. If the object also has to be placed in a superior coordinate system, absolute orientation becomes necessary, too. If the superior coordinate system is earth fixed this is also called georeferencing (Pfeifer & Briese, 2007b). Because of the great number of points, the visualization of the raw point clouds enables basic variation, displacement and deformation tendencies to be defined (Slob et al., 2005; Abellán et al., 2009). When compared to traditional methods, point clouds provide a significantly higher level of true geometric completeness and detail of the site virtually eliminating costly site re-visits to gather more detail or collect omitted features (Slob & Hack, 2004).

Classification of terrestrial laser scanner is difficult to some extent, since there is no one universal laser scanner for all conceivable applications. Different principles can be used to measure the distance between sensor system and target. Fröhlich and Mettenleiter (2004) verify two forms for laser scanners classification, either based on the measurement principle (general) or based on the technical specifications achieved (specific). Herein, the former will be highlighted in the coming paragraph, while the latter is slightly mentioned since it is most appropriate for particular-, and/or industrial-use specifications. The distance measurement system correlates to both the range and the resulting accuracy of the system. In this direction, three different technologies for laser range finding measurements are used with laser scanners:

- Time-of-flight (TOF) principle: The pulsed method measures the time it takes a pulse or short burst of laser energy to "fly" from its source to a surface and return to a detector at the source instrument, hence the term time-of-flight. The distance to the measured surface is computed by multiplying the time it takes for the whole flight of each pulse by the speed of light and then dividing by two to account for two flights (to the measured surface and back to the instrument). This technique allows unambiguous measurements of distances up to several hundred of meters. The advantage of long ranges implies reasonable accuracy.
- Phase-based measurement principles: The phase-based method measures a shift in a continuously emitted and returned phase (sine wave) of the laser. The instrument computes a distance to the measured surface based on the magnitude of the phase shift. The range is restricted to one hundred meters. This system offers a measurement rate of 500 kHz (i.e. 500000 per sec.) and more precision and accuracy are in the order of ± 1 mm.
- Triangulation methods: For the sake of completeness, several close range laser scanners with ranges up to few meters are available. But, they are more for the use in industrial applications and reverse engineering (online monitoring in construction processes). The used distance measurement

principle is optical triangulation. In this case, range is not determined directly, but via angle measurements. Accuracies down to some micrometers can be achieved with this technology. In addition, classifications by technical properties are more useful as they indicate the possibilities and the performance of the individual system.

In general, the differences in terrestrial scanners between TOF and phase-shift measurements scanners are therefore: higher range for TOF and higher measurement speed and better precision for phase-based laser scanners (Pfeifer & Briese, 2007b). Accordingly, each application discipline is best described by one technique or another, where, for instance, for topographic survey work TOF based scanners are most common, while phase-measurements technique are best adapted in engineering and heritage applications. Recently, advances in both measurements have allowed for the application in all science disciplines. Accuracy measurements depend on several elements that include reflectivity of the scanned object and the incidence angle. The accuracy of distance measurements depends mainly on the intensity of the reflected laser light and therefore directly on the reflectivity of the object surface. The reflectivity depends on the angle of incidence, and surface properties. At present, most laser scanner sensors provide an additional measurement pertaining to the strength (intensity) of the returned laser beam (e.g. ScanStation 2 of Leica), which is variable according to the material surface measured and the optical wavelength of the laser used (Buckley et al., 2008).

The selection of the appropriate laser technology should be chosen in relation to the main purpose of the work. In this direction, scale, resolution and the structure complexity (brightness and material type) are the most important. Studies on landform structures in general and channel networks in particular could be realized at different scales and resolutions, whilst these structures are scale invariant with the absent of the geological control, and vice versa (e.g. Rodriguez-Iturbe & Rinaldo, 1997; Schoorl et al., 2000). It is highly acceptable that first order streams of channel networks are shifted up or down in relation to the source map scale (i.e. topographic maps) or DEM resolution (i.e. grid dimensions). For example, first order streams defined at 1:50000 topographic maps could be shifted up to second or even third order streams (Chorley et al., 1984; Mark, 1983). Whereas, DEMs capture the topography and landform structure in function of the unit dimension, that is its resolution. Main valleys and channels are best determined by mid- to coarse- resolutions (e.g. >10m), whereas channel heads are too sparse to be captured at such dimensions, which often are only decimetres in size at their tips (Dietrich et al., 1993). Moreover, channel heads are related to dominant hydrological processes; that is, the position where hillslopes end and channels begin is the transition between upslope diffusive processes and the downslope incisive fluvial processes (Montgomery & Dietrich, 1988, 1989; Dietrich & Dunes, 1993). Hence, medium to long range accuracy techniques could be used in main valleys and channels (up to 1000 m range and 0.01 m accuracy), whereas close-range scanners with a much higher measurement precision for fingertips or point deflection between

dominant process seems to be the best approach. Of course, the latter is highly constrained by a much smaller area than the former since laser range is somewhat short (< 100 m).

It is clear that the terrestrial laser scanning opens up the opportunities to investigate morphology and processes, as well as structures and forms in the fluvial systems. Data acquisition and details may be obtained at different scales and resolutions ranging from fine structures of grain-scale ($10^{-3} \times \text{m}^2$) through hillslope-scale ($10^3 \times \text{m}^2$) (figure 6.4), where the operator bias and interpolation error are significantly reduced (Heritage & Hetherington, 2007). The main advantage of laser scanning can be observed in measurements that cannot be executed by traditional methods or would make the evaluation unaffordable. The point density of the laser-scanned point cloud enables the modelling of the studied relief and hence the definition and evaluation of its structure.

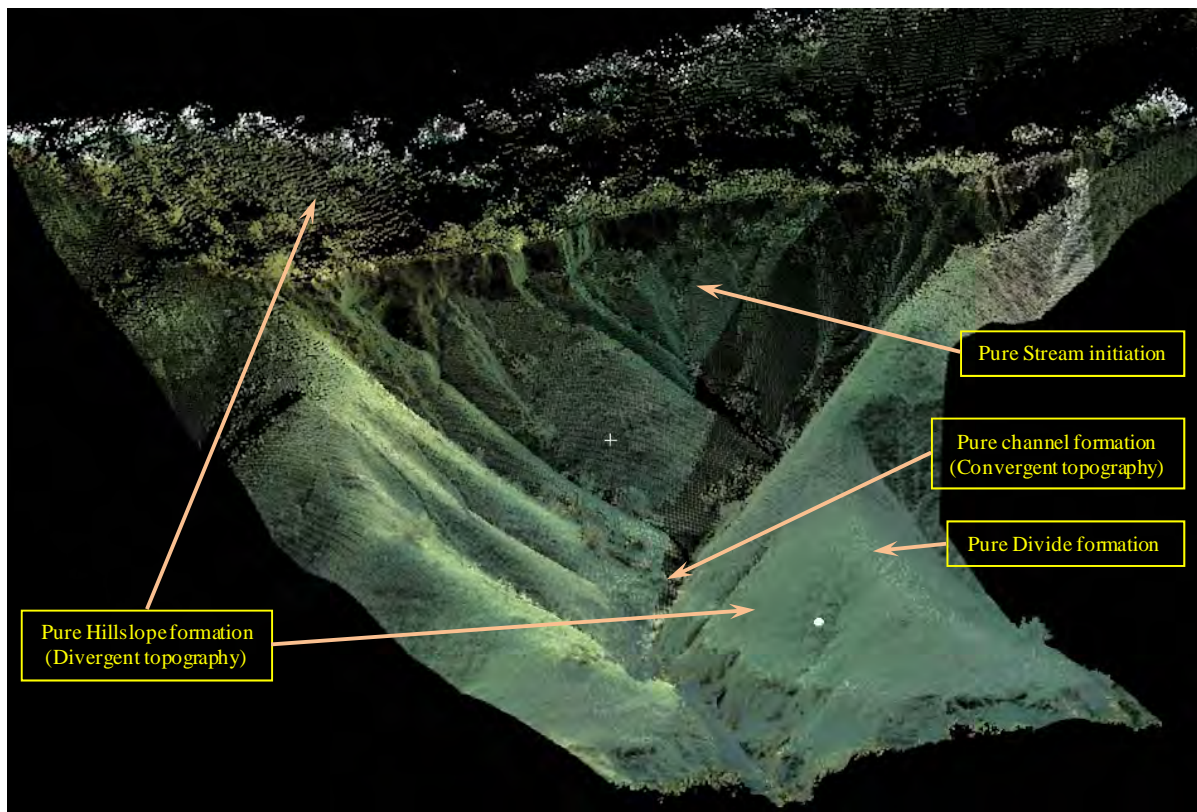


Figure 6.4 A “point cloud” representing a hydrographic unit basin with perfect examples of different landform structure formations captured at 0.5 mm initial grid dimension.

6.2.4. Workflow for *TLS* data

The *TLS* used in this research is a “*Leica ScanStation 2*”, the technical specifications of the scanner are presented in table 6.1. Original and final datasets were handled and treated in combination of different software, each corresponds to the stage and needs of the work, e.g. Cyclone (Leica Geosystems) for data acquisition and filtering, ARCGIS (from ESRI) for DEM generation, TauDEM (Tarboton & Ames, 2001) for stream network delineation, and *GS+* (Gamma Design Software) and “*R*” (<http://cran.r-project.org>) for the geostatistical analysis. In order to provide a complete insight on procedures and methods used to obtain the final dataset, a systematic workflow was developed to

acquire and process *TLS* data. This workflow has three main stages: field data collection; data processing; and model creation.

6.2.4.1. Field data collection

In order to obtain a complete topographical description of landform structure, *TLS* datasets of different points of view were acquired. The result of a single scan is a dense 3D data (termed as “point cloud”) of the subject surface, where each point in the dataset with *xyz* value relative to the scanner position. The raw data (scans) require several stages of treatment that include pre-, in- and post-processing (e.g. filtering, removing unwanted objects, etc.). The individual scans are then combined using special procedures to reduce the alignment error between scans. Finally, the 3D model structure is georeferenced in relation to a real georeference system using referenced points in the studied site (GPS or known vertices). As laser scanning is somewhat a newly technique in geomorphologic and hydrologic studies, data acquisition and treatment should be realized with special care and attention. A number of important factors must be considered before a survey scanning is carried out, in order to fulfil the aims of the study and the reasons for using such technologies.

Data collection should be realized in order to satisfy all necessary elements that permits a comprehensive and realistic conclusion over stream and channel limits in the landscape. Such elements should, from one hand, satisfy the main objectives and aims of the work and, on the other hand, permit the least possible treatment of obtained raw data (e.g. filtering, correction, elimination of vegetation, etc.), since part of the analysis will be realized over the unhandled data. It should be taken in mind that conditions and requirements for data acquisition from a *TLS* need to be adapted to the laser scan device. As acquisition and measurement of surveyed data is realized from a fixed platform (usually tripod instrument), scanning process requires the following. First, a clear line of sight from the instrument to the target surface is needed. A scan position should be chosen to allow for the maximum coverage of the study site, within the maximum range and angular field of view of the instrument (Buckley et al., 2008). Moreover, manufacture specification should be taken in mind in the scanning processes (e.g. surface material reflectivity, precision and accuracy, range of the beam, atmospheric conditions, etc.). Second is the orientation of the scanner devise in relation to the scanned surface so that it permits to attain the maximum exposure parts. Such requirement is achieved when the foreground details (e.g. vegetation, gravels, rocks, etc.) don't interfere with the line of sight of the scanner; otherwise, more scans will be needed and more errors will be induced, as well as more complex filtering processes are required. It is important to underline that usually several scans are needed for one surface, depending on the outcrop and the complexity of the relief surface, the more complex the terrain is the more the surface details are obscured as the measurement become more oblique to normal, and hence more than one scan is needed. Generally, in field experiment and under complex topographic conditions, it is usual to capture more than one scan from different positions in order to fulfil for hidden parts and to ensure shadows kept to minimum.

6.2.4.2. Data processing

Data processing includes the initial condition or parameters applied on the scanned object, combination of point clouds or “data registration”, and filtering and cleaning of the 3D surface object.

Specifications	Measures
1) General:	
1.1) Instrument type:	Pulsed, dual-axis compensated, very-high speed laser scanner, with survey-grade accuracy, range, and field-of-view
2) System performance:	
2.1 Accuracy of single measurement:	
2.1.1 Position	6mm
2.1.2 Distance	4mm
2.1.3 Angle (horizontal/vertical)	60 μ rad/60 μ rad
2.2 Modelled surface precision/noise:	2 mm
2.3 Target acquisition:	2 mm std. deviation
2.4 Dual-axis compensator:	Resolution 1'', dynamic range +/- 5'
2.5 Data integrity monitoring	Periodic self-check during operation and start-up
3) Laser Scanning System	
3.1 Type:	Pulsed; proprietary microchip
3.2 Colour:	Green
3.3 Laser Class:	3R (IEC 60825-1)
3.4 Range:	300 m @ 90%; 134 m @ 18% albedo
3.5 Scan rate:	
3.5.1 maximum instantaneous rate:	up to 50,000 points/sec
3.5.2 average:	dependent on specific scan density and field-of-view
4) Scan Resolution	
4.1 Spot size:	From 0 - 50m:4mm (FWHH-based); 6mm (Gaussian-based)
4.2 Selectability:	Independently, fully selectable vertical and horizontal point-to-point measurement spacing
4.3 Point spacing:	i) Fully selectable horizontal and vertical; ii) <1 mm minimum spacing; and iii) single point dwell capability
4.4 Sample density	<1 mm maximum, through full range

Table 6.1 Specifications and system performance characteristics of Leica ScanStation 2 Laser System.

1. *Data resolution:*

TLSs applications may differ considerably in relation to its accuracy and precision, and hence spatial resolution is an important aspect of any laser scanning survey. Spatial resolution governs the level of identifiable detail within a scanned point cloud and it is particularly important for recording of

features of fine details (Lichti & Jamatsho, 2006). But, capability of new advanced scanners to identify a feature may be beyond the required by the application. Hence, there is a prior need to set and adjust the resolution of the scanning system to a sensible level, defined by the scale of the features to be measured. For *TLSs*, the resolution of the grid spacing in the cloud point is user defined where it can be decoupled into range and angular components. The former is the ability of a rangefinder to resolve two objects on the same line of sight and is governed by pulse length for a pulsed system (Wehr & Lohr, 1999), which is a distance unit representing the actual grid spacing of the point cloud. The latter is the ability to resolve two objects on adjacent sight lines, and is a function of spatial sampling interval and the laser beamwidth (Lichti & Jamtsho, 2006); that is, the angular units representing the separation between the point measurements. Since the spatial resolution, or separation between the grid points, varies with distance, range resolution becomes so complicated to determine while angular resolution remained constant. In laser scanning, emphasis on resolution is often placed on the finest possible sampling interval (i.e. 1 mm in the Leica ScanStation 2), which is often much smaller than the laser beamwidth (i.e. 4 mm in the Leica ScanStation 2). Moreover, beamwidth divergence is not constant and varies with distance of the scanned surface and the angle incidence of the reflected beam. Under these conditions, the laser beam spot size is a limiting factor leading to correlated sampling, and hence giving the appearance of higher resolution. The effect of this is that if a resolution is chosen that is too high, the fine details may become blurred as the laser beamwidth overlaps between point readings (Buckley et al., 2008).

2. Data registration

Also could be referred to as relative orientation, in which registration is putting more emphasis on the active role of the point cloud rather than in the process itself (Brenner et al., 2008), while relative orientation refers to the relation between device coordinate system (Pfeifer & Briese, 2007a). In many situations, multiple scans are required from different locations to cover the whole object. So, for building a complete *3D* model of different scanning data, transformation of the local *xyz* coordinates from each scan into a common reference frame should be realized. Registration is commonly performed by the Iterative Closest Point (*ICP*) algorithm, Least Squares *3D* Surface Matching (*LS3D*), or the homologous explicit tie features. These features could be natural or artificial in forms of points, lines or even surfaces. Natural tie elements can be identified with lower accuracy in the intensity images by visual inspection or automatic procedures, while artificial ties elements, and due to the high intensity value, can be found automatically (Pfeifer & Briese, 2007a & b). Such process can be realized directly by overlapping geometry of the point cloud itself (Brenner et al., 2008) or with the aid of photogrammetry (Al-Manasir & Fraser, 2006). *ICP* algorithm has been early suggested by Besl and McKay (1992), in which the procedure does not require homologous points, rather the orientation differences between sets of scans is iteratively reduced by matching a number of points on one surface with the closest points on the other surface and minimizing the sum of squares of

the spatial offset distances. Finally, the *LS3D* method (Gruen & Akca, 2005) is based on a minimization of the sum of squares of the Euclidean distance between the different datasets. The *LS3D* method is of little use in current *TLS* commercial devices because it requires a large overlap between the point clouds.

3. Data filtering

Since scanning a site capture everything in the selected field-of-view, the acquiesced raw data, in the form of a point cloud, registered or not, requires farther filtering due to various factors, mainly the interactions of the scanner precision and the complex geometry of the studied surface. The scanner precision is customer-defined for some parameters and fabricant-defined for others (table 6.1). The resolution of the captured-structure determines the degree of complexity in these structures. Herein, two important factors affect the degree of noise in the point could, these are edge-effect and the complexity of the studied surface.

The edge effect is an inevitable phenomenon since the laser spot cannot be focused to point size (Boehler & Marbs, 2003). Even at maximum resolutions and well focus, the laser beam on the object-structure will have a certain size. When the spot hit an object edge, only part of it will be reflected there, and the rest may be reflected from the adjacent surface, a different surface behind the edge, or not at all (i.e. when no further object is present within the possible range of the scanner). Almost, all scanner types produce a variety of wrong points (i.e. errors) in the vicinity of the edges. The range error may vary from just a fraction of millimetre to values larger than the initial spot size. *3D* structures of complex relief need more than one scan to construct a complete formation of the related object. Each scan includes the point cloud, which describes the object, and the corresponding errors and noises related to edge effect and the accuracy of the instrument. So, scans when registered, noise or error points will increases in relation to earlier-mentioned factors.

Usually, in order to identify and remove unwanted observation from the point cloud, two procedures could be applied, manual and automatic filtering. The manual procedure consists of looking for error points manually through comparing the scanned structure with possible reference definition for the object, a photo for instance, and tries to remove or clean the points that do not pertain to the object-structure. While automated filters include a group of tools and models that is developed and /or incorporated in the software and are used generally in the preparation of the point cloud. Herein, the process of removing “noise” was carried out exclusively in the Cyclone software modules, either manual or automated. Such algorithms include local filters (e.g. distance from a point, density, trim edges, etc.) or regional ones (e.g. “region grow”).

6.2.4.3. Model creation

The final stage of the workflow is to convert the point clouds into the required end product; that is generating a model from the point cloud. This model can be applied for different purposes. The

simplest is the point cloud itself, e.g. distances, angles, or even stochastic modelling (Pfeifer & Briese, 2007 b). Whilst complex models include generating a surface from the point cloud, which may include Digital Surface Models (DSMs) and Digital Terrain Models (DTMs) or DEMs variables. For the generated point clouds, in addition to its precision, one of the special advantages is the possibility to generate DEMs without need to complex interpolation procedures that usually introduce considerable errors in the generated matrix data (Desmet, 1997; Heritage & Hetherington, 2007). Direct rasterization is possible if the number and spatial distances between points in the point cloud are, to some extent, homogeneous. In particular, The DEM surface quality is a function of the precision and accuracy of the data points used to fit the surface, the point density and the point distribution relative to the morphology (Lane, 1998). Based on the extraction procedure of the digital data and the final aims, the DSM will define a digital terrain model (DTM) or a digital elevation model (DEM). For the generation of DTM's a separation between ground points and non ground points is required. Whereas, for DEM's generation TINs, interpolation procedures or gridding based approaches are required. The scanning process depicts all available objects in the sight of the laser light, which in one way or another permit the detection of the smallest details in the scanned surface that may even include particle-suspended dust in the air. So, considerable processing is necessary to extract the DTM or DEM from the DSM. Due to their measurement principle, laser scanners support an entirely digital processing. Therefore, laser scanning techniques is the appropriate choice for a largely automatic DEM generation (Lohr, 1998). Even without post-processing the calculated raster DEMs can form a basic dataset for a GIS used to perform monitoring and/or simulation tasks.

Advantages in LiDAR technology for DEM or DTM generation over conventional methods (e.g. photogrammetrically or from topographic maps) are boundless, mainly the improvements in resolution and accuracy standpoints (Hodgson et al., 2003; Schiess & Krogstad, 2003). LiDAR-DEMs with sufficient precision and resolution have been used in microtopographic analysis (Aguilar et al., 2009), to extract and monitor local gully morphologic information (Betts & DeRose, 1999; James et al., 2007), volumetric assessments of geomorphic change (Thoma et al., 2005), morphological changes in barrier islands (White & Wang, 2003), flood modelling (Mason, et al., 2007; Schumann et al., 2008), mapping detention basins (Liu & Wang, 2008), geomorphological mapping (Jones et al., 2007), modelling stream networks (Murphy et al., 2008), and to improve base map information such as slope and drainage density (Vianello et al., 2009). Moreover, LIDAR-DEMs have great potential to improve hydrologic modelling (MacMillan et al., 2003). The conventional DEM surface is typically interpolated from the initial elevation point grid to a grid of higher resolution (e.g. from 50 m to 10 m grid spacing) for improved resolution of flow accumulation. However, the DEM surface still reflects the topographic surface defined by the initial points. In contrast, with LiDAR, the initial point elevations are typically acquired at high resolution (e.g. 1-2 m), requiring relatively little interpolation. The original DEM grid can be further enhanced by overlaying and 'burning' hydrographic details such

as streams, lakes, and shorelines into this grid, to ensure that the modelled flow is forced to conform to already mapped surface water features, i.e. a hydrologically corrected DEM (Saunders & Maidment, 1996; Simley, 2004). So, LiDAR technology is competing with or replacing these data sources (Wehr & Lohr, 1999).

6.3. Aims and objectives

In the present work, we will try to describe a geostatistical framework that is specifically intended for landform definition, mainly stream channels and hillslope formations, and thus allows geomorphic concepts to be incorporated into the terrain modelling process. The proposed approach has three key objectives.

- The first is to fully take advantage of the geometric information contained in the multi-spatial *TLS* point clouds acquired over a given area in order to maximize measurement sensitivity to semivariograms.
- The second is to verify the capacity of spatial analysis procedure in detecting landform elements. These two objectives will lead to a third objective, which is the essence of the current work; that is, to look for changes in structure relief forms that allow for channel-initiation detection.

In order to achieve these aims the following procedures have been realized:

- i)* a geostatistical analysis of dimensional and directional semivariograms was performed to show what information can be derived from models of spatial variation and to describe the spatial structure of stream channels and hillslope formations;
- ii)* definition of the exact spatial patterns that controls landform elements (convergent and divergent topography), first within the formation itself and second between the elements; and finally,
- iii)* verifying scale effect (i.e. scaling-up and down) over the topographic formations and limits between them.

6.4. Data acquisition and site location

6.4.1. Introduction to site location

With the selection of this particular site, we try to validate not only landform components but also relation between processes and structures, which allows for an indirect validation for models used in stream network delineation. The selected study area is located within the Cautivo catchment area (figure 6.5). A small mini-basin was verified and selected with area size of 956.02 m². The survey site is a badlands system that comprises clear and perfect examples of varying types of incised channels and hillslope formations. In addition, we tried to look for a site with active geomorphological processes (runoff and erosion), for future monitoring of stream network evolution. Evidence of erosion is observed in the catchment, with gullying at stream heads and clear sheet erosion on hillslopes. Rills are also observed en the lower left part of the catchment indicating smooth channel initiation

structures. The channel network system of the site is perfectly dendritic that penetrates and cuts the hillslopes in two forms. In the first one, the stream links vanish gradually throughout the hillslope with no clear edge formation (e.g. upper parts of the catchment). The second case consists of channels and streams with clear bounds and limits that vanish abruptly (e.g. lateral parts of the catchment) leading to clear separation bounds between the terrain features.

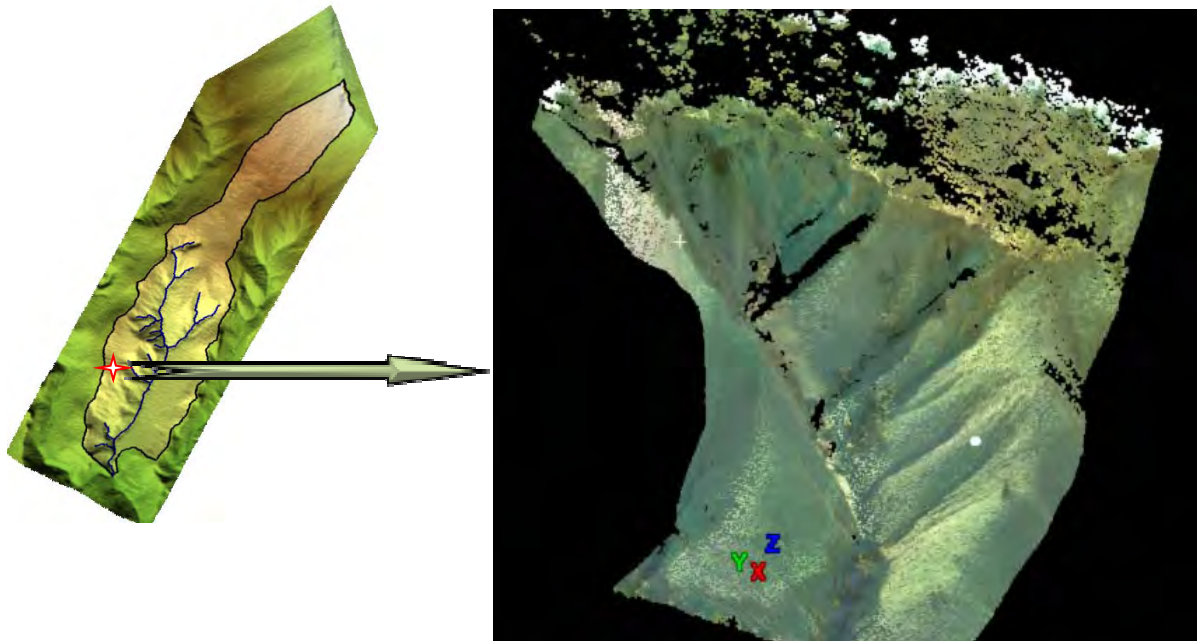


Figure 6.5 Location of the study area and its position within El Cautivo field site

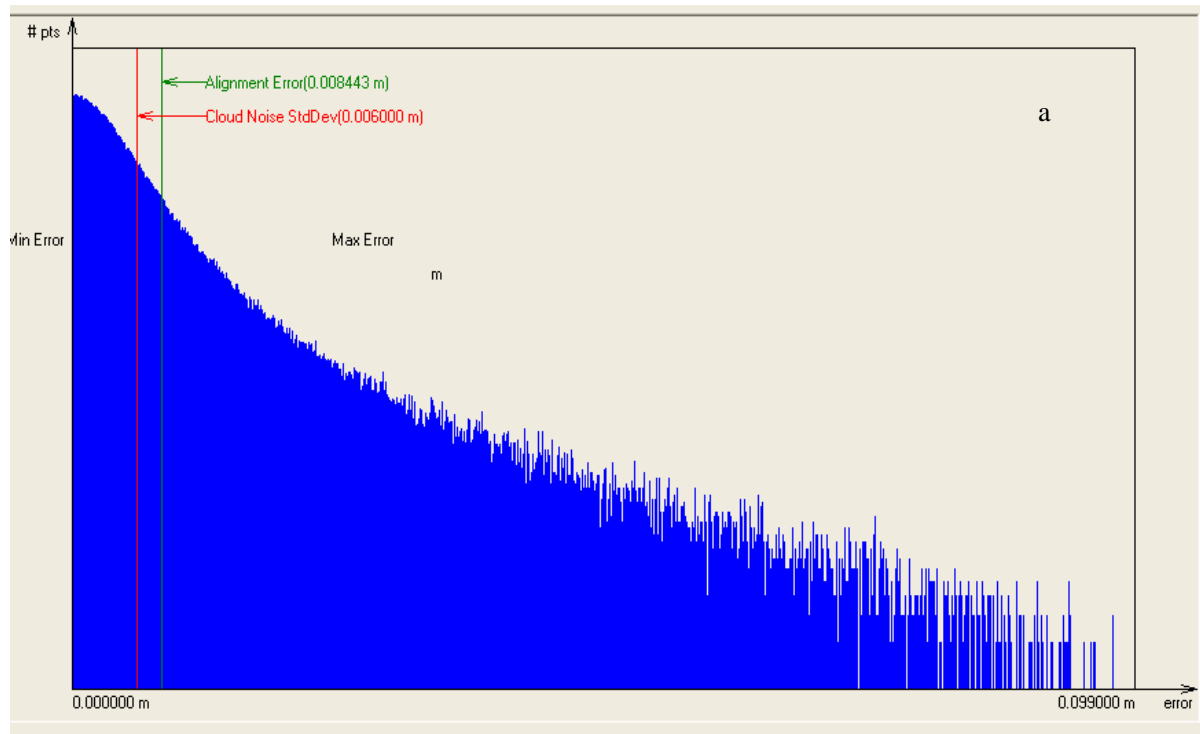
6.4.2. Data acquisition and preparation

A minimum of two stations were necessary to cover the basin area of the studied location. These scans were verified in order to minimize shadow effect and ensure a complete scanning cover of the terrain, since channels and stream incite the presence of a lot of shaded areas, mainly in highly dissected terrains, such as the Cautivo area. Laser scanning is relatively a simple way of obtaining a fine-detailed and high resolution digital dataset to describe smallest terrain formations. Of course, several factors should be considered before a LiDAR survey is carried out, so that the aims of the study are fulfilled, and so that the reason for using this technology is justified. Morphological considerations, in particular the minimum scale of interest and surface complexity are primary factors in selecting the point separation within a *TLS* scan scene (Dunning et al., 2009). So, grid spacing or the spatial resolution must be chosen to meet the established aims and define the optimum limits between features in the studied terrain. Features to be measured are purely hillslope formation, incised rills, small streams, and formation between both. In this direction, the 5 mm grid spacing has been established in the laser scanner in order to achieve the best approximation between the finest relief forms and unnecessary information (gravels and vegetation), as well as to avoid overlapping in point cloud.

Two point clouds of two scans have been carried out, each of which contain at least more than 1,200,000 points. The first step of the processing was the integrating of all point clouds into a common

coordinate system (i.e. registration). In the present work, the registration process was carried out by the Cyclone software using a 3D bundle-adjustment algorithm that uses a least-squares approach to define a transformation which minimizes the errors of the points in the final coordinate system (Hodge et al., 2009). Such process could be realized either by artificial known targets (i.e. ties) observed in each scan, or by the overlapping geometry of the point cloud of each scans when target data are not available or missing, using the *ICP* algorithm. Herein, both transformations procedures were used in order to obtain the highest accuracy registration, as well to reduce errors and uncertainties to the minimum. The implementation of the process includes the use of 5 artificial fixed targets. The adjustment procedure calculates a transformation for each point cloud such that the errors of the survey targets in the final point cloud are at minimum. The registration of the scanned surfaces revealed a varying error between 1-6 mm in all target objects (figure 6.6). All ties with error higher than 5 mm were rejected and the point cloud was registered again. The point cloud was then limited to the area of interest. It is highly observed that the density of the point cloud is dissimilar in the observed landform structures, where high densities are observed in perpendicular facet surfaces to the device and low ones in shade-complex structures (figure 6.7).

After the registration process, a smooth filtering step was realized (i.e. removing noise of all point clouds). As mentioned earlier, scanners, in general, blankets the entire selected site, for which undesired objects are also collected (e.g. vegetation, people, etc.). Since the selected site is formed by almost completely naked soil mantled surface, a smooth filtering procedure has been realized, mainly to remove the dispersed annuals that may be encountered in the site. Manual selection and intensity of reflectance were the unique filters applied to the available point cloud. The final product of the entire scanning, registration and filtering processes was a DLSM with spacing of approximately 1-6 cm between points in the 3D space. Later on, a DEM was extracted from this data using the Inverse Distance Weighted (*IDW*) approach. The reason for using *IDW* in this work is attributed to its simplicity and efficiency (Merwade et al., 2006; Villatoro et al., 2008). Characterization of data uncertainty obtained by such devices at such high resolution is somewhat difficult, since validation requires comparison between the derived surface and a second, more accurate surface (Brasington et al., 2003). While acquisition of this second surface is difficult or even is not possible, hence validation is usually based on quantifying model uncertainty through diagnostic surface visualization or field ground truthing (Wechsler, 2000; Heritage & Hetherington, 2005; Heritage et al., 2009). In the present study, the original data was obtained at a fixed initial resolution of 5mm giving rise in some parts of the terrain (mainly vertical and directly facing the *TLS*) to an ordered grid of approximately fixed dimensions of about 9-10 mm, which was used as the second surface to compare with. Although we consider such step is of least important since the final error is directly related to the errors produced through the capturing of data and processing process.



Status: VALID Registration

Mean Absolute Error:
for Enabled Constraints = 0.2345 cm
for Disabled Constraints = 12.1098 cm

b

Database name : Carcavas

ScanWorlds:

ScanWorld 1

ScanWorld 2 (Leveled)

Constraints

Name	ScanWorld	ScanWorld	Type	On/Off	Weight	Error	Error Vector	Horz	Vert
TargetID: T1	ScanWorld 1	ScanWorld 2	(Leveled) Coincident: Vertex-Vertex	Off	1.0000	12.1098 cm	(-0.7246, 2.6445, -11.7953) cm	2.7420 cm	-11.7953 cm
TargetID: T3	ScanWorld 1	ScanWorld 2	(Leveled) Coincident: Vertex-Vertex	On	1.0000	0.2014 cm	(-0.1678, 0.0981, -0.0525) cm	0.1944 cm	-0.0525 cm
TargetID: T2	ScanWorld 1	ScanWorld 2	(Leveled) Coincident: Vertex-Vertex	On	1.0000	0.2435 cm	(0.1622, -0.1487, 0.1045) cm	0.2200 cm	0.1045 cm
Cloud/Mesh 1	ScanWorld 1	ScanWorld 2	(Leveled) Cloud: Cloud/Mesh-Cloud/Mesh	On	1.0000	0.2586 cm	aligned [0.8443 cm]		
Cloud/Mesh 1	[ScanWorld 1 : ScanWorld 2		(Leveled)]						

Objective Function

Value: 0.254664 sq cm

Iterations: 51

Overlap Point Count: 915433

Overlap Error Statistics

RMS: 0.844269 cm

AVG: 0.501627 cm

MIN: 9.66443e-006 cm

MAX: 9.23956 cm

Overlap Center: (-2040.1009, 419.0608, 193.8819) cm

Error after global registration: 0.035191 sq cm

Translation: (271.4079, -1524.8355, -3.9328) cm

Rotation: (-0.0001, -0.0001, 1.0000):-71.214 deg

ScanWorld Transformations:

ScanWorld 1

translation: (0.0000, 0.0000, 0.0000) cm

rotation: (0.0000, 1.0000, 0.0000):0.000 deg

ScanWorld 2 (Leveled)

translation: (271.9501, -1524.5781, -4.0196) cm

rotation: (-0.0000, -0.0000, -1.0000):71.210 deg

Figure 6.6 Data registration for the 2 point clouds of the studied area; a) error histogram for cloud constraints in the registered point clouds; and, b) related statistical values obtained from the registration process.

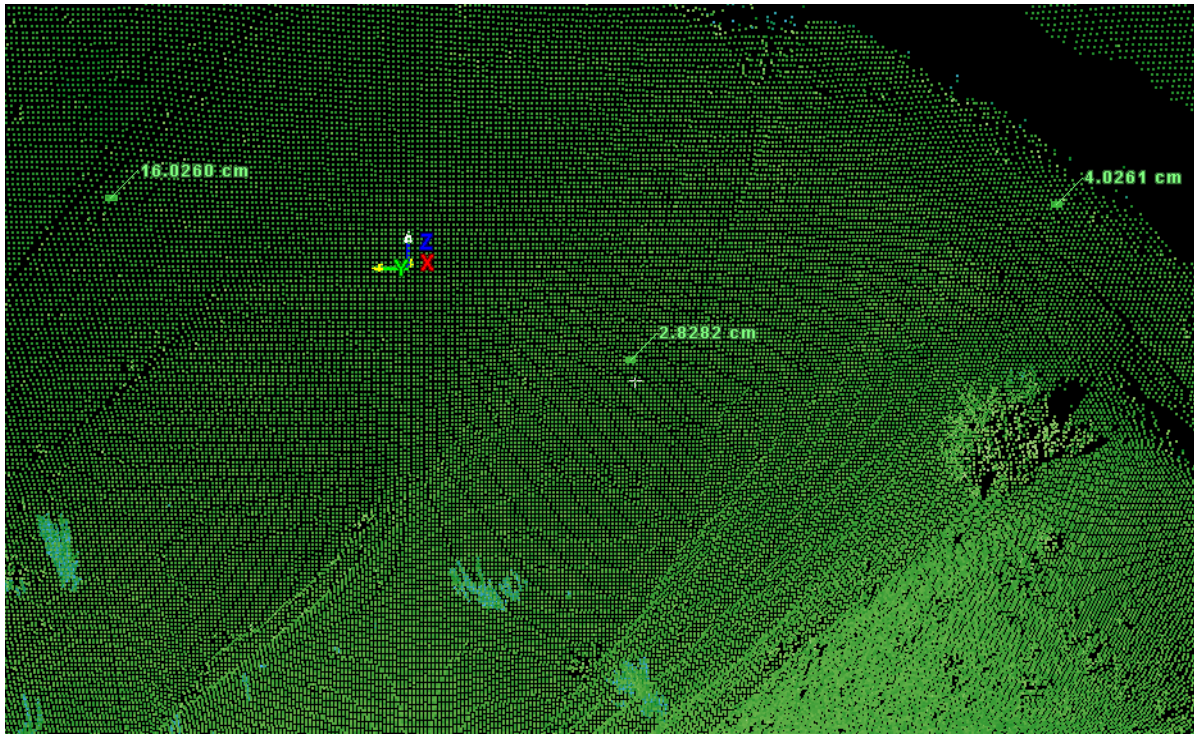


Figure 6.7 Dissimilarity in point cloud density in relation to the direction and orientation of the landform and the laser scanner position. In addition to variation between points, vegetation cover is highly detected from the data composition.

6.5. Methodology

Early assumptions of regionalized variable theory (Matheron, 1963) allowed for several conclusions on embodied predictions for trend surface analysis. The most interesting is the intrinsic hypothesis where the mean and the variance of the differences for most spatial variation in any attribute are both stationary. Such variance can be defined by a function of semivariograms (Eq. 6.1 & 6.2). Oliver et al., (1989a) appointed out that where the intrinsic hypothesis holds, the semivariogram contains all the information about the spatial variation of the attribute of interest. Furthermore, it enables the semi-variances (i.e. $\gamma(h)$) to be estimated from a sample of a single realization of the underlying process. Sill, nugget, range and the model applied to fit spatial data distribution can provide important information on the type and the structure of the studied phenomenon (e.g. landform attributes, soil type and content, mining, etc.) as well as dominant processes within these formations (Oliver et al., 1999b; Madej, 1999). Moreover, if it is possible to distinguish more than one variogram component in the same dataset, scale effect could be underlined by sub-variograms of its own set of parameters (Issaks & Srivastava, 1989). For which, the early idea of this work has been evolved in order to use such knowledge in landform detection under varying scale of high resolution, i.e. captured data of laser scanning technique (*LST*).

In general, researchers (e.g. Burrough et al., 2001; Pennock, 2003; MacMillan & Shary, 2009) used to classify landform elements to discrete units based on direct segmentation of individual hillslopes into more or less homogenous classes along a catena sequence (i.e. toposequence) from

ridge to valley following concepts outlined by Ruhe and walker (1968). In contrary to other modes of landform classification that rely upon morphological measures, the current work adapts a geospatial approach of semivariograms to define spatial structure variations within relief formations that allows for landform delineation based on prevailing processes within these elements. Such notion will be used to define, and hence validates landform elements in general, and stream networks and their source areas in particular, which is the main aim of the current chapter.

Landform elements or terrain components (i.e. elements and components are synonyms that will be used alternatively throughout the coming paragraphs) are usually extracted or defined from Digital Elevation Models (DEMs), i.e. primary inputs for morphometric analysis (Pike et al., 2009). Errors and uncertainties in such structures are of great concerns since it determine the quality of the procedure analysis and the capacity of the defined structures to simulate natural ones. Florinsky (1998) underlines that quality of land-surface objects and parameters are widely related to several factors, e.g. land-surface roughness, the sampling density, data resolution (vertical and horizontal), and DEM gridding algorithm. These are highly optimized by the *LSTs*. Advantages of such approaches are countless, but the main convenience consists of its capacity to verify the highest details of landform elements needed to achieve the main objective for the current work. This is to define landform types and elements using the geospatial analysis of terrain formations under real and simulated landscape conditions. The former is represented by the Digital Land Surface Models (DLSMs) whereas the latter is denoted by the DEMs. Herein, the *TLS* has been used to capture the topography at 5 mm initial spatial resolution, which provides a DLSM and DEM with approximately 2 cm grid spacing. The final errors in the generated models contain initial device errors with values that approximate to ± 4 mm and data preparation errors (i.e. ± 8 mm related to the registration process on the point clouds).

The methodology of the current work is based on a general hypothesis which assumes that relief formations have distinctive spatial dependencies and that each landform element contains concrete spatial properties maintained by the prevailing processes and giving rise to the current relief component that they sustain. Hence, in order to verify spatial structure variations within the landscape components, a directional analysis has been adapted. First, the anisotropy between landform components has been analysed using a hierarchical approach of varying dimensions (i.e. scaling down in a sample dataset of known dimensions). In a small controlled catchment, the terrain was divided to four basic elements: these are divide, hillslope, stream, and stream-hillslope connecting area (i.e. upstream area or channel initiation zone). Justification of such classification is attributed to the direct effect of these formations in the definition of flow direction and accumulation, and hence runoff generation. Second, In order to evaluate the directional effect in the defined landform units, the anisotropic semivariance surface (*ASS*) was verified and the principal anisotropic axis was fitted to the maximum and minimum spatial continuity in the sample dataset. The former is related to the lowest semivariance value (i.e. the major axis of the anisotropic variogram model), while the latter is related

to the minimum spatial continuity which defines the highest semivariance value and correspond to the minor axis of the variogram model. Consequently, the semivariograms have been constructed and the parameters of the experimental models have been fitted in 18 directions (0°-170° clockwise from north – unit circle).

In each studied formation, in addition to the type of the semivariogram applied, the following parameters are determined: nugget ($C0$), sill ($C0+C1$), range of spatial dependence, both major (A) and minor (B) ranges, and the ratio of both ($A:B$). These parameters were plotted graphically for each terrain unit in order to infer the main properties of spatial variations (i.e. form and type of the dominant pattern) at each studied unit. Corresponding mathematical models (i.e. defined earlier in Eq. 6.3–6.6) were adjusted to the experimental semivariograms, which allowed for the visualization of the nature of the spatial variation of the examined formation structure.

In nature, hypsometry or slope effect is the most dominant between spatial trends, for which the analysis was repeated with detrending of the sampled datasets. This is important because the results might be an excessive smooth version of reality, and one could lose detail of interest. Moreover, trend component of the spatial structure variation may yield useful and complementary information on the morphology of the landform element. With hypsometric trend, several morphometric aspects that are relevant at the watershed level could be highlighted. However, the weight of the trend masks the effect of the underlying processes that causes such morphometry. For which, and in order to detect such processes, the relief must be examined without trend, because underlying dominant processes (e.g. diffusive runoff on hillslopes and concentrated flow within stream channel system) will be enough apparent to be detached. The channel initiation area, which is the main focus of the work, is a critical zone since both coarse and fine morphometric aspects are essential, and for which the topography should be analysed with and without trend. Accordingly, each hierarchical sub-scale has been analyzed two times: the first with prevailing trend of hypsometry and the second without any trend.

The area has been sampled by a laser scanner at 0.5 mm of initial resolution, which has allowed for the capturing of a dense point cloud that describes all surface details (DLSMs) in the studied catchment. Each terrain feature may contain one or more prevailing pattern that characterizes runoff behaviour. Hence, pure terrain units (i.e. features) are needed to identify spatial trends and prevailing patterns. Consequently, each unit was subjected to verification and studied at four hierarchical sub-scales of the following diameters: 3-, 2-, 1-, and 0.5-m. The reason for such scaling is to determine the optimum dimension for detecting prevailing pattern and trend, because in high detailed data prevailing processes are dominant by the scale of the dataset dimensions. Results of the semivariograms within and between hierarchical sub-scales were registered and prevailing patterns and processes at each scale have been underlined. Type of spatial variation, dominant patterns and prevailing processes within each formation is verified and accepted as a reference form for similar

landform components. Later on, such knowledge was used to characterize each landform element in a toposequence profile of sample datasets that undergoes from a pure convergent topography to reach adjacent hillslope passing through the transition between both (i.e. channel initiation zone). In this case, the centre of the sample dataset is located to coincide with the centre of the channel with enough diameters to ensure the presence of a hillslope formation in the analyzed semivariograms.

In general, two groups of dataset will be analysed: *i)* The first includes the DLSTM and represents real landscape components; and, *ii)* The second comprises the DEM and represents simulated landscape conditions (i.e. interpolated data). In each dataset the analysis was carried out twice: with and without trend. Of course, these repetitions were applied once to discrete landform elements and second to the toposequence profile. It is important to recall that the data set of the terrain was used in its original format; just only the vegetation cover has been filtered and eliminated. Such conditions allows for a direct determination of the landform component as well as the prevailing processes in each one.

The above procedure is a physically-justified qualitative approach to validate landscape depiction, in general, and limits of stream networks, in particular. In the past chapter, validation of channel network limits was handled partially since the digitized-*BLs*, used as valid representation of natural streams, maintains considerable subjectivity in first and second order streams. The presented approach provides a more consistent objective validation method than the *BLs* because landform definition is based on real terrain characteristics contained in the spatial properties of landform features. Accordingly, the channel network in the studied area was delineated using the *CDA* and the $R'_A t$ techniques and their limits was subjected to directional analysis to check for the type of prevailing topography (i.e. convergent, divergent and the transition zone). Moreover, because of the high resolution of the original data (i.e. 6 mm), the contrasts between relief formations and the limited size of the studied basin (i.e. 956 m²) the visualization processes may form a valid and valuable source of information to detach limits between landform elements.

6.6. Analysis and results

6.6.1. Introduction

In the presented study, a geospatial approach has been applied to delineate major landform elements based on spatial structure variations in relief formations. This implies the use of the semivariograms and its parameters as the main tool for such classification. The experimental protocol includes the use of Terrestrial Laser Scanner (*TLS*) to capture the topography at fine details to construct a point cloud that represents real landscape components and designated as Digital Land Surface Model (DLSTM). Later on, the directional analysis is applied to delineate main landform components and limits between them, mainly for stream sources or channel initiation zone. In general, quantitative classification methods of landform components is carried out by means of algorithms that

uses interpolated data structures (i.e. DEMs) and not raw one (DLSDMs), for which the analysis was repeated on a DEM that simulates the original landscape. Accordingly, all the analysis and results will contain two replicates carried out on real and simulated datasets, which will be compared frequently throughout the context both with tables and graphics.

6.6.2. Spatial analysis in ridge formations

In a general commonplace definition, a ridge (or a divide) is a morphometric feature that describes a line which delimited two opposite hillslopes. Indeed, exact description and identification of ridge structure is beyond the object of this study (e.g. Band, 1999; Smith & Mark, 2001; Mark & Smith, 2004) and we will accept the visual interpretation of these formations for limited purposes. Herein, a pure ridge or a divide line in the studied catchment was verified in relation to the above simple definition (figure 6.8). As mentioned earlier, each structure formation was analyzed with and without hypsometric trend, through which ridge formation provided the following results.

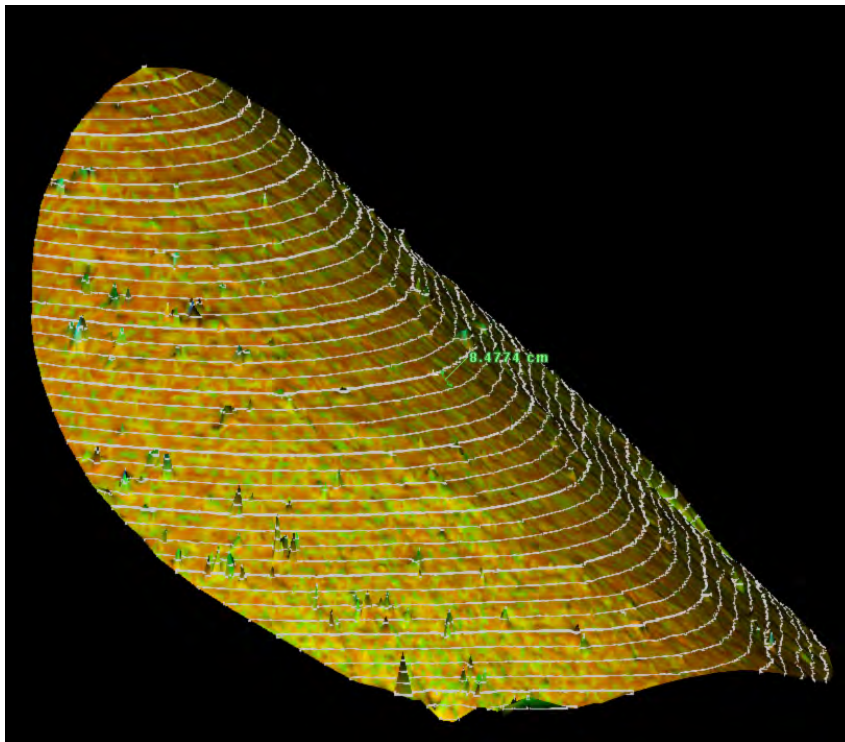


Figure 6.8 A pure ridge formation or a divide line from the mini-catchment in the study area.

6.6.2.1. Ridge analysis with trend

The original data structure for ridge formation was analyzed at the four mentioned sub-units (i.e. 3-, 2-, 1-, and 0.5m) and the related parameters were highlighted separately. For the highest scale (i.e. 3 m), posting of data values against ASS reveals an interesting result in which the axes of minimum spatial continuity coincides with the direction of the divide line, while the contour lines occupy the direction of the maximum spatial continuity (figure 1a, appendix 1). Scaling down in the hierarchical formations underlines the presence of the same tendencies in all the sub-sample sets

(figure 1b, c & d, appendix 1). Table (6.2) shows the studied sample parameters at the different analyzed scales, where 0° indicates the axes of maximum spatial continuity in the sample dataset. While major and minor ranges highlighted trivial information on sample pattern, sill variance and anisotropic ratio provided a lot of information over the shape of the landform unit and the prevailing pattern within it. Hence, these parameters, in addition to the type of the fitted model were plotted and studied separately for each scale and later on combined for the four sub scales. Moreover, the presence of a Gaussian-fitted model in all the directions underline a gradual smooth change in the prevailing pattern, which could be attributed to the smooth variation in the structure shape of the studied sample datasets. The nugget ($C0$) highlights the relatively small noise effect in the analyzed data.

Angle (α)	Model type	Nugget ($C0$)	Sill ($C0+C1$)	Range Minor (B)	Range Major (A)	Anisotropy ratio ($A:B$)
3 m						
0	Gaussian	0.001	0.0402	1.3096	2.0703	1.5808
30	Gaussian	0.001	0.1912	3.5214	4.4136	1.2533
60	Gaussian	0.001	0.4246	5.1393	5.1953	1.0108
90	Gaussian	0.001	0.4914	4.9295	4.9295	1
120	Gaussian	0.001	0.4057	4.7139	4.7139	1
150	Gaussian	0.001	0.1552	2.8428	3.7015	1.3020
2 m						
0	Gaussian	0.001	0.0205	1.0914	1.7928	1.6426
30	Gaussian	0.001	0.1419	1.9999	2.8583	1.4292
60	Gaussian	0.001	0.3741	3.1888	3.2005	1.0036
90	Gaussian	0.001	0.4566	3.1542	3.1542	1
120	Gaussian	0.001	0.6371	3.1361	3.1706	1.0110
150	Gaussian	0.001	0.1159	1.7327	2.4771	1.4296
1 m						
0	Gaussian	0.0001	0.0153	0.2799	0.7846	2.8031
30	Gaussian	0.0001	0.0793	0.7806	1.0303	1.3198
60	Gaussian	0.0001	0.2037	1.1161	1.1161	1
90	Gaussian	0.0001	0.2655	1.0977	1.0977	1
120	Gaussian	0.0001	0.2037	1.0928	1.0928	1
150	Gaussian	0.0001	0.0836	0.8101	1.0581	1.3061
0.5 m						
0	Gaussian	0.0001	0.0159	0.1885	0.5138	2.725
30	Gaussian	0.0001	0.0653	0.4141	0.5863	1.4158
60	Gaussian	0.0001	0.1853	0.6247	0.6247	1
90	Gaussian	0.0001	0.2561	0.6464	0.6464	1
120	Gaussian	0.0001	0.1915	0.6343	0.6343	1
150	Gaussian	0.0001	0.0859	0.4662	0.6456	1.3848

Table 6.2 Parameters of the anisotropic models fitted to experimental variograms in six directions (0° , 30° , 60° , 90° , 120° , and 150° counter-clockwise from axis of maximum continuity) for the ridge formations with trend at the four analyzed sub-hierarchical scales.

Plotting sill and anisotropic ratios for the ridge formation at each sub-scale separately (figure 6.9) shows a clear prevailing trend in the ridge formation dominated by the contour-lines direction; that is the maximum rate of change or maximum spatial continuity. Such prevailing trend is variable between units (figure 6.9) giving rise to clear dominant pattern with varying interpretations related to the corresponding parameters. The $A:B$ ratio reveals similarities between two different sub-scales. The first contains ridge units that extends between 0.5- and 1-m, at this scale the $A:B$ ratio is characterized by an extremely varying ratio within the studied range (0-180°) that oscillates between 1 and 2.8 for the highest anisotropy. Indeed, the extreme values are just located within the range of 150-30° and the rest of the values approximate to unity (figure 6.9a). The second level includes the highest units of 2- and 3-m, which underlines the presence of smoothness in the ridge formation. In this case, the anisotropic ratio revealed little variation (i.e. $A:B$ oscillates between 1-1.6) between the analyzed directions and the curve plot shows a semi-circle aspect (figure 6.9a). It worth to underline that in both defined scales the anisotropic ratio maintains constant (i.e. a values of 1) in the direction of the ridge line indicating greatest change with separation distance, which may be interpreted as higher changes in the formation unit is founded across the ridge line and less one across the contour lines (figure 6.8).

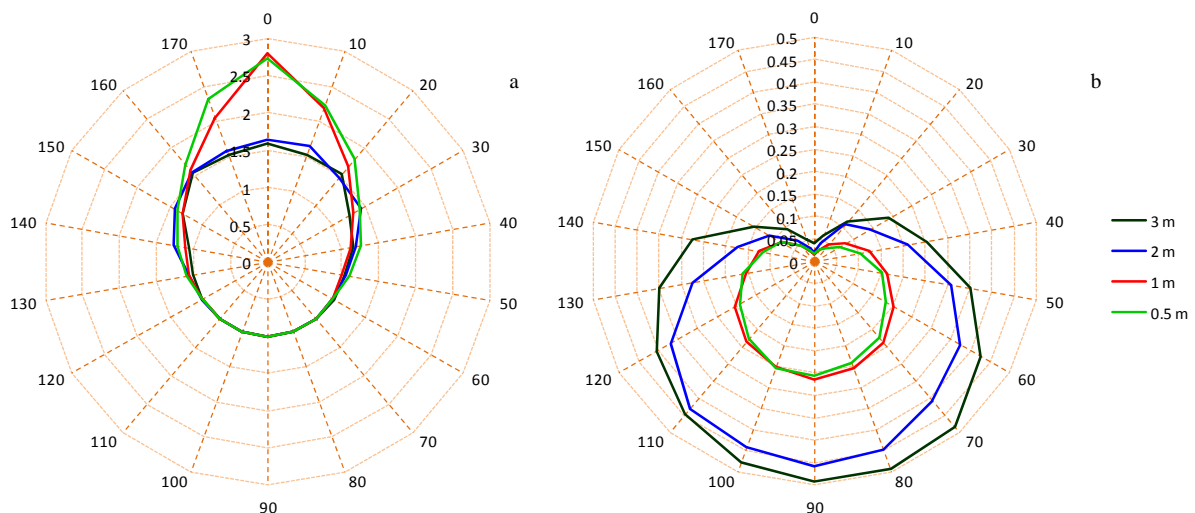


Figure 6.9 Parameters of the directional analysis used in the direct comparison between the different sub-hierarchical scales of ridge formation with trend, organized as follows: a) anisotropic ratio; and, b) sill variance.

The sill variances highlighted varying patterns in the curve tendencies and discern again the presence of two different scales, at 0.5-1 m and 2-3 m, respectively (figure 6.9b). The first two scales of 0.5- and 1-m reveal a moderate variation in sill variance of values that oscillate between 0.0159-0.2561 m and 0.0153-0.2655 m, respectively. Whereas, the 2- and 3-m sample datasets exposed a more sever change in the curve variation that varies between 0.0205-0.4566 m and 0.0402-0.4933 m, respectively. In both cases, sill variations adapted a heart curve aspect with the highest variation in the direction of the ridge line. Such variation, moderate or extreme, indicates the presence of two contradictory forces. The first acts a long ridge divide and is characterized by greater variations with separation distance leading to easier water movement in the opposite direction. The second acts across

the ridge divide and along the contour lines and characterized by least variation with separation distance, suggesting easier movement and less resistance forces for water movements. These results explain water movement on ridge formations, where water movement to adjacent hillslopes requires less energy expenditure rather than to continue in the direction of the divide line. In general, the above results highlighted the presence of a scale breaking point (i.e. 0.5-1 and 2-3) at which the prevailing pattern, and hence the underlying dominant processes, could be slightly altered. Hence, special attention should be taken to sample dimensions utilized in landform attributes definition and verification.

It is important to underline that the direct comparison of the semivariogram parameters between scales is not the ideal and is somewhat subjective, since magnitude of the sill ($C0+C1$) is related directly to the active lag distance, specifies the interval over which semivariance will be calculated. Hence, the form of the sill is a good indication of the anisotropic effect in the sample dataset but not as an exclusive indicator. In order to handle such a problem, an initial active lag distance of about $80\% \pm 10$ was set to be used as the base for all the variance analysis. Such step allows for the detection of pattern change over scaling sample datasets.

6.6.2.2. Ridge analysis without trend

In relation to ridge formation without trend, comparison between plots of data values and the ASS map revealed a completely converse tendency to ridge formations with trend. In this case the, the maximum spatial continuity was a lined to the divide line, whereas the minimum spatial continuity is located in the direction of the contour lines (figure 2, appendix 1). Such change in the direction of variation is widely related to hypsometry, which is of great importance in the spatial analysis since patterns in topography are highly related to hypsometric variations. This is somewhat contradictory to similar formations with trend, which may highlight different interpretation of water movement on these formations. Herein, water movement in hypothetically non-inclined divides is along the divide line and not to adjacent hillslopes. This is somewhat rare in nature, where divides and ridges always maintain a kind of inclination in the direction of the catchment outlet or to neighbour-basin borders.

On the other hand, the semivariograms parameters of anisotropic ratio and sill variation (figure 6.10) provided indispensable and complementary information on the prevailing pattern in relation to change in scale. While the same tendency effect was clearly observed in the anisotropic ratio and sill values, the direct comparison between scales confirms again the presence of a moderately breaking scale, but in this case is located in the unit formation of 0.5 m (figure 6.10b). Once more, interpretation of such observation could be attributed to change in the effect of prevailing process detectable by the sample size and the corresponding resolution (i.e. spaces between sample values). In this case, resolution effect is directly detached by change in sill variance where datasets are sampled

hierarchically. This means that although the samples have initially the same resolution, larger scale dimensions are needed in order to detect the same prevailing process.

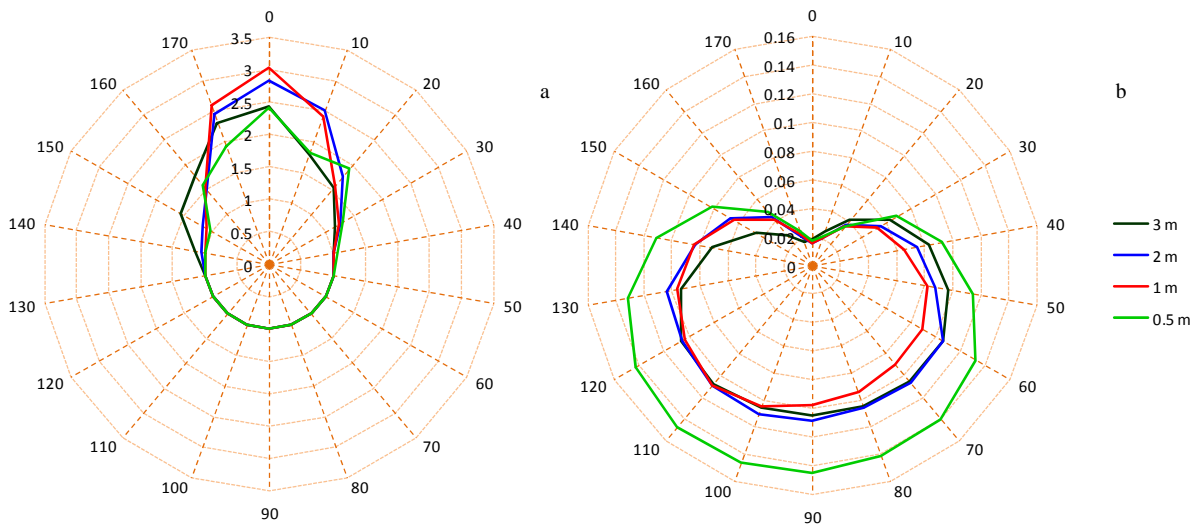


Figure 6.10 Parameters of the directional analysis used in the direct comparison between the different sub-hierarchical scales of ridge formation with trend, organized as follows: a) anisotropic ratio; and, b) sill variance.

6.6.3. Spatial analysis in hillslope formations

In the studied mini-catchment, delimiting a hillslope was a direct and easy task, since terrain and relief characteristics allow for a direct selection with simple eyes. The studied sample dataset was selected in the lower part of the catchment between a stream and a ridge formations (figure 6.11), and not in the upper part of the catchment. This criterion was applied in order to verify the effect of neighbouring and adjacent terrain formations.

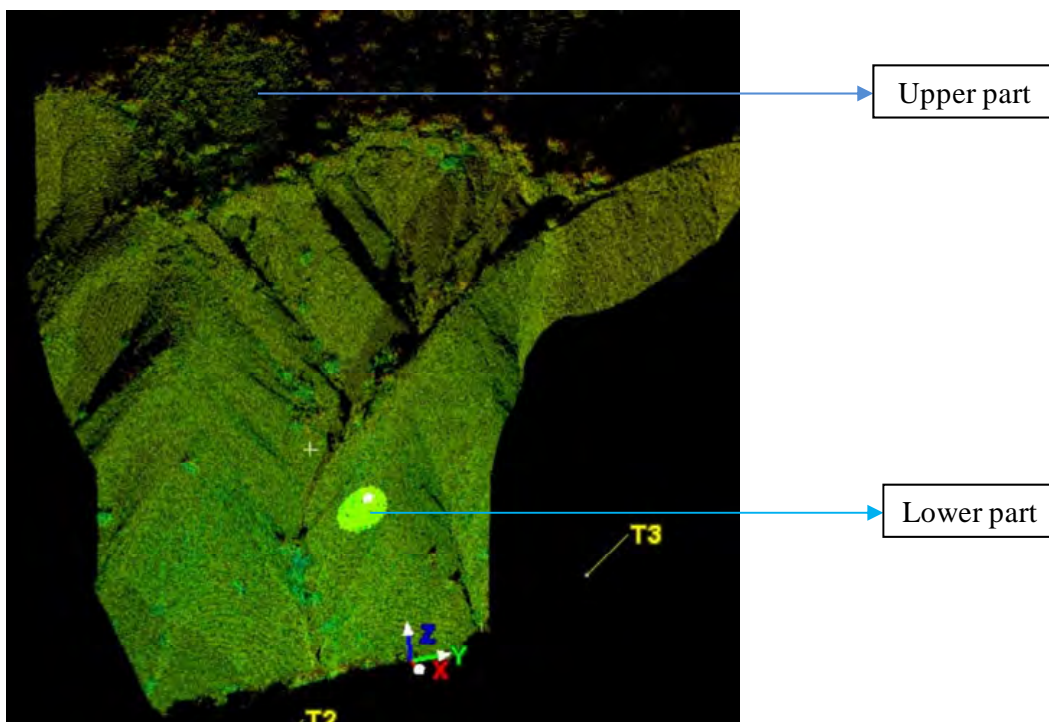


Figure 6.11 Hillslope sample data set location in the studied mini catchment

6.6.3.1. Hillslope formations with trend

Herein, posting of data values against their ASS plot (figure 3, appendix 1) shows a clear anisotropy in the sample datasets for all the hierarchical sub-scales, in which the maximum spatial continuity occupies the direction of the hypsometry. Again, maximum energy expenditure will be in the direction of the contour lines, leading to direct movement of water in the direction of hypsometric change.

It seems that the prevailing patterns and tendencies in hillslope formations maintain constant between scales, with both anisotropic ratios and sill values (figures 6.12). The sill variance adapted a heart curve aspect with a considerable change in sill value that extends between 0.02-0.48 m for 0° and 90°, respectively (table 6.3). This drastic change may be attributed to the presence of a unique prevailing pattern of one dominant process. Of course, hypsometry and gravity are the main factors that control and explain such behaviour. On the other hand, the semivariograms of the different sample datasets have shown a completely Gaussian fitted model, which confirms a smooth structure form, and the absence of unexplained spatial variability proved by the small nugget values (tables 6.3.).

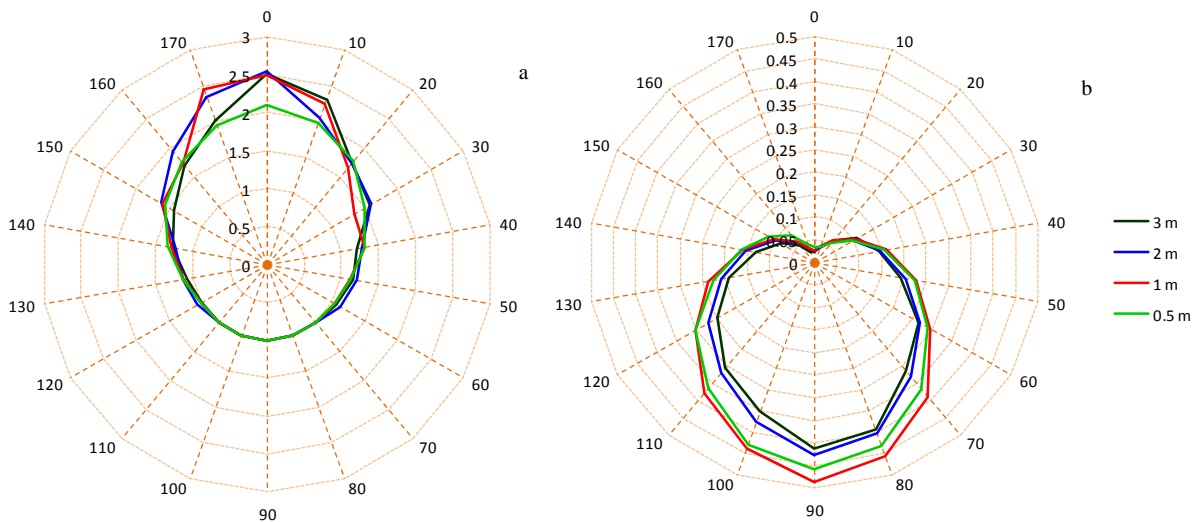


Figure 6.12 Parameters of the directional analysis used in the direct comparison between the different sub-hierarchical scales of hillslope formation with trend, organized as follows: a) anisotropic ratio; and, b) sill variance.

Angle (α)	Model type	Nugget (C0)	Sill (C0+C1)	Range Minor (B)	Range Major (A)	Anisotropy ratio (A:B)
3m						
0	Gaussian	0.001	0.0231	1.4103	3.5422	2.5116
30	Gaussian	0.001	0.1072	2.0672	3.2373	1.5660
60	Gaussian	0.001	0.2645	3.1667	3.3462	1.0566
90	Gaussian	0.001	0.4121	3.5945	3.5945	1
120	Gaussian	0.001	0.2460	3.0639	3.0639	1
150	Gaussian	0.013	0.0836	1.9617	2.7893	1.4218
2m						
0	Gaussian	0.001	0.0249	0.8099	2.0625	2.5466
30	Gaussian	0.001	0.0963	1.3701	2.1851	1.5948
60	Gaussian	0.001	0.2691	2.0748	2.3076	1.1170
90	Gaussian	0.001	0.4275	2.5077	2.5077	1
120	Gaussian	0.001	0.2683	2.0947	2.2471	1.0727
150	Gaussian	0.001	0.0976	1.2676	2.0622	1.6268
1m						
0	Gaussian	0.001	0.0254	0.4237	1.0586	2.4984
30	Gaussian	0.001	0.1041	0.7711	1.0321	1.3384
60	Gaussian	0.001	0.2951	1.0771	1.1171	1.0370
90	Gaussian	0.001	0.4867	1.2559	1.2559	1
120	Gaussian	0.001	0.3025	1.1105	1.1251	1.0131
150	Gaussian	0.001	0.1031	0.6574	1.0466	1.5920
0.5m						
0	Gaussian	0.0001	0.0347	0.3075	0.6459	2.1004
30	Gaussian	0.0001	0.0958	0.3671	0.5467	1.4892
60	Gaussian	0.0001	0.2881	0.5709	0.5901	1.0336
90	Gaussian	0.0001	0.4575	0.6677	0.6677	1
120	Gaussian	0.0001	0.3026	0.5982	0.6041	1.0098
150	Gaussian	0.0001	0.1149	0.3651	0.5723	1.5675

Table 6.3 Parameters of the anisotropic models fitted to experimental variograms in six directions (0°, 30°, 60°, 90°, 120° and 135° counter-clockwise from axis of maximum spatial continuity) for the hillslope formations with trend at the four analyzed hierarchical sub-scales.

6.6.3.2. Hillslope formations without trend

In this case, the sample dataset and the anisotropic semivariance analysis have revealed new insights in the forms and the patterns that control hillslope formations. For the first and highest unit (i.e. 3 m), plotting of data values against their ASS plot reveal the presence of a slight trend controlled by the contour lines that forms at the borders of the sample data set (figure 4a, appendix 1). Such control is widely reflected by the anisotropic semivariance surface (figure 4b, appendix 1), which reveals a clear directional effect that extended between east-western directions in the sample dataset. Under these conditions, water movement is expected to be in the horizontal direction, which produces minimum energy expenditure. Scaling down in the sample datasets generates new conditions of

patterns and tendencies. In the second sub-scale with the sample dataset of 2 m, the prevailing trend is completely vanished and the data reveals no clear tendencies (figure 5a, appendix 1). Posting of data values highlights the absence of any particular trend, such lack of pattern dominance leave the surface structure under the control of micro relief formations, which can be attributed to the degree of roughness in the studied element. Moreover, the *ASS* plot underlines the presence of no directional effect in the sample dataset, rather the presence of approximately “omnidirectional effect”. Again, scaling down in the sample datasets of 1 and 0.5 m, confirms the presence of no prevailing pattern in the studied units (figure 5b & c, appendix 1). Herein, the omnidirectional effect is repeated again in these two scales highlighting the presence of approximately isotropic effect.

The sill variance is characterized by extreme small values (table 6.4), indicating a smooth formation governed by a slightly roughed aspect. Moreover, in the 1 m sample dataset both anisotropic ratio and sill variance (figures 6.13) approximates to unity (i.e. no change with direction) giving rise to a mixture of pure geometric and zonal anisotropy, which is a structure form rarely observed in nature (Isaaks & Srivastava, 1989). Another important aspect is the type of change in the fitting model throughout the change of direction (table 6.4). Except the unit of 1 m, the rest of sub-scales showed an interchangeable fitting model in relation to direction change between spherical and Gaussian functions. This is widely acceptable since roughness or micro-topography is the limiting factor, which is translated to different curve fitting in relation to the type and roughness of each micro-relief formation within each sub-scale. Gaussian fit represents smooth transition while spherical fit represents a clear transition point; both are presented in each hierarchical sub-scale. Again, nugget variances reveal small values (table 6.4) indicating limited noise effect in the sample datasets. Under these conditions of isotropy, water movement is unpredictable and is widely controlled by local micro-relief. In addition, energy expenditure and optimality criteria of water movement in stream basins (Rodriguez-Iturbe et al., 1992) are little perceived.

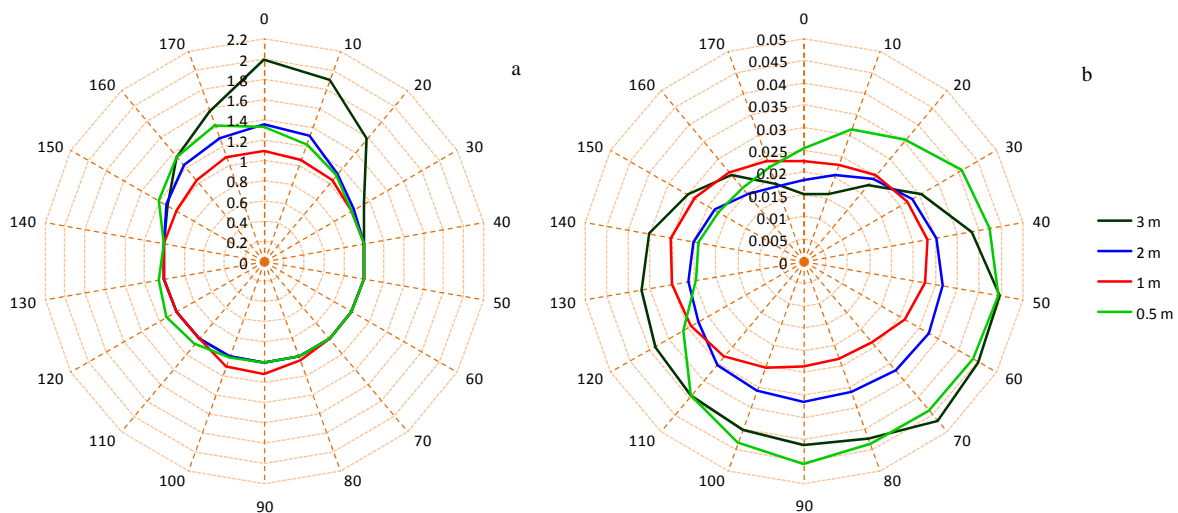


Figure 6.13 Parameters of the directional analysis used in the direct comparison between the different sub-hierarchical scales of hillslope formations without trend, organized as follows: a) anisotropic ratio; and, b) sill variance.

Angle (α)	Model type	Nugget (C0)	Sill (C0+C1)	Range Minor (B)	Range Major (A)	Anisotropy ratio (A:B)
3 m						
0	Gaussian	0.0004	0.0151	0.7105	1.4164	1.9935
30	Gaussian	0.0004	0.0304	1.2231	1.3968	1.1420
60	Spherical	0.0006	0.0453	1.2508	1.2508	1
90	Spherical	0.0012	0.0412	1.0135	1.0135	1
120	Spherical	0.0012	0.0384	1.0461	1.0461	1
150	Gaussian	0.0011	0.0301	1.2322	1.3654	1.1080
2 m						
0	Spherical	0.0015	0.0182	0.4783	0.6461	1.3508
30	Spherical	0.0015	0.0281	0.7551	0.7758	1
60	Spherical	0.0015	0.0324	0.6991	0.6991	1
90	Gaussian	0.0015	0.0314	0.6152	0.6152	1
120	Spherical	0.0015	0.0273	0.5883	0.5883	1
150	Spherical	0.0015	0.0231	0.6007	0.6709	1.1168
1 m						
0	Spherical	0.0008	0.0225	0.4333	0.4729	1.0913
30	Spherical	0.0011	0.0267	0.5164	0.5164	1
60	Spherical	0.0045	0.0263	0.4465	0.4465	1
90	Spherical	0.0022	0.0235	0.4501	0.4913	1.0915
120	Spherical	0.0015	0.0292	0.6131	0.6131	1
150	Spherical	0.0015	0.0283	0.6185	0.6185	1
0.5 m						
0	Spherical	0.0051	0.0203	0.5041	0.5041	1
30	Spherical	0.0039	0.0185	0.4119	0.5546	1.3464
60	Gaussian	0.0075	0.0225	0.3743	0.3743	1
90	Spherical	0.0035	0.0321	0.5593	0.5593	1
120	Gaussian	0.0081	0.0331	0.5874	0.5874	1
150	Spherical	0.0057	0.0291	0.6859	0.6859	1

Table 6.4 Parameters of the anisotropic models fitted to experimental variograms in six directions (0°, 30°, 60°, 90°, 120° and 135° counter-clockwise from axis of maximum continuity) for the hillslope formations without trend in the four analyzed hierarchical sub-scales.

It worth's to highlight that in the above analysed feature the tiny value of sill variations may deduce a fractional Brownian surface and hence unbounded model fit. But the fitted semivariogram shows a bounded type model for the four analysed hillslope units (figure 6.14). Herein, the sill reached asymptotic at value between 9.4×10^{-5} - 3×10^{-3} m, which is an extremely small to reflect variation in the spatial structure. This is a periodic variation type, which could be attributed to resolution effect in relation to the relief. In this case, the sill may convey data uncertainty rather than spatial structure variation. Under these conditions McBratney and Webstar (1986) explained that however the small sampling intervals, if the supports are smaller than the interval there is always some variation. These results bear a corollary interpretation that any surface could be Brownian (i.e. fractional Brownian motion) and contain unbounded variogram if it is properly examined at an adequate resolution (i.e.

threshold). That is analysing any surface feature require a threshold resolution to be examined accurately. If this is the case, then the surface is fractal and its variance is derived by

$$E[z(x) - z(x+h)]^2 = k(|h|)^{2H} \tag{6.10}$$

where $E[]$ denotes the statistical expectation, $z(x)$ is the height of the surface at coordinates denoted by the vector x , h is a displacement vector, k is a constant, $|h|$ is the magnitude (length) of the displacement vector, and H is a parameter in the range 0 to 1 (Goodchild & Mark, 1987).

and its fractal dimension (i.e. the Hausdorff-Besicovetch dimension) is defined by

$$D=3-H \tag{6.11}$$

In nature, D takes values between 2 and 3, where 2 represents a completely smooth surface and 3 completely rugged surface.

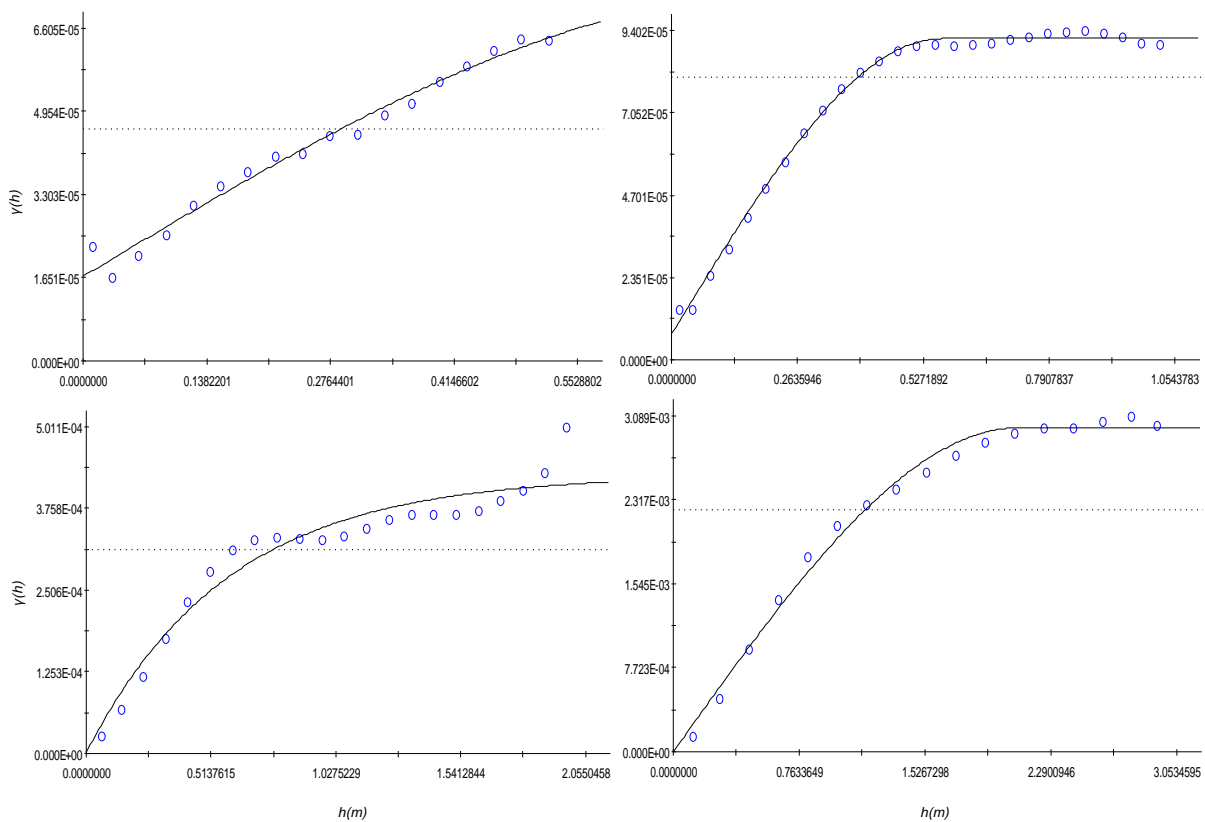


Figure 6.14 Semivariograms of the hillslope feature of the 1 m unit showing a spherical bounded model of sill variance of 0.026 m.

In the analysed sub-hierarchical scales, H values oscillates between 0.1781-0.44 (table 6.5), which indicates considerably significant variations between the surfaces. Taking into account that the analyzed units are hierarchically contained, theoretically that means the surfaces should be identical, whereas the results indicate the contrary. The fractal values of such surfaces suggest the smaller the terrain is the higher the roughness is, that is, highly rugged terrain with rough local relief (figure 6.15).

Under these conditions, the analysed unit formations present clear self-similarity underlined by tiny varying in D values. Burrough (1983) suggests that changes in D values are widely related to local variation; higher D values indicates short-range variations, and vice versa. In the analysed units,

the average D values suggest moderate- to short-range variations in surface roughness, which is widely appreciated in the 3D representation of figure (6.15). The causes of these large D values in this case just can be attributed to the microrelief, and hence the short-range variations can explain the roughness of the terrain. Table (6.5) shows that the smaller the sample size the higher the variation is, and vice versa. Mandelbrot (1977) reported that for landform element $D \approx 1.1$ (i.e. in two dimensional profile analyses), which means that: *i*) topographic roughness is completely independent and unexplained by the general relief, or *ii*) the sample resolution is too coarse to resolve the pattern adequately. In this case, the sill values of the analysed sample datasets (figure 6.14) seem to reflect a type of uncertainty in the analysed patterns rather than variations, which should be analysed deeply in future works directed for studying resolution effect on topographic surface roughness.

Diameter of landform element (m)	D	H
0.5	2.8219	0.1781
1	2.7363	0.2637
2	2.6442	0.2558
3	2.56	0.44

Table 6.5 Values of fractal dimension and the Brownian motion for the analysed sub-scales.

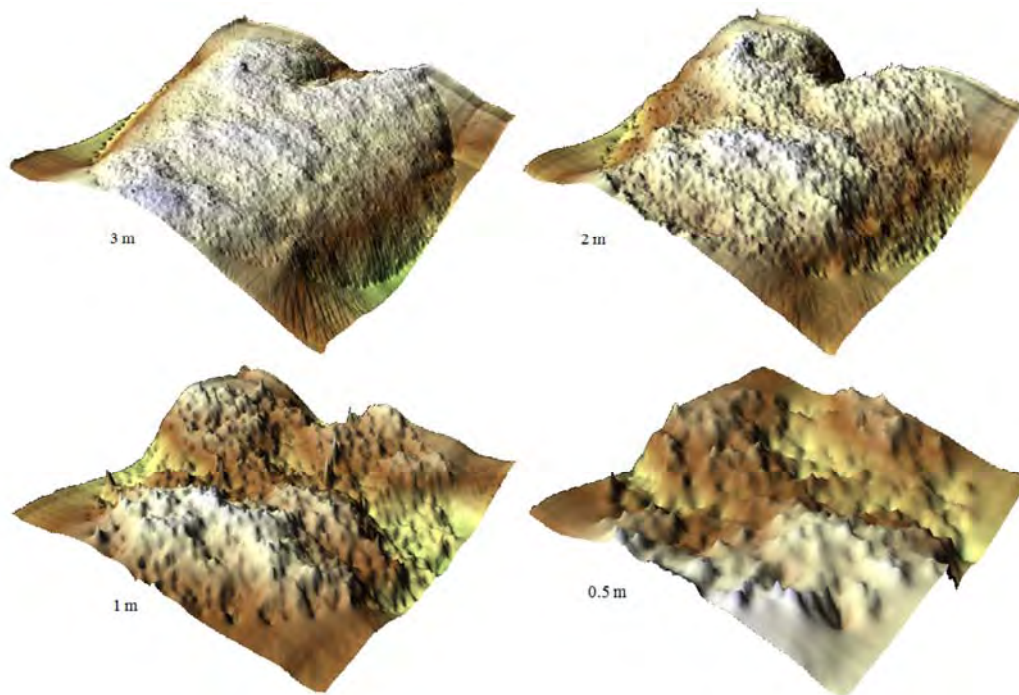


Figure 6.15 3D representations of hillslope formations without trend for the four sub-units and the corresponding self-similar surfaces and their fractal dimension.

6.6.4. Spatial analysis in channels and valley formations

The sample dataset, which represents a complete stream unit, is located in the central part of the mini-catchment with a slope of about 25° (figure 6.16). Both sides of the stream (i.e. stream banks) have no other formations (e.g. rills, stones, etc.), in order to fit the character of a pure landform. Just

have no other formations (e.g. rills, stones, etc.), in order to fit the character of a pure landform. Just only, the upper left side of the sampled unit contains a small intrusion of rill formation. The stream units were analyzed with and without the hypsometric trend, and the following results have been highlighted.

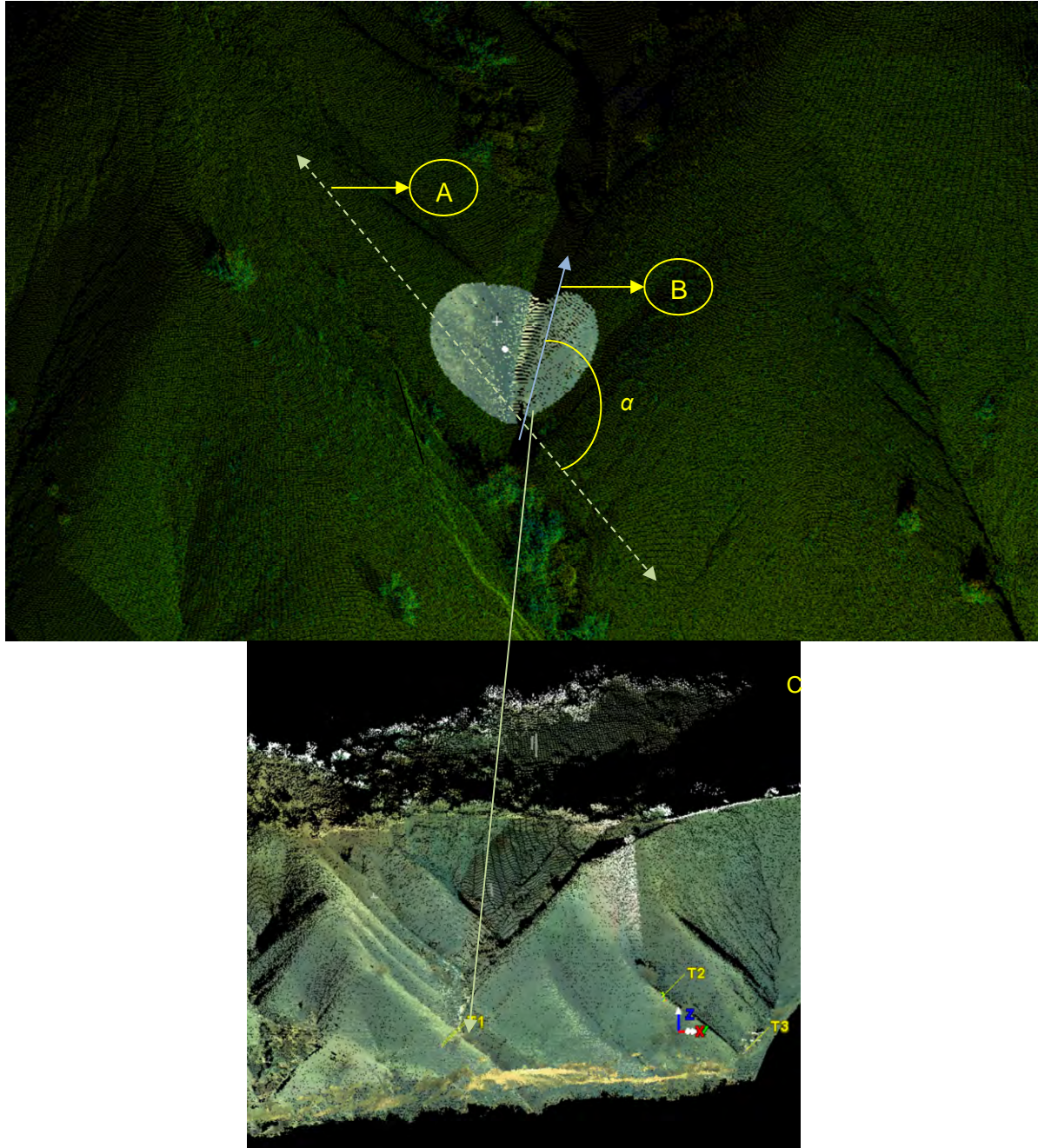


Figure 6.16 Location, form and limits of the channel sample dataset within the studied catchment. A) Indicates the direction of the basin outlet, streams, and longest hillslopes; B) indicates the direction of the analyzed stream in relation to the outlet; and α) is the angle between the two directions. C) Generalized view for the basin outlet, rills and longest hillslope direction in the studied catchment.

6.6.4.1. Channel formations with trend

Again using the same procedure, comparison between direct data posting and ASS maps highlighted a clear prevailing pattern in relation to the size of the sample datasets. In the first scale (i.e.

3 m), the maximum spatial continuity coincides well with the direction of the main stream line (figure 6a, appendix 1); that is, the prevailing pattern is widely related to convergent topography. These findings confirm to our expectation that the direction of maximum variation is across the channels, whilst the direction of minimum variation was found along the streams. Scaling down in the comparison process reveal similar variations in the sample datasets where again greatest continuity coincides well with the stream line direction (figures 6b, c, & d, appendix 1). This explains why water movement in channel formations is always along the stream lines.

The constructed semivariograms shows a clear directional effect in these formations (figure 6.17). The anisotropic ratios reveal approximately similar shape structure for the different sub-scales (figure 6.17a), which tends to have the same tendency along the analyzed directions (figure 6.17a). The maximums in $A:B$ ratios are decreased with size, while minimums maintain constant across stream lines (figure 6.17a). In all cases, the variation is concentrated to the direction of maximum spatial continuity, mainly between 170° - 20° , suggesting that such formations are widely dominated by a clear prevailing pattern that acts along these ranges, giving rise to the actual shape of stream formation. A deeply insight in the plot curves of the different scales underline that the highest scale owns a smoother anisotropic ratio than smaller ones (figure 6.17a) suggesting that channels and stream are readjusted in shape as the dimension of analysis is enlarged. All the analyzed scales, with exception of the smallest one, have shown a bulk form in the directions between 150° - 0° (figure 6.17a), suggesting the presence of another pattern in the studied samples. Closer inspection to this sample data underlines the presence of a small stream that connect to the sample data from in the left upper side, which is widely appreciated in figure 6.16 and pointed out by an arrow in figure 6a (appendix 1).

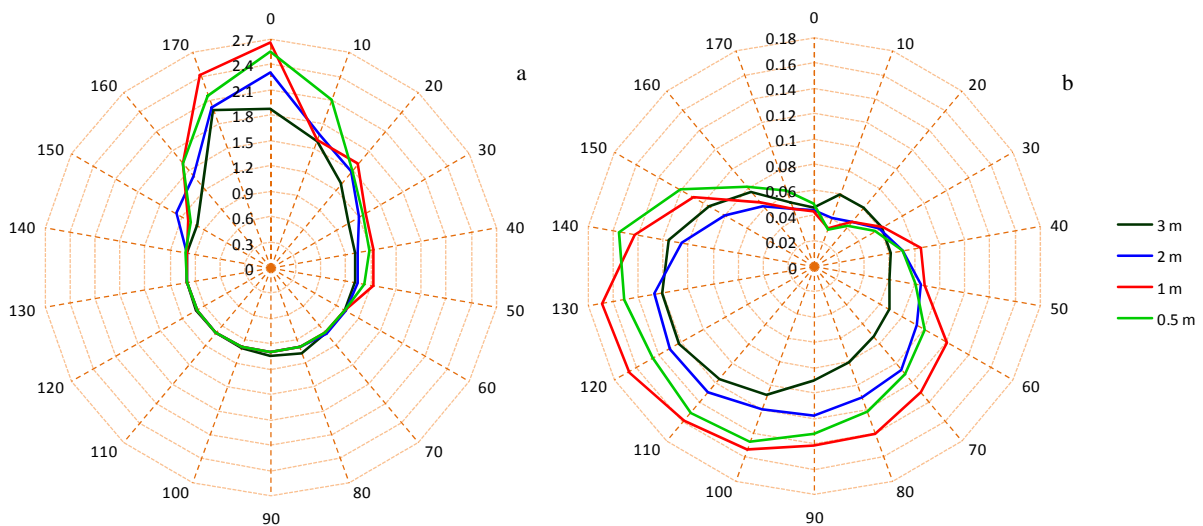


Figure 6.17 Parameters of the directional analysis used in the direct comparison between the different sub-hierarchical scales of stream formations with trend organized as follows: a) anisotropic ratio; and, b) sill variance.

In the same direction, the analyzed sample datasets have large sill variance across the channel streams that extend between 0.15-0.16 m and 0.12-0.13 m for the smallest and highest scales,

respectively (figure 6.17b). In general, the sill variation adapts the aspect of an ellipsoid rose variogram where the maximum sill variation is localized between 80-140° (figure 6.17b), suggesting one prevailing process, which doesn't act in the direction of minimum variation (i.e. along the channel stream), rather is somewhat inclined. This inclination coincides well with the direction of the longest hillslopes and the outlet of the catchment (figure 6.16). A close inspection to the studied basin reveals that this coincides with the majority of the existing streams and rills in the analyzed mini-catchment (figure 6.16). This change in direction could be explained by the erodibility of the materials presented in each location that acts as a barrier leading to a considerable deviation in stream direction. Usually, these are southwest-facing slopes, characterized by active morphologic process and more received radiations than northeast-facing slopes (Solé-Benet et al., 2009), giving rise to more frequent and develop rills (Cantón et al., 2001, 2003).

6.6.4.2. Channel formations without trend

In order to verify the weight of the contour-line effect these comparisons were repeated again without the hypsometric trend. Again, the hypsometric trend has been counteracted by removing the major slope line of the sample datasets, and the same analysis procedures were repeated for all the sampled scales. The comparison between posting of data values and ASS plot reveals a similar tendency effect in all the studied sub-scales (figures 7, appendix 1). In all these scales, the maximum spatial continuity coincides well with the direction of the stream line, whereas the minimum spatial continuity is lined with the contour lines. Such spatial continuity is widely represented by a clear prevailing anisotropic effect (figure 6.18a), which highlighted a similar shape structure controlled by a clear prevailing pattern for the different scales. Such prevailing pattern explains the possible spatial function of a convergent topography within a hydrological unit structure. The sill variance (figure 6.18b) confirms such trend, where all the plotted values show the same directional distribution. It seems that differences between channel formations with and without trend are somewhat trivial and its effect is insignificant either in the shape structure or in the prevailing trend, where in both cases values maintain approximately the same variation range (figures 6.17 & 6.18). Such characteristics ensure downward movement of water maintained by the gravitational potential energy of water obtained in the upper areas of the catchment.

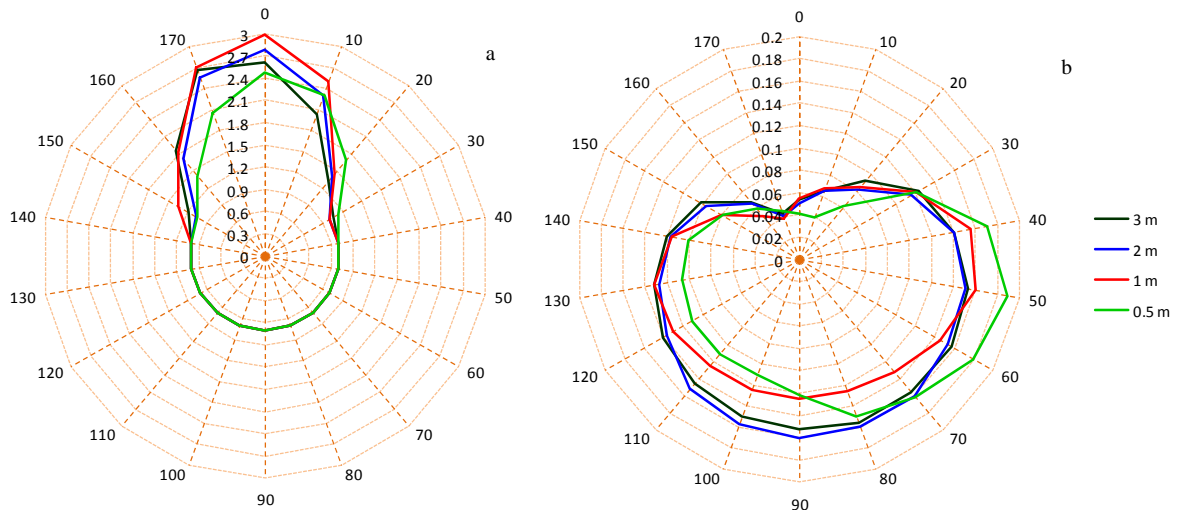


Figure 6.18 Parameters of the directional analysis used in the direct comparisons between the different sub-hierarchical scales of channel stream formations without trend, organized as follows: a) anisotropic ratio; and, b) sill variance.

6.6.5. Spatial analysis in channel heads (channel initiation)

In general, the visual definition of channel initiation in the field is fairly ambiguous, and in some cases could be arbitrary. Topographic contrasts and scale extend are essential factors in such definition. From one hand, under high relief contrast stream borders and channel initiation is more appreciated than smooth relief formations. On the other hand, the scale of observation may lead to contradictory conclusions on the type of the defined landform if the total relief element has not been included in the verification process. So, care should be taken in the extracting and definition procedure. Under these limitations, we accept a relief element as a pure upstream area or channel initiation if it only shows a clear change from convergent to divergent topography; that is a structure form with a clear hillslope formation and clear stream borders (figure 6.19). Figure 6.19 shows a clear topographic formation for channel initiation or upstream valley, which is a sample dataset with a gradual vanishing of a channel formation to approximately gradual intrusion in hillslope formation. In the studied area, the maximum possible size for a pure upstream formation was a sample dataset of about 200 cm, which is considered as the coarsest scale to be analyzed under the present classification methodology. In this case, the sample data set was divided into three sub-hierarchical units, each with a diameter of 200, 100, and 50 cm.

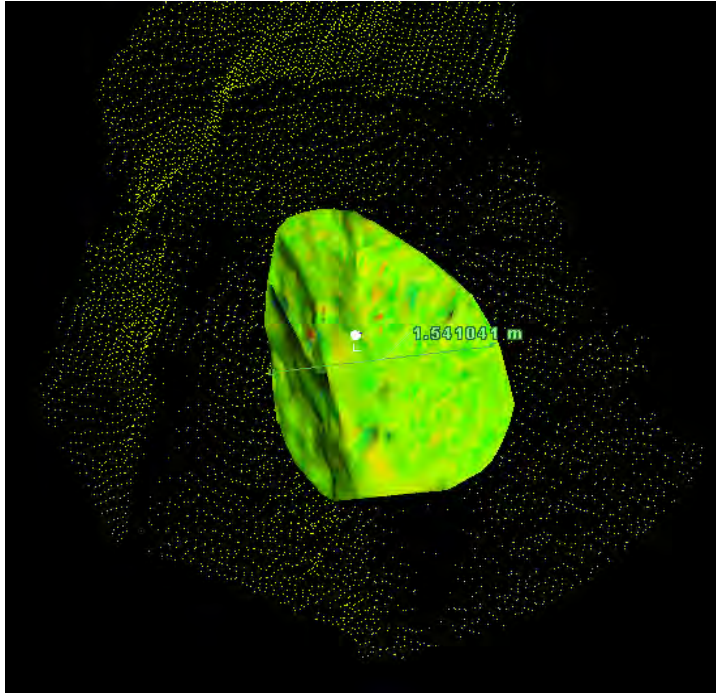


Figure 6.19 A Sample data set of channel initiation form with clear borders between a vanishing stream and a new hillslope formation.

6.6.5.1. Channel head formations with trend

Again, maximum and minimum variation of the analyzed sample datasets were carried out and preliminary results underlined a varying trend in relation to scale. Posting of data values against their ASS plot shows a maximum spatial continuity in the direction of the contour lines in the 0.5-m unit (figure 8a, appendix 1). Such spatial continuity is completely vanished and fairly detected in the 1- and 2-m units, respectively (figure 8b & 8c, appendix 1). In this case, the direction of minimum variation is in the direction of the channel stream, suggesting higher effect for the stream over the hillslopes at this scale.

The semivariogram analysis of the different sample datasets shows irregular results in relation to scale size and the analyzed parameters (i.e. anisotropic ratio and sill variance). First, the $A:B$ values show a smooth anisotropy at the highest scale with rates that oscillate between 1-1.45 (figure 6.20a), which is not localized in a unique direction rather is distributed between two range directions (100–150° and 160-20°) suggesting a kind of interrelation between adjacent features, whereas sill values maintain a smooth variation that oscillate between 0.052-0.092 m (figure 6.20a & b). Second, at the 1-m unit, the anisotropic ratio and sill variance approximates to unity (figure 6.20a) suggesting a completely rounded and smooth formation. Under these conditions the anisotropy is vanished and the structure is fairly isotropy or contains a nearly perfect omnidirectional effect. Finely, scaling down to 0.5-m unit, the perfect omnidirectional aspect of the $A:B$ values is altered and the fit curves adapted an ellipsoid rose aspect (figure 6.20a), in which the maximum variation is a lined with the channel direction (figure 6.20a). Likewise, the sill variance revealed a clear anisotropy (figure 6.20b), which

extends between 0.04-0.16 m suggesting the presence of a dominant process at this scale. This change in the directional effect could be attributed to the dimension and/or the resolution of the sample dataset. In the first case, it seems that a unit of 0.5 m is not enough to detect an initiation zone, where part of the sample dataset is disappeared and the constructed semivariograms recognized a hillslope or a stream formation. While in the second case, the resolution of the sampled dataset seems to be entirely insufficient to define the transition from divergent to convergent topography and the semivariogram detect approximately hillslope-like structure form.

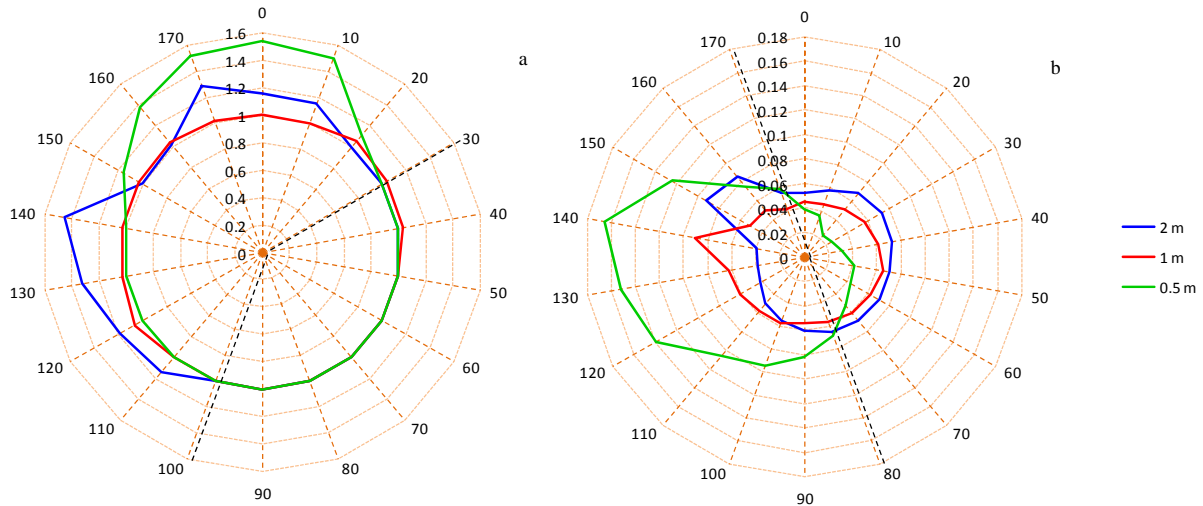


Figure 6.20 Parameters of the directional analysis used in the direct comparison between the different sub-hierarchical scales of channel initiation with trend, organized as follows: a) anisotropic ratio; and, b) sill variance. Dotted black lines in both curve lines indicate the limits between unity and directional effect in the analyzed sample data.

The comparison of all studied parameters in figure (6.20) underlines three important points: a) scale has major influence on anisotropic ratio than sill variance values: this is explained by the sensibility of anisotropic ratio to changes in the structure shape of the studied landform as scale increased, whereas sill is more appropriate to indicate the presence of a prevailing process in the landform structure; b) sill variance and $A:B$ ratios contain variable but complementary information, suggesting that in spatial analysis of landform components both are necessary for any structural study; and, c) finally, the 1-m sample dataset exhibits sufficient information to represent shape type and dominant patterns in channel initiation landform. So, it seems that a sample dataset of 1 m is an acceptable and appropriate scale at which channel initiation can provide substantial information on landform properties and may be used for structure-relief definition. So, in a wide general sense, the 1 m is an acceptable reference for the definition of channel initiation, where down which sample dataset highlights little (i.e. insufficient) information on stream initiation (i.e. transition from divergent to convergent topography) and up which data may contain surplus or unnecessary information.

Of course, anisotropic ratio and sill variance provide different conclusions, but in a general sense highlight a change in process control for each scale that maybe explained separately. Such results are completely different to those obtained from the previous semivariogram analysis of ridge,

hillslope and even channel stream formations. Hence, structure forms of channel initiation should contain to large degree sufficient information in relation to the variogram parameters that allows for a certain separation between such formations. From one hand, ridge, hillslope and channel formations have a clear anisotropy and high variation values for both ($A:B$) and ($C0+C1$) suggesting varying and considerable changes with separation distance along the axes of analysis. On the other hand, channel initiation contain trivial variation in sill variance (i.e. absence of prevailing pattern) and $A:B$ ratio (i.e. omnidirectional aspect). This suggests that such landforms behave as a structure of unbiased state, where the different prevailing forces act in opposite directions in order to nullify each other.

6.6.5.2. Channel head formations without trend

Again, the same analysis procedures have been applied to channel head formations after trend removal and results revealed relatively different insights on the form and type of prevailing patterns to channel initiation with trend. First posting of data vales against their ASS maps underline the presence of a clear anisotropic effect for all studied scales with a maximum spatial continuity in the direction of the concavity lines (figure 9, appendix 1), which forms as a result of trend removal. The directional effect was observed in the analyzed semivariogram parameters and in all studied scales. The $A:B$ ratios vary considerable with maximums that oscillate between 2.13-2.96 (figure 6.21a). Nevertheless, sill values show a clear scale effect, where scaling up and down in the analyzed sample datasets reveal different levels of variation (figure 6.21b). The unit of 3 m unit includes the highest variations in sill variance with values that oscillate between 0.055-0.165 m. Indeed, these values approximate to that observed earlier in channel formations. The medium scale contains moderate variations in sill values that extend between 0.03-0.097 m. Herein, these values are much similar to channel initiation than a pure stream formation. Finally, scaling down to the smallest sample unit reveals an extremely smooth variation that oscillates between 0.017-0.064 m. In fact, visualization of these sub-scales in 3D using kriging interpolation reveals that these formations are altered from a similar stream formation in the highest scale to approximately channel initiation form in the lowest one (figure 6.22). This may explains the above variations in sill variance for the different scales, which again highlights the importance of dimension in the analyzed sample datasets.

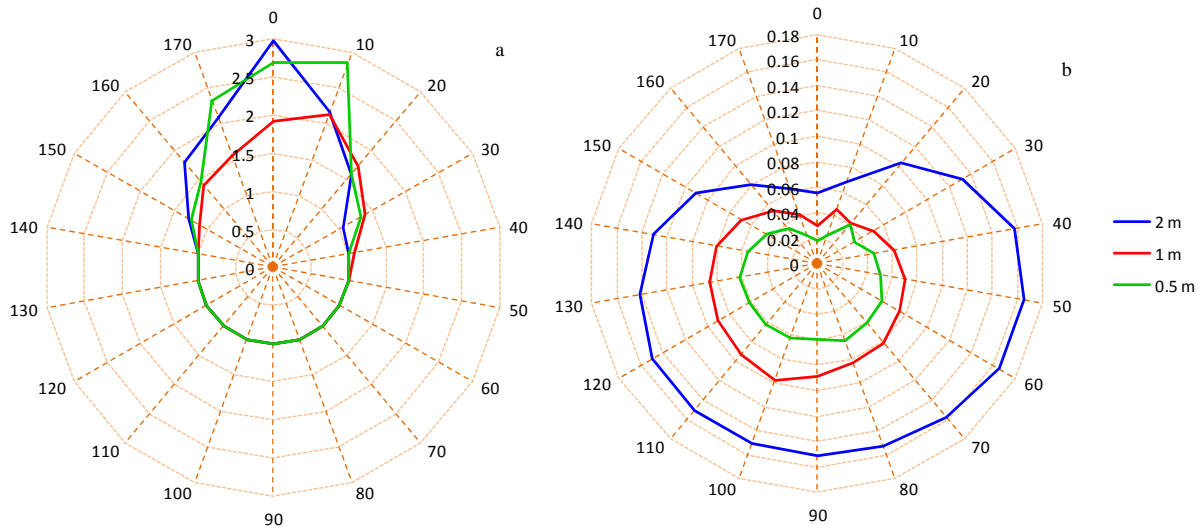


Figure 6.21 Parameters of the directional analysis used in the direct comparison between the different sub-hierarchical scales of channel initiation without trend, organized as follows: a) anisotropic ratio; and, b) sill variance.

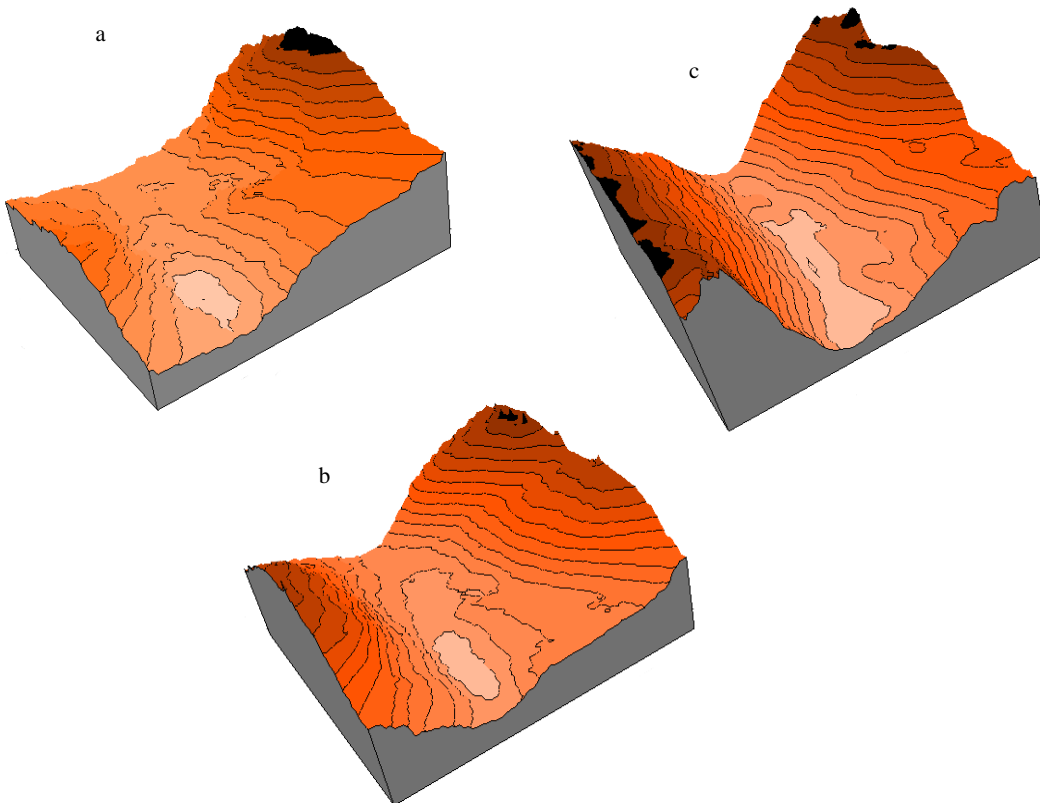


Figure 6.22 3D representations of the analyzed sample datasets of channel initiation without trend by kriging. Semivariograms was calculated at, a) 50 cm; b) 100 cm; and, d) 200 cm.

6.6.6. Interpretation of the directional analysis for the examined formations

It should be highlighted that the comparison process in general implies some certain risk because a perfect comparison should be realized between semivariograms that encompass all the sample data set. This is not the case, since the active lag distance is selected in relation to the best model fit and to the presence of anisotropy for each dataset. The fitted model parameters for these

variograms at the sample data of 1-m unit are given in table 6.6. All variograms were fitted best (in the least squares sense) by bounded models indicating that the range of spatial dependence is within the scale of this investigation (Webster & Oliver, 1990; Chappell, 1996). The studied variograms have demonstrated varying sill variance and range values, which is highly related to the dimensions of the analyzed formations leading in some cases to geometric anisotropy (i.e. similar shape and sill variance but different range values) or a mixture of zonal and geometric anisotropy.

In general, table 6.6 highlighted different information over the variation and the spatial continuity extent and type for each landform component that worth to be analyzed deeply. First, all formations revealed a small Nugget variance values (C_0) indicating absence of measurement errors and spatial variations at distances smaller than the shortest sampling intervals (i.e. the initial resolution of the scanning process). Thus, the spatial variability within the formations itself are well explained and verified. Secondly, Bounded models generally fitted all variograms best. The dominance of the bounded models is explained by the short-range trend and the stationary underlying processes that characterize these formations. All these parameters are good indicators of the limited spatial errors and that the spatial structure of these formations is well conveyed by the data sampling intervals. Gaussian curve fit is the prevailing model function within the studied formations, suggesting a smoothly varying pattern property. Just only the hillslope formation without trend is represented by a spherical model fit that vary in relation to change in the direction of the spatial continuity indicating smoothness or short-range variability. This is true in these formations since hillslope without trend is, indeed, a plane formation with a blurred prevailing pattern. But at high resolutions of 0.5-2 cm, gravels and stones as well as sinks of considerable dimensions (i.e. ≥ 10 cm) will form a nested landform structure with new geospatial properties. In fact, this is the roughness property of the analyzed formation. Furthermore, with the exception of channels, all formations with trend have higher sill variances than those without trend, which underline the importance of trend in semivariograms and geospatial analysis. Such geospatial property of stream channels indicates that such formations maintain the same behaviour independently of its steepness. Indeed, the smooth sill variation in landforms without trend indicates moderate prevailing process that could be altered easily with small changes in shape structure. Finally, all the studied sample datasets of the distinct relief formations was organized and summarized in order to verify prevailing patterns in the different landform components (table 6.7). This table shows each formation with the corresponding maximum and minimum continuity, scale effect, and the presence/absence of internal structures determined by the type of existing models.

Model parameters	Direction of Spatial continuity	Type of landform element							
		Ridge		hillslope		Channel networks		Stream initiation	
		Trend presence							
		with	without	with	without	with	without	with	without
Model type	0	Gaussian	Gaussian	Gaussian	Spherical	Gaussian	Gaussian	Gaussian	Gaussian
Nugget	0	0.0001	0.0001	0.001	0.0008	0.0001	0.0005	0.001	0.0005
Sill	0	0.0153	0.0159	0.0254	0.0225	0.0431	0.0551	0.0451	0.0301
Anisotropic ratio	0	2.8031	3.0224	2.4984	1.0913	2.6615	2.985	1.2186	1.9197
Model type	45	Gaussian	Gaussian	Gaussian	Spherical	Gaussian	Gaussian	Gaussian	Gaussian
Nugget	45	0.0001	0.0001	0.001	0.0035	0.0001	0.001	0.001	0.0005
Sill	45	0.1423	0.0751	0.1917	0.0283	0.0867	0.1529	0.0632	0.0655
Anisotropic ratio	45	1.1005	1.1	1.1216	1	1.2233	1	1	1
Model type	90	Gaussian	Gaussian	Gaussian	Spherical	Gaussian	Gaussian	Gaussian	Gaussian
Nugget	90	0.0001	0.0001	0.001	0.0022	0.0001	0.001	0.001	0.0025
Sill	90	0.2655	0.0971	0.4869	0.0235	0.1541	0.1246	0.0538	0.0886
Anisotropic ratio	90	1	1	1	1.0915	1	1	1	1
Model type	135	Gaussian	Gaussian	Gaussian	Spherical	Gaussian	Gaussian	Gaussian	Gaussian
Nugget	135	0.0001	0.0001	0.001	0.0016	0.0001	0.001	0.001	0.0015
Sill	135	0.1036	0.0739	0.1381	0.0292	0.1221	0.0918	0.0736	0.0781
Anisotropic ratio	135	1.2078	1.0112	1.4485	1	1.0581	1.1632	1.1027	1

Table 6.6 Parameters of the anisotropic models fitted to experimental variograms in four directions (0°, 45°, 90° and 135°) for each unit formation at 1 m.

Formation type	Model type	Axes of continuity		Scale effect	Observations
		Maximum	Minimum		
Ridge with trend	Gaussian	Contour lines	Ridge line	Available	Water flow is from ridge lines to adjacent hillslopes
Ridge without trend	Gaussian	Ridge lines	Contour lines	Available	Water flow through the ridge line and not to adjacent features
Hillslope with trend	Gaussian	hypsometry	Contour lines	None	Prevailing processes are relatively homogeneous at all scales
Hillslope without trend	Spherical/ unbounded	Blurred		Scale invariant	Local topography is the dominant factor (surface roughness)
Channels with trend	Gaussian	Stream line	Contour lines	Trivial	Prevailing processes and patterns are widely appreciated in the analyzed variogram
Channels without trend	Gaussian	Stream line	Contour lines	Moderate	Prevailing processes and patterns are widely appreciated in the analyzed variogram
Channel initiation with trend	Gaussian	Blurred		None	No prevailing trends and isotropy is widely appreciated
Channel initiation without trend	Gaussian	Stream line	Contour lines	Available	Contains characteristics of convergent topography and channel initiation

Table 6.7 Summary of semivariogram parameters and their interpretations deduced from the different analyzed formations of the studied area.

6.6.7. Spatial analysis in a stream-hillslope transect (toposequence profile)

In the studied mini-catchment, an exhaustive directional analysis was performed for the main landforms within the basin area. Such analysis allows for a detailed verification of the spatial structure as well as the prevailing patterns and trends that domain fluvial and flow movement within such formations. In the toposequence profile analysis we used the unit of 1 m as a constant dimension, which promises an acceptable compromise between the verified patterns in all the studied relief forms. At this scale, the all formations highlighted a clear representing trend over the rest of the sampled datasets (i.e. sample units). Further to that, and under the terrain conditions of the study area (i.e. badlands formations), 1 m is an acceptable dimension for visualizing conditions.

Previous results verified main geospatial properties of the main relief formations in the current studied landscape. Consequently, definition of convergent or divergent topography and the transition zone between them should be a foreseeable task. So, and in order to prove such conclusions a transect analysis, designated as toposequence profile, was realized in the small mini-catchment in the studied area. The toposequence profile undergoes from a pure channel formation to a clear hillslope passing through a transition zone of channel initiation area (figure 6.23). Herein, and in order to avoid repetition in figures presentation we pick out just only the transition zone (or what we believe to be a transition zone) and the two immediately adjacent samples from both sides, upward and downward. These sample datasets were selected to represent a pure channel and hillslope formations as well the intermediate zone between them; that is, channel initiation. This methodology was repeated in all stream links in the studied basin and results of two stream profiles were presented and discussed (figure 6.23). The first one is represented by the case (*A*), which is highly contrasted and the transition zone (i.e. channel initiation) is easily distinguished by eye observation. The second case (i.e. case *B*) is smoothly contrasted and the transition zone is hardly appreciated by eye observation.

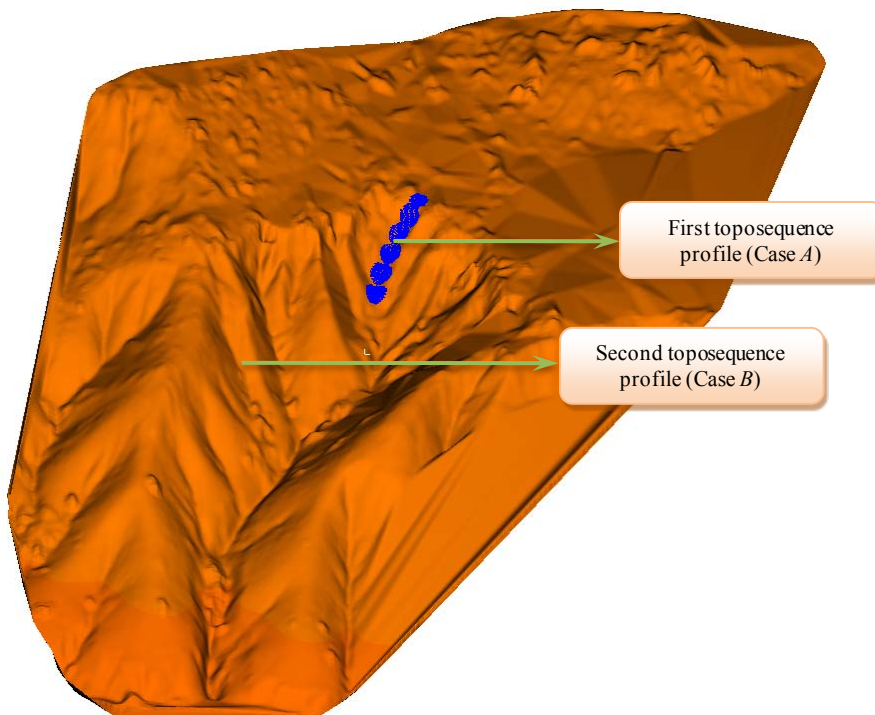


Figure 6.23 Location of the profile transects (toposequence profiles) in the studied mini-catchment. Case (A) represents a clear transitional area from a perfect stream to a complete hillslope form, whereas Case (B) shows a smooth transition between formations.

6.6.7.1. Toposequence profile with clear limits (case A)

The analysis of the sample datasets along the toposequence profile (A) revealed two breaking points between the three formations that allows for a clear definition of the limits of each one. First, in channel formations, the semivariogram analysis showed a clear anisotropic effect highlighted by the $A:B$ ratio (figure 6.24a). Such anisotropy is widely evident by the shape of the two curves and the magnitude of the ratio values in these formations, which approximate to 2.3 and 2.56 for stream 1 and stream 2, respectively (table 6.8). Moreover, a Gaussian fit model has been observed in all the examined directions highlighting the presence of a smooth and gradual change between directions. Likewise, values of sill variance maintain a directional effect with smooth anisotropy that oscillate between 0.032-0.111 and 0.024-0.127 for stream 1 and 2, respectively (table 6.8), which is in well agreement with previous results on channel-formation analysis.

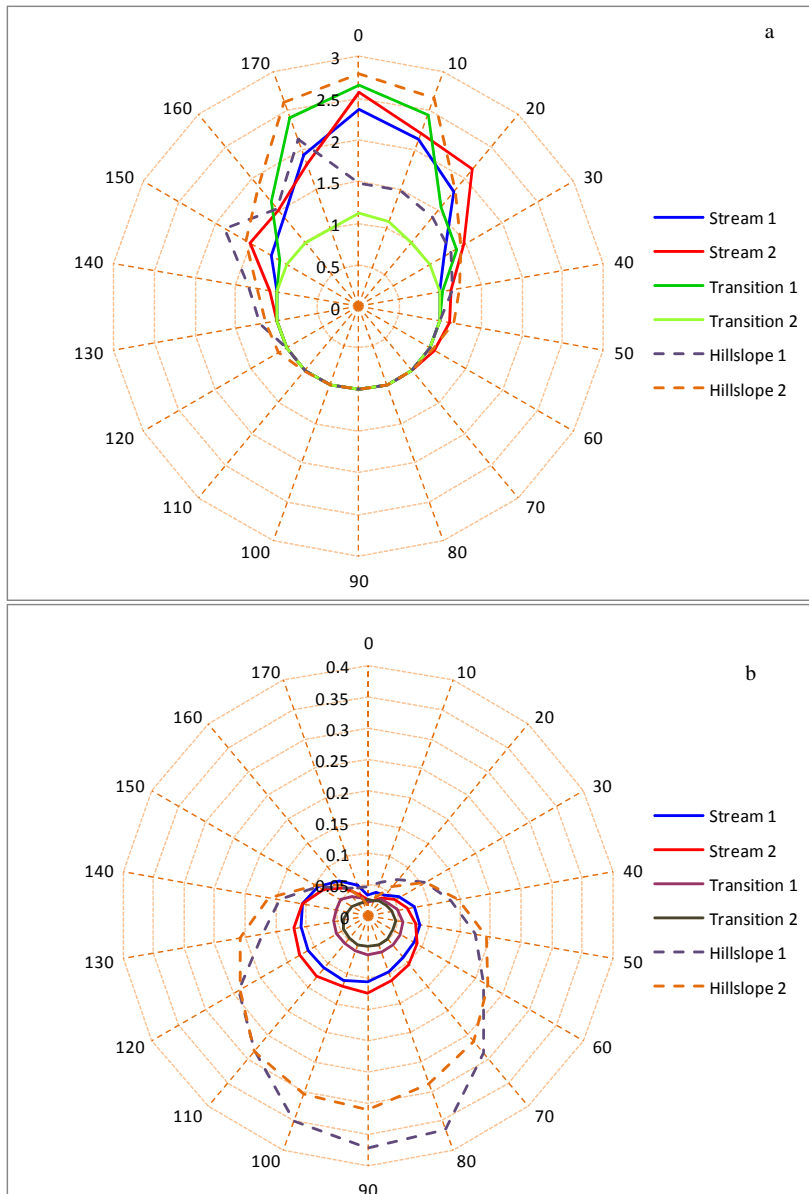


Figure 6.24 Schematic representations for the semivariogram parameters of (a) anisotropic ratio and (b) sill variance for the analyzed landforms within the toposequence profile A in the studied area.

Model parameters	Direction of Spatial continuity	Type of landform element					
		Stream 1	Stream 2	Transition 1	Transition 2	Hillslope 1	Hillslope 2
Model type	0	Gaussian	Gaussian	Gaussian	Spherical	Gaussian	Spherical
Nugget	0	0.0001	0.0001	0.0019	0.005	0.0033	0.0001
Sill	0	0.0328	0.0245	0.0208	0.0252	0.0454	0.0162
Anisotropic ratio	0	2.3622	2.5664	2.9472	1.1219	1.4811	2.7991
Model type	45	Gaussian	Gaussian	Gaussian	Spherical	Gaussian	Gaussian
Nugget	45	0.0001	0.001	0.0023	0.003	0.0035	0.001
Sill	45	0.0866	0.0781	0.0528	0.0427	0.1546	0.1673
Anisotropic ratio	45	1.0105	1.2731	1.0333	1	1.0511	1.2011
Model type	90	Gaussian	Gaussian	Gaussian	Spherical	Gaussian	Gaussian
Nugget	90	0.0001	0.004	0.0001	0.002	0.0022	0.004
Sill	90	0.1114	0.1273	0.0624	0.0493	0.3715	0.3119
Anisotropic ratio	90	1	1	1	1	1	1
Model type	135	Gaussian	Gaussian	Gaussian	Spherical	Gaussian	Gaussian
Nugget	135	0.0001	0.001	0.001	0.006	0.0032	0.001
Sill	135	0.1079	0.1115	0.0558	0.0331	0.1622	0.1213
Anisotropic ratio	135	1	1.0041	1	1	1.2745	1.1973

Table 6.8 Parameters of the anisotropic models fitted to experimental variograms in four directions (0°, 45°, 90° and 135°) for each unit formation in the toposequence profile.

Moving upward throughout the transect profile, the transition zones reveal varying information and results. For the first transition zone, the semivariance analysis shows a fairly high anisotropic ratio of 2.94 (figure 6.24a), similar or even higher than those observed in channel formations, while sill variance decreases to values that oscillate between 0.02-0.063 (figure 6.24b). This change or smoothness in sill variance and the maintenance of anisotropic ratio may be explained by the presence or the initiation of a new formation. In this case, the shape structure of the stream formation is maintained while a new prevailing process is initiated giving rise to the beginning of a new formation. This change in pattern formation is confirmed totally by the results of the second transition zone, where both parameters and even type of fitted model is altered completely (table 6.8).

In transition zone 2, two important points have been observed: first, the analyzed transect seems to contain more than one structure present, i.e. the variogram has a nested form (figure 6.24a). Since the analyzed structure contains a directional effect, the best fitting model could be an alteration between double spherical and Gaussian functions (table 6.8). Herein, the semivariogram was decomposed into 2 main components: the short-range component has a range of about 0.27 m and the long-range component is about 0.78 cm (figure 6.25b & c). These results indicate a complex structure shape marked by a sink-like formation (figure 6.26). Such structure form is the direct responsible for the presence of two fit-curve models (i.e. Gaussian and spherical) in such small dimensions. The short-range component corresponds to the sink structure whereas the long-range is related to the complete sample. Second, in the whole sample, the anisotropic ratio approximates to unity, giving rise to smoothly altered shape structure. Whereas, the sill variance maintains similar values to the first transition zone or even smoother (figure 6.24b) giving rise to approximately zonal anisotropy (figure 6.27). The smooth sill variance in these cases may be explained by the presence of two contradictory forces that acts in different directions leading to smooth variation throughout the analyzed directions.

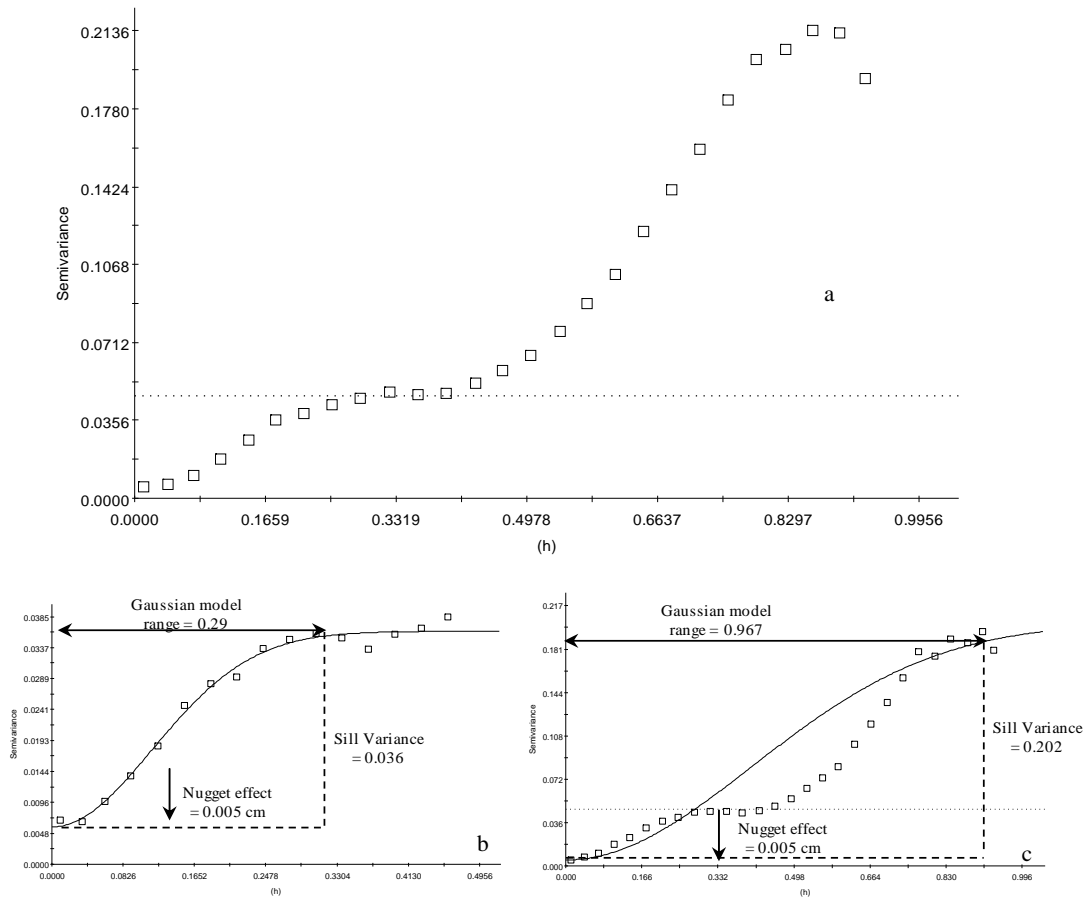


Figure 6.25 Nested-curve structure formed in the second transition zone of the analysed toposequence; a) the spatial variance of total data in the analysed unit, b) the variogram parameters of the sink-like formation, and c) the variogram parameters of the total unit.

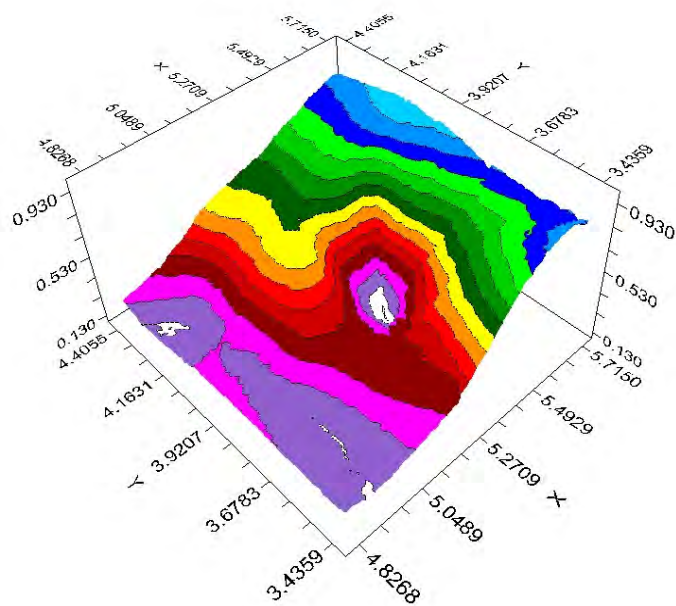


Figure 6.26 Kriging interpolation for the second transition zone. The sink-like formation is well appreciated in the centre of the figure.

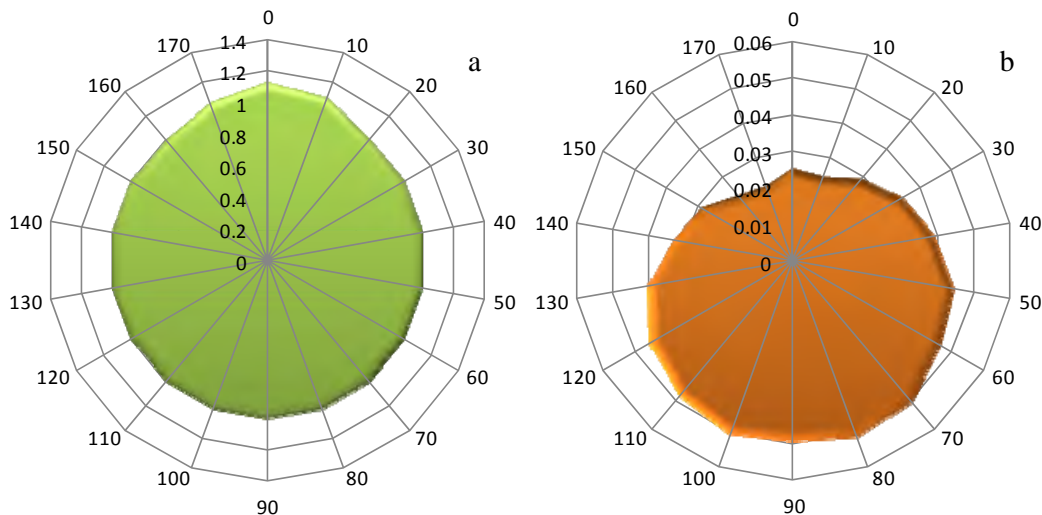


Figure 6.27 Zonal anisotropy observed in the second transition zone; a) Rose plot curve for anisotropic ratio; and, b) Elliptical rose plot curve for sill variance.

Finally, moving 1 m upward we will go into a new component that is completely different to the anterior ones. The semivariogram parameters of $A:B$ ratio and sill variance adapted new positions indicating new breaking point and hence a new formation. First, anisotropic ratio adapted an intermediate position between channels and transition zones of values that oscillate between 1-2.12 (i.e. concentrated between 130-40°) and 1-2.79 (i.e. concentrated between 120-50°), for hillslope 1 and 2, respectively (figure 6.24a). This change within these directions suggests a considerable elongation in the opposed direction of the contour lines. This is somewhat explained by the position of the first hillslope sample dataset in the studied catchment, which is a very abrupt inclined hillslope of 88.53°. Again, Gaussian fit model is the dominant in these formations highlighting a continuously smooth change within these components (table 6.8). Finally, sill variance demonstrates a clear breaking point and a sever change in variance values in relation to the past formations with values that oscillate between 0.045-0.371 and 0.016-0.31 for hillslopes 1 and 2, respectively (figure 6.24b). Such abrupt change in sill variance is attributed to the maximum spatial continuity throughout the contour lines and minimum continuity along the hypsometry suggesting high variability with elevation change. This explains why drop water continues downward controlled by gravity and in the direction of elevation change but in no way concentrated in real streams. While in stream formations variation in channels are controlled by more than one process (i.e. concentrated flow within the channel, lateral flow over the banks of the channels, hypsometry in the direction of the stream and in the directions of lateral banks), which acts in different directions giving rise to smoother sill variations as observed in earlier formations analysis. Yet again, these values are in good agreement with previous results of hillslope formations presented earlier.

It is widely evident that sill behaviour in channel initiation forms take a regular tendency with smooth variations between directions (figure 6.24b) highlighting little information about prevailing pattern or processes. As mentioned earlier, $A:B$ ratio or sill variance of a semivariogram highlighted

parts of the information related to the structure form and prevailing processes, for which it is necessary the use of both parameters for such verification. Thus, it is widely acceptable that in nature where landscape formation presents a considerable change between anterior and posterior datasets in a toposequence analysis the components under study belongs to different formations. So, in relation to toposequence (A) direct comparisons between anisotropic ratio and sill value as well as changes in model fit in the studied formations confirm that channel initiation is presented at this point.

Herein, the different variations in sill values in the distinct formations presented in figure (6.24b) could be attributed to changeable prevailing processes at each level. In channel formation the sill values reach a summit at 0.116 and 0.123 for stream 1 and 2, respectively, which is a sound indicator of the presence of a moderate prevailing process attributed to different runoff types (table 6.9). The moderate effect of runoff in these formations is explained by the small lateral banks of streams, which is about 60 cm to nearest ridge of the stream bottom. Such prevailing pattern tend to vanish as we are moving up toward the transition zones, or stream initiation, where, in this case, sill values reach a summit at 0.062 and 0.051 for transition 1 and 2, respectively. This small variation in sill values may be explained by the presence of unclear domain trend between divergent and convergent topography, where in channel initiation prevailing processes tend to disappear at this scale, or higher resolutions may be needed in order to explain underlying processes in these formations. While moving up toward hillslope formations, two types of formations are encountered. First, an approximately vertical hillslope (table 6.9) with sill values that oscillate between 0.045-0.3715 (table 6.8) was configured directly up the second transition zone. Second, a smooth to moderate hillslope formation of about 15.25° and a sill variance that oscillates between 0.016-0.31 (table 6.8) is verified exactly above the vertical hillslope formation. The high values of sill variance in the hillslopes are attributed to the hypsometric effect, which is perpendicular to the axis of minimum spatial continuity of the contour lines. It seems that although the two hillslope types vary greatly in slope, sill variance maintains approximately constant within these formations. The same is observed with streams and their initiation zones. This suggests that same structure formations are smoothly altered with slope in relation to the type of prevailing process. In fact, in convergent and divergent topography, prevailing processes are widely controlled by the runoff type, which in turn control sediment movement within these formations. Indeed, slope is responsible for acceleration rate of runoff and the transported sediment amounts in channels and hillslopes formations (Chorley et al., 1984) and not the runoff type.

The above findings underline the presence of breaking points between the different formations, e.g. stream, hillslope and the transition zone. Channels and hillslopes possess particular scale characteristics represented by similar values of sill variances for similar structures of similar local conditions. Maximum values of sill variance oscillate between 0.11-0.12 and 0.37-0.31 for channel and hillslope formations, respectively. These values represent minimum change in sill variance between similar formations. While in channel initiation the situation is completely different

where maximum sill variance reaches 0.063 and 0.051 for channel initiation 1 and 2, respectively. The low values indicate the presence of a smooth and gradual change in dominant process in the transition zone or channel initiation (i.e. the stream initiation area where runoff changes from divergent-dominance to convergent-prevailing pattern). These smooth changes in sill variance and even the small average variance value combined with anisotropic ratio will form the bases of selection criteria to define limits of stream networks or channel initiation zones. This fact could be attributed to the behaviour of relief formations, which varies considerably in relation to the internal structure of the formation, its position in the analyzed transect (e.g. stream, transition, hillslope, and vice versa), and type of prevailing processes within such elements. From one hand, resemblance in $A:B$ values may be explained by similarity in shape structure, prevailing materials, and/or the dimension of the sample datasets. On the other hand, pure prevailing processes may sustain approximately similar sill variance, although it occupies varying forms and aspects of the same formations (e.g. hillslopes of different inclinations or positions in the basin unit). In addition, similarity in prevailing materials as well as the dimension of the sample datasets may clarify such similarities in the obtained values. These factors should be taken into account in result interpretations in landform definition by semivariograms.

Profile section	Slope (degree)	sill variance		Prevailing runoff type
		minimum	maximum	
Stream 1	33.39	0.0328	0.1115	Concentrated flow within the channel and lateral flow over the channel banks
Stream 2	34.57	0.0245	0.1264	
Transition 1	41.44	0.0208	0.0631	Divergent to convergent runoff
Transition 2	39.03	0.0252	0.0513	
Hillslope 1	88.53	0.0454	0.3715	Divergent runoff
Hillslope 2	15.25	0.0162	0.3119	

Table 6.9. Slope and sill variance of the profile sample datasets in the studied area.

6.6.7.2. Toposequence profile with smooth limits (case B)

Actually, defining what we believe to be a channel head for the sample analysis is also another complicated task. Because channel heads could be strictly limited or smooth vanishing structures. In the first case, selection is direct and stream initiation should be the point exactly above that limit or the limit itself. Conversely, in smooth vanishing limits channel initiation is blurred or fuzzy and defining where stream begins is extremely complicated. Indeed, the second case is the wide probably to meet since in nature localizing the exact point of channel initiation would be a tedious and a complicated task. In this case, stream limits or the transition zone is the area at which semivariogram parameters are shifted from one spatial characteristic to another. So, a fairly smooth channel structure has been selected within the analyzed catchment (case B in figure 6.23), which represents an indefinite channel initiation zone. In this case, 4 sample datasets were studied, which extends from a pure channel to a clear hillslope formation (Figure 6.28). The semivariogram analysis revealed the presence of a clear

“breaking point” between streams and hillslope formations, even when the visualized elements was not clear enough to depict the limits of stream formation. Such breaking point is widely evident in sill variance (figure 6.29b), indicating different prevailing processes between the two formations. Even what we believe to be initiation zones (indicated by the SI-1 and SI-2 in figure 6.28) were aligned with the neighbour formations and not as separated ones indicating high similarity in the dominant processes with these elements (figure 6.29b). The anisotropic ratio highlighted trivial information on the limits between formations (figure 6.29a) confirming that anisotropic ratio or range parameter is best suitable to describe the shape of landform components. These results don’t confine the use of both parameters to verify the limits between formations, where shape of relief forms contains enough contrasts to be distinguished, as we saw earlier. The four studied formations have been interpolated separately in order to enhance the contrast in landform visualization (figure 6.30).

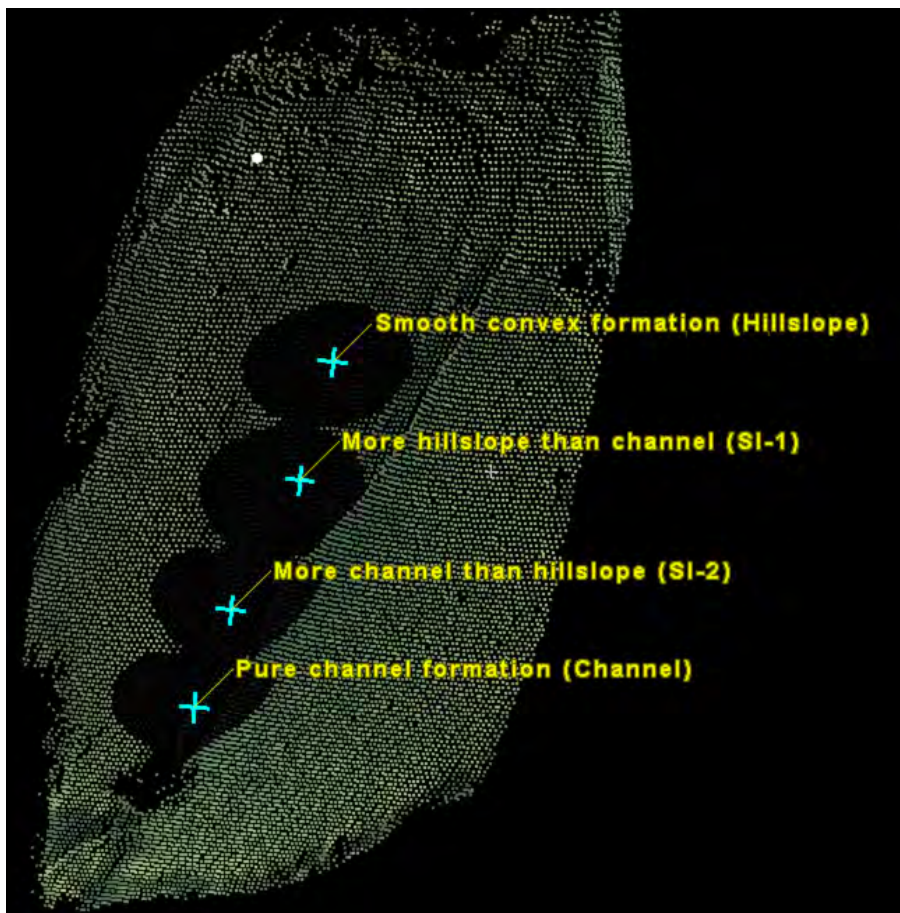


Figure 6.28 Channel-hillslope toposequence for a smooth transition zone presented as case B in figure (6.23).

In general, the common product utilized in the analysis and derivation of landform components are DEMs and not the digital land surface models (DLSMs) obtained directly from laser scanning technique. So, the above methodology and analysis were repeated on the same formations (i.e. the same profile transects) using gridded-DEM data, in order to understand the effect of the interpolation on landform behaviour. First, all the catchment has been interpolated using the *IDW* approach. Second, the same toposequence profiles have been extracted and the same methodology

analysis was repeated for each sample location, e.g. 6 samples for the first transect and four for the second one. Results of the geospatial analysis and the semivariograms are presented and contrasted between the two formations (i.e. real and simulated forms).

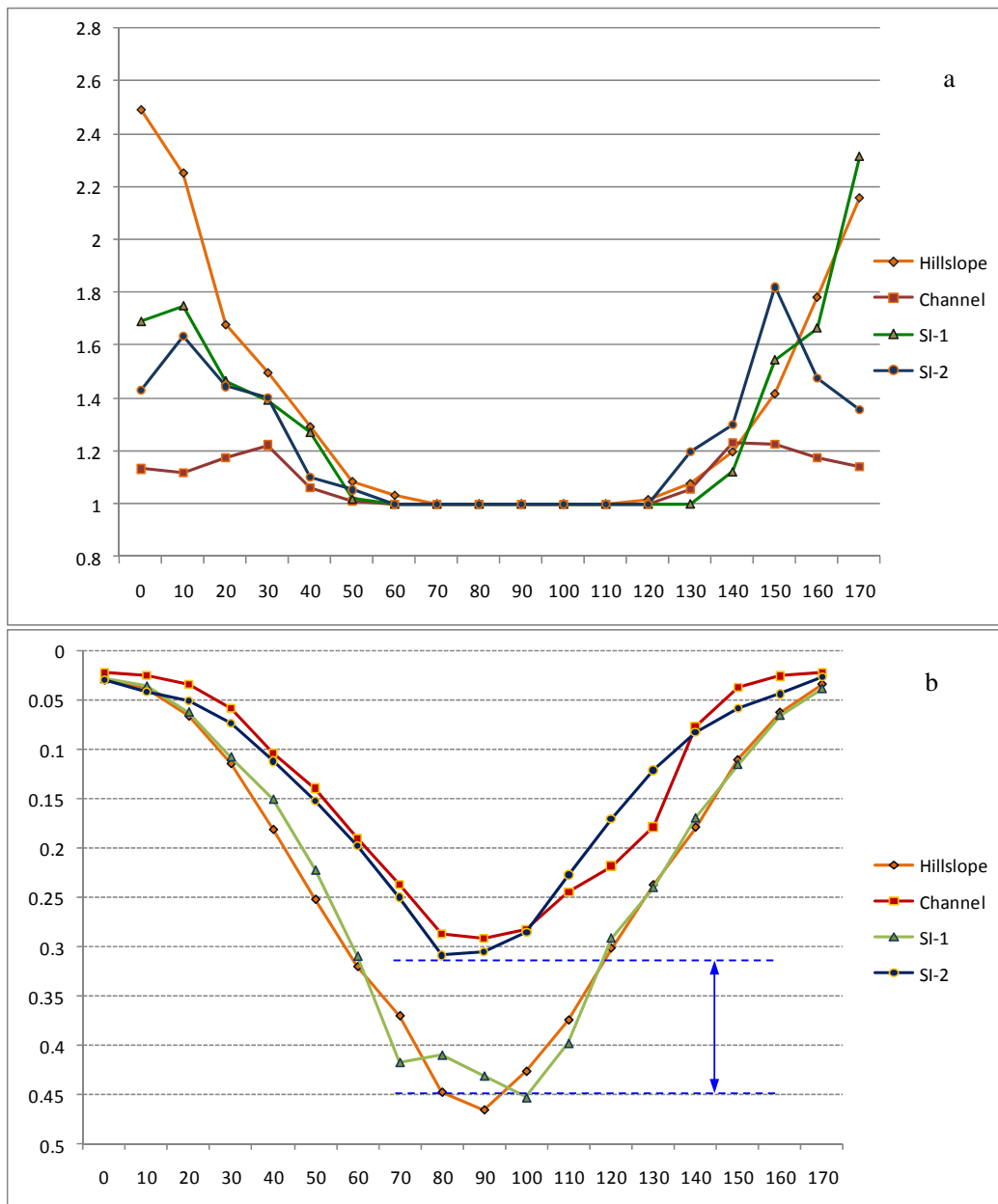


Figure 6.29 Schematic representations for the semivariogram parameters of a) anisotropic ratio and b) sill variance in the toposquence profile *B*. Dotted blue lines indicate the separation distance between the analyzed formations.

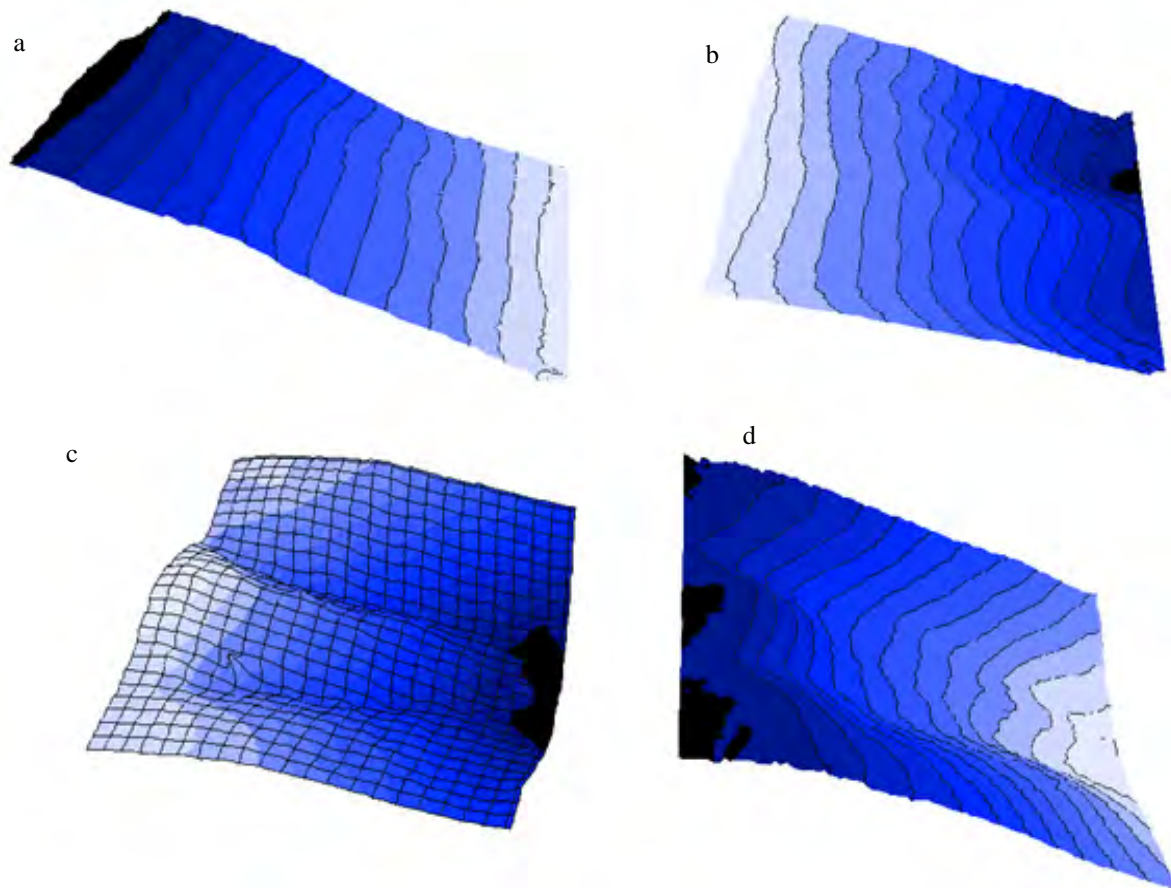


Figure 6.30 Interpolation of the sample datasets in the toposequence profile of case (B), organized in a descending form as follows: a) pure hillslope formation; b) first transition zone (SI-1); c) second transition zone (SI-2); and d) a pure channel formation.

6.6.8. Spatial analysis in simulated landscape (DEMs)

In order to avoid redundancy in data analysis, we opted for analyzing the stream-hillslope profile only because it provides a comprehensive understanding of landform behaviour under simulation conditions. The 6 sample datasets that form the stream-hillslope profile of the toposequence (A) have been analyzed and the semivariogram parameters were depicted and detached (figure 6.31). The initial results demonstrated again the presence of a breaking scale that separate channel formation from hillslope structure forms, clearly presented in sill variance (figure 6.31b). Once more, this behaviour could be attributed to the presence of different prevailing processes within each structure formation leading to such breaking scales. However, the anisotropic ratios provided trivial information on the presence of a clear separation between landform structures and indistinct breaking scales were observed (figure 6.31a). The $A:B$ values for each structure formation showed the presence of a clear anisotropy in all data structures. While these values are smooth for channel formations, hillslope structures demonstrated extremely directional effect. These results confirm again that hillslope formations maintain a more uniform shape structures, whereas streams are more complex landforms with varying shape formations (e.g. bed form, stream banks, etc.).

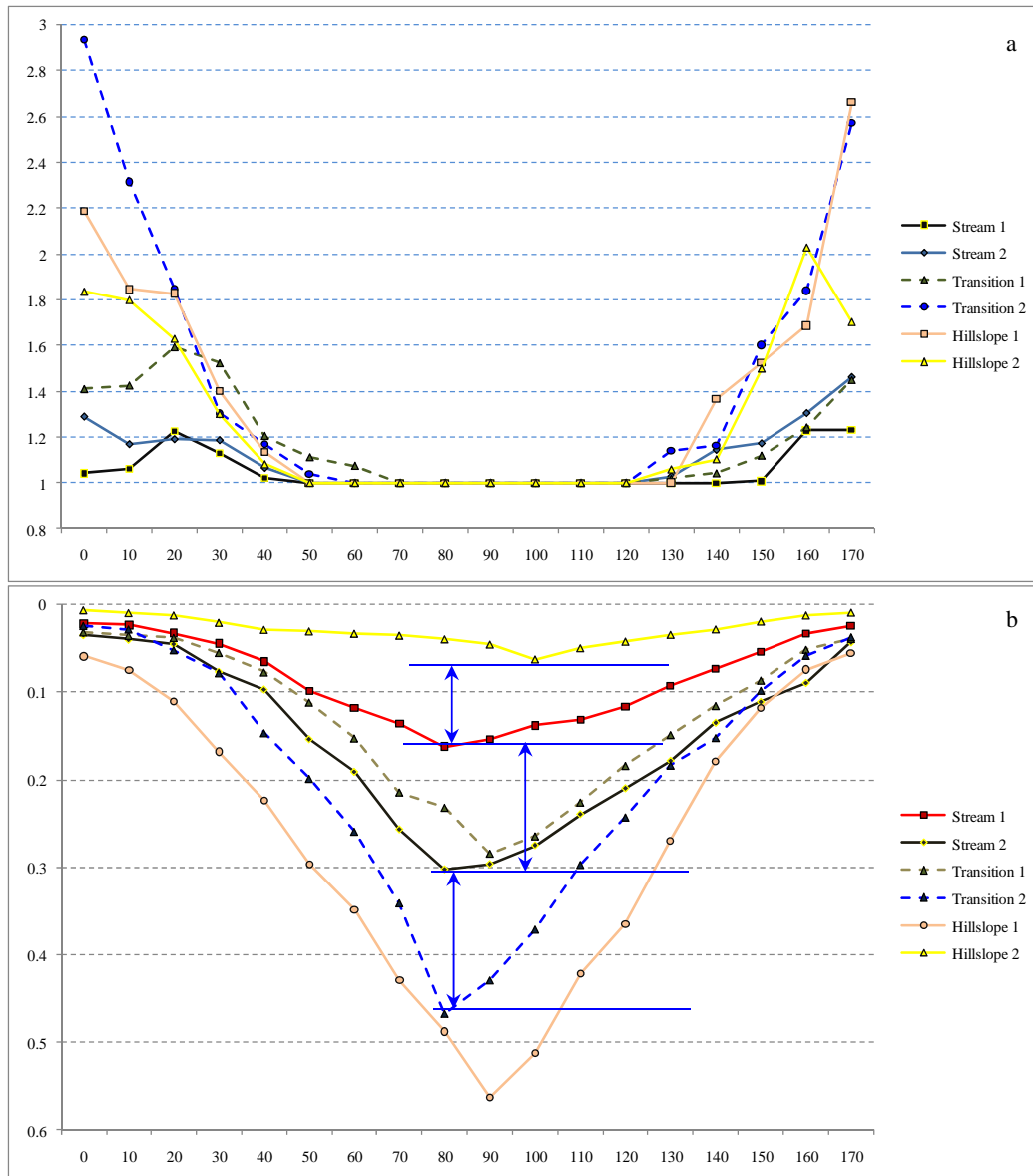


Figure 6.31 Schematic representations for the semivariogram parameters of (a) anisotropic ratio and (b) sill variance for the analyzed landforms within the toposequence profile A in the studied area using DEM data. The continuous blue lines indicate the breaking scale between values.

While channel and hillslope structure formations revealed similar tendencies in the geospatial analysis for real and simulated datasets, transition zones (i.e. channel initiation) confirmed varying behaviours. First, the spatial characteristics have been disappeared and the transition zones adapted neighbouring-formation properties, that is, channel or hillslope. The interpolation processes have smoothed these formations leading to new characteristics underlined by the type of prevailing processes. If the interpolated transition zone demonstrates geospatial characteristics that approximate to the general tendency of streams then it was classified as channel formations, and vice versa. This is widely appreciated in the two analyzed transition zones, where sill variations were altered in relation to neighbour formations. The curve of the first transition zone, with dotted green line in figure 6.31b, is located between the ranges of the two stream formations highlighting the presence of stream-like structure in this formation, and hence classified as channels. Conversely, the second transition zone

was shifted up from the first one and situated near the ranges of hillslope sill values (dotted blue line in figure 6.31b) indicating a hillslope formation. This is widely acceptable since the first transition zone is situated next to the channel stream formation; whereas the second transition zone is located between the hillslope and the first transition zone giving rise to more divergent topographic structure property. Such findings and results are similar to those obtained in the analysis of the smooth stream-hillslope profile, which confirms the smoothing effect of the interpolation processes (Burrough & McDonnell, 1998). Of course, such findings should be contrasted with other interpolated data of different interpolation procedures (e.g. IDW vs. kriging, or ANUDEM vs. kriging) in order to confirm these effects.

Moving upward, the final structure in the analyzed profile revealed completely different characteristic properties in comparison to the other formations. First, variations in sill variance are reduced to oscillate between 0.0062-0.0625, but in the same time maintain a strong directional effect (figure 6.32a). In the same direction, the anisotropic ratios show a considerable directional effect that coincide well with hillslope 1 (figure 6.32b). The considerable differences between the two structures can be explained by the detailed inspection of the two formations. While the first hillslope formation sustains a high inclination of 55.31° , the hillslope 2 formation is maintains a moderate inclination of 21.25° (figure 6.33). Such characteristics highlighted the presence of a new component, that is, a plane and smooth relief formation with a low fractal dimension of 2.19, which characterizes such surfaces. Herein, local relief or microtopographic effect is prevailed, and the directional effect is related to the slope direction. Water movement in these formations is similar to water drop in plane surfaces, where water drops maintain a random movement controlled by the microtopography and trend direction. The different categories of the grouped formations are well appreciated by the continuous blue lines in figure (6.31b), where 3 structured groups are well appreciated: the smooth hillslopes (i.e. plane element), typical hillslopes and stream channel formations.

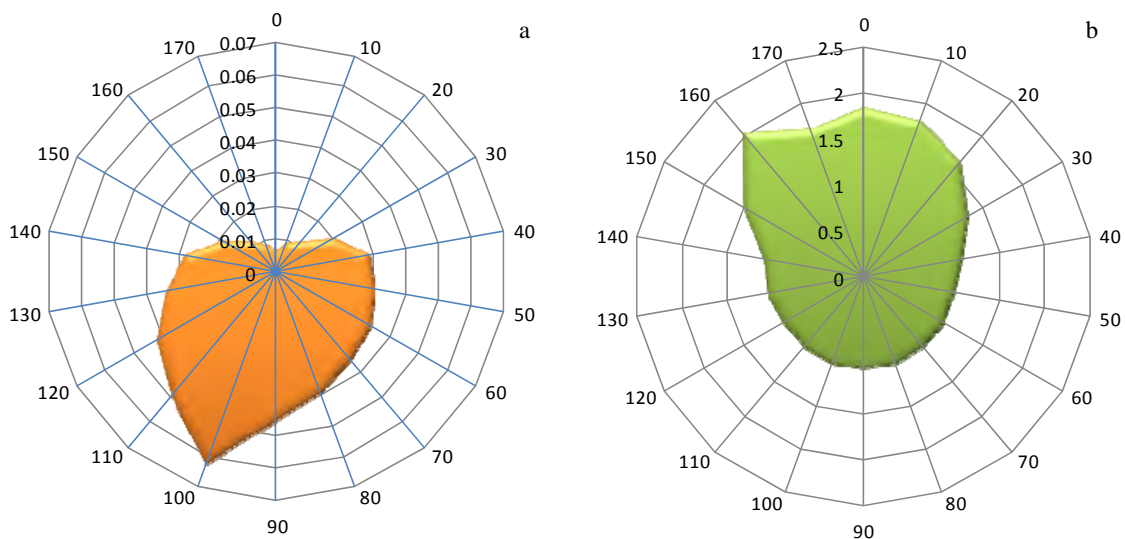


Figure 6.32 Semivariogram parameters of (a) sill variance and (b) anisotropic ratio from hillslope formation 2 in the analyzed profile fitted in 18 directions (0° - 170° clockwise from north – unit circle).

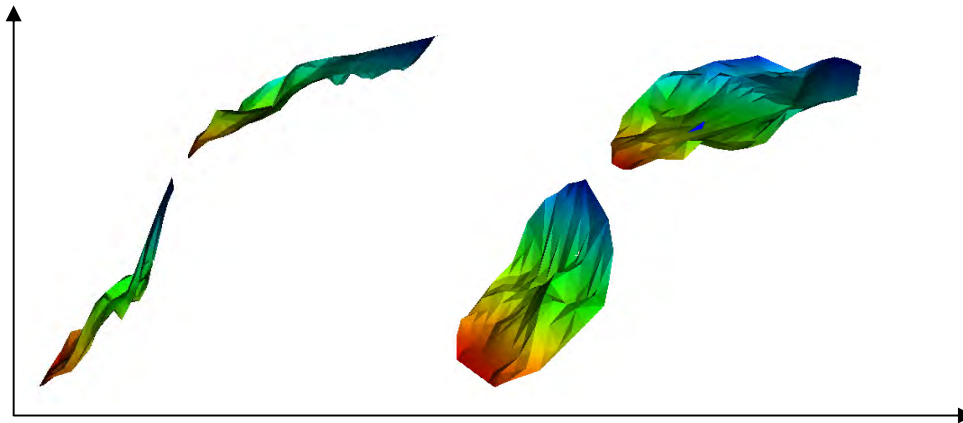


Figure 6.33 Degree of inclination in the two sample datasets that represents hillslope 1 & 2 used in the toposequence analysis of simulated landscape.

Another important aspect that was observed in simulated datasets is the direction of variations in stream river formations. All stream formations revealed unclear tendency, where minimum and maximum altered in relation to the sample dataset position in the landscape (figure 10, appendix 1). First stream formation (figure 10a, appendix 1) shows that the direction of the stream line is exactly perpendicular to the x axes in the posted data. Whereas in the map of maximum spatial continuity, the minimum variation has two scales: the first is within the 0.59 cm and the second is extended in all the sample dataset (i.e. 1 m). In the first scale, the directions of minimum variations are altered between the N-S and the E-W directions. In the second scale, the minimum variation is a lined with the E-W direction. These results imply isotropy in the short scale and clear anisotropy in the longest scale. Moving up in the profile analysis, the rest of the analyzed stream formations revealed a minimum variation in a diagonal direction between E-W and N-S directions (figure 10b & c, appendix 1). These results are somewhat contradictory to the earlier findings that maximum variations are prevailed across stream lines suggesting more water movement from the stream bank to the bed river than along the stream itself. Such effect could be explained by the smooth inclination of the stream banks in relation to the stream bed (figure 6.34). Herein, the interpolated surfaces are smoothed enough to provide stream banks that seems to be a kind of continuation to the stream bed rather than a clear stream bank. These effects provided a maximum continuity a cross river direction and maximum variation along the stream line. So, attention should be given to the type and dimension of the analyzed data in geospatial analysis of landform units. Finally, the hillslope formations revealed a similar behaviour to real datasets, where minimum variations are located perpendicular to the contour lines and in the direction of steepest inclination (figure 11, appendix 1).

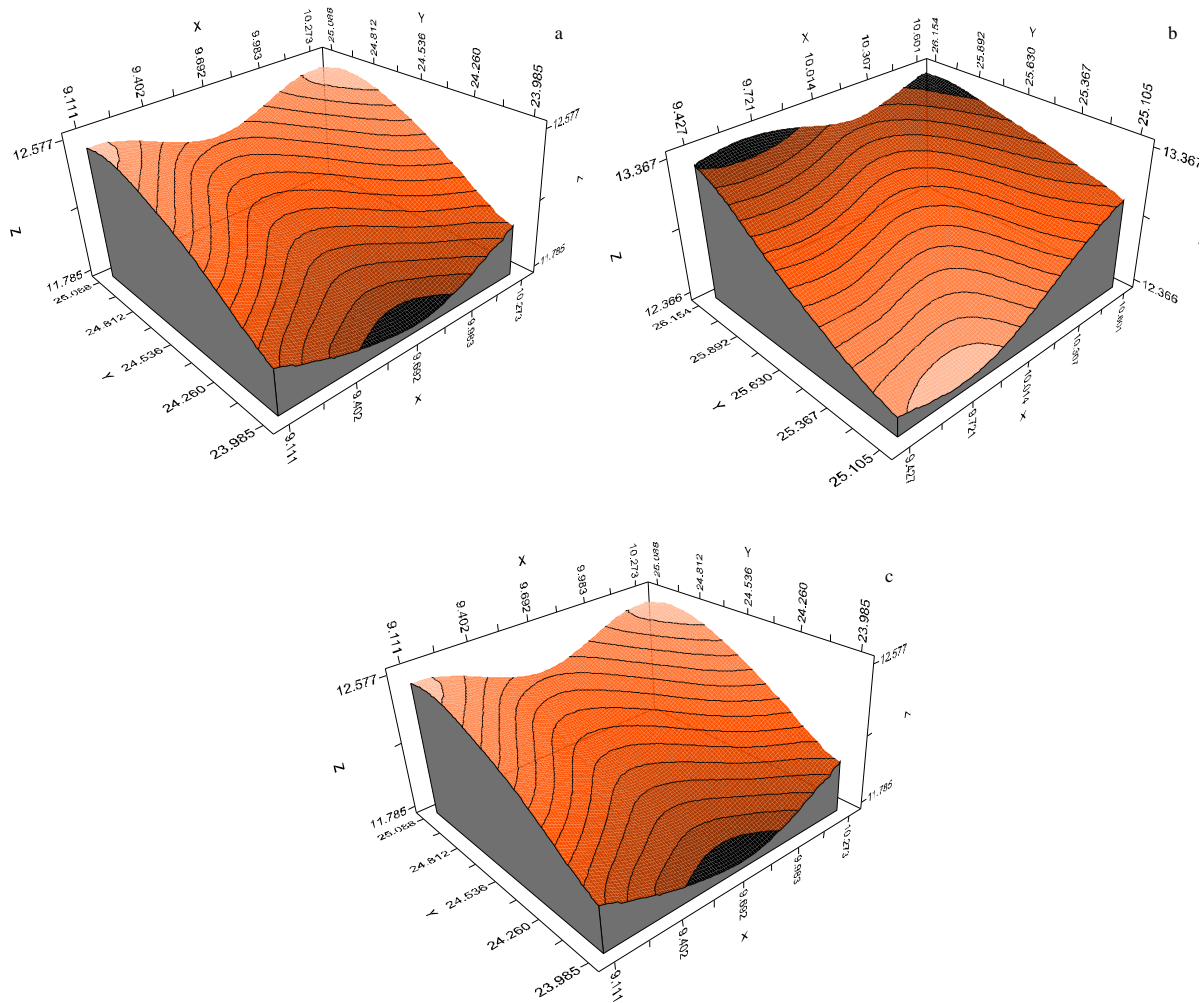


Figure 6.34 3D reconstructions of stream formations representing variations between stream bank and stream bed of the analysed units of (a) stream 1, (b) stream 2, and (c) transitions zone 1.

6.6.9. Delineation and validation of stream network limits

First, the curvature method (Ames & Tarboton, 2001) has been applied to code cells in the DEM either as channelled or unchannelled formations. Second, Stream networks in the analysed mini-catchment were delineated by the *CDA* and the $R'_A t$ techniques (described earlier in chapter five). With the *CDA* procedure, a value of 108 cells has been defined as the appropriate threshold (A_S) to define stream limits leading to a well-developed stream system but with clear false surplus in the upper part of the catchment (figure 6.35). A quick inspection to the constructed 3-dimensional landscape of figure (6.35) reveals with no doubt an erratic A_S value that depict well drainage network dissection in the mid and lower part of the catchment, but with a clear invasion of stream limits in the hillslopes of the basin. Again, such results confirm the limited capacity of the *CDA* technique under particular landscape conditions of homogeneity. Alternatively, the $R'_A t$ technique delineated channel network limits by A_S value of 375 cells leading to a moderately dissected stream system (figure 6.36). In this case, the defined streams are localised within the drainage system and did not invade the hillslope formations.

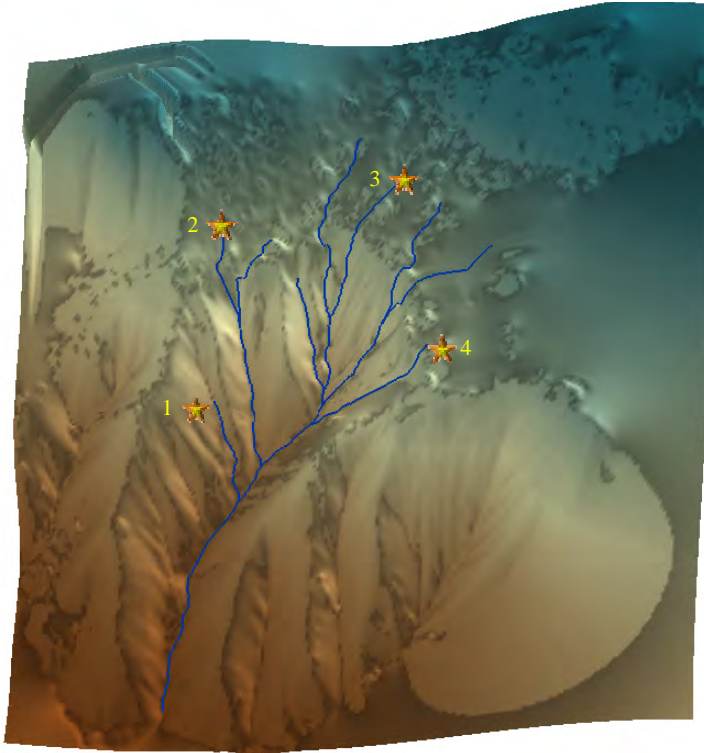


Figure 6.35 3D representation of the analysed mini-catchment and the corresponding channel network delineated by the Constant Drop Analysis (*CDA*) approach. Stars and numbers indicate the location of the analysed stream heads.

Confirmation of such affirmations is widely obtained by the spatial analysis and semivariograms in stream heads and in some toposequence profiles in both generated channel networks. Accordingly, in both automated drainage networks various stream limits were selected (figures 6.35 & 6.36) and the source area of each link (i.e. represented by a circle terrain unit where its centre coincides with the stream source) was tested. Tables (6.10 & 6.11) underline the semivariogram parameters of the four analysed stream heads with the two compared techniques. For the *CDA*, just only the first stream head confirms a channel-like structure whereas the rest confirms clear hillslope formations. Conversely, the semivariogram parameters prove that all stream heads defined by the $R'_A t$ technique correspond to channel and stream formations. Although the anisotropy is usually higher in hillslope formations, it was the sill variance that allows for a straightforward separation between formations (hillslopes vs. streams). Such effect is widely attributed to the interpolation process used to generate the regular-gridded data (i.e. DEM), which may smooth or crease the surface leading to biased conclusions.

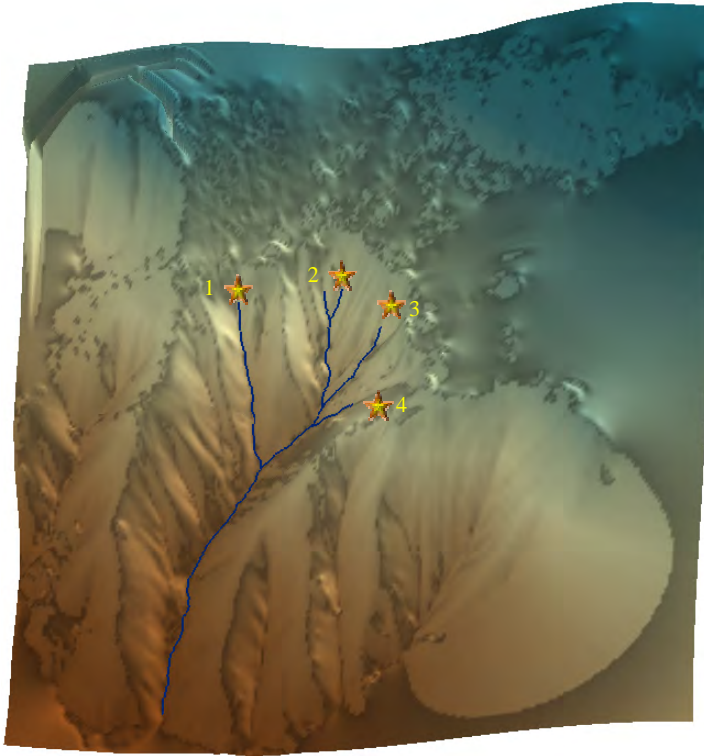


Figure 6.36 3D representation of the analysed mini-catchment and the corresponding channel network delineated by the $R'_A t$ approach. Stars and numbers indicate the location of the analysed stream heads. Stars and numbers indicate the location of the analysed stream heads.

Finally, both automated drainage networks defined from the 6-cm and 1-m DEM resolution were compared and overlapped in order to test and verify the capacity of the applied techniques (i.e. $R'_A t$ vs. CDA). Figure (6.37a & b) describes channels location of the compared techniques of the two scale units (i.e. 19040 m² vs. 956 m²) for the different resolutions (i.e. 6 cm vs. 1 m). Both techniques depicted well the main channel segment in the low resolution, which corresponds to first order link in the high scale units. In the higher resolution and low scale unit, such segment was defined as second and third order links for $R'_A t$ and CDA techniques, respectively. In both scales and resolutions, the CDA technique provided a channel network system well developed but with a clear erratic aspect in some parts of the catchment, translated in feathering or invasion in the hillslope formations, leading to doubt efficiency in defining stream limits or channel heads. Conversely, $R'_A t$ technique provided a robust drainage aspect, where landscape dissection is well described by the delineated stream networks with a clear vanishing for the erratic aspects observed in the CDA approach, again in both scales and resolutions.

Angle (α)	Model type	Nugget ($C0$)	Sill ($C0+CI$)	Range Min. (B)	Range Maj. (A)	Anisot. ratio ($A:B$)
Stream head 1						
0	Gaussian	0.0016	0.0302	30.02	43.64	1.2461
45	Gaussian	0.0017	0.1213	78.94	88.71	1.1237
90	Gaussian	0.0012	0.2972	117.7	117.7	1
135	Gaussian	0.0011	0.1078	79.2	89.6	1.1313
Stream head 2						
0	Gaussian	0.0001	0.0215	58.61	167.2	2.8527
45	Gaussian	0.0001	0.2838	199.4	220.8	1.1073
90	Gaussian	0.0001	0.6263	235.6	235.6	1
135	Gaussian	0.0001	0.2865	206.9	218.9	1.0579
Stream head 3						
0	Gaussian	0.001	0.0208	65.21	166.4	2.5519
45	Gaussian	0.001	0.3489	204.0	215.4	1.0559
90	Gaussian	0.001	0.9353	268.5	268.5	1
135	Gaussian	0.001	0.3488	205.8	224.9	1.0928
Stream head 4						
0	Gaussian	0.011	0.0188	40.14	104.8	2.611
45	Gaussian	0.001	0.1933	160.1	175.6	1.096
90	Gaussian	0.001	0.7535	266.3	266.3	1
135	Gaussian	0.001	0.7495	310.8	357.6	1.1503

Table 6.10 Parameters of the anisotropic models fitted to experimental variograms in four directions (0°, 45°, 90°, and 135° counter-clockwise from axis of maximum continuity) for stream heads delineated with CDA technique and marked with stars in figure 6.35.

Angle (α)	Model type	Nugget ($C0$)	Sill ($C0+CI$)	Range Min. (B)	Range Maj. (A)	Anisot. ratio ($A:B$)
Stream head 1						
0	Gaussian	0.0001	0.0468	45.73	70.48	1.5412
45	Gaussian	0.0001	0.1037	84.3	84.3	1
90	Gaussian	0.0001	0.1981	127.2	127.2	1
135	Gaussian	0.0001	0.1957	177.05	195.1	1.1022
Stream head 2						
0	Gaussian	0.001	0.0327	45.74	59.3	1.2966
45	Gaussian	0.001	0.1314	115.8	124.4	1.0742
90	Gaussian	0.001	0.3013	155.8	155.8	1
135	Gaussian	0.001	0.2316	151.4	151.4	1
Stream head 3						
0	Gaussian	0.0016	0.0605	46.99	56.21	1.1962
45	Gaussian	0.0010	0.0883	72.1	79.57	1.1036
90	Gaussian	0.0016	0.2284	113.4	113.4	1
135	Gaussian	0.0017	0.1342	82.56	82.56	1
Stream head 4						
0	Gaussian	0.001	0.0303	43.21	63.9	1.4788
45	Gaussian	0.001	0.1165	97.04	106.7	1.0995
90	Gaussian	0.001	0.2946	141.6	141.6	1
135	Gaussian	0.001	0.1646	124.9	124.9	1

Table 6.11 Parameters of the anisotropic models fitted to experimental variograms in four directions (0°, 45°, 90°, and 135° counter-clockwise from axis of maximum continuity) for stream networks delineated with $R'_A t$ approach and marked with stars in figure 6.36.

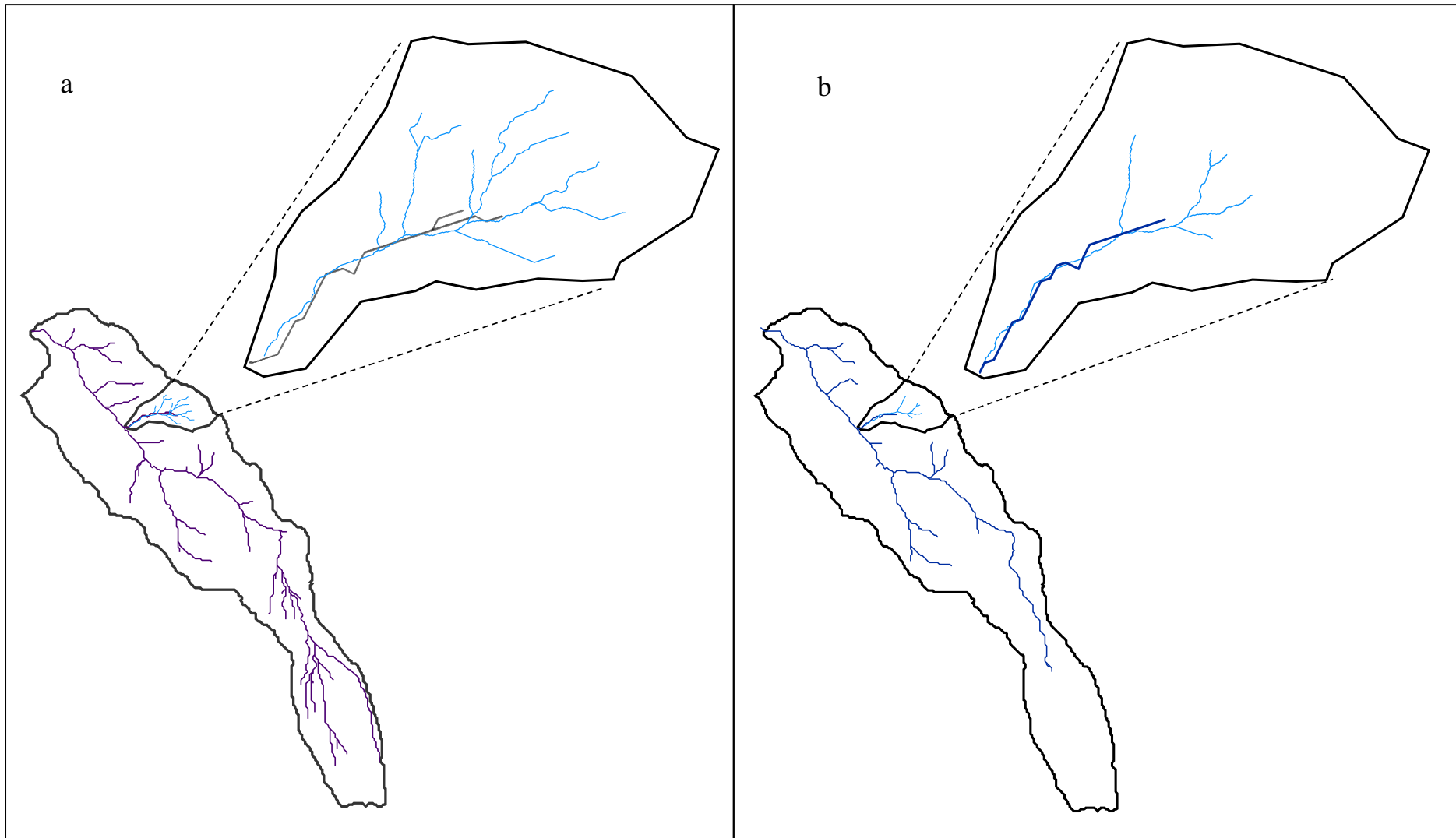


Figure 6.37 Stream networks delineated by (a) the Constant Drop Property (*CDP*) and (b) the $R'_A t$ approach in the Cautivo catchment using two landscape units. The lower part is generated by a DEM of 1 m resolution and a catchment area of 19040 m², whereas the higher part is generated by a DEM of 6 cm grid dimension and a catchment area of 956 m².

6.7. Discussion

6.7.1. Introduction

In order to verify prevailing patterns and processes in the basic elements of terrain formations, spatial variations between landform types have been analyzed using a hierarchical approach of varying dimensions, i.e. scaling down in a sample dataset of known dimensions. Results of the semivariograms within and between hierarchical sub-scales were registered and prevailing patterns and processes at each sub-scale have been underlined. Dominant patterns and prevailing processes within each formation is verified and accepted as a reference form for similar landform elements. Later on, such knowledge was used to characterize each landform type in a toposequence profile of sample datasets, which includes a pure convergent and divergent topography and the transition zone between them; that is channel initiation.

Results of this chapter highlighted several important points. The first one is the presence of a clear domain pattern in each formation that could be used to identify similar landform components. Secondly, such prevailing patterns are highly sensitive to the scale of the sample dataset (i.e. the dimension of the landform element) and the separation distance between the sampled points (i.e. the resolution). Third, the semivariograms demonstrated a great capacity in accurately identifying a dominant pattern in each formation and the corresponding scale for such pattern. The semivariogram parameters of anisotropic ratio and sill variance, between others, consistently reflected the presence of pattern- and scale-dependent structures that should be taken into account in any spatial analysis of landform components, results that have been confirmed earlier by scientists (Oliver et al., 1989b; Madej, 1999; Dungan et al., 2002; Chappell et al., 2003; Cai & Wang, 2006; Legleiter & Kyriakidis, 2008). Thirdly, earlier results highlighted the presence of a spatial threshold below which landform elements are controlled by local variability giving rise to wide alteration in water movement and hence runoff generation within these components. Finally, validation of stream limits under such knowledge provided a qualitatively compromising approach for models and algorithms used in channel head definition.

6.7.2. Landform analysis in real data structures

In pure landform components, semivariogram parameters of sill and anisotropic ratio provided different information that highlighted the presence of a prevailing pattern in each formation. Ridge revealed a clear control of the contour lines (i.e. greatest continuity or the minimum variation with lag distance) over elevation change along the ridge or divide line (figure 1, appendix 1). The anisotropy varies considerably within a directional analysis giving rise to a projectile and rose diagram-aspect of varying ranges and sills, i.e. geometrical and zonal anisotropy (figure 6.9). First, the $A:B$ ratios altered considerably with direction giving rise to values that range between 2.8 and 1 for the greatest least continuity axes, respectively, in the 1 m sample dataset. These values vary fairly between scales,

where the maximum $A:B$ values decreased with scale (2.1 and 1.8 for 2 and 3 m scales, respectively) and maintained approximately the same for the 0.5 m sample dataset (i.e. 2.7257). This indicates that ridge formations are generally expanded in their shapes, a spatial characteristic that could be altered with scale (i.e. usually scaling up in these formations), which normally smoothed such anisotropy. Second, the sill variances in the higher scales are larger than the smaller ones (0.5- and 1-m scale). The differences in the variability between scales appear to be due to the different response of prevailing process within each formation. Variations in the lower scales are approximately half to those observed in the higher ones (table 6.2). Moreover, such spatial variation explains the forces that controls flow direction on a ridge or a divide line, where water moves to adjacent hillslopes and not in the direction of the divide line. On the other hand, trend removal had led to complete changes in the directions of maximum and minimum variations leading to a different landform element of completely plane summit or divide line. This formation will generate a deceptive landform where water movement is more efficient on the divide line than to adjacent hillslopes, which is somewhat rare to find in nature. Herein, the directional analysis highlights a clear anisotropy in semivariogram parameters with unclear differences between scales indicating high similarities in the shape and the prevailed processes (i.e. unmodified element behaviour).

In hillslope formations, the situation is approximately similar to ridge elements with a clear anisotropic effect in the semivariogram parameters. In this case, hypsometry or difference in elevation seems to be the unique controlling factor over these elements leading to a clear omnidirectional movement of runoff and sediment. Differences in sill variances and anisotropic ratios are approximately constant at all scales suggesting the presence of a unique prevailing pattern in such formation. Herein, scaling up or down didn't affect dimensions and shapes of prevailing patterns, and all hierarchical scales maintained high similarity in the analyzed parameters. On the other hand, trend removal from hillslope formations has led to the emergence of new patterns and the disappearance of the prevailed one. Under these conditions two possible theories may explain spatial structure behaviour. First, if the analysed surface is fitted to transitive models, then the spatial variations within these formations are analysed in relation to a bounded semivariogram fit. Second, if the surface variation is unbounded and the spatial structure varies increasingly without limit as the area increased. In this case, the fractional Brownian motion function explains the spatial variation within the landform.

In case of transitive models, the anisotropic effect is widely observed within the analysed formations, where fitted models changed in relation to direction (table 6.4). Herein, changes in semivariogram parameters are unpredictable and provide little information about the presence of a dominant pattern. Sill variances and anisotropic ratios of the directional variogram are spatially independent suggesting a mixture of patterns or irrelevant information in the studied formation. This is explained by the presence of interchangeable curves of spherical and gaussian fit models in relation to

direction change within each sample dataset. Such changes in the semivariogram parameters may correspond to local micro-relief (structure roughness) or smooth formation with no trend. Under such condition, different scales and resolutions are needed in order to verify prevailing patterns on such formations. In case of unbounded model fit, the fractional Brownian motion explains spatial structure variations. Herein, fractal values (table 6.5) shows a significant scale variance effect, which may highlight a complete microtopographic control on surface roughness or the presence of uncertainty in the analysed dataset (i.e. the resolution effect). The above interpretation and the doubt over the type of the fit model lead us again to McBratney and Webstar (1986) interpretation that any surface could be transitive or unbounded variogram if it properly examined at an adequate resolution. A matter that should be handled deeply in future works. But in both cases, the local micro-relief effect may be detached as the key control factor in area roughness interpretation.

In channel and valley formations, a clear directional effect has been registered at the different hierarchical scales, in both with and without trend removal. In all cases, maximum variation is observed across the channel system, whereas minimum variation was found along the stream. This confirms that such formations are free transporting structures independently of their inclination. The anisotropic ratios vary between scales in trend-contained formations and maintains approximately constant between trend-free ones. The variations in $A:B$ ratios increased from 1.98 to 2.3, 2.66 and 2.55 for the units 3-, 2-, 1- and 0.5-m, respectively. These results reveal that channel structures are readjusted in shape with increasing dimensions suggesting more interacting processes than smaller streams. The readjustment in $A:B$ values with scale may suggest changes in the shape of the stream channel or even smoothness in the original shape, which may be attributed to an increase in channel bed width or a decrease in slope in the lateral sides of the channel. All these alterations may be related directly to change in runoff or sediment amount that is usually presented in channel formations. Such findings may underline the capacity of the $A:B$ ratio to indicate changes in sediment, runoff or even preferential lateral flow throughout the channel and valley streams. This is important for measurements reliability, where selection of the appropriate location for measuring tools may provide results with least uncertainties. Likewise, sill variance has demonstrated similar behaviour to anisotropic ratio. The direct comparison between the different scales reveals similar tendencies for the analyzed datasets with moderate sill variance that didn't exceed 0.16. In addition, sill variance maintained similar tendencies between contained- and free-trend formations. These results highlighted two important conclusions: first, in channels and streams prevailing processes are slightly affected by slope change. Second, within the channel formations lateral processes in stream banks moderate the effect of central processes in channel bed; that is, significant lateral anisotropy may reflect prominent directionality in the depositional settings, e.g. along and perpendicular to channels.

Researches on semivariogram analysis highlighted different directional effect in the channel networks (e.g. Chappell et al., 2003; Legleiter et al., 2007), mainly along and cross river directions.

These are directly related to the shape of the channel and the prevailing processes that occupy each section (e.g. roughness of bedforms, flow velocity, lateral flow, etc.). These studies have demonstrated that maximum variations are hold in crosswise river direction, whereas minimum variations are localized with the streamwise direction. These conclusions were interpreted in terms of scale dimensions. Lamerre and Roy (2005) concluded that large-scale variations prevail over reach-scale effect, that is, flow field is organized by coherent patterns of large scale variations. Likewise, Legleiter et al., (2007) highlighted that patterns of flow are controlled by the gross morphology of the channel and exhibit a reasonable degree of organization. In this direction, the semivariogram parameter of sill variance emphasized the large-scale variations over local-scale effect. The maximum sill variance was reached at ranges between 90-140° from the direction of the stream line (figures 6.17), which coincides with the angle of the basin outlet (i.e. α in figure 6.16). Herein, the dotted line indicates the direction of the outlet, longest streams and hillslopes, which coincide with maximum sill variances. In this case, local variations highlighted much about the presence and direction of prevailing processes (i.e. final direction flow). The anisotropic effect of sill variance reveals an active pattern process, whereas its direction is a good indicator of the final morphology of the channel system (i.e. direction of the basin outlet). While in stream-controlled trends, the maximum sill variances are controlled by local topography, that is, local-scale effect is the prevailing factor of the final direction flow in the catchment unit.

In channel initiation or transition zones, the variation and directional effect is completely different to stream formations. First, in maintained-trend formations, directional effect was completely vanished and the different sub-hierarchical scales underline an omnidirectional effect, mainly in 1- and 2-m sample datasets (figures 8b & c, appendix 1). The 0.5-m sample unit revealed a smooth anisotropic effect of maximum variation in the direction of the contour lines (figure 8a, appendix 1), which may be attributed to insufficient sampling to detect embedded processes with such dimensions. These results underline the importance of scale (i.e. dimension) and resolution (i.e. sampling distance) in channel initiation areas, where small variation in initial datasets may lead to erroneous conclusions. Second, the $A:B$ ratio and sill variance showed smooth variations between scales, but in general approximates to unity, mainly in the 1 m sample dataset suggesting an omnidirectional effect and a rounded type formation. Herein, sill variance oscillates between 0.041-0.09 m (figure 6.20b), a considerably low values in comparison to the rest of the analyzed landforms. Just only, the hillslope formations without trend provided similar values, where micro-relief effect was the controlling factor. While the actual channel initiation contains a considerable inclination of about 88.5°, sill values maintained small variations suggesting completely different prevailing pattern and processes. In free-trend hillslopes, micro-topography is the dominant pattern, whereas in channel initiation prevailing patterns are changed from divergent-dominant topography to completely convergent prevailing processes. This change in prevailing patterns could explain the smooth variation in sill values

suggesting an unbiased-state element. Under this state, prevailing patterns of different directions nullify each other producing a neutral formation, and again controlled by micro-relief. Thus, free-trend hillslopes and channel initiation with trend (i.e. varying steepness) occupy different topographic positions, but reveal similar effect of prevailing patterns on local relief (i.e. similar semivariograms). Hence, care should be taken in derived conclusions of analyzed formations, since under fixed scales similar semivariogram parameters doesn't mean similar landform elements, but similar relief formations should provide similar variogram parameters. Finally, stream initiation without trend provided varying conclusions in relation to the dimension of the analyzed sample dataset. In general, 3-m sample dataset registers channel formation behaviour; whereas 2- and 1-m sample dataset underline the presence of channel initiation form properties.

Another important aspect that may be induced from the above analysis is scale and resolution effect on water movement in and within landform elements. Several studies (e.g. Zhang & Montgomery, 1994; Schoorl et al., 2000; Wolock & McCabe, 2000; Tarolli & Fontana, 2009) underlined and explained resolution and scale effect on topographic and hydrologic attributes that may affect runoff generation. Their main conclusions confirm the presence of a threshold value above which the hydrological response is widely altered and slightly transferable to other scales. While different studies on sediment yield, runoff and soil erosion (Kalin et al., 2003; Cerdan et al., 2004; Chaubey et al., 2005; Cantón et al., 2011) confirms a more generalized effect of scale and resolution and pointed out to the presence of the optimum effect rather than a threshold one.

In the current work, the major results of the directional analysis highlighted the presence of a breaking scale (i.e. threshold effect) above which water redistribution is unpredictable and widely altered by local relief. Such scale should insure and support the presence of prevailing spatial structure properties of the analysed landform element. In the examined area of El Cautivo, this scale approximates to 1 m, where down which the spatial properties are highly sensitive to data structure uncertainty and above which the spatial variation highlighted little information about the prevailing pattern (i.e. data redundancy).

Again, such breaking point may be affected by the resolution of the analysed data structure. However, the effect of scale and resolution is not constant and is directly changed in relation to the type of the landform element (table 6.7), where scaling up and down between the analysed formations showed varying sensitivity. Herein, hillslopes and channel formations revealed a slight alteration in relation to scale effect, which could be attributed to the dominant effect of the prevailing divergent and convergent processes within these elements. Conversely, channel initiation zone and ridge lines showed considerable alteration in relation to scale explained by absence of clear domain process within these formations. These results confirm earlier findings on multi-fractal aspect of landform properties (e.g. De Bartolo et al., 2004; Lam & Quattrochi, 2005) where constant thresholds are often not met in natural watersheds.

6.7.3. Toposequence profile analysis in real landscapes

The above results have provided a general guide lines for the verification of the spatial behaviour of landform formation using semivariogram parameters as a characterizing index. Under particular scale and resolution, each relief form compromises sufficient spatial characteristics that should allow for an objective (i.e. qualitative and quantitative) separation with adjacent formations. Emphasize on such evidences could be applied directly to real terrain elements, where natural landscapes are well registered and defined. As highlighted earlier, previous results demonstrated that 1-m dimension is an acceptable scale to define embedded information in each landform type.

With the exception of ridge formations, the main landform types of hillslope, channel networks, and the transition zone between them were analyzed in a succession form using semivariograms. In order to obtain a comprehensive understanding of landform behaviour, two toposequence transects of different topographic conditions were analyzed: the first is characterized by a smooth transition between formations, whereas the second describes wide-contrast topography. The results of the profiles analysis revealed clear breaking points between the analyzed elements, which could be used as a rule of set to define each formation. In the high contrast topography, semivariogram parameters revealed with no doubt the presence of various formations of different characteristic length scale (figure 6.24). Both parameters of $A:B$ ratio and sill variance underline a breaking point that allow for the separation between three main formations: stream, hillslope, and the transition zone between them. Each of these formations holds particular characteristics of directional effect and autocorrelation that reflects its shape and prevailing patterns in the terrain. While sill variance maintains a strict separation between formations, $A:B$ ratio revealed less sensitivity to variation between landform elements. This is because the former is related to the prevailing processes within each formation, whereas the latter is more appropriate to describe the shape of landform components (Chappell et al., 2003).

In the Cautivo basin, hillslopes are characterized by multiple prevailing processes of overland flow and sheet erosion, which, in addition to hypsometry, provides a directional sill variance that oscillates between 0.04-0.37 (figure 6.24b). Whereas in stream formations, convergence processes are prevailed with concentrated flow in stream beds and lateral flow in stream banks (e.g. rill and gully erosion are the most evident in first order streams), and average variation of elevation is across and along the channel stream. So, different process with varying directions will lead to moderate sill variances (e.g. between 0.03-0.11 and 0.02-0.12 for stream one and two, respectively), which is the most evident in all analyzed streams in the studied basin. In transition zones (i.e. exact channel initiation), divergent and convergent process are encountered and hence no prevailing process is registered since both nullify each other and the final effect approximates to omnidirectional property. In summary, variability of elevation effect is minimized and sill variance approximates to unity with values that oscillate between 0.02-0.05, which is widely related to the effect of the micro-relief.

Likewise, anisotropic ratio reflects range variations, which seems to be more appropriate to describe feature shape than changes in dominant processes. All the analyzed elements demonstrated a directional effect of varying $A:B$ ratios, with the exception of stream initiation 2 (transition 2) (figure 6.24a). In this case, the $A:B$ ratios approximate to unity in all directions giving rise to rounded and smooth formation, that is similar to a completely plane hillslope form. Such landform is approximately isotropic with omnidirectional effect. In natural landscapes, hillslopes are anisotropic and variation of elevation is directional. Herein, it seems that this is true with the exception of stream initiation zone where omnidirectional effect is the widely prevailing aspect.

In the smooth-contrast toposequence, the transition zone was somewhat indefinite, for which the sampled datasets were defined regularly upward from stream to hillslope (figure 6.28). Again, the semivariogram parameters highlighted a breaking point between formations, but in this case with no clear identification of the transition zone (figure 6.29). These results could be attributed to the fact that channel initiation may be located between the selected samples and the defined samples itself, e.g. between SI-1 and SI-2. Herein, the breaking point identified the limits between hillslope and channel formations directly without passing with the transition zones. Indeed, the initials of SI-1 and SI-2 were assigned to indicate possible transition zones, but the final results revealed that their spatial parameters pertain to adjacent formations (hillslope or channel). In this case two important points should be underlined: first, the anisotropic ratio highlighted trivial information on the limits between formations (figure 6.29a); and second, stream formation is characterized by relatively high sill variance values that approximates to 0.30 (figure 6.29b). These observations maybe explained by the two line streams observed within the channel formation (figure 6.30d).

6.7.4. Toposequence profile analysis in simulated landscapes

Despite of the widely limitations of regular gridded data, mainly DEMs, it is still increasingly the most effective mode for encoding the topography for landscape modelling. One of the main limitations of these formations is its incapacity to adapt surface topography with spatially varying complexities (Hutchinson, 1996). So, finest resolutions are needed to represent the prevailed terrain complexity. Thus, issues of scale problem are raised mainly in hydrological and other earth surface models. Practical implications include data acquisition and storage and the algorithms used to generate the final data structure. In the present work, real landscape and prevailing complexity was describe by a 1-6 cm point cloud that was generalized later to 6 cm of regular spatial resolution (i.e. simulated landscape) using the *IDW* approach.

The semivariograms and the geospatial analysis for the stream-hillslope profile highlighted various differences between real and simulated landforms, mainly in stream networks and channel initiation zones. First, at the level of a unique component form, regular gridded data is deeply susceptible to terrain complexity leading in some cases to erroneous interpretation of the hydrological

behaviour within these elements. Maximum and minimum variations within stream formations have been widely altered and erroneous interpretation of water movement along stream component was concluded. While water movement with minimum variations were always registered along the stream lines in the real data analysis, simulated streams revealed that such behaviour is widely related to the scale of analysis. So, a unit sample dataset of 1 m within a stream may provide distinct hydrological interpretations between regular DEMs and real data surface. Here, it worth's to underline that earlier studies (e.g. Merwade et al., 2006) have confirmed the directional effect in channel bed morphology, where variability is higher in the transverse direction than along the flow direction. But, they also detached that such anisotropy in river bed is not consistent; rather it varies with the flow direction, which is related to river channel sinuosity. While this is not the case in the present study, it may explain part of the change in maximum and minimum variations in channel network components. In the two formations, not only the direct information but also embedded one is significantly distinct. In real data, general stream aspect and the basin outlet direction are well deduced from the semivariogram parameters. Whereas regularly gridded data conceals the implicit information embedded in the analyzed elements. Thus, higher scales or resolutions are needed to explain basin behaviour from landform components.

On the other hand, transition zones verified earlier in real datasets disappeared completely when landforms were analyzed after the interpolation processes. Both $A:B$ ratio and sill variance that characterized these formations vanished completely and new properties were perceived. It seems that channel initiation zones are sensible formations that are greatly affected by interpolation procedures giving rise to new forms influenced by neighbouring elements. In nature, stream initiation is a complex landform element that is widely related and influenced by surrounding environmental factors, giving rise to distinct initiation processes of different channel head types and locations (Bull & Kirkby, 2002). So, depending on the analyzed sample size and the exact location of the stream head, with semivariograms these formations may be classified as a ridge, hillslope or channel structure form. This is because channel initiation zones or channel heads, mainly in the studied area, are generally formed near such formations.

Once again, the semivariogram parameters under real landscape demonstrated great capacity in depicting landform properties. Both landform shape and prevailing patterns were distinguished in relation to the general geospatial properties (figure 6.31). Depending on position and the prevailing processes in the analyzed terrain, landforms are classified to convergent topography of moderate directional effect or divergent hillslopes of more severe dominant aspect. Within the same hydrologic catchment unit, any landform element may be grouped with other formations in relation to the geospatial properties or similarity in semivariogram parameters and fitted models. All these parameters should be evaluated since variations between structures may lead to erroneous conclusions, such as the case in hillslope 2 in figure 6.31.

In general, it seems that the information derived from digital models varies in relation to type of data processing and interpolation. Although simulated datasets (i.e. interpolated data) provide sufficient information on main landform components that is widely dominant by clear prevailing processes (e.g. ridge, hillslope, divide), its capacity may be questionable in transitional areas where limited information was registered. In these cases, although scale and spacing are limiting control factors, real datasets that capture (depict) the topography in relation to the original landform element are the best approach to describe landscape patterns and properties. Interpolation methods not only predict values of spatial phenomena in unsampled locations but also introduce some uncertainties in forms of regular data dimension that may hinder the tiny topography of some formations leading to incomplete conclusions. These conclusions are widely conditioned to the sensibility of the semivariance analysis, which demonstrated a great capacity in the verification of landform components based on the combination of both shape and embedded prevailing process within these formations.

6.7.5. Validation of stream limits based on directional analysis

In order to validate and compare how closely stream heads generated by the constant drop analysis (*CDA*) and the $R'_A t$ techniques mimic natural ones, a 956 m² watershed was chosen where the main stream link was detected by the two approaches at 1-m grid dimension. The generated drainage networks at 6 cm grid resolution and delineated by the *CDA* (figure 6.35) shows a high detailed stream network of 9 first order links (i.e. magnitude = 9), but with varying stream-limit conditions. First, the visualization process reveals with no doubt that 7 stream heads are located within hillslope formations and just 2 links are situated within convergent topography. Conversely, the $R'_A t$ technique depicts a drainage network where all stream heads are localized within convergent formations (figure 6.36). Comparisons of the two scales and resolutions (figure 6.37) confirm that validation is more efficient under comprehensive approaches that include qualitative and quantitative methods. Of course, visualization procedure may provide a reasonable approach for stream head validation, but it does not provide a quantitative description of how the stream limit approximates the channel initiation zone or the stream source area.

The directional analysis used in the validation of stream heads delineated by the compared techniques demonstrated that convergent and divergent topography maintained different properties that allows for a straightforward separation between these formations. Within a toposequence profile analysis or even for the stream formations itself, the semivariogram parameters revealed that all stream heads generated by the $R'_A t$ technique correspond to convergent topography. Conversely, the directional analysis of stream heads delineated by the *CDA* technique demonstrated that part of these formations hold divergent-topographic properties. It is worth to underline that a reliable drainage network system is the formation that verify all stream segments within convergent topography and their sources within stream initiation zone. So, it seems that an appropriate threshold value (A_S) for

stream delineation is the value that roughly estimates drainage network, best approximate to source areas, and minimizes local errors defined as feathering and/or specious limits. Feathering and invasion of stream limits in hillslope formations in addition to correct stream location are important aspect to take into account in any validation approach. While the first two aspects are related to the capacity of the technique used in stream delineation, the last is related to data errors and the method used for channel network generation (e.g. O'Callaghan & Mark, 1984; Tarboton & Ames, 2001). Herein, both delineated drainage network from *CDA* and $R'_A t$ technique didn't depict all divergent formation within the studied catchment, which may slightly affect the variations between natural and automated drainage networks. Such drawbacks should be treated by deeper insights on the automated approaches of stream delineation.

It seems that definition of the exact location of stream heads is still a highly complicated task and is widely affected by several factors (e.g. data resolution, interpolation procedure, models used to capture stream head, etc.), which makes the concept of reliability somewhat subjective. In general, the spatial analysis has, when used with real datasets, demonstrated high capacity in defining convergent/divergent topography and limits between them, and hence stream head or channel initiation zone. This is because semivariogram parameters define topographic elements not only in relation to changes in the shape but also in relation to the dominant processes within these formations. Such capacity is reduced in interpolated datasets leading to less sensitivity that effects mainly stream heads, since prevailing processes within these formations are distorted. In this case, the reliability in channel networks validation is to define the cells that approximate to channel heads and not overcome it, since hydrological parameters are rationally biased. Under such criteria, the $R'_A t$ technique shows sufficient capacity to delineate stream limits under varying condition of variability (i.e. resolution, scale, landform heterogeneity) that makes it a more reliable approach for stream limits delineation.

Finally, it worth to underline that validation of channel heads delineated by automated techniques is still a matter of debate between scientists (e.g. Tucker et al., 2001a; McMaster, 2002; Heine et al., 2004; Hancock & Evans, 2006; Lashermes et al., 2007; Tarolli & Fontana, 2009). The origin and wide aspect of these techniques require the use of one or various approach based on data availability and the main objectives of the work under scope. Field measurements, blue lines (*BLs*), *3D* visualization, general statistics, and the actual method of directional analysis may be used separately, interchangeably or even combined in order to achieve a rational approximation to natural streams and their limits extracted and delineated by digital terrain models and their derivatives (e.g. DEMs).

6.8. Conclusions and Recommendations

Division of landscape into landform elements is important because it provides information on the size and the scale of landform features, which in turn may affect the amount of energy available for geomorphic, pedogenic and hydrological processes (MacMillan & Shary, 2008). Automated

classification of landforms is contained into those that attempt to recognize and classify repeating types of landforms and those that attempt to partition landforms into landform elements along a toposequence from divide to channel. In the present work, the latter has been adapted, since it fulfils the general aim of an objective definition of limits between channels and hillslopes. In contrary to other modes of landform classification that rely upon morphological measures, this work adapts a geospatial approach of semivariograms to define elements or type patterns and prevailing processes within such structures. DEMs have been the main source of data for landform classification, mainly automatic extraction of channel networks and other landform types. While these datasets suffer of severe inconveniences (e.g. errors and uncertainties of the original data, scale and resolution, etc.), Digital Land Surface Models (DLSMs) provide a detailed replication of landform structures with the least possible errors. Herein, DLSMs has been accepted to represent real landforms, whereas DEMs were treated as simulated landscape.

In the current work, the analysed toposequence was reduced to 4 main structures: these are divide, hillslope, stream, and channel initiation. Usually, the first three are directly extracted from DEMs; whereas the transition zones are fuzzy elements and their definition are widely related to several extrinsic and intrinsic factors. The former are related to the local surrounding environment (e.g. geology, vegetation cover, land use, etc.), whereas the latter are related to DEMs reliability (i.e. errors and uncertainties) and the capacity of the applied algorithms to define such elements. Hence, the DLSMs have been used to overcome such inconveniences and to introduce new dimensions to the study of stream limits. In river basin hydrology, delineation of channel networks is a major problem, where stream limits are highly related to scale and resolution of initial data used in their definition. These fuzzy zones are easy detected by the geospatial analysis, where basic characteristics of shape structure and prevailing patterns are widely verified by semivariogram parameters. Hence, two toposequences of varying complexity were classified in relation to change in autocorrelation between its geomorphic units. First using DLSMs extracted from Terrestrial Laser Scanners (*TLS*) and second with DEM interpolated from the first data structure at regular resolution of 6 cm.

The geostatistical analysis of landform types with high detailed data from laser scanners has provided a valuable tool for precise landform depiction. The definition of the semivariogram parameters and the type of prevailing anisotropy may form appropriate guide to determine landform element in real landscapes. While such formations are not the same under distinct environmental conditions, results may provide a proper line for future studies of complex-structure patterns. The semivariogram parameters of anisotropic ratio, sill variance and the type of fitted model revealed a considerable enhancement in landform depiction and, hence, classification. Each of these parameters provided valuable and necessary information to be used for element definition. Not only shape structure but also prevailing processes within these forms, based on the basic hydrological unit that they embedded (i.e. catchment area), have been highlighted giving rise to objective understanding of

water movement within and between formations. The spatial analysis and the geostatistical approach have reasonably identified the appropriate scale of autocorrelation associated with each component, which best describe its shape and the prevailing processes within it. Moreover, it provided a basis upon which one can compare variability of landform elements within the feature itself and between units in a toposequence model.

Main results of the present work revealed that in real data structure (i.e. DLSM) the semivariogram parameters highlighted a particular characteristic length scale that allows for an objective separation between landform elements. Stream channels, hillslopes, ridges and channel initiation area showed clear geospatial characteristics that allows for their classification and definition as an independent elements. Such particular characteristics have been analyzed under a toposequence profile and the preliminary results provided a structural pattern of separated curve lines for each formation. Hence, within a toposequence profile that goes from the channel outlet to the divide line, but always passing through a channel line to the next hillslope, a semivariogram analysis may provide valuable information on limits and borders between such formations.

In simulated landscapes (i.e. regular gridded data), again, the semivariogram provided a considerable information on spatial characteristics of the main formations (i.e. stream, hillslope and ridge) and irrelevant ones over secondary landforms (i.e. channel initiation zone). It seems that the initiation zone of stream head contains particular characteristics of spatial variations that make it more susceptible to generalizing processes resulted from the interpolation procedures used in DEM generation. From one hand, the spatial characteristics of main landform elements are scale invariance and slightly affected by resolution change. On the other hand, channel initiation is a vulnerable formation that is widely altered to variations in scale and resolution of initial data. Thus, depending on the data type, DLSM or DEM, the influence of scale, resolution and the generalizing process can seriously affect the results of the semivariograms in relation to upstream area. Although interpolation techniques (e.g. *IDW*, kriging, etc.) are powerful tools for regular grid generation, spatial characteristics are modified when data is generalized and some information may be lost.

In addition to the above findings, captured data of *TLS* have provided a detailed, reliable and accurate solution to represent real terrain elements (i.e. real landscape) in comparison to simulated ones of DEMs. DLSMs with semivariograms highlighted valuable conclusions over prevailing patterns and processes as well as their corresponding scale. Structural information derived from *TLS* revealed significant enhancement in depicting and highlighting transitional zones between main landform units, which should be considered for future investigation on fuzzy elements in landscape studies. This information has direct and indirect implications on validation approaches, both models and structures (e.g. numerical models setup, monitoring geomorphic processes, precise delineation of landform components, etc.).

The capacity of semivariograms to depict terrain elements is widely observed in their variations in relation to minimum changes in these components. Main relief formations (e.g. hillslope, channels, and ridges) and secondary elements of unclear prevailing domain (e.g. channel initiation, transition zones, etc.) were underlined by the semivariogram parameters under real datasets. Landscape configuration under real data approach is less sensitive to scale and spacing between datasets, whereas interpolated formations are more susceptible to such limits and to the simulation approach used in DEM construction (i.e. interpolation process). These results underline the sensitivity of the semivariogram parameters as a relatively robust tool for landform depiction. Moreover, not only local information was inferred from the semivariograms but also the broad hydrological characteristics were detached. Directions of outlet, longest stream, major hillslopes, and the total drainage network were all deduced from the directional analysis, mainly sill variance type and direction. While this information is well highlighted from DLSMs, again DEMs failed to provide such details.

Water movement within and between landforms are well explained under the geostatistical approach. Spatial-variability direction (i.e. maximum and minimum variations), type (i.e. type of fitted model) and related parameters (i.e. sill variance and anisotropic ratio) may explain water movement and redistribution at hillslope scale. In ridge formations, a water drop moves to adjacent hillslopes and not in the direction of the divide line giving more weight to variations across the contour lines. In hillslopes and under the absence of local controlling factors, hypsometry is the unique control factor at the hillslope scale leading to parallel flow movements in the descent gradient. Herein, trend removal will lead to new formation controlled by microtopography or surface roughness that may be used in understanding infiltration capacity in such formations. The semivariograms confirms stream channels as free transporting components controlled by the total drainage network within a hydrological unit (i.e. catchment unit) independently of local stream gradient. Moreover, changes in sediment, runoff or even preferential lateral flow throughout the channel and valley streams are well indicated by $A:B$ ratio and sill variance changes with direction. This is important for measurements reliability, where selection of the appropriate location for measuring tools may provide results with least uncertainties. Moreover, within the channel formations lateral processes in stream banks moderate the effect of central processes in channel bed; that is, significant lateral anisotropy may reflect prominent directionality in the depositional settings, e.g. along and perpendicular to channels. Conversely, channel initiations are free prevailing elements, where convergent and divergent processes produce a nullify-dominant effect giving rise to approximately hydrologic static state.

Semivariogram analysis of main landform components studied in the present landscape context highlighted new insights on shape dimension and structure-functions effect on prevailing processes within it. First, ridges are dynamic elements, characterized by varying hydrological response controlled by scale and gradient. Such spatial variation explains the forces that control flow direction to adjacent hillslopes or along the divide line. Secondly, hillslopes are static landform components,

usually controlled by one prevailing process giving rise to flow direction altered by the slope gradient. Third, channel formations are readjusted in shape with scale leading to more interacting effect between prevailing processes. Changes or even smoothness of the original shape component are directly detached by the semivariogram parameters, which enclose straightforward information on runoff generation and transported sediment within these formations. Finally, in channel initiation the omnidirectional effect is widely prevailed (i.e. isotropic formations). Based on formation type, landform elements revealed varying susceptibility to change in scale and resolution, which could lead to erroneous conclusions if treated with the unsuitable dimensions. These conclusions are widely conditioned to the sensibility of the semivariance analysis, which demonstrated a great capacity in the verification of landform elements based on the combination of both shape and embedded prevailing process within these formations.

Implications of the above findings are included in their direct capacity as a validation procedures for landform elements, both shape and limits. The toposequence approach with the semivariograms demonstrated a reasonable potential in defining stream limits under varying landscape conditions that can be used as a rule of set for element delineation. Such verification is based not only shape but also on the embedded information that they contain (e.g. divergent hillslope processes vs. convergent flow on stream channels). Herein, the limiting effect of scale and resolution may diverge in two affirmations. Scale effect was deeply explained by the semivariogram approach. This is because the fractal nature of stream networks and other landscape components are well described by the examined datasets, which may be considered as efficient indicators, not only for the formation itself but also the higher landscape components. However, the resolution effect was explained in relation to type of the data structure (i.e. differences between DLSMs and DEMs), but not sufficiently in relation to the optimum resolution, where semivariograms may provide deeper insights. The preliminary results of this work highlighted some information on resolution effect, but we believe that providing concrete values on the optimal resolution is still awaiting task that should be handled and treated in future works.

Finally, from the above-described settings, results confirm the potential of the topographic information as a valid tool, contained within the digital terrain and surface models (e.g. DLSMs, DEMs, etc.), for landscape depiction. Landforms elements of streams and hillslopes maintain concrete geomorphic properties that allows for their direct validation by such tools. Moreover, limits between elements are also verified, where main processes of runoff and soil erosion maintain a blurred dominant aspect. In this case, local factors of relief (e.g. roughness, slope, etc.) as well as scale and resolution exerted a limiting effect in the definition of such formations.

Chapter 7

GENERAL CONCLUSIONS

7.1. Introduction

In this concluding chapter, the approach is summarized in the first place, including its methods and the quality of the used data. Then, the synthesis conclusion of the work is presented, followed by the partial conclusions emerging from the different components of this study. Finally, some remarks and suggestions for further research are given.

The problem addressed in this thesis is related to the capacity of DEMs to delineate channel networks and stream limits under limiting conditions of data availability and landscape complexity. Another related problem is the way in which these limits should be validated. Hence, the essence of the present work is to answer four main questions: i) Can DEMs provide with sufficient information to delineate channel networks? ii) Is it necessary more than one validation method for channel network definition? iii) What are the appropriate quantitative descriptors (hydrologic and geomorphic) for defining the scale effect over catchment behaviour? And iv) What is the appropriate resolution for the study of a landscape?

The study was conducted at the Tabernas Basin, which consists of several landscape systems associated with different lithologic and tectonic formations, which in turn involve different hydrologic and geomorphic dynamics. In Tabernas, model testing and validation was carried out upon two major level scales. First, the Tabernas basin, representing a highly heterogeneous landscape, was worked out as a whole using a DEM of 30 m grid resolution. Second, two sub-basins of rather homogeneous landscapes but of distinct relief formations, represented by the El Cautivo and Rambla Honda sites, were approached using respective DEMs of 1 m grid resolution. The reason for selecting two landscape units was that their relative internal homogeneity did facilitate the examination of hillslope-stream limits, and both units, which are different from each other, enabled comparing the robustness of the applied procedure. In addition, the model application at Tabernas Basin level did allow for testing model flexibility.

7.2. Evaluation of the data and the proposed approach

While a DEM is a representation of geographic reality, this capacity is reduced by the contained errors and uncertainties, mainly in derivative products (e.g. stream networks, topographic variables, etc.). Usually, DEM data is evaluated globally by the root mean square error (RMSE) or locally by conditional stochastic simulation. The present work used a mixture of these approaches, which allow for enhancing DEMs capacity and sensitivity in relation to channel network extraction;

that is, DEM assessment in relation to the final aims and objectives. The extracted streams and valleys from both original and corrected DEMs were highlighted and compared visually and using previous knowledge of the area.

Based on the intrinsic properties (topologic and geometric) of drainage networks, a new algorithm has been constructed (i.e. the R'_A or the “*adaptive model*”) to delineate stream limits. In nature, landscapes are characterized by varying complexity and heterogeneity, giving rise to different scale dimensions (i.e. simple or multifractal structures). For this purpose, the adaptive model was combined with a recursive stratification process in order to yield critical threshold values in relation to the DEM resolution and to the diversity of dominant landforms. The resulted procedure was symbolized and designated as the $R'_A t$ approach. In general, the adaptive model function is based on the basic notions of Schumm (1973, 1977) that attributed stream network evolution to extrinsic control factors (e.g. climate, tectonics, land use, etc) and other intrinsic ones of strong geomorphic controls. These factors are best described by the topologic and geomorphic properties of the stream networks combined in the proposed model. Hence, the final results of the model is a drainage networks that describe the optimum equilibrium point between these factors represented by a critical threshold value (A_S), which defines the optimum drainage density in relation to DEM resolution and landscape complexity.

The resulting stream networks were compared and validated in different forms. Herein, a new approach has been established in order to achieve a comprehensive methodology for a more real and vigorous comparison procedure. Thus, three major procedures were used and compared: the automated approach represented both by the adaptive model and the constant drop property, whereas natural streams were assumed to be represented by the digitized-*BLs*. In general, the comparisons were carried out qualitatively and quantitatively. The former revealed various drawbacks related to subjectivity and the scale of the work. The latter provided a rational physically-justified base by using geomorphometrical parameters, which describe structure properties of natural drainage networks. In order to avoid weighted effects of these parameters, selected descriptors were compared directly by the Gower Metric index that allows for pair-wise comparisons.

Usually, the geomorphometric parameters are derived from stream networks delineated by a critical threshold value (A_S), where uncertainties in DEM data may directly affect these descriptors. To avoid such shortcoming, a more robust validation approach was used to validate stream limits, based on spatial structure variations in real datasets. The directional analysis of semivariograms has provided quantitative parameters to define limits between landform elements, based on spatial variations in shape structure or change of prevailing processes within these formations. Such knowledge was applied on real data obtained by laser scanning technology (*LST*) that capture relief details at a very high resolution. Currently, Laser scanners, both terrestrial and aerial, are one of the important source

of digital data that can provide different type of data of different complexity but with high precision ranges (e.g. 1 mm) and, hence require complex treatment procedures. In theory, these datasets are free of common errors presented in DEMs data, which makes it a more reliable replicate of geographic reality. So, the obtained results did serve to validate the proposed technique and the critical threshold values provided, as well as the degree of uncertainty in the DEM data itself (e.g. interpolation procedure, resolution and scale effect, etc.).

7.3. Synthesis conclusion

The final results of the present study provide a consistent approach, designated as the “*Adaptive Model*”, which delineates stream limits in relation to data resolution and dominant processes. By such approach, the automatic delineated stream networks approximate well to natural ones leading to a more optimal quantification of landform components and corresponding processes, mainly hydrologic and geomorphic ones. Such approximation is reflected by a completely vanishing of feathering on smooth landforms or more drainage density in highly dissected sectors of the landscape and, hence provides more like aspect to the digitized-*BLs*. Moreover, channel networks extracted by different critical thresholds of the same DEM affect strongly the geomorphometric parameters, which strongly influence hydrological modelling results. Hence, automated channel network delineated by one approach or another could be scale-dependent. Such dependencies are also altered by the resolution and diversity of the DEM data. In nature, stream and channel networks are scale-independent and multifractal structures. Such knowledge assumes that more than one critical threshold area is needed to depict the correct landscape dissection, a matter that has been achieved by the adaptive model. In fact, independently of the DEM resolution or/and prevailing heterogeneity, the adaptive model maintained a consistent methodology in stream delineation highlighted by the definition of an acceptable critical threshold value in all the analysed basins.

The geomorphometric indices are highly specialized parameters that describe drainage network morphometry and hence widely used in the comparison between different stream systems. Their efficiency and capacity to determine one property or another is altered in relation to the mode in which they applied. First, Hack’s and Melton’s fractal values are broad descriptors (i.e. describe shape and frequency in relation to basin size, respectively) that are related to the general structure of the drainage network system, for which they are useless in one-to-one comparison of first order basins. Second, it seems that compound parameters (e.g. Dd , OCN , E , Isd , F_S , and k) are more sensible to stream variations and hence more efficient in stream comparison than simple ones (e.g. Ω , μ , La). Third, ratio parameters (e.g. K_i , R_B , F_S , inR_A) hold a moderate importance and provided particular insights on stream structure properties, where they occupied all the factors in the Principal Components Analysis. Finally, simple geometric and topologic properties (e.g. Ω , La , μ , D_{obs} , $p(\mu)$, $TPLC$, $TDCN$) occupy the same component of variation with similar loading weights, although they describe different characteristic length scale but their effect in the comparison seems to be similar.

Hence, one or two parameters of each property may provide the desirable effect and should perform well in any comparison and validation approach.

The validation procedure is not less important than the definition of the optimum A_S value, since both are interrelated, where the definition of the optimum A_S value requires a robust validation procedure. How and what to validate are the core subject in a robust methodological validation approach. Whilst the comparison tests, both qualitative and quantitative ones, employed in the analysis procedure have shown clear drawbacks that may deduce scantiness for depicting stream limits. From one hand, the qualitative approach is highly subjective where cartographer experience and background, terrain complexity and original data scale are limiting factors. On the other hand, the quantitative approach is greatly susceptible to random errors generated in the original data or/and resulted from the algorithms used to delineate the channel networks (e.g. sink area, slope direction, contributing area, etc). Finally, the data obtained from *LS* provided an optimal validation approach for landform components, in which stream-hillslope transition zones were depicted and verified precisely based on the spatial variation within and between elements. Moreover, the visualization process, obtained by such data, has provided a complementary and a powerful validation tool, which may add more emphasis on such approach. Both the geospatial analysis and the visualization process applied to *LS* data should form the future aspect for a real validation process in order to determine precise limits between landform components.

Based on these conclusions, some of the above highlighted questions can be answered. First, DEMs are suitable structures to describe and delineate stream networks, making it the best-to-date ones for the automatic extraction of these formations. Second, optimum scale and resolution are related to the level of details needed to cope with the general aims of the study. Third, in addition to scale and resolution, extrinsic and intrinsic factors (tectonics, climatic conditions, vegetation cover, prevailing runoff and soil erosion, geomorphic processes, land use) exert limiting effects on stream network delineation, for which models and algorithms should take into account such effects. Finally, a combination of different validation procedures is needed to ensure the optimal comparison between compared drainage networks, mainly between manual and automated extracted ones.

As any other approach, the adaptive model endures some drawbacks that may affect its capacity. The procedure itself is an iterative process of calculation that requires the definition of all possible A_S values used to construct a channel network of $\Omega \geq 2$ and hence the curve relationship of the stability zone (SZ), which, in large catchments, may be time and effort consuming. Conversely, in homogeneous terrain of a unique SZ, the curve relationship is altered by errors and uncertainty in the DEM data, which from one hand may modify the delineated drainage network but also may provide a good indicator for local deformation in the original data. Finally, the adaptive model itself is a ratio that require the presence of exterior and interior stream links, which is achieved at minimum of three segments and hence stream basin of $\Omega \geq 2$. In this case, the direct comparison with the digitized-*BLs* is

somewhat recursive. Unless the original assumptions of the model construction are modified for A_S value acceptance in the case of a unique SZ (i.e. primary conditions of the flowchart in figure 5.2), this drawback is the most serious and should form the challenge for future work.

7.4. Partial conclusions

1. Errors and uncertainties are inherent to DEM datasets and their treatment should be performed throughout the analysis stages and in concordance with the main aims of the study under scope. The final judgment to determine whether certainty in a DEM will affect results from specific analysis should be the responsibility of the DEM user. The global error (RMSE) of the DEM matrix was integrated with stochastic simulation approach and local uncertainties within depression areas was modified. Areas of high vegetation cover (northern faces) and valley bottoms demonstrated considerable uncertainties and hence were corrected and modified in order to produce a more realistic drainage network that reflect prevailing natural stream of the zone.
2. The importance of optimum resolution, in addition to cope with the final aims and objectives, is widely related to the relief grain and the size of area under study, mainly whenever DEMs are the unique source of information for catchment delineation. In the area of Tabernas, a DEM of ≤ 120 m resolution should be used in order to describe a rational drainage network system that could assure a realistic description of the smallest possible landform element in relation to major prevailing processes within these formations.
3. Geomorphometric indices are powerful tools to describe channel network structure properties and their bias and importance are widely related to the parameters they are made of. Moreover, these indices should form part of any quantitative description of the channel network morphology. However, the importance and significance of each attribute is to be evaluated in relation to the mode of validation and type of the test used in these processes. While in some cases few parameters may achieve significant conclusions, a wide range of descriptors is desirable in the description of fluvial systems, because geomorphometric indices are specialized parameters that may describe single or compound structure properties.
4. Stream network delineation is achieved by a critical threshold value (A_S). However, natural landscape dissection is widely related to extrinsic and intrinsic factors that should be taken into account in the delineation process, and hence simple or multiple critical A_S values are to be provided in relation to such factors.
5. The *adaptive model* is a powerful technique for depicting landscape dissection under varying conditions of landscape heterogeneity, being at the same time objective and easy to implement. Such capacity resides in the intrinsic properties that control its function. In addition, it could form an assessment index of hydrological unit similarities, where units of similar curve tendencies are comparable and may comprise the same prevailing features and processes.

6. Validation processes in channel networks should include quantitative and qualitative procedures that allow for a broad recognition of stream location and limits, as well as the dominant properties of stream network structure. In addition, type and form of the design-test used are of great importance because of the various factors that control stream channel initiation and even definition.
7. Geomorphometric parameters vary considerably with A_S values, and hence caution must be exercised in interpreting parameter variations.
8. The digitized-*BLs* provides a general guide and a reasonable source of information for hydrological and geomorphological studies, but also contains significant drawbacks that may lead to erroneous conclusions. The main shortcoming resides in the complete objectivity of stream limits definition leading, when compared to subjective approach, to considerable deficiencies and potential lost in automated extraction approaches. Hence, their use in validation processes should be combined with other sources of information to reduce such inconveniences mainly in first or even second order streams.
9. Channel initiation zones are fuzzy elements and their definition is related to the intrinsic and extrinsic factors that control their formation. Concretely, the initiation zone of stream head may contain particular characteristics of spatial variations that make it more susceptible to scale, resolution and the interpolation procedures used in the matrix-data construction. Thus, depending on the data type, DLSM or DEM, the influence of these factors can seriously affect the results of the semivariograms in relation to upstream area.
10. The capacity of LS data in depicting landform components provide a detail, reliable and accurate solution to real terrain representation (i.e. real landscape) in comparison to simulated ones of DEMs, mainly concerning the limits between components.
11. The semivariograms parameters (i.e. sill, range, nugget and type of fitted model) are powerful indicators of spatial variations within landscape components and hence landform limits. Not only the shape structure, but also the prevailing processes within these elements can be highlighted. Hence, water movement and redistribution within and between landforms are well explained under the geostatistical approach. The direct implications of such findings include the direct capacity of semivariograms as a validation procedures for landform elements, both shape and limits.
12. Landform elements revealed varying susceptibility to scale and resolution effect. While dominant convergence- or divergence-formations highlighted trivial effect, blurred or fuzzy formations, such as channel initiation zones, showed considerable alterations in relation to scale and resolution. Thus, scale of the sample dataset may conceal part of the landform spatial-properties leading to biased conclusions.

7.5. Suggestions for further research

Automated channel network extraction and stream limits delineation are widely related to DEM data structures, the critical threshold values and the validation approach used in their

comparison. All these factors were highlighted in this work, but it seems that more research is necessary to better understand and optimize their effect.

Stream and channel networks structure properties are best described by geometric, topologic, fractal, optimal, and complex properties, which should be taken into account in the delineation process. The adaptive model uses geometrical and topological characteristics, for which the integration of the remaining properties may enhance model function to approximate natural stream conditions.

The validation procedure is the main aspect to decide whether or not a particular drainage network extracted automatically is a reliable object. Usually, such a process is carried out by using a group of quantitative and/or qualitative properties that compares natural streams with the automatically delineated ones. While the latter is widely subjective and depends mainly on field visits and visual interpretations, the former, based on the use of the geomorphometric indices, seems to be the most objective in hydrological and geomorphological studies. The geomorphometric attributes are highly susceptible to errors and uncertainties of the DEMs data and to the A_s value used to extract and delineate the drainage network from which they defined. In published literature, little is found in relation to such problem and additional approaches may provide more lights over these effects.

The effect of DEM grid resolution was studied throughout the presented work in order to examine the model efficiency and to construct the best detailed drainage networks. But, little is underlined over the optimum resolution. Grid resolutions of 30-, 1-, 0.06-m were examined, and delineated drainage networks revealed that while considerable information can be gained, geomorphometric parameters showed to be sensitive not only to A_s value but also to the applied resolution. Moreover, the geospatial analysis highlighted considerable information on resolution effect and the presence of data redundancy at particular landform components. These observations confirm that it is possible to delineate landscape components within a multi-scale framework by changing the resolution where each element may be related to an appropriate resolution. Although several studies tackled on the optimum resolution (e.g. Artan et al., 2000; Thompson et al., 2001; Hancock, 2005), we believe that deeper insights are still needed in order to define a more realistic landscape, mainly the connection between optimum resolution and type of landscape element.

The *LST* provides valuable datasets for enhanced landform depiction, either quantitatively by providing a huge amount of digital points in a short time or qualitatively by the high precision of these data points. Such datasets should be submitted to complex processes of treatment (e.g. registration, filtering, etc.) that should be taken into account in the final desired product (e.g. DLSM, DEM or DTM). Moreover, the potential of these data is so far slightly examined and more studies are needed mainly in topographic applications and landscape quantification. Items, such as channel initiation properties, general and particular characteristics of relief components (i.e. grain and texture) at high details of centimetres, exact simple or multi fractal dimensions for prevailing landforms, water

movement and runoff generation and the effect of relief roughness at the plot scale, amount of error and uncertainties in data provided by other sources, between others should form part of future-lines investigation.

Finally, channel initiation zones or stream sources are highly complex structures and are widely affected by local factors of initial data resolution and related intrinsic and extrinsic factors. The former is underlined by the geomorphic control whereas the latter is related to the environmental conditions that lead to their actual shape structure. Herein, the geomorphic and visual perception of these areas is somewhat ambiguous, where the local relief and topographic contrasts seems to be determinant. However, theoretically, hillslope ends when convergent processes overcome the divergence domain and, hence direction of water movement is inherently to accumulate downward generating a runoff of sufficient energy to form a fine rill structure. These fingertips are just only appreciated at high topographic details and under particular soil characteristics (e.g. physically-altered soil structures). However, at lower details and resolutions rill initiation is slightly appreciated and the convergence/divergence process is still detached and stream sources are completely valid formations. While in landscape configuration, channel initiation zone may be considered as a homogeneous distinct entity with a unique fractal dimension, whereas their geomorphometric dimensions and spatial variations appear to be little predictable and highly scale dependent (i.e. cell dimension of the used DEM). These complexities, together with our current, far from complete, understanding of the exact prevailing processes, means that stream sources or, more precisely channel initiation zones are fuzzy element. Concretely, these are real when defined in relation to spatial structure variation underling the limits between prevailing process in the domain and fake elements when visualized in relation to shape structure under varying scales and resolutions.

BIBLIOGRAPHY

- Abellán, A. Jaboyedoff, M. Oppikofer, T. & Vilaplana, J.M. 2009. Detection of millimetric deformation using a terrestrial laser scanner: experiment and application to a rockfall event. *Natural Hazards and Earth System Sciences*, 9, pp: 365-372.
- Abellán, A. Vilaplana, J.M. & Martínez, J. 2006. Application of a long-range Terrestrial Laser Scanner to a detailed rockfall study at Vall de Núria (Eastern Pyrenees, Spain). *Engineering Geology*, 88(3-4), pp: 136-148.
- Abrahams, A.D. & Flint, J.J. 1983. Geological controls on the topological properties of some trellis channel networks. *Geological Society of America Bulletin*, 94(1), pp: 80-91.
- Abrahams, A.D. & Miller, A.J. 1982. The mixed gamma model for channel link lengths. *Water Resources Research*, 18(4), pp: 1126-1136.
- Abrahams, A.D. & Parsons, A.J. 1991. Relation between infiltration rate and stone cover on a semiarid hillslope, Southern Arizona. *Journal of Hydrology*, 122, pp: 49-59.
- Abrahams, A.D. 1972. Factor analysis of drainage basin properties: Evidence for stream abstraction accompanying the degradation of relief. *Water Resources Research*, 8, pp: 624-633.
- Abrahams, A.D. 1977. The factor of relief in the evolution of channel networks in mature drainage basins. *American Journal of Science*, 277(5), pp: 626-646.
- Abrahams, A.D. 1980. Channel Link Density and Ground Slope. *Analysis of the Association of American Geographers*, 70(1), pp: 80-93.
- Abrahams, A.D. 1984a. Channel Networks: A Geomorphological Perspective. *Water Resources Research*, 20(2), pp: 161-168.
- Abrahams, A.D. 1984b. Tributary development along winding streams. *American Journal of Science*, 284, pp: 863-892.
- Adediran, A.O. Parcharidis, I. Poscolieri, M. & Pavlopoulos, K. 2004. Computer-assisted discrimination of morphological units on north-central Crete (Greece) by applying multivariate statistics to local relief gradients. *Geomorphology*, 58, pp: 357-370.
- Afana, A. Del Barrio, G. & Puigdefábregas, J. 2003. Monitoring and Evaluation of Changes in Vegetation Density in Arid Zones: Implications and Involvements on Land Degradation. Edafología. Reference: RV5504/S.
- Aguilar, M.A. Aguilar, F.J. & Negreiros, J. 2009. Off-the-shelf laser scanning and close-range digital photogrammetry for measuring agricultural soils microrelief. *Biosystems Engineering*, 103(4), pp: 504-517.
- Alexander, R. & Millington, A.C. 2000. Vegetation Mapping: from patch to planet. John Wiley & Sons, Chichester. Pp. 339.

- Alexander, R.W. Harvey, A.M. Calvo, A. James P.A. & Cerdá, A. 1994. Natural stabilization mechanisms on badlands slopes: Tabernas, Almeria, Spain. In: Millington, C. & Pye, K. (eds.). *Environmental Change in Drylands: Biogeographical and Geomorphological Perspectives*. Wiley, Chichester, UK, pp: 85-111
- Allen, J.R.L. 1970. Physical processes of sedimentation. *Earth Science Series*, 1, Elsevier, New York, 248 p.
- Al-Manasir, K. & Fraser, C. 2006. Registration of terrestrial laser scanner data using imagery. *The Photogrammetric Record*, 21(115), pp: 255-268.
- Armstrong, J.S. 1969. Derivation of theory by means of Factor Analysis or Tom Swift and his electric Factor Analysis Machine. *American Statistician*, 21, pp: 17-23.
- Artan, G.A. Neal. C.M.U. & Tarboton, D.G. 2000. Characteristic length scale of input data in distributed models: Implications for modeling grid size. *Journal of Hydrology*, 227, pp: 128-139.
- Atkinson, P.M. 1997. Scale and spatial dependence. In Gardingen, P.R. Foody, G.M. & Curran, P.J. (eds.), *Scalling-Up from Cell to Landscape*. Cambridge University Press: pp: 35-60.
- Atkinson, P.M. Webster, R. & Curran, P.J. 1994. Cokriging with airborne MSS imagery. *Remote Sensing Environment*, 50, pp: 335-345.
- Bak, P. & Paczuski, M. 1995. Complexity, contingency, and criticality. *Proceedings of the National Academy of Sciences of the United State of America*, 92(15), pp: 6689-6696.
- Bak, P. Tang, C. & Wiesenfeld, K. 1987. Self-organized criticality: an example of $1/f$ noise. *Physical Review Letter*, 59, pp: 364-374.
- Bak, P. Tang, C. & Wiesenfeld, K. 1988. Self-organized criticality. *Physical Review A*, 38(1), pp: 364-374.
- Band, L.E. & Wood, E.F. 1988. Strategies for large-scale, distributed hydrologic-simulation. *Applied Mathematics and Computation*, 27(1), pp: 23-37.
- Band, L.E. 1986. Topographic partition of watersheds with digital elevation models. *Water Resources Research*, 22(1), pp: 15-24.
- Band, L.E. 1989. A Terrain-based watershed information systems. *Hydrological Processes*, 3, pp: 151-162.
- Band, L.E. 1999. Spatial hydrography and landforms. In: Longley, P.A. Goodchild, M.F. Maguire, D.J. & Rhind, D.W. (eds.), *Geographical Information Systems: Principles, Techniques, Managements and Applications*. New York: John Wiley & Sons, 2nd edition, pp: 527-542.
- Bastin, L. Fisher, P.F. & Wood, J. 2002. Visualizing uncertainty in multi-spectral remotely sensed imagery. *Computers & Geosciences*, 28(3), pp: 337-350.
- Bates, R.L. & Jackson, J.A. (Eds.) 2005. *Glossory of geology*. 5th edition. American Geological Institute, NewYork.
- Bauer, A. Paar, G. & Kaltenböck, A. 2005. Mass movement monitoring using Terrestrial Laser Scanner for rock fall management. In: Oosterom, P.V. Zlatanova, S. & Fendel, E.M. (eds.), *Geo-information for Disaster Management*. Springer, Berlin, pp: 393-406.

- Beauvais, A.A. & Montgomery, D.R. 1996. Influence of valley type on the scaling properties of river planforms. *Water Resources Research*, 32(5), pp: 1441-1448.
- Bellian, J.A. Kerans, C. & Jennette, D.C. 2005. Digital outcrop models: application of terrestrial scanning LiDAR technology to monitor landslide in stratigraphic modelling. *Journal of Sedimentary Research*, 75(2), pp: 166-167.
- Besl, P.J. & McKay, N.D. 1992. A method for registration of 3-D shapes. *IEEE Transactions on Pattern Analysis and Machine Intelligence*, 14(2), pp: 239-256.
- Betts, H.D. & DeRose, R.C. 1999. Digital elevation models as a tool for monitoring and measuring gully erosion. *International Journal of Applied Earth Observation and Geoinformation*, 1(2), pp: 91-101.
- Beven, K. & Wood, E.F. 1983. Catchment geomorphology and the dynamics of runoff contributing areas. *Journal of Hydrology*, 65(1-3), pp: 139-158.
- Beven, K.J. & Kirkby, M.J. 1979. A physically-based, variable contributing area model of basin hydrology. *Hydrological Science Bulletin*, 24, pp: 43-69.
- Beven, K.J. & Moore, I.D. 1993. *Terrain Analysis and Distributed Modelling in Hydrology*. Wiley, New York.
- Beven, K.J. 1989. Changing ideas in hydrology: the case of physically-based models. *Journal of Hydrology*, 105, pp: 157-172.
- Beven, K.J. 1995. Linking parameters across scales: Sub-grid parameterizations and scale dependent hydrological models. *Hydrological Processes*, 9(5-6), pp: 507-525.
- Beven, K.J. 2002. Towards an alternative blueprint for a physically based digitally simulated hydrologic response modelling system. *Hydrological Processes*, 16(2), pp: 189-206.
- Biasion, A. Bornaz, L. & Rinaudo, F. 2005. Laser Scanning Applications on Disaster Management. In: Van Oosterom, P. Zlatanova, S. & Fendel, E.M. (eds.), *Geo-information for Disaster Management*. Springer, Berlin, pp: 19-33.
- Bischetti, G.B. Gandolfi, C. & Whelan, M.J. 1998. The definition of stream channel head location using digital elevation data. *Hydrology, Water Resources and Ecology in Headwaters*, Proceedings of the HeadWater Conference
- Bishop, T.F.A. & McBratney, A.B. 2002. Creating Field Extent Digital Elevation Models for Precision Agriculture. *Precision Agriculture*, 3(1), pp: 37-46.
- Bitelli, G. Dubbini, M. & Zanutta, A. 2004. Terrestrial laser scanning and digital photogrammetry techniques to monitor landslide bodies. In *Proceedings of the XXth ISPRS Congress*, Istanbul: 6.
- Blöeschl, G. & Sivapalan, M. 1995. Scale issues in hydrological modeling: A review. *Hydrological Processes*, 9(3-4), pp: 251-290.
- Blöschl, G. & Grayson, R. 2002. Spatial observations and interpolation. In: Grayson, R. & Blöschl, G. (eds.), *Spatial patterns in catchment hydrology: observations and modelling*. Cambridge University Press, Cambridge, pp: 17-50.

- Bocco, G. 1991. Gully erosion: process and models. *Progress in Physical Geography*, 15, pp: 392-406.
- Boehler, W. & Marbs, A. 2003. Investigating Laser Scanner Accuracy. WWW: <http://scanning.fh-mainz.de>.
- Boer, M. & Puigdefábregas, J. 2004. Effects of spatially structured vegetation patterns on hillslope erosion in a semiarid Mediterranean environment: a simulation study. *Earth Surface Processes and Landforms*, 30, pp: 149-167.
- Bolongaro-Crevenna, A. Torres-Rodríguez, V. Sorani, V. Frame, D. & Arturo, M.O. 2005. Geomorphometric analysis for characterizing landforms in Morelos State, Mexico. *Geomorphology*, 67(3-4), pp: 407-422.
- Bourennane, H. King, D. Chery, P. Bruand, A. 1996. Improving the kriging of a soil variable using slope gradient as external drift. *European Journal of Soil Science*, 47, pp: 473-483.
- Brändli, M. 1996: Hierarchical models for the definition and extraction of terrain features. In Burrough, P. & Frank, A.U. (eds.), *Natural objects with indeterminate boundaries*. Taylor & Francis, London, pp. 257–70.
- Brandt, C.J. & Thornes, J.B. 1996. *Mediterranean Desertification and Land Use*. Wiley, Chichester, UK.
- Brasington, J. Langham, J. & Rumsby, B. 2003. Methodological sensitivity of morphometric estimates of coarse fluvial sediment transport. *Geomorphology*, 53(3-4), pp: 299-316.
- Brassel, K.E. & Weibel, R. 1988. A review and conceptual framework of automated map generalization. *International Journal of Geographical Information Science*, 2(3), pp: 229-244.
- Breilinger, R. Duster, H. & Weingartner, R. 1993. Methods of catchment characterization by means of basin parameters (assisted by GIS) - empirical report from Switzerland: Report - UK Institute of Hydrology, v. 120, pp: 171-181.
- Brenner, C. Dold, C. & Ripperda, N. 2008. Coarse orientation of terrestrial laser scans in urban environments. *ISPRS Journal of Photogrammetry and Remote Sensing*, 63, pp: 4-18.
- Broscoe, A.J. 1959. *Quantitative Analysis of Longitudinal Stream Profiles of Small Watersheds*. Office of Naval Research, Project NR 389-042, Technical Report No. 18, Department of Geology, Columbia University, New York.
- Brown, D.G. & Bara, T.J. 1994. Recognition and reduction of systematic error in elevation and derivative surfaces from 7 1/2-minute DEMs. *Photogrammetric Engineering and Remote Sensing*, 60(2), pp: 189-194.
- Bruneau, P. Gascuel-Oudou, C. Robin, P. Merot, P. & Beven, K. 1995. Sensitivity to space and time resolution of a hydrological model using digital elevation data. *Hydrological Processes*, 9, pp: 69-81.
- Brzank, A. Heipke, C. Geopfert, J. & Soergel, U. 2008. Aspects of generating precise digital terrain models in the Wadden Sea from lidar-water classification and structure line extraction. *Photogrammetry & Remote Sensing*, 63, pp: 510-528.
- Buckley, S.J. Howell, J.A. Enge, H.D. & Kurz, T.H. 2008. Terrestrial laser scanning in geology: data acquisition, processing and accuracy consideration. *Journal of the Geological Society*, 165, pp: 625-638.

- Bull, L.J. & Kirkby, M.J. 2002. Channel heads and channel extension. In: Bull, L.J. & Kirkby, M.J. (eds), *Dryland Rivers: Hydrology and Geomorphology of Semi-arid Channels*. John Wiley and Sons: Chichester, pp: 263-298.
- Bull, W.B. 1979. Threshold of critical power in streams. *Geological Society of America Bulletin*, 90(5), pp: 453-464.
- Burgess, J.A. 1990. The sorties paradox and higher-order vagueness. *Synthese*, 85(3), pp: 417-74.
- Burrough, P.A. & McDonnell, R.A. 1998. *Principles of Geographical Information Systems*, Oxford, Oxford University Press.
- Burrough, P.A. 1981. Fractal dimensions of landscapes and other environmental data. *Nature*, 294, pp: 240-242.
- Burrough, P.A. 1983. Multiscale sources of spatial variation in soil. I. The application of fractal concepts to nested levels of soil variation. *European Journal of Soil Science*, 34(3), pp: 577-597.
- Burrough, P.A. GIS and geostatistics: Essential patterns for spatial analysis. *Environmental and Ecological Statistics*, 8, pp: 361-377.
- Cai, X. & Wang, D. 2006. Spatial autocorrelation of topographic index in catchments. *Journal of Hydrology*, 328, pp: 581-591.
- Calver, A. 1978. Modelling drainage headwater development. *Earth Surface Processes*, 3(3), pp: 233-241.
- Cantón, Y. 1999. Efectos hidrológicos y geomorfológicos de la cubierta y propiedades del suelo en paisaje de cárcavas. PhD Thesis, University of Almería, Spain, pp. 210.
- Cantón, Y. Del Barrio, G. Solé-Benet, A. & Lázaro, R. 2004. Topographic controls on the spatial distribution of ground cover in the Tabernas Badlands of SE Spain. *Catena*, 55, pp: 341-365.
- Cantón, Y. Domingo, F. Solé-Benet, A. & Puigdefábregas, J. 2001. Hydrological and erosion response of a badlands system in semi-arid SE Spain. *Journal of Hydrology*, 252, pp: 65-84.
- Cantón, Y. Solé-Benet, A. & Lázaro, R. 2003. Soil-geomorphology relations in gypsiferous materials of the Tabernas desert (Almería, SE Spain). *Geoderma*, 115(3-4), pp: 193-222.
- Cantón, Y. Solé-Benet, A. de Vente, J. Boix-Fayos, C. Calvo-Cases, A. Asensio, C. & Puigdefábregas, J. 2011. A review of runoff generation and soil erosion across scales in semiarid south-eastern Spain. *Journal of Arid Environments*, in press.
- Cantón, Y. Solé-Benet, A. Queralt-Mitjans, I. & Pini, R. 2001. Weathering of a gypsum-calcareous mudstone under semi-arid environment at Tabernas, SE Spain: laboratory and field-based experimental approaches, *Catena*, 44, pp: 111-132.
- Carbonneau, P.E. Lane, S.N. & Bergeron, N.E. 2003. Cost-effective non-metric close-range digital photogrammetry and its application to a study of coarse gravel river beds. *International Journal of Remote Sensing*, 24(14), pp: 2837-2854.
- Carter, J.R. 1988. Digital representation of topographic surfaces. *Photogrammetric Engineering and Remote Sensing*, 54(11), pp: 1577-1580.

- Castillo, S.V. 1986. Caracterización morfológica de los paisajes fluviales madrileños. *Papeles de Geografía Física*, 11, pp: 53-62.
- Cavalli, M. Tarolli, P. Marchi, L. & Fontana, G.D. 2008. The effectiveness of airborne LiDAR data in the recognition of channel-bed morphology. *Catena*, 73, pp: 249-260.
- Cayley, A. 1859. On contour and slope lines. *The London, Edinburgh, and Dublin Philosophical Magazine and Journal of Science*. XVIII, pp: 264-268.
- Cerdan, O. Le Bissonnais, Y. Govers, G. Lecomte, V. van Oost, K. Couturier, A. King, C. & Dubreuil, N. 2004. Scale effect on runoff from experimental plots to catchments in agricultural areas in Normandy. *Journal of Hydrology*, 299(1-2), pp: 4-14.
- Chandler, J. 1999. Technical communication effective application of automated digital photogrammetry for geomorphological research. *Earth Surface Processes and Landforms*, 24, pp: 51-63.
- Chang, H.H. 1988. *Fluvial Processes in River Engineering*. John Wiley & Sons, New York, pp. 432.
- Chapman, C.A. 1952. A new quantitative method of topographic analysis. *American Journal of Science*, 250, pp: 428-452.
- Chappell, A. & Agnew, C.T. 2001. Geostatistical analysis of west African Sahel Rainfall. In: Conacher, A. (eds.), *Land Degradation*. Kluwer, Dordrecht, pp: 19-36.
- Chappell, A. & Oliver, M.A. 2000. Using geostatistics to improve ¹³⁷Cs-derived net soil flux maps. In: Foster, I.D.L. (eds.), *Tracers in Geomorphology*. Wiley: Chichester; pp: 221-240.
- Chappell, A. 1996. Modelling the spatial variation of processes in the redistribution of soil: digital terrain models and ¹³⁷Cs in southwest Niger. *Geomorphology*, 17, pp: 249-261.
- Chappell, A. 1998. Mapping ¹³⁷Cs-derived net soil flux using remote sensing and geostatistics. *Journal of Arid Environments*, 39, pp: 441-455.
- Chappell, A. Heritage, G.L. Fuller, I.C. Large, A.R.G. & Milan, D.J. 2003. Geostatistical analysis of ground-survey elevation data to elucidate spatial and temporal river channel change. *Earth Surface Processes and Landforms*, 28, pp: 349-370.
- Chappell, A. Oliver, M.A. Warren, A. Agnew, C.T. & Charlton, M. 1996. Examining the factors controlling the spatial scale of variation in soil redistribution processes from south-west Niger. In: Anderson, M.G. & Brooks, S.M. (eds.), *Advances in Hillslope Processes*. Wiley: Chichester; pp: 429-449.
- Chappell, A. Seaquist, J.W. & Eklundh, L.R. 2001. Improving geostatistical noise estimation in NOAA AVHRR NDVI images. *International Journal of Remote Sensing*, 22(6): pp: 1067-1080.
- Chaubey, I. Cotter, A.S. Costello, T.A. & Soerens, T.S. 2005. Effect of DEM data resolution on SWAT output uncertainty. *Hydrological Processes*, 19(3), pp: 621-628.
- Chorley, R.J. & Beckinsale, R.P. 1980. Gilbert's Geomorphology. In: Yochelson, E.L. (eds.), *The Scientific ideas of G.K. Gilbert*. *Geological Society of America Special Paper*, 183, pp: 129-142.

- Chorley, R.J. & Dale, P.F. 1972. Cartographic problems in stream channel delineation. *Cartography*, 7, pp: 150-162.
- Chorley, R.J. Malm, D.E. & Pogorzelski, H.A. 1957. A new standard for estimating drainage basin shape. *American Journal of Science*, 255(2), pp: 138-141.
- Chorley, R.J. Schumm, S.A. & Sugden, D.E. 1984. *Geomorphology*. Methuen, London, pp. 605.
- Chorowicz, J. Ichoku, C. Riazanoff, S. Kim, Y. & Cervelle, B. 1992. A combined algorithm for automated drainage network extraction. *Water Resources Research*, 28, pp: 1293-1302.
- Clarke, J.I. 1966. Morphometry from maps. In: Dury, G.H. (eds.), *Essays in geomorphology*. Elsevier, London, pp: 235-274.
- Coates, D.R. 1958. Quantitative geomorphology of small drainage basins in southern Indiana. Technical Report, No. 10, Nevada Research Project, Department of Geology, Columbia University, New York, USA.
- Coffman, D.M. Keller, E.A. & Melhorn, W.N. 1972. New topologic relationship as an indicator of drainage network evolution. *Water Resources Research*, 8(6), pp: 1497-1505.
- Coniglio, A. & Zannetti, M. 1989. Multiscaling and multifractality. *Physica D*, 38, pp: 37-40.
- Costa-Cabral, M.C. & Burges, S.J. 1994. Digital Elevation Model Networks (DEMON): A Model of Flow Over Hillslopes for Computation of Contributing and Dispersal Areas. *Water Resources Research*, 30(6), pp: 1681-1692.
- Cox, K.G. 1989. The role of mantle plumes in the development of continental drainage patterns. *Nature*, 342, pp: 873-877.
- Crave, A. & Davy, P. 1997. Scaling relationships of channel networks at large scales: Examples from two large-magnitude watersheds in Brittany, France. *Tectonophysics*, 269, pp: 91-111.
- Creed, I.F. Sanford, S.E. Beall, F.D. Molot, L.A. & Dillon, P.J. 2003. Cryptic wetlands: integrating hidden wetlands in regression models of the export of dissolved organic carbon from forested landscapes. *Hydrological Processes*, 17(18), pp: 3629-3648.
- Cressie, N. 1985. Fitting variogram models by weighted least squares. *Mathematical Geology*, 17(5), pp: 563-586.
- Curran, P. Foody, G. M. & van Gardigen, P.R. 1997. Scaling-up. In: van Gardigen, P.R. Foody, G. M. & Curran, P. (eds.). *Scaling-up: from cell to landscape*. Cambridge: Cambridge University Press, pp: 1-5.
- Curran, P.J. 1988. The semivariogram in remote sensing: An introduction. *Remote Sensing of Environment*, 24, pp: 493-507.
- Da Ros, D. & Borga, M. 1997. Use of Digital Elevation Model data for the derivation of the geomorphological instantaneous unit hydrograph. *Hydrological Processes*, 11(1), pp: 13-33.
- Daniel, M. Willsky, A. McLaughlin, D. & Rossi, D. 1995. A multi-resolution approach for imaging hydraulic conductivity. *International Conference on Image Processing (ICIP'95)*, 1, pp: 637-640.

- Darnell, A.R. Tate, N.J. & Brunson, C. 2008. A tool for assessing error in digital elevation models from a user's perspective. *Computers Environment and Urban Systems*, 32(4), pp: 268-277.
- Darwin, C. 1968. *The Origin of Species by Means of Natural Selection*, First Edition. (Reprint) London: Penguin. First published 1859. London: John Murray.
- Davis, J.C. 2002. *Statistics and Data Analysis in Geology*. Third Edition, John Wiley and Sons.
- Davis, W.M. 1899. The Geographical Cycle. *Geographical Journal*, 14, pp: 423-434.
- Davis, W.M. 1909. *Geographical essays*, Ginn, Boston (republished) 1954, Dover, New York.
- De Bartolo, S.G. Gabriele, S. & Gaudio. R. 2000. Multifractal behavior of river networks. *Hydrology and Earth System Sciences*, 4(1), pp: 105-112.
- De Bartolo, S.G. Gaudio, R. & Gabriele, S. 2004. Multifractal analysis of river networks: a sand-box approach, *Water Resources Research*, 40, p. W02201, doi:10.1029/2003WR002760.
- De Bartolo, S.G. Veltri, M. & Primavera, L. 2006. Estimated generalized dimensions of river networks. *Journal of Hydrology*, 322, pp: 181-191.
- De Pedraza, G.J. 1996. *Geomorfología: principios, métodos y aplicaciones*. Rueda,
- DeBarry, P.A. 2004. *Watersheds: Processes, Assessment and Management*. John Wiley & Sons, New Jersey, USA.
- Dehn, M. Gärtner, H. & Dikau, R. 2001. Principles of semantic modeling of landform structures. *Computers & Geosciences*, 27, pp: 1005-1010
- Del Barrio, G. Alvera, B. & Díez, J.C. 1993: The choice of cell size in Digital Terrain Models: an objective method. In: Robinson, M. (eds.), *Methods of Hydrological Basin Comparison*. Institute of Hydrology, IH Report 120, Wallingford, pp: 190-196.
- Deng, Y. Chen, X. Chuvieco, E. Warner, T. & Wilson, J.P. 2007. Multi-scale linkages between topographic attributes and vegetation indices in a mountainous landscape. *Remote Sensing of Environment*, 111(1), pp: 122-134.
- Desmet, P.J.J. 1997. Effects of interpolation errors on the analysis of DEMs. *Earth Surface Processes and Landforms*, 22, pp: 563-580.
- Deutsch, C.V. & Wang, L.B. 1996. Hierarchical object-based stochastic modeling of fluvial reservoirs. *Mathematical Geology*, 28, pp: 857-880.
- Devereux, B. & Amable, G. 2009. Airborne LiDAR: Instrumentation, Data Acquisition and Handling, in: Heritage, G.L. & Large, A.R.G. (eds.), *Laser Scanning for the Environmental Sciences*, Wiley-Blackwell, Oxford, UK.
- Dietrich, W.E. & Dune, T. 1993. The channel head. In: Beven, K. & Kirkby, M.J. (eds.), *Channel Network Hydrology*. John Wiley & Sons Ltd, Chichester, pp: 175-219.
- Dietrich, W.E. Wilson, C. Montgomery, D. & Mckean, J. 1993. Analysis of erosion thresholds, channel networks and landscape morphology using a digital terrain model. *Journal of Geology*, 101, pp: 259-278.

- Dietrich, W.E. Wilson, C.J. Montgomery, D.R. McKean, L. & Bauer, R. 1992. Erosion thresholds and land surface morphology. *Geology*, 20, pp: 675-679.
- Dikau, R. 1989. The Application of Digital Relief Model to Landform Analysis in Geomorphology. In: Raper, J. (eds.), *Three Dimensional Applications in Geographical Information Systems*. Taylor & Francis, London. pp: 51-77.
- Dikau, R. Brabb, E.E. Mark, R.K. & Pike, R.J. 1995. Morphometric landform analysis of New Mexico. *Zeitschrift für Geomorphologie*, Supplement Band, 10, pp: 109-126.
- Döll, P. & Lehner, B. 2002. Validation of a new global 30-min drainage direction map. *Journal of Hydrology*, 258(1-4), pp: 214-231.
- Drăguț, L. & Blaschke, T. 2006. Automated classification of landform elements using object-based image analysis. *Geomorphology*, 81(3-4), pp: 330-344.
- Dungan, J.L. Perry, J.N. Dale, M.R.T. Legendre, P. Citron-Pousty, S. Fortin, M.-J. Jakomulska, A. Miriti, M. and Rosenberg. M.S. 2002. A balanced view of scale in spatial statistical analysis. *Ecography*, 25, pp: 626-640.
- Dunne, T. & Leopold, L.B. 1978, *Water in Environmental Planning*. San Francisco, W.H. Freeman Co. pp.818.
- Dunne, T. 1980. Formations and controls of channel networks. *Progress in Physical Geography*, 4, pp: 211-239.
- Dunning, S.A. Massey, C.I. & Rosser, N.J. 2009. Structural and geomorphological features of landslides in the Bhutan Himalaya derived from Terrestrial Laser Scanning. *Geomorphology*, 103, pp: 17-29.
- Ebisemiju, F.S. 1979a. A reduced rank model of drainage basin morphology. *Geografiska Annaler. Series A, Physical Geography*, 61(1/2), pp: 103-112.
- Ebisemiju, F.S. 1979b. An objective criterion for the selection of representative basins. *Water Resources Research*, 15(1), pp: 148-158.
- Etzelmqller, B. Sulebak, J.R. 2000. Developments in the use of Digital Elevation Models in periglacial geomorphology and glaciology. *Physische Geographie*, 41, pp: 35-58.
- Evans, I.S. 1972. General geomorphometry, derivatives of altitude, and descriptive statistics. In: Chorley, R.J. (eds.), *Spatial Analysis in Geomorphology*. Methuen & Co. Ltd. London, pp: 17-90.
- Evans, I.S. 1980. An integrated system of terrain analysis and slope mapping. *Zeitschrift für Geomorphologie*, 36, pp: 274-295.
- Evans, I.S. 1984. Correlation structures and factor analysis in the investigation of data dimensionality: statistical properties of the Wessex land surface, England, *International Symposium on Spatial Data Handling*, Zurich, 1, pp: 98-116.
- Evans, I.S. Dikau, R. Tokunaga, E. Ohmari, H. & Hirano, M. 2003. Concepts and modelling in geomorphology: International perspectives. TERRAPUB, Tokyo.
- Fairfield, J. & Leymarie, P. 1991. Drainage networks from grid digital elevation models. *Water Resources Research*, 27 (5), pp: 709-717.

- FAO-ISRIC-ISSS, 1998. World Reference Base for Soil Resources. FAO Soils Bulletin No. 84. FAO, Rome, p. 88.
- Felicísimo, A.M. 1994. A parametric statistical method for error detection in digital elevation models. *ISPRS Journal of Photogrammetry and Remote Sensing*, 49(4), pp: 29-33.
- Felicísimo, A.M. 1996. Modelos digitales del terreno. Introducción y aplicaciones en ciencias ambientales. WWW: <http://www.etsimo.uniovi.es/~feli/TextosP.html>.
- Felicísimo, A.M. Cuartero, A. & Ariza, F.J. 1995. A method for the improvement elevation data generated from automated photogrammetric methods into SIS. Commission VI, WG VI/4.
- Fisher, P. 1993. Algorithm and implementation uncertainty in viewshed analysis. *International Journal of Geographical Information Systems*, 7(4), pp: 331-34.
- Fisher, P. 1998. Improved Modelling of elevation error with geostatistics. *GeoInformatica*, 2, pp: 215-233.
- Fisher, P. Wood, J. & Cheng, T. 2004. Where is Helvellyn? Fuzziness of Multiscale Landscape Morphometry. *Transactions of the Institute of British Geographers*, 29(1), pp: 106-128.
- Fix, R.E. & Burt, T.P. 1995. Global positioning system: An effective way to map a small area or catchment. *Earth Surface Processes and Landforms*, 20(9), pp: 817-827.
- Flint, J.J. & Proctor, J.R. 1979. Tributary diameter in topologically random channel networks. *Water Resources Research*, 15(2), pp: 484-486.
- Flint, J.J. 1974. Stream gradient as a function of order, magnitude, and discharge. *Water Resources Research*, 10(5), pp: 969-973.
- Florinsky, I.V. 1998. Accuracy of local topographic variables derived from digital elevation models. *International Journal of Geographical Information Science*, 12(1), pp: 47-61
- Food Agricultural Organization. 1977. Guías para la descripción de perfiles de suelos. Technical Report, FAO.
- Foody, G.M. & Curran, P.J. 1994. Scale and environmental remote sensing. In: Foody, G.M. & Curran, P.J. (eds.), *Environmental Remote Sensing from Regional to Global Scales*. Chichester: Wiley, pp: 223-232.
- Freeman, T.G. 1991. Calculating catchment area with divergent flow based on a regular grid. *Computers & Geosciences*, 17(3), pp: 413-422.
- Fröhlich, C. & Mettenleiter, M. 2004. Terrestrial Laser Scanning – New Perspectives in 3D Surveying. In: Thies, M. Koch, B. Spiecker, H. Weinacker, H. (eds.), *Laser-Scanners for Forest and Landscape Assessment*. International Archives of Photogrammetry, Remote Sensing and Spatial Information Sciences Vol. XXXVI-8/W2.
- Gallant, J.C. & Dowling, T.I. 2003. A multiresolution index of valley bottom flatness for mapping depositional areas. *Water Resources Research*, 39, pp: 1347-1360.
- Gallant, J.C. & Wilson, J.P. 2000. Primary topographic attributes. In: Wilson, J.P. & Gallant, J.C. (eds.), *Terrain Analysis: Principles and Applications*. New York, Wiley: pp 51-72.

- Gallant, J.C. Moore, I.D. Hutchinson, M.F. Gessler, P. 1994. Estimating Fractal Dimension of Profiles - A Comparison of Methods. *Mathematical Geology*, 26(4), pp: 455-481.
- Gallart, F. Solé-Benet, A. Puigdefábregas, J. & Lázaro, R. 2002. Badland Systems in the Mediterranean. In: Bull, L. & Kirkby, M.J. (eds.), *Dryland Rivers: hydrology and geomorphology of semi-arid channels*. John Wiley & Sons, pp: 299-326.
- Gandolfi, C. & Bischetti, G.B. 1997. Influence of the drainage network identification method on geomorphological properties and hydrological response. *Hydrological Processes*, 11, pp: 353-375.
- Garbrecht, J. & Martz, L.W. 1994. Grid Size Dependency of Parameters Extracted from Digital Elevation Models. *Computers and Geosciences*, 20(1), pp: 85-87.
- Garbrecht, J. & Martz, L.W. 2000. Digital elevation model issues in water resources modeling. In: Maidment, D.D. (eds.), *Hydrologic and hydraulic modelling support with geographic information systems*. Redlands, CA: ESRI Press, pp: 1-27
- Gatzliolis, D. & Fried, J.S. 2004. Adding Gaussian noise to inaccurate digital elevation models improves spatial fidelity of derived drainage networks. *Water Resources Research*, 40, W02508, doi:10.1029/2002WR001735.
- Gerla, P.J. 1999. Estimating the ground-water contribution in wetlands using modelling and digital terrain analysis. *Wetlands*, 19, pp: 394-402.
- Gessler, P.E. McKenzie, N.J. & Hutchinson, M.F. 1996. Progress in soil-landscape modeling and spatial prediction of soil attributes for environmental models. In: NCGIA (eds.), *Third International Conference/Workshop on Integrating GIS and Environmental Modelling*. Santa Barbara, CA: University of California, National Center for Geographic Information and Analysis (NCGIA).
- Ghose, B. Pandey, S. Singh, S. & Lal, G. 1967. Quantitative geomorphology of drainage basins in the central Luni basin in western Rajasthan. *Zeitschrift Für Geomorphologie*, 11, pp: 146-160.
- Gilbert, G.K. 1909. The convexity of hillslopes. *Journal of Geology*, 17, pp: 344-350.
- Gilbert, L.E. 1989. Are topographic data sets fractal? *Pure and Applied Geophysics*, 131(1-2), pp: 241-254.
- Gilvear, D.J. & Bryant, R. 2003. Analysis of aerial photography and other remotely sensed data. In: Kondolf, G.M. & Piégay, H. (eds.), *Tools in Fluvial Geomorphology*. Wiley: New York. pp: 135-170.
- Glock, W.S. 1931. The development of the drainage systems and the dynamic cycle. *The Ohio Journal of Science*, 31(5), pp: 309-334.
- Goodchild, S. 2008. *Geospatial Analysis - a comprehensive guide*. 2nd edition, Longley.
- Goolchild, M.F. & Mark, D.M. 1987. The fractal nature of the geographic phenomena. *Annals of the Association of the American Geographers*, 77(2), pp: 265-278.
- Gooverts, P. 1997. *Geostatistics for natural resources evaluation*. Oxford University Press, New York, NY.
- Gousie, M.B. 2005. Digital Elevation Model Error Detection and Visualization. In: Gold, C. (eds.), *The 4th Workshop on Dynamic & Multi-dimensional GIS*. Pontypridd, Wales, UK, ISPRS, pp: 42-46.
- Gower, J.C. 1971. A General Coefficient of similarity and some of its properties. *Biometrics*, 27(4), pp: 857-871.

- Graham, S.T. Famiglietti, J.S. Maidment, D.R. 1999. Five-minute, 1/2, and 1 degree data sets of continental watersheds and river networks for use in regional and global hydrologic and climate system modelling studies. *Water Resources Research*, 35, pp: 583-587.
- Gray, D.M. 1961. Interrelationships of watershed characteristics. *Journal of Geophysical Research*, 66(4), pp: 1215-1223.
- Grayson, R.B. & Blöschl, G. 2000. Spatial patterns in hydrological processes: observations and modelling. Cambridge, UK: Cambridge University Press.
- Grayson, R.B. Blöschl, G. Barling R.D. & Moore, I.D. 1993. Process, scale and constraints to hydrologic modeling in GIS. In: Kovar, K. & Nachtnebel, H.P. (eds.), Application of Geographic Information Systems in Hydrology and Water Resources. Proceedings of the HydroGIS 93 held in Vienna, April. Willingford, UK. International Association of Hydrogeological Sciences Publication No. 211, pp: 83-92.
- Grayson, R.B. Moore, I.D. & McMoahn, T.A. 1992a. Physically based hydrological modelling: 1. A terrain based model for investigative purpose. *Water Resources Research*, 28(10), pp: 2639-2658.
- Grayson, R.B. Moore, I.D. & McMoahn, T.A. 1992b. Physically based hydrological modelling: 2. Is the concept realistic? *Water Resources Research*, 28(10), pp: 2659-2666.
- Gregory, K.J. & Gardiner, V. 1975. Drainage density and climate. *Zeitschrift Für Geomorphologie*, 19, pp: 287-298.
- Gregory, K.J. 1976. Drainage networks and climate. In: Derbyshire, E. (eds.), Geomorphology and Climate. John Wiley, New York, pp: 289-315.
- Gruber, S. & Peckham, S. 2009. Land-Surface Parameters and Objects in Hydrology. *Developments in Soil Science*, 33, pp: 171-194
- Gruen, A. & Akca, D. 2005. Least squares 3D surface and curve matching. *ISPRS Journal of Photogrammetry and Remote Sensing*, 59(3), pp: 151-174.
- Gupta, V.K. & Waymire, E. 1989. Statistical self-similarity in river networks parameterized by elevation. *Water Resources Research*, 25(3), pp: 463-476.
- Gupta, V.K. Waymire, E. & Rodriguez-Iturbe, I. 1986. On scale, gravity and network structure in basin runoff. In: Gupta, V.K. Rodriguez-Iturbe, I. & Wood, E.F. (eds.), Scale problems in hydrology. Reidel, Dordrecht, pp: 159-184.
- Gurnell, A.M. 1997. Channel change on the River Dee meanders, 1946-1992, from the analysis of air photographs. *Regulated Rivers Research and Management*, 13, pp: 13-26.
- Guth, P.L. 2003. Eigenvector Analysis of Digital Elevation Models in a GIS: Geomorphometry and Quality Control. In: Evans, I.S. Dikau, R. Tokunaga, E. Ohmari, H. & Hirano, M. (eds.), Concepts and modelling in geomorphology: International perspectives. TERRAPUB, Tokyo.
- Gutiérrez, E.M. 1994. Geomorfología de España, Editorial Rueda.

- Gutiérrez, L.C. 2000. Estructura y Productividad en la Vegetación de Estepa Mediterránea Semiárida en Relación con la Variabilidad Climática: El Sistema de Ladera en Rambla Honda (Almería). Estación Experimental De Zonas Áridas (CSIC). Almería, Spain.
- Gyasi-Agyei, Y. Willgoose, G. & De Troch, F.P. 1995. Effects of vertical resolution and map scale of digital elevation models on geomorphological parameters used in hydrology. *Hydrological Processes*, 3(4), pp: 363-382.
- Hack, J.T. 1957. Studies of longitudinal stream profiles in Virginia and Maryland: U.S. Geological Survey Professional Paper 294-B, 97p.
- Haila, Y. 2002. Scaling environmental issues: problems and paradoxes. *Landscape & Urban Planning*, 61, pp: 59-69.
- Halsey, T.C. Meakin, P. & Procaccia, I. 1986. Scaling structure of the surface layer of diffusion-limited aggregates. *Physical Review Letters*, 56, pp: 854-857.
- Hamond, E.H. 1965. What is a landform? Some further comments. *The Professional Geographer*, 17(3), pp: 12-14.
- Hancock, G.R. & Evans, K.G. 2006. Channel head location and characteristics using digital elevation models. *Earth Surface Processes and Landforms*, 31, pp: 809-824.
- Hancock, G.R. & Willgoose, G.R. 2002. The use of a landscape simulator in the validation of the SIBERIA landscape evolution model: transient landforms. *Earth Surface Processes and Landforms*, 27(12), pp: 1321-1334.
- Hancock, G.R. 2005. The use of DEMs in the identification and characterization of catchments over different grid scales. *Hydrological Processes*, 19, pp: 1727-1749.
- Harvey, A.M. 1984a. Aggradation and dissection sequences on Spanish alluvial fans: influence on morphological development. *Catena*, 11, pp: 289-304.
- Harvey, A.M. 1984b. Geomorphological response to an extreme flood: a case from SE Spain. *Earth Surface Processes and Landforms*, 9, pp: 267-279.
- Harvey, A.M. 1987. Patterns of Quaternary aggradational and dissectional landform development in the Almería region, southeast Spain: a dry-region, tectonically active landscape. *Die Erde*, 118, pp: 193-215.
- Harvey, A.M. 1996. The role of alluvial fans in mountain fluvial systems of southeast Spain: implications of climatic change. *Earth Surface Processes and Landforms*, 21, pp: 543-553.
- Harvey, A.M. 2002. Effective timescales of coupling in fluvial systems. In: Gupta, A. (eds.), *Geomorphology on Large Rivers*. *Geomorphology*, 44, pp: 175-201.
- Harvey, A.M. Foster, G. Hannam, J. & Mather, A.E. 2003. The Tabernas alluvial fan and lake system, southeast Spain: applications of mineral magnetic and pedogenic iron oxide analyses towards clarifying the Quaternary sediment sequences. *Geomorphology*, 50, pp: 151-171.

- Hehn, M. Gärtner, H. & Dikau, R. 2001. Principles of semantic modeling of landform structures. *Computer & Geoscience*, 27, pp: 1005-1010.
- Heine, R.A. Lant, C.L. & Sengupta, R.R. 2004. Development and comparison of approaches for automated mapping of stream channel networks. *Annals of the Association of American Geographers*, 94(3), pp: 477-490.
- Helmlinger, K.R. Kumar, P. & Foufoula-Georgiou, E. 1993. On the use of digital elevation model data for Hortonian and fractal analyses of channel networks. *Water Resources Research*, 29, pp: 2599-2613.
- Hengl, T. & Rossiter, D.G. 2003. Supervised Landform Classification to Enhance and Replace Photo-Interpretation in Semi-Detailed Soil Survey. *Soil Science Society of America Journal*, 67, pp: 1810-1822.
- Heritage, G. & Hetherington, D. 2005. The use of high-resolution field laser scanning for mapping surface topography in fluvial systems. *International Association of Hydrological Scientists Red Book Publication*, 291, pp: 269-277.
- Heritage, G. & Hetherington, D. 2007. Towards a protocol for laser scanning in fluvial geomorphology. *Earth Surface Processes and Landforms*, 32(1), pp: 66-74.
- Heritage, G.L. Milan, D.J. Large, A.R.G. & Fuller, I.C. 2009. Influence of survey strategy and interpolation model on DEM quality. *Geomorphology*, 112(3-4), pp: 334-344.
- Hetherington, D. 2009. Laser Scanning: Data Quality, Protocols and General Issues. In: Heritage, G.L. & Large, A.R.G. (eds.), *Laser Scanning for the Environmental Sciences*. Wiley-Blackwell, Oxford, UK.
- Hirano, A. Welch, R. & Lang, H. 2003. Mapping from ASTER stereo image data: DEM validation and accuracy assessment. *Journal of Photogrammetry & Remote Sensing*, 57, pp: 356-370.
- Hodge, R. Brasington, J. Richards, K. 2009. In situ characterization of grain-scale fluvial morphology using Terrestrial Laser Scanning. *Earth Surface Processes and Landforms*, 34(7), pp: 954-968.
- Hodgson, M.E. Jensen, J.R. Schmidt, L. Schill, S. & Davis, B. 2003. An evaluation of LiDAR- and IFSAR-derived digital elevation models in leaf-on conditions with USGS Level 1 and Level 2 DEMs. *Remote Sensing of Environment*, 84, pp: 295-308.
- Holmes, K.W. Chadwick, O.A. & Kyriakidis, P.C. 2000. Error in a USGS 30-meter digital elevation model and its impact on terrain modeling. *Journal of Hydrology*, 233, pp: 154-173.
- Hopkinson, C. Hayashi, M. & Peddle, D. 2009. Comparing alpine watershed attributes from LiDAR, Photogrammetric, and Contour-based Digital Elevation Models. *Hydrological Processes*, 23, pp: 451-463.
- Horton, R.E. 1945. Erosional development of streams and their drainage basins; hydrophysical approach to quantitative morphology. *Geological Society of America Bulletin*, 56, pp: 275-370.
- Howard, A.D. 1967. Drainage analysis in geologic interpretation: A summation. *Bulletin-American Association of Petroleum Geologists*, 51, pp: 2246-2259.
- Howard, A.D. 1971a. Optimal angles of stream junction: geometric stability to capture and minimum power criteria. *Water Resources Research*, 7, pp: 863-873.

- Howard, A.D. 1971b. Simulation of stream networks by headward growth and branching. *Geographical Analysis*, 3, pp: 29-50.
- Howard, A.D. 1971c. Simulation model of stream capture. *Geological Society of America Bulletin*, 82, pp: 1355-1363.
- Howard, A.D. 1990. Theoretical model of optimal drainage networks. *Water Resources Research*, 26(9), pp: 2107-2117.
- Howard, A.D. 1994. A detachment-limited model of drainage basin evolution. *Water Resources Research*, 30(7), pp: 2261-2285.
- Hurtrez, J.-E. Sol, C. & Lucazeau, F. 1999. Effect of drainage area on hypsometry from an analysis of small-scale drainage basins in the Siwalik Hills (Central Nepal). *Earth Surface Processes and Landforms*, 24(9), pp: 799-808.
- Hutchinson, M.F. & Dowling, T.I. 1991. A continental hydrological assessment of a new grid-based digital elevation model of Australia. *Hydrological Processes*, 5(1), pp: 45-58.
- Hutchinson, M.F. & Gallant, J.C. 2000. Digital elevation models and representation of terrain shape. In Wilson, J.P. & Gallant, J.C. (eds.), *Terrain analysis: principles and applications*. John Wiley & Sons, Canada, pp: 29-49.
- Hutchinson, M.F. 1988. Calculation of hydrologically sound digital elevation models. *Proceedings of the Third International Symposium on Spatial Data Handling*. Sydney, Columbus: International Geographical Union, pp: 117-133.
- Hutchinson, M.F. 1989. A new procedure for gridding elevation and stream line data with automatic removal of spurious pits. *Journal of Hydrology*, 106, pp: 211-232.
- Hutchinson, M.F. 1996. A locally adaptive approach to the interpolation of digital elevation models. In: NCGIA (eds.), *Proceedings of the Third International Conference Integrating GIS and Environmental Modeling*. Santa Fe, New Mexico. Santa Barbara, CA: University of California, National Center for Geographic Information and Analysis: CD and www.
- Ibbitt, R.P. Willgoose, G.R. & Duncan, M. J. 1999. Channel network simulation models compared with data from the Ashley river, New Zealand. *Water Resources Research*, 35, pp: 3875-3890.
- Ichoku, C. Karnieli, A. & Verchovsky, I. 1996a. Application of fractal techniques to the comparative evaluation of two methods of extracting channel networks from digital elevation models. *Water Resources Research*, 3, pp: 389-399.
- Ichoku, Ch. Karnieli, A. Meisels, A. & Chorowicz, A. 1996b. Detection of drainage channel networks on digital satellite images. *International Journal of Remote Sensing*, 17(9), pp: 1659-1678.
- Ijjász-Vásquez, E.J. & Bras, R.L. 1995. Scaling regimes of local slope versus contributing area in Digital Elevation Models. *Geomorphology*, 12, pp: 299-311,
- Ijjász-Vásquez, E.J. Bras, R.L. & Rodríguez-Iturbe, I. 1993a. Hack's relation and optimal channel networks: The elongation of river basins as a consequence of energy minimization. *Geophysical Research Letters*, 20(15), pp: 1583-1586.

- Ijjász-Vásquez, E.J. Bras, R.L. Rodríguez-Iturbe, I. Rigon, R. & Rinaldo, A. 1993b. Are river basins optimal channel networks? *Advances in Water Resources*, 16(1), pp: 69-79.
- Ijjász-Vásquez, E.J. Rodríguez-Iturbe, I. & Bras, R.L. 1992. On the multifractal characterization of river basins. *Geomorphology*, 5(3-5), pp: 297-310.
- Isaaks, E.H. & Srivastava, R.M. 1989. An introduction to applied geostatistics. New York: Oxford University Press.
- Jaeger, K. 2004. Channel-Initiation and Surface Water Expression in Headwater Streams of Different Lithology. MSc Thesis, University of Washington.
- James, L.A. Watson, D.G. & Hansen, W.F. 2007. Using LiDAR data to map gullies and headwater streams under forest canopy: South Carolina, USA. *Catena*, 71, pp: 132-144.
- James, W.R. & Krumbein, W.C. 1969. Frequency distribution of stream link lengths. *Journal of Geology*, 77, pp: 544-565.
- Jarvis, R.S. 1972. New measure of the topologic structure of dendritic drainage network. *Water Resources Research*, 8, pp: 1265-71.
- Jarvis, R.S. 1975. Law and order in stream networks. Cambridge University, PhD thesis.
- Jarvis, R.S. 1976a. Stream orientation structures in drainage networks. *Journal of Geology*, 84, pp: 563-582.
- Jarvis, R.S. 1976b. Link length organization and network scale dependencies in the network diameter model. *Water Resources Research*, 12(6), pp: 1215-1225.
- Jarvis, R.S. 1977. Drainage network analysis. *Progress in Physical Geography*, 1, pp: 271-295.
- Jensen, J.R. 1995. Issues involving the creation of digital elevation models and terrain corrected orthoimagery using soft-copy photogrammetry. *Geocarto International*, 10(1), pp: 5-21.
- Jenson, S.K. & Domingue, J.O. 1988. Extracting topographic structure from Digital Elevation Data for Geographic Information System analysis. *Photogrammetric Engineering and Remote Sensing*, 54(11), pp: 1593-1600.
- Johnson, D. 1993. Available relief and texture of topography, a discussion. *Journal of Geology*, 41(3), pp: 293-305.
- Jones, A.F. Brewer, P.A. Johnstone, E. & Macklin, M.G. 2007. High-resolution interpretative geomorphological mapping of river valley environments using airborne LiDAR data. *Earth Surface Processes and Landforms*, 32, pp: 1574-1592.
- Jordan, G. Meijninger, B.M.L. Hinsbergen, D.J.J. Meulenkamp, J.E. & Dijk, P.M. 2005. Extraction of morphotectonic features from DEMs: Development and applications for study areas in Hungary and NW Greece. *International Journal of Applied Earth Observation and Geoinformation*, 7(3), pp: 163-182.
- Journel, A.G. & Huijbregts, Ch.J. 1978. Mining Geostatistics. Academic Press, London, pp. 600.
- Kalin, L. Govindaraju, R.S. & Hantush, M.M. 2003. Effect of geomorphologic resolution on modeling of runoff hydrograph and sedimentograph over small watersheds. *Journal of Hydrology*, 276(1-4), pp: 89-111.

- Kelley, A.D. Malin, M.C. & Nielson, G.A. 1988. Terrain simulation using a model of stream erosion. *ACM SIGGRAPH Computer Graphics*, 22(4), pp: 263-268.
- Kenward, T. Lettenmaier, D.P Wood, E. F. & Fielding, E. 2000. Effects of Digital Elevation Model accuracy on hydrologic predictions. *Remote Sensing of Environment*, 74(3), pp: 432-444.
- Keylock, C.J. 2003. Mark Melton's geomorphology and geography's quantitative revolution. *Transactions of the Institute of British Geographers*, 28, pp: 142-157.
- Kidner, D.B. Ware, J.M. Sparkes, A.J. & Jones, C.B. 2000. Multiscale terrain and topographic modelling with the implicit TIN. *Transactions in GIS*, 4(4), pp: 361-378.
- Kienzle, S.W. 2004. The effect of DEM raster resolution on first order, second order and compound terrain derivatives. *Transactions in GIS*, 8, pp: 83-111.
- Kilian, J. Haala, N. & Englich, M. 1996. Capture and evaluation of airborne laser scanner data. *International Archives of Photogrammetry and Remote Sensing*, 31, pp: 383-388.
- Kirchner, J.W. 1993. Statistical inevitability of Horton's laws and the apparent randomness of stream channel networks. *Geology*, 21, pp: 591-594.
- Kirkby, M.J. & Chorley, R. 1967. Throughflow, overland flow and erosion. *Bulletin of the International Association of Scientific Hydrology*, 12, pp: 73-80.
- Kirkby, M.J. 1971. Hillslope process-response model based on the continuity equation. *Institute of British Geographers Space Publications*, 3, pp: 15-30.
- Kirkby, M.J. 1976. Tests of the random model and its application to basin hydrology. *Earth Surface Processes and Landforms*, 1, pp: 197-212.
- Kirkby, M.J. 1986. A two-dimensional simulation model for slope and stream evolution. In: Abrahams, A.D. (eds.), Hillslope Processes. Allen and Unwin, London, pp: 203-222.
- Kirkby, M.J. 1993. Long term interactions between networks and hillslopes. In: Beven, K. & Kirkby, J. (eds.), Channel network Hydrology. Wiley, New York, pp: 253-293.
- Klemes, V. 1983. Conceptualization and scale in hydrology. *Journal of Hydrology*, 65, pp: 1-23.
- Kleverlaan, K. 1989. Neogene history of the Tabernas basin (SE Spain) and its Tortonian submarine fan development. *Geologie en Mijnbouw*, 68, pp: 421-432.
- Kraus, K. & Pfeifer, N. 1998. Determination of terrain models in wooded areas with airborne laser scanner data. *Journal of Photogrammetry & Remote Sensing*, 53, pp: 193-203.
- Kumler, M.P. 1994. An intensive comparison of Triangulated Irregular Networks (TINs) and Digital Elevation Models (DEMs), *Cartographica, Monograph*, 31(2), pp: 1-99.
- Kyriakidis, P.C. Shortridge, A.M. & Goodchild, M.F. 1999. Geostatistics for conflation and accuracy assessment of digital elevation models. *International Journal of Geographical Information Science*, 13, pp: 677-707.
- Lam, N. S. & Quattrochi, D.A. 1992. On the issues of scale, resolution, and fractal analysis in the mapping sciences. *The Professional Geographer*, 44(1), pp: 89-99.

- Lam, N.S. & Quattrochi, D.A. 2005. On the issues of scale, resolution, and fractal analysis in the mapping sciences. *The Professional Geographer*, 44(1), pp: 88-98.
- Lamarre, H. & Roy, A.G. 2005. Reach scale variability of turbulent flow characteristics in a gravel-bed river. *Geomorphology*, 68 (1-2), pp: 95-113.
- Lark, R.M. & Webster, R. 2006. Geostatistical mapping of geomorphic variables in the presence of trend. *Earth Surface Processes and Landforms*, 31, pp: 862-874.
- Lashermes, B. Foufoula-Georgiou, E. & Dietrich, W.E. 2007. Channel network extraction from high resolution topography using wavelets. *Geophysical Research Letters*, 34, doi:10.1029/2007GL031140.
- Lavellée, D. Lovejoy, S. Schertzer, D. & Ladoy, P. 1993. Nonlinear variability of landscape topography: multifractal analysis and simulation. In: Lam, N.S. & De Cola, L. (eds.), *Fractals in geography*. Prentice Hall, Englewood Cliffs, NJ, pp:158-192.
- Lázaro, R. 1995. Relaciones entre vegetación y geomorfología en el área acarcavada del Desierto de Tabernas. PhD Thesis, Facultad de Biología, Universidad de Valencia, Valencia.
- Lázaro, R., Rodríguez-Tamayo, M.L. Ordiales, R. & Puigdefábregas, J. 2004. El Clima. In: Mota, J. Cabello, J. Cerrillo, M.I. & Rodríguez-Tamayo, M.L. (eds.), *Subdesiertos de Almería: naturaleza de cine*, pp: 63-79. Consejería de Medio Ambiente, Junta de Andalucía. Almería.
- Lea, N.L. 1992. An aspect driven kinematic routing algorithm. In: A.J. Parsons & A.D. Abrahams, (eds.), *Overland Flow: Hydraulics and Erosion Mechanics*. Chapman & Hall, New York, pp: 147-175.
- Lee, J. Snyder, P.K. Fisher, P.F. 1992. Modelling the effect of data errors on feature extraction from digital elevation models. *Photogrammetric Engineering and Remote Sensing*, 58(10), pp: 1461-1467.
- Leenaers, H. Okx, J.P. & Burrough, P.A. 1990. Employing elevation data for efficient mapping of soil pollution on floodplains. *Soil Use and Management*, 6(3), pp: 105-114.
- Legleiter, C.J. & Kyriakidis, P.C. 2008. Spatial prediction of river channel topography by Kriging. *Earth Surface Processes and Landforms*, 33(6), pp: 841-867.
- Legleiter, C.J. Phelps, T.L. & Wohl, E.E. 2007. Geostatistical analysis of the effects of stage and roughness on reach-scale spatial patterns of velocity and turbulence intensity. *Geomorphology* 83, pp: 322-345.
- Leighty, R.D. 2001. Automated IFSAR terrain analysis system. Final Report. U.S. Army Aviation & Missile Command Under, Defense Advanced Research Projects Agency (DOD) Information Sciences Office, Arlington, VA 22203-1714.
- Lejot, J. Delacourt, C. Piégay, H. Fournier, T. Trémélo, M-L. & Allemand, P. 2007. Very high spatial resolution imagery for channel bathymetry and topography from an unmanned mapping controlled platform. *Earth Surface Processes and Landforms*, 32(11), pp: 1705-1725.
- Leopold, L.B. & Langbein, W.B. 1962. The Concept of Entropy in Landscape Evolution. U.S. Geological Survey Professional Paper, 500-A, pp. 20.

- Leopold, L.B. & Maddock T.J. 1953. The hydraulic geometry of stream channels and some physiographic implications. U.S. Geological Survey Professional Paper, 252, pp. 56.
- Leopold, L.B. & Miller, J.P. 1956. Ephemeral streams-hydraulic factors and their relation to the drainage net. Geological Survey Professional Paper, 282-A.
- Leopold, L.B. Wolman, M.G. & Miller, J.P. 1964. Fluvial Processes in Geomorphology. W.H. Freeman and Co., San Francisco, pp. 522.
- Lichti, D.D. & Jamtsho, S. 2006. Angular resolution of terrestrial laser scanners. *The Photogrammetric Record*, 21(114), pp: 141-160.
- Lindsay, J.B. & Creed, I.F. 2005. Removal of artefact depressions from DEMs: towards a minimum impact approach. *Hydrological Processes*, 19, pp: 3113-3126.
- Lindsay, J.B. & Evans, M.G. 2008. The influence of elevation error on the morphometrics of channel networks extracted from DEMs and the implications for hydrological modelling. *Hydrological Processes*, 22, pp: 1588-1603.
- Lindsay, J.B. 2004. *Coping with topographic depression in digital terrain analysis*. PhD thesis, University of Western Ontario.
- Lindsay, J.B. 2005. The Terrain Analysis System: a tool for hydro-geomorphic applications. *Hydrological Processes*, 19(5), pp: 1123-1130.
- Lindsay, J.B. 2006. Sensitivity of channel mapping techniques to uncertainty in digital elevation data. *International Journal of Geographical Information Science*, 20(6), pp: 669-692.
- Liu, H. & Wang, L. 2008. Mapping detention basins and deriving their spatial attributes from airborne LIDAR data for hydrological applications. *Hydrological Processes*, 22, pp: 2358-2369.
- Loewenherz, D. S. 1991. Stability and the initiation of channelized surface drainage: a reassessment of the short wavelength limit. *Journal of Geophysical Research*, 96(B5), pp: 8453-8464.
- Lohr, U. 2003. Digital elevation models by laser scanning. *Photogrammetric Record*, 16(91), pp: 105-109.
- Lubowe, J.R. 1964. Stream junction angles in the dendritic drainage pattern. *American Journal of Science*, 262, pp: 325-339.
- Luo, B.W. Stepinski, T.F. & Qi, R.Y. 2007. Drainage Density and Controlling Factors in Cascade Range, Oregon, USA. To appear in proceedings of Geoinformatics 2007. Nanjing, China.
- Luoto, M. & Hjort, J. 2006. Scale matters-A multi-resolution study of the determinants of patterned ground activity in subarctic Finland. *Geomorphology*, 80, pp: 282-294.
- Mackaness, W. & Beard, K. 1993. Use of graph theory to support map generalisation. *Cartography and Geographical Information Systems*, 20(4), pp: 210-221.
- MacMillan, R.A. & Shary, P.A. 2009. Landforms and landform elements in geomorphometry. In: Hengel, T. & Reuter, H.I. (eds.), *Geomorphometry: Concepts, Software, Applications*. Developments in Soil Science, 33, pp: 227-254.

- MacMillan, R.A. Pettapiece, W.W. Nolan, S. & Goddard, T.W. 2000. A generic procedure for automatically segmenting landforms into landform elements using DEMs, heuristic rules and fuzzy logic. *Fuzzy Sets and Systems*, 113, pp: 81-109.
- Madej, M.A. 1999. Temporal and spatial variability in thalweg profiles of a gravel-bed river. *Earth Surface Processes and Landforms*, 24, pp: 1153-1169
- Mandelbrot, B.B. 1977. *Fractals: Form, Chance and Dimension*. San Fransisco, WH Freeman.
- Mandelbrot, B.B. 1982. *The Fractal Geometry of Nature*. New York: WH Freeman
- Mandelbrot, B.B. 1985. Self-affine fractals and fractal dimension. *Physica Scripta*, 32, pp: 257-260.
- Mandelbrot, B.B. 1989. Multifractal measures, especially for the geophysicist. *Pageoph*, 131(1-2), pp: 5-42.
- Mantilla, R. Gupta V.K. & Mesa, O.J. 2006. Role of coupled flow dynamics and real network structures on Hortonian scaling of peak flows. *Journal of Hydrology*, 322, pp: 155-167.
- Marcus, A. 1980. First-order drainage basin morphology-definition and distribution. *Earth Surface Processes and Landforms*, 5(4), pp: 389-398.
- Maritan, A. Rinaldo, A. Region, R. Giacometti, A. & Rodríguez-Iturbe, I. 1996. Scaling laws for river networks. *Physical Review E*, 53, pp: 1510-1515.
- Mark, D.M. & Averack, R. 1984. Link length distributions in drainage networks with lakes. *Water Resources Research*, 20(4), pp: 457-462.
- Mark, D.M. & Church, M. 1977. On the misuse of regression in earth science. *Mathematical Geology*, 9(1), pp: 63-75.
- Mark, D.M. & Smith, B. 2004. A science of topography: bridging the qualitative-quantitative divide. In: Bishop, M.P. & Shroder, J.F. (eds.), *Geographic Information Science and Mountain Geomorphology*. Chichester: Springer-Praxis, pp: 75-100.
- Mark, D.M. 1975. Geomorphometric parameters: a review and evaluation. *Geografiska Annaler Series A-Physical Geography*, 57, pp: 165-177.
- Mark, D.M. 1983. Relations between field-surveyed channel networks and map-based geomorphometric measures, Inez, Kentucky. *Annals of the Association of American Geographers*, 73(3), pp: 358-372.
- Mark, D.M. 1984. Automated detection of drainage networks from digital elevation models. *Auto-Carto*, 6, pp: 169-178.
- Martz, L.W. & Garbrecht, J. 1992. Numerical definition of drainage network and sub-catchment areas from digital elevation models. *Computers & Geosciences*, 18(6), pp: 747-761.
- Martz, L.W. & Garbrecht, J. 1998. The treatment of flat areas and closed depressions in automated drainage analysis of raster digital elevation models. *Hydrological Processes*, 12, pp: 843-855.
- Mason, D.C. Horritt, M.S. Hunter, N.M. & Bates, P.D. 2007. Use of fused airborne scanning laser altimetry and digital map data for urban flood modelling. *Hydrological Processes*, 21(11), pp: 1436-1447.

- Mather, R.M. & Doornkamp, J.C. 1970. Multivariate Analysis in Geography, with Particular Reference to Drainage Basin Morphometry. *Transactions of the Institute of British Geographers*, 51, pp: 163-187.
- Mather, R.M. 1972. Areal classification in geomorphology. In: Chorley, R.J. (eds.), *Spatial Analysis in Geomorphology*. Methuen & Co. Ltd., London, pp: 305-322.
- Matheron, G. 1963. Principles of geostatistics. *Economic Geology*, 58, pp: 1246-1266.
- Maxwell, J.C. 1870. On contour lines and measurements heights. *The London, Edinburgh and Dublin Philosophical Magazine and Journal of Science*, 40, pp: 421-427.
- Maxwell, J.C. 1960. Quantitative geomorphology of the San Dimas Experimental forest, California. Department of Geology, Columbia University. Technical Report, No. 19.
- McBratney, A.B. & Webster, R. 1986. Choosing functions for semivariograms of soil properties and fitting them to sampling estimates. *European Journal of Soil Science*, 37(4), pp: 617-639.
- McCaffrey, K.J. Jones, R.R. Holdsworth, R.E. Wilson, R.W. Clegg, P. Imber, J. Holliman, N. & Trinks, I. 2005. Unlocking the spatial dimension: Digital technologies and the future of geoscience fieldwork. *Journal of the Geological Society*, 162(6), pp: 927-938.
- McMaster, K.J. 2002. Effects of digital elevation model resolution on derived stream network positions. *Water Resources Research*, 38(4), doi: 10.1029/2000WR000150.
- Meisel, J.E. & Turner, M.G. 1998. Scale detection in real and artificial landscapes using semivariance analysis, *Landscape Ecology*, 13, pp: 347-362.
- Melton, M.A. 1957. An analysis of the relations among elements of climate, surface properties, and geomorphology. Technical Report, No. 11, Department of Geology, New York Columbia University.
- Melton, M.A. 1958a. Geometric properties of mature drainage systems and their representation in an E4 phase space. *Journal of Geology*, 66, pp: 35-56.
- Melton, M.A. 1958b. Correlation structure of morphometric properties of drainage systems and their controlling agents. *The Journal of Geology*, 66(4), pp: 442-460.
- Merwade, V.M. Maidment, D.R. & Goff, J.A. 2006. Anisotropic considerations while interpolating river channel bathymetry. *Journal of Hydrology*, 331, pp: 731-741.
- Mesa, O.J. & Gupta, V.K. 1987. On the main channel length-area relationships for channel networks. *Water Resources Research*, 23(11), pp: 2119-2122.
- Miall, A.D. 1996. *The geology of fluvial deposits: Sedimentary facies, basin analysis, and petroleum geology*. New York, Springers.
- Miesch, A.T. 1975. Variograms and variance components in geochemistry and ore evaluation. *Geological Society of America*, 142, pp: 333-340.
- Miller, D.J. & Burnett, K.M. 2007. A probabilistic model of debris-flow delivery to stream channels, demonstrated for the Coast Range of Oregon, USA. *Geomorphology*, 94(1-2), pp: 184-205.

- Milne, B. Gupta, V. & Restrepo, C. 2002. A scale invariant coupling of plants, water, energy, and terrain. *Ecoscience*, 9, pp: 191-199
- Mock, S.J. 1971. A Classification of Channel Links in Stream Networks. *Water Resources Research*, 7(6), pp: 1558-1566.
- Moffat, A.J. Catt, J.A. Webster, R. & Brown, E.H. 1986. A re-examination of the evidence for a Plio-Pleistocene marine transgression on the Chiltern Hills. I. Structures and surfaces. *Earth Surface Processes and Landforms*, 11, pp: 95-106.
- Moglen, G.E. Elfatih A. Eltahir, B. & Bras, R.L. 1998. On the sensitivity of drainage density to climate change. *Water Resources Research*, 34(4), pp: 855-862.
- Molnar, P. & Ramirez, J.A. 2002. On downstream hydraulic geometry and optimal energy expenditure: case study of the Ashley and Taieri Rivers. *Journal of Hydrology*, 259, pp: 105-115.
- Molnar, P. 2006. On geometrical scaling of Cayley trees and river networks. *Journal of Hydrology*, 322, pp: 199-210.
- Montgomery, D.R. & Dietrich, W.E. 1988. Where do channels begin? *Nature*, 336, pp: 232-234.
- Montgomery, D.R. & Dietrich, W.E. 1989. Source area, drainage density, and channel initiation. *Water Resources Research*, 25, pp: 1907-1918.
- Montgomery, D.R. & Dietrich, W.E. 1992. Channel Initiation and the Problem of Landscape Scale. *Science*, 255, pp: 826-830.
- Montgomery, D.R. & Dietrich, W.E. 1994. Landscape dissection and drainage area-slope thresholds. In: Kirkby, M.J. (eds.), *Process Models and Theoretical Geomorphology*. John Wiley and Sons Ltd, pp: 221-246.
- Montgomery, D.R. & Foufoula-Georgiou, E. 1993. Channel network source representation using Digital Elevation Model. *Water Resources Research*, 29(12), pp: 3925-3934.
- Montgomery, D.R. 2003. Predicting landscape-scale erosion rates using DEMs. *Compts Rendus Geoscience*, 335, pp: 1121-1130.
- Montgomery, D.R. Dietrich, W.E. Torres, R. Anderson, S.P. Heffner, J.T. & Loague, K. 1997. Hydrologic response of a steep, unchanneled valley to natural and applied rainfall. *Water Resources Research*, 33(1), pp: 91-109.
- Moore, I.D. & Grayson, R.B. 1991. Terrain-based catchment partitioning and runoff prediction using vector elevation data. *Water Resources Research*, 27, pp: 1177-1191.
- Moore, I.D. Gessler, P.E. Nielsen, G.A. & Peterson, G.A. 1993. Soil attributes prediction using terrain analysis. *Soil Society Science of America Journal*, 57, pp: 443-452.
- Moore, I.D. Grayson, R.B. & Ladson, A.R. 1991. Digital terrain modelling: A review of hydrological, geomorphological and biological applications. *Hydrological processes*, 5, pp: 3-30.
- Moore, I.D. O'Loughlin, E. & Burch, G. 1988. A contour based topographic model for hydrological and ecological applications. *Earth Surface Processes and Landform*, 13, pp: 305-320.

- Morgan, R.P.C. 1973. The influence of scale in climatic geomorphology: A case study of drainage density in West Malaysia. *Geographical Analysis*, 55, pp: 107-115.
- Morisawa, M.E. 1957. Accuracy of determination of stream lengths from topographic maps. *Transactions, American Geophysical Union*, 38, pp: 86-88.
- Murphy, P.N. Ogilvie, J. Meng, F. & Arp, P. 2008. Stream network modelling using LIDAR and photogrammetric digital elevation models: a comparison and field verification. *Hydrological Processes*, 22, pp: 1747-1754.
- Myers, A.K. Marcarelli, A.M. Arp, Ch.D. Baker, M.A. & Wurtsbaugh, W.A. 2007. Disruptions of stream sediment size and stability by lakes in mountain watersheds: potential effects on periphyton biomass. *Journal of the North American Benthological Society*, 26(3), pp: 390-400.
- Nash, D.J. & Smith, R.F. 2003. Properties and development of channel calcretes in a mountain catchment, Tabernas Basin, southeast Spain. *Geomorphology*, 50, pp: 227-250.
- Neumann, H. 1961. El clima del sudeste de España. *Estudios Geográficos*, 21(79), pp: 171-209.
- Niedermeier, A. Hoja, D. & Lehner, S. 2005. Topography and morphodynamics in the German Bight using SAR and optical remote sensing data. *Ocean Dynamics*, 55(2), pp: 100-109.
- O'Callaghan, J.F. & Mark, D.M. 1984. The extraction of drainage networks from digital elevation data. *Computer Vision, Graphics and Image Processing*, 28, pp: 323-344.
- Odeh, I.O. McBratney A.B. & Chittleborough, D.J. 1994. Spatial prediction of soil properties from landform attributes derived from a digital elevation model. *Geoderma*, 63, pp: 197-214.
- Oksanen, J. & Sarjakoski, T. 2005. Error propagation analysis of DEM-based drainage basin delineation. *International Journal of Remote Sensing*, 26(14), pp: 3085-3102.
- Olea, R.A. 1975. Optimum Mapping Techniques Using Regionalized Variable Theory. *Series on Spatial Analysis*, 3, Lawrence, Kansas.
- Olea, R.A. 1977. Measuring spatial dependence with semi-variograms. *Series on Spatial Analysis*, 3, Lawrence, Kansas.
- Oliver, M.A Webster, R. & Gerrard, J. 1989a. Geostatistics in physical geography. Part I: theory. *Transactions of the Institute of British Geographers*, 14, pp: 259-269.
- Oliver, M.A Webster, R. & Gerrard, J. 1989b. Geostatistics in physical geography. Part II: theory. *Transactions of the Institute of British Geographers*, 14, pp: 270-286.
- Oliver, M.A. & Webster, R. 1986. Semi-variograms for modelling the spatial patterns of landform and soil properties. *Earth Surface Processes and Landforms*, 11, pp: 491-504.
- Oliver, M.A. 1987. Geostatistics and its applications to soil science. *Soil Use and Management*, 3, pp: 8-20.
- Oliver, M.A. 2001. Determining the spatial scale of variation in environmental properties using the variogram. In: Tate, N.J. & Atkinson, P.M. (eds.), *Modelling scale in geographical information science*. Wiley, Chichester.

- Oliver, M.A. Webster, R. & Slocum, K. 2000. Filtering SPOT imagery by kriging analysis. *International Journal of Remote Sensing*, 21(4), pp: 735-752.
- Olivera, F. 2001. Hydrologic Modelling System. (WWW: <http://www.crrw.utexas.edu/gis/gishyd98/class/-prepro/webfiles/prepro.htm>)
- O'Loughlin, E.M. 1986. Prediction of surface saturation zones in natural catchments by topographic analysis. *Water Resources Research*, 22(5), pp: 794-804.
- O'Neill, R.V. De Angelis, D.L. Waide, J.B. & Allen, T.F. 1986. A Hierarchical Concept of Ecosystems. Princeton University Press, Princeton, NJ, pp. 254
- Oppikofer, T., Jaboyedoff, M., Blikra, L. H., & Derron, M.-H. 2008. Characterization and monitoring of the Aknes rockslide using terrestrial laser scanning. In: Locat, J. Perret, D. Turmel, D. Demers, D. & Leroueil, S. (eds.), Proceedings of the 4th Canadian Conference on Geohazards: From Causes to Management. Presse de l'Université Laval, Quebec, Canada, pp: 211-218.
- Ortofotografía digital en color de Andalucía. 2007. Consejería de Medio Ambiente, Junta de Andalucía.
- Oyonarte, C. 2004. La diversidad edáfica. In: Mota, J. Cabello, J. Cerrillo, M.I. Rodríguez-Tamayo, M.L. (eds.). Los subdesiertos de Almería. Naturaleza de cine. Consejería de Medio Ambiente, Junta de Andalucía, pp: 51-62.
- Pajarola, R. 1998. Large Scale Terrain Visualization Using the Restricted Quadtree Triangulation. *Ninth IEEE Visualization*, vis, pp: 19.
- Palacio Pemberty, J.F. 2002. Assessment of morphodynamic processes and soil pollution as indicators of land degradation, a case study in the Tabernas area, southeastern Spain. Master Thesis. International Institute for Geo-information Science and Earth Observation (ITC), Enschede, The Netherlands.
- Parsons, M. & Thoms, M.C. 2007. Hierarchical patterns of physical-biological associations in river ecosystems. *Geomorphology*, 89(1-2), pp: 127-146.
- Peckham, S.D. 1995. Self-Similarity in the Three-Dimensional Geometry and Dynamics of Large River Basins. PhD Thesis, Program in Geophysics, University of Colorado.
- Peckham, S.D. 1998. Efficient extraction of river networks and hydrologic measurements from digital elevation data. In: Barndorff-Nielsen, O.A. (eds.), Stochastic Methods in Hydrology: Rain, Landforms and Floods. World Scientific River Edge, N. J. pp: 173-203.
- Pennock, D.J. 2003. Terrain Attributes, Landform Segmentation, and Soil Redistribution. *Soil & Tillage Research*, 69, pp: 15-26.
- Pennock, D.J. Zebarth, B.J. & De Jong, E. 1987. Landform classification and soil distribution in hummocky Terrain, Saskatchewan, Canada. *Geoderma*, 40(3-4), pp: 297-315.
- Pérez Pujalte, A. & Oyonarte, C. 1987. Proyecto LUCDEME, Mapa de Suelos Escala 1:100.000, Tabernas-1030. ICONA-CSIC.
- Pesci, A. Loddo, F & Conforti, D. 2007. The first terrestrial laser scanner application over Vesuvius: High resolution model of a volcano crater. *International Journal of Remote Sensing*, 28(1), pp: 203-219.

- Peucker, T.K. & Douglas, D.H. 1975. Detection of Surface-Specific Points by Local Parallel Processing of Discrete Terrain Elevation Data. *Computer Graphics and Image Processing*, 4, pp: 375-387.
- Peucker, T.K. Fowler, R.J. Little, J.J. & Mark, D.M. 1978. The triangulated irregular network. Proceedings of the ASP Digital Terrain Models (DTM) Symposium. Falls Church, Virginia, pp: 516-540.
- Pfeifer, N. & Briese, C.B. 2007a. Geometrical aspects of airborne laser scanning and terrestrial laser scanning. *IAPRS*, XXXVI, Part 3 / W52, pp: 311-319.
- Pfeifer, N. & Briese, C.B. 2007b. Laser scanning: principles and applications. 3rd International Exhibition & Scientific Congress on Geodesy, Mapping, Geology, Geophysics, Cadaster.
- Phillips, J.D. 1993. Instability and Chaos in Hillslope Evolution. *American Journal of Science*, 293(1), pp: 25-48.
- Pike, R.J. 1988. The geometric signature: Quantifying landslide-terrain types from digital elevation models. *Mathematical Geology*, 20(5), pp: 491-511.
- Pike, R.J. 2000. Geomorphometry -diversity in quantitative surface analysis. *Progress in Physical Geography*, 24 (1), pp: 1-20.
- Pike, R.J. 2002. A bibliography of terrain modelling (geomorphometry), the quantitative representation of topography –suplement 4.0. *Open-File Report 02-465, United States Geological Survey, Menlo Park, California*.
- Pike, R.J. Evans, I.S. Hengl, T. 2009. Geomorphometry: a Brief Guide. In: Hengl, T. & Reuter, H.I. (eds.), *Geomorphometry: Concepts, Software, Applications. Developments in Soil Science*, 33, Elsevier, pp: 1-28.
- Pillips, J.D. 1998. Earth surface systems: complexity, order and scale. Blackwell, Oxford.
- Pitlick, J. 1994. Relation between peak flows, precipitation, and physiographic for five mountainous regions in the western USA. *Journal of Hydrology*, 158, pp: 219-240.
- Playfair, J. 1802. Illustrations of the Huttonian theory of the earth. Edinburgh: W. Creech.
- Puigdefábregas, J. Alonso, J.M. Delgado Castilla, L. Domingo, F. Cueto, M. Gutiérrez, L. Lázaro, R. Nicolau, J.M. Sánchez, G. Solé-Benet, A. & Vidal, S. 1996. The Rambla Honda field site: interactions of soil and vegetation along a Catena in semi-arid southeast Spain. In: Brandt, C.J. & Thornes, J. (eds.), *Mediterranean desertification and land use*. Wiley, Chichester, UK, pp: 137-168.
- Puigdefábregas, J. Cueto, M. Domingo, F. Gutierrez, L. Sanchez, G. & Solé-Benet, A. 1998a. Rambla Honda, Tabernas, Almería, Spain. In: Mairota, P. Thornes, J.B. & Geeson, N.A. (eds.), *Atlas of mediterranean environments in Europe: the desertification context*. John Wiley & Sons, London, pp: 110-112.
- Puigdefábregas, J. Del Barrio, G. Boer, M. Gutiérrez, L. & Sólé-Benet, A. 1998b. Differential Responses of Hillslope and Channel Elements to Rainfall Events in a Semi-arid Area. *Geomorphology*, 23, pp: 337-351.
- Puigdefábregas, J. Solé-Benet, A. Gutiérrez, L. del Barrio, G. & Boer, M. 1999. Scales & processes of water and sediment redistribution in drylands: results from the Rambla Honda field site in SE Spain. *Earth-Science Reviews*, 48(1-2), pp: 39-70.

- Puigdefábregas, J., Solé-Benet, A. Lázaro, R. Sánchez, G. Cantón, Y. Cueto, M. Moro, M. Boer, M. Armas, C. Vidal, S. Gutiérrez, L. Domingo, F. Delgado, L. Incoll, L.D. Clark, S.C. Brenner, A.J. Pugnair, F.I. Haase, P. Beven, R. 1994. MEDALUS II - Field Guide -Almería Meeting- Estación Experimental de Zonas Áridas (CSIC) & University of Leeds. Almería, Spain.
- Quinn, P. Beven, K. Chevallier, P. & Planchon, O. 1991. The prediction of hillslope flow paths for distributed hydrological modeling using digital terrain models. *Hydrological Processes*, 5, pp: 59-79.
- Quinn, P. F. Beven, K. J. & Lamb, R. 1995. The $\ln(a/\tan b)$ Index: How to Calculate it and how to use it Within the TOPMODEL Framework. *Hydrological Processes*, 9, pp: 161-182.
- Rabus, B. Eineder, M. Roth, A. & Bamler, R. 2003. The shuttle radar topography mission-a new class of digital elevation models acquired by space-borne radar. *ISPRS Journal of Photogrammetry & Remote Sensing*, 57, pp: 241-262.
- Rahbek, C. 2005. The role of spatial scale and the perception of large-scale species-richness patterns. *Ecology Letters*, 8, pp: 224-239.
- Rayburg, S.C. & Neave, M. 2008. Assessing morphologic complexity and diversity in river systems using three-dimensional asymmetry indices for bed elements, bedforms and bar units. *River Research and Applications*, 24(9), pp: 1343-1361.
- Reddy, G.P.O. Maji, A.K. & Gajbhiye, K.S. 2004. Drainage morphometry and its influence on landform characteristics in a basaltic terrain, Central India - a remote sensing and GIS approach. *International Journal of Applied Earth Observation and Geoinformation*, 6(1), pp: 1-16.
- Renschler, C.S. Doyle, M.W. & Thoms, M. 2007. Geomorphology and ecosystems: Challenges and keys for success in bridging disciplines. *Geomorphology*, 89(1-2), pp: 1-8.
- Richards, K.S. 1976. The morphology of riffle-pool sequences. *Earth Surface Processes*, 1(1), pp: 71-88.
- Richards, K.S. 1982. Rivers: Form and Process in Alluvial Channels. Methuen, London, pp. 358.
- Rigon, R. Rinaldo, A. & Rodriguez-Iturbe, I. 1994. On landscape self-organization. *Journal of geophysical research*, 99(6), pp: 11971-11993.
- Rigon, R. Rinaldo, A. Rodriguez-Iturbe, I. Bras, R.L. & Ijjasz-Vasquez, E.J. 1993. Optimal channel networks: a framework for the study of river basin morphology. *Water Resources Research*, 29 (6), pp: 1635-1646.
- Rigon, R. Rodriguez-Iturbe, I. Giacometti, A. Maritan, A. Tarboton, D. & Rinaldo, A. 1996. On Hack's Law. *Water Resources Research*, 32, pp: 3367-3374.
- Rinaldo A, Rodriguez-Iturbe, I. Rigon, R. Ijjasz-Vasquez, E. & Bras, R.L. 1993. Self-organized fractal river networks. *Physical Review Letters* 70, pp: 822-825.
- Rinaldo, A. Rodriguez-Iturbe, I. Rigon, R. Bras, R.L. Ijjasz-Vasquez, E.J. & Marani, A. 1992. Minimum energy and fractal structures of drainage networks. *Water Resources Research*, 28(9), pp: 2183-2195.

- Rinehart, R.E. & Coleman, E.J. 1988. Digital elevation models produced from digital line graphs. In *Proceedings of the ACSM-ASPRS Annual Convention*, 2, pp: 291-299. American Congress on Surveying and Mapping, American Society for Photogrammetry and Remote Sensing.
- Robert, A.R. & Richards, K.S. 1988. On the modelling of sand bedforms using the semivariogram. *Earth Surface Processes and Landforms*, 13(5), pp: 459-473.
- Robert, A.R. 1988. Statistical properties of sediment bed profiles in alluvial channels. *Mathematical Geology*, 20(3), pp: 205-225.
- Rodriguez-Iturbe, I. & Escobar, L.A. 1982. The dependence of drainage density on climate and geomorphology. *Hydrological Science*, 27, pp: 2-6.
- Rodriguez-Iturbe, I. & Rinaldo, A. 1997. Fractal river basins: chance and self-organization, Cambridge University Press, U.K., 1997.
- Rodriguez-Iturbe, I. & Valdes, J.B. 1979. Geomorphologic structure of hydrologic response. *Water Resources Research*, 15(6), pp: 1409-1420.
- Rodriguez-Iturbe, I. Rinaldo, A. Rigon, R. Bras, R.L. Marani, A. & Ijjasz-Vasquez, E.J. 1992. Energy dissipation, runoff production, and the three-dimensional structure of river basins. *Water Resources Research*, 28(4), pp: 1095-1103.
- Romero, D.A. & Lopez, B.F. 1987. Morfometría de redes fluviales: Revisión crítica de los parámetros más utilizados y aplicación al alto Guadalquivir. *Papeles de Geografía (Física)*, 12, pp: 47-62.
- Rosgen, D.L. & Silvey, H.L. 1996. Applied River Morphology. Wildland Hydrology Books, Fort Collins, CO.
- Rosgen, D.L. 1994. A classification of natural rivers. *Catena*, 22, pp: 169-199.
- Rosgen, D.L. 2001. A stream channel stability assessment methodology. Proceedings of the Seventh Federal Interagency Sedimentation Conference, 25 to 29th of March, 2001, Reno, Nevada.
- Rossel, J.W. 1988. Conversion of Cartesian coordinates from and to generalized balance ternary addresses. *Photogrammetric Engineering and Remote Sensing*, 54(11), pp: 1565-1570.
- Rosser, N.J. Petley, D.N. Lim, M. Dunning, S.A. & Allison, R.J. 2005. Terrestrial laser scanning for monitoring the process of hard rock coastal cliff erosion. *Quarterly Journal of Engineering Geology & Hydrogeology*, 38(4), pp: 363-375.
- Ruhe, R.V. & Walker, P.H. 1968. Hillslope models and soil formation. I. Open systems. *Transactions of the 9th International Congress of Soil Science*, Adelaide, 4, pp: 551-560.
- Sainsbury, R.M. 1989. What is a vague object? *Analysis*, 49, pp: 99-103.
- Samet, H. Rosenfeld, A. Shaffer, C.A. & Webber, R.E. 1984. A geographic information system using quadtrees. *Pattern Recognition*, 17(6), pp: 647-656.
- Sandmeier, S. & Itten, K.I. 1997. A physically-based model to correct atmospheric and illumination effects in optical satellite data of rugged terrain. *IEEE Transactions on Geoscience and Remote Sensing*, 35(3), pp: 708-717.

- Sanz de Galdeano, C. Shanov, S. Galindo-Zaldívar, J. Radulov, A. & Nikolov, G. 2006. Neotectonics in the Tabernas Desert (Almería, Betic Cordillera, Spain). *National Conference "Geosciences 2006" (5th National Geophysical Conference & Annual Scientific Conference of the Bulgarian Geological Society*, pp: 75-78. Sofia, Bulgaria.
- Saura, S. Gómez-Plaza, A. & Castillo, V.M. 2000. Extracción Automatizada de la red de drenaje a partir de Modelos Digitales de Elevaciones. *Revista Cuaternario y Geomorfología*, 14(34), pp: 25-37.
- Scheidegger, A.E. 1991. *Theoretical Geomorphology*, 3rd ed. Springer-Verlag, Berlin.
- Schiess P, & Krogstad F. 2003. LiDAR-based topographic maps improve agreement between office-designed and field-verified road locations. In: *26th Annual Meeting of the Council on Forest Engineering*, Bar Harbor, Maine.
- Schmidt, J. & Andrew, R. 2005. Multi-scale landform characterization. *Area*, 37(3), pp: 341-350.
- Schmidt, J. & Hewitt, A. 2004. Fuzzy land element classification from DTMs based on geometry and terrain position. *Geoderma*, 121, pp: 243-256.
- Schmidt, J. Hennrich, K. & Dikau, R. 2000. Scales and similarities in runoff processes with respect to geomorphometry. *Hydrological Processes*, 14, pp: 1963-1979.
- Schneider, B. 2001. Phenomenon-based Specification of the Digital Representation of Terrain Surfaces. *Transactions in GIS*, 5(1), pp: 39-52.
- Schoorl, J.M. Sonneveld, M.P.W. & Veldkamp, A. 2000. Three dimensional landscape process modelling: the effect of DEM resolution. *Earth Surface Processes and Landforms*, 25(9), pp: 1025-1034.
- Schumann, G. Matgen, P. Cutler, M.E. Black, A. Hoffmann, L. & Pfister, L. 2008. Comparison of remotely sensed water stages from LiDAR, topographic contours and SRTM. *ISPRS Journal of Photogrammetry & Remote Sensing*, 63, pp: 283-296.
- Schumm, S.A. & Licity, R.W. 1965. Time, space and causality in geomorphology. *American Journal of Science*, 263, pp: 110-119.
- Schumm, S.A. 1956. Evolution of drainage systems and slopes in Badlands at Perth Amboy, New Jersey. *Bulletin of the Geological Society of America*, 67(5), pp: 597-646.
- Schumm, S.A. 1973. Geomorphic thresholds and complex response of drainage systems. In: Morisawa, M. (eds), *Fluvial Geomorphology. A Proceedings Volume of the Fourth Annual Geomorphology Symposia Series*, Binghamton, New York. George Allen & Unwin Ltd.
- Schumm, S.A. 1977. *The Fluvial System*: John Wiley, N.Y., p. 338.
- Schumm, S.A. Harvey, M.D. & Watson, C.C. 1984. *Incised Channels: Morphology, Dynamics and Control*. Water Resources Publications, Littleton, CO.
- Shan, J. & Toth, C.K. 2008. *Topographic Laser Ranging and Scanning: Principles and Processing*. CRC Press: Boca Raton, FL. pp: 590.

- Shaw, L.C. 1984. Pennsylvania Gazetteer of Streams Part II. Water Resources Bulletin No. 16, Prepared in Cooperation with the United States Department of the Interior Geological Survey, 1st Edition, Harrisburg, PA: Commonwealth of Pennsylvania, Department of Environmental Resources.
- Shreve, R.L. 1966. Statistical law of stream numbers. *Journal of Geology*, 74, pp: 17-37.
- Shreve, R.L. 1967. Infinite topologically random channel networks. *Journal of Geology*, 77, pp: 397-414.
- Shreve, R.L. 1969. Stream lengths and basin areas in topologically random channel Networks. *Journal of Geology*, 77, pp: 397-414.
- Shreve, R.L. 1974. Variation of mainstream length with basin area in river networks. *Water Resources Research*, 10(6), pp: 1167-1177.
- Shreve, R.L. 1975. The probabilistic topologic approach to drainage-basin geomorphology. *Geology*, 3, pp: 527-529.
- Simley J. 2004. The geodatabase conversion. *USGS National Hydrography Newsletter*, 3(4). USGS.
- Simon, A. & Thomas, R.E. 2002. Processes and forms of an unstable alluvial system with resistant, cohesive streambeds. *Earth Surface Processes and Landforms*, 27, pp: 699-718.
- Skidmore, A.K. 1990. Terrain position as mapped from a gridded digital elevation model. *International Journal of Geographical Information Systems*, 4(1), pp: 33-49
- Slob, S. & Hack, R. 2004. 3D Terrestrial Laser Scanning as a New Field Measurement and Monitoring Technique. In: Hack, R. Azzam, R. & Charlier, R. (eds.), *Engineering Geology for Infrastructure Planning in Europe. A European Perspective. Lecture Notes in Earth Sciences*. Springer, Berlin / Heidelberg, pp: 179-190.
- Slob, S. Van Knapen, B. Hack, R. Turner, K. & Kemeny, J. 2005. Method for automated discontinuity analysis of rock slopes with three-dimensional laser scanning. In: *Proceedings of the Transportation Research Board 84th Annual Meeting*, Washington DC.
- Smart, J.S. & Moruzzi, V.L. 1971a. Computer Simulation of Clinch Mountain drainage networks. *Journal of Geology*, 79, pp: 572-584.
- Smart, J.S. & Moruzzi, V.L. 1971b. Random-walk model of stream network development. *IBM Journal of Research Development*, 15, pp: 197-203.
- Smart, J.S. 1968. Statistical Properties of stream lengths. *Water resources Research*, 4(5), pp: 1001-1014.
- Smart, J.S. 1969a. Topological properties of channel networks. *Geological Society of America Bulletin*, 80(9), pp: 1757-1774.
- Smart, J.S. 1972a. Channel Networks. *Advances in Hydroscience*, 8, pp: 305-346.
- Smart, J.S. 1972b. Quantitative characterization of channel network structure. *Water Resources Research*, 8(6), pp: 1487-1496.
- Smart, J.S. 1974. The Random model in fluvial geomorphology. In: Morisawa, M.E. (eds.), *Fluvial Geomorphology*, Publications in geomorphology. Binghamton, N.Y. pp: 27-49.

- Smart, J.S. 1978. The Analysis of drainage network composition. *Earth Surface Processes and Landforms*, 3(2), pp: 129-170.
- Smart, J.S. 1981. Link lengths and channel network topology. *Earth Surface Processes and Landforms*, 6 (1), pp: 77-79.
- Smith, B. & Mark, D.M. 2001. Geographic categories: an ontological investigation. *International Journal of Geographical Information Science*, 15(7), pp: 591-612.
- Smith, T.R. & Bretherton, F.P. 1972. Stability and the conservation of mass in drainage basin evolution. *Water Resources Research*, 8(6), pp: 1506-1529.
- Smith, T.R. 1950. Standards for grading texture of erosional topography. *American Journal of Science*, 248, pp: 655-658.
- Smith, T.R. Birnir, B. & Merchant, G.E. 1997. Towards an elementary theory of drainage basin evolution: I. The theoretical basis. *Computers & Geosciences*, 23(8), pp: 811-822.
- Snell, J.D. & Sivapalan, M. On geomorphological dispersion in natural catchments and the geomorphological unit hydrograph. *Water Resources Research*, 30(7), pp: 2311-2323
- Solé-Benet, A. & Cantón, Y. 2004. Estabilidad de los agregados de suelos franco-arenosos sobre micasquistos como indicadora de su erosionabilidad. In: Benito, G. & Diez Herrero, A. (eds.), Riesgos Naturales y Antrópicos en Geomorfología (VIII Reunión Nacional de Geomorfología), II, SEG-CSIC, pp 299-309.
- Solé-Benet, A. Calvo, A. Cerdà, A. Lázaro, R. Pini, R. & Barbero, J. 1997. Influences of micro-relief patterns and plant cover on runoff related processes in badlands from Tabernas (SE Spain). *Catena*, 31, pp: 23-38.
- Solé-Benet, A. Cantón, Y. Lázaro, R & Puigdefábregas, J. 2009. Meteorización y erosión en el sub-desierto de Tabernas, Almería. *Cuadernos de Investigación Geográfica*, 35(1), pp: 141-163.
- Speight, J.G. 1974. A parametric approach to landform regions. In: Brown, E.H. & Waters, R.S. (eds.), Progress in Geomorphology. London, Alden, pp: 213-230.
- Stein, A. 1998. Analysis of space-time variability in agriculture with geostatistics. *Statistica Neerlandica*, 52(1), pp: 18-41.
- Stojic, M. Chandler, J.H. Ashmore, P. & Luce, J. 1998. The assessment of sediment transport rates by automated digital photogrammetry. *Photogrammetric Engineering and Remote Sensing*, 64(5), pp: 387-395.
- Strahler, A.N. 1950. Equilibrium theory of erosional slopes approached by frequency distribution analysis, Part I. *American Journal of Science*, 248, pp: 673-696.
- Strahler, A.N. 1952a. Dynamic basis of geomorphology. *Geological Society American Bulletin*, 63, pp: 923-938.
- Strahler, A.N. 1952b. Hypsometric (area-altitude) analysis of erosional topography. *Geological Society of America Bulletin*, 63, pp: 1117-1142.
- Strahler, A.N. 1954. Statistical analysis in geomorphic research. *Journal of Geology*, 62, pp: 1-25.
- Strahler, A.N. 1956. Basic principles of quantitative geomorphology. *Annals of the Association of American Geographers*, 46(2), pp: 275-275

- Strahler, A.N. 1957. Objective field sampling of physical terrain properties. *Annals of the Association of American Geographers*, 47(2), pp: 179-180.
- Strahler, A.N. 1958. Dimensional analysis applied to fluvially eroded landforms. *Geological Society of America Bulletin*, 69, pp: 279-300.
- Strahler, A.N. 1964. Quantitative geomorphology of drainage basins and channel networks. In: Chow, V.T. (eds.), *Handbook of applied hydrology*. McGraw-Hill, New York.
- Sulebak, J.R. Etzelmüller, B. & Sollid, J.L. 1997. Landscape regionalization by automatic classification of landform elements. *Nor Geogr Tidsskr*, 51(1), pp: 35-45.
- Tarboton, D. 2001. Terrain Analysis Using Digital Elevation Models (TAUDEM). (WWW: <http://hydrology.usu.edu/taudem/taudem5.0/index.html>).
- Tarboton, D.G. & Ames, D.P. 2001. Advances in the mapping of flow networks from digital elevation data. In: *World Water and Environmental Resources Congress*, Orlando, Florida, May 20-24, ASCE.
- Tarboton, D.G. 1997. A New Method for the Determination of Flow Directions and Contributing Areas in Grid Digital Elevation Models. *Water Resources Research*, 33(2), pp: 309-319.
- Tarboton, D.G. 2003. Terrain analysis using Digital Elevation Models in hydrology. ESRI Users Conference, San Deigo, July 7-11.
- Tarboton, D.G. Bras, R.L. & Rodriguez-Iturbe, I. 1988. The fractal nature of river networks. *Water Resources Research*, 24(8), pp: 1317-1322.
- Tarboton, D.G. Bras, R.L. & Rodriguez-Iturbe, I. 1989. Scaling and elevation in river networks. *Water Resources Research*, 25, pp: 2037-2051.
- Tarboton, D.G. Bras, R.L. & Rodriguez-Iturbe, I. 1991. On the extraction of channel networks from Digital Elevation Data. *Hydrologic Processes*, 5(1), pp: 81-100.
- Tarboton, D.G. Bras, R.L. & Rodriguez-Iturbe, I. 1992. A physical basis for drainage density. *Geomorphology*, 5(1/2), pp: 59-76.
- Tarolli, P. & Fontana, G.D. 2009. Hillslope-to-valley transition morphology: New opportunities from high resolution DTMs. *Geomorphology*, 113(1-2), pp: 47-56.
- Tate, E.C. Maidment, D.R. Olivera, F. & Anderson, D.A. 2002. Creating a terrain model for floodplain mapping. *Journal of Hydrologic Engineering*, 7(2), pp: 100-108.
- Thieken, A.H. Lücke, A. Diekkrüger, B. & Richter, O. 1999. Scaling input data by GIS for hydrological modeling. *Hydrological Processes*, 13, pp: 611-630.
- Thoma, D.P. Gupta, S.C. Bauer, M.E. & Kirchoff, C.E. 2005. Airborne laser scanning for riverbank erosion assessment. *Remote Sensing of Environment*, 95, pp: 493-501.
- Thompson, J.A. Bell, J.C. & Butler, C.A. 2001. Digital Elevation Model resolution: Effects on terrain attribute calculation and quantitative soil-landscape modelling. *Geoderma*, 100, pp: 67-89.

- Thornes, J.B. 1976. Semi-Arid Erosional Systems. Geographical Papers, 7. London School of Economics, London.
- Thornes, J.B. 1996. Introduction. In: Brandt, C.J. & Thornes, J.B. (eds.), Mediterranean Desertification and Land Use. Chichester: John Wiley, pp: 1-11.
- Ting, Z. Guo-an, T. Xuejun, L. Yi, Z. Dunxin, J. 2007. Spatial pattern of channel network in Jiuyuangu drainage basin. Key Laboratory of Virtual Geographic Environment. Ministry of Education, Nanjing, China
- Toutin, T. & Gray, L. 2000. State-of-the-art of elevation extraction from satellite SAR data. *ISPRS Journal of Photogrammetry & Remote Sensing*, 55, pp: 13-33.
- Tribe, A. 1991. Automated recognition of valley heads from digital elevation models. *Earth Surface Processes and Landforms*, 16(1), pp: 33-49.
- Tribe, A. 1992. Automated recognition of valley lines and drainage networks from grid digital elevation models: a review and new method. *Journal of Hydrology*, 139, pp: 263-293.
- Tsakiri, M. Lichti D. & Pfeifer, N. 2006. Terrestrial Laser Scanning for deformation monitoring. 3rd IAG / 12th FIG Symposium, Baden.
- Tsukamoto, Y. Ohta, T. & Noguchi, H. 1982. Hydrological and geomorphological studies of debris slides on forested hillslopes in Japan. In: Recent Developments in the Explanation and Prediction of Erosion and Sediment Yield. IAHS Publication, 13, pp: 89-98.
- Tucker, G.E. & Slingerland, R. 1997. Drainage basin response to climate change. *Water Resources Research*, 33(8), pp: 2031-2047.
- Tucker, G.E. Bars R.L. 1998. Hillslope processes, drainage density, and landscape morphology. *Water Resources Research*, 34(10), pp: 2751-2764.
- Tucker, G.E. Catani, F. Rinaldo, A. & Bras, R.L. 2001a. Statistical analysis of drainage density from digital terrain data. *Geomorphology*, 36, pp: 187-202.
- Tucker, G.E. Lancaster, S.T. Gasparini, N.M. Bras, R.L. & Rybarczyk, S.M. 2001b. An object-oriented framework for distributed hydrologic and geomorphic modeling using triangulated irregular networks. *Computers & Geosciences*, 27, pp: 959-973.
- Turcotte, D.L. 1999. Self-Organized Criticality. *Reports on Progress in Physics*. 62, pp: 1377-1429.
- Turner, M.G. & Gardner, R.H. 1991. Quantitative Methods in Landscape Ecology. Springer-Verlag, New York, New York, USA.
- Turner, M.G. 1989. Landscape ecology: The effect of pattern on process. *Annual Review of Ecological Systems*, 20, pp: 171-197.
- Twigg, D.R. 1998. The global positioning system and its use for terrain mapping and monitoring. In: Lane, S.N. Richards, K.S. & Chandler, J.H. (eds.), Landform Monitoring, Modelling and Analysis. New York: Wiley, pp: 37-62.

- USGS. 1987. Digital Elevation Models Data Users Guide. Technical Instructions, Data Users Guide 5, National Mapping Program, United States Geological Survey, Reston, VA.
- Van Rompaey, A. Govers, G. & Baudet, M. 1999. A strategy for controlling error in distributed environmental models by aggregation. *International Journal of GIS*, 13 (6), pp: 577–590.
- Vandekerckhove, L. Poesen, J. Oostwoud, D. Gyssels, G. Beuselinck, L. & de Luna, E. 2000. Characteristics and controlling factors of bank gullies in two Mediterranean semi-arid environments. *Geomorphology*, 33, pp: 37-58.
- Varzi, A.C. 2001. Vagueness in geography. *Philosophy and Geography*. 4, pp: 49-65.
- Vendrusculo, L.C. Magalhães, P.S.G. Vieira, S.R. & Carvalho, J.R.P. 2004. Computational System for Geostatistical Analysis. *Scientia Agricola*, 61(1), pp: 100-107.
- Verdin, K. L. & Jenson, S.K. 1996. Development of Continental Scale DEMs and Extraction of Hydrographic Features. Integrating GIS and Environmental Modeling, Sante Fe, New Mexico: National Center for Geographic Information and Analysis (NCGIA).
- Vianello, A. Cavalli, M. & Tarolli, P. 2009. LiDAR-derived slopes for headwater channel network analysis. *Catena*, 76, pp: 97-106.
- Vicsek, T. 1992. Fractal Growth Phenomena. Singapore, World Scientific Publishing, Co. Ltd.
- Viessmann, W. & Lewis, G.L. 1996. Introduction to Hydrology. New York, HyperCollins College Publishers.
- Villatoro M. Henríquez, C. & Sancho, F. 2008. Comparación de los interpoladores IDW y kriging en la variación espacial de pH, Ca, CICE y P del suelo. *Agronomía Costarricense*, 32(1), pp: 95-105.
- Vogt, J.V. Colombo, R. & Bertolo, F. 2003. Deriving drainage networks and catchment boundaries: a new methodology combining digital elevation data and environmental characteristics. *Geomorphology*, 53(3-4), pp: 281-298.
- Voudouris, V. Wood, J. & Fisher, P. 2005. Collaborative geo-visualization: Object-field representations with semantic and uncertainty information. *Lecture Notes in Computer Science*, 3762, pp: 1056-1065.
- Walker, J.P. & Willgoose, G.R. 1999. On the effect of digital elevation model accuracy on hydrology and geomorphology. *Water Resources Research*, 35, pp: 2259-2268.
- Walsh, S.J. Butler, D.R. & Malanson, G.P. 1998. An overview of scale, pattern, process relationships in geomorphology: a remote sensing and GIS perspective. *Geomorphology*, 21(3-4), pp: 183-205.
- Wang, X. & Yin, Z.Y. 1998. A comparison of drainage networks derived from digital elevation models at two scales. *Journal of Hydrology*, 210(1-4), pp: 221-241.
- Ware, J.M. & Jones, C.B. 1997. A Triangle-Based Surface Model for 3D-GIS. Proceedings 5th ACM Workshop on Advances in GIS, Las Vegas, ACM Press, pp: 20-23.
- Webster, R. & Oliver, M.A. 1990. Statistical methods in soil and landscape resources survey. Oxford University Press, Oxford.
- Webster, R. & Oliver, M.A. 2001. Geostatistics for Environmental Scientists. John Wiley and Sons, Chichester.

- Wechsler, S.P. & Kroll, C. 2006. Quantifying DEM Uncertainty and its Effect on Topographic Parameters. *Photogrammetric Engineering and Remote Sensing*, 72, pp: 1081-1090.
- Wechsler, S.P. 2000. Effect of DEM Uncertainty on Topographic Parameters, DEM Scale and Terrain Evaluation, State University of New York College of Environmental Science and Forestry, Syracuse, NY, Ph.D. Dissertation, pp. 380.
- Wechsler, S.P. 2003. Perceptions of Digital Elevation Model Uncertainty by DEM Users, *URISA Journal*, 15, pp: 57-64.
- Wechsler, S.P. 2007. Uncertainties associated with digital elevation models for hydrologic applications: a review. *Hydrology and Earth System Science*, 11, pp: 1481-1500.
- Wehr, A. & Lohr, U. 1999. Airborne laser scanning-an introduction and overview. *ISPRS Journal of Photogrammetry and Remote Sensing*, 54(2/3), pp: 68-82.
- Weibel, R. & Heller, M. 1991. Digital Terrain Modeling. In: Maguire, D.J. Goodchild, M.F & Rhind, D.W. (eds.), *Geographic Information Systems, Vol. 1: Principles*. Harlow: Longman: pp: 269-297.
- Weijermars, R. 1991. Geology and tectonics of the Betic zone, SE Spain. *Earth Science Review*, 31, pp: 153-236.
- Werner, C. & Smart, J.S. 1973. Some new methods of topologic classification of channel networks. *Geographical Analysis*, 5, pp: 271-95.
- Wharton, G. 1994. Progress in the use of drainage network indices for rainfall-runoff modelling and runoff prediction. *Progress in Physical Geography*, 18(4), pp: 539-557.
- White, S.A. & Wang, Y. 2003. Utilizing DEMs derived from LIDAR data to analyze morphologic change in the North Carolina coastline. *Remote Sensing of Environment*, 85, pp: 39-47.
- Wiens, J.A. 1989. Spatial scaling in ecology. *Functional Ecology*, 3, pp: 385-397.
- Willgoose, G.R. & Hancock, G. 1998. Revisiting the hypsometric curve as an indicator of form and process in transport-limited catchment. *Earth Surface Processes and Landforms*, 23, pp: 611-623.
- Willgoose, G.R. & Perera, H.J. 2001. A simple model for saturation excess runoff generation based on geomorphology, steady state soil moisture. *Water Resources Research*, 37, pp: 147-156.
- Willgoose, G.R. Bras, R.L. & Rodriguez-Iturbe, I. 1991. A physical explanation of an observed link area-slope relationship. *Water Resources Research*, 27(7), pp: 1697-1702.
- Wilson, J.P. & Gallant, J.C. 1998. Terrain-based approaches to environmental resource Evaluation. In: Lane, S.N. Richards, K.S. & Chandler, J.H. (eds.), *Landform Monitoring, Modelling and Analysis*. New York: Wiley, pp: 219-240.
- Wilson, J.P. & Gallant, J.C. 2000. Digital Terrain Analysis. In: Wilson, J.P. & Gallant, J.C. (eds.), *Terrain Analysis: Principles and Applications*. New York, Wiley, pp: 1-28.
- Wilson, J.P. & Repetto, L. & Snyder, R.D. C. 2000. Effect of data source, grid resolution, and flow-routing method on computing topographic attributes. In: Wilson, J.P. & Gallant, J.C. (eds.), *Terrain Analysis: Principles and Applications*, New York, Wiley, pp: 133-161.

- Wilson, J.P. Spangrud, D.J. Nielsen, G.A. Jacobsen, J.S. & Tyler, D.A. 1998. Global positioning system sampling intensity and pattern effects on computed topographic attributes. *Soil Science Society of America Journal*, 62(5), pp: 1410-1417
- Wimmer, C. Siegmund, R. Schwäbisch, M. Moreira, J. 2000. Generation of high-precision DEMs of the Wadden Sea with airborne interferometric SAR. *IEEE Transactions on Geoscience and Remote Sensing*, 38, pp: 2234-2245.
- Wise, S.M. 1998. The Effect of GIS interpolation errors on the use of DEMs in Geomorphology. In: Lane, S.N. Richards, K.S. & Chandler, J.H. (eds.), *Landform Monitoring, Modelling and Analysis*. Wiley, Chichester, pp: 139-164.
- Wise, S.M. Thornes, J.B. & Gilman, A. 1982. How old are the badlands? A case study from south-east Spain. In: Bryan, R.B. & Yair, A. (eds.), *Badlands geomorphology and piping*. Geo Books, Norwich, pp: 259-277.
- Wolf, G.W. 1991. A FORTRAN subroutine for cartographic generalization. *Computers & Geosciences*, 17(10), pp: 1359-1381.
- Wolock, D.M. & McCabe, G.J. 2000. Differences in topographic characteristics computed from 100- and 1000-m resolution digital elevation model data. *Hydrological Processes*. 14(6), pp: 987-1002.
- Wolock, D.M. & Price, C.V. 1994. Effects of digital elevation model map scale and data resolution on a topography-based watershed model. *Water Resources Research*, 30(11), pp: 3041-3052.
- Wood, J.D. 1990. Automated surface feature detection from digital elevation data. Part two: Implementation. *Midlands Regional Research Laboratory Research Report no. 21*. Midlands Regional Research Laboratory, Leicester, England.
- Wood, J.D. 1993. Measuring and reporting the accuracy of Ordnance Survey digital elevation data. Ordnance Survey Technical Report, Ordnance Survey, Southampton.
- Wood, J.D. 1995. Scale-based characterization of Digital Elevation Models. Proceedings, 3rd National Conference on GIS Research UK (GISRUK '95), Newcastle.
- Wood, J.D. 1996a. The geomorphologic characterization of digital elevation models. PhD Dissertation, University of Leicester, UK.
- Wood, J.D. 1996b. Scale-based characterization of digital elevation models in Parker D *Innovations in GIS 3* Taylor & Francis, London, pp: 163-175.
- Wood, J.D. 1998. Modelling the continuity of surface form using Digital Elevation Models. In: Proceedings of the 8th International Symposium on Spatial Data Handling. Simon Fraser University, Burnaby, British Columbia, pp: 725-736.
- Wood, J.D. 2002. Visualizing the structure and scale dependency of landscapes. In: Fisher, P. & Unwin, D. (eds.), *Virtual reality in geography*. Taylor & Francis, London, pp: 163-174.

- Wood, J.D. Dykes, J. & Slingsby, A. 2007. Interactive visual exploration of a large spatio-temporal dataset: Reflections on a geovisualization mashup. *IEEE Transactions on Visualization and Computer Graphics*, 13(6), pp: 1176-1183.
- Woorcock, C.E. & Strahler, A.H. 1987. The factor of scale in remote sensing. *Remote Sensing of Environment*, 21, pp: 311-322.
- Wu, J. 1999. Hierarchy and scaling: Extrapolating information along a scaling ladder. *Canadian Journal of Remote Sensing*, 25, pp: 367-380.
- Wu, J. 2004. Effects of changing scale on landscape pattern analysis: scaling relations. *Landscape Ecology*, 19(2), pp: 125-139.
- Wu, J. Jelinski, E.J. Luck, M. & Tueller, P.T. 2000. Multiscale analysis of landscape heterogeneity: Scale variance and pattern metrics. *Geographic Information Sciences*, 6(1), pp: 6-16.
- Yang, D. Herath S. & Musiake, K. 2001. Spatial resolution sensitivity of catchment geomorphologic properties and the effect on hydrological simulation. *Hydrological Processes*, 15, pp: 2085-2099.
- Yang, D. Herath, S. & Musiake, K. 2000. Comparison of different distributed hydrological models for characterization of catchment spatial variability. *Hydrological Processes*, 14, pp: 403-416.
- Yoeli, P. 1983. Digital terrain models and their cartographic and cartometric utilization. *The cartographic Journal*, 20(1), pp: 17-22.
- Yu, S. Kreveld, M.V. & Snoeyink, J. 1997. Drainage queries in TINs: from local to global and back again. In: Kraak, M.J. & Molenaar, M. (eds.), *Advances in GIS Research II: Proceedings of the 7th International Symposium on Spatial Data Handling*. London: Taylor & Francis, pp: 829-842.
- Zaluski, M.H. & Moe, M.J. 2008. Analytical element method for modeling of groundwater flow in anisotropic aquifer. *Proceedings of the 2008 Spring simulation multiconference*, Ottawa, Canada, pp: 209-213.
- Zevenbergen, L.W. & Thorne, C.R. 1987. Quantitative Analysis of Land Surface Topography. *Earth Surface Processes and Landforms*, 12, pp: 47-56.
- Zhang, W. & Montgomery, D. 1994. Digital elevation model grid size, landscape representation, and hydrologic simulation. *Water Resources Research*, 30, pp: 1019-1028.
- Zhang, X. Drake, N.A. Wainwright, J. & Mulligan, M. 1999. Comparison of slope estimates from low resolution DEMs: Scaling issues and a fractal method for their solution. *Earth Surface Processes and Landforms*, 24, pp: 763-779.
- Zhou, H. Sun, J. Turk, G. & Rehg, J.M. 2007. Terrain Synthesis from Digital Elevation Models. *Transactions on Visualization and Computer Graphics*, 13, 4: pp: 834-848.
- Zwolinski, Z. 2003. Streams and river Lab: An introduction to fluvial geomorphology. <http://resweb.llu.edu/~rford/courses/ESSC500/fluvial/fluvial.html>.

Appendix 1:

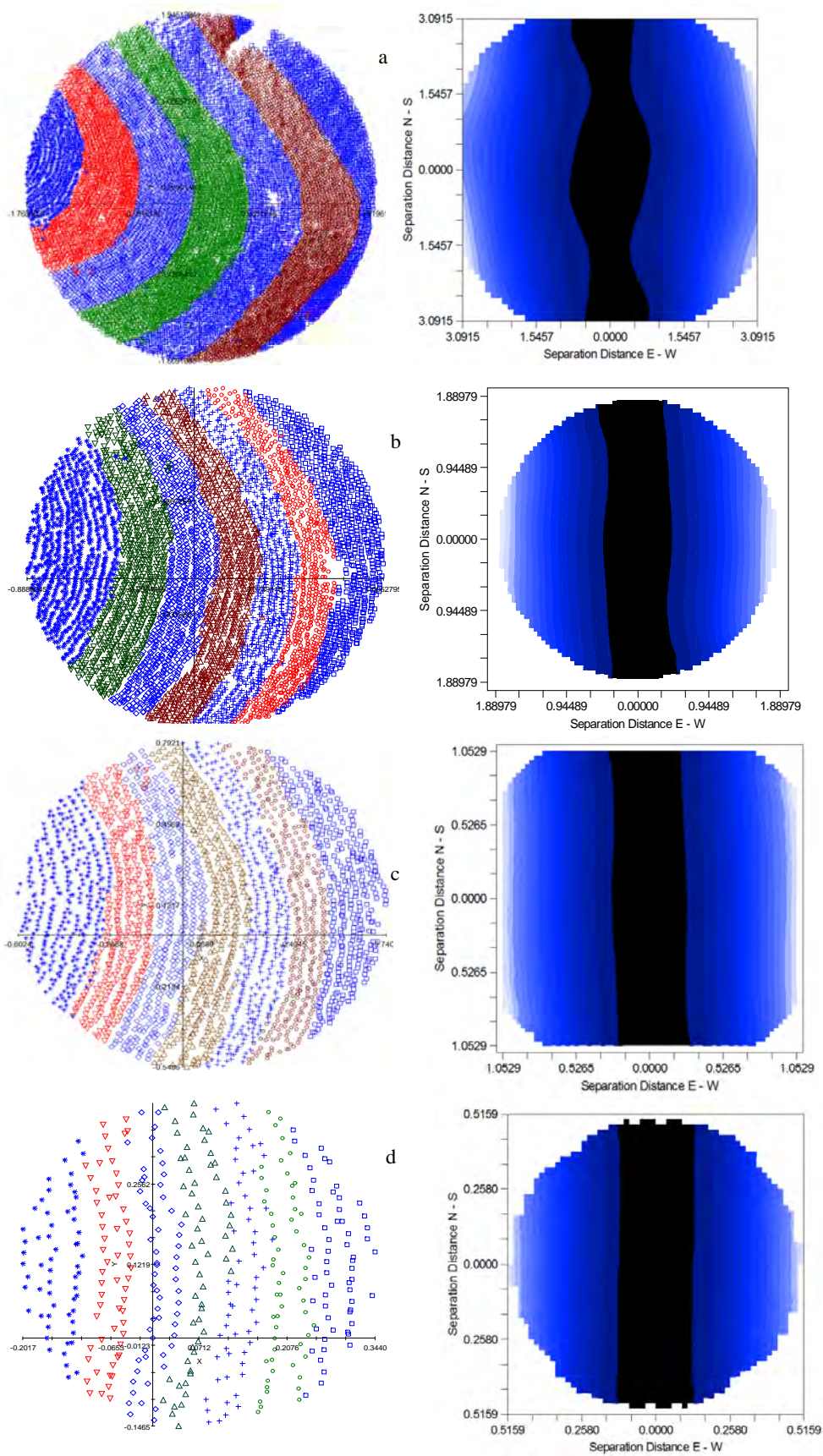


Figure 1 Posting of data values against their anisotropic semivariance surface (ASS) in ridge formation with trend, for the sub-hierarchical scales organized as follows: a) 3 m; b) 2 m; c) 1 m; and, d) 0.5 m.

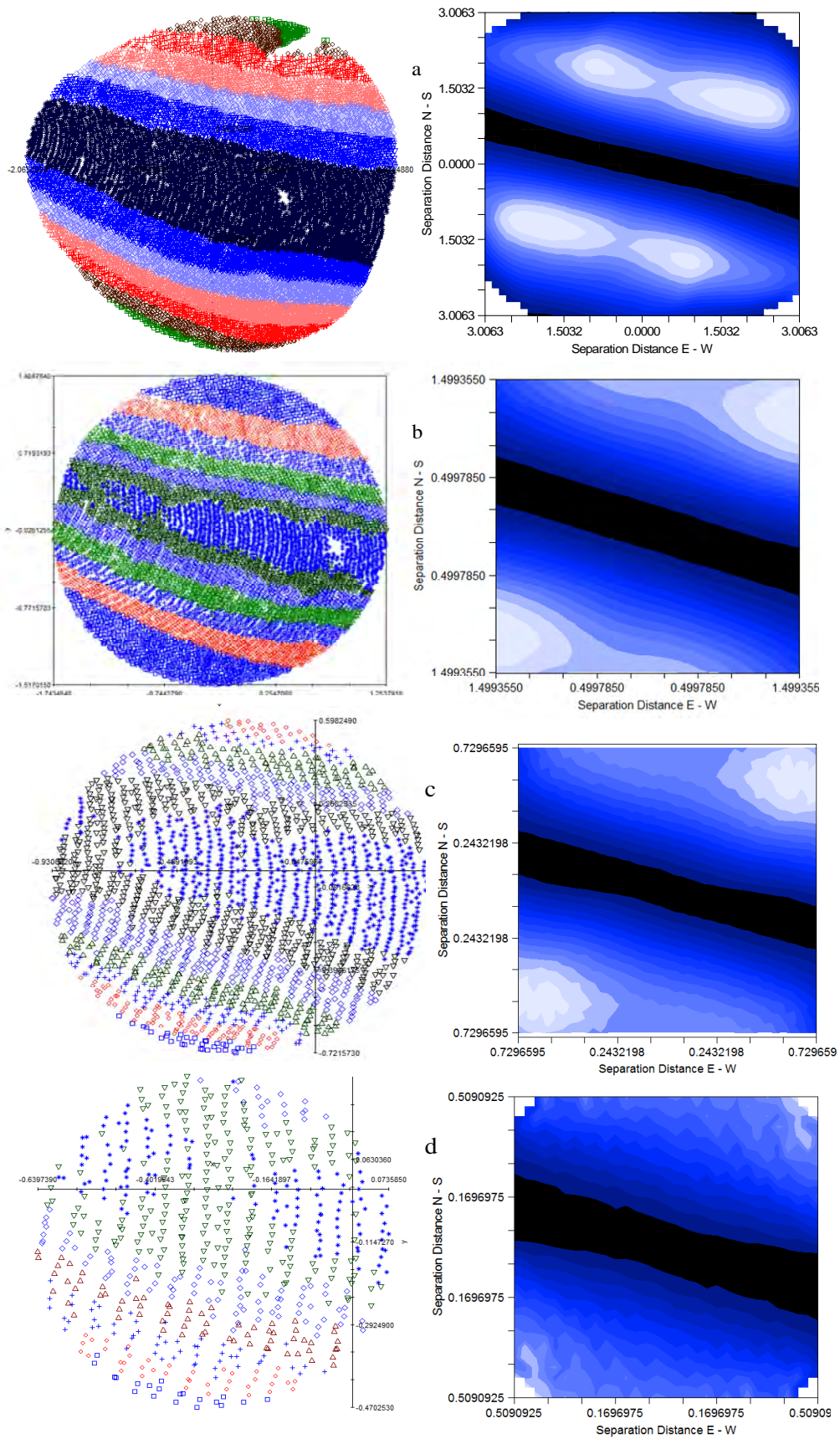


Figure 2 Posting of data values against their anisotropic semivariance surface (ASS) in ridge formations without trend, for the different sub hierarchical scales organized as follows: a) 3 m; b) 2 m; c) 1 m; and, d) 0.5 m.

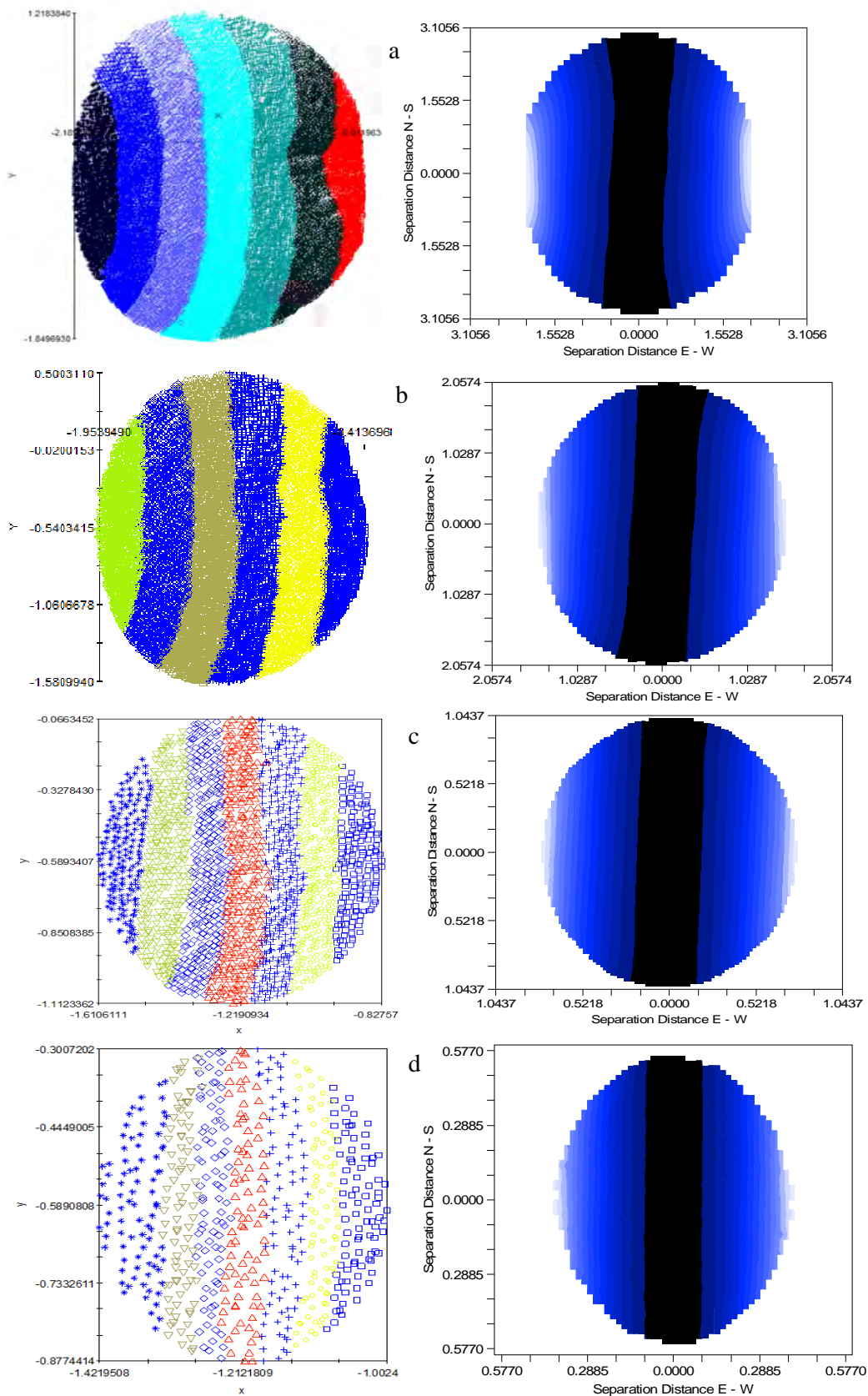


Figure 3 Posting of data value against their corresponding anisotropic semivariance surface (ASS) in hillslope formations with trend, for the different sub-hierarchical scales organized as follows: a) 3 m; b) 2 m; c) 1 m; and, d) 0.5 m.

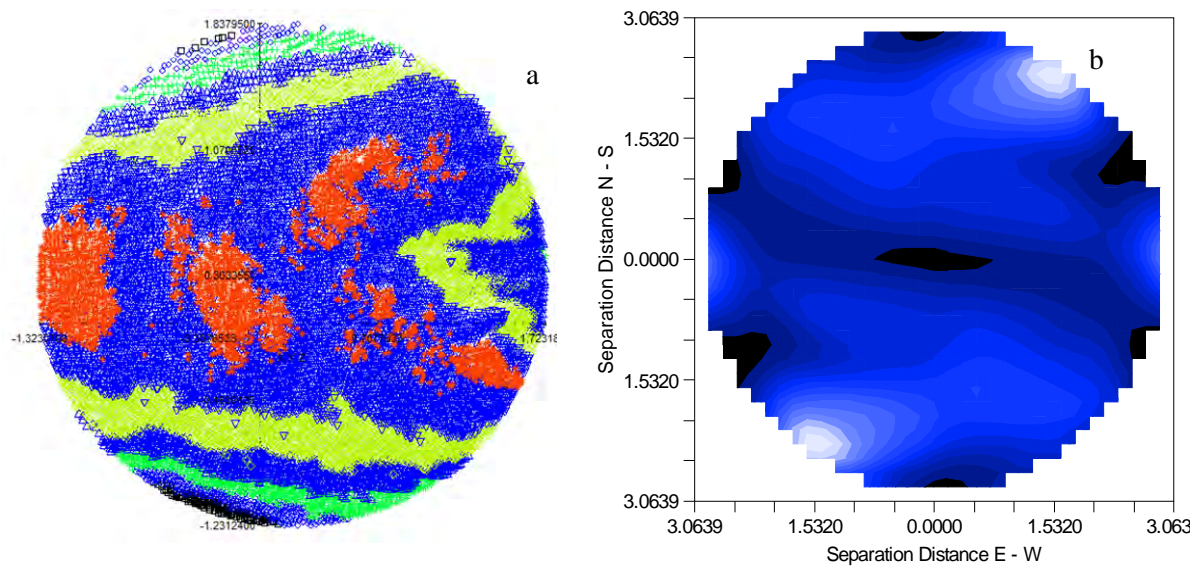


Figure 4 Directional autocorrelation in hillslope formation without trend in the studied sample dataset of 3 m; a) map of data posting values; and, b) map of anisotropic semivariance surface (ASS).

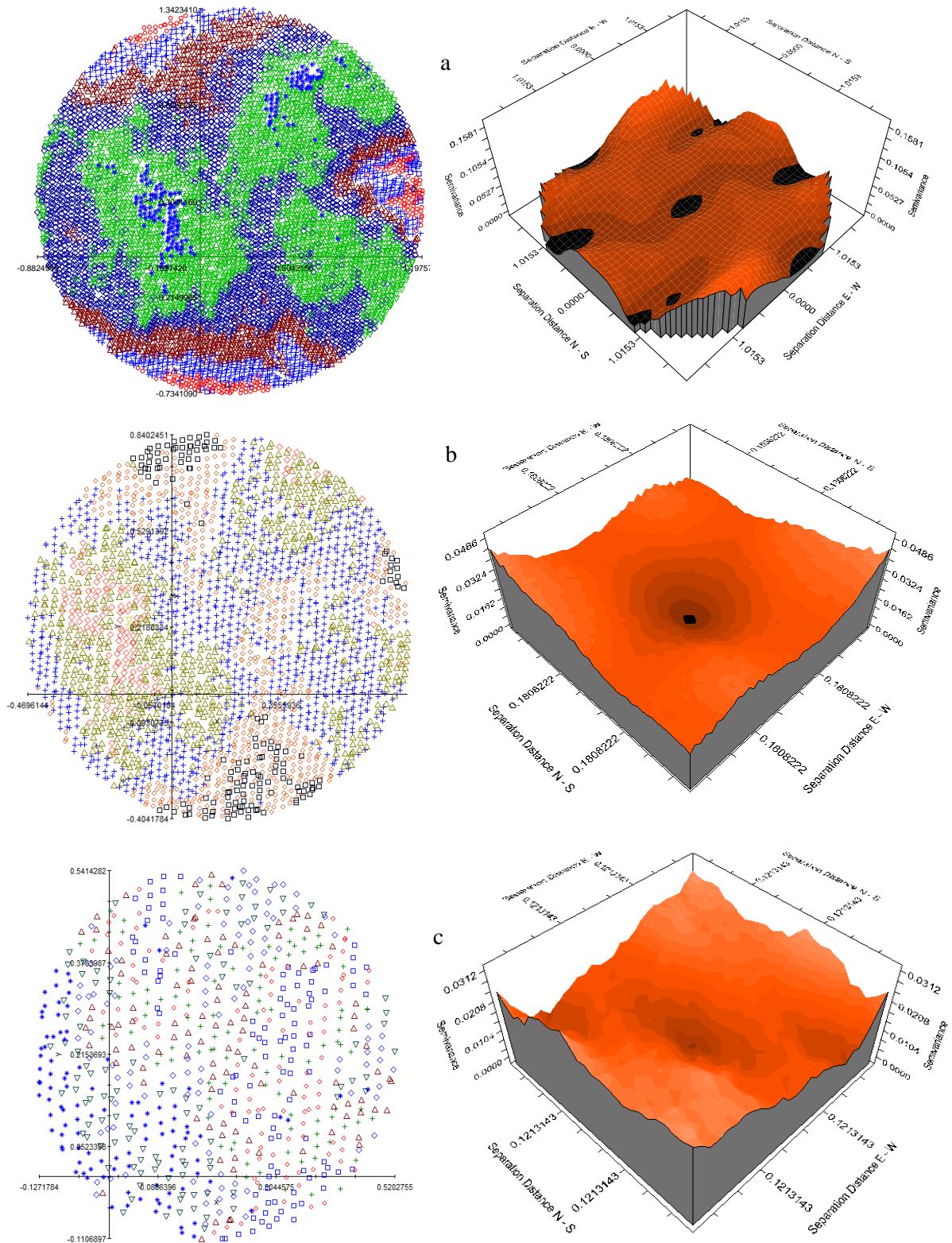


Figure 5 Posting of data values against their anisotropic semivariance surface (ASS) in hillslope formation without trend, for the different sub-hierarchical scales organized as follows: a) 2 m; b) 1 m; and, c) 0.5 m.

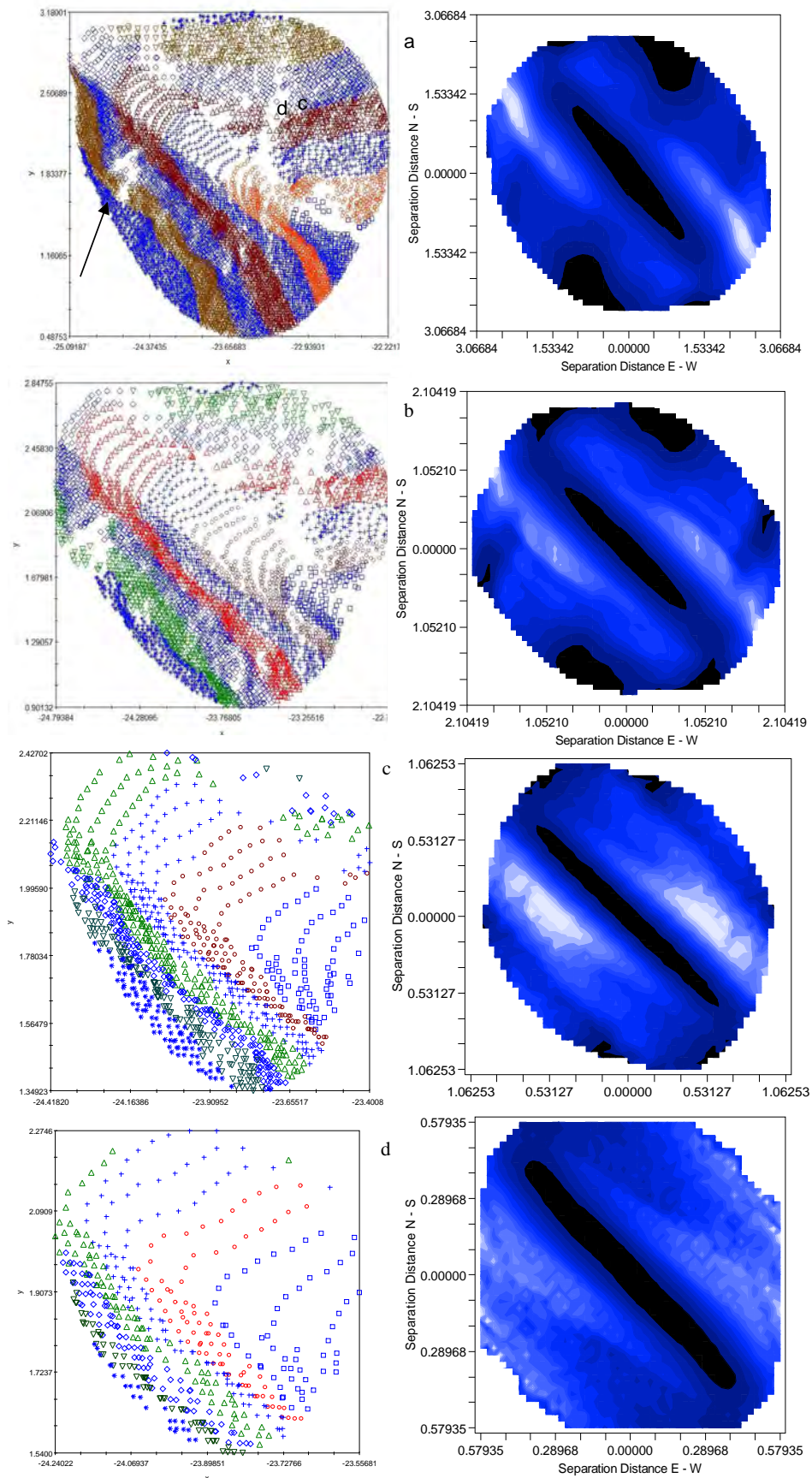


Figure 6 Posting of data values against their anisotropic semivariance surface (ASS) in stream formations with trend, for the different sub-hierarchical scales organized as follows: a) 3 m; b) 2 m; c) 1 m; and, d) 0.5 m.

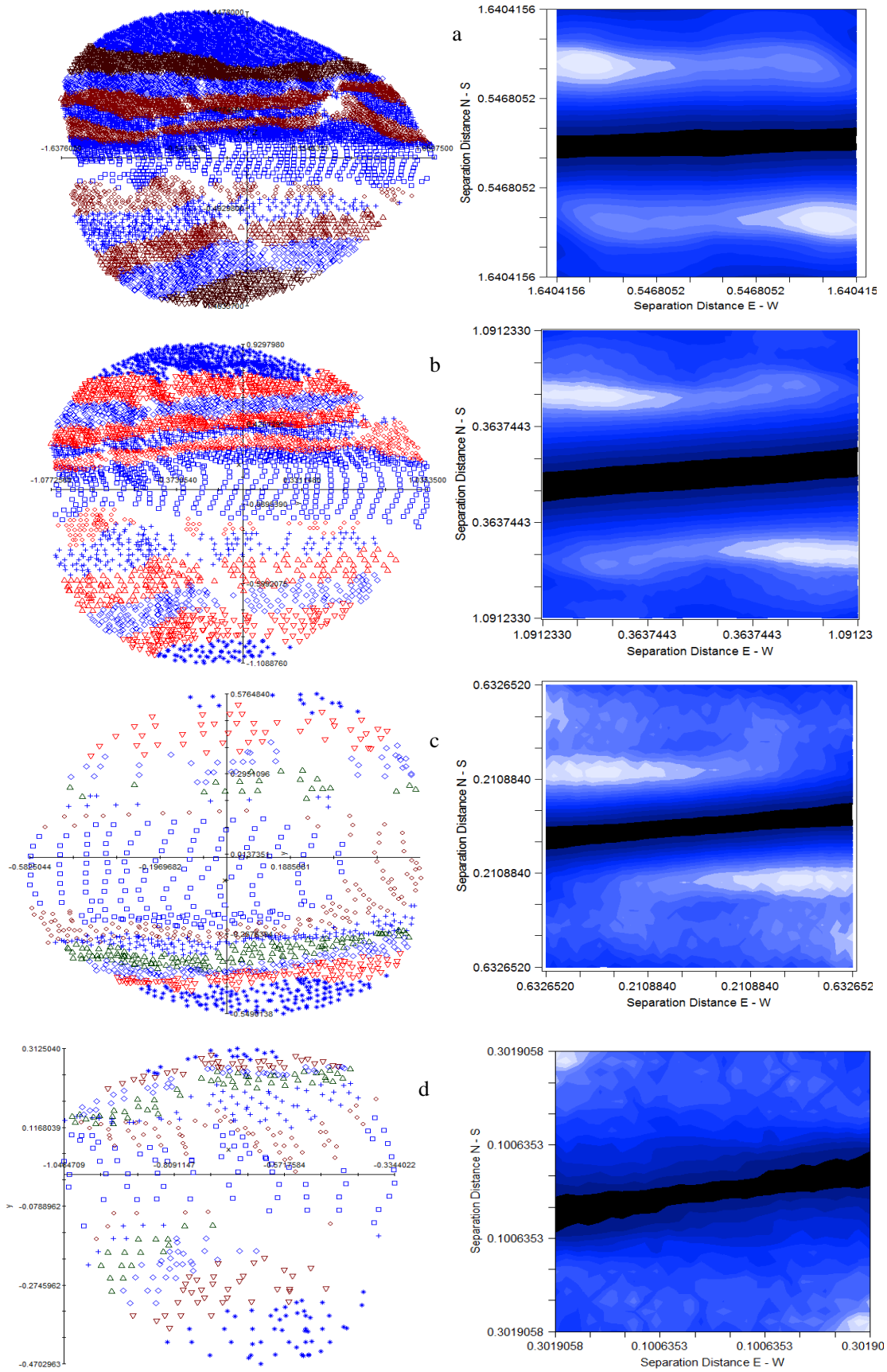


Figure 7 Posting of data value against their anisotropic semivariance surface (ASS) in stream formation without trend, for the different sub-hierarchical scales organized as follows: a) 3 m; b) 2 m; c) 1 m; and, d) 0.5 m.

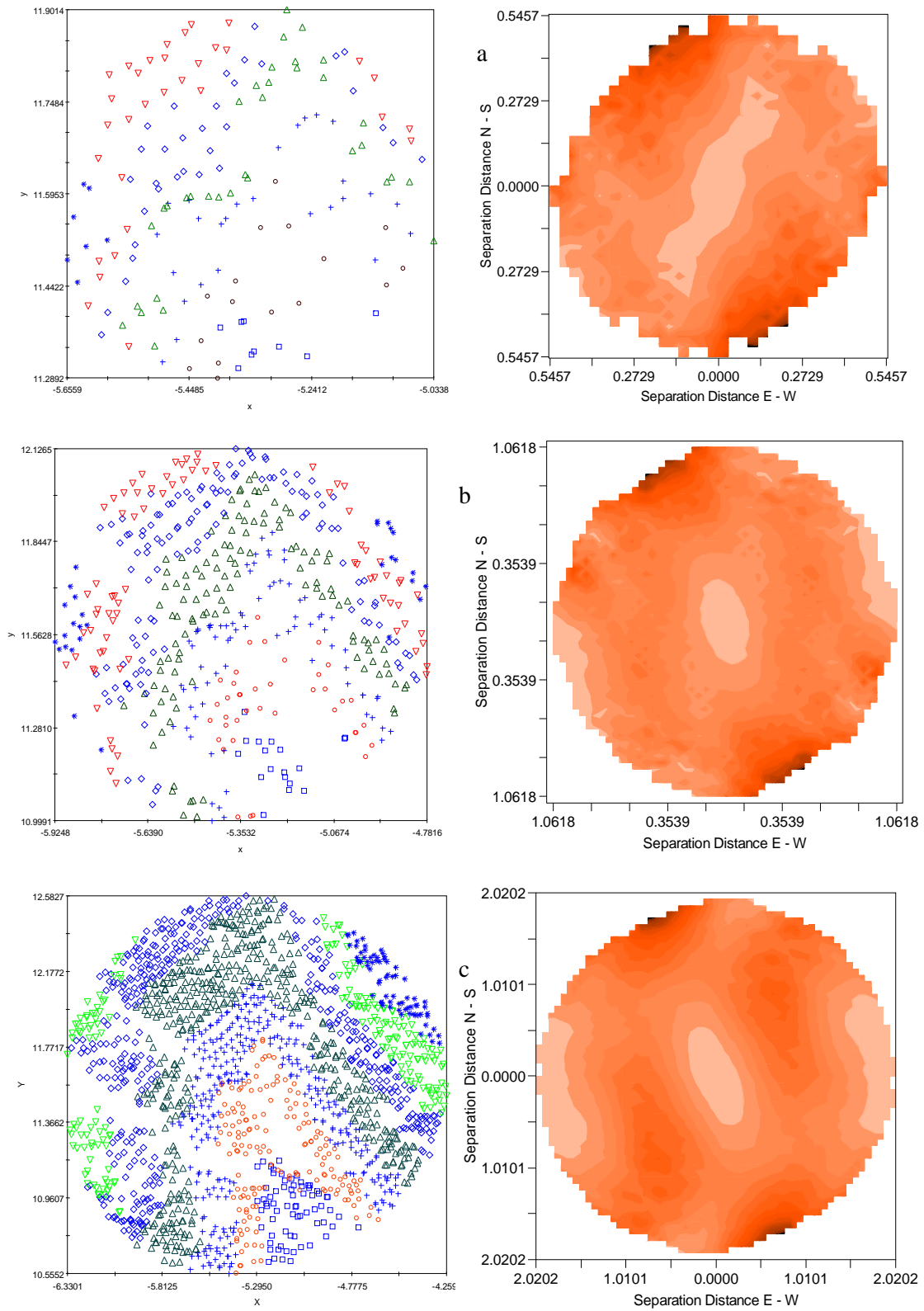


Figure 8 Posting of data values against their anisotropic semivariance surface (ASS) in channel initiation with trend, for the different sub-hierarchical scales organized as follows: a) 2 m; b) 1 m; and c) 0.5 m.

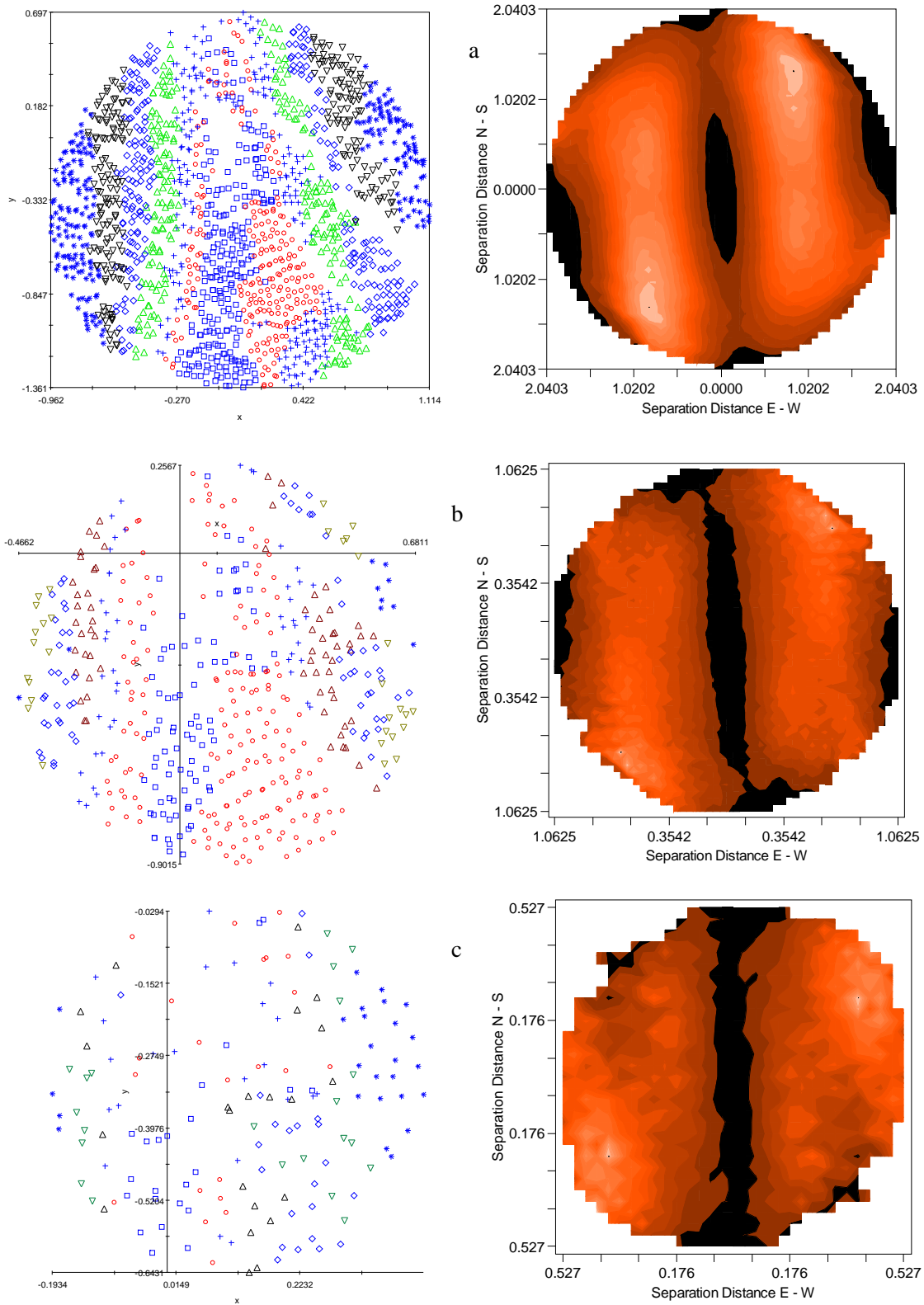


Figure 9 Posting of data value against their anisotropic semivariance surface (ASS) in channel initiation without trend, for the different sub-hierarchical scales organized as follows: a) 2 m; b) 1 m; and, c) 0.5 m.

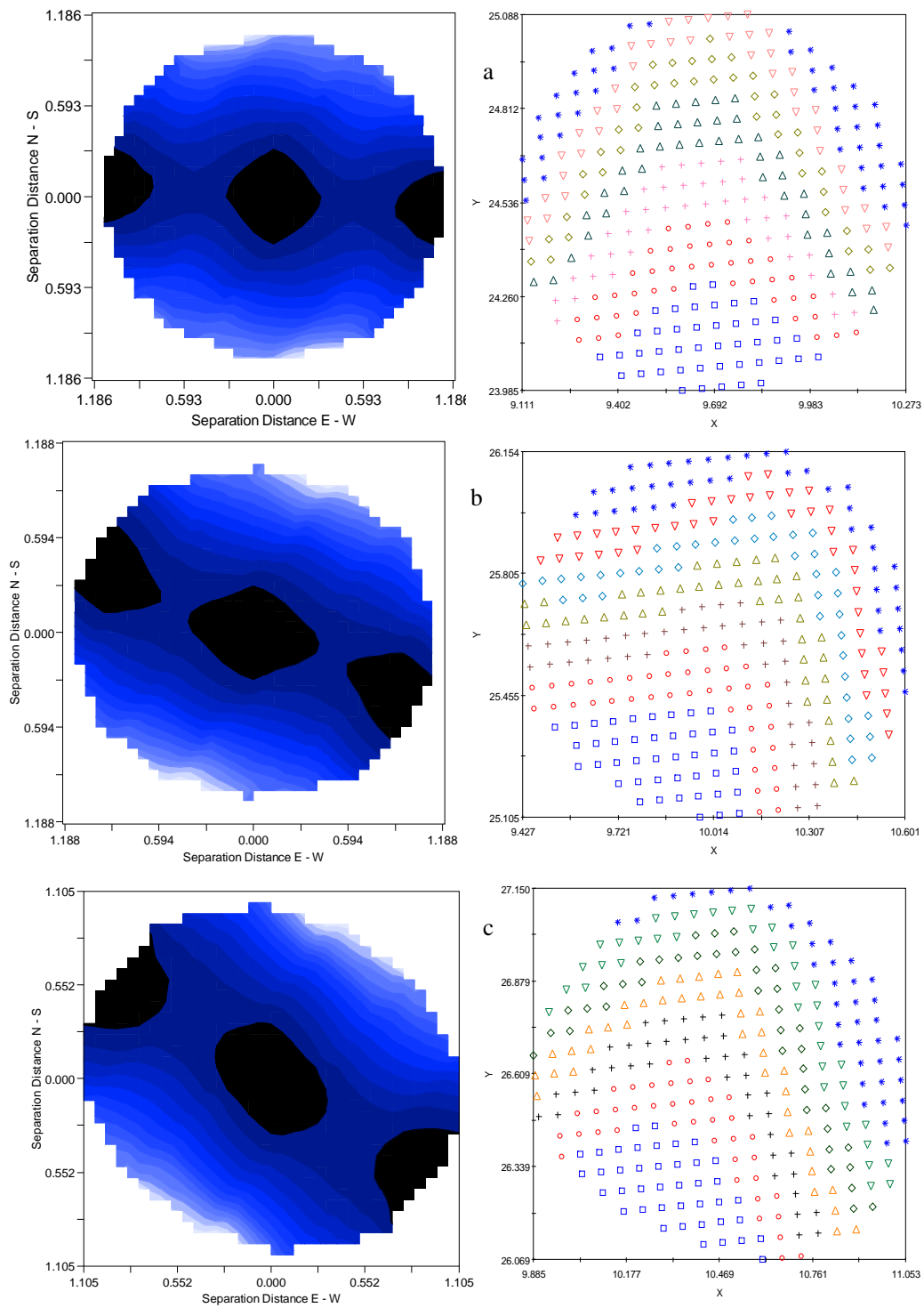


Figure 10 Posting of data values against their corresponding anisotropic semivariance surface (ASS) in the interpolated stream formations organized as follows: a) Stream 1; b) stream 2; and, c) transition zones 1.

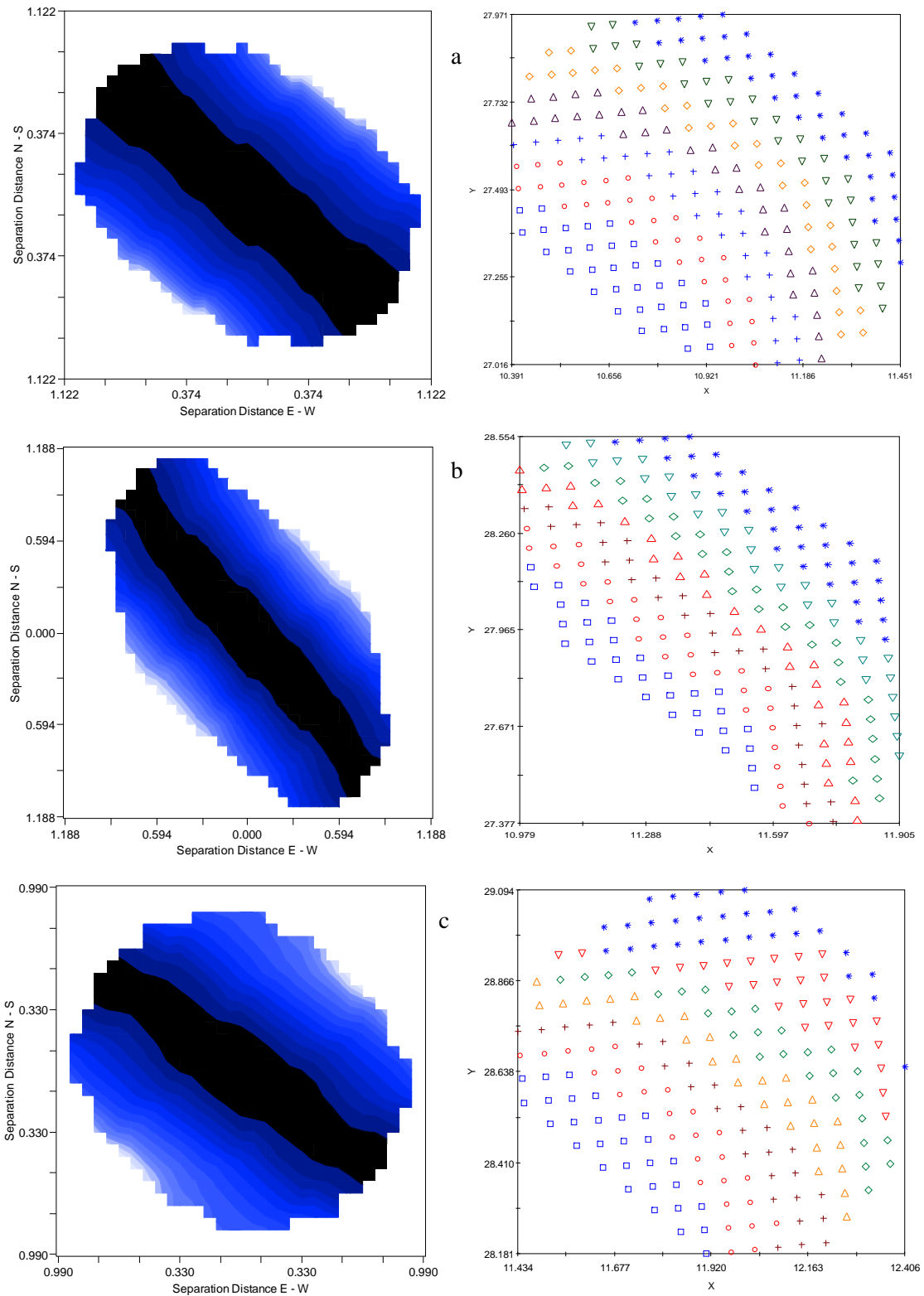


Figure 11 Posting of data values against their corresponding ASS representation for the interpolated hillslope formations; a) transition zone 2; b) hillslope 1; and, c) hillslope 2.

